Akademie věd České republiky

Disertace
k získání vědeckého titulu "doktor věd"
ve skupině věd Chemické vědy

Interfacing microchannel separations with electrospray mass spectrometry

……
název disertace

Komise pro obhajoby doktorských disertací v oboru Analytická chemie

Jméno uchazeče: Ing. František Foret, CSc.

Pracoviště uchazeče: Ústav analytické chemie AV ČR, v.v.i., Veveří 97, 602 00 Brno

V Brně dne 30. 6. 2017

Table of Contents

Summary

This dissertation describes development and application of interfaces for coupling of microchannel separations with electrospray mass spectrometry. The text, based on 20 selected publications, covers mainly electrophoretic separations coupled to electrospray mass spectrometry for both capillary arrangements and chip based devices. The papers document my research activities in electrospray mass spectrometry interfacing over the past 24 years and were selected from over 100 other studies published during the 1993 – 2016. The presented work is highly experimental and since each arrangement has its own specifics, I have divided the papers into two separate sections (although both parts of the work have overlapped in time). The first part deals with capillary electrophoresis-mass spectrometry and includes eleven research papers covering various aspects of interfacing of capillary electrophoresis, performed in standard fused silica capillaries, with electrospray mass spectrometry. The second part documents the evolution of different approaches and instrumentation for on-line coupling of microfabricated devices with electrospray mass spectrometry.

List of symbols and abbreviations

BGE	Background electrolyte
CE-MS	capillary electrophoresis-mass spectrometry
EOF	electroosmotic flow
ESI	Electrospray ionization
GC	gas chromatography
HPLC	high performance liquid chromatography
HV	high voltage
IC	ion chromatography
ID	internal diameter
IEF	isoelectric focusing
ITP	isotachophoresis
LOD	limit of detection
MS	Mass spectrometry
OD	outer diameter
pI	isoelectric point
PTFE	polytetrafluoroethylene
S/N	signal-to-noise
TOF	time-of-flight

Introduction

In the late 1980 – early 1990 the mass spectrometry witnessed a paradigm change when John Fenn published a series of papers describing electrospray ionization[1]. Suddenly, the analysis of large molecules, including biopolymers, could be easily achieved without fragmentation. Moreover, the multiply charged ions of peptides and proteins could be analyzed on mass spectrometers with limited mass/charge range. Within few years the mass spectrometry, once dominating only in laboratories dealing with inorganic and/or small organic molecules analyses, became an important tool for bioanalysis.

At about the same time another revolution was growing in molecular biology related to the invention of new tools for DNA analysis. In 1990 the Human Genome Project officially started[2] and after its completion little over a decade later, the outcomes are changing the way biology and medicine is practiced today. Also in the same time, capillary electrophoresis has emerged as an interesting separation tool for rapid and highly efficient analysis of ionogenic compounds[3]. In that period I was finishing my CSc. (PhD in today's world) with the focus on theory, instrumentation and applications of capillary electrophoresis[4] under the direction of Prof. Petr Boček. When the first papers, indicating the potential of CE for rapid separations of DNA fragments, have just been published[5-6] we have also started to look into the technology [7]and in 1991 I was lucky to get a postdoctoral position at the Northeastern University in Boston. Originally, my intention was to work on the research related to the Human Genome Project[8-10] with Prof. Barry L. Karger at the Barnett Institute; however, during the first year the laboratory received a brand new TSQ700 triple quadrupole electrospray mass spectrometer from Finnigan and I was asked to interface it with capillary electrophoresis. That was the start of my diversion towards the mass spectrometry coupling territory, which extended for another 10 years of my stay in Boston and continues as one of the main research activities even today in Brno. The following text will briefly review the development of both capillary electrophoresis-electrospray mass spectrometry (CE-ESI/MS) and coupling of microfluidic devices with ESI/MS. The text is largely based on review papers, which I have co-authored, but are not included in the papers selected for the presented thesis[11-14].

1. Mass spectrometry interfacing

The advances in the mass spectrometric instrumentation provide tools for high resolution and high throughput analyses of broad range of biological analytes. Given the resolving power of the new time of flight (TOF), the Fourier transform mass spectrometers (FT-MS) and Orbitrap instruments one might question the need for sample separation prior to the MS analysis. Indeed, instruments with the resolution of several hundreds of thousands have clearly demonstrated the capability for analyses of crude mixtures of hundreds of proteins and protein digests[15-16]. Although impressive, the resolution of the mass spectrometer itself does not guarantee a successful analysis. Besides the need to separate isobaric species, isomers and isoforms, the ionization suppression effects are the main limiting factors for practical

use of direct MS analysis. Both main interfacing techniques used in biological mass spectrometry, the electrospray (ESI) and matrix assisted laser desorption/ionization (MALDI), suffer from these problems. It is frequently observed, that the detected MS signals of individual species in a mixture do not correspond to their respective concentrations. In some cases the presence of a certain (often major) sample component completely suppresses the signal of other components. Although, the ionization processes are still not fully understood, it is known that signal suppression can be eliminated by separating the interfering compounds, e.g., by chromatography or electrophoresis. An example of the observed signal suppression is shown in Fig. 1.

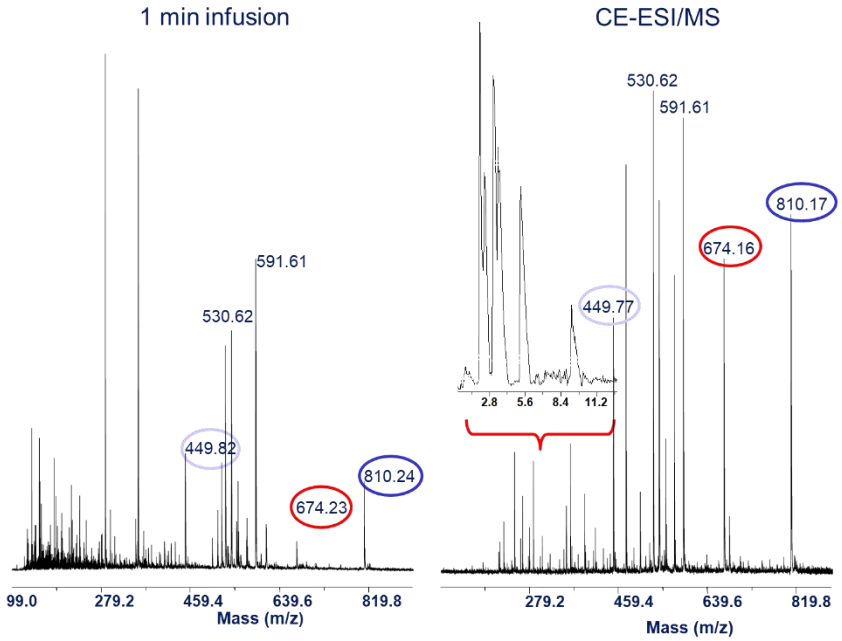

Fig. 1 Demonstration of the signal suppression in ESI/MS analysis. The left panel shows an ESI/MS spectrum averaged during a 1 min infusion of a peptide mixture. The right side shows the ESI/MS spectrum of the same sample injected into a CE capillary in 10x smaller volume and separated by CE-MS. The mass spectra behind the total ion current CE-MS trace shown in the inset were summed up to provide the corresponding total sample mass spectrum. The circled numbers were selected to point out some of the clear differences in the signal intensity. F. Foret, unpublished results.

This example is typical for practically all complex samples where the minor sample components can be completely obscured by compounds with higher concentration and/or higher ionization efficiency, e.g., higher proton affinity in the gas phase. Thus coupling of liquid-phase separation techniques with mass spectrometry (MS) is the main way for obtaining identity and structural information in many fields of bioanalysis including proteomics. Although dominated by the maturing LC/MS technology there are also other techniques playing important roles in specific bioanalytical areas. Capillary electrophoresis (CE) offers different selectivity, higher efficiency and often also shorter analysis time compared to HPLC. In addition, working with narrow, open

separation capillaries and very small (nL) injection volumes may be an advantage when the sample amount is limited or for a second dimension in multidimensional separations. Finally, once optimized, electrophoretic separation protocols can be easily scaled either for obtaining higher injected amount in longer capillaries or for speed in shorter columns or microfluidic chips.

The above mentioned arguments have been documented in a number of original and review articles dealing with CE-MS. Review articles focused on the instrumental[17-18] and wet chemistry[19] aspects as well as CE-MS application in various fields such as proteomics[20-24], glycomics[25], metabolomics[26], biomarker discovery[27-30], amino acid analysis acids[31] and/or chiral CE-MS[32]. Other CE-MS reviews specialized on the use of capillary coatings in CE-MS[33], CE-TOF/MS[34], or on-line coupling of electrokinetic chromatography and mass spectrometry[35]. Selected instrumentation as well as CE-ESI/MS applications are discussed below.

2. Instrumentation for CE-ESI/MS

A variety of ionization methods such as atmospheric pressure chemical ionization (APCI), atmospheric pressure photoionization (APPI), sonic spray ionization (SSI), thermospray ionization (TSI), matrix-assisted laser desorption/ionization (MALDI) or continuous-flow fast atom bombardment (CF-FAB) have been attempted for CE-MS coupling[36]; however, electrospray (ESI) is by far the most popular ionization technique. In principle, a CE-MS interface should accomplish four important features: (i) electrical connection for adjusting ESI potential, (ii) electrical connection to close the electrophoresis separation current, (iii) suitable outlet for direct spray of separated analytes, and (iv), in some cases, introduction of a spray liquid and nebulizing gas. For reproducible separation and stable ESI, the optimal CE/ESI/MS interface device should effectively decouple the CE and MS processes so that each could work under optimal conditions without negatively affecting the other. Physical robustness, ease of use with maximal stability and sensitivity for analyte detection as well as maintaining CE separation efficiency represent practical key characteristics required for CE-MS interfaces. A number of different interfaces to hyphenate CE and ESI/MS have been described which can be classified into the three main categories: (i) sheathless, (ii) sheath liquid (flow), and (iii) liquid junction interfaces – Fig.2. The specific class is represented by microfabricated CE devices (microchips) with integrated spray emitters. The detail discussion of most of the microfabricated (microchip) CE-MS interfacing is summarized in review articles[14,37-39] and will be detailed in the section 3.

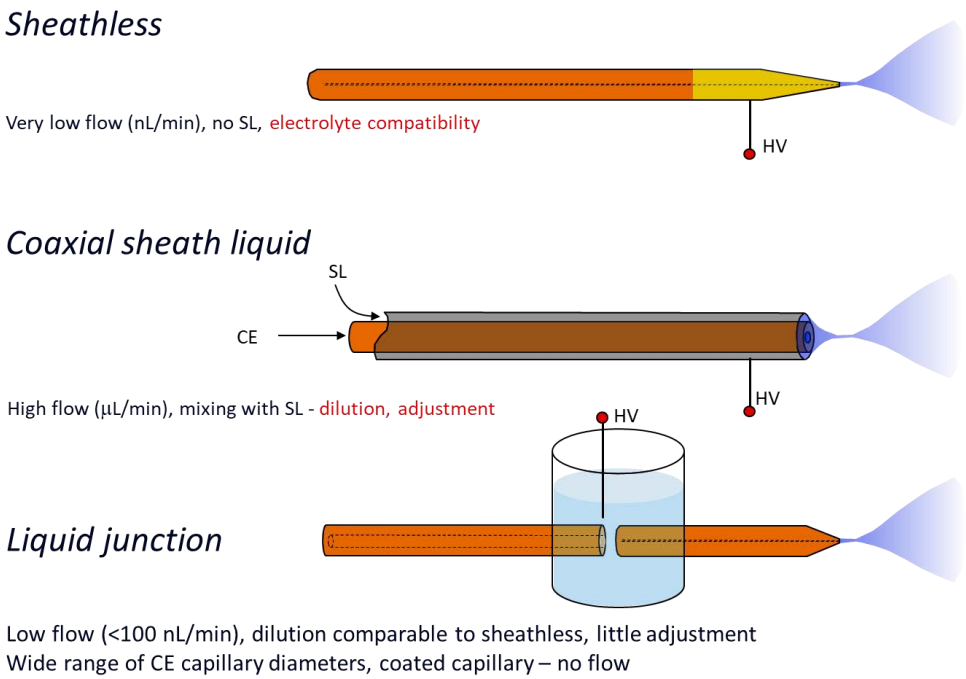

Fig. 2 Scheme of the sheathless (top), sheath liquid (middle) and liquid junction interfaces

2.1 Sheathless interfaces

The sheathless interfacing for CE-MS coupling has been pioneered by the group of Smith in the late 1980s. In the first reported sheathless interface design, a fused silica capillary was terminated in a stainless steel capillary[40], and later a metalized fused silica capillary was directly used as an ESI emitter[41]. Since in the sheathless interface the fused silica capillary serves as both the separation capillary and the electrospray emitter, several methods for creating electrical contact at the ESI end of the CE capillary have been developed. The most common approaches include metal coating of the tip, inserting an electrode inside the capillary outlet, use of porous etched capillary walls or the use of a microdialysis junction[42]. Sheathless interfaces do not suffer from the dilution effect by the sheath liquid; however, as there is only one background electrolyte for separation and ionization, the separation/ionization conditions must be optimized accordingly to fulfill both needs. Reduction of the flow compared to the sheath liquid based interfacing significantly improves ionization efficiencies as well as reduces ion suppression of co-migrating analytes.

Based on the porous membrane design[43], a new front-end separation and ionization technology called CESI 8000 module with the OptiMS sprayer has recently been developed in the laboratories of Beckman Coulter. In this sheathless interface, the 3-4 cm of the distant end of the separation capillary is etched with hydrofluoric acid. The etching procedure creates a capillary with an outer diameter (OD) at the etched portion of 40 µm with a ~5 µm thick porous wall[44]. Since the porous tip is not internally tapered, the sprayer presents a good ability to spray at low flow rates while reducing the potential for clogging. The porous tip is located within a housing comprising of a

stainless steel needle, which protects the tip from physical damage. The electrical contact for the CE is achieved through the ESI needle, which is filled with a conductive liquid and for the ESI by the porous capillary protruding from the needle. The developed OptiMS sprayer technology is compatible with several mass spectrometers, plugging directly to the nanospray sources or by using specific adapters.

The porous tip interface is compatible with a very wide range of electrophoretic conditions (electrophoretic mobilities ranging from 2.9 to 233×10^{-9} $m^2V^{-1}s^{-1}$, which covers most of the conditions generally encountered in CE[45]. The direct comparison with a sheath liquid interface clearly proved the benefits of the sheathless interfaces including generation of a very stable and robust ESI at flow rates in the nL/min range, reduced ion suppression and improved sensitivity[46]. Additional advancements in the design of the sprayer may further improve the performance in the future. For example, a number of reports dealing with multisprayers formed by frits, membranes and/or channel arrays, has been covered by a review article[47].

2.2 Sheath liquid interfaces

Coaxial sheath liquid interfaces, based on the triple tube, design developed by Smith et al.[48], are currently used on most of the commercially available instruments. The CE separation capillary itself is the center tube of the sprayer and it is surrounded by two metal tubes. The inner steel tube delivers the sheath liquid and the outer one delivers the nebulizing gas assisting in the spray stability. The sheath liquid completes an electrical circuit of the CE system and generates the necessary flow for a stable electrospray. Most of the interfaces utilize a stainless steel spray needle; however, stainless steel can oxidize and generate metal ions interfering with the analysis. The electrolysis behavior of the metal electrospray needles has been known for over 20 years[49] and the electrochemical reactions and ionization processes occurring during the ESI ionization has recently been reviewed[50]. These processes can cause clogging of the separation capillary as well as form complexes with analyzed anions resulting in decreased detection sensitivity. Therefore, other material such as platinum was found as a more suitable, especially for analysis of negative ions[51].

The sheath liquid interface allows independent optimization of the sheath liquid and the background electrolyte (BGE) compositions; however, a significant dilution of the sample occurs at the interface needle since the CE electrolyte flow rate is usually significantly lower (nL/min) than the sheath liquid (μL/min). Furthermore, a number of parameters such as CE capillary protrusion from the sprayer needle, positioning of the interface with respect to the MS orifice, applying adequate voltages for electrospray, sheath liquid composition as well as flow rates of the sheath liquid and the nebulizing gas is required to be optimized to create a stable electrospray and maintain separation efficiency and detection sensitivity[52]. Another drawback of many of the sheath liquid CE-MS instruments is the requirement to use relatively long separation capillary due to the instrument configuration (40 cm or more, typically with the inner diameter (ID) of 50 or 75 μm), leading to long separation times. Unfortunately, the requirement to use long separation capillaries is dictated by the design of the commercial instruments where the separation capillary has to reach out from the CE instrument to be

connected to the external ESI interface. Thus, while the UV absorbance can be monitored just few centimeters past the injection, the distance to the ESI interface is almost an order of magnitude greater. This contrasts with the potential for CE separation on the timescale of seconds demonstrated with capillaries narrower than 50 μm[53]. In the recent nanospray sheath-flow interface design a stable spray is achieved with very low sheath flow rates and without a pump or nebulizing gas[54]. Here, the separation capillary is placed inside a tapered glass emitter (2-10 μm id) and ESI voltage is applied via a platinum electrode placed in the sheath liquid reservoir. The capillary, the electrospray emitter, and the sheath-liquid tubing are connected via a PEEK cross. Sheath liquid is driven by electroosmosis produced by the zeta potential at the emitter surface. The sheath liquid flows over the end of the separation capillary, closing the circuit and mixing with the capillary effluent inside the tip. This design, although described as sheath liquid arrangement by the authors, may be also classified as the liquid junction arrangement.

In another, but similar design, the separation capillary was secured in a microtee assembly serving as the body of another nebulizer-free sheath liquid interface described by Lapainis et al.[55]. The PEEK tee incorporated a stainless steel metal tubing opposing the port in which the CE capillary was secured, serving as the sheath liquid tube and ESI needle. The design of these scale-down interfaces allows achieving a stable electrospray at significantly lower flow rates (250 nL/min - 2 μL/min) than commercially available sheath liquid interfaces typically operating at 4-10 μL/min flow of the sheath liquid. Although in some cases one can lower the flow in the sheath liquid interface down to a μL/min this may require a careful positioning of the separation capillary at the exit of the sheath liquid tube. Even in such a case the stability of the sheath liquid electrospray process is compromised. This can be attributed to the larger size (diameter) of the electrospray tip resulting in lower and less homogeneous electric field. The sheath liquid electrospray has to be positioned at a greater distance from the mass spectrometer sampling orifice leading to larger ESI plume size. Since the sampling orifice of current mass spectrometers is limited by the pumping speed of the vacuum system only a very small part of the ESI plume can enter the mass analyzer. Using of the nanospray emitter not only reduces the liquid flow and the size of the electrospray tip, but also allows easier spatial optimization of its position in front of the mass spectrometer resulting in enhanced ion transfer efficiency and detection sensitivity. Similar low sheath flow interfaces were described with a removable ESI sprayer for capillary and chip-based CE-MS applications[56-58].

2.3 Liquid junction interfaces

Since the first paper dealing with a liquid junction interface[59], a plethora of designs has been developed. The bodies of the liquid junction interfaces are mainly made from glass[60-61] or plastic materials such as polypropylene[62-63], polycarbonate[64] and polysulfone[65]. The use of inert materials such as glass or polysulfone minimizes the ESI chemical noise caused by plastic softeners or material degradation. In the liquid junction interface, the separation and electrospray capillaries aligned axially are separated by a small gap (20-200 μm) permanently filled with a spray liquid[66]. A fused

silica capillary with the ID of 10–50 μm with a sharpened and polished tip is usually used as the ESI emitter. The spray liquid reservoir is equipped with the electrode for connection of the ESI potential. This arrangement provides independent optimization of the CE separation and ESI conditions.

A pressurized version[67] of the liquid junction interface is capable to work with a nanospray needle (10 μm id) at flow rates of tens of nL/min[60-61,65]. To avoid a pressure driven flow in the separation capillary, both the background electrolyte reservoir and the liquid junction ESI solution reservoir are maintained at the same pressure. The detail numerical analysis describing the mass transport of analytes through the liquid junction interface has recently been presented[68]. It has been shown, that the most important parameters of the liquid junction interface effecting the transfer of analyte zones between the separation and the spray capillaries are (i) the electric field strength that controls the migration of analytes in the CE capillary and in the gap, and (ii) the pressure exerted on the gap that controls the liquid flow rate through the spray capillary. On the other hand the interface geometry, i.e., the gap width between the separation and spray capillaries can be varied in relatively broad range (20-200 μm) without a detrimental effect on the separation.

A recent design of the liquid junction interface called a junction at the tip interface consisting of the separation capillary (365 μm od) inserted as far as possible into the stainless steel hollow ESI emitter with a beveled tip has been developed by Chen and coworkers[69-71]. A space enclosed by the CE capillary exit and the inner surface of the stainless steel tip forms a flow-through microvial acting as the outlet vial and the terminal electrode. The junction is filled with a spray liquid, supplied from the reservoir at a flow rate of ~100 nL/min, supporting a stable electrospray with minimized sample zone dilution. Numerical simulation describing the mass transport of the analyte through the junction at the tip interface was verified by CE-MS experiments[72], proving the laminar flow profile in the microvial with no broadening of the analyte zone (peak shape) by the spray liquid.

3. Microfluidics

In the early 1990 the Human Genome Project was still searching for technologies suitable for analyzing the (then) immense amounts of Sanger sequencing products. Many bet on the new developments in mass spectrometry and while impressive results were obtained early on especially with MALDI-TOF instruments[73], the obstacles related to the total time of analysis, data processing, instrument size and cost finally led to the development of different technologies. One technology many groups moved into was microfabrication using photolithography developed originally for electronics. In fact it was already tested for microfabrication of a gas chromatograph as early as in 1979[74], as shown in Fig. 3.

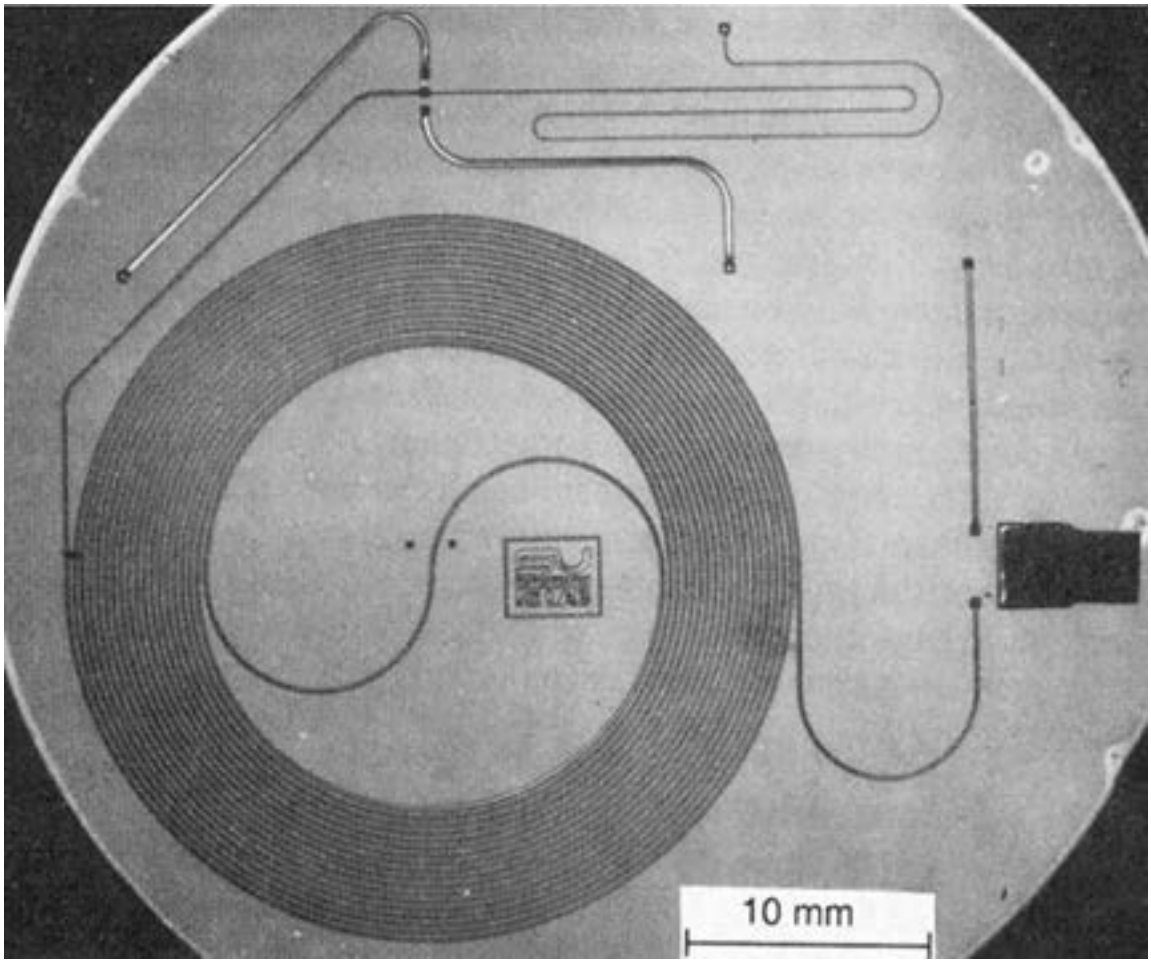

Fig. 3 A Gas Chromatographic Air Analyzer Fabricated on a Silicon Wafer[74].

The main advantage of miniaturization was in the possibility of creating highly parallel systems with a small footprint and high speed of operation. Indeed, the results of this research have materialized in the next generation of DNA sequencers being used today. In mid 1990s several groups published exciting papers on microfabrication of parallel channel capillary electrophoresis systems for high throughput DNA sequencing. One example of such a system as described by Mathies et al.[75] is in Fig. 4.

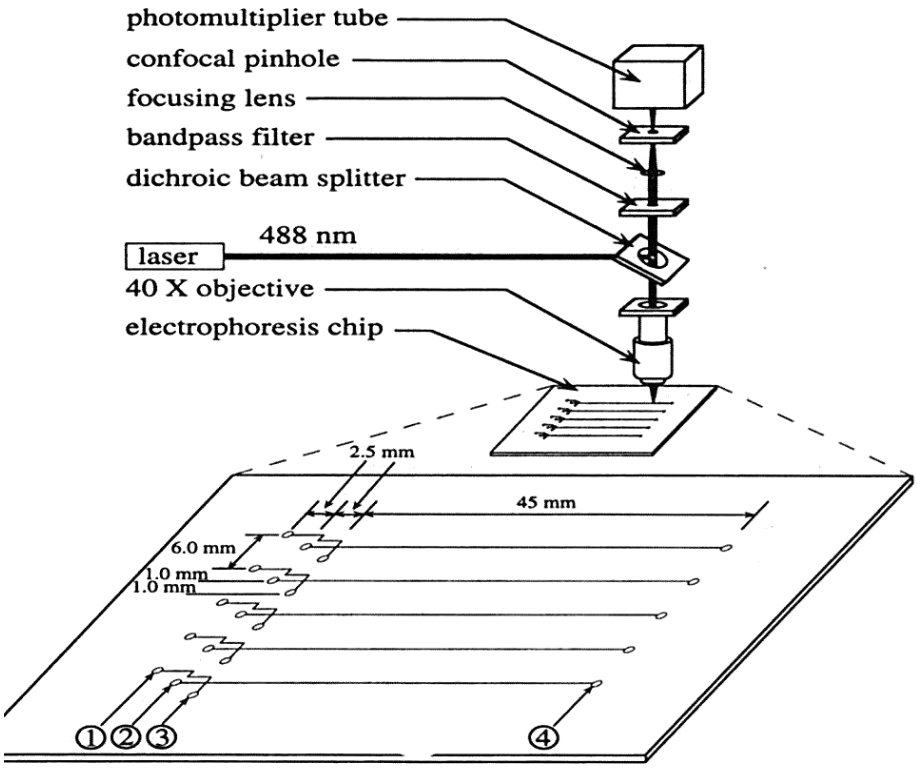

Fig. 4 Ultra-high-speed DNA fragment separations using microfabricated capillary array electrophoresis chips[75].

At that time we were developing a capillary array DNA sequencing technology and felt that we might be missing out on the microfabrication. As a group Leader at the Barnett Institute, I was under increasing stress to move into microfluidics. Since we had neither experience nor the equipment, I have resisted for some time. Eventually, I realized that microfluidics could be potentially useful for the electrospray mass spectrometry and filed an invention disclosure. Soon we have filled a full patent application[76] with colleagues from the electrical engineering microfabrication lab and a new postdoc was hired to work on the project. What seems quite logical today was quite difficult to start then and we had to improvise, especially in the early stages of the work. It is interesting to note that the Human Genome Project was eventually finished with the standard capillary array technology at both the Celera Genomics (private part of the DNA sequencing) and Molecular Dynamics (the government funded part); however, the research on microfluidic sequencers generated a basis of a new area of analytical instrumentation, including mass spectrometry coupling. The basic arrangements of the devices we were testing at that time as disclosed in the patent are in Fig. 5.

Since microfabrication of pointed electrospray tips in glass was difficult, our first devices used a simple channel opening on the polished surface (sometime silanized) of the glass chip edge. While such an arrangement was not suitable for coupling with separations, infusion experiments worked quite well. Soon it turned out that the timing of the work was right since all major instrument manufacturers licensed the technology and eventually brought commercial instruments to the market.

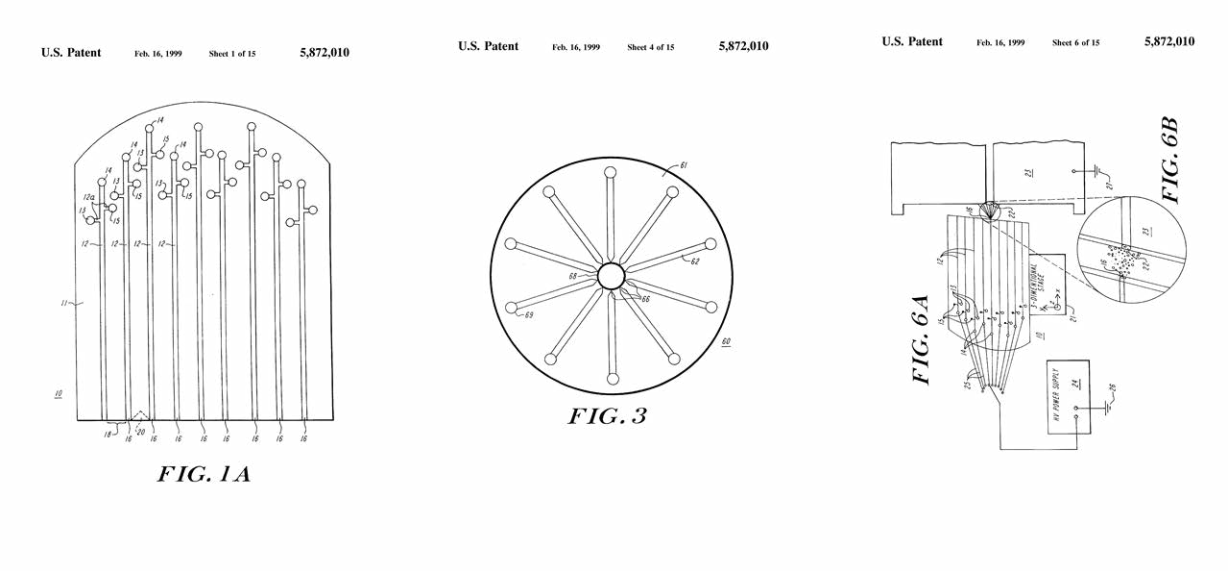

Fig. 5 Microflidic designs for coupling with ESI/MS[76].

3.1. Microfluidics interfacing with ESI-MS

There are three important issues that must be addressed in the design of a microchip-MS interface. First, an approach must be developed to ensure high electrospray ionization efficiency from the microfabricated device, in order to obtain high sensitivitiy. Second, if separations are to be performed on the chip, the contribution of the interface to band broadening must be minimized. Third, since most of current applications use electrical forces to control fluid flows on the chip and since MS detection occurs off-chip, an effective approach must be found to direct the fluids towards the MS interface.

Spray generation from the microchip flat surface.

In early reports where microdevices were used for infusion ESI-MS analysis, electrospray was initiated directly from the channel opening on the flat surface of the chip[77-79]. The open channel electrospray properties were studied in more detail for devices made of a dielectric, non-wetting material[80]. In accord with previous experimental results[81], it was concluded that the electrospray activated from a small opening on a flat hydrophobic surface can have performance close to that of a needle arrangement[82]. Although the ability to generate electrospray directly from the chip surface was clearly demonstrated, the flat edge may not be suitable for direct coupling with on-chip separations. Close inspection of the electrospray cone revealed a volume of tens of nL – Fig. 6. Thus,for microchip separations where peak volumes are typically below ~5 nL, any separation would be lost in the dead volume of the electrospray cone. As with column separations, a sharp electrospray tip is required in order to minimize dead volumes and to improve ionization efficiency.

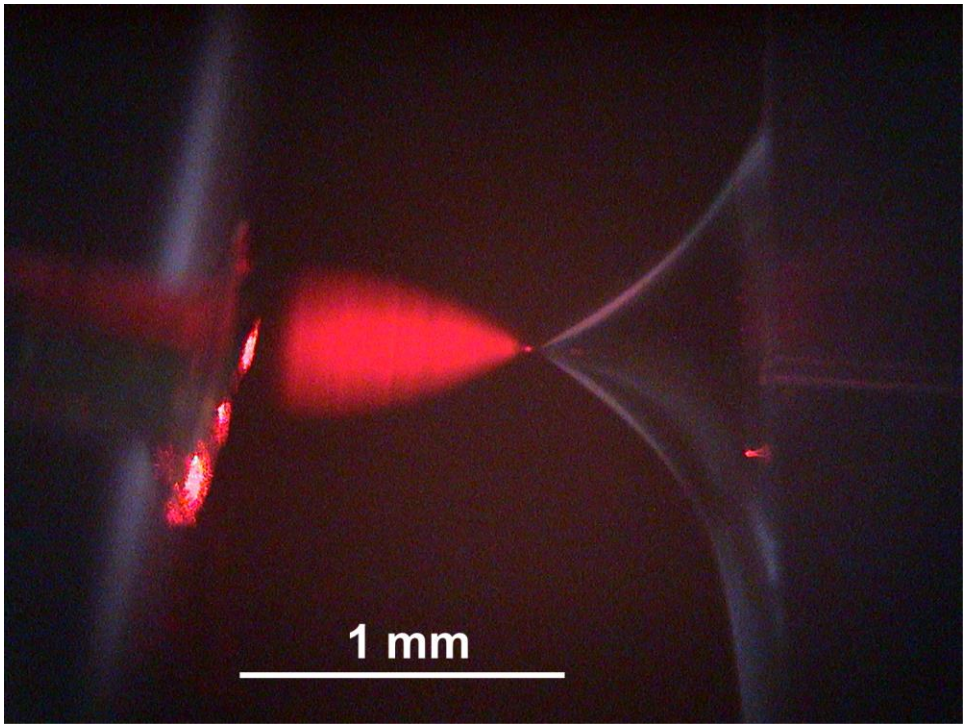

Fig. 6 Image of the electrospray plume (illuminated by a red laser) generated off the microchannel ending on the edge of the glass chip. The droplet formed at the channel exit is clearly visible. F. Foret – unpublished.

Spray generation from capillary emitters inserted in the microchip.

A variety of approaches have been taken to generate electrospray by inserting capillary emitters in the microchip device, resulting generally in performances comparable to those found for microcolumn separations. Either an electrospray tip or a fused silica capillary transfer line was inserted in the microchip body[83-84] or a liquid junction configurations with a removable electrospray tip have been developed[85-86]. Some of the arrangements developed during my work form part of this thesis – papers 14-17.

Microfabricated electrospray emitters.

Batch-generation of microchips with integrated electrospray emitters/tips can result in improved emitter reproducibility, and the potential for simple, disposable devices. However, the microfabrication of fine electrospray tips as an integral part of a microdevice is not a trivial task, and suitable microfabrication procedures are still under development. Robust, hollow needle structures (electrospray emitters with tapered tips having 5 x 10 µm rectangular openings, that extended 1 mm beyond the edge of the substrate), were fabricated from parylene polymer layers deposited on a silicon substrate[87] and microfabricated electrospray nozzles with high aspect ratio (10 µm ID x 50 µm depth) were constructed on the planar surface of a silicon substrate using deep reactive ion etching[88-89]. These silicon ESI Chips™ in a 100 nozzle format are presently commercialized - www.advion.com. Alternative techniques have used a combination of low pressure chemical vapor deposition, pattern transfer, reactive ion

etching and sacrificial layer etching for the fabrication of miniaturized polysilicon-based ESI emitters[90].

The microfabrication of disposable plastic microdevices is attractive from the commercial perspective and a number of fabrication procedures can be found in the literature. For electrospray generation, the parylene film was micromachined in a triangular shape by lithography and etching[91]. In another approach, the microfluidic system and the electrospray exit nozzle were fabricated by plasma etching in polyimide[92]. In addition, electrospray emitters were fabricated from SU-8 epoxy resin by photolithography[93], from polyethylene terephthalate[94] and polycarbonate substrates[95] by laser ablation, from poly(dimethylsiloxane) by casting[82], from poly(methylmethacrylate) by injection molding [96-97], micromilling[98] and/or mechanical cutting[99]. Plastic systems are also attractive for low volume multiple channels systems as documented for glutamate release from neuronal cells[100] or small-volume proteomics[101].

It is interesting to note that glass, the most common material in microfluidics, has only recently been rediscovered as a material for integrated ESI devices. For laboratory use the group of Detlev Belder uses a mechanical cutting of the glass around the channel exit followed by flame pulling. While this approach may not be suitable for mass production it brings a good potential for high quality “proof-of-principle” research, including MS studies of rapid chemical synthesis[102] and or chip based HPLC[103]. A more streamlined way of fabrication of glass microdevices with integrated was recently developed by R. Kostiainen et al.[104 -105]. The group of M. Ramsey has been probably the most active group in the development of CE-ESI/MS microdevices, which are now commercially available via the 908devices company – www.908devices.com. Their works cover a wide area of systems for both electrophoresis[106-108] and two dimensional separations combining the CE with chromatography[109].

4. Concluding remarks

Electrospray/MS coupling is one of the most important tools in the current (bio)analytical instrumentation. Mature CE equipment has been on the market for quite a while and new generation of instruments is under development. It is worth noting that at the peak of the “irrational exuberance” of the stock market around the year 2000 microfabrication and microfluidics were the banners for success. Many startup companies made their fortunes overnight when going public at that time. Several years later only a few of the “old timers” remained in the business; however, new startups are still being formed. In his editorial “Microfluidics, the Ultrahigh-Throughput Underachiever” in the GenomeWeb News (5/14/03) the senior editor John S. MacNeil calls this period as a time of“ frantic search for the one application that will force reluctant customers in academia, biotech, and big pharma to go whole hog on microfluidics, since the whole concept might just be too powerful not to succeed eventually.”

As the success of the number of next generation sequencers documents, the new technologies are and will continue changing many fields in the science, technology and medicine. Take the applications of microfluidics in chemical analysis as an

example. Although the first examples of the development of the microfabricated instrumentation can be traced back to the mid-seventies, without any doubt the major trend of miniaturization and integration of analytical processes and instrumentation has been witnessed only in the past ten years, or so. The figure shown below clearly demonstrates the trend – Fig.6.

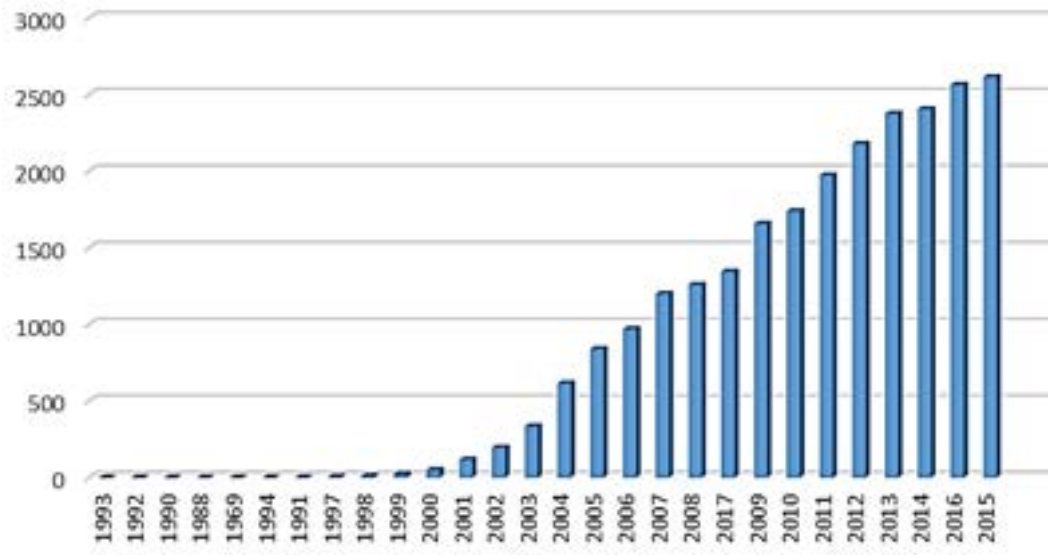

Fig. 6. Plotting the occurrence of the word „microfluidic“reveals that the number of scientific articles listed in the PubMed database (www.ncbi.nlm.nih.gov/PubMed) started increasing exponentially in just the same time when the stock market bubble burst. Data from June 8, 2017.

It is anticipated that microfluidics[110] (Lab-on-a-chip) will play an important role in the new instrumentation for high-sensitivity/high-throughput analyses. The main advantages of the technology include speed of analysis, minimum consumption of reagents and samples, integration of functional elements and possibility to create massively parallel systems for high throughput. Another important feature of the microfabrication technology from the prospective of a separation scientist is the fact that leak-free, zero dead volume junctions can easily be produced. Additionally, the reduction of the instrument size leads to lower requirements for the laboratory space. In an increasing number of cases, mass spectrometry coupling is required and this trend will keep growing as documented by the recent successful introduction of the zip-chip CE-MS device by the 908 devices company[111]. Fabrication technologies include the processes used commonly in electronics, e.g., photolithography and wet chemical etching or reactive ion etching in glass or silicon. Structures as small as few nm can currently be fabricated in microelectronics; however, two to three orders of magnitude larger structures are more common in microfluidics. Precision injection molding can be used for replication in plastic materials. The advantages of the new technologies are clear and the potential applications are endless.

The Human Genome Project finished well ahead of schedule thanks also to the massive application of capillary electrophoresis. While the majority of today’s analytical applications relate to HPLC separations, with capillary electrophoresis being

a niche use, the general belief is that CE might grow rapidly in the near future for applications in protein (top-down proteomics), glycan and larger biopolymers separations in general. With the current advances in life sciences there is a continuously increasing need for new analytical tools. Besides chromatographic techniques, capillary electrophoresis is the only high resolution separation alternative. New protocols are being developed for CE separations of proteins (e.g., antibodies), peptides and oligosaccharides, where the separation efficiency typically exceeds that of chromatography. While the sample loading capacity of CE is often mentioned as a serious drawback, it can be significantly improved by on-line preconcentration techniques. In addition, this lower sample capacity turns into an advantage when dealing with limited sample quantities. The electrospray interfacing is clearly the key component required for the successful deployment of the CE-MS in practice. While one can argue that many of the interfaces are alike, it is the technical details, designer/operator skills and a particular application, which lead to the use of a particular design. Many interface designs have been described in the past 20 years; however, a universal solution to all the needs is difficult to find. The following selected papers describe some of our contributions to the field.

5. Brief description, impact factors and numbers of citations of papers used in the dissertation

Part one – papers on capillary electrophoresis-electrospray/mass spectrometry

1.
Thompson, T. J., Foret, F., Vouros, P., Karger, B. L. Capillary Electrophoresis-Electrospray Ionization Mass Spectrometry: Improvement of Detection Limits Using On-column Transient Isotachophoretic Sample Preconcentration. Anal.Chem., 1993, 65, 900-906.
IF = 4.075; 174 CIT

This work belongs to a series of papers addressing the limited loading capacity of CE. Based on the knowledge of ITP principles we have developed a protocol for on-column sample concentration allowing injections of much larger sample volumes than common in regular CE. The term transient ITP, used in this work, later became widespread in the literature. Mixtures of model proteins have been separated in the cationic mode using a coated capillary and have been analyzed by mass spectrometry coupled on-line to an electrospray interface with a coaxial sheath flow arrangement. An interesting phenomena was observed in zones of lactoglobulins forming a non-covalent complex with the 6-aminocaproic acid present in the BGE. Compared to regular CE the detection limits could be improved by at least a factor of 100. Advantages and limitations of the technique with respect to the very narrow ITP zones were discussed.

2.
Foret, F., Thompson, T. J., Vouros, P., Karger, B. L., Gebauer, P., Bocek, P. Liquid sheath effects on the separation of proteins in capillary electrophoresis electrospray mass spectrometry. Anal. Chem., 1994, 66, 4450-4458.
IF = 4.609; 133 CIT

In previous experiments, we have noticed that different compositions of the BGE and sheath liquid can influence the migration of zones in CE-ESI/MS. In this joint study between the Barnett Institute, Boston and IACH, Brno we have described the ionic migration in CE-ESI/MS with a coaxial sheath liquid interface. Formation of moving ionic boundaries inside the separation capillary was observed. These ionic boundaries, which can lead to delays, inversions in migration order and/or loss of resolution, were studied both theoretically and experimentally. Based on the results of the modelling of the ionic migration it was shown that even difficult to-spray electrolytes (such as phosphate-containing buffers) can be used for the CE separation with properly selected background electrolyte counterions.

3.
Foret, F., Kirby, D. P., Vouros, P., Karger, B. L. Electrospray Interface for Capillary Electrophoresis-Electrospray Mass Spectrometry with Fiber-Optic UV Detection Close to the Electrospray Tip. Electrophoresis, 1996, 17, 1829-1832.
IF = 2.467; 12 CIT

This technical work takes advantage of experimenting with optical fibers and UV absorbance detection back at IACH in Brno. The early ESI/MS instruments suffered

from frequent instabilities and putting a UV detector just a couple of centimeters from the exit of the separation capillary was very useful in troubleshooting the problems since it provided precise information about the time when UV-active zones enter the electrospray and allowed easy location of analyte mass information in the ion current profile. In addition the integration of the fiber optic detector directly into the ESI interface allowed using of short separation capillaries, saving experimental time on an expensive instrument shared by several users.

4.
Foret, F., Zhou, H., Gangl, E., Karger, B. L. Subatmospheric electrospray interface for coupling of microcolumn separations with mass spectrometry. Electrophoresis, 2000, 21, 1363-1371.
IF = 3.385; 51 CIT

As the experiments with different interface concepts proceeded, it was clear that a single pointed electrospray tip with minimum diameter provides the best stability and ionization efficiency. Such ESI tips can be used in the liquid junction arrangement. A low flow rate of a spray fluid is needed for the transport of electrophoretic zones into the ESI tip. Here the flow was generated by lowering the pressure in the electrospray chamber creating a subatmospheric electrospray. The previously developed fiber optic UV detector was also incorporated into the system and a chain of optically controlled photoresistors was used to adjust the electrospray voltage without the need for an additional high voltage power supply. Since the electrospray did not depend on fluid delivery from the separation column, coated capillaries without electroosmotic flow as well as capillaries with electroosmotic flow could be used for CE and capillary LC separations with separation efficiencies reaching several hundreds of thousands theoretical plates. At the time of publication these were probably the best results in its class.

5.
Křenková, J., Bílková, Z., Foret, F. Characterization of a monolithic immobilized trypsin microreactor with on-line coupling to ESI-MS. J. Sep. Sci. 2005, 28, 1675-1684.
IF = 1.829; 57 CIT

After the return back to Brno in 2001, we have started looking for new research directions for adding functionality into the CE-MS protocols. It was the time when proteomics techniques were under rapid development and enzymatic digestion was one of the most important processes. In this work we have prepared and characterized a miniaturized trypsin flow-through capillary reactor for on-line coupling with an ESI-TOF mass spectrometer. The enzyme was covalently immobilized on poly(glycidyl methacrylate-co-ethylene dimethacrylate) monolith prepared in a 75 μm ID fused silica capillary resulting in a bioreactor with high local concentration of the proteolytic enzyme. Although one can expect that some trypsin molecules got inactivated during the immobilization (the enzyme immobilization was not oriented), at flow rates of 50–300 nL/min complete protein digestion was achieved in less than 30 s at 25° C with the sequence coverage of 80% (cytochrome c). This is comparable to a 3 h digestion in solution at 37°C. Besides the good performance at laboratory temperature, the

bioreactor also performed well at lower pH compared to the standard in-solution protocols.

6.
Kusý, P., Klepárník, P., Aturki, Z., Fanali, S., Foret, F. Optimization of pressurized liquid junction nanoelectrospray interface between capillary electrophoresis and mass spectrometry for reliable proteomic analysis. Electrophoresis, 2007, 28, 1964-1969.
IF = 3.609; 20 CIT

During a joint project with our long-term Italian collaborators, we have designed liquid junction CE-ESI/MS interface for use at the CNR in Rome. The pressurized system was designed for easier operation with the available mass spectrometer and was optimized for analyses of proteins and peptides with the separation and spray capillaries fixed in a pressurized spray liquid reservoir equipped with the electrode for connection of the electrospray potential. During optimization, the transfer of the separated zones between the separation and electrospray capillaries was monitored by UV absorbance and contactless conductivity detectors placed at the outlet of the separation capillary and inlet of the electrospray tip, respectively. This arrangement allowed independent monitoring of the effects of pressure, CE voltage and geometry of the liquid junction on the spreading and dilution of the separated zones during passage through the interface.

7.
Krenkova, J., Kleparnik, K., Foret, F. Capillary electrophoresis mass spectrometry coupling with immobilized enzyme electrospray capillaries. J. Chromatogr. A, 2007, 1159, 110-118.
IF = 3.641; 48 CIT

Based on the experience with the monolithic immobilized enzymatic reactors we have tested the use of narrow capillaries with the enzyme immobilized on the fused silica surface. These open tubular capillary enzyme reactors were tested for rapid protein digestion and on-line integration into a CE-ESI/MS system. Narrow bore (10 μm ID) capillaries were used to minimize the diffusion time of analyte molecules towards the surface immobilized enzyme and to maximize the surface-to-volume ratio. Extremely small protein amounts (atto-femtomoles loaded) could be digested within few seconds transition time. Thus, a protein mixture was injected and after the CE separation individual separated proteins were digested by pepsin prior to entering the ESI/MS.

8.
Krenkova, J., Kleparnik, K., Grym, J., Luksch, J., Foret, F. Self-aligning subatmospheric hybrid liquid junction electrospray interface for capillary electrophoresis. Electrophoresis 2016, 37, 414–417.
IF = 2.482; 3 CIT

In an attempt to design a user friendly instrumentation we have designed a self-aligning subatmospheric hybrid liquid junction electrospray interface for CE eliminating the need for manual adjustment by guiding the separation and electrospray capillaries in a microfabricated liquid junction glass chip at a defined angle. Both the ESI and

separation capillaries were inserted into the microfabricated part until their ends touched. The resulting distance between the capillary openings was defined by the angle between capillaries. The microfabricated part contained channels for placement of the capillaries and connection of the external electrode reservoirs. It was fabricated using standard photolithographic/wet chemical etching techniques followed by thermal bonding. The liquid junction was connected to a subatmospheric electrospray chamber inducing the flow inside the ESI needle. After presenting the results at the ASMS conference in Minneapolis we were approached by Agilent Technologies with an offer of a joint research grant. The collaboration continues with significant financial and instrumental support from Agilent. Two master degree thesis were finished during the work, one German student has worked in Brno for a month and another will spend winter semester in Brno this year. It is anticipated, that this research will lead to a commercialization of the interface.

9.
Tycova, A., Foret, F. Capillary electrophoresis in an extended nanospray tip–electrospray as an electrophoretic column. J.Chromatogr. A, 2015, 1388, 274–279.
IF = 3.926; 12 CIT

The most challenging instrumental aspect in CE-MS is striking the balance between the stability and reproducibility of the signal and required sensitivity of the analysis in terms of both the concentration LOD and minimum injected amount. One of the long term goals of our work is development of tools for chemical analyses of single cells. The use of very narrow emitters is necessary to minimize dilution of the cell content. Since at constant voltage the current in CE is inversely proportional to the second power of the capillary diameter we have speculated that at certain low diameter (depending on the conductivity of the BGE) the CE current could equal the ESI current. Under such a condition the CE-MS coupling would not require any interface since the CE separation would be driven by the ESI current. In this work we have explored such an "interface-free" approach, where the CE-MS analysis was performed in narrow bore (<20 μm ID) electrospray capillaries ending in an electrospray. The performance of this simplest possible CE-MS system was tested on peptide separations from the cytochrome c tryptic digest. The subnanoliter sample consumption and sensitivity in the attomole range was achieved.

10.
Tycova, A., Prikryl, J., Foret, F. Reproducible preparation of nanospray tips for capillary electrophoresis coupled to mass spectrometry using 3D printed grinding device. Electrophoresis 2016, 37, 924-30.
IF = 3.981; 1 CIT

The outcome of the work described in the previous and following papers strongly depends on the use of high quality fused silica capillary nanospray tips. Achieving of reliable and reproducible electrospray/MS signal is critical; however, reproducible (laboratory) preparation of such tips is a challenging task. In this work, we have designed a low-cost grinding device assembled from 3D printed and commercially easily available components allowing to achieve maximum symmetricity, surface smoothness and repeatability of the conus shape. Moreover, the presented grinding

device brings the possibility to fabricate the nanospray emitters of desired dimensions and tip angle. The prepared tips were tested and compared for analyses of reserpine, rabbit plasma, and aminoacids mixture. It was shown that the best results can be obtained with the lowest tip angle (below 30^{o}).

11. Tycova, A., Vido, M., Kovarikova, P., Foret, F. Interface-free capillary electrophoresis-mass spectrometry system with nanospray ionization—Analysis of dexrazoxane in blood plasma. J.Chromatogr. A, 2016, 1466, 173-179.
IF = 2.744; 5 CIT

The newly developed interface-free capillary electrophoresis-nanospray/mass spectrometry system (CEnESI/MS) was applied for rapid analysis of the cardioprotective drug dexrazoxane and its hydrolysed form ADR-925 in deproteinized blood plasma samples. The aim of this study was to test the simplest possible CE-nESI/MS instrumentation for analyses of real samples. This interface-free system, utilizing single piece of a narrow bore capillary as both the electrophoretic separation column and the nanospray emitter, was operated at a flow rate of 30 nL/min. Excellent electrophoretic separation and sensitive nanospray ionization was achieved with the use of only one high voltage power supply. In addition, hydrophobic external coating was developed and tested for additional stability of the nanospray ionization. To our knowledge this is the first study devoted to the analysis of dexrazoxane and ADR-925 by capillary electrophoresis-mass spectrometry.

Part two – papers on microfluidics-electrospray/mass spectrometry

12.
Xue, Q., Foret, F., Dunayevskiy, Y. M., Zavracky, P. M., McGruer, N. E., Karger, B. L. Multichannel Microchip Electrospray Mass Spectrometry. Anal.Chem., 69, 1997, 426-430.
IF = 4.743; 323 CIT

This is the first published study demonstrating direct electrospray coupling of a microfabricated glass chip with mass spectrometer (ESI-MS). The microchip device was fabricated by standard photolithographic, wet chemical etching, and thermal bonding procedures and the ESI high voltage was applied individually from each reservoir for spraying sample sequentially from each channel. With the sampling orifice of the MS grounded, it was found that a liquid flow of 100-200 nL/min was necessary to maintain a stable electrospray. The detection limit of the microchip MS experiment for myoglobin was found to be in the nanomolar range. Samples in 75% methanol were successfully analyzed with good sensitivity, as were aqueous samples.

13.
Xue, Q. F., Dunayevskiy, Y. M., Foret, F., Karger, B. L. Integrated multichannel microchip electrospray ionization mass spectrometry: Analysis of peptides from on-chip tryptic digestion of melittin. Rapid Commun. Mass Spectrometry 1997, 11, 1253-1256.
IF = 3.343; 90 CIT

In continuation of our work to develop an integrated multichannel microchip interfaced to electrospray mass spectrometry (ESI-MS), this paper demonstrates one of several applications of this approach in monitoring tryptic digestion products. The multichannel microchip allowed integration of sample preparation onto the microchip to facilitate the analysis process. Melittin was selected as a model oligopeptide because it possesses a cluster of four adjacent basic residues which enable probing the site specificity of trypsin as a function of digest times. Reactions were performed on-chip in different wells for specific time periods and then analyzed by infusion from the microchip by ESI-MS, using leucine enkephalin as internal standard. The rate of formation and disappearance of the molecular ion and individual fragments was followed for a melittin to trypsin concentration ratio of 300:1. The results indicate the potential of integrating enzymatic reactions with multichannel microchip ESI-MS for automated optimization of reaction conditions while consuming only small amounts of sample.

14.
Zhang, B., Liu, H., Karger, B. L., Foret, F. Microfabricated devices for capillary electrophoresis-electrospray mass spectrometry. Anal. Chem., 1999, 71, 3258-3264.
IF = 4.555; 200 CIT

This work described two fundamental approaches for the coupling of microfabricated devices to electrospray mass spectrometry (ESI-MS). Both approaches integrated sample inlet ports, preconcentration sample loops, the separation channel, and a port for ESI coupling. In one design, a modular, reusable microdevice was coupled to an external subatmospheric electrospray interface using a liquid junction and a fused silica transfer capillary. The transfer capillary allowed the use of an independent electrospray interface as well as fiber optic UV detection. In the second design, a miniaturized pneumatic nebulizer was fabricated as an integral part of the chip, resulting in a very simple device. The on-chip pneumatic nebulizer provided control of the flow of the electrosprayed liquid and minimized the dead volume associated with droplet formation at the electrospray exit port. Thus, the microdevice substituted for a capillary electrophoresis instrument and an electrospray interface - traditionally two independent components.

15.
Zhang, B., Foret, F., Karger, B. L. A Microdevice with integrated liquid junction for facile peptide and protein analysis by capillary electrophoresis/electrospray mass spectrometry Anal. Chem., 2000, 72, 1015-1022.
IF = 4.587; 149 CIT

This work extends the previous design into an design integrating (a) sample inlet ports, (b) the separation channel, (c) a liquid junction, and (d) a guiding channel for the insertion of the electrospray capillary, which was enclosed in a miniaturized subatmospheric electrospray chamber of an ion trap MS. The replaceable electrospray capillary was precisely aligned with the exit of the separation channel by a microfabricated guiding channel. No glue was necessary to seal the electrospray capillary. This design allowed simple and fast replacement of either the microdevice or the electrospray capillary. The performance of the device was tested for CE-MS of peptides, proteins, and protein tryptic digests. On-line tandem mass spectrometry was used for the structure identification of the protein digest products. High-efficiency/high-resolution separations could be obtained on a longer channel (11 cm on-chip)

microdevice, and fast separations (under 50 s) were achieved with a short (4.5 cm on-chip) separation channel with the separation efficiency comparable to that obtained from conventional capillary electrophoresis.

16.
Liu, H., Felten, C., Xue, Q., Zhang, B., Jedrzejewski, P., Karger, B. L., Foret, F. 2000. Development of multichannel devices with an array of electrospray tips for high-throughput mass spectrometry. Anal. Chem., 2000, 72, 3303-3310.
IF = 4.587; 93 CIT

This work, describing multichannel devices with an array of electrospray tips for high-throughput infusion electrospray ionization mass spectrometry (ESI-MS), has an interesting origin. The prototype plastic devices were fabricated by casting from a solvent-resistant resin which we were using a decade earlier at the institute in Brno. The sample wells on the device were arranged in the format of the standard 96-microtiter well plate, with each sample well connected to an independent electrospray exit port via a microchannel with imbedded electrode. A second plastic plate with distribution microchannels was employed as a cover plate and pressure distributor. Nitrogen gas was used to pressurize individual wells for transport of sample into the electrospray exit port. The device was placed on a computer-controlled translation stage for precise positioning of the electrospray exit ports in front of the mass spectrometer sampling orifice and allowed very high throughput and duty cycle, as well as elimination of any potential sample carryover. High-throughput ESI-MS was demonstrated by analyzing 96 peptide samples in 480 s, corresponding to a potential throughput of 720 samples/h. As a model application, the device was used for the MS determination of inhibition constants of several inhibitors of HIV-1 protease. The photograph of the device was presented on the cover of Analytical Chemistry.

17.
Zhang, B., Foret, F., Karger, B. L. High throughput microfabricated CE/ESI-MS: automated sampling from a microwell plate Anal. Chem., 2001, 73, 2675-2681.
IF = 4.532; 98 CIT

In this work we have developed a prototype for automated high-throughput CE-ESI/MS incorporating not only the CE separation and ESI ionization but also sample injection and channel flushing after analyses. The samples were injected directly from a standard microwell plate and a miniaturized subatmospheric electrospray interface was used for ESI ionization. The microdevice was attached to a polycarbonate manifold with external electrode reservoirs equipped for electrokinetic and pressure fluid control. A computer-activated electropneumatic distributor was used for both sample loading from the microwell plate and washing of channels after each run. Removal of the electrodes and sample reservoirs from the microdevice structure significantly simplified the chip design and eliminated the need both for drilling access holes and for sample/buffer reservoirs. The external manifold also allowed the use of relatively large reservoirs that are necessary for extended time operation of the system.

18.
*Grym, J., Otevřel, M., Foret, F. Aerodynamic mass spectrometry interfacing of microdevices without electrospray tips. Lab Chip, 2006, **6**, 1306-1314.*
IF = 5.821; 10 CIT

In the early 2000s we have started a collaboration between the Brno group and the Gyros AB in Uppsala, Sweden on adapting the ESI to the microfluidic devices fabricated in the compact disk format. After spending some time on the fabrication of ESI tips on the edge of the plastic microdevice, we have decided to test a flat channel opening and an external adapter assisting in formation and transport of the electrosprayed plume from the multichannel polycarbonate microdevice. The compact disk sized microdevice was designed with radial channels extending to the circumference of the disk. Electrospray was initiated directly from the channel openings by applying high voltage between sample wells and the entrance of the external adapter. The formation of the spatially unstable droplet at the electrospray openings was eliminated by air suction provided by a pump connected to the external adapter. Compared with the air intake through the original mass spectrometer sampling orifice, more than an order of magnitude higher flow rate was achieved for efficient transport of the electrospray plume into the mass spectrometer. Additional experiments with electric potentials applied between the entrance sections of the external adapter and the mass spectrometer indicated that the air flow was the dominant transport mechanism. Basic properties of the system were tested using computer modeling and characterized using ESI/TOF-MS measurements of peptide and protein samples.

19.
Tomas, R., Yan, L., Krenkova, J., Foret, F. Autofocusing and ESI-MS analysis of protein digests in a miniaturized multicompartment electrolyzer. Electrophoresis 2007, 28, 2283–2290.
IF = 3.609; 11 CIT

This paper is the result of an informal collaboration with the Swiss startup Diagnoswiss in Lausanne developing polyimide based microfluidics. That time we have also received a gift from the company BioRad of their newly introduced MicroRotofor™ multicompartment electrolyser. In the work we have studied a free-solution isoelectric focusing (IEF) of protein digests without the addition of carrier ampholytes. In this “autofocusing” mode the tryptic digest itself served as the mixture of ampholytes leading to the separation of the peptides with well-defined pI’s. The focusing process was monitored visually using colored pI markers. The resulting fractions were analyzed by CE and electrospray-TOF mass spectrometer using electrospray tips microfabricated in polyimide (Diagnoswiss). Although not all peptides in the protein digests have well defined pI’s the autofocusing process can separate many of them leading to higher S/N in the ESI/MS signals and improved protein sequence coverage.

20.
Jarvas, G., Grym, J., Foret, F., Guttman, A. Simulation-based design of a microfabricated pneumatic electrospray nebulizer. Electrophoresis 2015, 36, 386-92.
IF = 2.482; 3 CIT

In this work we have returned to the design of the previously developed microfabricated pneumatic electrospray nebulizer and evaluated two different geometries using computer simulations and experimental measurements of the MS signals. The microdevice was designed for electrospray MS interfacing without the need to fabricate an electrospray needle and can be used as a disposable or an integral part of a reusable system. The design of the chip layout was supported by computational fluid dynamics simulations. The tested microdevices were fabricated in glass using conventional photolithography, followed by wet chemical etching and thermal bonding. The performance of the microfabricated nebulizer was evaluated by means of TOF-MS with a peptide mixture. And the ESI plume shape and stability was monitored by a camera with laser scatter illumination. It was demonstrated that the nebulizer with converging gas channels operated at supersonic speed of the nebulizing gas and produced very stable nanospray (900 nL/min) as documented by less than 0.1% (SE) fluctuation in total mass spectrometric signal intensity.

6. References

[1] Fenn, J.B., Mann, M., Meng, C.K., Wong, S.F., Whitehouse, C.M. Electrospray Ionization for Mass-Spectrometry of Large Biomolecules. *Science* 1989, 246, 64-71.

[2] https://www.genome.gov/12011239/ (displayed on June 6., 2017)

[3] Jorgenson, J.W., Lukacs, K.D. Zone Electrophoresis in Open-Tubular Glass-Capillaries. *Anal.Chem.* 1981, 53, 1298-1302.

[4] Foret, F., Krivankova, L., Bocek, P. Capillary Zone Electrophoresis. Electrophoresis Library. (Editor Radola, B.J.) VCH, Verlagsgessellschaft, Weinheim, 1993.

[5] Heiger, D.N., Cohen, A.S., Karger, B.L. Separation of DNA Restriction Fragments By High-Performance Capillary Electrophoresis with Low And Zero Cross-Linked Polyacrylamide Using Continuous and Pulsed Electric-Fields. *J. Chomatogr.* 1990, 516, 33-48.

[6] Cohen, A.S, Najarian, D.R., Karger, B.L. Separation and Analysis of DNA-Sequence Reaction-Products by Capillary Gel-Electrophoresis. *J. Chromatogr.* 1990, 516, 49-60.

[7] Sudor, J., Foret, F., Bocek, P. Pressure Refilled Polyacrylamide columns for the Separation of Oligonucleotides by Capillary Electrophoresis. *Electrophoresis.* 1991, 12, 1056-1058.

[8] Pariat, Y.F., Berka, J., Heiger, D.N., Schmitt, T., Vilenchik, M., Cohen, A.S., Foret, F., Karger, B.L. Separation of DNA Fragments By Capillary Electrophoresis Using Replaceable Linear Polyacrylamide Matrices. *J.Chromatogr.* 1993, 652, 57-66.

[9] Mueller, O., Minarik, M., Foret, F. Ultrafast DNA analysis by capillary electrophoresis/laser-induced fluorescence detection. *Electrophoresis.* 1998, 19, 1436-1444.

[10] Kleparnik, K., Foret, F., Berka, J., Goetzinger, W., Miller, A.W., Karger, B.L. The Use of Elevated Temperature to Extend DNA Sequencing Read Lengths in Capillary Electrophoresis with Replaceable Polymer Matrices. *Electrophoresis.* 1996, 17, 1860-1866.

[11] Foret, F., Preisler, J. Liquid phase interfacing and miniaturization in matrix-assisted laser desorption/ionization mass spectrometry. *Proteomics*. 2002, 2, 360-372.

[12] Krenkova, J., Foret, F. On-line CE/ESI/MS interfacing: Recent developments and applications in proteomics. *Proteomics.* 2012, 12, 2978–2990.

[13] Foret, F., Kusý, P. Microdevices in mass spectrometry*. Eur. J. Mass. Spectrom.* 2007, 13, 41-44.

[14] Lazar, I.M., Grym, J., Foret, F. Microfabricated devices: A new sample introduction approach to mass spectrometry. *Mass Spectrom. Rev.* 2006, 25, 573-594.

[15] Bruce, J.E., Anderson, G.A., Wen, J., Harkewicz, R., Smith, R.D. High-Mass-Measurement Accuracy and 100 Sequence Coverage of Enzymatically Digested Bovine Serum Albumin from an ESI-FTICR Mass Spectrum. *Anal. Chem.* 1999, 71, 2595-9.

[16] Shen, Y., Tolic, N., Zhao, R., Pasa-Tolic, L., Li, L., Berger, S.J., Harkewicz, R., Anderson, G.A., Belov, M.E., Smith, R.D. *Anal. Chem.* 2001, 73, 3011-21.

[17] Klampfl, C.W. CE with MS detection: A rapidly developing hyphneated technique. *Electrophoresis.* 2009, 30, 83-91.

[18] Hommerson, P., Khan, A.M., de Jong, G.J., Somsen, G.W. Ionization techniques in capillary electrophoresis-mass spectrometry: Principles, design, and application. *Mass Spectrom. Rev.* 2011, 30, 1096-1120.

[19] Pantuckova, P., Gebauer, P., Bocek, P., Krivankova, L. Recent advances in CE-MS: Synergy of wet chemistry and instrumentation innovations. *Electrophoresis.* 2011, 32, 43-51.

[20] Metzger, J., Schanstra, J., Mischak, H. Capillary electrophoresis-mass spectrometry in urinary proteome analysis: current applications and future developments. *Anal. Bioanal. Chem.* 2009, 393, 1431-1442.

[21] Desiderio, C., Rossetti, D.V., Iavarone, F., Messana, I., Castagnola, M. Capillary electrophoresis-mass spectrometry: Recent trends in clinical proteomics. *J. Pharmaceut. Biomed. Anal.* 2010, 53, 1161-1169.

[22] Fonslow, B.R., Yates, J.R. Capillary electrophoresis applied to proteomic analysis. *J. Sep. Sci.* 2009, 32, 1175-1188.

[23] Haselberg, R., de Jong, G.J., Somsen, G.W. Capillary electrophoresis-mass spectrometry for the analysis of intact proteins 2007-2010. *Electrophoresis.* 2011, 32, 66-82.

[24] Dakna, M., He, Z., Yu, W.C., Mischak, H., Kolch, W. Technical, bioinformatical and statistical aspects of liquid chromatography-mass spectrometry (LC-MS) and capillary electrophoresis-mass spectrometry (CE-MS) based clinical proteomics: A clinical assessment. *J. Chromatogr. B.* 2009, 877, 1250-1258.

[25] Mechref, Y., Novotny, M.V. Glycomic analysis by capillary electrophoresis-mass spectrometry. *Mass Spectrom. Rev.* 2009, 28, 207-222.

[26] Ramautar, R., Mayboroda, O.A., Somsen, G.W., de Jong, G.J. CE-MS for metabolomics: Developments and applications in the period 2008-2010. *Electrophoresis.* 2011, 32, 52-65.

[27] Fang, X.P., Balgley, B.M., Lee, C.S. Recent advances in capillary electrophoresis-based proteomic techniques for biomarker discovery. *Electrophoresis.* 2009, 30, 3998-4007.

[28] Mischak, H., Schanstra, J. P. CE-MS in biomarker discovery, validation, and clinical application. *Proteomics Clin. Appl.* 2011, 5, 9-23.

[29] Ahmed, F. E. The role of capillary electrophoresis-mass spectrometry to proteome analysis and biomarker discovery. *J. Chromatogr. B.* 2009, 877, 1963-1981.

[30] Mischak, H., Coon, J. J., Novak, J., Weissinger, E. M. et al. Capillary electrophoresis-mass spectrometry as a powerful tool in biomarker discovery and clinical diagnosis: An update of recent developments. *Mass Spectrom. Rev.* 2009, 28, 703-724.

[31] Desiderio, C., Iavarone, F., Rossetti, D.V., Messana, I., Castagnola, M. Capillary electrophoresis-mass spectrometry for the analysis of amino acids. *J. Sep. Sci.* 2010, 33, 2385-2393.

[32] Simo, C., Garcia-Canas, V., Cifuentes, A. Chiral CE-MS. *Electrophoresis.* 2010, 31, 1442-1456.

[33] Huhn, C., Ramautar, R., Wuhrer, M., Somsen, G.W. Relevance and use of capillary coatings in capillary electrophoresis-mass spectrometry. *Anal. Bioanal. Chem.* 2010, 396, 297-314.

[34] Staub, A., Schappler, J., Rudaz, S., Veuthey, J.-L. CE-TOF/MS: Fundamental concepts, instrumental considerations and applications. *Electrophoresis.* 2009, 30, 1610-1623.

[35] Somsen, G.W., Mol, R., de Jong, G.J. On-line coupling of electrokinetic chromatography and mass spectrometry. J. Chromatogr A. 2010, 1217, 3978-3991.

[36] Hommerson, P., Khan, A. M., de Jong, G. J., Somsen, G.W. Ionization techniques in capillary electrophoresis-mass spectrometry: Principles, design, and application. *Mass Spectrom. Rev.* 2011, 30, 1096-1120.

[37] Koster, S., Verpoorte, E. A decade of microfluidic analysis coupled with electrospray mass spectrometry: An overview. *Lab on a Chip.* 2007, *7*, 1394-1412.

[38] Sikanen, T., Franssila, S., Kauppila, T. J., Kostiainen, R. et al. Microchip technology in mass spectrometry. *Mass Spectrom. Rev.* 2010, *29*, 351-391.

[39] Kitagawa, F., Otsuka, K. Recent progress in microchip electrophoresis-mass spectrometry. *J. Pharmaceut. Biomed. Anal.* 2011, *55*, 668-678.

[40] Olivares, J.A., Nguyen, N.T., Yonker, C.R., Smith, R.D. Online mass-spectrometric detection for capillary zone electrophoresis. *Anal. Chem.* 1987, 59, 1230-1232.

[41] Smith, R.D., Olivares, J.A., Nguyen, N.T., Udseth, H.R. Capillary zone electrophoresis mass-spectrometry using an electrospray ionization interface. *Anal. Chem.* 1988, 60, 436-441.

[42] Maxwell, E.J., Chen, D.D.Y. Twenty years of interface development for capillary electrophoresis-electrospray ionization-mass spectrometry. *Anal. Chem.* 2008, 627, 25-33.

[43] Moini, M. Simplifying CE-MS operation. 2. Interfacing low-flow separation techniques to mass spectrometry using a porous tip. *Anal. Chem.* 2007, 79, 4241-4246.

[44] Faserl, K., Sarg, B., Kremser, L., Lindner, H. Optimization and evaluation of a sheathless capillary electrophoresis-electrospray ionization mass spectrometry platform for peptide analysis: Comparison to iquid chromatography-electrospray ionization mass spectrometry. *Anal. Chem.* 2011, 83, 7297-7305.

[45] Busnel, J.M., Schoenmaker, B., Ramautar, R., Carrasco-Pancorbo, A. et al. High capacity capillary electrophoresis-electrospray ionization mass spectrometry: Coupling a porous sheathless interface with transient-isotachophoresis. *Anal. Chem.* 2010, 82, 9476-9483.

[46] Kawai, M., Iwamuro, Y., Iio-Ishimaru, R., Chinaka, S. et al. Analysis of phosphorus-containing amino acid-type herbicides by sheathless capillary electrophoresis/electrospray ionization-mass spectrometry using a high sensitivity porous sprayer. *Analyt. Sci.* 2011, 27, 857-860.

[47] Gibson, G.T.T., Mugo, S.M., Oleschuk, R.D. Nanoelectrospray emitters: trends and perspective. *Mass Spectrom. Rev.* 2009, 28, 918-936.

[48] Smith, R.D., Barinaga, C.J., Udseth, H.R. Improved electrospray ionization interface for capillary zone electrophoresis-mass spectrometry. *Anal. Chem.* 1988, 60, 1948-1952.

[49] Blades, A.T., Ikonomou, M.G., Kebarle, P. Mechanism of electrospray mass-spectrometry - electrospray as an electrolysis cell. *Anal. Chem.* 1991, 63, 2109-2114.

[50] Girault, H., Liu, B.H., Qiao, L.A., Bi, H.Y., Prudent, M., Lion, N., Abonnenc, M. Electrochemical reactions and ionization processes. *European J. Mass Spectrom.* 2010, 16, 341-349.

[51] Soga, T., Igarashi, K., Ito, C., Mizobuchi, K. et al. Metabolomic profiling of anionic metabolites by capillary electrophoresis mass spectrometry. *Anal. Chem.* 2009, 81, 6165-6174.

[52] Mokaddem, M., Gareil, P., Belgaied, J.E., Varenne, A. New insight into suction and dilution effects in CE coupled to MS via an ESI interface. II - Dilution effect. *Electrophoresis.* 2009, 30, 1692-1697.

[53] Grundmann, M., Matysik, F.M. Fast capillary electrophoresis-time-of-flight mass spectrometry using capillaries with inner diameters ranging from 75 to 5 μm. Anal. Bioanal. Chem. 2011, 400, 269-278.

[54] Wojcik, R., Dada, O.O., Sadilek, M., Dovichi, N.J. Simplified capillary electrophoresis nanospray sheath-flow interface for high efficiency and sensitive peptide analysis. *Rapid Commun. Mass Spectrom.* 2010, 24, 2554-2560.

[55] Lapainis, T., Rubakhin, S.S., Sweedler, J.V. Capillary electrophoresis with electrospray ionization mass spectrometric detection for single-cell metabolomics. *Anal. Chem.* 2009, 81, 5858-5864.

[56] Li, F.A., Huang, J.L., Her, G.R. Chip-CE-MS using a flat low-sheath-flow interface. *Electrophoresis.* 2008, 29, 4938-4943.

[57] Lee, W.H., Her, G.R. The development of a two-leveled two cross interface for on-line coupling solid-phase extraction and capillary electrophoresis-mass spectrometry. *Electrophoresis.* 2009, 30, 1675-1683.

[58] Lee, W.H., Wang, C.W., Her, G.R. Staggered multistep elution solid-phase extraction capillary electrophoresis/tandem mass spectrometry: a high-throughput approach in protein analysis. *Rapid Commun. Mass Spectrom.* 2011, 25, 2124-2130.

[59] Lee, E.D., Muck, W., Henion, J.D., Covey, T.R. Online capillary zone electrophoresis ion spray tandem mass-spectrometry for the determination of dynorphins. *J. Chromatogr.* 1988, 458, 313-321.

[60] Kusy, P., Kleparnik, K., Aturki, Z., Fanali, S., Foret, F. Optimization of a pressurized liquid junction nanoelectrospray interface between CE and MS for reliable proteomic analysis. *Electrophoresis.* 2007, 28, 1964-1969.

[61] Krenkova, J., Kleparnik, K., Foret, F. Capillary electrophoresis mass spectrometry coupling with immobilized enzyme electrospray capillaries. *J. Chromatogr. A.* 2007, 1159, 110-118.

[62] Thakur, D., Rejtar, T., Karger, B. L., Washburn, N.J. et al. Profiling the glycoforms of the intact alpha subunit of recombinant human chorionic gonadotropin by high-resolution capillary electrophoresis-mass spectrometry. *Anal. Chem.* 2009, 81, 8900-8907.

[63] Szabo, Z., Guttman, A., Rejtar, T., Karger, B. L. Improved sample preparation method for glycan analysis of glycoproteins by CE-LIF and CE-MS. *Electrophoresis.* 2010, 31, 1389-1395.

[64] Fanali, S., D'Orazio, G., Foret, F., Kleparnik, K., Aturki, Z. On-line CE-MS using pressurized liquid junction nanoflow electrospray interface and surface-coated capillaries. *Electrophoresis.* 2006, 27, 4666-4673.

[65] Hezinova, V., Aturki, Z., Kleparnik, K., D'Orazio, G. et al. Simultaneous analysis of cocaine and its metabolites in urine by capillary electrophoresis-electrospray mass spectrometry using a pressurized liquid junction nanoflow interface. *Electrophoresis.* 2012, 33, 653-660.

[66] Foret, F., Zhou, H., Gangl, E., Karger, B.L. Subatmospheric electrospray interface for coupling of microcolumn separations with mass spectrometry. *Electrophoresis.* 2000, 21, 1363-1371.

[67] Wachs, T., Sheppard, R. L., Henion, J. Design and applications of a self-aligning liquid junction electrospray interface for capillary electrophoresisi mass spectrometry. *J. Chromatogr. B.* 1996, 685, 335–342.

[68] Kleparnik, K., Otevrel, M. Analyte transport in liquid junction nano-electrospray interface between capillary electrophoresis and mass spectrometry. *Electrophoresis.* 2010, 31, 879-885.

[69] Maxwell, E.J., Zhong, X.F., Zhang, H., van Zeijl, N., Chen, D.D.Y. Decoupling CE and ESI for a more robust interface with MS. *Electrophoresis.* 2010, 31, 1130-1137.

[70] Maxwell, E.J., Ratnayake, C., Jayo, R., Zhong, X.F., Chen, D.D.Y. A promising capillary electrophoresis-electrospray ionization-mass spectrometry method for carbohydrate analysis. *Electrophoresis.* 2011, 32, 2161-2166.

[71] Zhong, X.F., Maxwell, E.J., Ratnayake, C., Mack, S., Chen, D.D.Y. Flow-through microvial facilitating interface of capillary isoelectric focusing and electrospray ionization mass spectrometry. *Anal. Chem.* 2011, 83, 8748-8755.

[72] Zhong, X.F., Maxwell, E.J., Chen, D.D.Y. Mass transport in a micro flow-through vial of a junction-at-the-tip capillary electrophoresis-mass spectrometry interface. *Anal. Chem.* 2011, 83, 4916-4923.

[73] Haff, L.A., Smirnov, I.P. Single-nucleotide polymorphism identification assays using a thermostable DNA polymerase and delayed extraction MALDI-TOF mass spectrometry. *Genome Res.* 1997, 7, 378-388.

[74] Terry, S.C., Jerman, J.H., Angell, J.B. A Gas Chromatographic Air Analyzer Fabricated on a Silicon Wafer. *IEEE Transactions on Electron Devices.* 1979, 26, 1880-86.

[75] Woolley, A.T., Mathies, R.A. Ultra-high-speed DNA fragment separations using microfabricated capillary array electrophoresis chips. *Proc. Natl. Acad. Sci. USA.* 1994, 91, 11348-11352.

[76] Karger, B.L., Foret, F., Qifeng, X., Dunayevski, Y., Zavracki, P., McGruer, N. Microscale Fluid Handling System U.S. Patent # 5, 872, 010, 1999.

[77] Xue, Q.F., Foret, F., Dunayevskiy, Y., Zavracky, P., McGruer, N.E., Karger, B.L. Multichannel microchip electrospray mass spectrometry. *Anal. Chem.* 1997, 69, 426-430.

[78] Xue, Q.F., Dunayevskiy, Y., Foret, F., Karger, B.L. Integrated multichannel microchip electrospray ionization mass spectrometry: Analysis of peptides from on-chip tryptic digestion of melittin. *Rapid Commun. Mass Spectrom.* 1997, 11, 1253-1256.

[79] Ramsey, R.S., Ramsey, J.M. Generating electrospray from microchip devices using electroosmotic pumping. Anal. Chem. 1997, 69, 1174-1178.

[80] Lozano, P., Martinez-Sanchez, M., Lopez-Urdiales, J.M. Electrospray emission from nonwetting flat dielectric surfaces. J Coll. *Inter. Sci.* 2004, 276, 392-399.

[81] Huikko. K., Ostman, P., Grigoras, K., Tuomikoski, S., Tiainen, V.M., Soininen, A., Puolanne, K., Manz, A., Franssila, S., Kostiainen, R., Kotiaho, T. Poly(dimethylsiloxane) electrospray devices fabricated with diamond-like carbon-poly(dimethylsiloxane) coated SU-8 masters. *Lab on a Chip.* 2003, 3, 67-72.

[82] Svedberg, M., Veszelei, M., Axelsson, J., Vangbo, M., Nikolajeff, F. Poly(dimethylsiloxane) microchip: microchannel with integrated open electrospray tip. *Lab on a Chip.* 2004, 4, 222-327.

[83] Figeys, D., Aebersold, R. Microfabricated modules for sample handling, sample concentration and flow mixing: Application to protein analysis by tandem mass spectrometry. J. Biomech. *Engineering.* 1999, 121, 7-12.

[84] Bings, N.H., Wang, C., Skinner, C.D., Colyer, C.L., Thibault, P., Harrison, D.J. Microfluidic devises connected to fused-silica capillaries with minimal dead volume. *Anal. Chem.* 1999, 71, 3292-3296.

[85] Wachs, T., Henion J. Electrospray device for coupling microscale separations and other miniaturized devices with electrospray mass spectrometry. *Anal. Chem.* 2001, 73, 632-638.

[86] Deng, Y.Z., Zhang, N. W., Henion, J. Chip-based quantitative capillary electrophoresis/mass spectrometry determination of drugs in human plasma. *Anal. Chem.* 2001, 73, 1432-1439.

[87] Licklider, L., Wang, X.Q., Desai, A., Tai, Y.C., Lee, T.D. A micromachined chip-based electrospray source for mass spectrometry. *Anal. Chem.* 2000, 72, 367-375.

[88] Schultz, G.A., Corso, T.N., Prosser, S.J., Zhang, S. A fully integrated monolithic microchip electrospray device for mass spectrometry. *Anal. Chem.* 2000, 72, 4058-4063.

[89] Sjödahl, J., Melin, J., Griss, P., Emmer, Å., Stemme, G., Roeraade, J. Characterization of micromachined hollow tips for two-dimensional nanoelectrospray mass spectrometry. *Rapid Commun Mass Spectrom*. 2003, 17, 337-341.

[90] Arscott, S., Legac, S., Rolando, C. A polysilicon nanoelectrospray-mass spectrometry source based on a capillary microfluidic slot. *Sens Actuators*. 2005, B 106, 741-749.

[91] Kameoka, J., Craighead, H.G., Zhang, H.W., Henion, J. A polymeric microfluidic chip for CE-MS determination of small molecules. *Anal. Chem.* 2001, 73, 1935-1941.

[92] Lion, N., Gellon, J.O., Girault, H.H. Flow-rate characterization of microfabricated polymer microspray emitters. *Rapid Commun Mass Spectrom.* 2004, 18, 1614-1620.

[93] Le Gac, S., Arscott, S., Rolando, C. A planar microfabricated nanoelectrospray emitter tip based on a capillary slot. *Electrophoresis.* 2003, 24, 3640-3647.

[94] Rohner, T.C., Rossier, J.S., Girault, H.H. Polymer microspray with an integrated thick-film microelectrode. *Anal. Chem.* 2001, 73, 5353-5357.

[95] Tang, K.Q., Lin, Y.H., Matson, D.W., Kim, T., Smith, R.D. Generation of multiple electrosprays using microfabricated emitter arrays for improved mass spectrometric sensitivity. *Anal. Chem.* 2001, 73, 1658-1663.

[96] Svedberg, M., Pettersson, A., Nilsson, S., Bergquist, J., Nyholm, L., Nikolajeff, F., Markides, K. Sheathless electrospray from polymer microchips. *Anal. Chem.* 2003, 75, 3934-3940.

[97] Muck, A., Svatos, A. Atmospheric molded poly(methylmethacrylate) microchip emitters for sheathless electrospray. *Rapid Commun Mass Spectrom.* 2004, 18, 1459-1464.

[98] Schilling, M., Nigge, W., Rudzinski, A., Neyer, A., Hergenroder, R. A new on-chip ESI nozzle for coupling of MS with microfluidic devices. *Lab on a Chip.* 2004, 4, 220-224.

[99] Yuan, C.H., Shiea, J. Sequential electrospray analysis using sharp-tip channels fabricated on a plastic chip. *Anal. Chem.* 2001, 73, 1080-1083.

[100] Wei, H. B., Li, H. F., Gao, D., Lin, J.M. Multi-channel microfluidic devices combined with electrospray ionization quadrupole time-of-flight mass spectrometry applied to the monitoring of glutamate release from neuronal cells. *Analyst.* 2010. 135, 2043-2050.

[101] Mao, P., Gomez-Sjoberg, R., Wang, D.J. Multinozzle Emitter Array Chips for Small-Volume Proteomics. *Anal. Chem.* 2013, 85, 816-819.

[102] Fritzsche, S., Ohla, S., Glaser, P., Giera, D.S., Sickert, M., Schneider, C., Belder, D. Asymmetric Organocatalysis and Analysis on a Single Microfluidic Nanospray Chip. *Angew. Chem., Int. Ed.* 2011, 50, 9467-9470.

[103] Lotter, C., Heiland, J. J., Thurmann, S., Mauritz, L., Belder, D. HPLC-MS with Glass Chips Featuring Monolithically Integrated Electrospray Emitters of Different Geometries. *Anal. Chem.* 2016, 88, 2856-2863.

[104] Sainiemi, L., Sikanen, T., Kostiainen, R. Integration of Fully Microfabricated, Three-Dimensionally Sharp Electrospray Ionization Tips with Microfluidic Glass Chips. *Anal. Chem.* 2012, 84, 8973-8979.

[105] Sainiemi, L., Nissila, T., Kostiainen, R., Franssila, S., Ketola, R.A. A microfabricated micropillar liquid chromatographic chip monolithically integrated with an electrospray ionization tip. *Lab on a Chip.* 2012, 12, 325-332.

[106] Batz, N.G., Mellors, J.S., Alarie, J.P., Ramsey, J.M. Chemical Vapor Deposition of Aminopropyl Si lanes in Microfluidic Channels for Highly Efficient Microchip Capillary Electrophoresis-Electrospray Ionization-Mass Spectrometry. *Anal. Chem.* 2014, 86, 3493-3500.

[107] Mellors, J.S., Black, W.A., Chambers, A.G., Starkey, J.A., Lacher, N.A., Ramsey, J.M. Hybrid Capillary/Microfluidic System for Comprehensive Online Liquid Chromatography-Capillary Electrophoresis-Electrospray Ionization-Mass Spectrometry. *Anal. Chem.* 2013, 85, 4100-4106.

[108] Mellors, J.S., Jorabchi, K., Smith, L.M., Ramsey, J.M. Integrated Microfluidic Device for Automated Single Cell Analysis Using Electrophoretic Separation and Electrospray Ionization Mass Spectrometry. *Anal. Chem.* 2010, 82, 967-973.

[109] Chambers, A.G., Mellors, J.S., Henley, W.H., Ramsey, J.M. Monolithic Integration of Two-Dimensional Liquid Chromatography-Capillary Electrophoresis and Electrospray Ionization on a Microfluidic Device. *Anal. Chem.* 2011, 83, 842-849.

[110] Dittrich, P.S., Manz, A. Lab-on-a-chip: microfluidics in drug discovery. *Nat. Rev. Drug Discov.* 2006, 5, 210-218.

[111] http://908devices.com/products/zipchip/ Displayed on June 12, 2017

Capillary Electrophoresis/Electrospray Ionization Mass Spectrometry: Improvement of Protein Detection Limits Using On-Column Transient Isotachophoretic Sample Preconcentration

Toni J. Thompson, Frantisek Foret,† Paul Vouros, and Barry L. Karger*

Barnett Institute, Department of Chemistry, Northeastern University, Boston, Massachusetts 02115

On-column transient isotachophoretic sample preconcentration has been utilized for decreasing concentration detection limits in capillary electrophoresis (CE)/electrospray ionization mass spectrometry analysis (ESI/MS) of protein samples. Mixtures of model proteins have been separated in the cationic mode using a coated capillary and have been analyzed by mass spectrometry coupled on-line to an electrospray interface with a coaxial sheath flow arrangement. Complex formation, between β-lactoglobulins A and B and the BGE, was found to occur under certain conditions. The detection level was evaluated using capillary zone electrophoresis (CZE)/MS, capillary isotachophoresis (CITP)/MS and the on-column combination of transient CITP/CZE/MS. In CZE/MS, the sample concentration necessary to obtain a reliable full scan spectrum was in the range of 10^{-6} M (~500 fmol injected in a 75-μm-i.d. capillary). In the CITP/MS mode, a sample could in principle be preconcentrated by several orders of magnitude. The isotachophoretically stacked zones overlapped one another, and the minor components, focused to very narrow zones of less than 1 s, could not be reliably identified. However, isotachophoresis represents an ideal preconcentration technique for CZE whereby the benefits of both CITP and CZE are maintained. By proper selection of running buffers, the on-column combination of both CITP and CZE (transient CITP/CZE) was used to decrease the concentration detection limits for a full scan CZE/MS analysis by a factor of 100 to ~10^{-7} M. Such an approach can be employed with currently available commercial CE equipment.

INTRODUCTION

There is currently a great deal of interest in the development of capillary electrophoresis/mass spectrometry (CE/MS) for the separation and identification of charged species ranging from small ions to proteins.[1-5] The importance of this combination stems from the advantageous features of both CE and MS. Capillary electrophoresis provides significant separation efficiency and analytical speed for a broad range of substances in solution, while mass spectrometry provides peak identification. Furthermore, the flow rates from the capillary column are compatible with on-line coupling to MS.

In an early report on coupling capillary electrophoresis to a mass spectrometer,[6] an on-line valve was used to transfer CITP-separated zones into a mass spectrometer equipped with an electron ionization source. Although this technique should properly be referred to as an off-line technique, the potential of mass spectrometry for identification of analytes separated by capillary electrophoresis was clearly demonstrated. The first reports of the on-line coupling of CZE to MS used an electrospray source for the ionization and transfer of analyte ions into a quadrupole mass spectrometer.[1,2] Later, fast atom bombardment (FAB) was also employed for the ionization and sample transfer into the mass spectrometer.[4,7-9] Recently, other types of mass spectrometers such as time of flight[10] and ion trap[11] have been tested for coupling to CE.

For the determination of high molecular weight ions, electrospray ionization has an advantage in the formation of multiply-charged ions that can be conveniently analyzed by a mass spectrometer in the m/z range up to 4000. Exact molar masses can then be easily calculated from the observed distribution of charge states of the molecule.[12] With respect to coupling of CE to MS, electrospray has the further advantage of operating at atmospheric pressure so that hydrodynamic flow in the separation capillary (with its attendant parabolic flow profile) does not result or can be simply overcome.

Mass detection levels for proteins determined by CZE/MS are typically in the high femtomole range,[3] but when the concentration of the sample injected is considered, the detection level is frequently insufficient (~10^{-5} M). One solution to this detection level problem is the use of selected ion recording,[13] which is known to significantly decrease the detection limits as compared to full scan analyses; however, this method requires prior knowledge of ions that will be present in the sample. In cases where detection limits of a CE/MS analysis are an issue, sample preconcentration, preferably in an on-line arrangement, should be considered as a possible method to improve detection without the loss of accuracy. Several approaches for decreasing the concentration detection limits for CE analyses by on-column preconcentration have been described. Principally, they can

* Author to whom correspondence should be addressed.
† On leave from Institute of Analytical Chemistry, Veveri 97, 611 42 Brno, Czechoslovakia.

(1) Olivares, J. A.; Nguyen, N. T.; Yonker, C. R.; Smith, R. D. *Anal. Chem.* **1987**, *59*, 1232-1236.
(2) Lee, E. D.; Muck, W.; Henion, J. D.; Covey, T. R. *J. Chromatogr.* **1988**, *458*, 313-321.
(3) Thibault, P.; Paris, C.; Pleasance, S. *Rapid Commun. Mass Spectrom.* **1991**, *5*, 484-490.
(4) Moseley, M. A.; Deterding, L. J.; Tomer, K. B.; Jorgenson, J. W. *Anal. Chem.* **1991**, *63*, 109-114.
(5) Garcia, F.; Henion, J. D. *Anal. Chem.* **1992**, *64*, 985-990.
(6) Kenndler, E.; Kaniansky, D. *J. Chromatogr.* **1981**, *209*, 306-309.
(7) Moseley, M. A.; Deterding, L. J.; Tomer, K. B.; Jorgenson, J. W. *J. Chromatogr.* **1989**, *480*, 233-245.
(8) Moseley, M. A.; Deterding, L. J.; Tomer, K. B.; Jorgenson, J. W. *Rapid Commun. Mass Spectrom.* **1989**, *3*, 87-96.
(9) Wolf, S.; Norwood, C.; Jackim, E.; Vouros, P. *J. Am. Soc. Mass Spectrom.* **1992**, *3*, 757-761.
(10) Hallen, R. W.; Shumate, C. B.; Siems, W. F.; Tsuda, T.; Hill, H. H., Jr.; *J. Chromatogr.* **1989**, *480*, 233-245.
(11) Schwartz, J. C.; Jardine, I. Poster presented at The 40th ASMS Conference on Mass Spectrometry and Allied Topics, Washington, DC, (TP67) May 31-June 5, 1992.
(12) Fenn, J. B.; Mann, M.; Meng, C. K.; Wong, S. F.; Whitehouse, C. M. *Science* **1989**, *246*, 64-71.
(13) Moseley, M. A.; Jorgenson, J. W.; Shabanowitz, J.; Hunt, D. F.; Tomer, K. B. *J. Am. Soc. Mass Spectrom.* **1992**, *3*, 289-300.

0003-2700/93/0365-0900$04.00/0

be divided into two classes—sorption[14,15] and electrophoretic techniques.[16-20] While the sorption techniques require a precolumn and somewhat complex instrumentation, the use of electrophoretic techniques is simpler and more general.

This study has as its goal the development of a simple preconcentration technique for CZE/MS where higher sample volumes could be injected. The use of sample stacking via low conductivity sample matrices as a means of increasing injection volume[16] was first tested. Next, CITP was investigated, followed by a combination of CITP and CZE. The on-line coupling of CITP to ESI/MS has been previously demonstrated.[21] While the concentrating capability of CITP is excellent, the optimization of separation conditions, particularly in the case of protein analysis, is not straightforward. On the other hand, when ITP is used solely as a preconcentration technique, the selection of leading and terminating electrolytes can be easily accomplished. The coupling of CITP as a preconcentration step to CZE was already explored with UV[18-20,22] and fluorescence[23] detectors and recently with a mass spectrometer.[24] So far, coupled column systems were solely explored where preconcentration was carried out in a CITP wide bore preseparation tube connected to a CZE capillary of smaller internal diameter. This technique permits sample preconcentration by at least 3 orders of magnitude; however, it requires somewhat complicated instrumentation. Recently we have demonstrated the possibility of on-column transient CITP preconcentration of protein samples where both CITP preconcentration and CZE separation proceed in one capillary on a commercial instrument equipped with a UV detector.[22]

The present work reports results on the use of on-column transient CITP sample preconcentration for decreasing the detection limits of protein determination by CE/ESI/MS. This method is compared to sample stacking via low conductivity sample matrices and CITP alone. It will be shown that transient CITP provides a simple means of decreasing detection limits by 2 orders of magnitude over normal CZE.

EXPERIMENTAL SECTION

Mass Spectrometer and Interface. The mass spectrometer was a Finnigan MAT TSQ700 (Finnigan, San Jose, CA) triple quadrupole equipped with an electrospray ionization source. Several modifications to the electrospray interface (Figure 1) were necessary to couple CE with ESI/MS. The stainless steel needle supplied with the instrument was replaced with a polyimide coated fused silica capillary used in CE. This change was made to eliminate any junctions that could be detrimental to the separation and to enable the end of the capillary to be located at the electrospray needle tip. The interface utilized a coaxial liquid sheath, as shown previously,[25] as well as a coaxial gas sheath.[2] The liquid sheath tube supplied by the manufacturer was replaced by stainless steel tubing (Small Parts, Inc., Miami Lakes, FL) of ~0.4-mm i.d. and ~0.7-mm-o.d., and the gas sheath tip was also replaced with a tip having an orifice of 1.0-mm i.d. The liquid sheath tip was narrowed to ~0.5 mm to improve the electrospray stability.[26] The fused silica separation capillary terminated 0.5 mm inside the liquid sheath tip. A silicone septum was also added to prevent back flow of sheath liquid along the capillary.

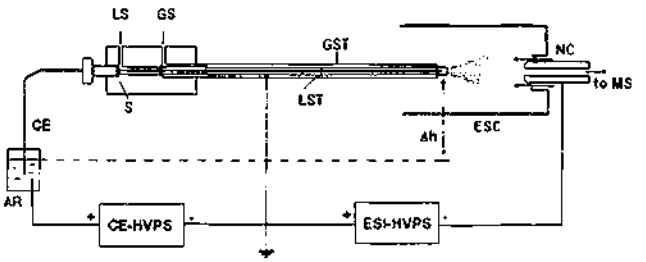

Figure 1. Diagram of the capillary electrophoresis/electrospray interface. S is septum, LST is liquid sheath tube, LS is liquid sheath entry port, GST is gas sheath tube, GS is gas sheath entry port, AR is anode reservoir, CE is CE capillary, NC is nitrogen curtain drying gas, ESC is cylindrical electrospray electrode, ESI-HPVS is the electrospray high voltage power supply, Δh is the height difference between the anode and cathode ends of the column, and CE-HPVS is the capillary electrophoresis high-voltage power supply. See the Experimental Section for further details.

Figure 1 further shows that the difference in height (Δh) between the anode reservoir and the tip of the electrospray needle (the cathode end of CZE column) was ~10 cm. A partial vacuum was created due to the flow of the gas sheath at the capillary tip, and with the ends of the capillary at equal height, a significant bulk liquid flow toward the cathode took place. In order to compensate for this pressure drop, the level of the anode reservoir was lowered. Capillary isotachophoresis was employed to determine the level at which no bulk flow occurred. The capillary was first filled with the leading electrolyte (0.01 M ammonium acetate, pH 5), and then ~150 nL of 10^{-3} M methyl green dye was siphon injected. The injection end of the capillary was then placed in the terminating electrolyte reservoir (0.001 M acetic acid), and the current was applied. The current was turned off when the dye had focused into a narrow 2-mm-long band. Movement of the zone could easily be observed through the polyimide coating of the capillary, due to the high concentration of this focused dye. The height of the reservoir was adjusted until no movement of the dye was observed in either the forward or the reverse direction.

The electrospray needle, as shown in Figure 1, was maintained at ground potential while the sampling orifice was at about −4000 V when operating in the positive ion mode. The drying gas (nitrogen curtain) for the electrospray was maintained at about 100 °C at a flow rate of 6 L/min, while the sheath gas flow was set at approximately 2 L/min. The liquid sheath consisted of 1% acetic acid in 50% 2-propanol/water, flowing at a rate of 4.0 μL/min. Tuning and calibration of the mass spectrometer were performed using a 5 pmol/μL myoglobin solution. The third quadrupole of the mass spectrometer was scanned from m/z 600 to 2000 at 1 scan/s for all analyses while the first and second quadrupoles were operated in the rf only mode. The quadrupole manifold was heated to 70 °C, and the electron multiplier was set at 1.5 kV with the conversion dynode at −15 kV.

Capillary Electrophoresis. The electrophoresis apparatus was made in-house using a CZE1000R (Spellman, Plainview, NY) high-voltage power supply. The CE columns were fused silica capillaries (Polymicro Technologies, Phoenix, AZ) 75-μm i.d., 360-μm o.d., and 50-cm length, coated in-house with linear polyacrylamide.[27] The polyacrylamide coating minimized adsorption by proteins to the capillary walls and eliminated electroosmotic flow within the capillary. The voltage for the CZE and transient CITP analyses was 18 kV with a resultant current of 6 μA. The constant current applied during the CITP analyses was 6 μA with voltage increasing from 7 to 17 kV.

Solutions. The standard proteins were purchased from Sigma Chemical Co. (St. Louis, MO) and were used without further

(14) Guzman, N. A.; Trebilock, M. A.; Advis, J. P. *J. Liquid Chromatogr.* **1991**, *14* (5) 997-1015.
(15) Cai, J.; El Rassi, Z. *J. Liquid Chromatogr.* **1992**, *15* (6&7), 1179-1192.
(16) Aebersold, R.; Morrison, H. D. *J. Chromatogr.* **1990**, *516*, 79-88.
(17) Chien, R. L.; Burgi, D. S. *J. Chromatogr.* **1991**, 559, 141-152.
(18) Kaniansky, D.; Marak, J. *J. Chromatogr.* **1990**, *498*, 191-204.
(19) Foret, F.; Sustacek, V.; Bocek, P. *J. Microcol. Sep.* **1990**, *2*, 299-303.
(20) Stegehuis, D. S.; Irth, H.; Tjaden, U. R.; van der Greef, J. *J. Chromatogr.* **1991**, *538*, 393-402.
(21) Smith, R. D.; Fields, S. M.; Loo, J. A.; Barinaga, C. J.; Udseth, H. R.; Edmonds, C. G. *Electrophoresis* **1990**, *11*, 709-717.
(22) Foret, F.; Szoko, E.; Karger, B. L. *J. Chromatogr.* **1992**, *608*, 3-12.
(23) Stegehuis, D. S.; Tjaden, U. R.; van der Greef, J. *J. Chromatogr.* **1992**, *591*, 341-349.
(24) Tinke, A. P.; Reinhoud, N. J.; Niessen, W. M. A.; Tjaden, U. R., van der Greef, J. *Rapid Commun. Mass Spectrom.* **1992**, *6*, 560-563.
(25) Smith, R. D.; Barinaga, C. J.; Udseth, H. R. *Anal. Chem.* **1988**, *60*, 1948-1952.
(26) Chowdhury, S. K.; Chait, B. T. *Anal. Chem.* **1991**, *63*, 1660-1664.
(27) Hjerten, S. *J. Chromatogr.* **1985**, *347*, 191-197.

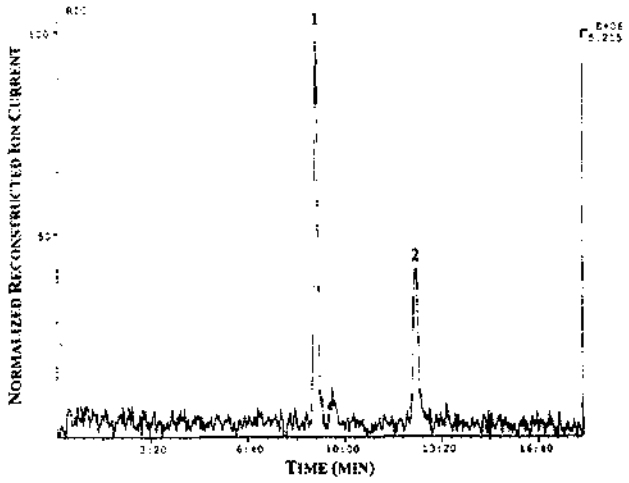

Figure 2. CZE/MS full scan (m/z 600–2000) reconstructed ion electropherogram of 9.0 μM cytochrome *c* (1) and 5.4 μM myoglobin (2) in the BGE. Injection volume: 50 nL (injected quantity of 450 and 270 fmol, respectively). BGE: 0.02 M 6-aminohexanoic acid + acetic acid, pH 4.4. CE conditions: constant voltage 18 kV, current 6 μA.

purification. The samples were dissolved in either the background electrolyte or distilled/deionized water for CZE separations. The CZE background electrolyte (BGE) was 0.02 M 6-aminohexanoic acid in water, adjusted to pH 4.4 with glacial acetic acid. The CITP leading electrolyte was 0.01 M ammonium acetate adjusted to pH 4.4 with glacial acetic acid, and the terminating electrolyte was 0.001 M acetic acid. For the transient CITP experiments, the samples were diluted in the CITP leading electrolyte buffer and the background electrolyte was the same as that used in the CZE experiments. All buffer chemicals were purchased from Sigma.

Sample Injection. The CE column was first washed with the background electrolyte or, in the case of CITP, with the leading electrolyte. The sample was then siphon injected by inserting the column into the sample vial and elevating the vial by 20 cm for 10–150 s, producing an injection volume of 50–750 nL.

RESULTS AND DISCUSSION

In order to provide a baseline from which to judge the preconcentration methods, initial studies were performed with CZE/MS, with the sample dissolved in the background electrolyte. Figure 2 shows the full scan reconstructed ion electropherogram (RIE) of 50 nL of a sample containing cytochrome c and myoglobin in which the proteins were diluted in the background electrolyte (6-aminohexanoic acid) to a concentration of $\sim 10^{-5}$ M. This injection volume of 50 nL is larger than typically used in CZE and was chosen so that reliable mass spectra could be obtained. In this figure, the signal to noise ratio (S/N) for cytochrome c is 12:1. An improved S/N may be obtained by dissolving the sample in water or low concentration buffer[17] with subsequent focusing of the larger volume injected. Figure 3a shows the full scan RIE of 150 nL of a sample containing lysozyme (1), cytochrome c (2), ribonuclease A (3), myoglobin (4), β-lactoglobulin A (5), β-lactoglobulin B (6), and carbonic anhydrase (7) dissolved in water. An example of the spectra obtained by averaging the scans under the peaks is shown in Figure 3b, and the deconvolution of that spectrum is shown in Figure 3c. Initial preconcentration across the sample/BGE boundary was responsible for improved detection signal of 3.5 times that of the sample dissolved in the BGE.

Few of the proteins in Figure 3a were still detectable in the RIE of a 1:10 dilution (10^{-6} M) of this sample with water as shown in Figure 4a. While mass spectra of separated proteins could still be obtained, clearly the zone identification of an unknown component at these concentrations would be difficult. The analysis time was significantly longer with, for

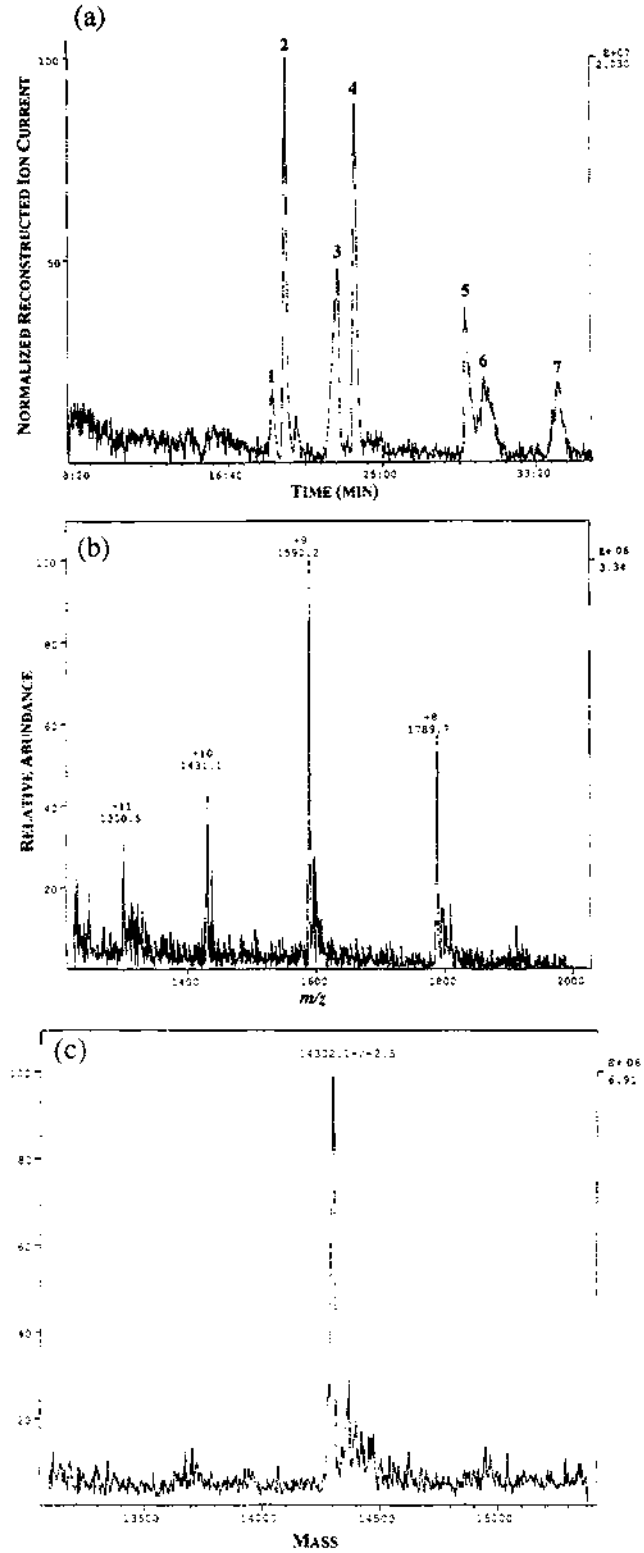

Figure 3. (a) CZE/MS full scan (m/z 600–2000) reconstructed ion electropherogram of a 150-nL injection of 12 μM each of lysozyme (1), cytochrome *c* (2), ribonuclease A (3), myoglobin (4), β-lactoglobulin A (5), β-lactoglobulin B (6), and carbonic anhydrase (7) dissolved in water. BGE: 0.02M 6-aminohexanoic acid + acetic acid, to pH 4.4; (b) spectrum of lysozyme taken from averaging the scans under the peak; (c) deconvoluted spectrum of lysozyme. M_r for lysozyme is 14 308.[34] CE conditions as in Figure 2.

example, cytochrome c eluting 12 min later in Figure 3a and 23 min later in Figure 4a than in Figure 2 where the sample was dissolved in the BGE. The increased migration time is due to the voltage drop across the initial sample zone caused by the low electrical conductivity of the zone compared with the BGE. The electric field strength is not uniform through-

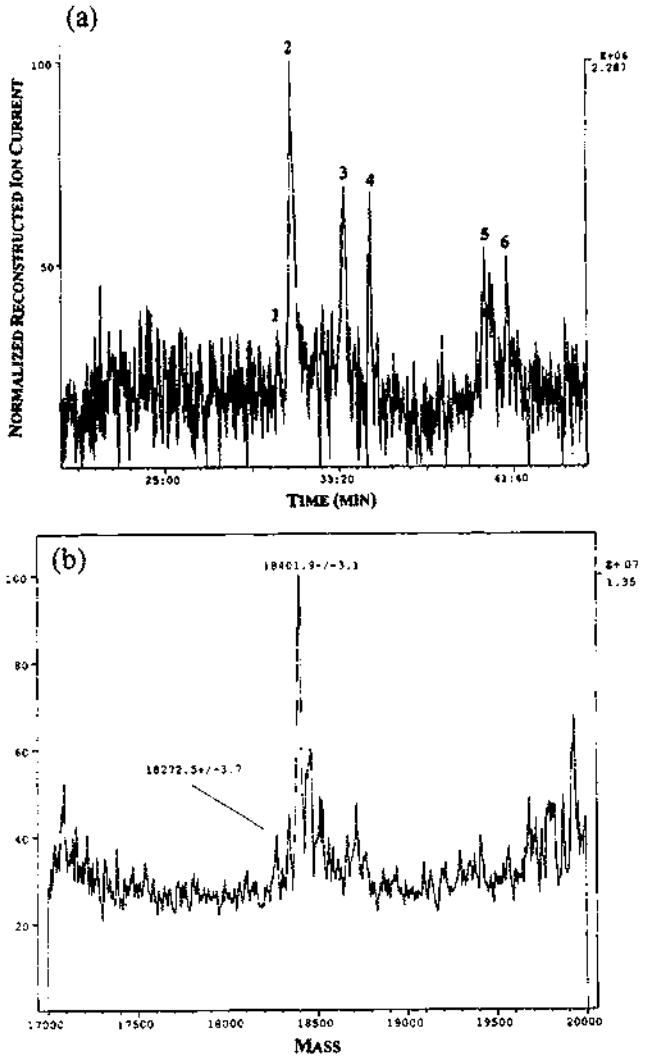

Figure 4. (a) CZE/MS full scan (m/z 600–2000) reconstructed ion electropherogram of a 150-nL injection of 1.2 μM each of lysozyme (1), cytochrome c (2), ribonuclease A (3), myoglobin (4), β-lactoglobulin A (5), β-lactoglobulin B (6), and carbonic anhydrase (not detected) dissolved in water. BGE: 0.02 M 6-aminohexanoic acid + acetic acid, pH 4.4; (b) deconvoluted spectrum of β-lactoglobulin B. M_r for β-lactoglobulin B is 18 277.[34] Note the complex formation at M_r = 18 401.9. The molecular weight of 6-aminohexanoic acid is 130. CE conditions as in Figure 2.

out the capillary but is lower in the BGE than in the original sample zone, resulting in slower migration of the sample ions. This could be overcome by working with constant current; however, excessive sample Joule heating would result. Thus, when a sample is dissolved in water or dilute electrolyte, sample deterioration may occur due to low ionic strength and increased Joule heat generation across the sample zone.[28]

The deconvolution of the spectra of both the β-lactoglobulin A and β-lactoglobulin B in Figures 3a and 4a led to the interesting observation of two values of mass, one at the correct mass for the protein and one at 130 mass units greater. The charge states corresponding to these peaks are identical, indicating that some form of complexation with the protein was occurring. Since 6-aminohexanoic acid (BGE constituent) has a molecular weight of 130, and the standard deviation of mass for both the complexed and uncomplexed protein was <3.0, the resulting increase of 130 in mass suggests the protein is complexing with the BGE. Figure 4b shows the deconvoluted spectrum of β-lactoglobulin B. At low concentrations the β-lactoglobulin/BGE complex was significantly more abundant than the uncomplexed species. This result indicates that one needs to be cautious in interpreting data obtained in CZE with buffered electrolytes. As has been reported,[29] it may be possible to eliminate complex formation by increasing the nozzle to skimmer voltage to break up a complex in the source; however, this was not pursued here since the intent of this study was not to explore complexation; moreover, in this process, the sample may be fragmented leading potentially to interpretation errors.

As noted, one drawback of CZE is the limited volume of the sample that can be injected into the column without deterioration of the separation. In this study, the maximum volume that could be injected when the sample was dissolved in the BGE was 50 nL, and when the sample was dissolved in water the maximum injection volume was 150 nL. Although the injection volume could in principle be further increased with water as the sample matrix, the injection volume was still limited by the fact that the analysis time would increase significantly with the water matrix. The analysis time could be decreased by using uncoated capillaries with attendant electroosmotic flow, but in this case some proteins could adsorb to the capillary wall. This would be especially true for the basic proteins in this study.

Capillary isotachophoresis was next tested in an attempt to increase further the volume injected. Figure 5a shows the CITP/MS reconstructed ion electropherogram of a sample containing lysozyme (1), ribonuclease A (2), and β-lactoglobulin A (3) with 6-aminohexanoic acid added as a low molecular weight spacer to separate ribonuclease A from β-lactoglobulin A. In this case, large amounts of sample (250 nL, 50 pmol) were injected. A region of increased signal is visible prior to the elution of the β-lactoglobulin A zone. The increased signal is likely due to detection of a mixed zone of 6-aminohexanoic acid and β-lactoglobulin A. The deconvoluted spectrum of this region is shown in Figure 5b. As in the CZE/MS electropherogram, the analysis of this region suggested that a complex was formed between the spacer and β-lactoglobulin A.

The analytes in CITP elute in a stack of narrow bands. In the analysis of samples of trace concentration, these bands could become extremely narrow such that the mass spectrometer could not scan over the necessarily wide m/z range at the speed required to prevent overlap of the eluting peaks. A typical example of the narrow zones possible in CITP with UV detection is in Figure 6, which shows the separation of the same proteins as in Figure 5a, but the amount injected was 5 times less. Narrow ITP zones could easily be detected since the time constant of the UV detector was 0.1 s. This sample amount injected (5 pmol of each) could not be reliably detected by the mass spectrometer under the conditions specified because the time-based length of all three protein zones was only 12 s and the shortest zone was only 2 s wide. With the requirement of at least 1 s/scan for full scan analysis, reliable mass spectra of individual trace components could not be obtained. In principle, the rate of elution of ITP zones could be slowed by decreasing the electric field so that wider bands in terms of time could allow MS scanning. However, lower fields would lead to poorer resolution and longer migration times in CITP. Furthermore, separation at high fields, with a subsequent reduction in the field strength after UV detection, would be difficult to precisely control. Finally, optimization of protein separations by CITP is not straightforward.

An advantage of CITP, however, is the possibility of injecting and focusing relatively large sample volumes. On

(28) Vinther, A.; Soeberg, L.; Nielsen, J.; Pedersen, J.; Biederman, K. *Anal. Chem.* **1992**, *64*, 1878–191.

(29) Loo, J. A.; Udseth, H. R.; Smith, R. D. *Rapid Commun. Mass Spectrom.* **1988**, *2*, 207–210.

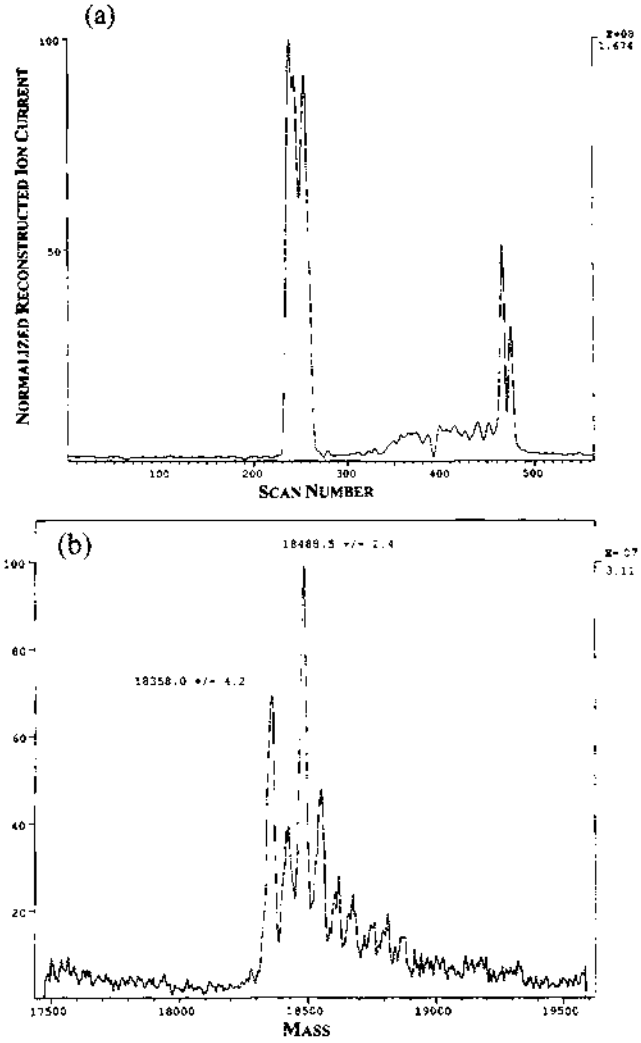

Figure 5. (a) CITP/MS full scan (m/z 600–2000) reconstructed ion electropherogram of a 250-nL injection of 200 μM of lysozyme, ribonuclease A, β-lactoglobulin A with 6-aminohexanoic acid added as a spacer. Leading electrolyte: 0.01 M ammonium acetate + acetic acid to pH 4.4. Terminating electrolyte: 0.001 M acetic acid. The β-lactoglobulin A peak is split in two due to instability in the electrospray process. (b) Deconvoluted spectrum of β-lactoglobulin A complexed with 6-aminohexanoic acid. CE conditions: constant current 6 μA, voltage increased from 7 to 17 kV. M_r = 18 362 for β-lactoglobulin A.

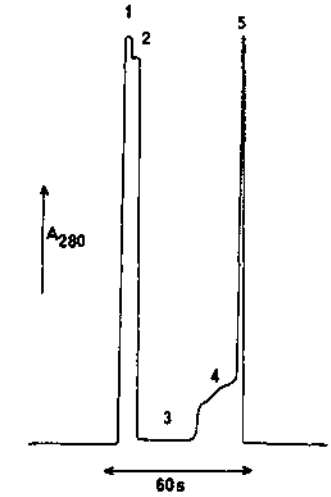

Figure 6. CITP analysis with UV detection of 25 nL of 200 μM lysozyme (1), ribonuclease A (2), 6-aminohexanoic acid (3), mixed zone of (3) and (5), and β-lactoglobulin A (5). A_{280} = UV absorbance at 280 nm. Leading electrolyte: 0.01 M ammonium acetate + acetic acid, pH 4.4. Terminating electrolyte: 0.001 M acetic acid, pH 4.4. CE conditions: constant current 6 μA, voltage increased from 7 to 17 kV.

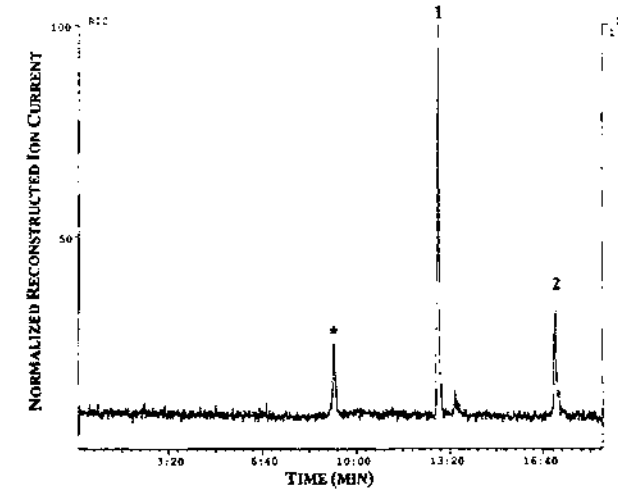

Figure 7. Transient CITP/MS full scan (m/z 600–2000) reconstructed ion electropherogram of 450 nM cytochrome c (1) and 270 nM myoglobin (2) in 0.005 M ammonium acetate buffer. The peak marked (•) is from the rear boundary of the ammonium zone. Injection volume = 750 nL (injected quantity of 337 and 202 fmol, respectively). BGE: 0.02 M 6-aminohexanoic acid + acetic acid, pH 4.4. CE conditions as in Figure 2.

the other hand, CZE offers the advantage of better peak separation, generally with peak widths of sufficient time for full scan MS of proteins. We, therefore, combined the advantages of CITP and CZE by employing transient CITP prior to CZE analysis.[22] Using a simple mixture of two standard proteins, the utility of transient CITP was tested. The sample was diluted in 5×10^{-3} M ammonium acetate with ammonium serving as the leading ion with the 6-aminohexanoate cation of the BGE acting as the terminating ion during the transient CITP migration.

Initially, the column was filled with the BGE, followed by siphon injection of 750 nL of the sample dissolved in ammonium acetate buffer. The end of the column was then returned to the BGE reservoir. The ammonium ions (which have high mobility) moved ahead of the sample ions when the field was applied. At this point the sample ions stacked behind the ammonium zone in a narrow band and began moving at constant velocity (as in CITP). The ammonium ions, however, continued to move through the slower BGE. Consequently, the concentration of ammonium ions in the ammonium zone rapidly decreased below the concentration necessary for ITP migration.[30] At this point, the zones separated as in CZE.

Using transient CITP, we were able to inject and detect sample concentrations that were significantly lower in magnitude than in CZE without preconcentration. Figure 7 shows the full scan reconstructed ion electropherogram of the protein sample containing cytochrome c (1) and myoglobin (2) diluted in 5×10^{-3} M ammonium acetate to a concentration of 10^{-7} M, which is roughly 100 times lower than in Figure 2 (sample dissolved in BGE) and is 30 times lower than Figure 3a (sample dissolved in water). Furthermore, under this condition, the peaks in Figure 7 are narrower and more intense than those in Figures 2 and 3a, resulting in higher signals; however, the comparison of separation efficiency is not possible since due to the focusing step, a shorter migration length is available for the consecutive CZE separation.

Next, transient CITP/MS of the protein mixture containing lysozyme (1), cytochrome c (2), ribonuclease A (3), myoglobin

(30) Gebauer, P.; Bocek, P.; Thormann, W. *J. Chromatogr.* **1992**, *608*, 47–57.

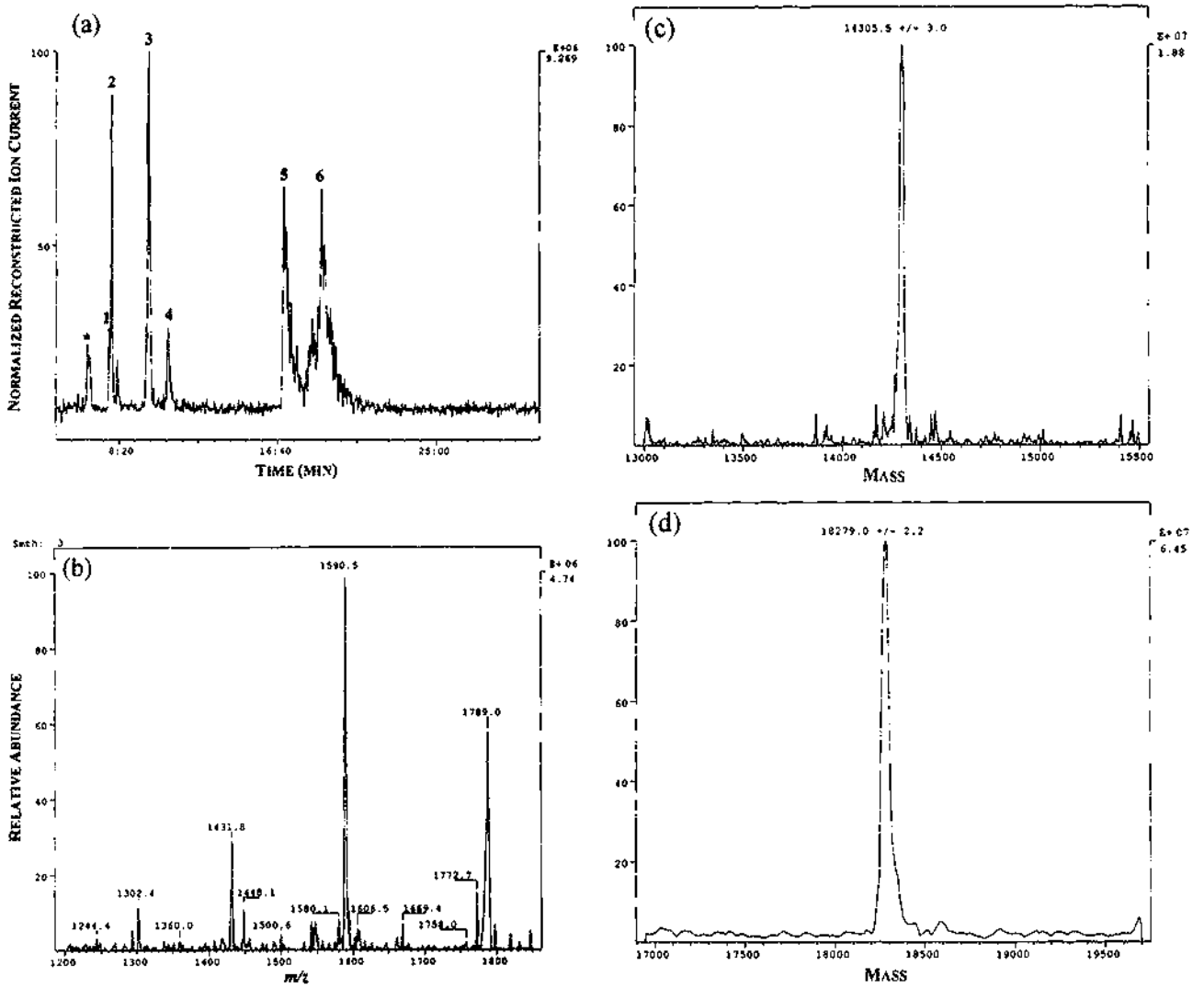

Figure 8. (a) Transient CITP/MS full scan (m/z 600–1850) reconstructed ion electropherogram of ~500 nM each of lysozyme (1), cytochrome c (2), ribonuclease A (3), myoglobin (4), β-lactoglobulin A (5), β-lactoglobulin B (6), and carbonic anhydrase (not detected) in 0.005 M ammonium acetate buffer. The peak marked (*) is from the rear boundary of the ammonium zone. Injection volume = 750 nL. BGE: 0.02 M 6-aminohexanoic acid + acetic acid, pH 4.5. CE conditions as in Figure 2. (b) The spectrum of lysozyme obtained by averaging the scans under the peak in the electropherogram. (c) The deconvoluted spectrum of lysozyme. (d) The deconvoluted spectrum of β-lactoglobulin B.

(4), β-lactoglobulin A (5), β-lactoglobulin B (6), and carbonic anhydrase (not labeled) was performed. The sample concentration was ~5×10^{-7} M for each protein. Figure 8a shows the full scan reconstructed ion electropherogram of the analysis of this mixture. When compared to Figure 3a, the increased sensitivity is apparent from the fact that the total ion currents for the peaks of greatest intensity are equivalent while the sample concentration is 24 times less in Figure 8a. In addition, the spectra, obtained from averaging the scans under the peaks shown in Figure 8b–d, indicate increased signal to noise ratios over what was obtained in Figures 3 and 4, and the biomasses calculated for these spectra are more accurate as a result of this greater signal to noise ratio.

Further examination of Figure 8a shows that there is an additional peak (*) eluting ahead of lysozyme (also in Figure 7). This peak is caused by the rear boundary of the ammonium zone, resulting in transient increase in the ion current of the electrospray at that point. In addition, in Figure 8d, the intensity of the complex of 6-aminohexanoic acid with β-lactoglobulin A is much lower when compared to Figure 4b since the protein concentration is significantly higher, due to sample focusing, in Figure 8d. At the same time, the concentration of 6-aminohexanoic acid in the protein zone is significantly lower due to the electroneutrality principle. β-lactoglobulins A and B in Figure 8 as in Figures 3a and 4a reveal broad bands probably due to the known multimer formation of these proteins in the pH range of 4–5.[31] Finally, carbonic anhydrase is missing in Figure 8 as a result of the fact that this protein does not preconcentrate under the specific conditions, because its effective mobility at this pH (7×10^{-5} cm^2/V·s as calculated from Figure 3a) is less than that of the BGE (15×10^{-5} cm^2/V·s). For preconcentrating proteins of low mobilities, the BGE would need to contain a co-ion with an effective electrophoretic mobility less than 6-aminohexanoic acid such as β-alanine (5×10^{-5} cm^2/V·s at pH 4.4). The selection of BGE co-ion can be made by comparing the electrophoretic mobilities of the sample components obtained by preliminary CZE experiments with those found in published tables.[32]

CONCLUSIONS

As found with UV detection,[22,33] on-column transient isotachophoretic sample preconcentration can be successfully used for improvement of the concentration detection limits

(31) Grinberg, N.; Blanco, R.; Yarmush, D. M.; Karger, B. L. *Anal. Chem.* **1989**, *61*, 514–520.
(32) Pospichal, J.; Gebauer, P.; Bocek, P. *Chem. Rev.* **1989**, *89*, 419–430.
(33) Foret, F.; Szoko, E.; Karger, B. L. *Electrophoresis*, submitted.
(34) Smith, R. D.; Loo, J. A.; Edmonds, C. G.; Barinaga, C. J.; Udseth, H. R *Anal. Chem.* **1990**, *62*, 882–899.

in CZE/ESI/MS. This enhancement is a result of the preconcentration of a large sample volume injected into the capillary. In the most simple case described here, two conditions must be fulfilled. First, the injected sample must be supplemented by co-ions with high electrophoretic mobility that can act as leading ions for the ITP migration in the early stages of the separation. In the case of cationic separation demonstrated here, ammonium can be selected as a universal leading ion since its electrophoretic mobility is among the highest of all cations. Furthermore, ammonium ion, unlike other highly mobile inorganic ions such as sodium or potassium, does not interfere with the electrospray process. Depending on the original salt concentration of the sample, the addition of an ammonium salt in a 0.001–0.01 M concentration will be generally satisfactory in practice. If necessary, a desalting pretreatment step can be performed prior to CE analysis. The second condition requires that the background electrolyte used for CZE separation contain a co-ion with low electrophoretic mobility that can serve as a terminating ion during the transient ITP migration. Suitable substances can be found among organic amines, amino acids, and Good's buffers, and the respective electrophoretic mobilities are listed in tables.[32] When the proper BGE is selected and a well-coated capillary is used to prevent adsorption, transient on-column ITP preconcentration provides reproducible and quantitative results. In a separate study,[33] quantitation of protein samples with concentrations less than 10^{-8} M was achieved using UV detection.

ACKNOWLEDGMENT

The authors thank Beckman Instruments for support of this work. The authors also acknowledge Finnigan MAT Corporation for their instrument support and helpful discussions. Contribution no. 542 from the Barnett Institute, Northeastern University, Boston, MA 02115.

RECEIVED for review August 11, 1992. Accepted December 30, 1992.

Anal. Chem. **1994**, *66*, 4450–4458

Liquid Sheath Effects on the Separation of Proteins in Capillary Electrophoresis/Electrospray Mass Spectrometry

František Foret, Toni J. Thompson, Paul Vouros,* and Barry L. Karger*

Barnett Institute, Northeastern University, Boston, Massachusetts 02115

Petr Gebauer and Petr Boček

Institute of Analytical Chemistry, Brno, Czech Republic

Ionic migration in capillary electrophoresis/electrospray mass spectrometry using a coaxial sheath liquid interface was investigated. Formation of moving ionic boundaries inside the capillary was observed due to migration of liquid sheath counterions into the separation capillary. Either sharp or diffuse ionic boundaries were created, leading to delays or inversions in migration order and, at times, loss of resolution. The conditions of formation and minimization of ionic boundaries have been studied both theoretically and experimentally. It has further been demonstrated that difficult-to-spray electrolytes (such as phosphate-containing buffers) can be used for capillary electrophoresis/mass spectrometry when liquid sheath counterions replace the background electrolyte counterions.

Capillary electrophoresis/mass spectrometry (CE/MS) is an attractive combination of two high-resolution techniques with the potential to solve complex analytical problems. While CE permits fast and efficient separations of a wide variety of charged species,[1-3] MS provides information about the mass and, potentially, the structure of the separated compounds.[4,5] A key point in this combination is the specific interface design which serves for the transport, vaporization, and ionization of the species separated by the capillary column in the vacuum region of the mass spectrometer.[6-8] Although a variety of ionization/vaporization procedures can be used,[9,10] the electrospray interface with a coaxial liquid sheath arrangement[11-14] is very often selected. In this arrangement, the end of the separation capillary is provided with a makeup flow of an electrolyte (sheath liquid) which provides electrical contact with the capillary for electrophoresis and simultaneously aids in the optimization of the electrospray conditions. For example, when the mass spectrometric determination of positively charged ions is desired, a typical sheath liquid will consist of a dilute solution of a volatile organic acid (~1% formic or acetic) in a mixed water–organic solvent. Here, the volatile acid maintains a low pH, enhancing formation of positively charged ions. In addition, the organic modifier (e.g., methanol) decreases the surface tension of the sheath liquid while increasing its volatility and thus enhancing the stability of the electrospray.

In CE, neutral, hydrophilic surface-coated capillaries with minimized electroosmotic flow are frequently used for efficient separation of proteins. For example, attachment of a layer of linear polyacrylamide is recommended for suppression of electroosmotic flow and minimization of adsorption of protein zones on the capillary surface.[15-17] In this case, the bulk flow inside the capillary is negligible, and the only transport mechanism is that due to the electromigration of ionic constituents. Electrically neutral (zwitterionic or uncharged) components will not move in a coated capillary without electroosmotic flow. This lack of migration enables the use of high concentrations of background electrolyte (BGE) additives without interfering with the electrospray mass spectrometric signal, since these constituents will not exit the separation capillary.[18]

In all capillaries, but especially in those with limited or zero electroosmotic flow, the electric charge transported by the ions exiting one end of the separation capillary must be substituted by a charge carried by ions of the same sign entering the opposite end of the capillary in order to maintain electroneutrality. Thus,

(1) Li, S. F. Y. *Capillary Electrophoresis*; Journal of Chromatography Library 52; Elsevier: New York, 1992.
(2) *Capillary Electrophoresis Technology*; Guzman, N. A., Ed.; Marcel Dekker: New York, 1993.
(3) Foret, F.; Křivánková, L.; Boček, P. *Capillary Zone Electrophoresis*; Electrophoresis Library: VCH Verlagsgesellschaft: Weinheim, 1993.
(4) Niessen, W. M. A.; van der Greef, J. *Liquid Chromatography–Mass Spectrometry*; Marcel Dekker: New York, 1992.
(5) Niessen, W. M. A.; Tjaden, U. R.; van der Greef, J. *J. Chromatogr.* **1993**, *636*, 3–19.
(6) Olivares, J. A.; Nguyen, N. T.; Yonker, C. R.; Smith, R. D. *Anal. Chem.* **1987**, *59*, 1230–1232.
(7) Smith, R. D.; Udseth, H. R.; Barinaga, C. J.; Edmonds, C. G. *J. Chromatogr.* **1991**, *559*, 197–208.
(8) Whitehouse, C. M.; Dreyer, R. N.; Yamashita, M.; Fenn, J. B. *Anal. Chem.* **1985**, *57*, 675–682.
(9) Caprioli, R. M.; Moore, W. T.; Martin, M.; DaGue, B. B.; Wilson, K.; Moring, S. *J. Chromatogr.* **1989**, *480*, 247–257.
(10) Moseley, M. A.; Deterding, L. J.; Tomer, K. B.; Jorgenson, J. W. *J. Chromatogr.* **1990**, *516*, 167–173.
(11) Mück, W. M.; Henion, J. D. *J. Chromatogr.* **1989**, *495*, 41–59.
(12) Moseley, M. A.; Jorgenson, J. W.; Shabanowitz, J.; Hunt, D. F.; Tomer, K. B. *J. Am. Soc. Mass Spectrom.* **1992**, *3*, 289–300.
(13) Garcia, F.; Henion, J. *J. Chromatog.* **1992**, *606*, 237–247.
(14) Gale, D. C.; Smith, R. D. *Rapid Commun. Mass Spectrom.* **1993**, *7*(11), 1017–1021.
(15) Hjertén, S. *J. Chromatogr.* **1985**, *347*, 191–197.
(16) Cobb, K. A.; Dolník, V.; Novotny, M. *Anal.Chem.* **1990**, *62*, 2478–2483.
(17) Schmalzing, D.; Piggee, C. A.; Foret, F.; Carrilho, E.; Karger, B. L. *J. Chromatogr.* **1993**, *652*, 149–159.
(18) Nashabeh, W.; Greve, K. F.; Kirby, D.; Foret, F.; Karger, B. L.; Reifsnyder, D. H.; Builder, S. E. *Anal. Chem.* **1994**, *66*, 2148–2154.

0003-2700/94/0366-4450$04.50/0

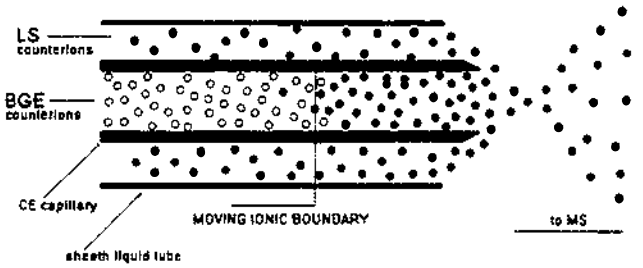

Figure 1. Expanded view of the electrospray tip with an ionic boundary propagating into the CE capillary. The empty and filled circles correspond to the background electrolyte (BGE) and liquid sheath (LS) counterions, respectively.

liquid sheath counterions will migrate through the separation capillary, replacing the original counterions of the electrolyte BGE. This substitution of ions can create ionic boundaries that significantly affect migration time and separation. The purpose of the present study is to investigate the influence of these effects on the analysis of protein samples in CE/MS.

THEORETICAL SECTION

During CE operation, sample ions and co-ions of the BGE exit the capillary at the electrospray interface, and, simultaneously, counterions from the liquid sheath (LS) enter the column and migrate toward the injection end. If the BGE contains different counterions than the LS, a moving ionic boundary will develop inside the capillary. This process is schematically shown in Figure 1, with an expanded view of the separation capillary exiting the liquid sheath tube at the electrospray tip. Here, the counterions of the BGE (○) and the LS (●) are assumed to be different, resulting in propagation of the LS counterions into the separation capillary. As discussed below, depending on the electrophoretic mobilities and the pK_a values of the respective ions, the boundary between the original BGE and the buffer formed by the replacement of the counterions may be either sharp or diffuse. In addition, the pH and conductivity of the new BGE behind the moving ionic boundary may differ significantly from the original BGE.

Since the sample zones migrate against the moving ionic boundary, sample components will experience two different separation environments during the CE analysis. At first, the sample ions migrate in the original BGE within the capillary. Depending on the velocity of the moving boundary and the electrophoretic velocity of individual sample zones, the zones will cross the ionic boundary at different positions inside the capillary. Once this crossing occurs, the sample zones will move in the region where the counterions are those from the LS. Depending on the change of the pH and conductivity in the newly formed BGE relative to the original one, the separation may be significantly altered from that in the original BGE. In the following discussion, it is assumed that any liquid flow inside the capillary (hydrodynamic, electroosmotic) is suppressed. However, the formation of ionic boundaries could also significantly affect the migration of ions in the presence of bulk liquid flow inside the capillary.

Two basic types of ionic boundaries are depicted in Figure 2. If the BGE counterions have a higher effective mobility than those of the LS ($\bar{u}_{BGE} > \bar{u}_{LS}$), a sharp isotachophoretic (ITP) boundary that moves opposite to the separating zones will be formed, Figure

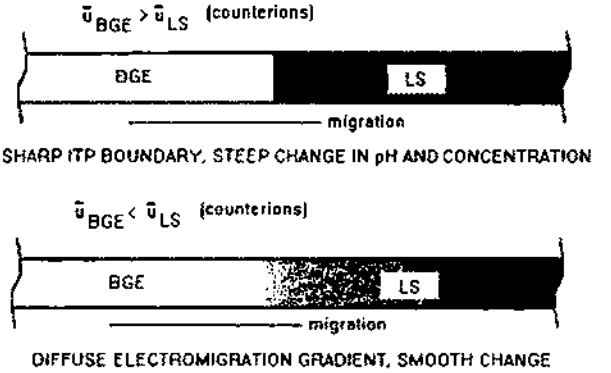

Figure 2. Basic types of the moving ionic boundaries occurring during CE-ESI/MS experiment. $\bar{u}_{BGE}$ and $\bar{u}_{LS}$ are the effective electrophoretic mobilities of the counterions of the background electrolyte and the liquid sheath, respectively. BGE, the original background electrolyte; LS, the new background electrolyte formed by replacement of the BGE counterions by counterions of the liquid sheath. ITP, isotachophoretic.

2, top.[19] This boundary will separate the original BGE from that formed by the LS counterions. The velocity, v, of the boundary, i.e., the velocity of the propagation of the LS counterions into the separation capillary, is given by the product of electric field strength in the BGE (E_{BGE}) and the effective electrophoretic mobility of its counterion, $\bar{u}_{BGE}$, on either side of the boundary:

$$v = \bar{u}_{BGE} E_{BGE} \tag{1}$$

The effective mobility, $\bar{u}_{BGE}$, is defined as the product of the ionic mobility, u_{BGE}, and the degree of ionization, α, of the counterion:[19]

$$\bar{u}_{BGE} = u_{BGE}\alpha \tag{2}$$

The velocity of the ionic boundary can be quite high. For example, for the BGE consisting of 20 mM β-alanine/formic acid at pH 3.4 ($\bar{u}_{form} = 16 \times 10^{-5}$ cm^2/Vs), the speed of penetration of acetate ions from the LS into the capillary will be equal to the velocity of the formate ions in the BGE. Assuming that the electric field strength in the BGE is 300 V/cm, this velocity can be estimated as 0.5 mm/s.

The conductivity of any buffer, κ, is related to the concentration and effective electrophoretic mobility, $\bar{u}_i$, of its constituents by a simple relationship,

$$\kappa = F\sum_i c_i \bar{u}_i \tag{3}$$

where F is the Faraday constant. Since, in ITP, ions with lower effective mobility migrate behind zones of ions of higher mobility, the conductivity of the newly formed BGE will be lower than that of the original BGE (eq 3). The electric field strength will be higher in this lower conductivity region, maintaining self-sharpening of the boundary. It should further be noted that the pH of the newly formed BGE may also be different than that of the original one. For the most part, the pH will be higher when anionic LS counterions migrate into the capillary (CE analysis of

(19) Bocek, P.; Deml, M.; Gebauer, P.; Dolnik, V. *Analytical Isotachophoresis*; VCH Verlagsgesellschaft: Weinheim, 1988.

cationic species) or lower with cationic counterions (CE analysis of anionic species).[19]

If, on the other hand, the effective electrophoretic mobility of the BGE counterions is lower than that of the LS counterions ($u_{BGE} < u_{LS}$), a diffuse ionic boundary will be formed, Figure 2, bottom. In this case, the conductivity of the newly formed BGE will be higher than that of the original one, and there may be a pH change, as well. The velocity of the LS counterions penetrating the separation capillary at the front of the boundary can be calculated from the effective electrophoretic mobility of the LS counterions and the electric field strength in the original BGE. For example, trifluoroacetate ions from the LS will migrate into the separation capillary filled with the 20 mM β-alanine/formic acid BGE at pH 3.4 with a velocity of approximately 1.2 mm/s (for $E = 300$ V/cm and $u_{TFA} = 40 \times 10^{-5}$ cm²/Vs).

Since the ionic boundary moves opposite to the analyte zones, a change in migration of the separated compounds can be expected due to a different pH, ionic strength, conductivity, and type and extent of ionic interactions. Indeed, this process can be used for a programmed change of the selectivity during the separation in a manner similar to gradient elution in HPLC.[20]

It is also worth noting that the formation of a moving ionic boundary enables the use of an initial BGE with nonvolatile and/or difficult-to-spray counterions. As an example, we can consider separation of cationic species in a phosphate-based BGE. When the liquid sheath containing formic acid is used, the formate ions will migrate into the separation capillary and replace phosphate ions which move toward the injection end, away from the electrospray. While the sample may not experience the phosphate buffer for its full travel through the column, a significant fraction of the column could still be traversed in the phosphate buffer.

The physicochemical properties of ionic boundaries in electrophoresis have been well documented in the literature,[21,22] and, in many cases, their exact properties can be analyzed by computer simulation.[23-25] In this case, the solution of the set of partial differential equations accounting for electromigration, diffusion, and chemical equilibria provide pH, concentration, and conductivity profiles along the migration path at given time intervals. Electric current density, electrophoretic mobilities, and pK_a values of all migrating ions serve as the input parameters for such calculations.

In this work we have used computer simulation to estimate the pH and conductivity changes which may develop inside the CE capillary during CE/MS analysis. The calculations were performed using the algorithm described in ref 22. The electrophoretic mobilities, pK_a values, and resulting effective mobilities of the BGE and LS constituents used for the simulations are listed in Table 1. The starting point of the simulation is a capillary filled partially with the BGE and the rest with the LS. After selection of the electric current density (typically 100 A/m²) and the time of migration (typically 10 min), the computer calculates the position, pH, and conductivity profile of the boundary between the BGE and LS inside the capillary.

Table 1. Acidity Constants and Ionic Mobilities of BGE and LS Constituents Used in This Work[33]

	pK_a	u (10^{-5} cm²/Vs)
acetic acid	4.8	42
formic acid	3.8	53
trifluoroacetic acid	<1	~40
hydrochloric acid	<0	79
phosphoric acid	2.1, 7.2, 12.3	34, 58, 72
β-alanine	3.5	37.5
ε-aminocaproic acid	4.4	30.0

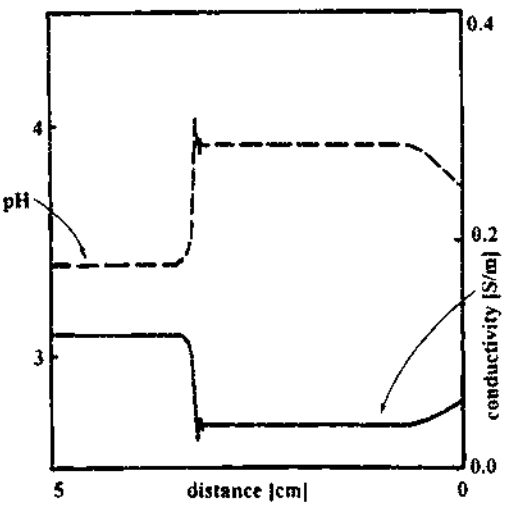

Figure 3. Computer simulation showing the pH and conductivity profiles of the ionic boundary after it had migrated 3 cm into the separation capillary during electrophoresis in 20 mM β-alanine/formic acid, pH 3.4, as BGE and 1% acetic acid as LS. In this case, $u_{BGE} > u_{LS}$. Conductivity is in siemens/meter.

An example of a calculated pH and conductivity profile that may develop inside the separation capillary with 20 mM β-alanine/formic acid BGE at pH 3.4 and a LS containing 1% acetic acid is shown in Figure 3. During the analysis, the acetate counterions from the liquid sheath migrate into the separation capillary and replace formate ions in the BGE. Since the effective electrophoretic mobility of acetate is lower than that of formate at pH 3.4 (see Table 1), the conductivity behind the moving boundary will also be lower (~70% lower), resulting in a higher electric field strength in the newly formed acetate zone. The moving boundary will have isotachophoretic properties with a self-sharpening effect. Thus, if the acetate ions penetrate into the formate BGE, the lower electric field strength at this position will slow down the migration of these acetate ions. On the other hand, formate ions penetrating into the acetate BGE behind the boundary will be accelerated by the higher electric field strength and will return to their side of the boundary. The simulation also shows that the pH in the acetate zone behind the boundary will be ~0.5 unit higher than that in the original BGE.

As already mentioned, the replacement of the BGE counterions by those of the LS permits the use of an initial buffer which might normally interfere with the electrospray process. Figure 4A shows the conductivity and pH profile which will develop inside the separation capillary during the analysis with 20 mM ε-aminocaproic acid/phosphoric acid, pH 4.4, as BGE and 20 mM acetic acid

(20) Boček, P.; Gebauer, P. In *Capillary Electrophoresis Technology*; Guzman, N. A., Ed.; Marcel Dekker: New York, 1993; pp 261–309.
(21) Mikkers, F. E. P.; Everaerts, F. M.; Verheggen, T. P. E. M. *J. Chromatogr.* **1979**, *169*, 1–10.
(22) Mosher, R. A.; Saville, D. A.; Thormann, W. *The Dynamics of Electrophoresis*; VCH Verlagsgesellschaft: New York, 1992.
(23) Bier, M.; Palusinsky, O. A.; Mosher, R. A.; Saville, D. A. *Science* **1983**, *219*, 1281–1287.
(24) Gaš, B.; Vacík, J.; Zelenský, I. *J. Chromatogr.* **1991**, *545*, 225–237.
(25) Ermakov, S. V.; Mazhorova, O. S.; Zhukov, M. Y. *Electrophoresis* **1992**, *13*, 838–848.

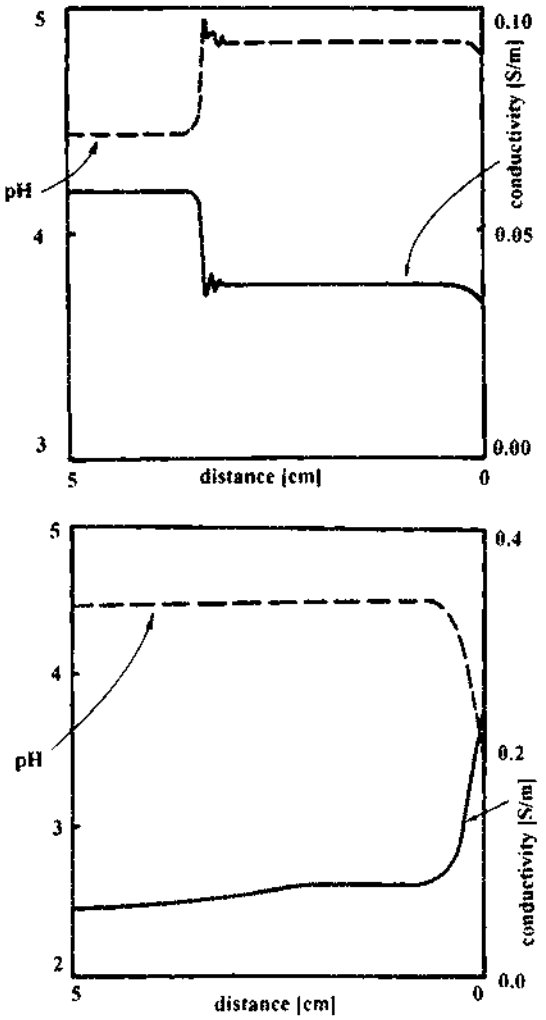

Figure 4. Computer simulation of the pH and conductivity profiles of the ionic boundary formed during electrophoresis in 20 mM ϵ-aminocaproic acid/phosphoric acid, pH 4.4, as BGE. Conductivity is in siemens/meter. (A, top) 1% acetic acid as LS. In this case, $\mathcal{D}_{BGE} > \mathcal{D}_{LS}$. (B, bottom) 1% formic acid as LS. In this case, $\mathcal{D}_{BGE} < \mathcal{D}_{LS}$.

as LS. During the analysis, the phosphate anions will move toward the anode (away from the sheath electrode), and, as in the previous case, a sharp ITP boundary will develop with a steep change in pH (~0.4 unit) and conductivity (40%).

It is clear that the above sharp changes in pH and conductivity can significantly affect separation (positively or negatively). The potentially adverse effects of ionic boundaries can be minimized by using the same counterion in both the BGE and LS. For example, an acetic acid-containing LS will be suitable for an acetate-containing BGE. If, for some reason, the LS cannot contain a common counterion with the BGE, the effects of formation of the ionic boundary can be minimized by selection of the liquid sheath counterion with an electrophoretic mobility and pK_a similar to those of the BGE counterion. Many such examples can be found in the literature.[33] As an illustration, the use of a phosphate/ϵ-aminocaproic acid BGE at pH 4.4 would lead to the formation of an ionic boundary with an acetate-containing LS; however, changes in pH and conductivity can be minimized by substituting formic acid for acetic acid in the LS. This situation is shown in Figure 4B, where the LS containing 1% formic acid was used for the computer simulation. The effective mobility of formic acid at this pH (~42×10^{-5} cm^2/Vs, as calculated according to eq 2 with data in Table 1) is close to the effective mobility of the phosphate in the BGE (34×10^{-5} cm^2/Vs). The resulting ionic boundary is diffuse, and the change of conductivity is small. The change in pH is also small since both formic acid and ϵ-aminocaproic acid have pK_a values close to the pH of the BGE, resulting in good buffering capacity.

EXPERIMENTAL SECTION

Capillary Electrophoresis. The capillary electrophoresis apparatus was constructed in-house using a CZE 1000R (Spellman High Voltage, Plainview, NY) high-voltage power supply operated in the constant voltage mode. Fused silica capillaries (Polymicro Technologies, Phoenix, AZ), 75 μm i.d., 360 μm o.d., were coated with linear polyacrylamide[17] to suppress electroosmosis and protein adsorption. The capillary length was 36 cm (27 cm to detector) for experiments with UV detection or 60 cm for experiments with ESI/MS detection. On-column UV detection was performed with a Spectra 100 (Spectra Physics, Fremont, CA) detector operating at 214 nm. The migration order of the protein zones was confirmed by spiking the sample with individual proteins.

Electrospray Mass Spectrometry. A Finnigan MAT TSQ700 (Finnigan MAT, San Jose, CA) triple quadrupole mass spectrometer was operated in the positive ion mode. The third quadrupole was scanned from m/z 600 to 2000 at 2 s/scan for all analyses, while the first and second quadrupoles were operated in the radio frequency only mode. The electron multiplier was set at 1.8 kV, with the conversion dynode at −15 kV. The mass spectrometer was equipped with a coaxial liquid sheath electrospray interface (Analytica of Branford, Branford, CT), modified in our laboratory for use with capillary electrophoresis.[26] The electrospray voltage was −4000 V, resulting in an electrospray current of ~200 nA. The sheath liquid (50% methanol/water, v/v) was supplied at a flow rate of 4 μL/min, and the sheath liquid modifiers were acetic, formic, and trifluoroacetic acid. The electrospray sheath gas (O_2) was supplied at 200 mL/min and the drying gas (N_2), preheated to 170 °C, at 6 L/min. Isotachophoretic migration of methylene blue was used to determine the anode reservoir height necessary to eliminate bulk liquid flow inside the separation capillary.[26] Samples were injected hydrodynamically, approximately 4 nL with UV detection and approximately 40 nL with ESI/MS detection.

Samples and Electrolytes. Standard proteins (lysozyme, cytochrome c, aprotinin, ribonuclease A, myoglobin, α-chymotrypsinogen A, β-lactoglobulin A and B, and carbonic anhydrase) were purchased from Sigma (St. Louis, MO) and used without further purification. Samples of 16−50 μM were made up in deionized water. CZE background electrolytes consisted of 20 mM ϵ-aminocaproic acid or β-alanine titrated to the desired pH with formic, acetic, or phosphoric acid. All BGE substances were also purchased from Sigma.

RESULTS AND DISCUSSION

During CE/MS studies on proteins, a substantial difference in the electrophoretic mobilities and separations obtained with standard UV and ESI/MS detection was frequently observed. This can be illustrated in a comparison of the UV separation of a model protein mixture in Figure 5A with that of ESI/MS with a liquid sheath of 1% acetic acid in 50% (v/v) methanol/water, shown in Figure 7A. Note in particular the good separation of β-lactoglob-

(26) Thompson, T. J.; Foret, F.; Vouros, P.; Karger, B. L. *Anal. Chem.* **1993**, *65*, 900−906.

ulin B (peak 6) and α-chymotrypsinogen (peak 9) with UV detection and the overlap of the bands with ESI/MS. Furthermore, the electrophoretic mobilities of all proteins are substantially lower in ESI/MS than with UV. (This can be easily seen in a comparison of the migration times for the two detection systems after correcting for the 2.2 times longer column length in ESI/MS.) As noted above, these differences for the two detector systems were expected to be due to the formation of ionic boundaries arising from counterions in the LS.

We decided to explore these effects in detail by examining on-column UV detection changes in separation that could occur using an experimental design in which the sheath liquid behavior could be simulated. Here, the cathodic electrode reservoir (at the detection end of the capillary) was filled with the various sheath liquids used for the CE/MS experiments. We could then easily examine the changes in separation as a function of sheath liquid.

A. Liquid Sheath with UV Detection. Figure 5A shows the standard separation of the protein mixture in which both electrode reservoirs contained the BGE: 20 mM β-alanine + formic acid, pH 3.4. Figure 5B presents the separation when 1% acetic acid solution in 50% methanol/water (v/v) was used in the cathodic electrode reservoir. It can be seen in Figure 5B that the migration time is ~30% longer and that separation has changed, in comparison to Figure 5A. Among the variations in selectivities, there is a shift in migration order of carbonic anhydrase (peak 8), which in Figure 5B coelutes with β-lactoglobulin B (peak 6), whereas in Figure 5A the protein coelutes with β-lactoglobulin A (peak 7). During electrophoretic migration in the experiment of Figure 5B, acetate anions from the cathode reservoir moved into the CE capillary and displaced formate anions. Since at the running buffer pH, acetate had a lower effective electrophoretic mobility than the BGE formate counterion (Table 1), a sharp ITP boundary developed during the separation, which could be detected as a sharp decrease of the background signal as the boundary traveled across the detector window. The average velocity of this boundary, as estimated from the time to travel the migration distance to the detection window, was 0.7 mm/s. From this velocity and the velocities of the protein zones in the initial BGE, it can be estimated that most of the protein bands met the boundary approximately at the midpoint of the capillary, beyond which they migrated at a higher pH. The experiment was performed at constant voltage (15 kV), and the observed decrease of the current during the separation (from 18 to 10 μA) corresponded to a decreased conductivity of the newly formed BGE behind the boundary, as shown in Figure 3. Thus, the electric field strength, as well as the pH, in the newly formed BGE propagating into the capillary was higher than that of the original BGE, leading to the change of the resolution and migration time.

Figure 5C displays the UV trace of the separation of the protein mixture when a solution of 20 mM trifluoroacetic (TFA) acid in 50% methanol/water (v/v) was placed in the cathode reservoir to simulate the LS. Trifluoroacetic acid is a relatively strong acid with a higher effective electrophoretic mobility than that of formate present in the BGE at pH 3.4 (see Table 1). Consequently, a diffuse boundary propagated through the capillary, resulting in the increase of conductivity of the background electrolyte. This increase was also indicated by the elevation of the separation current from 18 to 32 μA from the beginning to the end of the run. Since the change of the BGE composition resulted in an

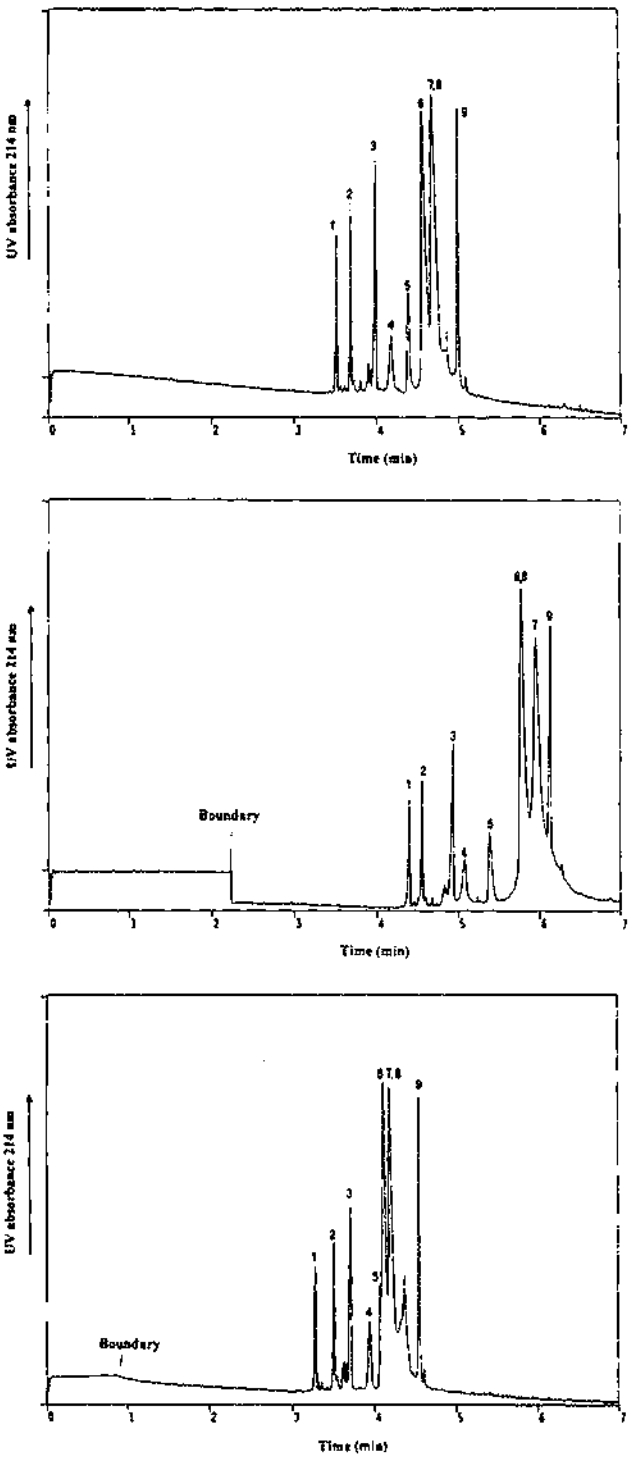

Figure 5. UV detection of ionic boundaries during the separation of the model protein sample. BGE, 20 mM β-alanine + formic acid, pH 3.4. Capillary, 36(27) cm × 75 μm i.d. Constant voltage, 15 kV. (A, top) Reference separation with the BGE in both electrode chambers; stable current, 18 μA. (B, middle) 1% acetic acid in 50% methanol/water in cathodic reservoir; continuously decreasing current, 18–10 μA. (C, bottom) 20 mM trifluoroacetic acid in 50% methanol/water in cathodic reservoir; continuously increasing current, 18–32 μA. The peak identification is 1, cytochrome *c*; 2, lysozyme; 3, aprotinin; 4, myoglobin; 5, RNase A; 6, β-lactoglobulin B; 7,8, β-lactoglobulin A + carbonic anhydrase; 9, α-chymotrypsinogen A; i, impurity from β-lactoglobulin B.

alteration, albeit small, in the background UV signal, the movement of the boundary could be detected as a decrease of the baseline signal. From this boundary, the velocity of the propaga-

tion of TFA anions through the capillary was calculated to be 1.7 mm/s. Since the protein zones moved with the speed of only 0.4–0.8 mm/s (based on the experiment in Figure 5A), the analyte zones migrated substantially in the modified BGE containing TFA as counterion. This effect resulted in a shorter migration time and a shift in selectivities compared to the standard separation shown in Figure 5A.

The previous separations were performed at relatively low pH. Often, however, a BGE with higher pH may be necessary for separation. A good resolution of a sample of basic proteins can be obtained in ϵ-aminocaproic acid/ phosphoric acid buffers at pH 4.2–5.2. Unfortunately, phosphate ions strongly destabilize the electrospray process, resulting in decreases in the electrospray current and excessive noise in the detection ion current. Thus, no useful signal for the determination of the MW could be obtained when the liquid sheath contained phosphoric acid. The use of a standard, acetic acid-based sheath liquid is an option to minimize the presence of phosphate ions in the electrospray; however, the development of a moving ionic boundary can be expected, as seen in the computer simulation of pH and conductivity profile, Figure 4. Phosphate, being a relatively strong acid ($pK_a \sim 2.1$; see Table 1), was replaced during migration by the much weaker acetate ions with a lower effective electrophoretic mobility. Consequently, an ITP boundary developed, resulting in an increase of pH inside the capillary ($\Delta pH \sim 0.4$). Since at pH 4.4 the proteins with low pI (β-lactoglobulins and carbonic anhydrase) are only partially protonated, any change in pH in this region could cause significant change in migration.

The standard separation obtained in 20 mM ϵ-aminocaproic acid/H_3PO_4, pH 4.4, BGE is shown in Figure 6A. The separation of the same protein mixture, with 1% acetic acid solution in 50% methanol/water (v/v) as the LS, is presented in Figure 6B. Here, again, the ionic boundary is detected as a sharp shift in the baseline. The last three zones corresponding to β-lactoglobulin B (peak 6), carbonic anhydrase (peak 8), and β-lactoglobulin A (peak 7) were well separated from the more basic proteins. Interestingly, the migration orders of the myoglobin (peak 4) and α-chymotrypsinogen (peak 9), as well as of carbonic anhydrase (peak 8) and β-lactoglobulin A (peak 7), were reversed compared to the standard separation in Figure 6A. This reversal was likely due to the fact that α-chymotrypsinogen has a higher pI and thus a higher positive charge than myoglobin at this pH. Carbonic anhydrase also has a higher pI than β-lactoglobulin A. The migration pattern of Figure 6A could be restored by changing the composition of the liquid sheath from acetic acid to formic acid, Figure 6C. Since formic acid is much closer to phosphoric acid than acetic acid (with respect to pK_a and effective electrophoretic mobility; see Table 1), the change of the BGE was not substantial. Although there is only a minor effect on separation, the transition of the boundary can still be detected on the UV trace. The result in Figure 6C is in agreement with the computer simulation shown in Figure 4B.

In both initial BGE systems examined, the co-ion was selected so that its pK_a value was close to the pH of the BGE. Since, in such a case, the co-ion had a high buffering capacity, the pH changes due to alterations in composition behind the moving ionic boundary were significantly moderated. If strong co-ions, such as sodium, were used for the preparation of the BGE, the variation in pH behind the ionic boundary could be much higher, resulting in even more dramatic changes in separation. However, the use of stronger and usually highly mobile co-ions is generally not desirable due to the potential for electromigration band broadening[27,28] and excessive Joule heating.

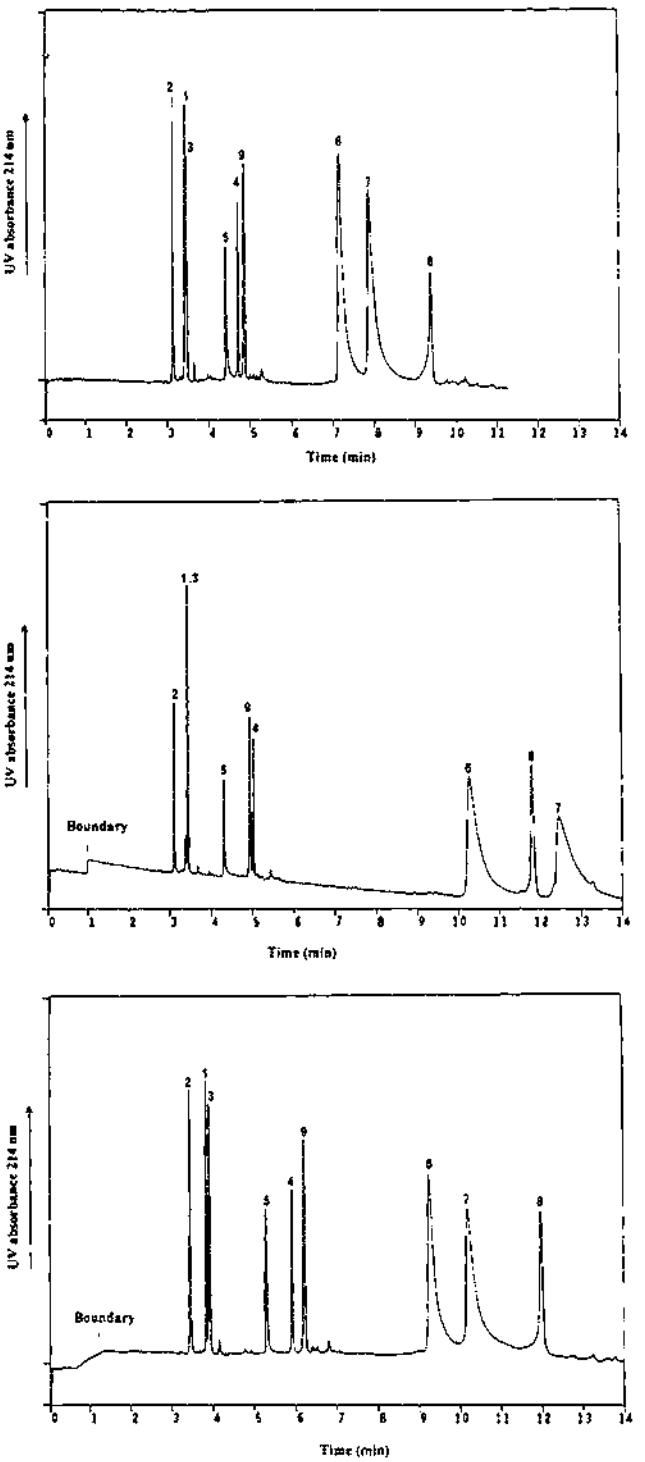

Figure 6. UV detection of ionic boundaries during the separation of the model protein sample. BGE, 20 mM ϵ-aminocaproic acid/ phosphoric acid, pH 4.4. Capillary, 36(27) cm × 75 μm i.d. Constant voltage, 25 kV. (A, top) Reference separation with the BGE in both electrode chambers; stable current, 13 μA. (B, middle) 1% acetic acid in 50% methanol/water in cathodic reservoir; continuously decreasing current, 13–6 μA. (C, bottom) 20 mM formic acid in 50% methanol/ water in cathodic reservoir; continuously increasing current, 12–18 μA. The peak identification is as in Figure 5.

(27) Mikkers, F. E. P.; Everaerts, F. M.; Verheggen, T. P. E. M. *J. Chromatogr.* **1979**, *169*, 11–20.
(28) Šustáček, V.; Foret, F.; Bocek, P. *J. Chromatogr.* **1991**, *545*, 239–248.

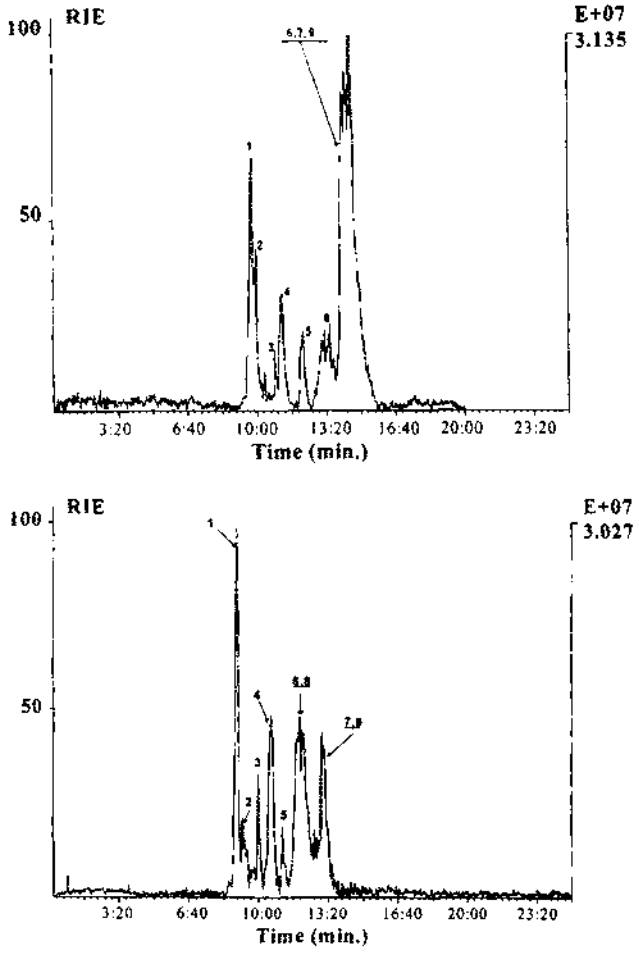

Figure 7. CE-ESI/MS analyses of the model protein mixture in 20 mM β-alanine/formic acid BGE at pH 3.4. Capillary, 60 cm × 75 μm i.d. Constant voltage, 25 kV. (A, top) LS, 1% acetic acid in 50% methanol/water. (B, bottom) LS, 20 mM trifluoroacetic acid in 50% methanol/water. The peak identification is as in Figure 5.

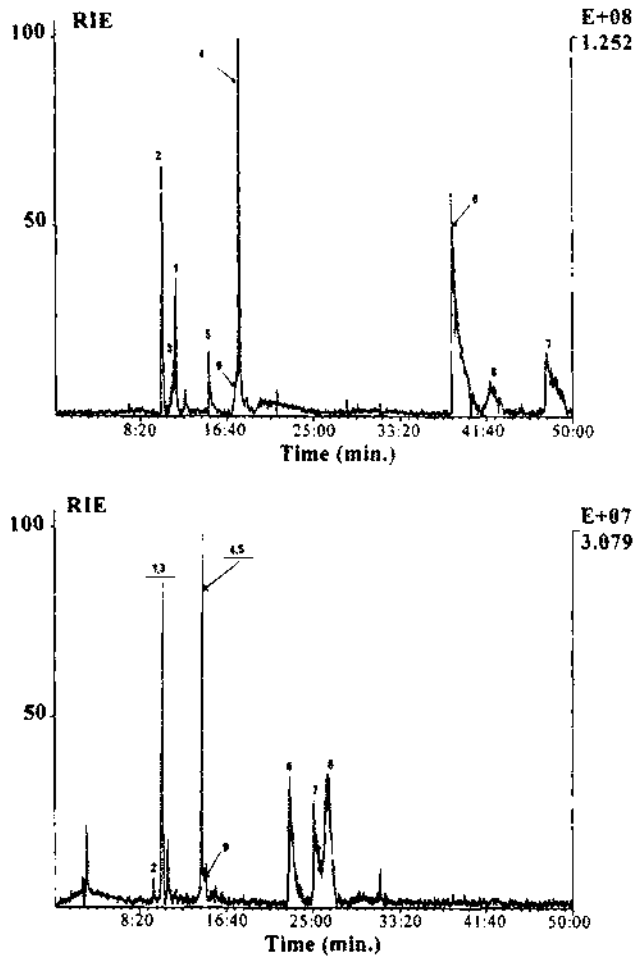

Figure 8. (A, top) CE-ESI/MS analyses of the protein mixture in 20 mM ε-aminocaproic acid/phosphoric acid BGE, using a liquid sheath containing 1% acetic acid. (B) CE-ESI/MS analyses of the protein mixture in 20 mM ε-aminocaproic acid/acetic acid BGE, using a liquid sheath containing 1% acetic acid. Capillary, 60 cm × 75 μm i.d. Constant voltage, 25 kV. The peak identification is as in Figure 5.

B. Liquid Sheath with ESI/MS Detection. Electrospray mass spectrometry is an on-line, but not on-column, detector for CE, and thus the existence of ionic boundaries cannot be directly observed inside the capillary. However, unlike UV detection, each analyte zone, as it exits the separation capillary, is identified according to its molecular mass. Hence, the effects of the ionic boundaries can be easily detected as changes in zone migration.

Figure 7 shows the CE-ESI/MS analyses of the protein mixture in 20 mM β-alanine/formic acid BGE at pH 3.4. In Figure 7A, an acetate liquid sheath was used, resulting in formation of an ITP moving boundary, see Figure 3. When a TFA-containing liquid sheath was employed, Figure 7B, only a minor change in the BGE properties was created, and the whole analysis was faster than in the previous example. The reversal in migration order of carbonic anhydrase (peak 8) and β-lactoglobulin B (peak 6) is especially to be noted.

In Figure 7, the separation efficiency does not approach that obtained with UV detection. Part of the reason for this result may be the influence of the electrospray interface on band broadening. Another potential reason, especially during fast separations, is the slow scanning rate of the quadrupole mass filter. In the present case, the scan rate limited the data collection to less than 1 point/s. This problem, which can reduce resolution in fast separations, can be overcome by using a fast-scanning mass spectrometer such as ion trap[29] or time of flight.[30] In spite of the above, the main source of band broadening in Figure 7 is believed to be the relatively low sensitivity of the mass spectrometric detection, requiring sample overloading in the CE separation. Compared to UV detection, more than an order of magnitude higher sample amounts were injected.

An increase in separation efficiency can be obtained by using a BGE with a co-ion matched to the electrophoretic mobility of the separated proteins. In such a case, relatively high concentrations of migrating zones may be tolerated without excessive band broadening.[27,28] This is illustrated for the BGE containing ε-aminocaproic acid as co-ion at pH 4.4, Figure 8. The effective electrophoretic mobility of ε-aminocaproate cations is ~15 × 10^{-5} cm^2/Vs, which is close to the effective mobilities of most of the sample proteins (e.g., from 25 × 10^{-5} (lysozyme) to 10 × 10^{-5} cm^2/Vs (carbonic anhydrase)). Figure 8A shows the reconstructed ion electropherogram obtained in 20 mM ε-aminocaproic acid/phosphoric acid BGE, using a liquid sheath containing 1% acetic acid. Resolved zones of basic proteins were obtained, with efficiencies exceeding 100 000 theoretical plates. In agreement

(29) Ramsey, R. S.; Goeringer, D. E.; McLuckey, S. A. *Anal. Chem.* **1993**, *65*, 3521–3524.
(30) Murray, K. K.; Russel, D. H. *J. Am. Soc. Mass Spectrom.* **1994**, *5*, 1–9.

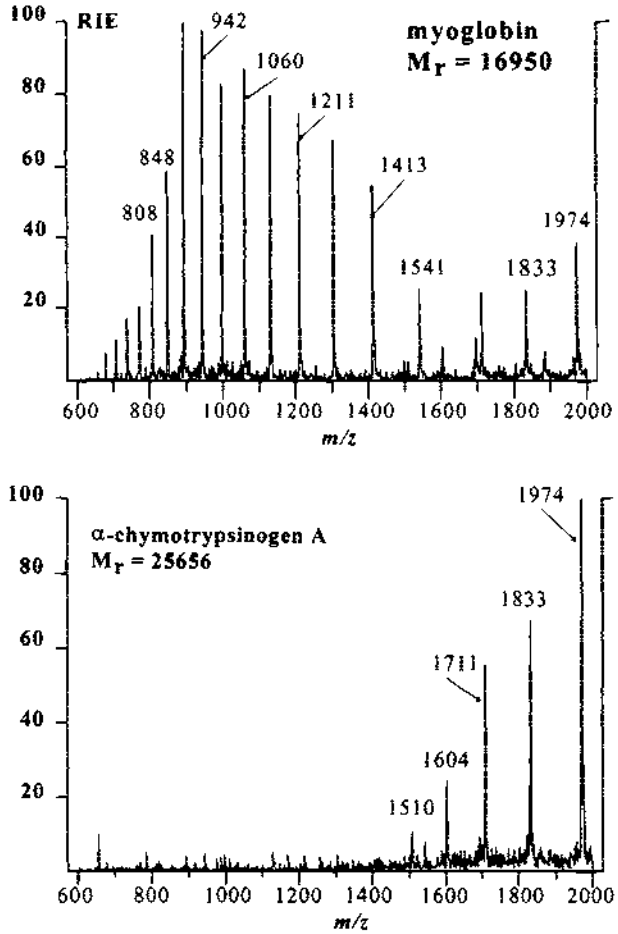

Figure 9. Unsmoothed full scan spectra corresponding to partly overlapping zones of myoglobin and α-chymotrypsinogen A obtained during the separation shown in Figure 8A. The injected amount was 600 fmol and 1.8 pmol for myoglobin and α-chymotrypsinogen A, respectively.

with the experiment shown in Figure 6, the zones of less basic proteins, although baseline resolved, elute late, with reversal of migration order of carbonic anhydrase (peak 8) and β-lactoglobulin A (peak 7). The lower separation efficiency in this case may be due to a combined effect of electromigration dispersion due to sample overloading and formation of molecular multimers of β-lactoglobulin.[31]

The migration order for the UV run, Figure 6A, can be restored when acetate instead of phosphate BGE is used. This is demonstrated in Figure 8B, where no ionic boundary was formed, since both the BGE and the LS contained the same counterion. The migration times of the most basic proteins were identical to those in Figure 8A, with only minor shifts. The main difference between Figure 8A and 8B is the faster migration of the last three zones in Figure 8B, with the loss in resolution. Clearly, the counterion of the BGE is important in affecting separation. It is important to note that the phosphate ions were replaced by acetate ions by electromigration during the analysis, which enabled monitoring of the protein mass spectra with excellent signal to noise ratio. Figure 9 shows unsmoothed full scan spectra corresponding to partly overlapping zones of myoglobin and α-chymotrypsinogen A obtained during separation in the phosphate buffer. Since the protein zones were effectively "cleaned" by electromigration from phosphate adducts, an excellent S/N ratio was obtained, allowing precise determination of molecular weights, see Table 2. The injected amounts were 300 fmol and 1.8 pmol for myoglobin and α-chymotrypsinogen A, respectively. This result can be translated into a full scan detection limit in the low femtomole region which would normally be impossible to obtain in the presence of phosphate ions.

(31) Grinberg, N.; Blanco, R.; Yarmush, D. M.; Karger, B. L. *Anal. Chem.* **1989**, *61*, 514–520.

Table 2. Isoelectric Points and Molecular Weights (Calcd and Expl)[36] of the Sample Proteins

protein	pI	MW calcd	MW expt	RSD (%)[a]
lysozyme	11.0	14 306	14 301.7 ± 2.4	−0.03
cytochrome *c*	10.7	12 230	12 239.6 ± 3.6	+0.078
ribonuclease A	9.5	13 682	13 676.3 ± 1.4	−0.04
α-chymotrypsinogen A	9.1	25 656	25 650.5 ± 2.3	−0.02
aprotinin		6 511	6 507.3 ± 0.7	−0.06
myoglobin	7.0	16 950	16 948.1 ± 1.5	−0.01
carbonic anhydrase	6.6	29 024	29 017.3 ± 3.3	−0.02
β-lactoglobulin A	5.1	18 363	18 359.8 ± 2.2	−0.017
β-lactoglobulin B	5.3	18 277	18 274.7 ± 0.9	−0.01

[a] Relative standard deviation.

CONCLUSION

When a sheath liquid-based interface is used for CE-ESI/MS analysis, the formation of moving ionic boundaries must be considered. The ionic boundary is formed when different BGE and LS counterions are used. Since the ionic boundary usually has optical properties (refractive index, UV absorbance) different from those of the original BGE, it can frequently be detected as a disturbance of the detector baseline. The formation of the boundary is especially important with low electroosmotic flow systems, such as hydrophilic polymer-coated capillaries, gels, or viscous separation matrices. The ionic boundary may significantly influence the CE separation. This influence must be considered when the CE protocol is optimized with a UV detector and then transferred to the CE-ESI/MS. Prediction of the migration pattern may be difficult but can be obtained experimentally. In some cases the formation of the ionic boundary may be beneficial for the separation (see Figure 6). In cases in which the changes in migration are not acceptable, several approaches for the minimization of the adverse effects of the BGE and LS interactions can be considered:

(i) use of a common counterion in both the BGE and the LS; (ii) use of a LS counterion with a pK_a and electrophoretic mobility similar to that in the BGE; (iii) use of a pressure difference between the capillary ends to induce hydrodynamic flow faster than propagation of the ionic boundary through the capillary; (iv) use of a capillary that creates sufficient electroosmotic flow.

It is to be noted that while uncoated and/or surface-charged capillaries with strong electroosmotic flow can reduce effects of ionic boundaries, the velocity of the moving boundary may still be faster than that of the electroosmotic flow. The counterions from the LS may still penetrate into the CE capillary, resulting in formation of the moving ionic boundary. Also, a sheathless electrospray interface might be used with electroosmotic flow.[6,32]

Finally, it should be noted that, besides CE/MS, the formation of ionic boundaries needs to be considered whenever sheath liquid systems are used, such as in coaxial postcolumn reaction[34] or collection devices.[35]

(32) Fang, L.; Zhang, R.; Zare, R. N. 6th International Symposium–HPCE'94, San Diego, CA, January 31–February 3, 1994; poster p-315.
(33) Pospichal, J.; Gebauer, P.; Bocek, P. *Chem. Rev.* **1989**, *89*, 419–430.
(34) Nickerson, B.; Jorgenson, J. W. *J. Chromtogr.* **1989**, *480*, 157–168.
(35) Schwer, C.; Lottspeich, F., submitted to *Anal. Chem.*

ACKNOWLEDGMENT

The authors wish to thank Dr. Wolfgang Thormann for providing the software package used for computer simulations. This work is contribution no. 606 from the Barnett Institute.

Received for review June 24, 1994. Accepted September 22, 1994.[⊗]

[⊗] Abstract published in *Advance ACS Abstracts*, November 1, 1994.

František Foret*
Daniel P. Kirby
Paul Vouros
Barry L. Karger

Barnett Institute and Department of Chemistry, Northeastern University, Boston, MA, USA

Electrospray interface for capillary electrophoresis-mass spectrometry with fiber-optic UV detection close to the electrospray tip

A miniaturized, integrated capillary electrophoresis-ultraviolet detection-electrospray ionization-mass spectrometry (CE-UV-ESI-MS) interface has been constructed and evaluated. The device incorporates a fiber optic detection cell close to the electrospray tip to allow UV monitoring of separated zones just prior to their admittance into the mass spectrometer. This configuration provides precise information about the time when UV-active zones enter the electrospray and allows easy location of analyte mass information in the ion current profile. The miniaturized dimensions of the interface allow the use of short capillaries for fast separations.

1 Introduction

During the development of a CE-ESI-MS method, CE conditions (buffer composition, field strength, sample injection, *etc.*) are usually optimized with off-line optical detection prior to coupling of the separation capillary to the MS. However, since CE-ESI-MS interfaces often do not contain optical detectors, the separation protocol developed off line cannot always be effectively transferred on line with only mass spectrometric detection. However, when a standard optical detector is incorporated into on-line CE-MS, its use requires significantly increased capillary length and results in long analysis times. Moreover, the size of commercial UV detectors does not allow detection of separated species close to the end of the separation capillary [1], and only a crude estimation of the time when separated species enter the mass spectrometer can be obtained. Optical detection close to the capillary tip has several advantages for CE-MS. First, precise knowledge of migration times obtained with optical detection allows easy location of relevant MS information without reference to MS ion current profiles. The presence of a real-time optical signal assists in the transfer and troubleshooting of on-line applications developed off line. Changes that may be required by an on-line procedure, such as increased sample loading or on-column preconcentration, can result in significant alteration of migration patterns [2]. In this case, the presence (or absence) of an optical signal just prior to zone migration into the MS can quickly differentiate between CE- or MS-related problems. Finally, simultaneous optical detection can provide useful information about the migration of sample matrix ions as well as disturbances due to electroosmosis, hydrodynamic flow, and ionic boundaries [3]. In this paper we describe the construction and evaluation of an electrospray interface which uses optical fibers to provide on-line UV detection close to the electrospray tip.

Correspondence: Dr. F. Foret, Barnett Institute and Department of Chemistry, Northeastern University, 360 Huntington Avenue, Boston, MA 02115, USA (Tel: +617-373-3877; Fax: +617-373-2855)

Nonstandard abbreviations: BGE, background electrolyte; **RIE**, reconstructed ion electropherogram

Keywords: Capillary electrophoresis / Mass spectrometry

2 Materials and methods

2.1 Mass spectrometry

A TSQ 700 triple quadrupole MS (Finnigan MAT, San Jose, CA) was used for this study. The ESI flange supplied with the Finnigan API source was removed and replaced with the laboratory-constructed CE-UV-ESI interface.

2.2 ESI interface

The construction of the interface is shown in Fig. 1. It was designed with a liquid sheath [4] and an optional gas sheath [5]. The L-shaped base (A) was made from two 50 × 50 × 6 mm aluminum plates. The bottom plate was mounted on a base (not shown) that attached to the "T" slide normally used to mount the ESI flange onto the TSQ 700. The front plate had a 1 mm hole with a 10 mm piece of stainless steel capillary (B) (HTX-22, Small Parts Inc., Miami Lakes, FL) glued in place as a guide for the CE capillary. Two pieces of HTX-22 stainless steel capillary (C) were glued on the surface of the front plate as guides for the optical fibers (FVP300330360, Polymicro Technologies, Phoenix, AZ). These guides were aligned under a microscope to intersect the axis of the capillary guide (B). A 20 × 20 × 2 mm piece (D) of polyvinyl chloride (PVC) separated the fiber optic cell and the electrospray block (E), which was fabricated from a 20 × 20 × 20 mm piece of Plexiglas. The electrospray block was drilled with 0.8 mm channels for liquid and gas sheaths. A 15 mm piece of HTX-22 stainless steel capillary (F) with tapered end was glued by epoxy resin inside the block as the liquid sheath tube (see inset, Fig. 1). A silicone septum (G) between the electrospray block and the PVC plate prevented back flow of the liquid sheath. A miniature positioning stage (E38531, Edmund Scientific, Barrington, NJ) with an attached pin vise (A-PV-6, Small Parts Inc.) was used to position the CE capillary with respect to the liquid sheath tube to obtain electrospray stability [6]. When the CE capillary and optical fibers were in place, the assembly was joined to the front plate with two nylon screws. The optical fibers were held in place with

* On leave from the Institute of Analytical Chemistry, Czech Academy of Sciences, Brno, Czech Republic

0173-0835/96/1212-1829 $10.00+.25/0

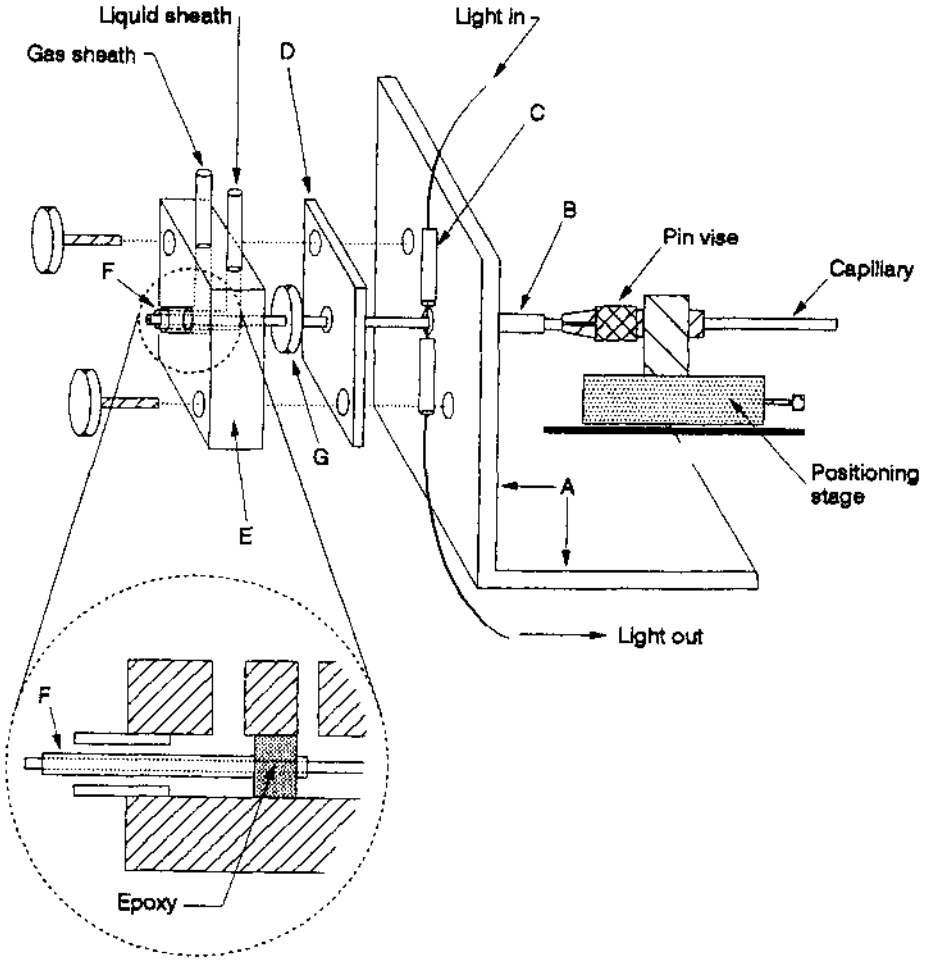

Figure 1. Scheme of the CE-UV-ESI-MS interface. See Section 2.2 for details.

a rubber-coated PVC plate (not shown) attached to the front plate. The CE and ESI power supplies were connected through the liquid sheath tube.

2.3 UV detection

An HPLC UV detector (LC 90, Perkin Elmer Corp., Cupertino, CA) was used for detection. The original flow cell was replaced with a bracket to hold the optical fibers in alignment with the sample and reference photodiodes inside the detector. The sample beam was carried from the UV source to the electrospray interface by a 60 cm fiber and from the interface to the detector by a second 60 cm fiber collecting the light transmitted through the separation capillary. The reference beam was transmitted by a 100 cm fiber from the source to the detector. The reference fiber was cut in the middle, and the ends thus formed were inserted into a 30 mm piece of stainless steel tubing. Adjustment of the gap between these ends attenuated the reference beam to equalize its intensity with that of the sample beam. Smooth fracture of the fiber ends was achieved with a standard sapphire cleaving tool (Supelco, Bellefonte, PA), and polishing of the fiber ends was not necessary. Since the original deuterium lamp in the UV detector did not provide sufficient intensity when used with the fiber optic cell in the interface, an external light source was substituted [7]. Detection at 214 nm was accomplished with a Zn lamp (BHK, Pomona, CA) and a band pass filter (CWL/BW214/10nm, Barr Associates, Inc., Westford, MA). Similarly, although not used in this work, detection at 254 and 280 nm could be accomplished with appropriate combinations of lamps and filters. The high intensity external source allowed the detector to function without loss of sensitivity. Short-term noise was $\sim 5 \times 10^{-5}$ AU, corresponding to the original detector specifications.

2.4 Capillary electrophoresis

Fused silica capillaries were purchased from Polymicro Technologies. Reagents and solvents were obtained from a variety of sources and were used as received. Peptides KRTLRR, RPKP and RPKPQQFFG and 2′-deoxyguanosine 5′-monophosphate were obtained from Sigma (St. Louis, MO). Deionized water was produced with a Compact Milli-Q® system (Millipore Corp., Marlborough, MA). A CZE 1000R high-voltage power supply (Spellman, Plainview, NY) was used for separations. Additional experimental conditions are noted in the figure captions.

3 Results and discussion

The interface described above is useful in applications that require precise information about zone exit time, and the design is similar to a fraction collector for capillary electrophoresis developed in this laboratory [8]. The

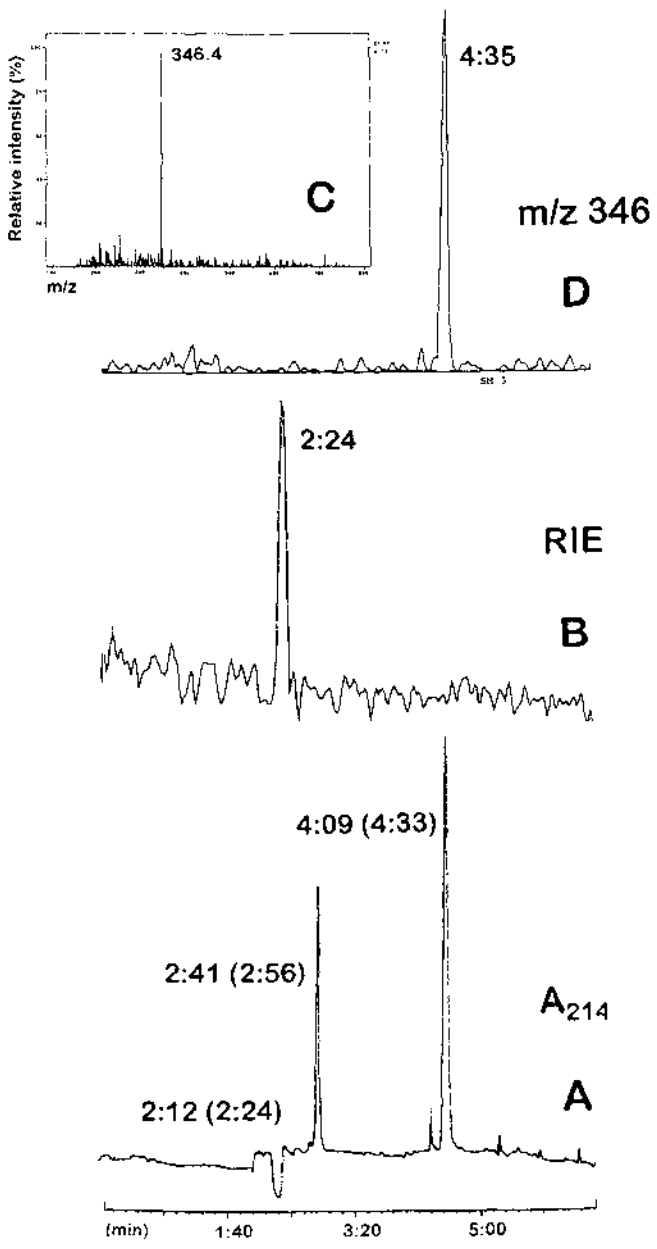

Figure 2. CE-UV-ESI-MS analysis of d-GMP. (A) UV_{214} electropherogram. Migration times in parentheses are t_{MS} values calculated from Eq. (1). (B) RIE. (C) Mass spectrum from co-added scans around t_{MS} 4:33. (D) Extracted ion electropherogram for $[M-H^-]$, *m/z* 346. Capillary: 38 cm × 360 μm OD × 75 μm ID, bare fused silica with fiber optic window 3.2 cm from the tip. Background electrolyte (BGE): 10 mM ammonium acetate, pH 9.5. Liquid sheath: 0.2% v/v NH_4OH in 50% v/v MeOH, 2 μL min. Analyte: 1 pmol injected hydrodynamically from 1×10^{-4} M aqueous solution. CE: 330 V/cm, 19 μA. MS: Negative ESI, −3.5 kV, scan 100 to 800 amu in 1.5 s.

fiber-optic detector close to the capillary end allows precise calculation of the zone exit time, and the detector signal can be used for computer control of subsequent events such as fraction collection, MS data acquisition, voltage programming, *etc.* The following examples demonstrate the use of the interface for simultaneous CE-UV-ESI-MS analyses. Figure 2A shows the UV signal from the CE analysis of 2′-deoxyguanosine 5′-monophosphate (d-GMP). The baseline drop corresponding to electroosmotic flow detected at 2 min 12 s (2:12) is followed by peaks at 2:41 and 4:09. Based on the migration distance to the fiber optic detection cell, X, and the total length of the capillary, L, the migration time of the zones entering the mass spectrometer, t_{MS}, can be calculated as [8]:

$$t_{MS} = (L/X)t_{UV} \quad (1)$$

where t_{UV} is the detection time of the UV signal. In Fig. 2A, t_{MS} values are shown in parentheses. Figure 2B is the reconstructed ion electropherogram (RIE) obtained during the same electrophoretic run with scanning ESI-MS detection. Based on its calculated t_{MS}, the single peak present in the RIE is associated with the EOF front, but there is no useful information in the RIE corresponding to the UV-active peaks. Without the information provided by the UV detector, one would assume that the single peak on the RIE trace is the analyzed d-GMP. In reality that peak may be caused by the electrospray instability due to the exit of the water zone (sample solvent) and provides no mass information for the sample. However, summing scans around t_{MS} 4:33 produced the mass spectrum shown in Fig. 2C and permitted the identification of the corresponding peak at t_{UV} 4:09 as d-GMP. The extracted ion electropherogram corresponding to the $[M-H]^-$ ion of d-GMP, *m/z* 346 (Fig. 2D) shows a peak at the measured migration time of 4:35, corresponding to the peak at the predicted time of 4:33 (Fig. 2A). In general, the agreement between predicted and measured migration times was better than 2%. The UV-active peak at 2:41 had no discernible mass spectrum and is most likely an impurity zone with very high UV absorbance.

Figures 3A–C illustrate the CE-UV-ESI-MS analysis of a peptide mixture. Figure 3A, the UV electropherogram, shows peaks corresponding to all three peptides; however, only one peak is observed in the reconstructed ion electrophoregram (Fig. 3B, bottom panel). As with the previous example, t_{MS} could be calculated for each UV-active peak with Eq. (1), and the relevant MS information could be located without reference to the RIE. Thus, spectra for all compounds (shown in Fig. 3C) were obtained by summing scans around the predicted t_{MS} values, as shown in Fig. 3C. Extracted ion electropherograms based on the mass spectra are shown in the upper panels of Fig. 3B.

4 Concluding remarks

The examples described above show optical detection close to the electrospray tip. Although the interface was demonstrated with UV detection, a similar design can be used for high sensitivity fluorescence detection as well. The interface was evaluated with a liquid sheath but can be adapted to sheathless operation [9]. There is no need to increase the capillary length to accommodate this detector, because the optical cell is part of the ESI interface and is separated from the detector electronics. Short capillaries can easily be used for rapid separations. In cases where the electrophoretic velocity changes during the run (large volume preconcentration, large salt content, isoelectric focusing, *etc.*), two spaced fiber-optic de-

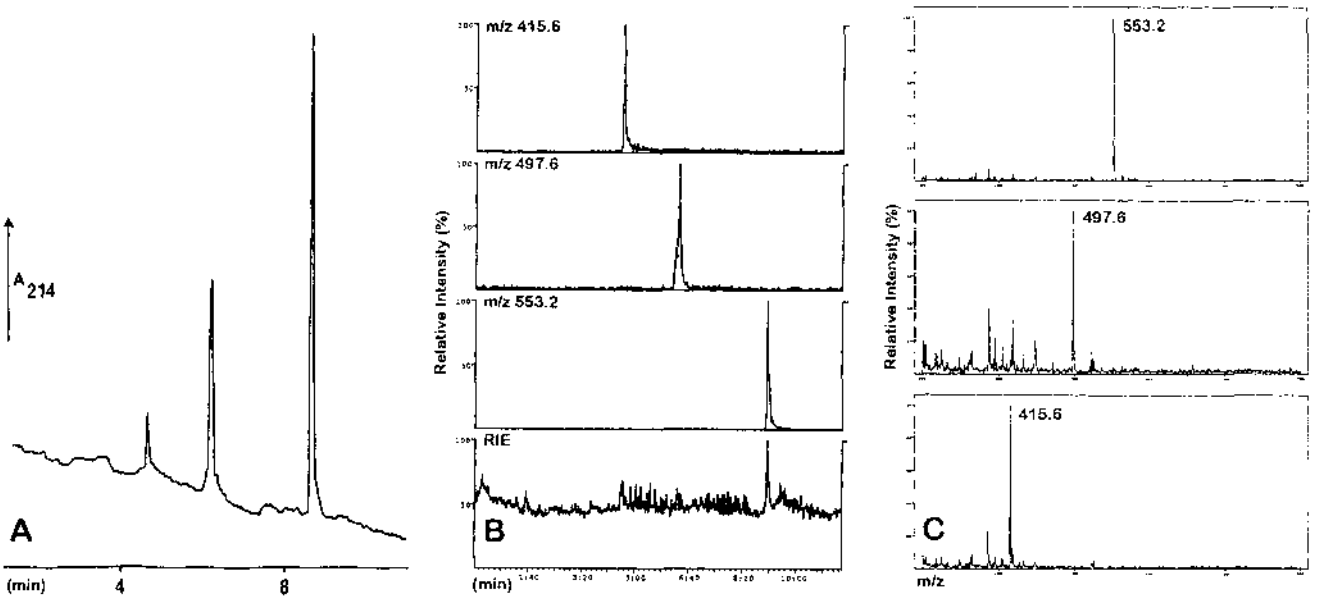

Figure 3. CE-UV-ESI-MS analysis of peptide mixture in order of increasing migration time: KRTLRR, RPKP and RPKPQQFFG. (A) UV_{214}-electropherogram. (B) RIE and extracted ion electropherograms. (C) Mass spectra of peptides. Capillary: 50 cm × 360 μm OD × 50 μm ID, bare fused silica with fiber-optic window 3.2 cm from the tip. BGE: 20 mM ε-amino caproic acid + acetic acid, pH 4.5. Liquid sheath: 25-75-0.05 v/v/v H_2O-MeOH-acetic acid, 2.5 μL/min. Analytes: 500 fm each injected hydrodynamically from 1×10^{-4} M aqueous solution. CE: 340 V/cm, 2 μA. MS: positive ESI, 3.2 kV, scan 300 to 800 amu in 1 s.

tection cells can be placed close to the capillary exit for precise measurement of the zone velocity prior to its exit. The detection signal can also be used for automation of CE-MS analyses. Thus, peak detection can be used for computer control of the start of data acquisition, change of scan range, and/or control of the separation voltage in the same manner as in the automated fraction collector [8].

This work, partially supported by NIH IROICA, 69390-01 (PV) and NIH GM15847 (BLK), was presented at the 43rd ASMS Conference on Mass Spectrometry and Allied Topics, Atlanta, GA, 1995. Contribution No. 680 from the Barnett Institute.

Received August 30, 1996

5 References

[1] Johansson, I. M., Huang, E. C., Henion, J. D., Zweigenbaum, J., *J. Chromatogr.* 1991, *554*, 311–327.

[2] Thompson, T. J., Foret, F., Vouros, P., Karger, B. L., *Anal. Chem.* 1993, *65*, 900–906.

[3] Foret, F., Thompson, T. J., Vouros, P., Karger, B. L., Gebauer, P., Boček, P., *Anal. Chem.* 1994, *66*, 4450–4458.

[4] Smith, R. D., Barinaga, C. J., Udseth, H. R., *Anal. Chem.* 1988, *60*, 1948–1952.

[5] Lee, E. D., Muck, W., Henion, J. D., Covey, T. R., *Biomed. Environ. Mass Spectrom.* 1989, *18*, 844–850.

[6] Kirby, D. P., Thorne, J. M., Gotzinger, W. K., Karger, B. L., *Anal. Chem.* 1996, in press.

[7] Foret, F., Deml, M., Kahle, V., Boček, P., *Electrophoresis* 1986, *7*, 430–432.

[8] Müller, O., Foret, F., Karger, B. L., *Anal. Chem.* 1995, *67*, 2974–2980.

[9] Olivares, J. A., Nguyen, N. T., Yonker, C. R., Smith, R. D., *Anal. Chem.* 1987, *59*, 1230–1232.

Frantisek Foret
Haihong Zhou
Eric Gangl
Barry L. Karger

Barnett Institute and
Department of Chemistry,
Northeastern University,
Boston, MA, USA

Subatmospheric electrospray interface for coupling of microcolumn separations with mass spectrometry

A modular subatmospheric electrospray interface with fiber optic UV detection close to the electrospray tip was developed for coupling of microcolumn separation techniques with mass spectrometry. The interface was based on a liquid junction with a removable microelectrospray tip. The electrospray tip was enclosed in a subatmospheric chamber attached in front of the sampling orifice of the mass spectrometer. The inlet of the liquid junction was maintained at atmospheric pressure, and thus no pressure drop developed across the separation column. The flow rate of the electrosprayed liquid from the liquid junction reservoir was adjusted by the pressure in the electrospray chamber. In this approach, a continuous and stable electrospray could be achieved without the use of an external pump. Since the electrospray did not depend on fluid delivery from the separation column, coated capillaries without electroosmotic flow as well as capillaries with electroosmotic flow could be used for capillary electrophoresis. In addition, the interface was found to be effective with capillary liquid chromatography. The use of a fiber optic UV detector placed close to the exit of the separation column provided additional detection information and a simple means of troubleshooting. The interface did not significantly influence the quality of the separation, even with columns generating several hundred thousand theoretical plates. Peptide samples in the submicromolar concentration range were detected, corresponding to a limit of detection in the attomole range.

Keywords: Subatmospheric electrospray interface / Microcolumn separation / Microelectrospray
EL 3806

1 Introduction

The initial reports on capillary electrophoresis – electrospray mass spectrometry (CE-ESI-MS) interfacing [1–3] triggered much interest in the MS coupling of microcolumn separation techniques such as CE, CEC, or packed capillary liquid chromatography (CLC). A number of ESI interfaces for the combination of capillary separations with MS have been described in the literature, based on a liquid sheath [4–6], liquid junction [7–9], or sheathless arrangement [10–12]. More detailed information can be found in recent reviews [13, 14].

In the liquid sheath approach, the exit of the separation column is generally positioned concentrically inside a tube supplied with a sheath fluid to maintain a stable ESI. The composition of the sheath fluid can be selected to optimize the ESI conditions (surface tension, additives, pH, *etc.*); however, the liquid sheath flow (typically > 1 μL/min) results in significant sample dilution. At the same time, the large outer diameter of the ESI tip, which has to accommodate the separation capillary, often requires manual adjustment to maintain a stable ESI [6]. The sheathless interface uses a fine ESI tip which can be part of the separation column or the tip can be attached to the column separately [15]. The sheathless arrangement requires a stable liquid flow inside the separation column, eliminating the use of capillaries with neutral wall coatings (without electroosmotic flow) that are often employed to minimize analyte wall adsorption in CE. The sheathless design is suitable for very low flow rates; however, the electrolyte solution required to optimize separation (pH, nonvolatile buffer components) may not be suitable for ESI.

The liquid junction interface, as developed for CE [16, 17], combines the advantages of independent optimization of the ESI and separation conditions with the use of a fine ESI tip for stable and sensitive ESI operation. In this approach, sample transport from the exit of the separation capillary into the ESI tip is typically achieved by applica-

Correspondence: Dr. Barry L. Karger, Barnett Institute and Department of Chemistry, Northeastern University, Boston, MA 02115, USA
E-mail: bakarger@lynx.neu.edu
Fax: +617-373-2855

Abbreviations: CLC, capillary liquid chromatography; **PVA**, poly(vinyl alcohol)

0173-0835/00/0707-1363 $17.50+.50/0

tion of positive pressure in the liquid junction. However, the resultant pressure drop along the separation capillary has to be compensated by pressurizing the sample inlet reservoir to avoid excessive band broadening [9], and the flow through the ESI tip may not be easy to control.

In this study, we report a new ESI interface for coupling the MS with microcolumn separations that is both simple to operate and robust. The interface uses a liquid junction for coupling of the separation column with a replaceable micro-ESI tip enclosed in a subatmospheric chamber. The lower pressure inside the ESI region leads to sample transport through the ESI needle without the need for positive pressure at the liquid junction. The construction allows simple turnkey operation without adjustments. Note that, unlike previous attempts for direct ESI in vacuum [18, 19], only modestly descreased pressure (50–90 kPa) was applied in this study [20]. The slight decrease in the ESI chamber pressure eliminates the problem of solvent freezing typical of deep vacuum ESI [18]. High efficiency and sensitive separations of peptide samples were obtained with both CE and packed CLC. The interface can also be used for coupling of microfabricated separation devices to MS [21].

2 Materials and methods

2.1 Instrumentation

2.1.1 MS and ESI interface

All experiments were conducted on an LCQ quadrupole ion trap mass spectrometer (Finnigan, San Jose, CA). The temperature of the heated desolvation capillary was 120°C, and the ESI voltage was 1.5 kV. A collision energy was set to 25% of the instrument maximum and used for all CID experiments. The design of the interface is shown in Fig. 1. The interface base and liquid junction reservoir were made of transparent polycarbonate resin (Small Parts, Miami Lakes, FL). Fused-silica capillaries (Polymicro Technologies, Phoenix, AZ), were employed for ESI emitters (20 μm ID × 360 μm OD × 44 mm). The tips of the emitters were etched in 40% hydrofluoric acid to a final diameter of ~ 40 μm. In addition, fine tips with a diameter of ~ 3 μm were prepared from the same fused-silica capillary using a modified pipette puller (P-87; Sutter Instruments, Novato, CA). The modification included the replacement of the original heating element with four turns of 0.25 mm Ir wire (Goodfellow, Berwyn, PA). Over 100 fused-silica tips could be pulled before having to replace the heating coil. The entire ESI chamber was sealed by a rubber O-ring between the interface base and the MS, allowing subatmospheric conditions in the ESI chamber. The volume of this chamber, created by enclosing the indentation around the sampling orifice of the mass spectrometer, was estimated to be ~ 300 mL. The pressure difference between the chamber and atmosphere was monitored by a digital manometer (TIF Instruments, Miami, FL) and regulated by a miniature plastic valve (731-8220; Bio-Rad, Hercules, CA). The air intake flow (~ 0.5 L/min at atmospheric pressure) was directed around the ESI tip by a needle guide to aid desolvation. By regulating the air flow, the pressure inside the chamber (pressure difference) was controlled together with the liquid intake.

2.1.2 CE

Fused-silica capillaries (75 μm ID × 360 μm OD × 40 cm; Polymicro Technologies) coated with poly(vinyl alcohol) (PVA) [22] were used for separation. The high voltage power supply (Model PS/EG 30 R; Glassman, Whitehouse Station, NJ), connected to a platinum electrode in

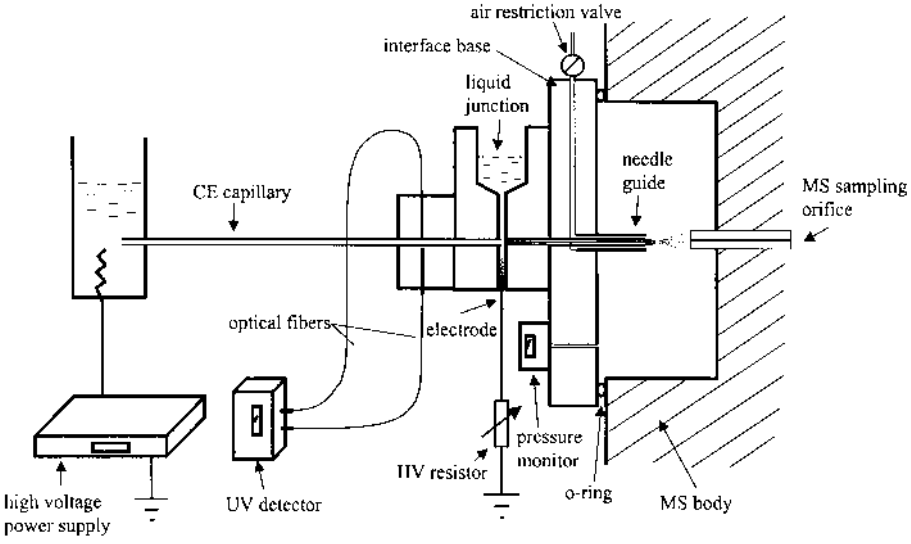

Figure 1. Diagram of the subatmospheric ESI interface. See Section 2.1.1 for details.

a vial containing background electrolyte (BGE), was operated in the constant voltage mode. An optically controlled high voltage resistor, consisting of a chain of 20 photoresistors (part # 699 9514; Allied Electronics, Forth Worth, TX) connected in series, was used to adjust the potential of the liquid junction and the ESI. The final resistance was adjusted to achieve the 1.5 kV ESI potential. This adjustment could easily be fixed in the range of ~ 1 MΩ to several TΩ by illuminating the photoresistors with a 5V incandescent lamp. Since the ESI current was typically a small fraction of the electrophoresis current, only one high voltage power supply was necessary for operation. The ESI process began simultaneously with the CE analysis without the need of a separate high voltage power supply. On-column UV detection was performed using a fiber optic detection cell made of a fiber optic adapter (SMA 905-120-5003; Amphenol, Lisle, IL). A 2 mm hole was drilled in the center of the adapter, which was then mounted in an aluminum block (17 × 17 × 17 mm) together with two 10 mm pieces of stainless steel tubing (HTX-22; Small Parts), used as a guide for the separation capillary. The mutual positions of the guiding tubes and optical fibers, used for directing the detection UV light (FVP300330370; Polymicro Technologies), were adjusted under a microscope and fixed by epoxy glue. The length of each of the optical fibers was 1 m. A modified variable wavelength UV detector (Spectra 100; Linear Instruments, Reno, NV) was used for detection at 214 nm. The modification included attachment of the optical fiber holders in place of the original flow cell and an increase in the amplification of the transimpedance amplifier of the detector by a factor of 100 in order to compensate for the loss in light intensity in the optical fiber. The UV detector output, connected to the user input of the LCQ mass spectrometer, was recorded simultaneously with the MS signal.

2.1.3 CLC

CLC was performed on a 14 cm × 75 μm ID (365 μm OD) fused-silica column that was slurry-packed with 5 μm C_{18} particles (218TP54; Vydac, Hesperia, CA). A sintered silica frit was used to retain the packing inside the column; no precolumn or entrance frit was needed. Solvent was delivered using an HP 1100 binary pump (Hewlett-Packard, Palo Alto, CA) set at a flow rate of 0.35 mL/min. Nanoliter flow rates were achieved by coupling the pump effluent to a precolumn splitter (Acurate, IC-400 Var; LC Packings, San Francisco, CA). The flow calibrator provided with the Acurate splitter was used to deliver flow rates of ~ 250 nL/min to the column, with a resulting split ratio of approximately 1400. An injector, equipped with a 200 nL internal loop (Model C4; Valco Instruments, Houston, TX), was employed for sample introduction. Samples consisted of protein digests of 1 μL volume. All mobile-phase solvents were degassed with helium prior to use, and the column was maintained at ambient temperature (~25°C). A two-stage linear gradient was employed to perform the separation; solvent A was 0.05% v/v trifluoroacetic acid (TFA) in water and solvent B, 0.05% v/v TFA in acetonitrile. The gradient was as follows: 4-40% B in 35 min, then 40-80% B in 15 min, with an additional 10 min hold at the final solvent composition. The HPLC column had an air initial pressure of 172 atm and a final pressure of 133 atm. The liquid junction buffer was 1% acetic acid in 50% methanol.

2.2 Reagents and materials

Peptide standards, bovine serum albumin (BSA), myoglobin, horse heart cytochrome *c* and L-1-tosylamide-2-phenylethyl chloromethyl ketone (TPCK)-treated trypsin were purchased from Sigma (St. Louis, MO) and used as received. Solvents and reagents were all analytical grade. Deionized water was produced with a compact Milli-Q^+ system (Millipore, Marlborough, MA).

2.3 Enzymatic digestion

Horse heart cytochrome *c* (*ca.* 100 μM) was digested with TPCK treated trypsin for 16 h at 37°C at a substrate-to-enzyme ratio of 12:1 w/w in 50 mM ammonium acetate buffer, pH 8.1. The pH of the buffer solution was adjusted with ammonium hydroxide. The digestion solution was then aliquoted and stored in a freezer (–20°C) for future use.

3 Results and discussion

3.1 Design strategy

The following parameters were considered in the design of the interface: (i) ESI stability and robustness; (ii) ease of optimization of operational parameters; (iii) compatibility with all modes of separation; (iv) ability to maintain high performance separation; and (v) sensitivity. The liquid junction arrangement was selected since in CE-MS it decouples the separation process from ESI, allowing independent optimization of each component. The ability to maintain high-performance separation required low dead volume. In the liquid junction interface, the internal volume of the ESI needle was minimized by using a short ESI needle. At the same time the taper on the exit side of the ESI needle maximized the electric field strength at that position, even at low applied voltage [23]. Good ionization efficiency could be obtained without the danger of a corona discharge.

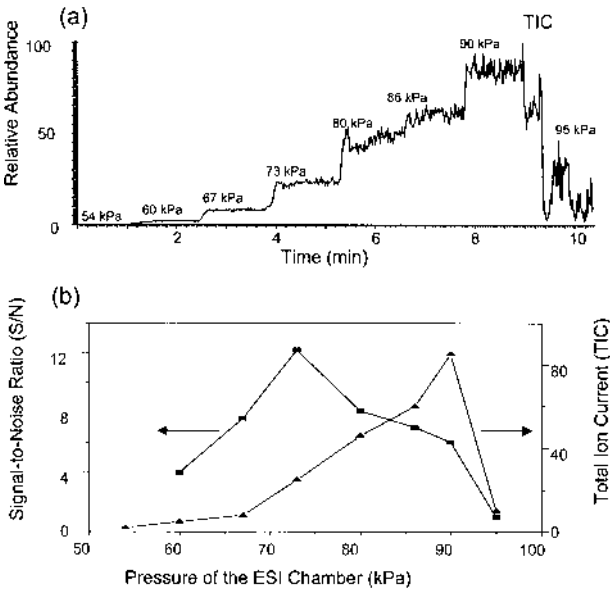

Figure 2. (a) Effect of the pressure of ESI chamber on the signal profile. (b) Plot of (■), the S/N ration; and (▲) total ion current. Sample, 0.1 mg/mL solution of myoglobin in 50% v/v methanol with 1% v/v acetic acid.

In our design, the liquid flow into the ESI needle was created by lowering the pressure inside the ESI chamber by restricting the air intake; no additional pump was necessary. The liquid junction outside the ESI chamber was maintained at atmospheric pressure. By varying the pressure in the ESI chamber, a wide range of flow rates through the ESI needle could be established. At the same time, the gas intake served as the gas sheath, aiding evaporation of the electrosprayed droplets. In contrast to the typical gas sheath arrangement where the sheath gas flow rate would greatly exceed the gas flow into the mass spectrometer, all the gas transporting the electrosprayed ions entered the MS sampling orifice.

In order to optimize the interface performance, we measured the effect of pressure in the ESI chamber (which influenced both the flow rate of the electrosprayed liquid and the gas intake into the MS) on the ESI signal. In this experiment, a 0.1 mg/mL solution of myoglobin in 50% v/v methanol with 1% v/v acetic acid was placed in the liquid junction reservoir, and the ESI mass spectrum was recorded at different pressures in the subatmospheric chamber. The separation capillary was not connected in this experiment. A plot of total ion current *versus* pressure in the ESI chamber in Fig. 2a revealed that the current had a maximum at approximately 90 kPa. However, the noise level increased with pressure, resulting in the optimum signal-to-noise ratio at 70 kPa (Fig. 2b). The higher noise at 90 kPa was likely caused by insufficient bulk liquid flow (~ 45 nL/min) resulting in ESI instability (although higher ion transmission into the mass spectrometer was achieved). At 70 kPa, the flow was sufficient for a stable ESI with a high S/N ratio in spite of lower ion transmission. The ESI signal was stable at lower pressures in the ESI chamber; however, the transport of gas-phase ions through the sampling orifice was significantly reduced, resulting in a lower S/N ratio. Note that the optimum pressure in the ESI chamber may be different for different mechanical arrangements, especially ESI capillary and sampling orifice dimensions, as well as for different solvents used in the spray liquid. Further sensitivity improvements could be expected using a larger MS sampling orifice internal diameter, as in a recent ion trap design [24].

The optimum pressure difference of ~ 30 kPa across the ESI tip generated a liquid flow of ~ 140 nL/min through the ESI capillary. This flow rate was sufficient to transport all the ions exiting the separation column into the ESI capillary (see Section 6). At the same time, dilution of the sample zones was negligible since the spray liquid volume flow rate was lower than the volumetric rate of electromigration (150–360 nL/min ion movement, no bulk flow; see Section 6). Note that the sample entered the ESI capillary *via* laminar flow of the spray liquid (*i.e.*, no turbulent mixing). This laminar flow caused spatial focusing of the sample in the center of the spray capillary in the same manner as in flow cytometry [25], thus minimizing zone dispersion.

Another important parameter of the ESI interface is the dimension of the ESI tip. According to the literature [16, 26], a small diameter (5–10 μm) tip will provide a 25-to 50-fold gain in sensitivity, as compared to a larger capillary tip (50–100 μm). The tips with lower diameter, prepared with a pipette puller (down to 3 μm), were successfully tested; however, the increased hydrodynamic resistance resulted in a decreased flow. In addition, no gain in sensitivity was observed compared to the 20 μm tapered ESI needle. Moreover, as found by others [16], the fine tips tended to plug even if all the solutions were thoroughly filtered. The best results in terms of spray stability and resistance to clogging were obtained with 15–20 μm tapered capillaries.

In our work, the tips, prepared by hydrofluoric acid etching, were found to work better than those made by mechanical grinding because the relatively rough surface caused by grinding was easily wetted, eventually leading to a surface for crystallization of nonvolatile buffers. Thus, tips made by grinding sometimes experienced clogging or an unstable spray. The 20 μm etched ESI tips used in this work were positioned 1–3 mm from the MS sampling orifice. As noted above, at only moderately decreased pressure (~70% atmospheric pressure), the ESI was not prone to corona discharge within the operating voltage range of 1.2–2.2 kV.

3.2 Separation efficiency

Figure 3 presents an on-line CE-UV-ESI-MS separation of 12 peptides using the subatmospheric interface with a 40 cm separation capillary and the 20 μm tapered ESI needle. Separation efficiencies as high as 170 000 total plates (measured at the peak half-height) were determined from the mass electropherogram (peak 10). The ESI tip and the exit end of the separation column in the liquid junction were spaced approximately 100 μm apart. In practice, the separation capillary was inserted into the liquid reservoir until it lightly touched the ESI tip and then pulled back slightly. The resulting gap allowed spray liquid to flow unrestricted into the ESI tip from the surrounding reservoir. The volume of the gap (~ 400 pL) was much smaller than the volume of the zones exiting the separation column (~ 10 nL), and no loss of efficiency was expected in this transfer step. The sample zones entering the laminar flow stream of the sheath fluid were hydrodynamically focused in the center of the capillary tip without band broadening [27, 28]. The total volume of the ESI tip was ~ 12 nL, and at the flow rate of 140 nL/min, the liquid flowed through the ESI tip in approximately 5s, minimizing diffusional band broadening. The corresponding peaks measured by the on-column UV detector and by the mass spectrometer revealed no change in peak shape, and the plate counts (measured at the peak half-height) agreed within experimental error (± 20%), supporting the above arguments.

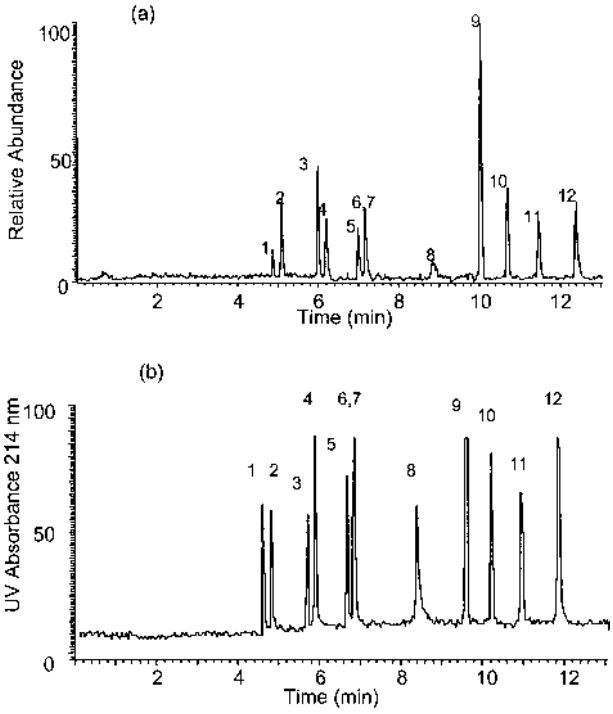

Figure 3. Mass electropherogram (*m/z* 500–1400) and on-line UV spectrum obtained for a mixture of angiotensins. Samples, 10 μg/mL each of: peak 1, angiotensin I des-Asp I; 2, angiotensin I goosefish; 3, angiotensin II; 4, angiotensinogen (1–14) human; 5, angiotensin I human; 6, angiotensin I [Val^5]-; 7, angiotensin I salmon; 8, angiotensinogen (1–14) porcine; 9, angiotensin III frag. 3–8; 10, angiotensin III frag. 1–7; 11, angiotensin III human, 12, angiotensin I bullfrog. Separation capillary, 40 cm (38.5 cm to UV detector), 75 μm ID, 365 μm OD, PVA-coated. BGE, 20 mM ε-aminocaproic acid titrated with acetic acid to pH 4.4. The sample was injected at 10 cm height difference for 10 s. Separation at a field of 560 V/cm. ESI capillary tip, 4.4 cm, 20 μm ID, 365 μm OD, fused-silica capillary; spray liquid, 1% v/v acetic acid in 50% v/v methanol; electrospray voltage, 1.5 kV; pressure in the ESI chamber, 70 kPa.

3.3 Sensitivity

Sensitivity, particularly with respect to solute concentration, is an important issue for on-line CZE-UV-ESI-MS. The use of a fine ESI tip in the subatmorspheric interface provided an improved S/N ratio in comparison to a standard coaxial liquid sheath arrangement. Typically, 10^{-5} M concentrations of the individual sample peptides separated by CE could be detected with a 10-50-fold better S/N ratio compared to the standard ESI interface supplied with the instrument (total ion current monitoring, no sample preconcentration). The detection limit for the analyzed peptides was in the submicromolar concentration range, corresponding to a mass detection limit in the low femtomole range (total ion current monitoring), or the attomole range (selected ion monitoring). Of course, one could employ a variety of sample preconcentration techniques in order to improve concentration detection limits even further [29].

3.4 Robustness

Since there are no mechanical adjustable parts, the operation of the interface was quite simple. Once attached to the mass spectrometer, the pressure inside the ESI chamber could be set in less than 1 min, and daily operation over one week or more could be achieved without change of the ESI tip. This is demonstrated in Fig. 4 where comparable mass electropherograms were obtained before and after replacement of both the ESI tips and CE capillaries on three consecutive days. The peak height variation of the zone at roughly 8 min, for angiotensinogen (1–14) porcine, the most basic peptide, was probably due to adsorption to the capillary wall. If required, both the separation capillary and the ESI tip could be replaced in less than 1 min without change in the CE-MS performance. In practice, it is also important that the CE-MS interface be able to analyze minor sample

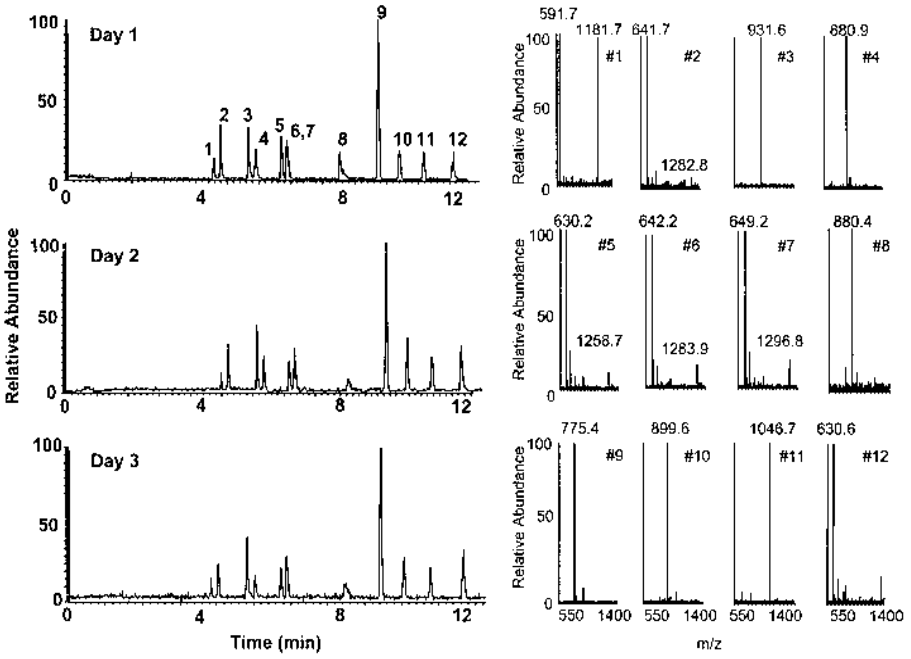

Figure 4. Mass electropherograms of a mixture of angiotensins from three CE columns with three ESI tips. Other conditions as in Fig. 3. Single scan mass spectra on the right correspond to the respective maxima of the numbered peaks.

components in the presence of large amounts of a major sample component. In an example of such an analysis (Fig. 5) the concentration of the major component was 800 μg/mL, while the minor sample constituents were present at only 5 μg/mL. Although 160 times higher in concentration, the major peak was clearly separated from the minor components. No "ghost" mass spectrometric signal was detected within the mass spectra of the minor sample components.

As another way of testing robustness, we have selected a microcolumn LC representing a different separation mode than CE. CLC is frequently interfaced to MS using a sheathless interface [30, 31]. The liquid junction, used in this work, provides a useful means for connection of the ESI high voltage. In practice the ESI liquid intake can be adjusted to match the LC effluent flow so that the interface operates in a sheathless mode. In case the LC effluent flow rate is higher than the liquid intake by the ESI capillary, part of the sample will be split away from the analysis; however, the MS response will not change, providing that the ESI-MS operates in the concentration-sensitive region [15]. In either case the actual solution in the liquid junction provides a useful means for connection of the ESI voltage and will not influence the MS signal. If the LC effluent flow is lower than the ESI capillary intake, both liquids will mix in the ESI capillary. The resulting signal will be influenced by the final electrosprayed sample composition and may be higher (spray composition optimized) or lower (dilution prevails) compared to the sheathless arrangement.

In this work we have analyzed cytochrome *c* tryptic digest by packed CLC-UV-ESI-MS at the LC flow rate higher (250 nL) than the ESI liquid intake (140 nL). The mass electropherogram obtained from tryptic digests of ~1.8 ng (~150 fmole) of the protein is shown in Fig. 6. MS/MS

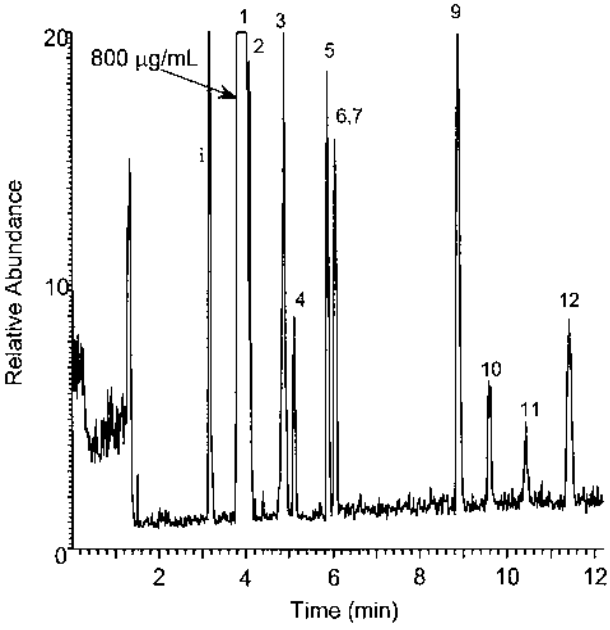

Figure 5. Mass electropherogram (*m/z* 500–1400) of a mixture of angiotensins. Samples, angiotensin I (des-Asp[1]) 800 μg/mL, and others 5 μg/mL each; i, impurity from peak 1. The conditions for separation and mass spectrometer were as in Fig. 3.

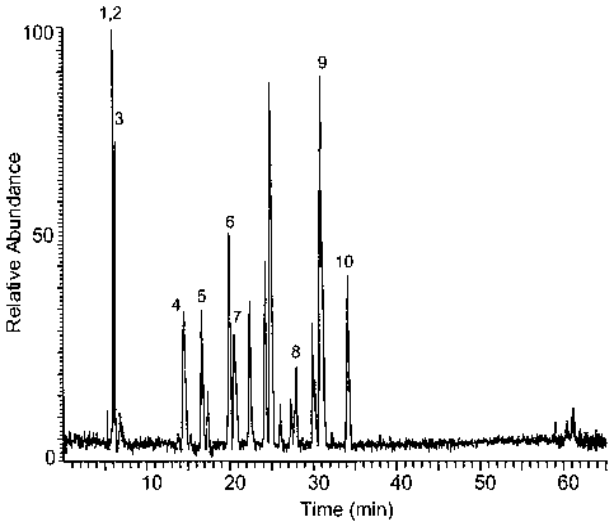

Figure 6. Packed CLC separation of a tryptic digest of cytochrome *c*. Mass chromatogram recorded in the range of *m/z* 100–1600. Peak identification: 1, GGK/NK; 2, Ac-GDVEK; 3, GITWK; 4, YIPGTK; 5, IFVQK; 6, TGQAPGF-TYTDANK; 7, GITWK; 8, MIFAGIK; 9, CAQCHTVEK + Heme; 10, EETLMEYLENPK. The gradient consisted of 0.05% v/v TFA in water (A) and 0.05% v/v TFA in acetonitrile (B); 4–40% B in 35 min, 40–80% B in 15 min, then hold, 10 min at final composition. Other conditions as in Fig. 3.

experiments in the data-dependent scan mode were performed on ions with intensities above a selected threshold value (1×10^6 counts). The resulting CID spectra were used to identify the protein by scanning sequence databases using the SEQUEST program [32]. The search results yielded correlation coefficients around 2 with the Δ correlation factors above 0.1, indicating a good match [32]. The identified peptide fragments can be found in the figure caption. Similar to the examples obtained with CE, the high efficiency of CLC was preserved.

4 Concluding remarks

The subatmospheric interface for microseparation-UV-ESI-MS was found to be simple to use. The interface was tested for MS coupling of CE and packed CLC. Since the liquid flow into the ESI needle can be adjusted, there can be little or no sample dilution. In fact, the liquid junction may also be used for sample preconcentration under certain circumstances (see Section 6). At the same time, the laminar flow inside the ESI needle causes spatial focusing of the analyte stream, thus minimizing zone band broadening. The separation efficiencies up to 170 000 plates were routinely obtained in the CE separations with the 40 cm long column. A limit of detection in the attomole range with selected ion monitoring was achieved for peptides separated by CE. Although not described in this study, the interface can also be readily applied for CIEF-UV-ESI-MS or CEC-UV-ESI-MS. Recently we have also used the interface for effective on-line MS coupling of microfabricated devices [21].

This work was supported by the National Institutes of Health, GM 15847. The authors thank Dr. Daniel P. Kirby for stimulating discussions and experimental help in the early stages of the project. Contribution # 773 from the Barnett Institute.

Received August 24, 1999

5 References

[1] Smith, R. D., Olivares, J. A., Nguyen, N. T., Udseth, H. R., *Anal. Chem.* 1988, *60*, 436–441.

[2] Smith, R. D., Barinaga, C. J., Udseth, H. R., *Anal. Chem.* 1988, *60*, 1948–1952.

[3] Lee, E. D., Muck, W., Henion, J. D., Covey, T. R., *J. Chromatogr.* 1988, *458*, 313–321.

[4] Garcia, F., Henion, J., *J. Chromatogr.* 1992, *606*, 237–247.

[5] Huggins, T. G., Henion, J. D., *Electrophoresis* 1993, *14*, 531–539.

[6] Kirby, D. P., Thorne, J. M., Goetzinger, W. K., Karger, B. L., *Anal. Chem.* 1996, *68*, 4451–4457.

[7] Lee, E. D., Muck, W., Henion, J. D., Covey, T. R., *Biomed. Environ. Mass Spectrom.* 1989, *18*, 844–850.

[8] Nichols, W., Zweigenbaum, J., Garcia, F., Johansson, M., Henion, J., *LC. GC* 1992, *10*, 676–686.

[9] Wachs, T., Sheppard, R. L., Henion, J., *J. Chromatogr. A* 1996, *685*, 335–342.

[10] Wahl, J. H., Gale, D. C., Smith, R. D., *J. Chromatogr. A* 1994, *659*, 217–222.

[11] Ramsey, R. S., McLuckey, S. A., *J. Microcol. Sep.* 1995, *7*, 461–469.

[12] Barnidge, D. R., Nilsson, S., Markides, K. E., Rapp, H., Hjort, K., *Rapid Commun. Mass Spectrom.* 1999, *13*, 994–1002.

[13] Cai, J., Henion, J., *J. Chromatogr. A* 1995, *703*, 667–692.

[14] Ding, J. M., Vouros, P., *Anal. Chem.* 1999, *71*, 378A–385A.

[15] Bateman, K. P., White, R. L., Thibault, P., *Rapid Commun. Mass Spectrom.* 1997, *11*, 307–315.

[16] Pleasance, S., Thibault, P., Kelly, J., *J. Chromatogr.* 1992, *591*, 325–339.

[17] Naylor, S., Ji, Q. C., Johnson, K. L., Tomlinson, A. J., Kieper, W. C., Jameson, S. C., *Electrophoresis* 1998, *19*, 2207–2212.

[18] Dohmeier, D. M., Thesis, University of North Carolina, Chapel Hill 1991.

[19] Sheenan, E. W., Willoughby, R. C., *Proceedings of the 45th ASMS Conference on Mass Spectrometry and Allied Topics*, Palm Springs, CA, June 1–5, 1997, p. 115.

[20] Foret, F., Kirby, D., Karger, B. L., *Proceedings of the 44th ASMS Conference on Mass Spectrometry and Allied Topics*, Portland, OR, May 12–16, 1996, p. 913.

[21] Zhang, B., Liu, H., Karger, B. L., Foret, F., *Anal. Chem.* 1999, *71*, 3258–3264.

[22] Karger, B. L., Goetzinger, W., *US Patent 5,840,388*, 1998.

[23] Wilm, M. S., Mann, M., *Int. J. Mass Spectrom. Ion Proc.* 1994, *136*, 167–180.

[24] LCQ™ DECA, Finnigan Corp., San Jose, CA.

[25] Ormerod, M. G., *Flow Cytometry*, 2nd Ed., Springer, New York 1999.

[26] Tetler, L. W., Cooper, P. A., Powell, B., *J. Chromatogr. A* 1995, *700*, 21–26.

[27] Kenis, P. J. A., Ismagilov, R. F., Whitesides, G. M., *Science* 1999, *285*, 83–85.

[28] Kutter, J. P., Jacobson, S. C., Ramsey, J. M., *Anal. Chem.* 1997, *69*, 5165–5171.

[29] Foret, F., Szoko, E., Karger, B. L., *Electrophoresis* 1993, *14*, 417–428.

[30] Gatlin, C. L., Kleemann, G. R., Hays, L. G., Link, A. J., Yates III, J. R., *Anal. Biochem.* 1998, *263*, 93–101.

[31] Davis, M. T., Stahl, D. C., Hefta, S. A., Lee, T. D., *Anal. Chem.* 1995, *67*, 4549–4556.

[32] Ducret, A., Van Oostveen, I., Eng, J. K., Yates III, J. R., Aebersold, R., *Prot. Sci.* 1998, *7*, 706–719.

[33] Janini, G. M., Metral, C. J., Issaq, H. J., Muschik, G. M., *J. Chromatogr. A* 1999, *848*, 417–433.

6 Appendix

Optimization of the flow rate in the liquid junction

In order to assure that analytes exiting the separation column are quantitatively transferred into the ESI needle, a sufficient liquid flow rate in the transfer capillary must be maintained. Using the geometry of the liquid junction, the definition of electrophoretic mobility and Ohm's law, the minimum required flow rate can be estimated from the mass flow balance, schematically shown in Fig. 7. The sample ions exiting the end of the CE capillary electromigrate toward the electrode in the liquid junction reservoir. At the same time, the hydrodynamic flow transports the ions into the ESI needle. For optimum transfer efficiency, this hydrodynamic flow rate should be larger than the electromigration in the gap between the separation column and ESI tip in the liquid junction.

The hydrodynamic flow velocity, v_f, through a surface of a cylinder defined by the radial distance x from the axis of the separation column and the distance of the gap d between the column and the electrospray capillary (see Fig. 7), can be written as

$$v_f = Q/2\pi xd \quad (1)$$

where Q is the volumetric hydrodynamic flow rate through the ESI tip. At the same time the electrophoretic velocity, v_e, of the ions electromigrating from the liquid junction gap, towards the electrode and against the hydrodynamic flow, will be

$$v_e = uE = uI/2\pi xd\kappa \quad (2)$$

where u is the analyte electrophoretic mobility, E the electric field strength at the distance x from the axis of the capillary, I is the electrophoretic current and κ the conductivity of the electrolyte in the liquid junction. To assure the transport of all ions exiting the separation column, the condition $v_f > v_e$ must be fulfilled. Thus, the minimum flow rate, Q, through the ESI tip can be estimated as

$$Q > uI/\kappa \quad (3)$$

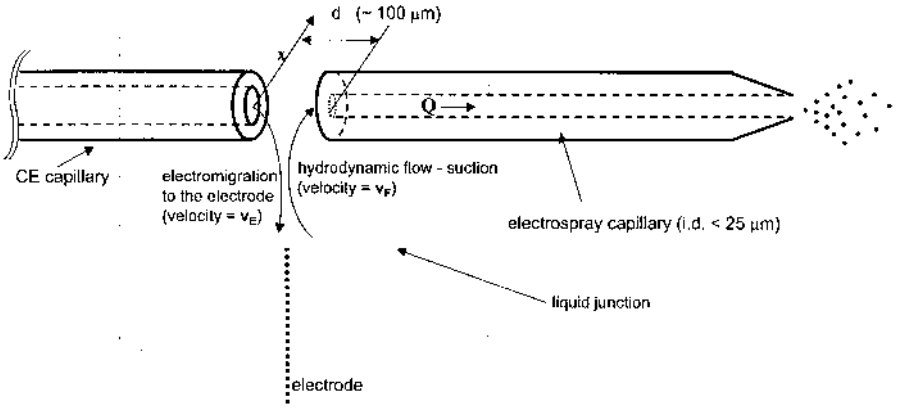

Figure 7. Schematic diagram of the mass transport in the liquid junction.

Assuming the conductivity κ to be 0.2 S/m (1% formic acid solution in 50% methanol/water), an electrophoretic mobility of 30×10^{-9} m^2/Vs and electrophoretic current of 10 μA, the minimum flow rate through the electrospray capillary should be higher than 90 nL/min. At the optimum pressure difference (70 kPa), the hydrodynamic flow rate through the ESI tip was measured to be ~ 140 nL/min, resulting in good transfer efficiency. Note that typical sample ions have electrophoretic mobilities below 30×10^{-9} m^2/Vs [33]. Only highly mobile inorganic ions with higher mobilities ($50–80 \times 10^{-9}$ m^2/Vs) will partially migrate toward the CE electrode in the liquid junction. In this respect, the liquid junction can also serve as a selective filter, preventing the highly mobile sample matrix (salt) ions from entering the ESI.

The discussion above deals only with the flow conditions necessary to transfer the analyte zones from the separation capillary into the ESI. The change of the electrosprayed sample concentration relative to its concentration inside the CE capillary can be estimated based on the comparison of the volumetric rate of electromigration inside the separation capillary and the hydrodynamic flow rate in the ESI capillary (note that due to different electrolyte compositions inside the capillary and in the liquid junction the corresponding electromigration rates may be different). The volume rate of electromigration Q_E in the separation capillary can be expressed as

$$Q_E = uE\pi r^2 = l/t\pi r^2 \quad (4)$$

where r is the radius of the separation capillary, l its length, and t the migration time. Based on the separation shown in Fig. 3 the rate of electromigration (ion movement, no bulk flow) was in the range of 150–360 nL/min. Providing that all the sample ions entered the ESI capillary, their ESI concentration (ESI tip flow rate, ~140 nL/min) was higher than during the separation. Thus, the liquid junction can also be viewed as a sample preconcentration device. Note that an increase in the sample concentration depends on the mobility of the sample ions and concentrations of the BGE and spray liquid and may not always be achieved. However, the fact that the sample ions are electrosprayed in a spray liquid optimized for the ESI instead of the separation buffer may be of much higher practical importance than the small concentration changes occurring during the ion transfer.

Jana Křenková[1,2]
Zuzana Bilková[2]
František Foret[1]

[1]Institute of Analytical Chemistry, Czech Academy of Sciences, Brno, Czech Republic
[2]Department of Analytical Chemistry, Faculty of Chemical Technology, University of Pardubice, Pardubice, Czech Republic

Characterization of a monolithic immobilized trypsin microreactor with on-line coupling to ESI-MS

The preparation and characterization of a miniaturized trypsin reactor using on-line coupling with an ESI-TOF mass spectrometer are described. L-1-Tosylamido-2-phenylethyl chloromethyl ketone-trypsin was covalently immobilized on poly(glycidyl methacrylate-*co*-ethylene dimethacrylate) monolith prepared in a 75 μm ID fused silica capillary resulting in a bioreactor with high local concentration of the proteolytic enzyme. Covalent immobilization of trypsin on this support was performed using the epoxide functional groups in either a one- or a multistep reaction. For on-line protein digestion-MS analysis the bioreactor was coupled with the mass spectrometer using a liquid junction microelectrospray interface. The performance of the reactor was tested using an on-line flow through the system with flow rates of 50–300 nL/min. The resulting protein consumption was in the atto- to low femtomole range. Proteolytic activity was characterized in a wide range of conditions with respect to the flow rate, pH, and temperature. Complete protein digestion was achieved in less than 30 s at 25°C with the sequence coverage of 80% (cytochrome c), which is comparable to 3 h digestion in solution at 37°C. Besides the good performance at laboratory temperature, the immobilized trypsin in the bioreactor also performed well at lower pH compared to the standard in-solution protocols.

Key Words: Immobilized enzymatic reactor; Immobilized trypsin; Mass spectrometry; Monolithic column

Received: April 14, 2005; revised: May 2, 2005; accepted: May 4, 2005

DOI 10.1002/jssc.200500171

1 Introduction

Immobilization of the proteins on surfaces or sorbent materials eliminates some of the disadvantages of the homogenous solution chemistries. High sensitivity enzyme linked immunoassays (ELISA), which belong to the most useful tools in clinical laboratories, may serve as the best example. With the advances in genomics and proteomics the bead (packing) materials with immobilized oligonucleotides, proteins, and enzymes for the sample preparation, enrichment, and digestion became widely adopted and are commercially available. The preparation of the immobilized enzymatic reactors (IMERs) inside capillaries or channels of the microfluidic devices represents another step in the development of the miniaturized systems for rapid analyses of very small sample sizes.

The significant part of the IMER applications is aimed at protein analysis by peptide mapping [1]. This technique is performed using enzymatic cleavage of the protein, and the peptide fragments in the resulting mixture are identified using ESI-MS or MALDI-MS [2]. Traditionally, enzymatic cleavage is performed in a homogeneous solution consisting of a mixture of the proteolytic enzyme and the protein of interest. This technique has several disadvantages, *e.g.*, long incubation time (3–24 h). The time of digestion can be reduced using a high concentration of the free enzyme; however, the enzymes in high concentration often lose their specificity and the enzyme autodigestion results in undesirable formation of additional peptides, which may lead to the ionization suppression in the MS analysis and complicate the interpretation of the data [3]. Immobilizing the enzyme on a porous support eliminates unwanted autodigestion and provides extremely high concentration of the proteolytic enzyme for rapid catalytic turnover. Works dealing with immobilization of trypsin can be traced back to the late 1970s [4].

A variety of methods are available for the trypsin immobilization including physical adsorption, biospecific adsorption, enzyme encapsulation using sol-gel technologies, or covalent binding minimizing of the leakage of the immobilized enzyme [1].

Some of the early reported microreactors were based on enzyme immobilization directly onto the surface of a fused

Correspondence: Dr. František Foret, Institute of Analytical Chemistry, Czech Academy of Sciences, Veveří 97, 611 42 Brno, Czech Republic. Fax: +420-532290242.
E-mail: foret@iach.cz.

Abbreviations: AIBN, 2,2′-azobisisobutyronitrile; **EDMA**, ethylene dimethacrylate; **GMA**, glycidyl methacrylate; **IMER**, immobilized enzymatic reactor; **TPCK**, L-1-tosylamido-2-phenylethyl chloromethyl ketone

Original Paper

silica capillary [5–10]. Since relatively large bore (50 μm ID) capillaries were used, a very low flow rate was required to allow sufficient time for diffusion of the protein sample to the capillary wall with the immobilized enzyme. Problems related to long diffusion times and rather low surface-to-volume ratio of the open-tubular IMER can be eliminated by packing the column or capillary with porous or nonporous particles [11–14].

In recent years, monolithic phases have emerged as an attractive and increasingly more popular alternative to packed columns due to simplicity of preparation as well as virtually unlimited choice of chemistries for the surface modification [15–19]. Several research groups have described enzyme reactors coupled to HPLC [13, 20] or CE [6–8, 21]. Recent applications include digestion of the proteins separated using HPLC [14] or 2-D PAGE [22]. Capillary or microfabricated IMERs can be directly combined on-line with ESI-MS [16, 23] or off-line with MALDI-MS [10, 15, 16, 24].

In this work, enzymatic reactors based on macroporous poly(glycidyl methacrylate-*co*-ethylene dimethacrylate) (GMA – glycidyl methacrylate; EDMA – ethylene dimethacrylate) monolith have been prepared with covalent coupling of L-1-tosylamido-2-phenylethyl chloromethyl ketone (TPCK)-trypsin using two different immobilization techniques. The effect of operational parameters such as flow rate, pH, or temperature on the enzymatic activity was studied using both off-line and on-line couplings of the reactors with ESI-MS for protein identification by peptide mapping.

2 Experimental

2.1 Chemicals and materials

Fused silica capillary (75 μm ID, 360 μm OD), with a polyimide outer coating, was purchased from Polymicro Technologies (Phoenix, AZ, USA). TPCK treated trypsin (EC 3.4.21.4) from bovine pancreas, cytochrome c (bovine), benzamidine hydrochloride, vinyltrimethoxysilane, and 2,2′-azobisisobutyronitrile (AIBN) were obtained from Sigma (St. Louis, MO, USA). GMA, EDMA, and sodium cyanoborohydride were obtained from Fluka (Buchs, Switzerland). Sodium periodate (Reanal, Budapest, Hungary) and the remaining chemicals supplied by Lachema (Neratovice, Czech Republic) were of analytical reagent grade. All buffers and solutions were filtered through 0.45 μm Millipore filters (Bedford, MA, USA) before use.

2.2 Preparation of poly(GMA-*co*-EDMA) monolithic column

Poly(GMA-*co*-EDMA) monolithic column was prepared in a 75 μm ID fused silica capillary. The internal surface of the capillary was first treated with vinyltrimethoxysilane to enable covalent attachment of the monolith to the wall [25]. The capillary (30 cm long) was first flushed with a 0.5 M sodium hydroxide solution for 30 min, and then washed with water for 5 min, followed by methanol for 5 min. In the next step the capillary was rinsed for 1 h with a solution consisting of 0.36 M hydrochloric acid and 14.3% v/v methanol in vinyltrimethoxysilane. Subsequently, the capillary was purged with nitrogen for 1 h at 100°C. The polymerization mixture consisting of 24% v/v GMA, 16% v/v EDMA, 54% v/v cyclohexanol, and 1% w/v AIBN was prepared according to Petro *et al.* [18] except for substituting the 6% dodecanol by 6% *n*-octanol in this work. After ultrasonication for 10 min, polymerization mixture was introduced into the vinylized capillary. The capillary was sealed at both ends with a rubber septum, and the polymerization was allowed to proceed in a GC oven at 60°C for 20 h. Next, 2–3 cm long sections were removed from both ends of the capillary, and the column was purged with nitrogen, washed with methanol, and purged again with nitrogen to eliminate any remaining polymerization solution. The monolithic columns were stored in a dry state at 4°C before use.

2.3 Immobilization of TPCK-trypsin on poly(GMA-*co*-EDMA) monolithic column

TPCK-trypsin was immobilized on a 2.5 cm long macroporous poly(GMA-*co*-EDMA) monolithic column using two different chemistries. Before immobilization the columns were equilibrated for 10 min by washing with immobilization buffer (50 mM carbonate buffer pH 10.5 for one-step immobilization and 50 mM phosphate buffer pH 7.0 for multistep technique) containing no trypsin.

2.3.1 One-step immobilization

TPCK-trypsin was dissolved (2 mg/mL) in 50 mM carbonate buffer pH 10.5 containing 0.2 mg/mL benzamidine. The enzyme solution was pumped through the monolith at a flow rate of 150 nL/min. After 4 h, the monolith conjugated with TPCK-trypsin was washed with 50 mM carbonate buffer pH 10.5 with 1 M NaCl to eliminate nonspecific physically adsorbed enzyme. The residual epoxide groups were blocked by 1 mg/mL aspartic acid in 50 mM carbonate buffer pH 10.5 for 1 h. The immobilization process was performed at room temperature.

The amount of immobilized TPCK-trypsin on the 2.5 cm long monolithic column was determined by the UV absorbance decrease of the enzyme solution at 280 nm before and after the immobilization process. Briefly, 500 μL of a 2 mg/mL TPCK-trypsin solution was prepared in 50 mM carbonate buffer pH 10.5; 250 μL of the solution was used for immobilization and another 250 μL was used as the standard. After immobilization, the column was flushed with 5 μL of 50 mM carbonate buffer pH 10.5 with 1 M NaCl. The eluent was collected and combined with the eluent from the immobilization, and diluted to 1 mL by the

carbonate buffer. The 250 μL of enzyme solution, kept as standard, was also diluted to 1 mL, and the absorptions at 280 nm of these solutions were measured. The amount of immobilized enzyme was calculated by the difference of the amount of TPCK-trypsin before and after immobilization.

2.3.2 Multistep immobilization

The monolithic column was first flushed with water for 10 min and then filled with 0.5 M hydrochloric acid. Both ends were sealed with a piece of rubber septum and kept at room temperature for 15 h. After hydrolysis of the epoxide groups, a 0.1 M sodium periodate solution was pumped through the column for 1 h, washed with water, and equilibrated with 50 mM phosphate buffer pH 7.0. TPCK-trypsin was dissolved (1 mg/mL) in 50 mM phosphate buffer pH 7.0 containing 0.1 mg/mL benzamidine and 3 mg/mL sodium cyanoborohydride. This enzyme solution was pumped through the monolith at a flow rate of 150 nL/min for 3 h. Finally, the reactor was sequentially washed with 50 mM phosphate buffer pH 7.0, with 50 mM phosphate buffer pH 7.0, with 1 M NaCl, and again with 50 mM phosphate buffer pH 7.0.

The immobilized monolithic columns were stored in 10 mM ammonium acetate solution, pH 6.7, containing benzamidine (0.1 mg/mL) at 4°C until use.

2.4 Characterization of the enzymatic microreactor

2.4.1 Off-line mode

Cytochrome c was dissolved to a concentration of 0.1 mg/mL in 10 mM ammonium acetate solutions containing 20% v/v methanol with the pH in the range 5.0–10.0 adjusted by concentrated acetic acid or ammonia, respectively. The protein solutions were pumped through the reactor at a flow rate of 150 nL/min using a syringe pump. The digestion was performed at 25°C. The solution containing the peptide fragments was collected into a microvial containing acetic acid (final concentration ~1%). Infusion MS analysis was conducted using a nanospray prepared from a 10 μm ID (360 μm OD) fused silica capillary with a polished tip.

2.4.2 On-line mode

Cytochrome c was dissolved in 10 mM ammonium acetate solution containing 20% v/v methanol (pH 6.7) to a concentration of 0.25 mg/mL. This protein solution was pumped through the reactor using a syringe pump at various flow rates (50–300 nL/min). Using a T- union the eluent from the IMER was continually mixed with a solution consisting of 50% aqueous ACN and 1% formic acid supplied at a constant flow rate of 1.2 μL/min. Peptide fragments were analyzed using ESI-TOF MS with a flow of nitrogen curtain gas set at 1.0 L/min and nitrogen nebulizer gas set at 0.25 L/min. The digestion was performed at various temperatures (25–37°C).

2.4.3 Protein digestion with soluble TPCK-trypsin

Cytochrome c was dissolved in 10 mM ammonium acetate solution containing 20% v/v methanol (pH 5.0–10.0) to a concentration of 0.2 mg/mL. TPCK-trypsin was added at a substrate-to-enzyme ratio of 50:1 w/w, and the solution was incubated at 25°C (37°C) for 3 h (9 h). The proteolysis was stopped by pH decreasing of the protein solution by addition of acetic acid. The protein digests were analyzed using ESI-TOF MS as described in Section 2.4.1.

2.5 MS

The Mariner TOF mass spectrometer (Applied Biosystems, CA, USA) was used in all experiments. The ESI-TOF measurements were carried out in positive ion mode with a scan range of 400–2500 *m/z*. Each mass spectrum was a sum of ten scans acquired within 2 s. The list of detected ions (*m/z*) was used for protein identification by the MS-Fit peptide mass fingerprinting tool of Protein Prospector protein digestion database (http://prospector.ucsf.edu).

3 Results and discussion

For the potential use as a component of an integrated microfluidic system it is important to know the stability and performance of the microreactors under different operational conditions. In this study we have tested the performance under different pH, flow rates, and temperatures using cytochrome c as a model protein without any modification (reduction or alkylation). Except for the temperature study all the digestion experiments were performed at 25°C.

From the variety of methods available for coupling of proteins onto the surfaces [1], we have decided to test two protocols for covalent binding, which eliminate any leakage of the immobilized enzyme. Both the immobilization protocols, described in Section 2, rely on the epoxide group present in the GMA. The epoxide functionalities can react directly with the amino groups of the protein molecule. While at neutral pH the reaction is slow and the binding can take several days [26], it is much faster at pH above 9 [27]. In this work we have allowed the reaction to proceed for several hours. Because the reaction of carboxylic functionalities with epoxides is not very efficient [28], we have attempted to mask the epoxide groups with amino groups of aspartic acid to increase the hydrophilic character of the pore surface. Another approach involves quenching the remaining reactive groups with ethanolamine [15]. Under the described conditions the amount of immobilized trypsin on the 2.5 cm long monolithic column

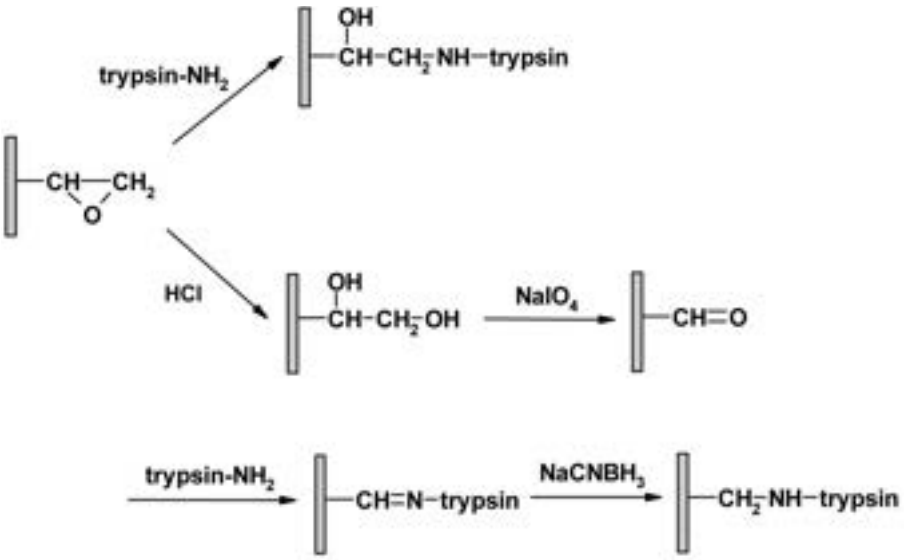

Figure 1. Scheme of the trypsin immobilization on the poly(GMA-*co*-EDMA) monolithic column.

was found to be approximately 35 μg, as determined by the UV spectrometric method.

For comparison we have also decided to test the enzyme reactor prepared by a multistep binding procedure. One of the most popular multistep immobilization techniques utilizing the epoxide group involves the modification of epoxide group with a diamine followed by activation using a glutaraldehyde [18, 19]. The disadvantage of this immobilization reaction is a potential for production of undesirable by-products, *e.g.*, homoconjugates and various polymers [27]. Thus, we have decided to test a different multistep binding procedure involving hydrolysis of epoxide groups using hydrochloric acid. During the work progress we have noted that sulfuric acid is also recommended for the reaction [29]. The hydrolysis was followed by oxidation of hydroxide groups and reaction with TPCK-trypsin molecule. To suppress the reversibility of the formed Schiff base and stabilize the bond with the enzyme, the immobilization was performed in the presence of a reducing agent, sodium cyanoborohydride. Both the procedures of TPCK-trypsin immobilization on the monolithic column are shown in Fig. 1. During the pilot experiments with both immobilization chemistries we have not observed any significant difference in the enzymatic activity or stability of the prepared reactors. Thus, the simpler one-step immobilization technique was applied for the preparation of the reactors used in this study.

The immobilization of trypsin was performed in the presence of benzamidine, a competitive inhibitor of trypsin, eliminating the binding *via* amino acids in the active center of the enzyme and stabilizing its tertiary structure. Further positive factor of immobilization in the presence of a competitive inhibitor is prevention of the undesirable autodigestion of the enzyme in solution during the immobilization process. The prepared reactors were stored at 4°C when not in use.

The poly(GMA-*co*-EDMA) monolithic column is relatively hydrophobic. Despite the elimination of the epoxide groups during the immobilization processes, we have still noted adsorption of the proteins and peptides causing losses of material during the first experiments. After testing several additives, including ACN and Triton X-100, we have found that addition of 20% methanol eliminates the nonspecific adsorption. Therefore, 10 mM ammonium acetate solution containing 20% of methanol was used as the digestion solution. Trypsin does not lose activity under these conditions, and this solution is also well suited for the consecutive ESI-MS analysis.

3.1 The effect of the pH

Buffer conditions, such as the composition and pH, are critical parameters influencing the trypsin activity in solution. For testing the pH influence on the reactor activity a 0.1 mg/mL cytochrome c solution was prepared in 10 mM ammonium acetate solutions containing 20% methanol as the carrier electrolyte. The pH was adjusted to 5.0, 6.0, 6.7, 8.5, and 10.0, and the flow rate of 150 nL/min was kept constant during the digestion. The collected digest was analyzed by MS in positive ion mode after addition of acetic acid. For simplicity the trypsin activities summarized in Table 1 were divided into three categories based on the appearance of protein and peptide peaks in the mass spectra. At pH 5.0 and 6.0 the enzymatic activity of immobilized trypsin was not detected; only the spectrum of the undigested protein was recorded. At the selected flow rate significant activity could be recorded only at pH > 6. Slightly increasing sequence coverages (79, 82, and 85%) were observed at pH 6.7, 8.5, and 10.0, respec-

Table 1. Trypsin activity at different pH

pH	IMER-trypsin[a)]	Soluble trypsin,[b)] 3 h	Soluble trypsin,[b)] 9 h
5.0	–	–	–
6.0	–	–	–
6.7	+	–	+
8.5	++	+	++
10.0	++	+	+

a) Cytochrome c (0.1 mg/mL); flow rate, 0.15 μL/min.
b) Trypsin/cytochrome c ratio 1:50 w/w, 0.2 mg/mL cytochrome c.
Digestion conditions: cytochrome c solution in 10 mM ammonium acetate/MeOH (80:20, v/v); temperature, 25°C; (–) no activity (only protein envelope); (**+**) peptide fragments, protein envelope; (**++**) only peptide fragments.

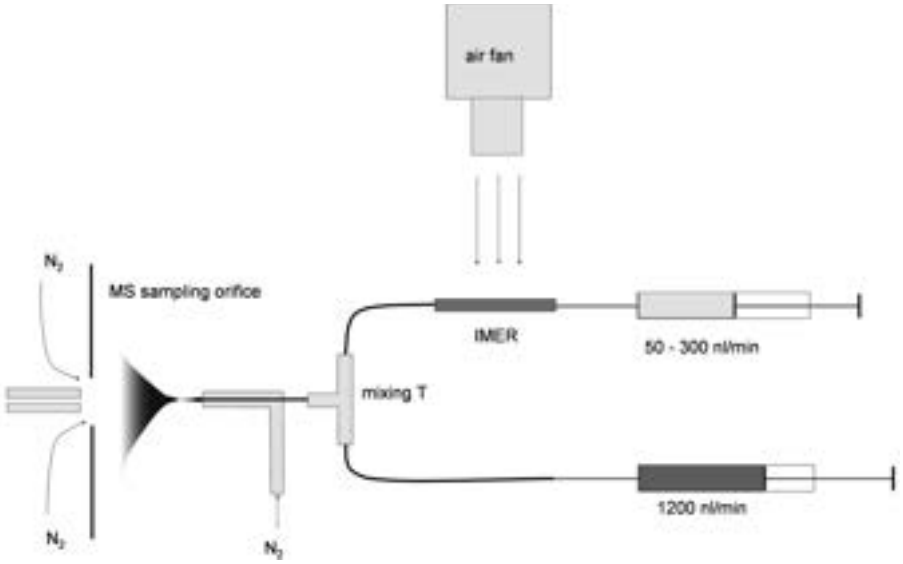

Figure 2. Experimental setup for the continuous monitoring of the IMER efficiency.

tively. For comparison a 3 h solution digestion with soluble trypsin was also performed. Practically on activity was detected under neutral pH at 25°C. Good digestion with the sequence coverage (78%) similar to that of the IMER was obtained in free solution only after extended digestion time (9 h) or increased digestion temperature to 37°C.

3.2 Time of the digestion

Another important factor influencing the extent of protein digestion inside the reactor is the protein residence time and its concentration. As expected, by increasing the flow rate, lower digestion yields were obtained due to a reduced contact time between the substrate and enzyme. For quantitative study the cytochrome c solutions (0.25 mg/mL) were introduced into the microreactor at various flow rates of 50–300 nL/min. The corresponding digestion times inside the reactor were between 10 and 60 s. These experiments were performed in the on-line arrangement with the continuous monitoring of the ESI-MS spectra. During the first experiments a simple experimental setup with a 10 μm ESI capillary was tested; however, the resulting signal was strongly influenced by the flow rate. Thus, we have assembled a system shown schematically in Fig. 2. In this arrangement the protein solution was pumped through the IMER at selected flow rates (50–300 nL), and the digestion products were mixed in a T-joint with a constant flow rate (1.2 μL/min) of the spray solution (50% aqueous ACN, 1% formic acid) supplied by the second syringe pump. The resulting stream was analyzed with the microspray interface supplied with the MS instrument. The absence of the protein envelope in the mass spectra implied near-complete protein digestion. Assuming the porosity of the monolith being 60% (based on the amount of the porogen used during the preparation) the minimum reaction time required for complete digestion of the sample protein at pH 6.7 in the 2.5 cm long reactor was less than 30 s. Examples of the MS spectra obtained at 100 and 150 nL/min are shown in Fig. 3. While at 100 nL/min (residence time 30 s) the digestion is practically complete, the appearance of the protein envelope indicates insufficient reaction time at 150 nL/min. The corresponding times can be decreased (higher flow rates) by increasing the pH as discussed in Section 3.1.

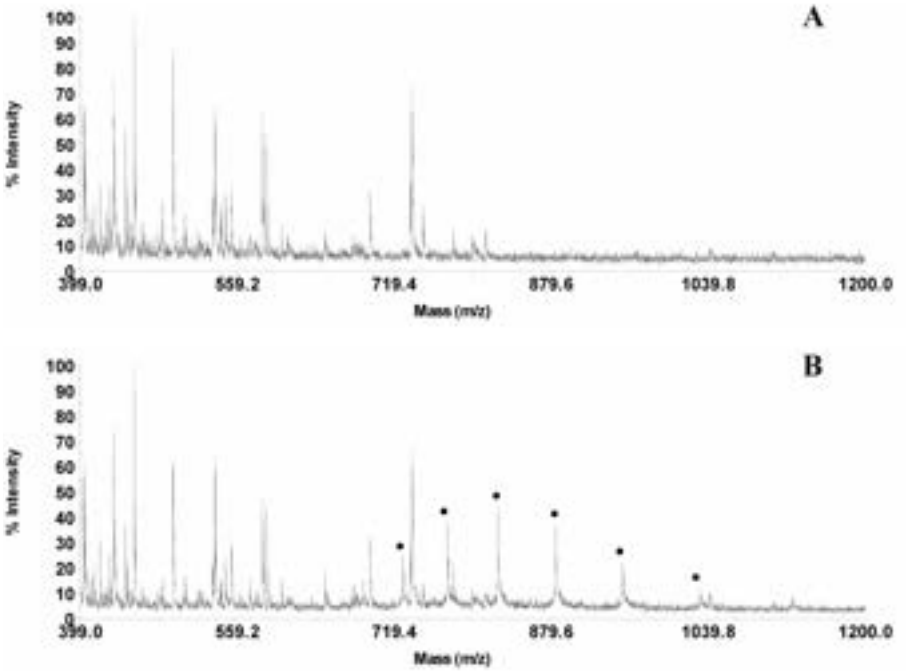

Figure 3. IMER enzymatic activity at different flow rates. Digestion conditions: 0.25 mg/mL cytochrome c (in 10 mM ammonium acetate/MeOH (80:20, v/v), pH 6.7; A – 100 nL/min (digestion time ~ 30 s), 25°C; B – 150 nL/min (digestion time ~ 20 s), 25°C; • indicates protein envelope.

Table 2. Comparison of the cytochrome c digestion using immobilized and soluble trypsin

	IMER			Soluble[a)]
	Off-line mode	On-line mode		
	25°C	25°C	37°C	37°C
Sequence coverage	79%	70%	83%	78%
	82/104 AA	73/104 AA	87/104 AA	81/104 AA
Missed cleavage	1.0	1.2	1.4	0.7
Reaction time	30 s	30 s	20 s	3 h

a) Enzyme/protein ratio 1:50 w/w, digestion solution 10 mM ammonium acetate/MeOH (80:20, v/v), pH 6.7; 3 h digestion at 37°C (no activity detected at 25°C).

3.3 Temperature

Although the optimum reaction temperature for trypsin is 37°C, the proteolysis using immobilized enzyme can be performed at lower temperature. This may simplify the integration of the IMER in the integrated microfluidic systems where the work at elevated temperature may be undesirable. Alternatively, increasing the digestion temperature provides the means of increasing the reactor efficiency at higher flow rate. The effect of the temperature was studied using hot air heating as shown in Fig. 2. Since the precise temperature control of the 2.5 cm long capillary reactor would be difficult, we have used the hot air blower for gradual increase of the IMER temperature. The actual temperature was monitored by a thermometer placed next to the IMER. The protein flow rate was set at 150 nL/min during this experiment, and the IMER efficiency was monitored continuously as the change in the intensity of the peaks characteristic for the protein (*m/z* 884.1) and one of the corresponding peptides (*m/z* 584.9) (Fig. 4). During the 7 min temperature increase from 25 to 37°C the corresponding ion currents indicated the change in the reactor efficiency. The total ion current remained practically constant during the measurement. It can be estimated that the temperature increase of 10° provides ~50% increase in the reactor efficiency. The corresponding MS spectra obtained at the beginning of this measurement at 25°C and later at 37°C indicate the degree of digestion.

3.4 Sequence coverage

The direct coupling of IMER with MS minimizes the risk of losses and contamination during manual handling of the sample. At the same time the immobilization chemistry as well as the monolith properties could, in principle, influence the specificity of the digestion and peptide identification. Thus, the ultimate performance test of the enzymatic reactor is the comparison of the experimentally obtained

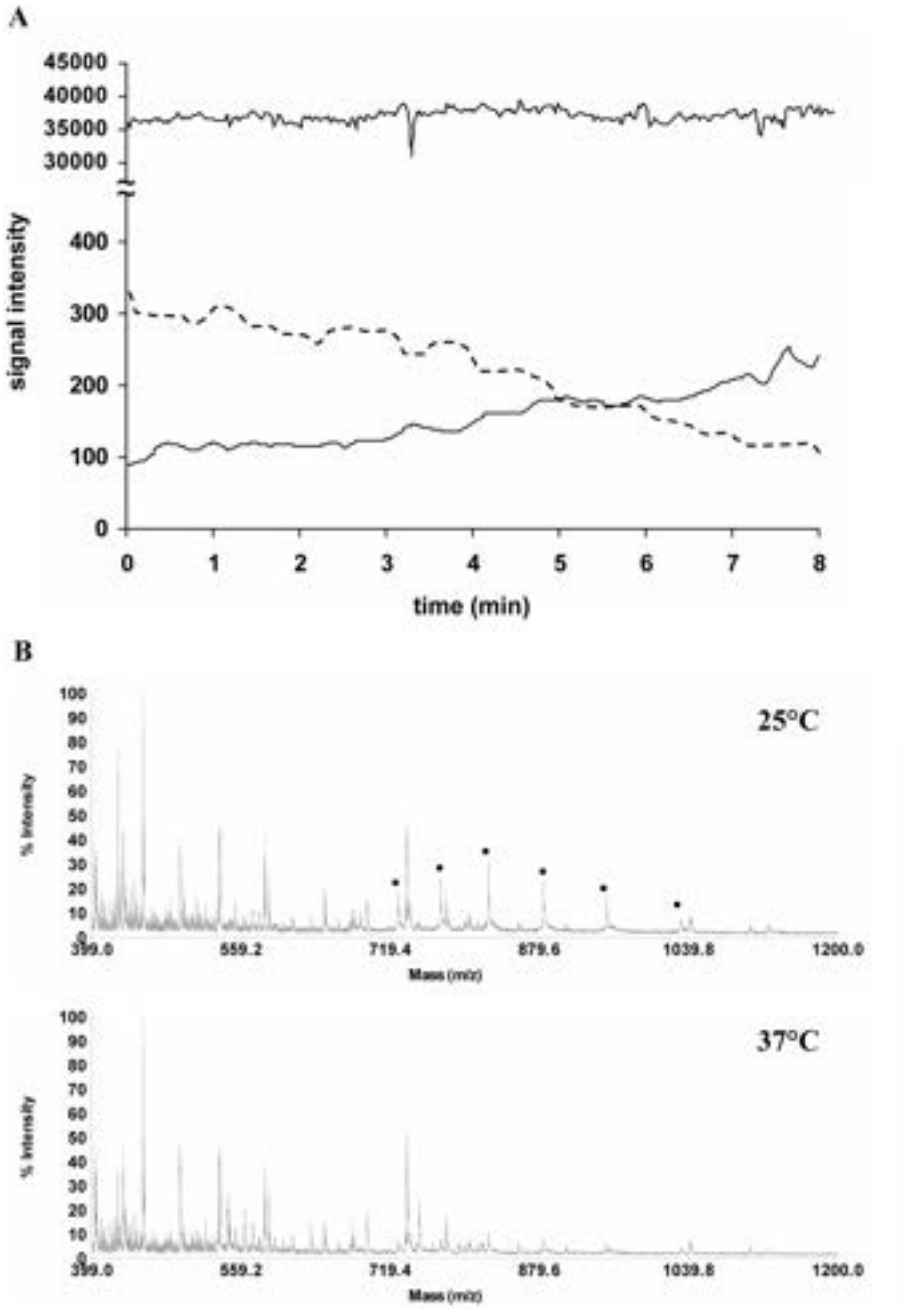

Figure 4. Temperature dependence of the protein digestion. Digestion conditions: 0.25 mg/mL cytochrome c (in 10 mM ammonium acetate/MeOH (80:20, v/v), pH 6.7; flow rate, 150 nL/min; temperature increase from 25 to 37°C in 7 min. A – The total ion current (top trace) and currents corresponding to the peptide fragment at *m/z* 584.9 and the 14+ charged protein ion at *m/z* 884.1 (dotted line). B – Typical MS scans obtained at 25 and 37°C; • indicates protein envelope.

sequence coverage using a database search, *e.g.*, using the Protein Prospector database (http://prospector.ucsf.edu). The comparison of the sequence coverage obtained with various digestion modes is summarized in Table 2. Typically, especially with short reaction time, less than 100% protein digestion efficiency is obtained with some of the peptide fragments still including cleavable amino acid sequences. The number of the missed cleavages is then averaged for all of the identified fragments. The sequence coverage obtained with the on-line protocol (70% coverage of cytochrome c sequence, missed cleavages 1.2 at 25°C, and 83% coverage, missed cleavages 1.4 at 37°C) was comparable to that obtained with IMER in the off-line protocol (79% coverage, missed cleavages 1.0 at 25°C). The typical mass spectrum obtained with the flow rate of 100 nL/min is shown in Fig. 5. Experimentally obtained molecular masses of the cytochrome c peptides are listed in the Table 3. These results are comparable with a standard digestion at 37°C – sequence coverage of 78% with an average of 0.8 missed cleavages. It is worth noting that compared with the free solution the digestion was 360 times faster with the IMER. Although one could expect decrease of the enzymatic activity due to the steric effects and nonoptimum digestion conditions

Table 3. Experimentally identified peptides from the bovine cytochrome c using the monolithic immobilized trypsin microreactor

Measured *m/z*	Peptide mass (MH^+)	Theoretical MH^+	Residues	Missed cleavages
434.1226	434.1226	434.1887	101–104	0
562.2320	562.2320	562.2837	100–104	1
634.3827	634.3827	634.3928	9–13	0
779.4077	779.4077	779.4490	80–86	0
403.6553^{+2}	806.3028	806.4776	73–79	1
454.1953^{+2}	907.3828	907.5439	80–87	1
482.6953^{+2}	964.3828	964.5355	92–99	0
546.7461^{+2}	1092.4844	1092.6305	92–100	1
584.7559^{+2}	1168.5040	1168.6227	28–38	0
432.8896^{+3}	1296.6531	1296.7177	28–39	1
436.1563^{+3}	1306.4532	1306.7007	89–99	1
653.7950^{+2}	1306.5822	1306.7007	89–99	1
478.8601^{+3}	1434.5646	1434.7957	89–100	2
717.8447^{+2}	1434.6816	1434.7957	89–100	2
717.8447^{+2}	1434.6816	1434.7957	88–99	2
478.8601^{+3}	1434.546	1434.7957	88–99	2
728.7980^{+2}	1456.5882	1456.6708	40–53	0
521.5631^{+3}	1562.6736	1562.8906	87–99	3
521.5631^{+3}	1562.6736	1562.8906	88–100	3
528.8557^{+3}	1584.5514	1584.7658	39–53	1
792.8502^{+2}	1584.6926	1584.7658	39–53	1
566.8715^{+3}	1698.5988	1698.8087	40–55	1
670.6058^{+3}	2009.8017	2009.9530	56–72	0
1005.4857^{+2}	2009.9636	2009.9530	56–72	0
713.3151^{+3}	2137.9296	2138.0480	56–73	1
1069.5444^{+2}	2138.0810	2138.0480	56–73	1

Digestion conditions: 0.25 mg/mL cytochrome c (10 mM ammonium acetate/MeOH (80:20, v/v), pH 6.7; flow rate, 100 nL/min (digestion time ~ 30 s); temperature, 25°C.

selected for the IMER operation, these effects are more than compensated by the much higher local concentration of the immobilized enzyme in the reactor (35 μg of the immobilized enzyme *vs.* 0.5 ng of the soluble enzyme present in the capillary of the same size).

4 Concluding remarks

Proteolytic activity of the IMERs was characterized in a wide range of conditions with respect to the flow rate, pH, and temperature. Complete protein digestion was achieved in less than 30 s at 25°C with the sequence coverage of 80% (cytochrome c), which is comparable to 3 h digestion in solution at 37°C. The single-step enzyme coupling chemistry tested in this work proved to be simple, reliable, and reproducible. The reactors could be used for peptide mapping with on-line coupling to the ESI-TOF MS. The use of the methanol containing digestion electrolyte did not significantly suppress the enzymatic activity and eliminated the unwanted protein and peptide adsorption on the monolithic support. The resulting protein consumption was in the attomole to low femtomole range. Besides the good performance at laboratory temperature, the immobilized trypsin in the bioreactor also performed well at lower pH compared to the standard in-solution protocols. This might be interesting for future use with separations requiring low pH environment. The preparation of miniaturized enzymatic reactors based on the monolithic supports seems to be very suitable for integration into more complex analytical systems. Based on the extended experience (tens of the reactors were prepared over the period of several months) it is also worth noting that the preparation, performance, as well as stability of the reactors are reproducible. Although our aim is the development

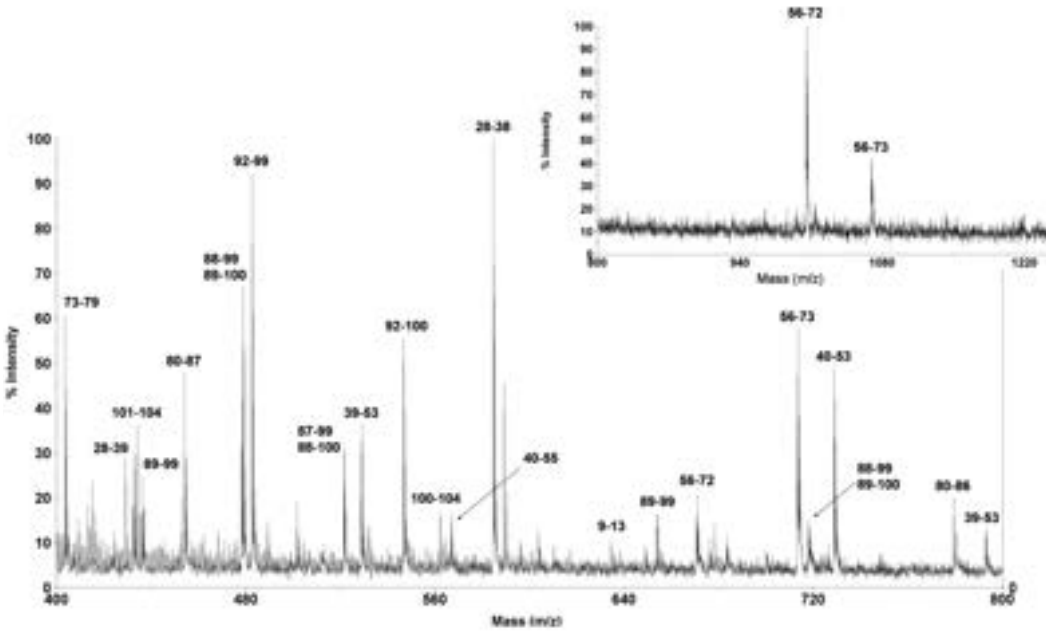

Figure 5. ESI-TOF mass spectrum obtained during the on-line tryptic digest of bovine cytochrome c. Digestion conditions: 0.25 mg/mL cytochrome c (in 10 mM ammonium acetate/MeOH (80:20, v/v), pH 6.7; flow rate, 100 nL/min (digestion time ~ 30 s); temperature, 25°C.

of inexpensive disposable devices, the reactors could be reused for several days without loss in performance.

Acknowledgments

The authors are grateful for donation of the mass spectrometer and support from the Applied Biosystems, Framingham, MA. This work was supported by the Institutional research plan Z40310501 from the Czech Academy of Sciences, grant MSM V2002/627502 and grant GAAV A 4003/0506.

5 References

[1] Krenková, J., Foret, F., *Electrophoresis* 2004, *25*, 3550–3563.

[2] Foret, F., Preisler, J., *Proteomics* 2002, *2*, 360–372.

[3] Lazar, I. M., Ramsey, R. S., Ramsey, J. M., *Anal. Chem.* 2001, *73*, 1733–1739.

[4] Turkova, J., Blaha, K., Malanikova, M., Vancurova, D., Svec, F., Kalal, J., *Biochem. Biophys. Acta* 1978, *524*, 162–169.

[5] Amankwa, L. N., Kuhr, W. G., *Anal. Chem.* 1992, *64*, 1610–1613.

[6] Amankwa, L. N., Kuhr, W. G., *Anal. Chem.* 1993, *65*, 2693–2697.

[7] Licklider, L., Kuhr, W. G., *Anal. Chem.* 1994, *66*, 4400–4407.

[8] Licklider, L., Kuhr, W. G., Lacey, M. P., Keough, T., Purdon, M. P., Takigiku, R., *Anal. Chem.* 1995, *67*, 4170–4177.

[9] Licklider, L., Kuhr, W. G., *Anal. Chem.* 1998, *70*, 1902–1908.

[10] Guo, Z., Xu, S., Lei, Z., Zou, H., Guo, B., *Electrophoresis* 2003, *24*, 3633–3639.

[11] Cobb, K. A., Novotny, M., *Anal. Chem.* 1989, *61*, 2226–2231.

[12] Wang, C., Oleschuk, R., Ouchen, F., Li, J., Thibault, P., Harrison, D. J., *Rapid Commun. Mass Spectrom.* 2000, *14*, 1377–1383.

[13] Samskog, J., Bylund, D., Jacobsson, S. P., Markides, K. E., *J. Chromatogr. A* 2003, *998*, 83–91.

[14] Slysz, G. W., Schriemer, D. C., *Anal. Chem.* 2005, *77*, 1572–1579.

[15] Peterson, D. S., Rohr, T., Svec, F., Fréchet, J. M. J., *Anal. Chem.* 2002, *74*, 4081–4088.

[16] Peterson, D. S., Rohr, T., Svec, F., Fréchet, J. M. J., *J. Proteome Res.* 2002, *1*, 563–568.

[17] Peterson, D. S., Rohr, T., Svec, F., Fréchet, J. M. J., *Anal. Chem.* 2003, *75*, 5328–5335.

[18] Petro, M., Svec, F., Fréchet, J. M. J., *Biotechnol. Bioeng.* 1996, *49*, 355–363.

[19] Ye, M., Hu, S., Schoenherr, R. M., Dovichi, N. J., *Electrophoresis* 2004, *25*, 1319–1326.

[20] Li, Y., Cooper, J. W., Lee, C. S., *J. Chromatogr. A* 2002, *979*, 241–247.

[21] Sakai-Kato, K., Kato, M., Toyo'oka, T., *Anal. Chem.* 2002, *74*, 2943–2949.

[22] Cooper, J. W., Lee, C. S., *Anal. Chem.* 2004, *76*, 2196–2202.

[23] Cooper, J. W., Chen, J., Li, Y., Lee, C. S., *Anal. Chem.* 2003, *75*, 1067–1074.

[24] Ekstrom, S., Onnerfjord, P., Nilsson, J., Bengtsson, M., Laurell, T., Marko-Varga, G., *Anal. Chem.* 2000, *72*, 286–293.

[25] Ivanov, A. R., Zang, L., Karger, B. L., *Anal. Chem.* 2003, *75*, 5306–5316.

[26] Vodopivec, M., Berovic, M., Jancar, J., Podgornik, A., Strancar, A., *Anal. Chim. Acta* 2000, *407*, 105–110.

[27] Hermanson, G. T., *Bioconjugate Techniques*, Academic Press, San Diego 1996.

[28] Drobnik, J., Vlasak, J., Pilar, J., Svec, F., Kalal, J., *Enzyme Microb. Technol.* 1979, *1*, 107–112.

[29] Svec, F., Hrudkova, H., Kalal, J., *Angew. Makromol. Chem.* 1978, *70*, 101–108.

etr Kus´
Kare K e árn k
eine turki
a vatore Fana i
František Foret

[1]Department of Bioanalytical Instrumentation, Institute of Analytical Chemistry, Academy of Sciences of the Czech Republic, Brno, Czech Republic
[2]Institute of Chemical Methodologies, National Council of Research, Rome Research Area, Monterotondo Scalo, Rome, Italy

Received October 4, 2006
Revised December 12, 2006
Accepted December 13, 2006

Research Article

ptimization of a pressurized liquid junction nanoelectrospray interface between CE and MS for reliable proteomic analysis

A pressurized liquid junction nanoelectrospray interface was designed and optimized for reliable on-line CE-MS coupling. The system was constructed as an integrated device for highly sensitive and selective analyses of proteins and peptides with the separation and spray capillaries fixed in a pressurized spray liquid reservoir equipped with the electrode for connection of the electrospray potential. The electrode chamber on the injection side of the separation capillary and the spray liquid reservoir were pneumatically connected by a Teflon tube filled with pressurized nitrogen. This arrangement provided precisely counterbalanced pressures at the inlet and outlet of the separation capillary. The pressure control system was driven by an electrically operated valve and maintained the optimum flow rate for the electrospray stability. All parts of the interface being in contact with the CEBGE, spray liquid and/or sample were made of glass or Teflon. The use of these materials minimized the electrospray chemical noise often caused by plastic softeners or material degradation. During optimization, the transfer of the separated zones between the separation and electrospray capillaries was monitored by UV absorbance and contactless conductivity detectors placed at the outlet of the separation capillary and inlet of the electrospray tip, respectively. This arrangement allowed independent monitoring of the effects of pressure, CE voltage and geometry of the liquid junction on the spreading and dilution of the separated zones after passage through the interface.

Keywords:
CE / Liquid junction interface / MS / Nanoelectrospray
DOI 10.1002/elps.200600640

1 Introduction

The development of ESI opened up new possibilities for on-line MS coupling. Although the resolution of modern mass spectrometers reaches 10^6 (*i.e.* two molecules with mass of about 10^4 Da differing in 0.01 Da can be resolved), coupling with liquid phase separations is mostly necessary to minimize ion suppression effects [1–3]. This is especially true for very complex samples such as in proteomic analyses where the loss of sensitivity due to the ion suppression would significantly reduce the number of identifiable proteins. In such cases, the analyte separation prior to the MS analysis may significantly improve the analysis output. Identification of hundreds or thousands of proteins in complex biological mixtures requires adequate sensitivity, peak capacity and dynamic range. These reasons motivate the intensive research and development of adequate instrumentation for the on-line coupling of liquid phase separation techniques with MS in the past few years [2–5].

A number of different approaches to the development of new analytical procedures and instrumentation have recently been described [6–13]. For example, two main directions can be distinguished in proteomics. In the top-down approach, the proteins are first isolated, and then identified after enzymatic digestion and collision-induced fragmentation inside the mass spectrometer. This approach depends on the ability to separate an isolate the individual sample proteins. Although protein HPLC [9, 14, 15] can be used, 1-D or 2-D SDS-PAGE [8, 16–18] is the dominant separation technique with CE having only a marginal importance [10, 19–24].

In the newer bottom-up approach, all proteins in the mixture are digested first, the resulting peptides separated and after the MS analysis assigned to corresponding proteins by database searching. Due to the extreme complexity of

Correspondence Dr. Karel Klepárník, Department of Bioanalytical Instrumentation, Institute of Analytical Chemistry, Czech Academy of Sciences, Veveří 97, CZ-611 42 Brno, Czech Republic
E-mail klep@iach.cz
Fax +42-0-541-212-113

Abbreviation FA, formic acid

such peptide mixtures, the use of a high-resolution technique (mostly in a 2-D arrangement) is mandatory [25]. Although off-line coupling of separation techniques to MS is also frequently used [6, 20, 21, 26–28], on-line analysis is prevailing with the electrospray arrangement [9, 11, 29].

The majority of the peptide separations are currently performed in the LC mode [30–32]. The use of CE for the high-resolution separations of peptides and coupling with MS is still under development [4, 5]. Although, in principle, the electrophoretic separation in free solution provides simplicity, very high separation efficiency and speed, it has also some limitations, which have to be taken into practical consideration. For example, the need for the use of electrospray compatible buffers limits the range of suitable BGE in the sheathless ESI interfacing. This limitation can be significantly decreased with the use of the liquid junction interface [33, 34].

In this report, optimization of a nanoelectrospray liquid junction interface for on-line coupling of the CE and MS is described. The interface was designed based on theoretical analysis of working parameters, including the width of the gap between the separation and spray capillaries, flow of the pressure-driven spray liquid and electric voltages controlling the electrophoresis and electrospray, respectively. The optimization was directed to achieve the maximum concentration of the analyte transferred from the separation into the electrospray capillary and robust operation at the flow rates of the spraying liquid ranging from 2 to 50 nL/min.

2 Materials and methods

2.1 Chemicals

ACN and formic acid (FA) of analytical grade were purchased from Lachema (Neratovice, Czech Republic) and used without any further purification. All peptides, angiotensin I (human), bradykinin and neurotensin, as well as cytochrome C (horse heart) were supplied by Sigma (St. Louis, MO, USA). All buffer solutions were filtered through disposable filter with 0.2-μm membranes purchased from Macherey-Nagel (D ren, Germany) and degassed by sonication.

2.2 Instrumentation

2.2.1 Interface setup

In this work, we have expanded on the experience with the previously described CE-ESI interfaces based on the liquid junction [34–36]. The CE system including electrode chambers and separation capillary was integrated with the body of the pressurized liquid junction interface. The scheme of the interface together with the electrical connection is depicted in Fig. 1. To avoid contamination with the commonly used plastic softeners, all parts in contact with the sample, CE

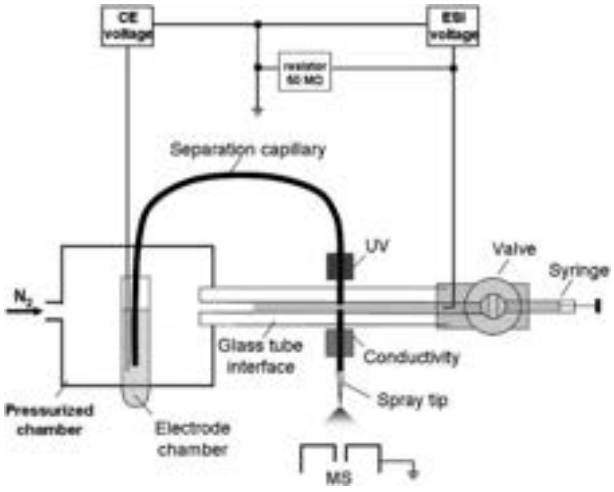

Figure 1. Scheme of the CE-ESI interface. For details, see Section 2.2.1.

BGE and spray liquid were made of glass or Teflon. The separation and spray capillaries were aligned axially and fixed in holes drilled perpendicularly through the walls of horizontally placed glass tubing (id 1 mm, od 8 mm). This glass tube formed the pressurized spray liquid reservoir. The photograph of the whole device is given in Fig. 2. The diameter of the holes (0.365 mm) fits the od of both the separation and spray capillaries (see the inset in Fig. 2). These capillaries were sealed on the outside wall of the glass tubing by silicon rubber gaskets inserted in a Plexiglass ring and compressed by hollow screws. The width of the gap between the capillaries could be approximately set under a microscope by comparing with their known diameters. Prior to analyses, the level of the spray liquid was adjusted by a Hamilton syringe (Hamilton, Bonaduz, Switzerland) connected *via* Luer lock to a Hamilton valve. The valve separating the syringe and the reservoir was closed whenever the nitrogen pressure was applied. The spray voltage was connected by a platinum electrode inserted into the spray liquid through the hole drilled in the Teflon body connecting the glass reservoir and the Hamilton valve. The CE electrode chamber was fixed to the opposite side of the glass tubing reservoir by a short Teflon channel furnished with the inlet fitting for the connection of pressurized nitrogen. Thus, the pressure was perfectly counterbalanced at the sealed inlet and outlet of the separation capillary. The precise laboratory constructed nitrogen pressure system, based on the compact electropneumatic regulator ITV 0050-3N- (SMC, Tokyo, apan), was used to control the flow of the spray liquid. The pressure could be set in the range from 10 to 250 kPa and was applied 1 min after the start of the CE separation. Electrode chamber was filled with the separation electrolyte consisting of 1% aqueous solution of FA, while the glass tubing was filled with 50% solution of ACN in 1% FA acting as the spray liquid. All parts of the interface were compressed by a C-clamp to avoid

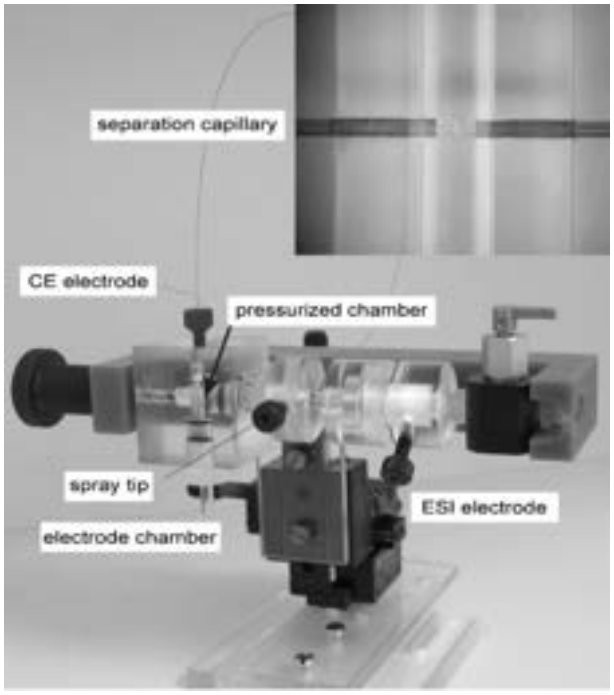

Figure 2. Photograph of the CE/ESI assembly. The inset shows the detail of the liquid junction gap (75 μm) between the separation and electrospray capillaries.

any leakage of gas or liquid. The whole CE/ESI system was attached to a *xyz*-stage, enabling precise positioning of the spray tip in front of the mass spectrometer sampling orifice.

2.2.2 Sample injection and detection

Samples were injected by electromigration at 10 kV for 10 s. To inject the sample, the inlet end of the separation capillary together with the electrode and rubber sealing were removed manually from the electrode chamber and inserted into the precisely leveled sample vial. Mixture of three peptides (angiotensin I, bradykinin, neurotensin) dissolved in distilled water at a concentration of 10 μM was used for the initial experiments. Signals of separated zones were monitored 12 cm before the outlet of the separation capillary by a UV detector at 210 nm (Spectra 100, Thermo Separation Products, USA) and 4 cm past the liquid junction in the electrospray capillary by a contactless conductivity detector (TraceDec, Strasshof, Austria). The signal from both detectors was acquired by an A/D converter and stored in a personal computer (CSW, Data Apex, Prague, Czech Republic).

During the experiments with the UV and conductivity detectors, the separation voltage of 10 kV was used for the CE separation (Spellman CZE 1000 R, Spellman, Valhalla, NY), while the spray electrode was grounded. The experiments with MS detection were performed at the same voltage on the separation capillary with the positive spray voltage set to 2.5 kV using a laboratory-constructed power source. Since the ESI power supply could not drain typical CE currents (2–20 μA), a 50-MΩ resistor was connected between the spray electrode and the ground (see the scheme in Fig. 1). In this way, both the separation and ESI voltages could be adjusted independently.

The developed CE-MS system was coupled to an orthogonal TOF mass spectrometer (Mariner, Applied Biosystems, Framingham, MA) working at potentials of 100 V -nozzle, 10 V - skimmer, 4000 V - acceleration and 1550 V - reflectron. The data acquisition time was 2 s per spectrum. The spray tip was positioned axially 5 mm from the MS orifice kept at 130°C. No drying gas was needed at the ESI flow rates used in this study.

2.2.3 Separation and spray capillaries

Coated capillaries, Guarant (Alcor Bioseparations, Santa Clara, CA), 50 cm long, with 375 μm od and 50 μm id were used for the CE separations. The electrospray tip was made of a 9 cm long uncoated capillary with 375 μm od and 10 μm id obtained from Polymicro Technologies (Phoenix, AZ). The tip was sharpened by a laboratory sharpener/polisher where the capillary, rotating around its axe, contacted under an angle of 45° a motor-driven rotating disk of fine abrasive paper. The tips were finally polished the same way using a fiber-optic polishing foil instead of the abrasive paper.

3 Results and discussion

Implementation of the liquid junction interface for the CE/MS coupling offers relatively simple means for independent optimization of the CE and electrospray with respect to both geometry and working parameters. Based on the previous studies [35, 33] and our recent experience with CE/MS applications [34] we have selected a pressurized device capable to work with a nanospray needle at flow rates of tens of nL/min. The most important feature of the interface is the ability to transfer analytes from the separation column into the spray tip in such a way that the concentration profiles of zones are not changed significantly, *i.e.* the dispersion and dilution of zones is minimized. It is evident that the width of the gap between the capillaries, pressure and electric field strength affect this transfer.

Although one can estimate the theoretical features of a given fluidic arrangement, direct measurement of the zone concentration profiles at different points of the system will provide the most useful data. For example, the optimization of the liquid junction operational parameters can be greatly improved by independent detection of the concentration profiles in the separation and electrospray capillaries before and past the liquid junction. In such a way, the net contribution of the interface to the total dispersion can directly be revealed by the subtraction of any disturbances in the separation capillary. For meaningful results, one should per-

form the measurements as close to the liquid junction as possible. In our previous work, we have employed optical fibers to bring the UV detection window as close to the liquid junction as possible [33]. While the UV absorbance detection can easily be performed in the 75-μm id separation capillary it is practically impossible to implement it on the 10-μm electrospray capillary. Since the conductivity response is not directly proportional to the capillary diameter, we have used the newly introduced [37, 38] contactless conductivity detector located at the entrance of the spray capillary to monitor the movement of the zones through the interface. The use of the mass spectrometer itself as the detector is not suitable for the pressure optimization, since the electrospray stability depends on the flow rate of the spray liquid. The signals of angiotensin I, bradykinin and neurotensin, registered by both the UV and conductivity detectors are compared in Fig. 3. The upper record shows the separation of the analytes in 50-cm long capillary at 10 kV, while the lower record monitored the zone passage through the 75-μm wide gap in the liquid junction. It is evident from the Figure that the resolution of zones is not affected, but there is a uniform shift in the separation time of individual peptides through the UV and conductivity detector. In this experiment, the pressure as low as 40 kPa induced the flow of about 2 mm/s (about 45 s of residence time) in the 9-cm long spray capillary. Consequently, this time shift was not caused only by a delay in the interface, but mainly due to the electromigration through the distance of 12 cm between the detection window and the separation capillary outlet. The preserved resolution of the separated zones detected by the conductivity detector indicated suitable working conditions.

The effect of the gap width on the resolution of the separated zones of the three model peptides is shown in Fig. 4. Here, the records of zones registered by the conductivity detector after their passage through the gaps of widths of 40, 75, 400 and 700 μm are compared. The optimum applied

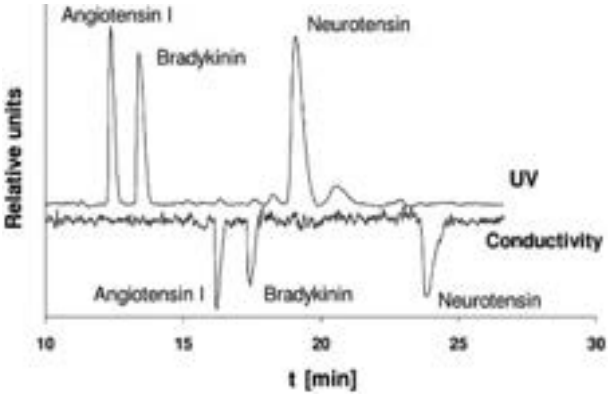

Figure 3. CE separation of angiotensin I, bradykinin and neurotensin. Upper record absorbance detection in the CE separation capillary (210 nm). Lower record conductivity detection in the electrospray capillary. CE voltage, 10 kV; capillary, 75 μm id, 365 μm od; injection, 10 s at 10 kV; pressure, 40 kPa; gap width 75 μm.

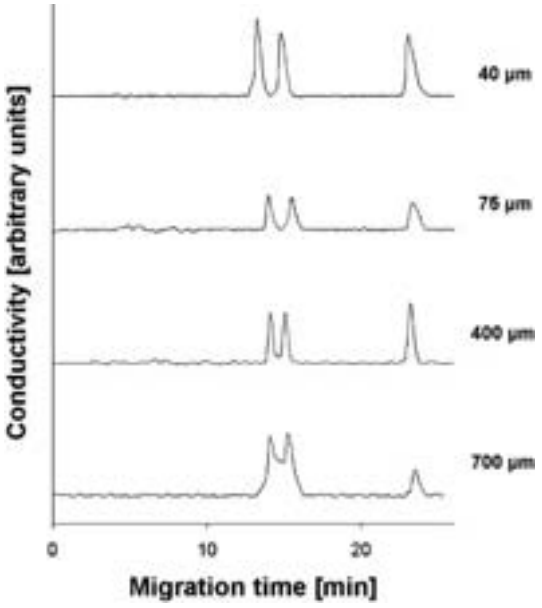

Figure 4. Separation resolution in the ESI capillary with the liquid junction gap of 40, 75, 400 and 700 μm. Records of conductivity detector. Pressure 100 kPa. Other conditions are the same as in Fig. 3.

pressure with respect to the spray was 100 kPa and other working conditions were identical to those in Fig. 3. The deterioration of the resolution was obvious for the gap widths wider than 400 μm. This phenomenon can be explained by the higher dispersion of zones leaving the separation capillary into the broad gap. If the electromigration of a zone in the electric field between the capillaries is not fast enough, an analyte does not fill the gap completely. Then, only the slower part of the hydrodynamic flow at the separation capillary outlet will transfer it into the spray capillary as a narrow filament confined in the outer flow of a pure liquid. This behavior is the reason of the zone dispersion and coincident dilution. The wider the gap, the weaker the electric field between the capillaries and the larger the volume of the spray liquid carrying no analyte. Thus, the gap width should be about 100 μm, which is easily achievable in practice. On the other hand, too narrow gap could cause a pressure drop, resulting in the excessive hydrodynamic flow inside the separation capillary.

It is interesting to note that an increased convective transport at an elevated pressure, can improve the analyte transport only partially. By increasing the pressure and flow rate through the spray capillary the convection is faster, but also the dilution of zones increases. The effect of pressure on the resolution is demonstrated in Fig. 5. The respective change is expressed here as the ratio of resolutions evaluated before and after the gap. The fact that the ratio is lower than 1 can be explained by the position of UV detector window 12 cm before the gap. Thus, in fact, the resolution at the end of the separation capillary was better than evaluated from the

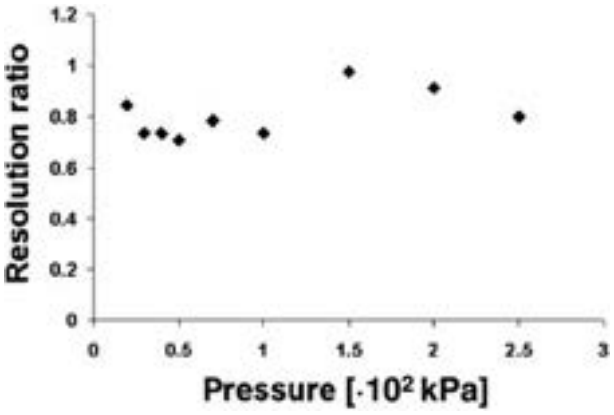

Figure 5. Dependence of the resolution ratio (resolution in the separation capillary/resolution in the electrospray capillary) on the applied pressure. Liquid junction gap, 75 μm. Other conditions are the same as in Fig. 4.

UV detector signal. In principle, the ratio must be higher than 1. Regardless of this, the dependence in Fig. 5 shows a little effect of the pressure in the range from 10 to 250 kPa on the dispersion of zones in the interface with the 75-μm gap at the given experimental conditions. Similarly, an increase in the electric field strength in the separation capillary did not bring any significant improvement in resolution or dilution of the separated zones after the passage through the interface (data not shown).

Based on these experiments, the CE-ESI-MS system was further operated with the gap of 75 μm, the electric field strength of 200 V/cm, spray voltage of 2.5 kV and pressure of 100 kPa. Figures 6 and 7 show the records of the total ion currents (TICs) of the separation of the calibration peptides (angiotensin I, bradykinin, neurotensin) and of a tryptic

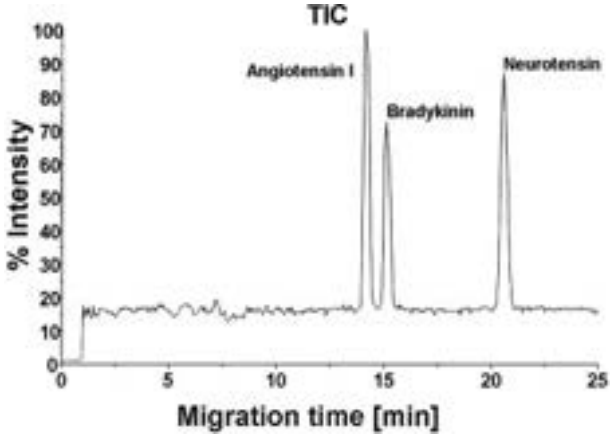

Figure . CE nanoESI MS analysis of a mixture of angiotensin I, bradykinin and neurotensin; 10^{-5} M each in distilled water. CE separation at 10 kV, (~ 40 μA) in 1% aqueous formic acid; capillary, 75 μm id, 365 μm od; 50 cm long; injection, 10 s at 10 kV; electrospray voltage, 2.5 kV; spray liquid, 1% formic acid in water, pressure, 100 kPa; liquid junction gap width, 75 μm.

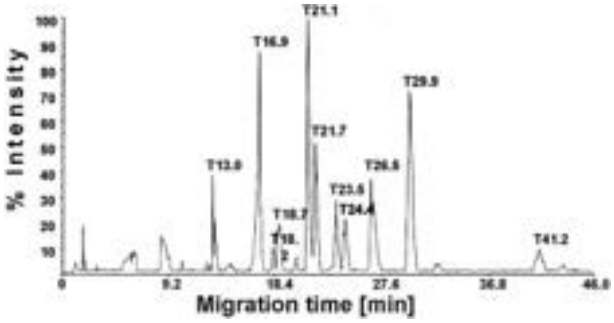

Figure . CE nanoESI MS analysis of a cytochrome C digest. Electrokinetic injection, 15 s at 10 kV. Other separation and detection conditions as in Fig. 6.

digest of cytochrome C. The peptides identified by the Protein Prospector MS Fit database (http://prospector.ucsf.edu) are listed in Table 1. It is important to note that both analyses were performed with the solution of 1% v/v FA serving as both the BGE for the CE separation and the spray liquid. Although no organic solvent was added to the spray liquid, the detection sensitivity was very good with the concentration detection limit in the 10^{-8} M range. The prerequisite of efficient spraying of purely aqueous solutions is the use of the nanospray capillary with id of 10 μm or less operating at the flow rate of 100 nL/min or less. In such a case, the spray tip can be positioned very close to the MS sampling orifice without the need for the use of drying gas.

Table 1. Identification of the peptides separated in Fig. 7

Time (min)	*m z*	Sequence
13.0	533.3314	KTER
16.9	403.7660^{+2}	KYIPGTK
18.2	405.2456	TER
18.7	454.3063^{+2}	MIFAGIKK
18.7	493.6573^{+3}	KTEREDLIAYLK
18.7	493.6573^{+3}	TEREDLIAYLKK
21.1	584.8348^{+2}	TGPNLHGLFGR
21.7	562.3085	KATNE
21.7	604.3788	GITWK
21.7	584.8639^{+2}	TGPNLHGLFGR
23.5	634.4261	IFV K
24.4	678.4280	YIPGTK
26.5	779.4936	MIFAGIK
26.5	799.9412^{+2}	KTG APGFTYTDANK
41.2	735.9133^{+2}	TG APGFTYTDANK

4 Concluding remarks

The system integrating CE separation with nanoelectrospray MS identification (Figs. 1 and 2) was optimized for the separation of peptides. However, it can be used for analysis of

any ions electromigrating under the experimental conditions. The most important working parameters of the interface with respect to an effective analyte transfer from the separation capillary into the spray tip are the interface geometry, separation voltage and pressure. The use of dual UV and conductivity detectors allowed independent experimental optimization of the system (Fig. 3). It is demonstrated that the crucial parameter of the interface is the gap width between the separation and spray capillaries. As a result of this study, the optimum was determined not to exceed the range of 50–200 μm (Fig. 4). Pressure is not an independent parameter for optimization since it influences both the electrospray stability and the mass transport in the liquid junction. Electric field strength in the separation capillary is an important parameter. It determines the electric field in the gap and is responsible for the transport of analytes into the fast moving regions of the spray liquid. With a gap width of 75 μm and at a pressure of 100 kPa at the inlet of a 10-μm id spray tip, the electric field strength of 200 V/cm was selected for minimum dispersion and dilution of separated zones (Fig. 6). The main advantage of the application of nanospray tip is the high ionization effectivity even when no organic additives are used in the electrosprayed liquid. Further reduction of the spray tip (*e.g.* down to 1 μm id) and the body of the interface to the dimensions of a microfluidic device is expected to bring additional improvement in performance.

The authors wish to thank the Grant Agency of the Academy of Sciences of the Czech Republic (grant A400310506), the Grant Agency of the Czech Republic (grant 203/06/1685) and the Ministry of the Education, Youth and Sports of the Czech Republic (grant LC06023). Travel support within the frame of the bilateral CNR-A CR agreement is also acknowledged.

5 References

[1] McLuckey, S. A., Wells, J. M., *Chem. Re .* 2001, *101*, 571–606.

[2] Tomer, K. B., *Chem. Re .* 2001, *101*, 297–328.

[3] Foret, F., Preisler, J., *Proteomics* 2002, *4*, 360–372.

[4] Schmitt-Kopplin, P., Englmann, M., *Electrophoresis* 2005, *26*, 1209–1220.

[5] Simpson, D. C., Smith, R. D., *Electrophoresis* 2005, *26*, 1291–1305

[6] Yu, W. J., Li, Y., Deng, C. H., Zhang, X. M., *Electrophoresis* 2006, *11*, 2100–2110.

[7] Yates, J. R., Cociorva, D., Liao, L. J., Zabrouskov, V., *Anal. Chem.* 2006, *2*, 493–500.

[8] Picariello, G., De Martino, A., Mamone, G., Ferranti, P. *et al.*, *J. Chromatogr. B* 2006, *1*, 101–108.

[9] Bergstrom, S. K., Dahlin, A. P., Ramstrom, M., Andersson, M. *et al.*, *Analyst* 2006, *7*, 791–798.

[10] Akashi, S., Suzuki, K., Arai, A., Yamada, N. *et al.*, *Rapid Comm n. Mass Spectrom.* 2006, *12*, 1932–1938.

[11] Wu, S. L., Jardine, I., Hancock, W. S., Karger, B. L., *Rapid Comm n. Mass Spectrom.* 2004, *19*, 2201–2207.

[12] Wang, Y. C., Choi, M. N., Han, J. Y., *Anal. Chem* 2004, *15*, 4426–4431.

[13] Hancock, W. S., Wu, S. L., Shieh, P., *Proteomics* 2002, *4*, 352–359.

[14] Wagner, K., Racaityte, K., Unger, K. K., Miliotis, T. *et al.*, *J. Chromatogr. A* 2000, *2*, 293–305.

[15] Wu, S. L., Kim, J., Hancock, W. S., Karger, B. L., *J. Proteome Res.* 2005, *4*, 1155–1170.

[16] Raikos, V., Hansen, R., Campbell, L., Euston, S. R., *Food Chem.* 2006, *4*, 702–710.

[17] Kitta, K., Ohnishi-Kameyama, M., Moriyama, T., Ogawa, T., Kawamoto, S., *Anal. Biochem.* 2006, *2*, 290–297.

[18] Smolka, M., Zhou, H. L., Aebersold, R., *Mol. Cell. Proteomics* 2002, *1*, 19–29.

[19] Liu, H. C., Yang, C., Yang, ., Zhang, W. B., Zhang, Y. K., *J. Chromatogr. B* 2005, *1*, 119–126.

[20] Rejtar, T., Hu, P., Juhasz, P., Campbell, J. M. *et al.*, *J. Proteome Res.* 2002, *2*, 171–179.

[21] Preisler, J., Hu, P., Rejtar, T., Moskovets, E., Karger, B. L., *Anal. Chem.* 2002, *1*, 17–25.

[22] Yeung, K. K. C., Kiceniuk, A. G., Li, L., *J. Chromatogr. A* 2001, *1–2*, 153–162.

[23] Kašička, V., *Electrophoresis* 2001, *19*, 4139–4162.

[24] Zhang, B., Liu, H., Karger, B. L., Foret, F., *Anal. Chem.* 1999, *15*, 3258–3264.

[25] Motoyama, A., Venable, J. D., Ruse, C. I., Yates III, J. R., *Anal. Chem.* 2006, *14*, 5109–5118.

[26] Wang, Y. C., Choi, M. N., Han, J. Y., *Anal. Chem.* 2004, *15*, 4426–4431.

[27] Chelius, D., Zhang, T., Wang, G. H., Shen, R. F., *Anal. Chem.* 2003, *23*, 6658–6665.

[28] Miliotis, T., Kjellstrom, S., Nilsson, J., Laurell, T. *et al.*, *J. Mass Spectrom.* 2000, *3*, 369–377.

[29] Preisler, J., Foret, F., Karger, B. L., *Anal. Chem.* 1998, *24*, 5278–5287.

[30] Aebersold, R., Mann, M., *Nat re* 2003, *422*, 198–207.

[31] Peiqing, H. P., Wall, D. B., Parus, S., Lubman, D. M., *J. Am. Soc. Mass Spectrom.* 2000, *11*, 127–135.

[32] Zhao, J., Zhu, K., Lubman, D. M., Miller, F. R. *et al.*, *Proteomics* 2006, 3847–3861.

[33] Foret, F., Zhou, H. H., Gangl, E., Karger, B. L., *Electrophoresis* 2000, *7*, 1363–1371.

[34] Fanali, S., D'Orazio, G., Foret, F., Klepárník, K., Aturki, Z., *Electrophoresis*, 2007, *28*, in press.

[35] Wachs, T., Sheppard, R. L., Henion, J., *J. Chromatogr. B* 1996, *2*, 335–342.

[36] Kelly, J. F., Ramaley, L., Thibault, P., *Anal. Chem.* 1997, *1*, 51–60.

[37] Zemann, A. J., Schnell, E., Volgger, D., Bonn, G. K., *Anal. Chem.* 1998, *3*, 563–567.

[38] Tanyanyiwa, J., Hauser, P. C., *Anal. Chem.* 2002, *24*, 6378–6382.

Available online at www.sciencedirect.com
ScienceDirect
Journal of Chromatography A, 1159 (2007) 110–118
JOURNAL OF CHROMATOGRAPHY A
www.elsevier.com/locate/chroma

Capillary electrophoresis mass spectrometry coupling with immobilized enzyme electrospray capillaries

Jana Křenková [a,b], Karel Klepárník [a], František Foret [a,*]

[a] *Institute of Analytical Chemistry, Academy of Sciences of the Czech Republic, Veveŕ 97, 602 00 Brno, Czech Republic*
[b] *Department of Analytical Chemistry, Faculty of Chemical Technology, University of Pardubice, Nám. Cs. Legiŕ 565, 532 10 Pardubice, Czech Republic*

Available online 2 March 2007

Abstract

Open tubular capillary enzyme reactors were studied for rapid protein digestion and possible on-line integration into a CE/ESI/MS system. The need to minimize the time of the analyte molecules to diffuse towards the surface immobilized enzyme and to maximize the surface-to-volume (*S*/*V*) ratio of the open tubular reactors dictated the use of very narrow bore capillaries. Extremely small protein amounts (atto-femtomoles loaded) could be digested with enzymes immobilized directly on the inside wall of a 10 μm I.D. capillary. Covalently immobilized L-1-tosylamido-2-phenylethyl chloromethyl ketone (TPCK)-trypsin and pepsin A were tested for the surface immobilization. The enzymatic activity was characterized in the flow-through mode with on-line coupling to electrospray ionization-time of flight-mass spectrometer (ESI/TOF-MS) under a range of protein concentrations, buffer pH's, temperatures and reaction times. The optimized reactors were tested as the nanospray needles for fast identification of proteins using CE-ESI/TOF-MS.

Keywords: Capillary enzyme reactor; Electrospray; Mass spectrometry; Capillary electrophoresis

1. Introduction

Current development of new analytical technologies follows the rapid advances in natural sciences, especially biology and medicine. For example proteomic research calls for new systems integrating and automating protein separation, digestion and identification. Although high resolution electrophoresis techniques followed by enzymatic digestion, liquid chromatography and mass spectrometry analysis address many of the needs in protein analysis [1], there are still numerous practical limitations waiting for improvement. Some of the common needs for increased speed and simplification of the complex sample handling of the (often very small) sample sizes relate to the proteolytic digestion of the analyzed proteins. Typically, the enzymatic digestion, performed using a soluble enzyme in a homogeneous solution, can take several hours to complete. Some of the problems of enzymatic cleavage in a homogeneous solution (speed, enzyme autolysis) can be eliminated by immobilization of the enzyme on a solid support to form an enzymatic reactor [2,3]. Additional practical advantage of immobilized enzymatic reactors is the possibility for direct coupling with separations and mass spectrometry [4–6].

Ultimately, for extremely small sample volumes, the enzymes can be immobilized directly on the wall of very narrow bore capillary. The first reported open tubular microreactors were prepared in 50 μm or 75 μm I.D. fused silica capillary [7–13] with the enzyme immobilized on the surface either by nonspecific or biospecific adsorption. Because of relatively small *S*/*V* ratio and long diffusion distances, a very low flow rate was needed to guarantee sufficient time (half an hour or more) for diffusion of the protein molecules to the immobilized enzyme. Problems related to long diffusion times and small *S*/*V* ratio of the open tubular bioreactor can be avoided by packing the capillary or channel of microfluidic chip with magnetic or non-magnetic particles [4,14–19] or using of monolithic support [20–25] that significantly increase the available surface area. Alternatively, the *S*/*V* ratio can be increased by using very narrow bore capillaries or microfluidics channels, e.g., with the inner diameter of 10 μm

Abbreviations: EDAC, 1-ethyl-3-(3-dimethylaminopropyl) carbodiimide hydrochloride; IMER, immobilized enzyme reactor; sulfo-NHS, sodium salt of *N*-hydroxysulfosuccinimide; TPCK, L-1-tosylamido-2-phenylethyl chloromethyl ketone; ESI, electrospray ionization; TOF, time of flight; IT, ion trap

* Corresponding author. Tel.: +420 532290242; fax: +420 532290242.
E-mail address: foret@iach.cz (F. Foret).

0021-9673/$ – see front matter © 2007 Elsevier B.V. All rights reserved.
doi:10.1016/j.chroma.2007.02.095

or less. Such bioreactors could find interesting practical applications in on-line coupling with separations such as capillary electrophoresis or chromatography. Previously such attempts were described for CE separation of peptide fragments after digestion process via a "fluid joint" [8,9] and also for off-line analysis of the separated peptide fragments by mass spectrometry [10]. Another approach used the sol–gel enzymatic reactor incorporated into the first part of the fused silica capillary also for the CE separation of peptide fragments [26,27].

In this work, the enzyme bioreactors were prepared with L-1-tosylamido-2-phenylethyl chloromethyl ketone(TPCK)-trypsin and pepsin A covalently immobilized on the wall of a 10 μm I.D. fused silica capillary. This open tubular enzyme reactor was on-line coupled with electrospray ionization-time of flight-mass spectrometer (ESI/TOF-MS) and the proteolytic activity was characterized in a range of protein concentrations, buffer pH's, temperatures and reaction times. The optimized reactors were tested as the nanospray needle in a liquid junction interface for CE-ESI/TOF-MS analysis of protein mixtures. On-line digestion of proteins on the capillary wall enables faster and fully automated protein identification using peptide mass fingerprinting suitable as an alternative approach to the commonly used methods for the identification of proteins and determination of posttranslational modifications.

2. Material and methods

2.1. Chemicals and materials

Fused silica capillary (10 μm I.D. and 75 μm I.D., 360 μm O.D.), with a polyimide outer coating, were purchased from Polymicro Technologies (Phoenix, AZ, USA). L-1-tosylamido-2-phenylethyl chloromethyl ketone (TPCK) treated trypsin (EC 3.4.21.4) from bovine pancreas, pepsin A (EC 3.4.23.1) from porcine stomach mucosa, cytochrome c (horse), myoglobin (horse), melittin (bee), beta-casein (bovine), γ-glycidoxypropyltrimethoxysilane, benzamidine hydrochloride and 1-ethyl-3-(3-dimethylaminopropyl) carbodiimide hydrochloride (EDAC) were obtained from Sigma (St. Louis, MO, USA). Sodium cyanoborohydride, (3-aminopropyl) trimethoxysilane and sodium salt of *N*-hydroxysulfosuccinimide (sulfo-NHS) were obtained from Fluka (Buchs, Switzerland). Sodium periodate (Reanal, Budapest, Hungary) and the remaining common chemicals supplied by Lachema (Neratovice, Czech Republic) were of analytical reagent grade. All buffers and solutions were filtered through 0.45 μm Millipore filter (Bedford, MA, USA) before use.

2.2. TPCK-trypsin immobilization

Selected length of 10 μm I.D. fused silica capillary was flushed with water for 5 min, with 0.1 M NaOH for 5 min and then with 0.1 M HCl for 5 min. After washing with water and methanol, the capillary was modified with a 10% (v/v) solution of (3-aminopropyl)trimethoxysilane in methanol for 24 h. The capillary was washed with methanol and continually purged with nitrogen for 1 h at 100 °C. After cooling to room temperature, the capillary was washed again with methanol to remove uncoupled reagent and equilibrated to 50 mM phosphate buffer pH 7.3. TPCK-trypsin (3 mg/ml) was dissolved in 50 mM phosphate buffer pH 7.3 containing benzamidine (0.3 mg/ml), EDAC (7 mg/ml) and sulfo-NHS (1.3 mg/ml). This enzyme solution was pumped through the capillary using a syringe pump (KDS model 100, KD Scientific Inc., MA, USA) at the flow rate of 50 nl/min for 5 h. The immobilization was performed at room temperature. The immobilization was carried out in the presence of benzamidine, a competitive inhibitor of trypsin, eliminating the binding via amino acids in the active center of the enzyme and stabilizing its tertiary structure. Further positive factor of immobilization in the presence of a competitive inhibitor is prevention of the undesirable autodigestion of the enzyme in solution during the binding process. Finally, the capillary reactor was washed with 50 mM phosphate buffer pH 7.3 to remove unbound material before storing the reactor at 4 °C. Twenty-five millimolar ammonium acetate pH 6.5 with benzamidine (0.1 mg/ml) was used as a storage solution.

2.2.1. Characterization of the TPCK-trypsin microreactor

Proteins were dissolved to a concentration of 0.1 mg/ml in 25 mM ammonium acetate solutions with the pH in the range of 6.5–9.5 adjusted by ammonia solution. These protein solutions were pumped through the open tubular reactor at selected flow rates (10–50 nl/min) using nitrogen pressure applied to the sample vial containing capillary inlet as described previously [25]. The digest was analyzed using ESI/TOF-MS. On-line MS analysis was conducted using a nanospray prepared from the 10 μm I.D. capillary reactor with a polished tip. The digestion was performed at selected temperatures in the range of 25–50 °C.

For comparison the tested proteins were also digested in solution using a soluble TPCK-trypsin. In this case the proteins were dissolved in 25 mM ammonium acetate (pH 6.5–9.5) to a concentration of 0.1 mg/ml. TPCK-trypsin was added at a substrate-to-enzyme ratio of 50:1 (w/w) and the solution was incubated at 37 °C for 16 h. Note, that the solution digestion time can be as short as 3 h; however, in this comparison we wanted to assure complete cleavage without the prior protein denaturation. The reaction products were stored in freezer at −20 °C until analysis. The protein digests were analyzed using ESI/TOF-MS equipped with a polished tip nanospray needle prepared from a 10 μm I.D. (360 μm O.D.) fused silica capillary.

2.3. Pepsin A immobilization

Selected length of the 10 μm I.D. fused silica capillary was flushed with 0.1 M NaOH for 5 min, with 0.1 M HCl for 5 min and then modified with 10% (v/v) solution of γ-glycidoxypropyltrimethoxysilane in methanol for 24 h. The treated capillary was flushed with water for 5 min and then with 0.5 M hydrochloric acid for 18 h. After hydrolysis of epoxide groups, a 0.1 M sodium periodate solution was pumped through the capillary for 1 h, washed with water and equilibrated with 50 mM acetate buffer pH 4.5. Pepsin A was dissolved (1 mg/ml) in 50 mM acetate buffer pH 4.5 containing 3 mg/ml sodium

cyanoborohydride. This enzyme solution was pumped through the capillary at flow rate of 30 nl/min for 4 h. Finally, the reactor was sequentially washed with 50 mM acetate buffer pH 4.5 and then with 1% formic acid solution. The immobilized pepsin A capillary was stored in 1% formic acid solution at 4 °C until the use.

2.3.1. Characterization of pepsin A microreactor

Proteins were dissolved to a concentration of 0.05 mg/ml in 1% formic acid solution. These protein solutions were pumped through the open tubular reactor at specified flow rates using pressurized nitrogen applied to the sample vial containing capillary inlet. The digest was analyzed using ESI/TOF-MS and ESI/IT-MS. On-line MS analysis was conducted using a nanospray prepared from the 10 μm I.D. capillary reactor with a polished tip. The digestion was performed at 25 °C.

2.4. MS analysis

2.4.1. ESI/TOF-MS

The Mariner TOF mass spectrometer (Applied Biosystems, MA, USA) was used in MS experiments. The measurements were carried out in positive ion mode with a scan range of 400–2500 *m/z*. Each mass spectrum was a sum of 10 scans acquired within 2 s. The list of detected ions (*m/z*) was used for protein identification by the MS-Fit tool of Protein Prospector database (http://prospector.ucsf.edu).

2.4.2. MS/MS analysis by ESI/IT-MS

The Esquire HCT (Bruker Daltonics, Germany) was used in MS/MS experiments. The ESI/IT-MS measurements were performed in positive ion mode with helium as the collision gas. The software Mascot (http://www.matrixscience.com) was used for peptide and protein identification based on the MS/MS product ions.

2.5. Immobilized capillary enzyme reactor as an electrospray needle for CZE-ESI/TOF-MS analysis

The CZE-ESI/TOF-MS experiments were performed using the Mariner TOF mass spectrometer and a laboratory made liquid junction interface for on-line capillary electrophoresis–electrospray ionization coupling [28]. This system was equipped with two high-voltage power supplies (Glassman High Volatge Inc., Model EH30P3, High Bridge, NJ, USA for CZE and ±6 kV regulated laboratory source with the E60 modules from EMCO High Voltage Corporation, Sutter Creek, CA, USA for the electrospray control). A 50 cm long fused silica capillaries (75 μm I.D., 365 μm O.D.) were used as separation columns. The CE separation capillaries were used either uncoated or with the inner surface coated with polyvinylalcohol to minimize protein adsorption [29]. Nanospray needles (10 cm long) were prepared from uncoated fused silica capillaries (10 μm I.D., 360 μm O.D.) with the ESI tip sharpened and polished with fiber optic polishing paper. The gap between the separation and spraying capillaries was set to 75 μm. The samples were injected by electromigration. In experiments integrating the protein separation with on-line digestion and ESI/MS analysis the experiments were performed using the same equipment except the nanospray needle. It was prepared from a selected length of 10 μm I.D. open tubular enzymatic reactor with immobilized TPCK-trypsin or pepsin A. The specific experimental conditions are shown in Section 3.

3. Results and discussion

A variety of methods are available for enzyme immobilization on the inner surface of a fused silica capillary, e.g., non-covalent binding using biotin–avidin coupling [7–11], metal-ion chelating system [12] or a photo-coupling procedure [13]. The reported open tubular microreactors utilized relatively wide bore fused silica capillaries with 50 or 75 μm I.D. with correspondingly small *S/V* ratio. Thus a very low flow rate was needed to permit time for diffusion of the protein molecule to the immobilized enzyme resulting in the digestion time of half an hour or more. Since the *S/V* ratio of the open capillary scales with 4/I.D., the decrease of the capillary I.D. from 75 to10 μm increases the *S/V* ratio 7.5 times (534 vs. 4000 cm^{-1}). Additionally, since the maximum diffusion time to the capillary wall decreases with the second power of the capillary I.D., it is reasonable to expect a significant increase in the digestion efficiency for the small I.D. reactors.

The enzyme reactors used in this work were prepared by covalent immobilization of TPCK-trypsin or pepsin A on the wall of a 10 μm I.D. fused silica capillary. The selected diameter represented a compromise between the required reactor efficiency and the ease of preparation and manipulation. In principle, smaller I.D. reactors could provide better operational parameters; however, it would require a complex re-design of the CE–MS interface used in our laboratory.

3.1. Characterization of TPCK-trypsin microreactor

The on-line coupling of reactor with the separation and mass spectrometry should eliminate the risk of losses and contamination of the sample during the sample handling. At the same time the reactor itself can serve as the electrospray needle without the need for the instrument modification. Additionally the requirements for the high performance of both the reactor and the electrospray tip are synergistic—both improve with the decreasing diameter.

The procedure of TPCK-trypsin immobilization on the capillary surface is shown in Fig. 1. The free amino groups on the surface of the capillary allow covalent attachment of the enzyme through the amide bond using the EDAC/sulfo-NHS technique. Enzyme was coupled to amino-modified capillary wall according to the simultaneous activation-conjugation method of Voyksner et al. [30]. The protocol was modified to include the use of sulfo-NHS and enhance the carbodiimide chemistry as described by Staros et al. [31].

When coupled with mass spectrometry the potential leakage of the immobilized enzyme from the reactor might ruin the system performance. Thus we have first conducted the enzyme leakage tests under different operational conditions.

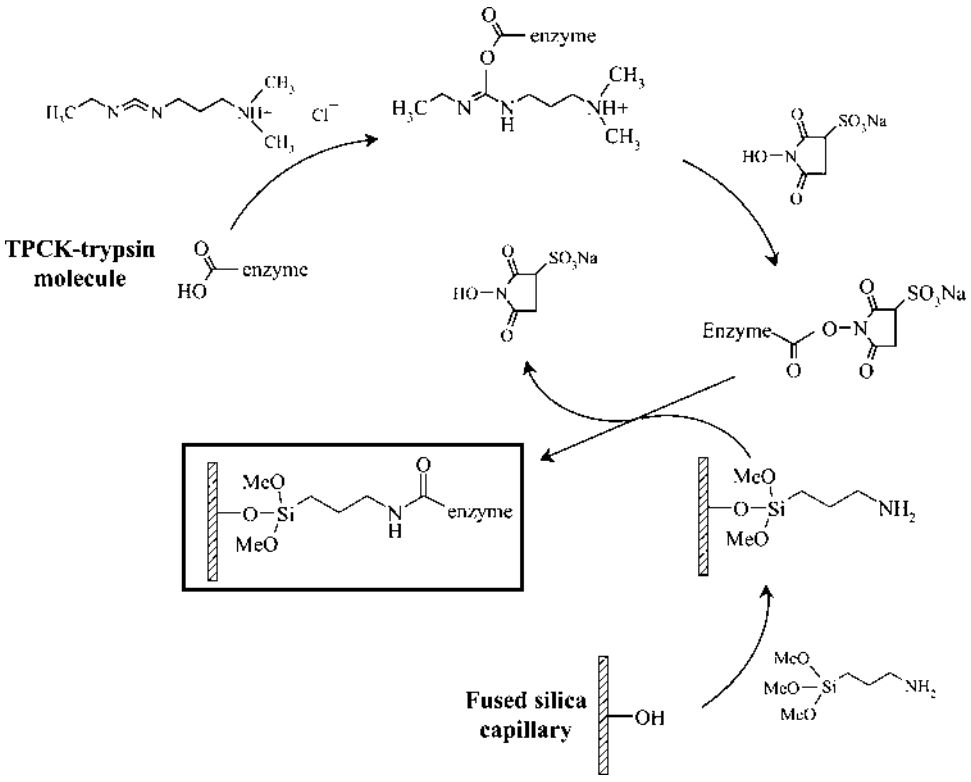

Fig. 1. Scheme of TPCK-trypsin immobilization on the wall of 10 μm I.D. fused silica capillary.

Cytochrome c (molecular weight 11 700, p*I* 9.6) and beta-casein (molecular weight 23 600, p*I* 5.1) were selected as model proteins. The digestion was performed on native proteins without any modification. The buffer composition, protein concentration, reaction time, temperature, and bioreactor length were selected as the experimental variables.

Since the optimum pH value of trypsin activity is at alkaline pH, the on-line protein digest-MS analysis should be performed preferably in the negative electrospray mode. We have tested this arrangement first; however, addition of high amounts (∼50%, v/v) of organic solvents (acetonitrile, isopropanol) was needed for obtaining a stable ESI signal. Unfortunately, under these conditions the enzymatic activity was drastically reduced. Thus we have opted for positive electrospray, detecting positively charged ions from the high pH aqueous solution, where a stable spray was observed. Positive electrospray ionization was also used in experiments with the immobilized pepsin, which has the optimum activity at low pH.

3.1.1. Digestion buffer composition

It is well-known that the selection of the digestion buffer has a significant impact on enzyme activity. At the same time the buffer composition is also critical for the ESI efficiency and stability. In this study, 25 mM ammonium acetate solution in water was chosen for all experiments with the immobilized trypsin since it had sufficient volatility and did not suppress the electrospray signal. As with the solution performed digestion and with the trypsin immobilized on a porous monolith [25] the optimal buffer pH value for the surface immobilized trypsin was found to be between 8 and 10. At higher pH, considerable amounts of siloxane bonds between silane and silica matrix were hydrolyzed resulting in decrease or loss of enzymatic activity. At lower (neutral) pH the enzymatic activity was slightly reduced; however, increasing the reaction temperature could restore and enhance the reactor performance. Enhanced thermal stability of the surface immobilized enzyme was observed up to 50 °C; however, for practical applications most of the experiments were performed at 25 °C.

3.1.2. Flow rate and sequence coverage

One of the most important factors in the flow-through open tubular reactor operation is the protein residence time, i.e., the sample flow rate. In the experiments with 0.1 mg/ml cytochrome c solutions the digestion times were between 30–150 s for 30 cm long reactor at 10–50 nl/min sample flow rate. The selected flow rate corresponded to the range where the electrospray was stable. As expected, lower proteolysis yields were obtained at higher flow due to the reduced contact time between the substrate and enzyme.

The selected length (30 cm) of the trypsin coated capillary was based on the preliminary experiments indicating a near-complete digestion of cytochrome c at room temperature. At the same time its total volume was 23 nl, a value which should not degrade the CE separation in a 75 μm I.D. capillary, planned for the consecutive experiments. The flow rate of the protein solution through the capillary was maintained at 30 nl/min. Under this condition the digestion time of the protein with immobilized enzyme was calculated to be about 46 s.

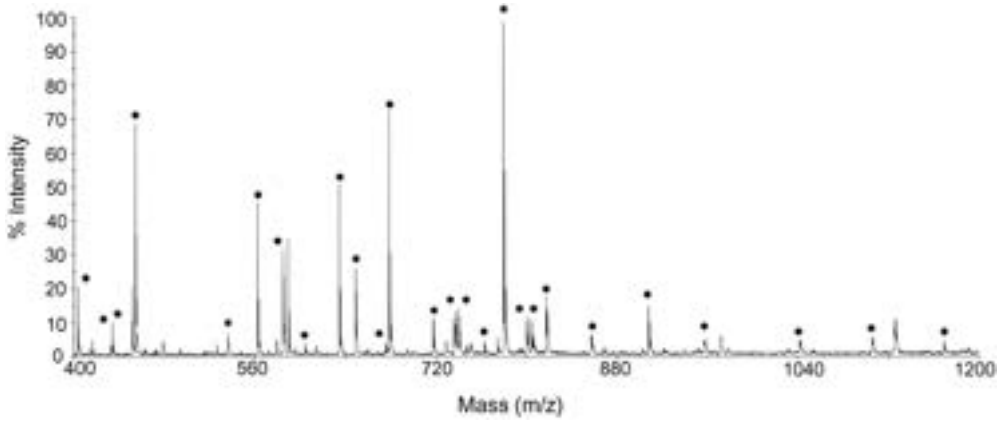

Fig. 2. ESI-TOF mass spectrum obtained during the on-line tryptic digest of horse cytochrome c. Digestion conditions: sample, 0.1 mg/ml cytochrome c in 25 mM ammonium acetate, pH 8.7; 10 μm I.D. IMER length, 30 cm; flow rate, 30 nl/min (digestion time ~50 s); temperature, 25 °C; * indicates the specific tryptic fragments from cytochrome c.

Similar results were obtained also with shorter capillary reactors (15 cm tested), providing that the protein digestion time was kept the same. Although approximately the same sequence coverage (see below) was achieved when digesting femtomole quantities of cytochrome c in the short reactor, the flow had to be kept at lower rates, reducing the useful range for the stable electrospray. In any case a significant speed improvement was achieved compared to the 1 m long (50 μm) capillary reactor needed in the previous reports [12].

The sequence coverage results of cytochrome c digestion using the capillary microreactor (90% coverage of cytochrome c sequence at 25 °C) were comparable with a standard in-solution technique (86% coverage at 37 °C); however with the advantage of much faster digestion speed. The typical mass spectrum obtained with the flow rate of 30 nl/min is shown in Fig. 2.

The correlation between the masses calculated for the enzymatic cleavage fragments and those observed in the mass spectrum is listed in Table 1. The similarity between the mass spectra obtained using immobilized and soluble trypsin indicates the preserved specificity of the enzyme immobilized on the silica wall. Repeated experiments demonstrated very good reproducibility of this procedure.

The cytochrome c digestion represents the simplest case without the potential interferences of posttranslational modifications and/or complex protein folding typical with large proteins. Apparently no protein denaturation or any other chemical treatment was needed prior to the flow through digestion. In practice, most proteins are more complex mostly requiring at least reduction and denaturation prior to the digestion. This can be demonstrated on a digestion of beta-casein selected as the second test protein the flow through digestion under the same conditions as with the cytochrome c, i.e., no denaturation or protein modification. Although a significant fragmentation was achieved—Fig. 3, only 41 of 209 amino acids (10 peaks) in the digest were positively identified (Table 2). The corresponding sequence coverage was 20% with an average of 0.4 missed cleavages. The same results were observed at higher reaction temperature (37–50 °C) or higher pH value (pH 8.5–9.5). Similarly, thermal denaturation (incubating at 60 and 90 °C, respectively for 10 min) of the protein sample prior the digestion did not improve the efficiency of the reactor. While deglycosylation (e.g., using PNGase F), denaturation, reduction of the disulfide bridges and subsequent alkylation are used in practice, these processes will require additional complexity of the on-line system.

Table 1
Experimentally identified peptides from the horse cytochrome c using the immobilized TPCK-trypsin microreactor

Measured *m/z*	Peptide mass (MH^+)	Theoretical MH^+	Residues	Missed cleavages
434.2195	434.2195	434.1887	101–104	0
562.3305	562.3305	562.2837	100–104	1
604.4107	604.4107	604.3459	56–60	0
634.4466	634.4466	634.3928	9–13	0
678.4504	678.4504	678.3827	74–79	0
762.5611	762.5611	762.4878	8–13	1
779.5272	779.5272	779.4490	80–86	0
403.7703^{+2}	806.5328	806.4776	73–79	1
454.3083^{+2}	907.6088	907.5439	80–87	1
907.6273	907.6273	907.5439	80–87	1
584.8680^{+2}	1168.7282	1168.6227	28–38	0
1168.7305	1168.7305	1168.6227	28–38	0
432.9438^{+3}	1296.8157	1296.7177	28–39	1
648.9188^{+2}	1296.8298	1296.7177	28–39	1
675.9282^{+2}	1350.8486	1350.7269	89–99	1
717.4604^{+2}	1433.9130	1433.7766	26–38	1
735.9232^{+2}	1470.8386	1470.6865	40–53	0
739.9789^{+2}	1478.9500	1478.8219	88–99	2
739.9789^{+2}	1478.9500	1478.8219	89–100	2
799.9775^{+2}	1598.9472	1598.7815	39–53	1
536.3537^{+3}	1607.0454	1606.9168	87–99	3
804.0347^{+2}	1607.0616	1606.9168	87–99	3
536.3537^{+3}	1607.0454	1606.9168	88–100	3
804.0347^{+2}	1607.0616	1606.9168	88–100	3
817.3934^{+2}	1633.7790	1633.8194	9–22	1
857.0015^{+2}	1712.9952	1712.8244	40–55	1
694.4014^{+3}	2081.1885	2081.0265	56–72	1
1041.1276^{+2}	2081.2474	2081.0265	56–72	1
1105.2200^{+2}	2209.4322	2209.1215	56–73	2
956.9329^{+3}	2868.7830	2868.4857	56–79	3

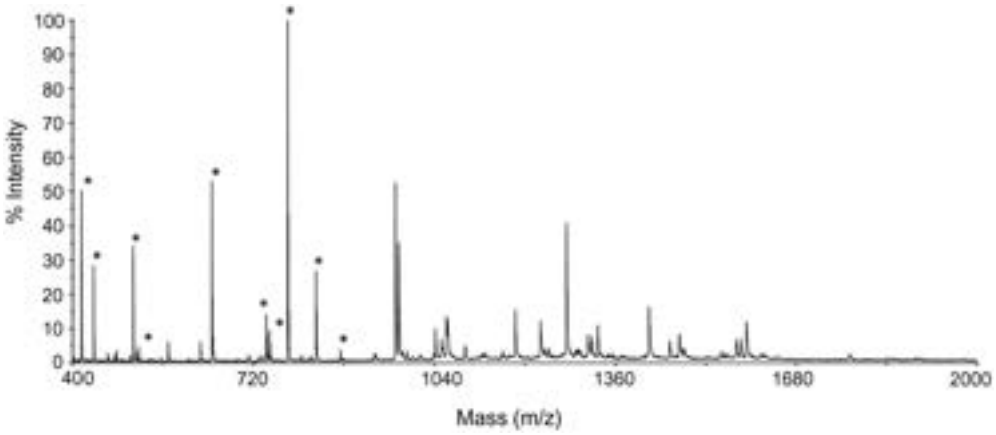

Fig. 3. ESI-TOF mass spectrum obtained during the on-line tryptic digest of bovine beta-casein. Digestion conditions: sample, 0.1 mg/ml cytochrome c in 25 mM ammonium acetate, pH 8.7; 10 μm I.D. IMER length, 30 cm; digestion time, 80 s; temperature, 25 °C; * indicates the specific tryptic fragments from beta-casein.

3.2. Pepsin A capillary microreactor

Unlike the trypsin pepsin is not commonly used in proteomics, mainly due to its low cleavage specificity. We have included it in this work for the ease of its immobilization and very good compatibility with the acidic electrospray solutions. Of the several pepsin variants designated A, B, C, and D Pepsin A, the major component, has a molecular weight of 35 000, an isoelectric point of 1.0, and an optimum pH of approximately 1.0–3.0. Since the optimal condition of the EDAC/sulfo-NHS immobilization technique is in neutral pH range and pepsin molecule is irreversibly inactivated (denaturation) above pH 6.0, a different multi-step immobilization technique was used for pepsin A immobilization on the silica surface. The binding procedure involved the capillary surface modification by γ-glycidoxypropyltrimethoxysilane and hydrolysis of epoxide groups using hydrochloric acid. The hydrolysis was followed by oxidation of the hydroxide groups and reaction with pepsin A molecules. To suppress the reversibility of the formed Schiff base and stabilize the bond with the enzyme, the immobilization was performed in the presence of a reducing agent, sodium cyanoborohydride. The procedures of pepsin A immobilization is shown in Fig. 4.

Table 2
Experimentally identified peptides from the bovine beta-casein using the immobilized TPCK-trypsin microreactor

Measured *m/z*	Peptide mass (MH^+)	Theoretical MH^+	Residues	Missed cleavages
517.3801	517.3801	517.3350	44–47	1
646.3738	646.3738	646.3234	115–120	0
742.4904	742.4904	742.4503	218–224	0
748.4127	748.4127	748.3704	123–128	0
780.5613	780.5613	780.4983	185–191	0
830.5111	830.5111	830.4525	192–198	0
415.7595^{+2}	830.5112	830.4525	192–198	0
437.2769^{+2}	873.5460	873.4868	113–120	1
873.5552	873.5552	873.4868	113–120	1
507.3030^{+2}	1013.5982	1013.5242	121–128	1

In the case of proteolytic enzyme immobilization, the competitive inhibitor should be used to block the autolytic activity of enzymes during the binding process. There is a wide range of specific inhibitors that can bind to the active site and effectively remove the activity of pepsin, e.g., pepstatin. Since pepsin adopts a native-like although catalytically inactive conformation in the 4.0–6.5 pH interval [32], the pepsin A immobilization was performed in 50 mM acetate buffer pH 4.5 without presence of a competitive inhibitor.

For testing the open tubular reactor was coupled on-line with ESI/TOF-MS using a nanospray interface as described in the previous section, and tested in the flow through mode with a solution of melittin, cytochrome c and myoglobin. Although the native reaction environment of pepsin is hydrochloric acid, the volatile and electrospray friendly formic acid can also be used with almost the same proteolytic activity [27]. Therefore 1% (v/v) formic acid solution was used as the digestion solution. An example of the on-line cytochrome c digestion is in Fig. 5.

Although complete fragmentation was observed, the database search (according to peptide mass fingerprinting data) using either the Protein Prospector database (http://prospector.ucsf.edu), ExPASy (http://www.expasy.org) or Mascot (http://www.matrixscience.com) resulted in no peptide identification. It should be noted that pepsin A is not a very specific enzyme and the protein database data differ in pepsin A specificity (e.g., Protein Prospector—F, W, A, I, L, and Y; ExPASy—at pH 1.3, F and L; at pH > 2, F, L, W, Y, A, E and Q). According to the IUBMB Enzyme Nomenclature, pepsin A cleaves proteins preferentially at carboxylic groups of F, L, and E. It does not cleave at V, A, or G. Other residues may be cleaved with very variable rates. Still different cleaving sites were described by Kato et al. [27] with pepsin cleaving the peptide bonds at carboxylic acid side of the A, L, F, and W amino acids. The high variability in the pepsin specificity has required a separate study to characterize the specificity of the immobilized pepsin A used in this work. Horse cytochrome c was selected as the sample protein flowing through the electrospray capillary with the surface immobilized pepsin A. The resulting MS/MS spectra were submitted to the Mascot database (http://www.matrixscience.com)

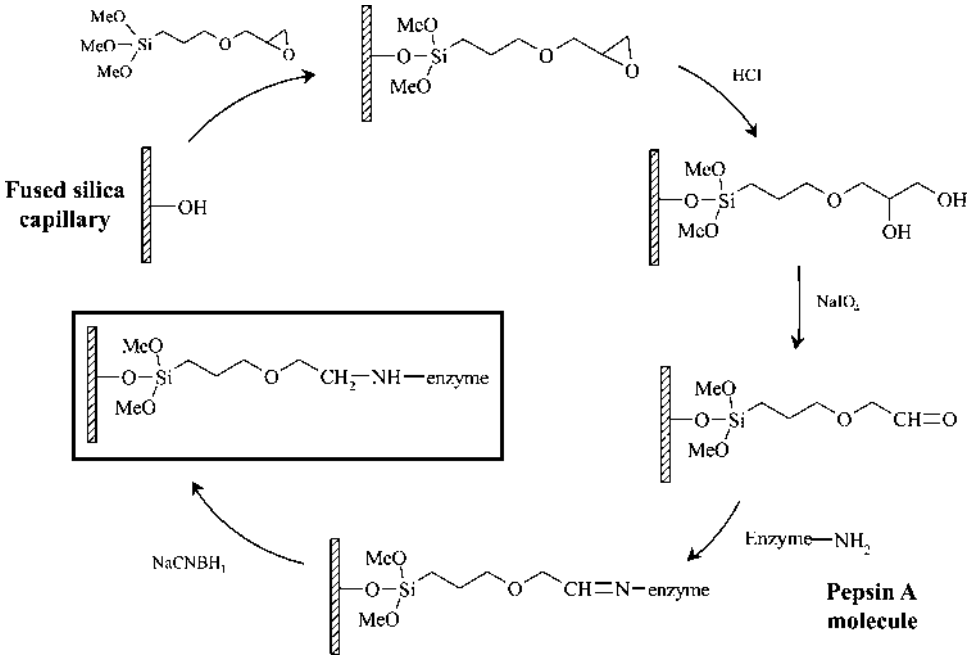

Fig. 4. Scheme of pepsin A immobilization on the wall of 10 μm I.D. fused silica capillary.

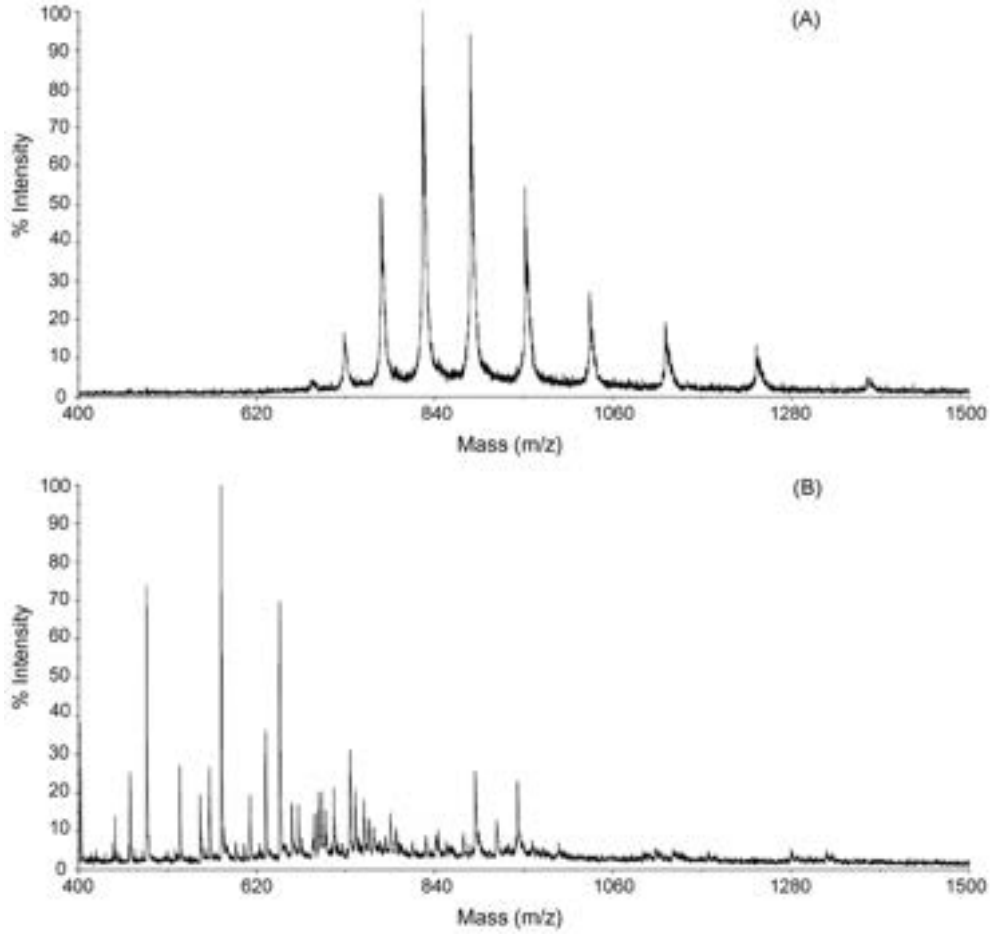

Fig. 5. ESI-TOF mass spectrum of horse cytochrome c (A) and its pepsin A digest (B). Conditions: sample, 0.05 mg/ml cytochrome c in 1% formic acid; 10 μm I.D. IMER length, 32 cm; digestion time, 126 s; temperature, 25 °C.

Table 3
Experimentally identified peptides from the horse cytochrome c using the immobilized pepsin A microreactor and MS/MS analysis

Measured mass	Peptide sequence	Residues
402.28^{2+}	(Y)LKKATNE(−)	98–104
463.31^{3+}	(F)AGIKKKTEREDL(I)	83–94
483.81^{2+}	(A)YLKKATNE(−)	97–104
524.72^{3+}	(F)AGIKKKTEREDLIA(Y)	83–96
550.06^{3+}	(M)IFAGIKKKTEREDL(I)	81–94
561.37^{3+}	(E)YLENPKKYIPGTKM(I)	67–80
575.90^{2+}	(L)IAYLKKATNE(−)	95–104
648.10^{3+}	(E) YLENPKKYIPGTKMIF(A)	67–82

for peptide sequence determination. Experimentally obtained molecular masses and identified peptide sequences are listed in Table 3. All identified peptides corresponded to the cleavages of the carboxylic acid side of the amino acids: F, L, E, M, Y, and A.

3.3. CZE-digestion-ESI/TOF-MS analysis

Since the requirements for the low diameter and flow rate are in line with the requirements for nanoelectrospray ionization the optimized enzyme reactor can be easily used as the nanoelectrospray needle. Here we have integrated it into the pressurized liquid junction nanoelectrospray interface for CE–MS [28]. The main requirement for such a coupling is the use of a BGE providing adequate electrophoretic separation of proteins and without disturbing the MS signal. In the first experiments the on-line CZE-trypsin digestion-ESI/TOF-MS was tested on a peptide mixture containing angiotensin I, bradykinin and neurotensin (10 μmol/l of each peptide). Since the pH optimum of the immobilized TPCK-trypsin is in the range of pH from 7.5 to 9.5, the electrophoretic separation of peptides was carried out in 25 mM ammonium acetate pH 8.0. Under these conditions, bradykinin (p*I* 12.00) and neurotensin (p*I* 9.70) were positively charged while angiotensin I (p*I* 6.92) was migrating as anion. Therefore, uncoated fused silica capillary (50 cm, 75 μm I.D., 360 μm O.D.) was used for the separation where all the zones were transported by the combination of electromigration and electroosmosis towards the ESI interface. The 9 cm long microreactor with immobilized TPCK-trypsin was used as the nanospray needle and the resulting separation-digestion-MS record is in Fig. 6. The 3D mass electropherogram was plotted in the total ion current mode. The theoretical sequences and isoelectric points, calculated based on the amino acid sequence (http://www.expasy.org) of the tryptic fragments, are in Table 4. Bradykinin has no cleaving site for trypsin and served as a marker of the immobilized TPCK-trypsin specificity.

From the record in Fig. 6 it is evident that the separation under alkaline conditions can be successfully coupled with the ESI-MS analysis performed in the positive ion mode. Unfortunately, the limitations related to the digestion of proteins in native state limit the use in the current simple arrangement. Alternatively, the CE separation can be performed on the mixture of the already denatured, reduced and alkylated, or otherwise modified proteins, which will be well processed by the trypsin microreactor. Based

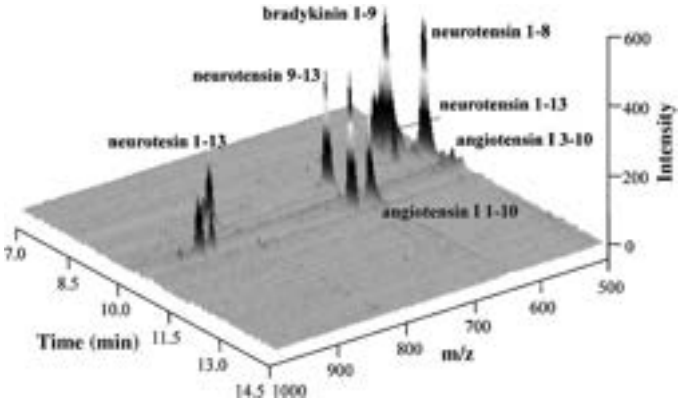

Fig. 6. CZE-trypsin digestion-ESI/TOF-MS analysis of the standard peptide mixture. Conditions: sample, 10 μM of each peptide; electrokinetic injection, 15 s at 10 kV; 75 μm I.D. uncoated capillary, total length, 50 cm; BGE, 25 mM ammonium acetate 8.0; applied CZE voltage, 10 kV; spray needle, 10 μm I.D. TPCK-trypsin IMER, length 9 cm; spray liquid, 25 mM ammonium acetate 8.0; applied ESI voltage, 3 kV; applied pressure, 100 kPa.

Table 4
Theoretical tryptic fragments of model peptides

Peptide mixture	Sequence		Molecular weight	Isoelectric point
Angiotensin I	1–10	DRVYIHPFHL	1296.49	6.92
	1–2	DR	289.29	5.84
	3–10	VYIHPFHL	1025.22	6.89
Bradykinin	1–9	RPPGFSPFR	1060.22	12.00
Neurotensin	1–13	QLYENKPRRPYIL	1672.92	9.70
	1–8	QLYENKPR	1030.12	8.59
	9–13	RPYIL	660.81	8.75

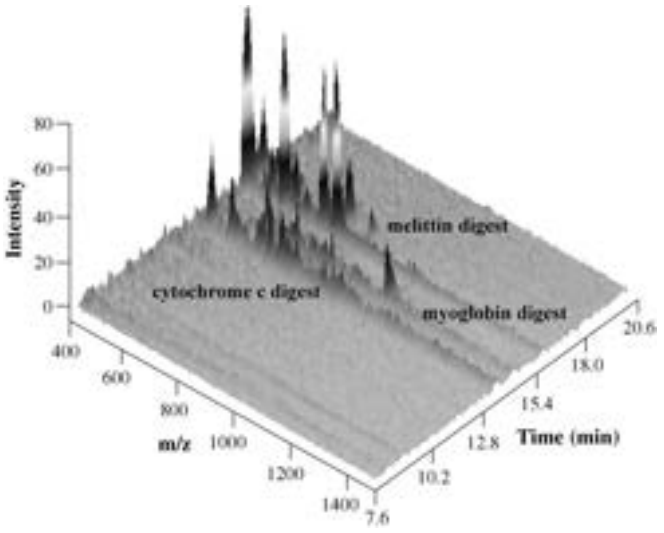

Fig. 7. CZE-pepsin A digestion-ESI/TOF-MS analysis of the protein mixture. Conditions: sample—cytochrome c and myoglobin (6.25 μg/ml), melittin (1.25 μg/ml); electrokinetic injection, 5 s at 10 kV; 75 μm I.D. PVA-coated capillary, total length, 50 cm; BGE, 1% formic acid; applied CZE voltage, 10 kV; spray needle, 10 μm I.D. pepsin A IMER, length 30 cm; spray liquid, 1% formic acid; applied ESI voltage, 2.5 kV; applied pressure, 200 kPa.

on our preliminary experiments it seems that a coated capillary will be necessary to minimize protein adsorption in this case as well as a reactor with larger *S*/*V* ratio.

Substituting the immobilized TPCK-trypsin with pepsin A provides better compatibility for the CE separation of wide range of proteins followed by high ionization efficiency of peptide fragments in positive electrospray mode. We have selected melittin (p*I* 11.1), cytochrome c (p*I* 9.6) and myoglobin (p*I* 7.3) as the model proteins for the experiments. The separation was performed in a PVA-coated capillary and 1% (v/v) formic acid solution was used as both the BGE and the spraying liquid. A 30 cm long capillary microreactor with immobilized pepsin A, as described in the Section 3.2 was incorporated as the ESI needle in the interface. It is worth noting, that the very narrow ESI needle operating at less than 100 nl/min, provided good ESI signals without the need for any organic additives in the spray fluid. The Fig. 7 demonstrates that effective on-line digestion of the separated proteins can be obtained with the pepsin A immobilized directly on the inner surface of the electrospray needle.

4. Conclusions

Although presented results are of preliminary nature it is clear that open tubular capillary enzyme reactors can be applied for rapid on-line protein digestion/MS analysis. The simple preparation procedure allows their direct use as the electrospray needle for infusion experiments where only a limited amount of sample is available. This eliminates both the extra step of the batch digestion and the sample handling, which otherwise always results in the sample loss. For example, the total volume of the 50 cm long 10 μm I.D. ESI reactor is less than 40 nl. Complete on-line digestion can be performed in a matter of seconds, basically without adding any extra time to the MS analysis. Such a low total volume also provides new possibilities for on-line integration into miniaturized separation systems, such as capillary chromatography or electrophoresis. In this respect the presented experiments with the CE/ESI/MS coupling show a very promising potential. Extremely small protein amounts (atto-femtomoles) loaded into the CE separation capillary could be digested on-line with the enzymes (trypsin and pepsin A) immobilized directly on the inside wall of the 10 μm I.D. ESI capillary. Alternatively, one can also envision, the use of this approach on microfabricated devices leading potentially to even faster analysis times.

Acknowledgments

The authors are grateful for donation of the mass spectrometer from the Applied Biosystems, Framingham, MA, USA. Additional support was obtained from the grants GAAV KJB400310604, GAAV A400310506, KAN400310651 (Grant Agency of the Academy of Sciences of the Czech Republic), 203/06/1685 (Grant Agency of the Czech Republic) and LC06023 (Ministry of Education, Youth and Sports). The institute research plan Z40310501 is also acknowledged.

References

[1] R. Aebersold, D.R. Goodlett, Chem. Rev. 101 (2001) 269.
[2] J. Křenková, F. Foret, Electrophoresis 25 (2004) 3550.
[3] F. Svec, Electrophoresis 27 (2006) 947.
[4] J. Samskog, D. Bylund, S.P. Jacobsson, K.E. Markides, J. Chromatogr. A 998 (2003) 83.
[5] Y. Li, J.W. Cooper, C.S. Lee, J. Chromatogr. A 979 (2002) 241.
[6] J.W. Cooper, C.S. Lee, Anal. Chem. 76 (2004) 2196.
[7] L.N. Amankwa, W.G. Kuhr, Anal. Chem. 64 (1992) 1610.
[8] L.N. Amankwa, W.G. Kuhr, Anal. Chem. 65 (1993) 2693.
[9] L. Licklider, W.G. Kuhr, Anal. Chem. 66 (1994) 4400.
[10] L. Licklider, W.G. Kuhr, M.P. Lacey, T. Keough, M.P. Purdon, R. Takigiku, Anal. Chem. 67 (1995) 4170.
[11] L. Licklider, W.G. Kuhr, Anal. Chem. 70 (1998) 1902.
[12] Z. Guo, S. Xu, Z. Lei, H. Zou, B. Guo, Electrophoresis 24 (2003) 3633.
[13] A. Bossi, L. Guizzardi, M.R. D'Acunto, P.G. Righetti, Anal. Bioanal. Chem. 378 (2004) 1722.
[14] K.A. Cobb, M. Novotny, Anal. Chem. 61 (1989) 2226.
[15] C. Wang, R. Oleschuk, F. Ouchen, J. Li, P. Thibault, D.J. Harrison, Rapid Commun. Mass Spectrom 14 (2000) 1377.
[16] G.W. Slysz, D.C. Schriemer, Anal. Chem. 77 (2005) 1572.
[17] Z. Bílková, M. Slováková, N. Minc, C. Fűtterer, R. Cecal, D. Horák, M. Beneš, I. Le Potier, J. Křenková, M. Przybylski, J.-L. Viovy, Electrophoresis 27 (2006) 1811.
[18] M. Slováková, N. Minc, Z. Bílková, C. Smadja, W. Faigle, C. Fűtterer, M. Taverna, J.-L. Viovy, Lab. Chip 5 (2005) 935.
[19] L.G. Rashkovetsky, Y.V. Lyubarskaya, F. Foret, D.E. Hughes, B.L. Karger, J. Chromatogr. A 781 (1997) 197.
[20] D.S. Peterson, T. Rohr, F. Svec, J.M.J. Fréchet, Anal. Chem. 74 (2002) 4081.
[21] D.S. Peterson, T. Rohr, F. Svec, J.M.J. Fréchet, J. Proteome Res. 1 (2002) 563.
[22] D.S. Peterson, T. Rohr, F. Svec, J.M.J. Fréchet, Anal. Chem. 75 (2003) 5328.
[23] M. Petro, F. Svec, J.M.J. Fréchet, Biotechnol. Bioeng. 49 (1996) 355.
[24] M. Ye, S. Hu, R.M. Schoenherr, N.J. Dovichi, Electrophoresis 25 (2004) 1319.
[25] J. Křenková, Z. Bílková, F. Foret, J. Sep. Sci. 28 (2005) 1675.
[26] K. Sakai-Kato, M. Kato, T. Toyo'oka, Anal. Chem. 74 (2002) 2943.
[27] M. Kato, K. Sakai-Kato, H. Jin, K. Kubota, H. Miyano, T. Toyo'oka, M.T. Dulay, R.N. Zare, Anal. Chem. 76 (2004) 1896.
[28] P. Kusý, K. Klepárník, Z. Aturki, S. Fanali, F. Foret, Electrophoresis 28 (in press).
[29] J.M. Thorne, W.K. Goetzinger, A.B. Chen, K.G. Moorhouse, B.L. Karger, J. Chromatogr. A 744 (1996) 155.
[30] R.D. Voyksner, D.C. Chen, H.E. Swaisgood, Anal. Biochem. 188 (1990) 72.
[31] J.V. Staros, Biochemistry 21 (1982) 3950.
[32] L.A. Campos, J. Sancho, FEBS Lett. 538 (2003) 89.

Jana Krenkova
Karel Kleparnik
Jakub Grym
Jaroslav Luksch
Frantisek Foret

Institute of Analytical Chemistry, CAS, v.v.i, Brno, Czech Republic

Received July 31, 2015
Revised August 18, 2015
Accepted August 18, 2015

Short Communication

Self-aligning subatmospheric hybrid liquid junction electrospray interface for capillary electrophoresis

We report a construction of a self-aligning subatmospheric hybrid liquid junction electrospray interface for CE eliminating the need for manual adjustment by guiding the capillaries in a microfabricated liquid junction glass chip at a defined angle. Both the ESI and separation capillaries are inserted into the microfabricated part until their ends touch. The distance between the capillary openings is defined by the angle between the capillaries. The microfabricated part contains channels for placement of the capillaries and connection of the external electrode reservoirs. It was fabricated using standard photolithographic/wet chemical etching techniques followed by thermal bonding. The liquid junction is connected to a subatmospheric electrospray chamber inducing the flow inside the ESI needle and helping the ion transport via aerodynamic focusing.

Keywords:
Capillary electrophoresis / Electrospray interfacing / Microfabrication
DOI 10.1002/elps.201500357

Electrophoresis in capillaries or microfluidic devices (CE) hyphenated with MS is an important tool for bioanalysis. A quarter of century long development of the combination of CE-MS [1] has brought numerous technical innovations and increasing number of published applications [2, 3]. While the ESI coupling is often performed using the sheath liquid interface, developed during the 1990s [4], it has been long known that the highest ionization efficiency can be obtained with pointed capillary emitters at submicroliter per minute flow rates [5]. Thus, a number of ESI interfaces operating in the low flow regime has been under development [2].

In one design the electrophoretic separation capillary was coupled to the nanoelectrospray emitter using a liquid junction [6–8]. This arrangement allows coupling electrophoretic separations regardless of the presence or absence of the flow (hydrodynamic, electroosmotic) inside the separation capillary during the separation. In addition, the ESI ionization can be optimized independently of the CE separation with regard to the composition of the spray liquid (SL) and its flow rate. In the previous designs of the liquid junction interfaces, the separation and ESI capillaries were mounted axially [9] inside an electrode reservoir serving for electrical connections of both the CE separation and ESI ionization and supplying the ESI liquid. While the exact distance between ends of the capillaries is not critical [7] and can wary in the range of tens to hundreds of micrometers [10], adjustment of this distance is sometimes considered to be difficult.

Correspondence: Frantisek Foret, Institute of Analytical Chemistry CAS, v.v.i., Veveri 97, Brno, Czech Republic
E-mail: foret@iach.cz.

Abbreviation: SL, spray liquid

Here, we describe a self-aligning liquid junction CE-MS interface eliminating the need for manual adjustment by guiding the capillaries in a microfabricated liquid junction glass chip at a defined angle. Both the ESI and separation capillaries are inserted into the microfabricated part until their ends touch. The distance between the capillary openings is defined by the angle at which the capillaries touch. The glass part contains channels for placement of the capillaries and connection of the external electrode reservoirs. It was fabricated using standard photolithographic/wet chemical etching techniques followed by thermal bonding. Briefly, two borofloat glass wafers with mirror images of identical structures were etched to the final diameter of the semicircular channels of ~200 μm. The two glass plates were thermally bonded to form circular channels with 400 μm id and cut to the final dimension of 3 × 4 cm. The etched channels enabled the positioning of the separation and ESI capillaries under the constant angle $\alpha = 30°$. The resulting distance between the capillary centers can be estimated as $\phi * \sin \alpha/2$, where ϕ is the outer diameter of the capillaries. For standard fused silica capillaries with 360 μm od this distance is 93 μm at the 30° angle. The glass liquid junction part was inserted into a holder machined from polypropylene and connected to an electrode block prepared from polysulfone resin with integrated SL reservoirs fitted with standard Luer syringe connectors. This external part of the interface was attached to the sampling orifice extension of the mass spectrometer via a subatmospheric ESI chamber made of polysulfone (PSU 1000, Tribon, Brno, Czech Republic). A laboratory made pinch valve was used for restriction of the air flow and the actual pressure

Colour Online: See the article online to view Figs. 1 and 2 in colour.

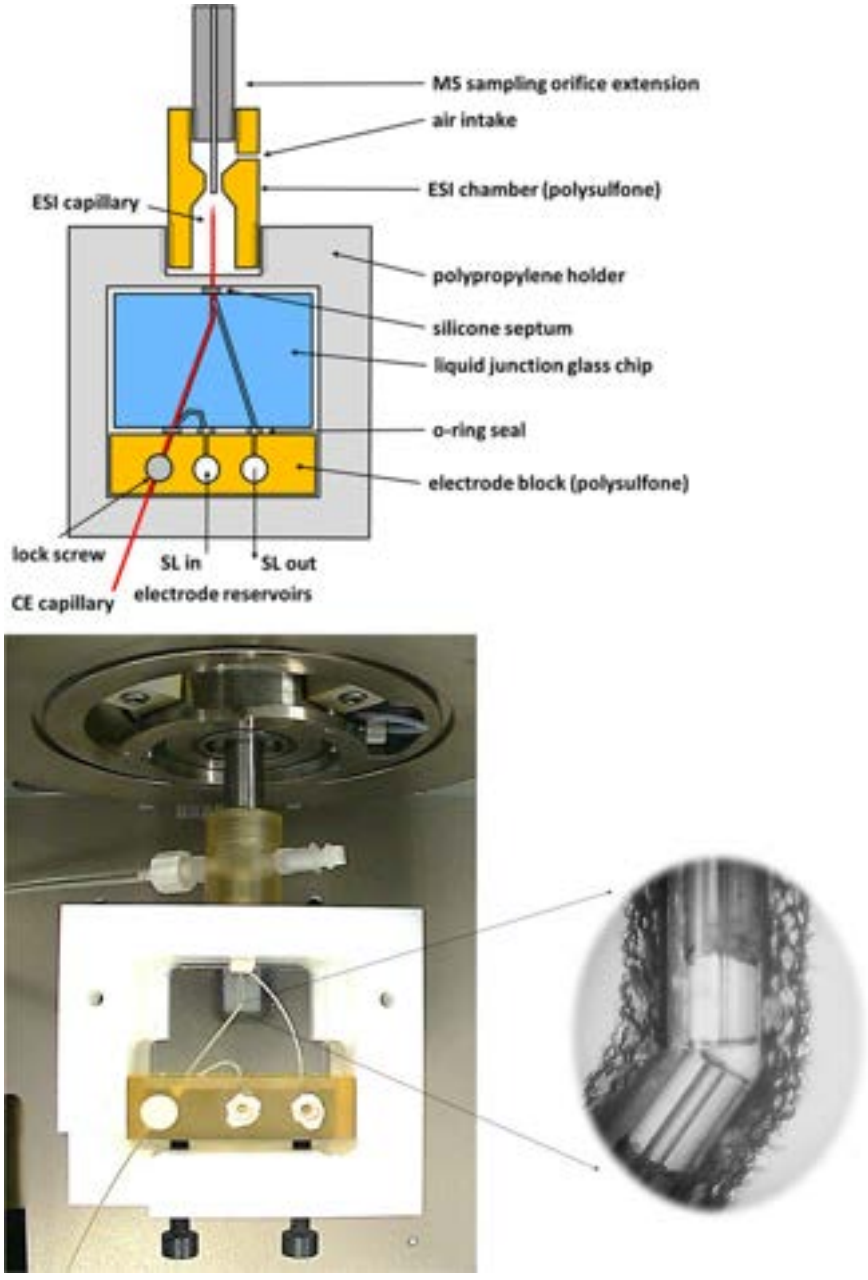

Figure 1. Scheme and photograph of the assembled interface attached to mass spectrometer.

inside the ESI chamber was monitored by a digital pressure meter (TIF Instruments, Miami, FL, USA).

All chemicals were obtained from Sigma-Aldrich (Prague, Czech Republic). Fused silica capillaries were obtained from Polymicro Technologies (Phoenix, AZ, USA). Capillaries (75 μm id × 40 cm) coated with polyacrylamide [11] were used for separations. Deionized water (18.2 MΩ.cm) was prepared using a Neptune system from Purite Limited (Thame, UK). Borofloat glass wafers (1.8 mm thick) were purchased from Nanofilm (Westlake, CA, USA). Positive photoresist ma-P 1225 and developer ma-D 331 were purchased from Micro Resist Technology (Berlin, Germany). A vacuum sputter coater (SCD 500) including the gold sputter target was obtained from Bal-TEC AG (Lichtenstein). Lithographic processes further included a spin coater WS-400B-6NPP/LITE, Laurell Technologies (North Wales, PA, USA) and a lithographic system μPG 101 from Heidelberg Instruments (Heidelberg, Germany). A dicing saw EC-400 purchased from MTI (Richmond, CA, USA) was used for cutting the glass device. A high voltage power supply for CE separation was obtained from Villa Labeco (Spisska Nova Ves, Slovakia) and connected to a platinum electrode in a vial containing the BGE and operated in the constant voltage mode. For the separation of peptides water solution of 0.5% formic acid for served as the BGE. For all other examples BGE containing 1% acetic acid in water was used.

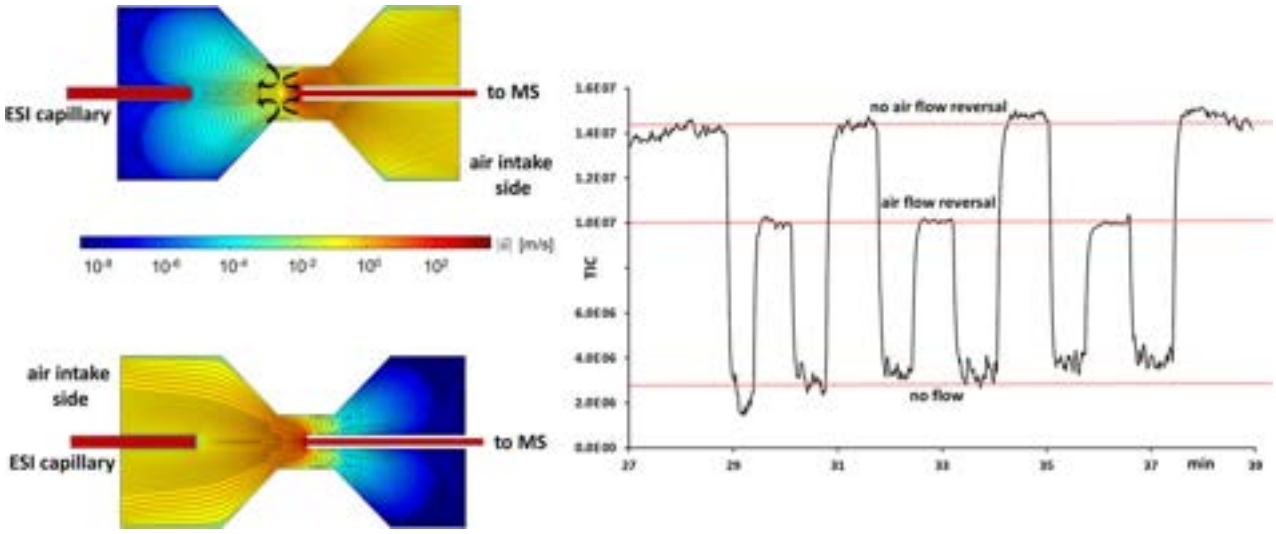

Figure 2. Left, computer simulation of aerodynamic focusing obtained with (top) and without (bottom) flow reversal air intake. Right, total ion current monitored during electrospray of 0.01 mM solution of bradykinin in the ESI chamber with and without air flow direction reversal.

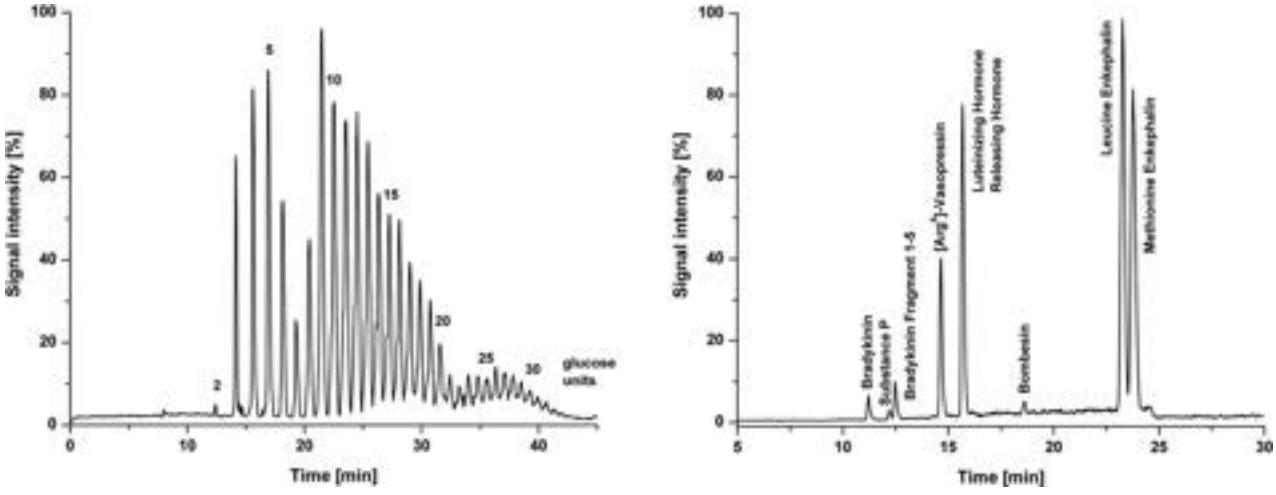

Figure 3. CE-MS analysis of AETMA labeled dextran ladder (left) and a 10 μM peptide mixture (right). See text for details.

CE-MS experiments were first conducted on a Mariner TOF mass spectrometer (ABI, Framingham, MA, USA) and repeated on an HCT ion trap impact mass spectrometer (BrukerDaltonics, Bremen, Germany). The ESI tip was made of a sharpened and polished fused silica capillary (25 μm id × 2.5 cm). The heated inlet capillary was maintained at 150°C. The ESI/MS was performed in the positive ion mode with an ESI voltage of 2 kV. The SL containing 1% acetic acid in 50% v/v isopropanol/water was used in all experiments.

The interface was constructed as a hybrid capillary/microfluidic system where the microfabricated glass part served as a manifold for attachment of the separation and ESI capillaries and for electrode connection. The design scheme on the left side of Fig. 1 shows the top view scheme with the liquid junction glass chip positioned in the polypropylene holder together with the polysulfone electrode block. The two reservoirs (SL in and out) contained 500 μL of the SL. A miniature connector with a platinum wire electrode was connected from the bottom (not shown in Fig. 1) and attached either to the ESI high voltage power supply of the MS (Mariner) or to the ground in case of the Bruker MS with the ESI high voltage at the MS entrance orifice. The electrode block also included a lock screw eliminating unwanted movement of the separation capillary. Prior to each analysis, the separation capillary was flushed with the BGE. Next, the liquid junction was flushed with the SL from the electrode reservoir "SL in" flowing through the glass liquid junction and exiting at the "SL out" reservoir. Note that channels of the glass liquid junction were slightly larger than the outside diameter of the separation and spray capillaries (400 μm vs. 360 μm) leaving sufficient clearance for the spray fluid flow. The connections between the glass chip and external parts

were sealed by rubber o-rings and silicone septa. The photograph in Fig. 1 shows the assembled interface and the detail of the liquid junction with the separation and spray capillaries. A 1 mm long section of the polyimide coating was removed from ends of the capillaries. The polypropylene holder was screwed on the ESI chamber machined from polysulphone and the whole assembly was attached on a 3 cm long MS sampling orifice extension machined from stainless steel with a 500 μm id stainless steel capillary in the center.

The SL flow through the ESI capillary was maintained at 100 nL/min by restricting the air intake into the closed ESI chamber. Under presented experimental conditions, this flow rate was achieved at the pressure of 86 kPa (0.85 atm) inside the ESI chamber. Since the air flow is the main mechanism of the transport of the ions into the vacuum region of the mass spectrometer, we have experimented with the airflow arrangements. The scheme in Fig. 1 shows an arrangement of the air intake where the direction of the air flow reverses by 180 degrees just in front of the ESI tip. We have expected this arrangement to help focusing the electrospray plume into the MS sampling orifice. While this design worked well, we have also done computer simulations and experiments comparing the flow reversal with the coaxial air intake without the flow reversal [7]. The results are summarized on the left side of Fig. 2 comparing the computer simulated (COMSOL, Burlington, MS, USA) velocity flow field obtained with (top) and without (bottom) the flow reversal air intake. The streamlines are supplemented by a color scale indicating the flow velocity. The simulation revealed formation of a vortex in the trajectory of the airflow with the direction reversal, potentially resulting in a decreased ion transport efficiency. The formation of a vortex is also evident in the case of the airflow without the direction reversal; however, in this case, the vortex is outside the trajectory of ESI ions.

While one could intuitively expect more effective drag toward the MS entrance in the case of the air counter flow, due to the vortex just behind the spray capillary, the ESI plume is spread and the number of ions reaching the MS orifice is reduced. The experimental results on the right side of Fig. 2 confirm that higher MS signal can be obtained without the airflow direction reversal.

An example in Fig. 3 shows the performance of the interface for separations of peptides and dextran ladder labeled with aminoethyltrimethylamine [12]. The sample injection was accomplished by hydrodynamic flow −10 cm height difference for 10–30 s. The separation voltage of 12.5 kV (312 V/cm) was used for the CE separation.

The presented results indicate that the current design performs similarly to our previous reports on the coaxial liquid junction interface [7, 13]. The separation performance of miniaturized interfaces with nano-ESI needles provides fast and highly sensitive identifications of analytes by CE-MS systems. Main benefit of the current version is the simplicity of the interface assembly without the need for the liquid junction adjustment. While the sensitivity in the ESI/MS is given mainly by the use of suitable nanospray emitters [14], we have shown that the air flow also affects the ESI sensitivity. Thus, the computer simulation approaches will be very useful in the future of CE-MS research and development [15, 16].

Financial support from the Grant Agency of the Czech Republic (P206/12/G014) and the institutional support RVO: 68081715 is acknowledged.

The authors have declared no conflict of interest.

References

[1] Smith, R. D., Barinaga, C. J., Udseth, H. R., *Anal. Chem.* 1988, *60*, 1948–1952.

[2] Tomas, R., Kleparnik, K., Foret, F., *J. Sep. Sci.* 2008, *31*, 1964–1979.

[3] Kleparnik, K., *Electrophoresis* 2015, *36*, 159–178.

[4] Cai, J. Y., Henion, J., *J. Chromatogr. A* 1995, *703*, 667–692.

[5] Marginean, I., Tang, K. Q., Smith, R. D., Kelly, R. T., *J. Am. Soc. Mass Spectrom.* 2014, *25*, 30–36.

[6] Pleasance, S., Thibault, P., Kelly, J., *J. Chromatogr. A* 1992, *591*, 325–339.

[7] Wachs, T., Sheppard, R. L., Henion, J., *J. Chromatogr. B* 1996, *685*, 335–342.

[8] Foret, F., Zhou, H., Gangl, E., Karger, B. L., *Electrophoresis* 2000, *21*, 1363–1371.

[9] Fanali, S., D'Orazio, G., Foret, F., Kleparnik, K., Aturki, Z., *Electrophoresis* 2006, *27*, 4666–4673.

[10] Kleparnik, K., Otevrel, M., *Electrophoresis* 2010, *31*, 879–885.

[11] Hjerten, S., *J. Chromatogr.* 1985, *347*, 191–198.

[12] Partyka, J., Foret, F., *J. Chromatogr. A* 2012, *1267*, 116–120.

[13] Krenkova, J., Kleparnik, K., Foret, F., *J. Chromatogr. A* 2007, *1159*, 110–118.

[14] Tycova, A., Foret, F., *J. Chromatogr. A* 2015, *1388*, 274–279.

[15] Jarvas, G., Grym, J., Foret, F., Guttman, A., *Electrophoresis* 2015, *36*, 386–392.

[16] Jarvas, G., Guttman, A., Foret, F., *Mass Spectrom. Rev.* 2015, *34*, 558–569.

Journal of Chromatography A, 1388 (2015) 274–279

Contents lists available at ScienceDirect

Journal of Chromatography A

journal homepage: www.elsevier.com/locate/chroma

Capillary electrophoresis in an extended nanospray tip–electrospray as an electrophoretic column☆

Anna Tycova[a,b], Frantisek Foret[a,c,*]

[a] Institute of Analytical Chemistry AS CR, v.v.i., Veveri 97, Brno, 602 00, Czech Republic
[b] Faculty of Science, Masaryk University, Kotlarska 2, Brno, 611 37, Czech Republic
[c] CEITEC - Central European Institute of Technology, Kamenice 753/5, 625 00 Brno, Czech Republic

ARTICLE INFO

Article history:
Received 6 November 2014
Received in revised form 13 February 2015
Accepted 14 February 2015
Available online 21 February 2015

Keywords:
Mass spectrometry
Separation
Interface
Capillary electrophoresis
Nanospray

ABSTRACT

Capillary electrophoresis coupled to mass spectrometry (CE/MS) is gaining its space among the most powerful tools in modern (bio)analytical laboratory. The most challenging instrumental aspect in CE/MS is striking the balance between the stability and reproducibility of the signal and sensitivity of the analysis. Several interface designs have been published in the past decade addressing the variety of instrumental aspects and ease of operation. Most of the interfaces can be categorized either into the sheath flow arrangement (considered to be a de facto standard), or sheathless interface, often expected to provide the ultimate sensitivity. In this work we have explored an "interface-free" approach, where the CE/MS analysis was performed in narrow bore (<20 μm ID) electrospray capillary. The separation capillary and electrospray tip formed one entity and the high voltage, applied at the injection end of the capillary served for both the separation and electrospray ionization. Thus the separation voltage was defined as the product of the electrospray current and resistivity of the separation electrolyte. Optimum conditions for the separation and electrospray ionization were achieved with voltage programming. The performance of this simplest possible CE/MS system was tested on peptide separations from the cytochrome c tryptic digest. The subnanoliter sample consumption and sensitivity in the attomole range predetermines such a system for analysis of limited samples.

1. Introduction

Since its introduction in the late 1980s, CE/MS has evolved into a research tool for separation and detection of wide range of ionic species [1]. While, in principle, matrix assisted laser desorption ionization can be also applied [2], electrospray is the most frequently used interfacing for online CE/MS coupling [3–5]. The two main electrospray arrangements include sheath flow interface and sheathless interface. In the sheath flow arrangement the sheath liquid (or make-up liquid) provides the electric contact to the exit end of the separation capillary as well as liquid flow to sustain stable electrospray conditions. The composition of the separation buffer and sheath liquid can be, to some extent, tuned independently [6]. This allows using high content of organic solvents (typically 20%–100%) supporting formation of stable electrospray plume and droplet desolvation. Sample dilution, decreasing the sensitivity, is often mentioned as a drawback of this technique [7]. In another approach, the sheathless interface, no sheath fluid is provided and separated zones must be delivered into the electrospray tip by liquid flow induced inside the separation capillary. At very low flow rates, on the order of 100 nL/min and less, the electrospray, commonly called nanospray, brings high ionization efficiency and sensitivity [8,9].

Since the nanospray needles are usually fabricated from glass or fused silica capillaries, the most challenging task is the electric connection to define potential gradient for electrophoretic separation and the electrospray voltage. Such connection can be maintained through supplementary component such as inserted wire [10], conductive coating of the tip [11,12] or recently developed porous capillary [13]. The use of the BGE for both the CE separation and electrospray ionization can limit the freedom in selection of the BGE composition.

In recent years there have been reports about the use of very narrow capillaries (with diameter of 10 μm or less) for electrophoretic separations [14–16]. Thin separation channel provides

☆ Presented at the 30th International Symposium on Chromatography (ISC 2014), Salzburg, Austria, 14–18 September 2014.

* Corresponding author at: Institute of Analytical Chemistry AS CR, v.v.i. Veveri 97, Brno, 602 00, Czech Republic. Tel.: +420 532 290 242; fax: +420 541 212 113.
E-mail address: foret@iach.cz (F. Foret).

http://dx.doi.org/10.1016/j.chroma.2015.02.042
0021-9673/

better capillary cooling, especially with high conductivity background electrolyte, minimizing the contribution of Joule heating to band broadening [16]. The reduced capillary volume allows working with very low sample amounts and in pressure assisted capillary electrophoresis the narrow capillaries exhibit much lower hydrodynamic flow band broadening [17].

It has been well known that nanospray prepared from a narrow capillary leads to finer electrospray plume, better ionization efficiency and sensitivity with less ion suppression effects [8,9,18]. It has also been accepted that nanospray is robust providing stable signal at relatively wide range of flow rates and voltages using small percentage or no organic solvent in the electrosprayed solution [19]. Integration of the separation capillary with the nanospray without using junctions or fittings has been previously described using flame pulled tips [20–22]. While the early results were far from optimum, the main advantage – the simplicity of the experimental setup, has been demonstrated. In this work we have studied CE/MS performed in capillaries of uniform diameter with the ESI tip prepared by polishing the capillary outer surface. In this arrangement there is no voltage loss associated with the constriction of the flame pulled ESI tip. Only one high voltage power supply was used supplying the electric current for both the electrophoretic separation and electrospray ionization leading to separations with extremely low sample consumption.

2. Matherial and methods

2.1. Chemicals

Cytochrome c and trypsin were purchased from Sigma–Aldrich (Czech Republic). Ammonium hydrogen carbonate and formic acid were obtained from Lach-Ner (Czech Republic).

2.2. Preparation of cytochrome c tryptic digest

The sample of cytochrome c tryptic digest was prepared from the protein (0.24 mg/mL) dissolved in ammonium hydrogen carbonate buffer (25 mM, pH = 8.0) and trypsin added at a protein-to-enzyme weight ratio of 50. Digestion run over night at 37 °C. The final digest solution was completely evaporated and later re-dissolved again in the background electrolyte to the desired concentration.

2.3. Current measurements

Knowledge of the electrophoretic (I_{ELF}) and electrospray (I_{ESI}) currents and voltages is useful for understanding of the electromigration/electrospray related phenomena within the capillary. During the experiment the electrophoretic current equals the electrospray current and can be directly measured. The voltages corresponding to the potential drop across the separation capillary and the electrospray plume can not be measured independently. Thus we have performed a set of measurements as shown in Fig. 1.

In the first measurement (Fig. 1A), the CE/MS capillary with the ESI tip was placed in front of an ESI receiving electrode, gas pressure was applied at the electrode reservoir causing liquid flow and high voltage was increased until reaching a stable electrospray was observed under microscope. The corresponding ESI current was recorded. In the second measurement the nanospray tip was placed into an electrode vial filled with the background electrolyte solution (Fig. 1B). The high voltage was maintained as in the previous case and the current was recorded. The potential drops across the ESI plume (V_{ESI}) and across the separation capillary can be calculated with the help of the Ohm's law according to Eq. (1):

$$V_{ESI} = V_{app}(1 - I_{ESI}/I_{CE}) \quad (1)$$

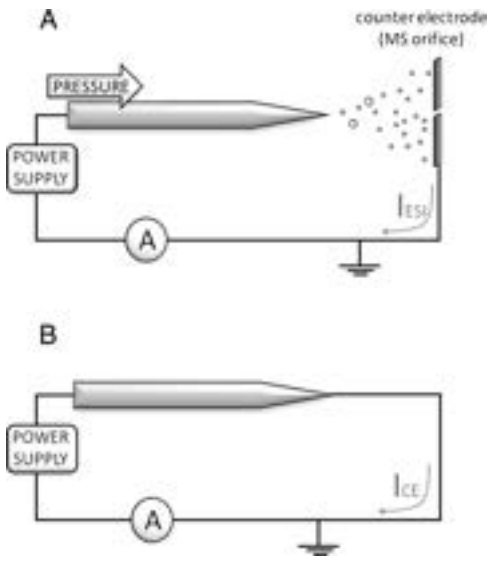

Fig. 1. Schematic electrical circuit for measurement of A – electrospray current; B – electrophoretic current.

where V_{app} is the applied high voltage and I_{ESI} and I_{CE} are the currents measured for the electrospray and electrophoresis, respectively.

2.4. Capillary electrophoresis/mass spectrometry

All CE/MS experiments were conducted on the Velos Pro Dual-Pressure Linear Ion Trap Mass Spectrometer (Thermo Fisher Scientific, Germany) in positive ionization mode. Electrophoretic separations were performed in a bare fused silica capillary with 375 μm OD (Polymicro Technologies, Phoenix, AZ, USA). The length of 60 cm was chosen as a compromise between the sufficient separation path and pressure needed for driving of analysis. Moreover, the fabrication of a symmetrical electrospray tip become challenging for much longer capillaries. The electrospray tip at the end of the capillary was prepared by grinding on fine sand paper and final polishing with fibre-optic lapping film (3M^{TM} Type H - 662XW, 3 M Electronics, St. Paul, MN). To achieve good tip symmetry both the capillary and the polishing paper (foil) were rotating during the preparation as described earlier [23]. The quality of the tip was inspected under a microscope and was visually comparable to the ones available commercially (www.newobjective.com). The ESI tip was positioned approximately 2 mm in front of the mass spectrometer orifice. The injection end of the capillary was placed in a laboratory constructed nitrogen pressurized chamber housing sample/buffer vials and platinum electrodes. The flow rate for the electrospray and sample injection was adjusted by the nitrogen pressure.

The high voltage power supply (0–30 kV, Villa Labeco, Slovakia) was connected to the platinum electrode in the pressurized chamber. Both the high voltage power supply and the mass spectrometer sampling orifice were grounded.

For some experiments a contactless conductivity detector (TraceDec, Innovative Sensor Technologies GmbH, Austria) was used to monitor conductivity changes during electrophoretic separations. Water solutions of formic acid were chosen as the background electrolyte with low pH value ensuring minimal sorption of positively charged analytes and negligible electroosmotic flow. Formic acid solutions of six different conductivities were prepared (Table 1).

Table 1
Conductivities and pH of used formic acid solutions.

Concentration of HCOOH (v/v)	0.01%	0.1%	0.5%	1.0%	2.5%	5.0%
Conductivity (S/m)	0.02	0.08	0.10	0.15	0.21	0.34
pH	3.15	2.75	2.35	2.23	1.91	1.65

3. Results and discussion

In the presented arrangement the background electrolyte used for the separation is directly electrosprayed from the column exit. Thus the choice of its composition is limited preferably to water solutions of the volatile acids (cationic separations). While addition of organic phases, such as the commonly used alcohols or acetonitrile, generally improves electrospray performance, it also significantly lowers the permittivity of the resulting solution. Lower permittivity decreases the degree of ionization of weak bases and acids resulting in slower migration and lower resolution. Thus organic phases are generally less suited for electrophoretic separations of weak electrolytes (peptides and proteins), unless dealing with analytes poorly soluble in water [24]. During our preliminary experiments we have found that water solutions require slightly higher voltage for the electrospray onset than the mixed water/organic solutions. At low voltage the droplets, forming on the ESI tip, form unstable bursts and the current sharply fluctuates. At higher voltage the Taylor cone is formed and stable current, suitable for recording mass spectra, is reached [25]. At even higher voltages the ESI current still rise; however, the plume splits resulting in a dramatic loss of useful MS signal. Since the pure water solutions have higher electric conductivity the electrospray current is also higher when compared to the water/organic based electrolytes.

To use electrospray capillary as a separation column (Fig. 1A) the electrospray current flowing from the injection end to the electrospray tip should result in sufficient electric field strength for the electrophoretic separation. Since the electrospray current is typically in the nanoampere region (even when spraying water solutions without organic additives) it cannot drive the separation in the most common capillary columns with diameters of 50–75 μm. The maximum achievable electrospray current can be estimated with the help of Faraday's law [26]:

$$I_{ESI} = FQ \sum n_i c_i \quad (2)$$

where n_i is the charge of the i-th ion, c_i is the molar concentration, F is the Faraday constant (96,485 C/mol) and Q the solution flow rate delivered to the ESI tip. Since the analyte concentration is typically orders of magnitude below that of the electrolyte (buffer) ions it does not influence the total electrospray current. In our measurements only formic acid was presented in the solution and the number of cations (hydronium, hydroxonium ions) as well as anions (formate) was given by the dissociation constant of the formic acid ($pK_a = 3.77$). For example, 1.0% (v/v) solution (conductivity 0.15 S/m) has pH = 2.23 corresponding to the concentration of hydroxonium ions of 5.89×10^{-3} mol/L. In a 10 μm ID capillary the maximum achievable current as calculated from Eq. (2) at $Q = 12$ nL/min (2.55 mm/s) is 110 nA whereas for a 25 μm capillary at $Q = 90$ nL/min (3 mm/s) it could reach 850 nA. The flow rates in these examples were selected based on experiments providing the most stable electrospray. For the low diameter ESI emitter the experimentally observed current could approach the theoretical value (especially with low conductivity solutions). With larger diameter capillaries, operating at higher flow rate, the electrospray current did not increase significantly. While reaching the electrospray current close to 1 μA as calculated for 25 μm capillary at $Q = 90$ nL/min was possible, the corresponding MS signal was unsuitable for practical analyses due to the excessively high ESI voltage and onset of the corona discharge resulting in the loss of useful MS signal. In contrary to the use of conductive (metal or metalized) electrospray tip, where the charge separation as well as the electrolyte redox reactions occur directly at the point of electrospray formation [27], in the insulating ESI capillary the high voltage electrode is decoupled from the electrospray plume and the ESI current has to pass through the solution inside the capillary. This ESI current creates a voltage drop across the capillary inducing electromigration of all ionic species. While the voltage drop is small in larger bore capillaries (e.g. 50 or 75 μm ID) [20–22] it could be sufficiently high for electrophoretic separation in very narrow capillaries. The voltage difference across such a separation channel results from the Ohm's law and can be easily calculated from experimental data [21] as depicted in Fig. 1.

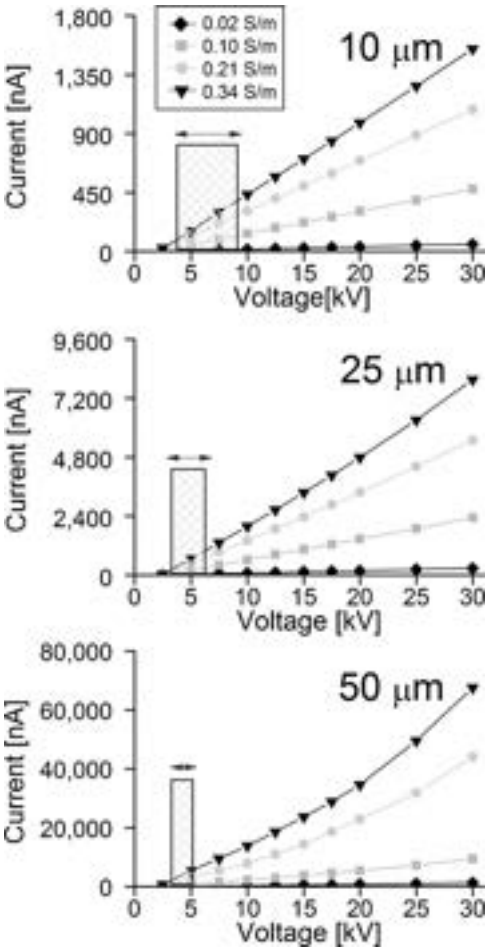

Fig. 2. Electrospray current measured for solution of different concentrations of formic acid. Nanospray was generated using 10 μm, 25 μm or 50 μm capillaries 40 cm long using 3.0 atm, 0.6 atm and 0.2 atm pressure applied at the inlet side, corresponding to flow rates of 12 nL/min, 90 nL/min and 600 nL/min (2.5 mm/s, 3.0 mm/s, 5.0 mm/s), respectively. The bars represent optimal voltage for stable MS signal.

Here we have measured the electrospray current in capillaries with internal diameters of 10 μm, 25 μm and 50 μm filled with formic acid solutions in water with concentrations of 0.01% (v/v), 0.1% (v/v) and 1.0% (v/v) as the background electrolyte. Fig. 2 depicts the ESI current versus the applied voltage.

It was experimentally observed that the ESI onset was practically the same in all instances - around 1900 V. With increasing voltage the current followed the Ohm's law and reached up to 70 μA in the 50 μm capillary. Such a high current is absolutely incompatible with electrospray and would lead to discharges at the electrospray tip and remarkable Joule heating. Flow rates indicated in Fig. 2 were kept constant during the experiments and were

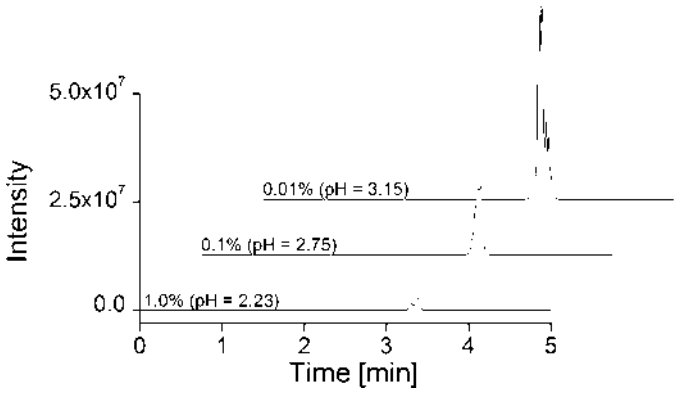

Fig. 3. Separations of cytochrome c tryptic digests (0.12 mg/mL) performed at three different BGE concentrations in the selected ion mode of all specific fragments. Flow rate: 30 nL/min at 2.2 atm pressure, capillary: 15 μm × 60 cm. Applied voltage: 5 kV.

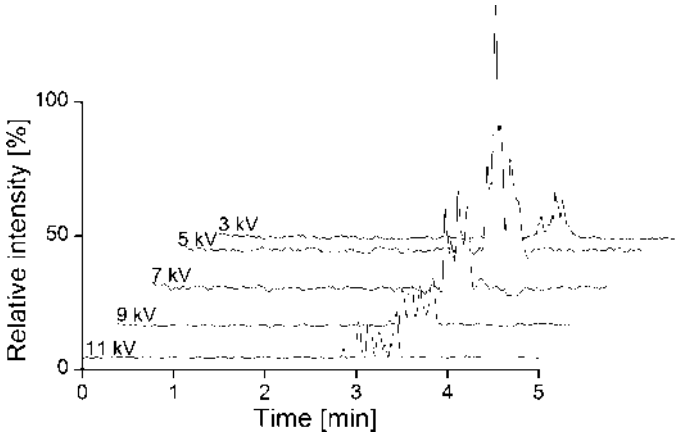

Fig. 4. Base peak electropherograms performed at different total applied voltages. Sample: tryptic peptides from 0.12 mg/mL cytochrome c. BGE: 0.01% HCOOH (v/v). Flow rate: 30 nL/min at 2.2 atm pressure, capillary: 15 μm × 60 cm.

selected for the most stable ESI/MS signal during the preliminary infusion experiments. From the plots it might seem that any capillary/electrolyte combination could be suitable for electrophoretic separation since the potential drop across the electrospray plume was relatively small and most of the applied voltage was available for electrophoretic separation.

Unfortunately, useful MS spectra could be recorded only at a limited range of applied voltages (indicated in Fig. 2 by bars). Outside of this region the Taylor cone stability rapidly deteriorated as the electrospray drifts towards the corona discharge or pulsing mode. The range of the stable ESI/MS signal depends on many experimental conditions, including the spray liquid composition and tip shape. Electrospray tip diameter plays an important role in the initial droplets size released from the jet of Taylor cone. Wider tip gives rise to larger droplets and the solvent is not able to evaporate before reaching mass spectrometer orifice. In contrast, the droplets from the capillaries of smaller ID are able to release bare ions more easily resulting not only in higher sensitivity but also in higher stability. Moreover, if the electrospray occurs in pulsing mode the narrower tip and lower flow rate lead to pulsation with higher frequencies (and smaller droplets) and to certain extended the signal can appear as stable [28]. Thus only the low ID capillaries (<20 μm, depending on the BGE conductivity) seem to be suitable for the CE separation in the ESI tip.

When using solution without any organic solvent as the separation buffer/electrospray liquid, low electrolyte concentration is needed for low conductivity. Solutions of volatile weak acids are commonly used for cationic ESI ionization (e.g. formic acid used here). Fig. 3 shows analysis performed at three different formic acid concentrations. As expected, the separation improves in the low conductivity electrolyte because of higher electric field strength inside capillary. Moreover also the detection signal significantly improves with decreasing formic acid concentration. This effect might be partly contributed to changes in the ESI charge states due to pH shifts. To exclude this effect the separations of cytochrome c digest was monitored in the selected ion mode (at any time only the specific fragments in all detected charge states in the mass spectrum were recorded). It should be mentioned that the experiments were performed in pure water. Lower electrolyte conductivity could also be obtained by mixed water/organic solutions; however, the lower ionization of the peptides in the sample resulted in no peptide separation. Thus the low conductivity solution of 0.01% HCOOH (v/v) was used as the separation/electrospray electrolyte for further experiments. Fig. 4 shows the separations performed at different total applied voltages. At 3 kV the signal, as well as the separation is low due to insufficient voltage for both the electrospray and separation. The best signal was obtained at 5 kV, where the electrospray operated under optimum conditions. It should be noted that at this total voltage about 2.5 kV was taken by the electrospray plume and the remaining 2.5 kV created the separation electric field strength of ~42 V/cm in the separation capillary. Further increase of the total applied voltage improved the electrophoretic separation; however, the signal intensity has deteriorated as the electrospray operated out of the optimum conditions.

From the presented experiments it is clear that the separation potential of the electrospray separation capillary for the separation of peptides is limited by the experimental conditions. Even in 10 μm ID capillary the electric field strength, generated by the electrospray current, may not be sufficient for high resolution separations. Using capillaries with even lower diameter should broaden the range of applicable voltages and achieve better separations. However, such narrow capillaries will require higher demands on solvent and sample preparation due to the risk of capillary clogging as well as the use of higher pressures, incompatible with our present instrumentation. On the other hand we have noticed that capillary clogging was not an issue when using the standard 0.45 μm syringe filters for the buffer and sample preparation. Of course, clean laboratory table without dust particles from the air ducts is also an important factor. As expected, the electrospray voltage can be rapidly switched from very high voltages to optimum conditions without any adverse effects on the quality of the spectra. This allowed easy voltage programming to achieve both the desired separation and sensitive electrospray detection as shown in Fig. 5.

In this mode high separation voltage was applied after the sample injection for a selected time interval and then reduced to obtain stable electrospray. With 60 cm long capillary we could apply the maximum voltage of our power supply (30 kV). Under these conditions the electrospray was operating in a multi jet or corona discharge conditions and none or very poor mass spectra could be obtained. On the other hand the current passing through the capillary generated sufficient voltage drop for the separation. Similar results could be obtained in a two-step operation where in the first step the capillary tip was placed in an electrode reservoir and the separation was conducted for 5 min. Afterwards the ESI tip was taken out from the electrode reservoir and positioned in front of the MS sampling orifice for the ESI analysis. While this procedure is feasible, the electrospray generated separation is much simpler and does not need any mechanical manipulation with the capillary during the analysis. This approach would be incompatible with the previously proposed setup, where separations were held in capillaries of 50 μm or 75 μm diameter with a pulled tip [20–22]. This would cause high currents and extensive Joule heating

Table 2
Ions observed in the analysis of cytochrome c tryptic digest. The corresponding retention times and full widths at half maximum (FWHM) are averages from five measurements. The separations were performed at ambient temperature and the relative standard deviations were between 2 and 10%.

Peptide mass	Observed charge	Peptide	Retention time [min]	FWHM [s]
146.08	1×	K	6.69	3.3
260.17	1×	GGK, NK	6.76	3.9
283.17	1×, 2×	HK	5.85	3.6
404.25	1×, 2×	TER	7.19	3.3
433.25	1×, 2×	ATNE	8.15	3.6
588.28	1×	GDVEK - acetylation	8.41	4.8
603.42	1×, 2×	GITWK	7.30	3.9
633.42	1×, 2×	IFVQK	7.45	3.9
677.43	1×, 2×	YIPGTK	7.50	4.2
778.43	1×, 2×	MIFAGIK	7.97	5.4
963.59	1×, 2×	EDLIAZLK	8.09	4.2
1469.68	2×	TGQAPGFTYTDANK	8.15	4.8
1494.70	2×	EETLMEYLENPK	8.68	5.4

in the constricted tip. While the BGE conductivity can be decreased by addition of an organic solvent, such a BGE composition is not compatible with most analytes (weak acids, bases,) due to shifts in dissociation constants leading to loss of charge, resolution and destruction of the peak shape [21]. Only substances with easily dissociated functional groups in low permittivity solvents might be separated under such conditions [20,22].

During our experiments the conductivity detector positioned 15 cm before the ESI tip allowed optimization of the timing of the voltage switching by monitoring the migration of the high mobility inorganic ions present in the sample. Unfortunately, this detector could not reliably detect the separated peptides. In the simplest case the voltage programming can be based on the migration of the fastest ions without the need for the conductivity detector. For example in a cationic separation no peptide will migrate faster than sodium ions with the electrophoretic mobility of 53×10^{-9} Vm/s^2 [17] and switch the voltage at the time when the sodium zone exits the separation capillary. In the 60 cm long capillary at the field strength of 500 V/cm this corresponds to the switching time of 230 s. Similar estimation can be made for anionic separations. Based on the preliminary experiments the applied voltage was reduced after 330 s to 5 kV and the MS base peak electropherogram was recorded with excellent sensitivity. Spectra of 13 specific fragments of cytochrome c together with peptides generated by trypsin miscleavages were detected. The sample solution separated in Fig. 5 was loaded for 10 s by pressure of 1 atm corresponding to the injected sample volume of 0.4 nL. Considering the starting protein concentration of 12 μg/mL (~1 μM) only 400 attomoles were injected and the detection limit (base peak recording) was in the low attomole range. Detected specific fragments are listed in Table 2.

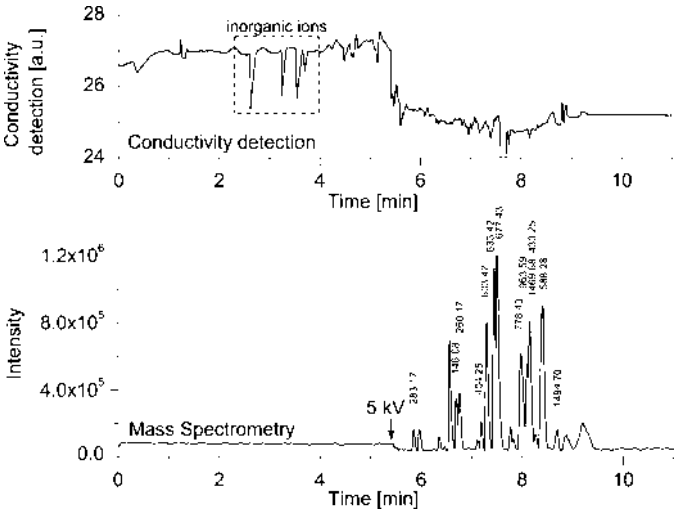

Fig. 5. Base peak electropherogram of cytochrome c tryptic digest (12 μg/mL) with voltage switching. Specific fragments are labelled by their masses. BGE: 0.01% HCOOH. Flow rate: 12 nL/min at 5.0 atm pressure. Capillary: 10 μm × 60 cm. Applied voltage: 30 kV (330 s), 5 kV (>330 s); the conductivity detector was positioned at 45 cm from the injection end.

Efficiency of a separation is given by capillary length (L) and total variance of an analyte zone (σ^2) [17]. The total variance is defined as the sum of all factors contributing to the band broadening. Joule heating, sorption, electromigration dispersion, diffusion, injection and hydrodynamic profile of the flow are typically considered as the main sources of band broadening in capillary electrophoresis. Some of the contributions can be suppressed by suitable experimental conditions. For example Joule heating is negligible in thin capillaries [16], whereas sorption is minimized in bare capillaries by low pH and by using neutral coatings. In the best case in our arrangement only the diffusion and hydrodynamic profile of the flow will be responsible for the band broadening.

The latter is function of capillary diameter (r), flow rate (v), the time of analysis (t) and diffusion coefficient (D) in terms of Eq. (3) [17]:

$$\sigma^2_{flow} = 2tr^2v^2/48D \quad (3)$$

Whereas, variance resulting from diffusion is given by the Einstein equation:

$$\sigma^2_{diff} = 2Dt \quad (4)$$

The best efficiency can be reached in very narrow capillaries [29]. For example 180,000 plates can be reached in a 60 cm × 10 μm ID capillary whereas in a 75 μm ID capillary, commonly used for electrophoretic separations, six times lower maximum efficiency would be achieved. In the described technique the first no-flow electromigration step, driving analytes towards the ESI tip decreases the contribution of hydrodynamic band broadening. On the other hand the flow conditions in the second step have positive effect on the speed of the analysis. However, in this approach it is not possible to calculate number of theoretical plates directly from retention time, since the main cause of motion has different nature in both steps. Whereas the first part of experiment is driven by electromigration, in the second step it is by hydrodynamic flow. The plate numbers corresponding only to the latter step reach on average 6000. This corresponds to about 140,000 plates per meter of the capillary. It should be stressed that such calculated separation efficiency is lowered by all the dispersion effects occurring during the first electromigration step, common for any electrophoretic separation, i.e., electromigration dispersion, adsorption on the capillary wall, injection and diffusion. Extremely fast separations may be achievable with shorter capillaries (providing a fast MS

instrument is available) or higher resolutions could be achieved using higher voltages with long separation capillary [30].

4. Conclusions

The described experimental setup represents the ultimate simplicity in the CE/MS instrumentation. The experiments clearly show the separation potential of the electrospray separation capillary. Since in commonly used capillaries the electric field strength, generated by the electrospray current, may not be sufficient for meaningful electrophoretic separations, using narrow bore capillaries is necessary. The use of such narrow capillaries should be especially suitable for analysis of limited samples (single cells) and, potentially, for multidimensional applications [31]. While the pressure sample injection needs precise high pressure control in the narrow capillaries, alternative methods including electric sample splitter [32] could be also useful for this application. In addition, the narrow capillaries have already been demonstrated as suitable on-line microreactors with surface immobilized enzymes [33]. While 100% water solutions may be necessary for good separations of weak electrolytes (e.g. peptides shown here) mixed water/organic electrolytes may be suitable for the separation of strong electrolytes ionisable in low permittivity solvents and for analysis of samples insoluble in pure water. It can be expected that capillaries with diameters of less than 10 μm should broaden the range of applicable voltages and achieve better more efficient separations. However, such narrow capillaries will require the use of higher pressures, incompatible with our present instrumentation. It is worth stressing that very low diameter sheathless capillary CE/MS should not be viewed as a substitute for the sheath liquid arrangement. While the sheathless interfaces operating at very low flow rates typically provide better sensitivity [34,35], the robustness of the sheath liquid arrangement may excel in applications requiring higher salt concentrations, gradients or ESI additives (standards, reagents). In this respect the liquid junction interfacing [36] may be also a good compromise.

Acknowledgements

Financial support from the Grant Agency of the Czech Republic (P206/12/G014) and the institutional support RVO: 68081715 is acknowledged. Part of the work was realized in CEITEC - Central European Institute of Technology with research infrastructure supported by the project CZ.1.05/1.1.00/02.0068 financed from European Regional Development Fund.

References

[1] J.A. Olivares, N.T. Nguyen, R.D. Smith, Capillary zone electrophoresis-mass spectrometry, Abstr. Pap. Am. Chem. Soc. 193 (1987) 204–210.
[2] F. Foret, J. Preisler, Liquid phase interfacing and miniaturization in matrix-assisted laser desorption/ionization mass spectrometry, Proteomics 2 (2002) 360–372.
[3] K. Klepárník, Recent advances in combination of capillary electrophoresis with mass spectrometry: Methodology and theory, Electrophoresis 36 (2015) 159–178.
[4] A. Hirayama, M. Wakayama, T. Soga, Metabolome analysis based on capillary electrophoresis-mass spectrometry, Trac-Trends Anal. Chem. 61 (2014) 215–222.
[5] G. Bonvin, J. Schappler, S. Rudaz, Capillary electrophoresis-electrospray ionization-mass spectrometry interfaces: Fundamental concepts and technical developments, J. Chromatogr. A 1267 (2012) 17–31.
[6] F. Foret, T.J. Thompson, P. Vouros, B.L. Karger, P. Gebauer, P. Bocek, Liquid sheath effects on the separation of proteins in capillary electrophoresis electrospray mass-spectrometry, Anal. Chem. 66 (1994) 4450–4458.
[7] M. Moini, Capillary electrophoresis mass spectrometry and its application to the analysis of biological mixtures, Anal. Bioanal. Chem. 373 (2002) 466–480.
[8] R. Juraschek, T. Dulcks, M. Karas, Nanoelectrospray - more than just a minimized-flow electrospray ionization source, J. Am. Soc. Mass Spectrom. 10 (1999) 300–308.
[9] J.S. Page, R.T. Kelly, K. Tang, R.D. Smith, Ionization and transmission efficiency in an electrospray ionization-mass spectrometry interface, J. Am. Soc. Mass Spectrom. 18 (2007) 1582–1590.
[10] P. Cao, M. Moini, A novel sheathless interface for capillary electrophoresis/electrospray ionization mass spectrometry using an in-capillary electrode, J. Am. Soc. Mass Spectrom. 8 (1997) 561–564.
[11] E.P. Maziarz, S.A. Lorenz, T.P. White, T.D. Wood, Polyaniline A conductive polymer coating for durable nanospray emitters, J. Am. Soc. Mass Spectrom. 11 (2000) 659–663.
[12] Y.Z. Chang, G.R. Her, Sheathless capillary electrophoresis/electrospray mass spectrometry using a carbon-coated fused silica capillary, Anal. Chem. 72 (2000) 626–630.
[13] J.T. Whitt, M. Moini, Capillary electrophoresis to mass spectrometry interface using a porous junction, Anal. Chem. 75 (2003) 2188–2191.
[14] J.H. Wahl, D.C. Gale, R.D. Smith, Sheathless capillary electrophoresis electrospray-ionization mass-spectrometry using 10 mu-m id capillaries - analyses of tryptic digests of cytochrome-c, J. Chromatogr. A 659 (1994) 217–222.
[15] M. Moini, B. Martinez, Ultrafast capillary electrophoresis/mass spectrometry with adjustable porous tip for a rapid analysis of protein digest in about a minute, Rapid Commun. Mass Spectrom. 28 (2014) 305–310.
[16] M. Grundmann, F.M. Matysik, Fast capillary electrophoresis-time-of-flight mass spectrometry using capillaries with inner diameters ranging from 75 to 5 μm, Anal. Bioanal. Chem. 400 (2011) 269–278.
[17] F. Foret, L. Křivánková, P. Boček, Capillary Zone Electrophoresis, Weinheim, New York, 1993.
[18] L. deJuan, J.F. delaMora, Charge and size distributions of electrospray drops, J. Colloid Interface Sci. 186 (1997) 280–293.
[19] B.R. Reschke, A.T. Timperman, A study of electrospray ionization emitters with differing geometries with respect to flow rate and electrospray voltage, J. Am. Soc. Mass Spectrom. 22 (2011) 2115–2124.
[20] L. Goodwin, J.R. Startin, B.J. Keely, D.M. Goodall, Analysis of glyphosate and glufosinate by capillary electrophoresis - mass spectrometry utilising a sheathless microelectrospray interface, J. Chromatogr. A 1004 (2003) 107–119.
[21] Y.T. Wu, Y.C. Chen, Sheathless capillary electrophoresis/electrospray ionization mass spectrometry using a pulled bare fused-silica capillary as the electrospray emitter, Anal. Chem. 77 (2005) 2071–2077.
[22] M. Mazereeuw, A.J.P. Hofte, U.R. Tjaden, J. vanderGreef, A novel sheathless and electrodeless microelectrospray interface for the on-line coupling of capillary zone electrophoresis to mass spectrometry, Rapid Commun. Mass Spectrom. 11 (1997) 981–986.
[23] P. Kusy, K. Klepárník, Z. Aturki, S. Fanali, F. Foret, Optimization of a pressurized liquid junction nanoelectrospray interface between ce and ms for reliable proteomic analysis, Electrophoresis 28 (2007) 1964–1969.
[24] E. Kenndler, A critical overview of non-aqueous capillary electrophoresis. Part i: Mobility and separation selectivity, J. Chromatogr. A 1335 (2014) 16–30.
[25] G.T.T. Gibson, S.M. Mugo, R.D. Oleschuk, Nanoelectrospray emitters: Trends and perspective, Mass Spectrom. Rev. 28 (2009) 918–936.
[26] A.T. Blades, M.G. Ikonomou, P. Kebarle, Mechanism of electrospray mass-spectrometry - electrospray as an electrolysis cell, Anal. Chem. 63 (1991) 2109–2114.
[27] G.S. Jackson, C.G. Enke, Electrical equivalence of electrospray ionization with conducting and nonconducting needles, Anal. Chem. 71 (1999) 3777–3784.
[28] J.F. Wei, W.Q. Shui, F. Zhou, Y. Lu, K.K. Chen, G.B. Xu, P.Y. Yang, Naturally and externally pulsed electrospray, Mass Spectrom. Rev. 21 (2002) 148–162.
[29] J.W. Jorgenson, E.J. Guthrie, Liquid-chromatography in open-tubular columns - theory of column optimization with limited pressure and analysis time, and fabrication of chemically bonded reversed-phase columns on etched borosilicate glass-capillaries, J. Chromatogr. 255 (1983) 335–348.
[30] S. Barany, Electrophoresis in strong electric fields, Adv. Colloid Interface Sci. 147–48 (2009) 36–43.
[31] F.J. Kohl, L. Sanchez-Hernandez, C. Neususs, Capillary electrophoresis in two-dimensional separation systems: Techniques and applications, Electrophoresis 36 (2015) 144–158.
[32] M. Deml, F. Foret, P. Bocek, Electric sample splitter for capillary zone electrophoresis, J. Chromatogr. 320 (1985) 159–165.
[33] J. Krenkova, K. Klepárník, F. Foret, Capillary electrophoresis mass spectrometry coupling with immobilized enzyme electrospray capillaries, J. Chromatogr. A 1159 (2007) 110–118.
[34] R. Ramautar, J.M. Busnel, A.M. Deelder, O.A. Mayboroda, Enhancing the coverage of the urinary metabolome by sheathless capillary electrophoresis-mass spectrometry, Anal. Chem. 84 (2012) 885–892.
[35] A.A.M. Heemskerk, J.M. Busnel, B. Schoenmaker, R.J.E. Derks, O. Klychnikov, P.J. Hensbergen, A.M. Deelder, O.A. Mayboroda, Ultra-low flow electrospray ionization-mass spectrometry for improved ionization efficiency in phosphoproteomics, Anal. Chem. 84 (2012) 4552–4559.
[36] F. Foret, H.H. Zhou, E. Gangl, B.L. Karger, Subatmospheric electrospray interface for coupling of microcolumn separations with mass spectrometry, Electrophoresis 21 (2000) 1363–1371.

Anna Tycova[1,2]*
Jan Prikryl[1]*
Frantisek Foret[1,3]

[1]Institute of Analytical Chemistry of the CAS, v. v. i., Brno, Czech Republic
[2]Faculty of Science, Masaryk University, Brno, Czech Republic
[3]CEITEC - Central European Institute of Technology, Brno, Czech Republic

Received October 19, 2015
Revised November 20, 2015
Accepted November 20, 2015

Research Article

Reproducible preparation of nanospray tips for capillary electrophoresis coupled to mass spectrometry using 3D printed grinding device

The use of high quality fused silica capillary nanospray tips is critical for obtaining reliable and reproducible electrospray/MS data; however, reproducible laboratory preparation of such tips is a challenging task. In this work, we report on the design and construction of low-cost grinding device assembled from 3D printed and commercially easily available components. Detailed description and characterization of the grinding device is complemented by freely accessible files in stl and skp format allowing easy laboratory replication of the device. The process of sharpening is aimed at achieving maximal symmetricity, surface smoothness and repeatability of the conus shape. Moreover, the presented grinding device brings possibility to fabricate the nanospray tips of desired dimensions regardless of the commercial availability. On several samples of biological nature (reserpine, rabbit plasma, and the mixture of three aminoacids), performance of fabricated tips is shown on CE coupled to MS analysis. The special interest is paid to the effect of tip sharpness.

Keywords:
Capillary electrophoresis / Grinding / Mass spectrometry / Nanospray tip / 3D printing
DOI 10.1002/elps.201500467

Additional supporting information may be found in the online version of this article at the publisher's web-site

1 Introduction

Since its introduction in the 1980s by John Fenn [1], ESI became the key ionization method in bioanalysis. Based on a continuous flow of solution through the electrospray tip and held at a constant potential difference (usually between 2 and 5 kV) with respect to the sampling orifice, ESI is especially suitable for online coupling of column separation techniques including CE. Since the ionization efficiency depends on the electric field strength, the electrospray capillary end is often sharpen into a narrow tip [2].

Besides the stainless steel emitters, frequently used in commercial instrumentations, in-house fabrication of non-conductive fused silica emitters is popular too especially for very low flow applications. Several protocols of fused silica capillary sharpening have been developed, which are based on pulling, etching, and grinding.

In the first case, a short segment of the capillary is heated close to the melting temperature and gently pulled to form a very sharp tip. Open flame [3], electric discharge [4], laser [5], or resistive electric heating wire [6, 7] can be used in this process. Unless precisely controlled the pulling often results in a tip closed with melted glass and reopening by etching in hydrofluoric acid [4, 5] or cutting [3] is needed. Pulling provides very thin emitters with inner diameter between 1 and 10 μm but emitters of less than 100 nm ID have also been reported [6]. Such narrow tips are most suitable for very low flow rates (sub-nL/min) resulting in very efficient ionization; however, clogging within the narrowing part often limits their lifetime. It should be noted that unless fully automated, reproducible tips preparation may be difficult.

In the etching approach, the capillary end, stripped off the outer polyimide coating, is etched by hydrofluoric acid. The acid solution creates a meniscus on the capillary surface defining the tip shape. Since the etching is isotropic, a

Correspondence: Dr. Frantisek Foret, Institute of Analytical Chemistry of the CAS, v. v. i., Veveri 97, Brno 602 00, Czech Republic
E-mail: foret@iach.cz
Fax: +420-541-212-113

Abbreviations: CE-MS, CE coupled to MS; **nano-ESI**, nanospray ionization

*Both authors contributed equally to this work.

Colour Online: See the article online to view Figs. 1–4 in colour.

symmetric tip is created. To prevent penetration of acid into the capillary, washing with water [8] or bubbling with inert gas [9] is recommended. The final shape is given by the time of etching and the depth of immersion and emitters with very thin walls (very fragile) can be prepared. It is worth noting that etching is also used for the creation of porous fused silica segments successfully utilized for the CE coupled to MS (CE-MS) interfacing [9].

Capillary grinding is often used for laboratory preparation of capillary tips with unaltered inner diameter [10–12]. Typically a fine sandpaper is used for manual grinding of the capillary tip. Capillary rotation during the fabrication is critical for obtaining symmetrical tip shape. The sharpness of the tip can be controlled by the angle under which is the capillary lead toward grinding medium [10]. Cheng et al. recently published a less common set-up, where the capillary rotated by an electrical drill was oriented perpendicularly toward the grinding medium. The angle was controlled by the distance between the drill and the grinding medium as well as by the elasticity of the capillary [13]. This operation required precise knowledge of capillary physical properties and thorough optimization. The main advantage of the grinding is no need for aggressive chemicals (etching) or complex and expensive instrumentations (pulling). In addition to the mechanical stability of the tips, the grinding process can be very reproducible with precise control of the tip angle. However, to our best knowledge commercially available grinding devices provide only beveled profile of tips, which are more suitable for biological applications rather than nanospray ionization (nano-ESI) emitters. The tips with symmetrical cone shape have to be therefore fabricated on laboratory-made instrumentations.

In the past decade, 3D printing also known as additive manufacturing or solid-freeform technology has become irreplaceable tool providing an efficient and rapid way of prototyping and manufacturing of laboratory devices [14–22]. The wide range of applicable materials includes photocurable resins, plastics [23, 24], biocompatible materials [25], ceramics [26], or even metals [27–29]. Electron beam melting or selective laser sintering represents the expensive high-end technology, whereas fused deposition modeling has become an inexpensive technology suitable for plastics [30].

In this work, we have developed a low-cost grinding device with adjustable angle arm for precise control of the grinding angle assembled from 3D printed plastic parts. The universal printing files in stl and skp format together with the detailed description of all used components are provided for easy replication. The device was used for sharpening fused silica capillary to obtain a nanospray tip with constant inner channel. It should be mentioned that currently the market with fused silica tips with constant inner channel is limited only to several dimensions (see, e.g. TaperTip™ by New Objective). Since the tip fabrication on proposed grinding device has practically no limitation as for capillary dimensions, it dramatically increases the variations of tips availability to nearly unlimited number. The aim of presented device is not to substitute the commercially available tips but to develop a tool allowing reproducibly fabricate the nano-ESI tips of desired dimensions regardless the commercial availability. The fabricated tips were inspected in terms of the shape reproducibility and performance as nano-ESI emitters for MS and coupling with CE.

2 Materials and methods

2.1 Grinding device construction

Based on the previous experience with the nanospray tips grinding, the device (Fig. 1) was designed using the user-friendly 3D-modeling software SketchUp (Trimble Navigation, Sunnyvale, CA, USA). The body of the grinding device serving also as a bench clamp was fabricated using the fused deposition modeling printer EASY3DMAKER (AROJA, s. r. o., Strážnice, Czech Republic) from white polylactic acid. A small drill (Micromot 50/EF, PROXXON, Niersbach, Germany) was attached to the body to control rotation of a round-shaped grinding support. The grinding medium was fixed to the support by double-sided adhesive tape. Another drill controlled the rotation of the capillary inserted in a PTFE tubing (1/16" OD×0.010"ID, Alltech Associates, Deerfield, IL, USA) and fixed in a quick-action chuck. A PEEK tubing (TPK115, 0.38 ID, VICI AG International, Schenkon, Switzerland) attached in an adjustable angle arm allowed setting of the grinding angle from 5° to 90° in 5° increments. The 3D printed parts were assembled using screws and o-rings without any thread cutting. For the detailed grinding device scheme, the list of purchased components, the assembling procedure as well as freely accessible files in stl and skp format, see the Support Information.

2.2 Tip grinding

A bare fused silica capillaries (Polymicro Technologies, Phoenix, AZ, USA) with 375 μm OD were used for the preparation of the tips. The inner diameter of used capillaries was 25 μm and 15 μm, respectively, and it is always specified in the text. In the first step, a sandpaper with grain size 2000 (Klingspor Abrasive, Hickory, NC, USA) was used, followed by polishing with a fiber-optic lapping film (3M™ Type H - 662XW, 3M Electronics, St. Paul, MN, USA). To assure maximal tip symmetricity, both the capillary and the support for grinding medium were rotating at 10 000 rpm and 7000 rpm, respectively. At constant rotational speed, the tangential speed was defined by the distance from the center of rotation. Therefore, the position of grinded capillary above the grinding support controlled the speed of the grinding as well as the direction of grinding. The rotation of grinding support and capillary were set to counterrun, minimizing the impact of the capillary flexibility on the grinding. For detailed grinding protocol, see the Support Information.

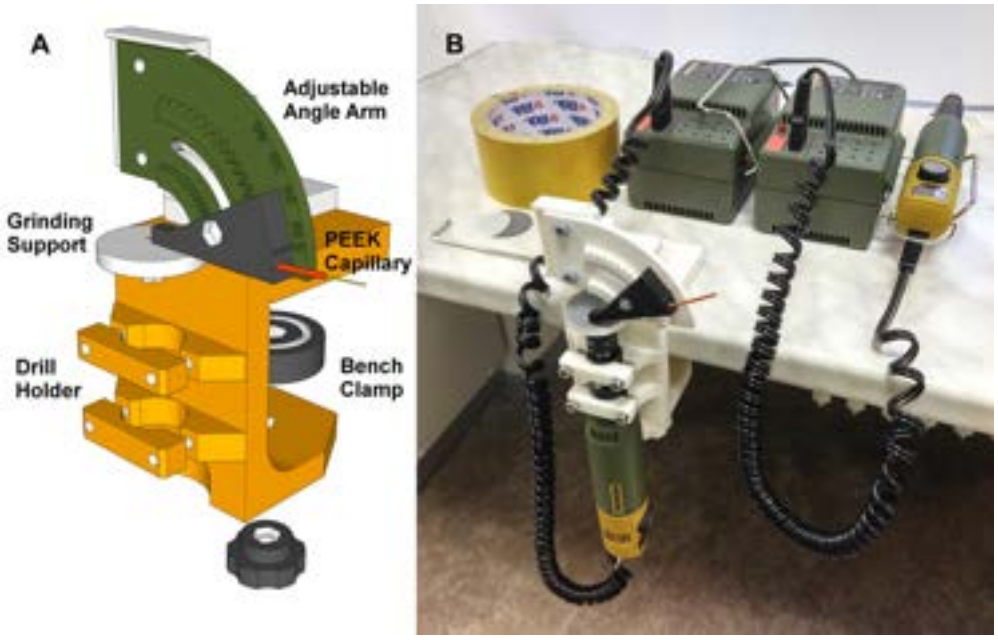

Figure 1. (A) Scheme of the 3D printed plastic parts; (B) photograph of the assembled grinding device.

2.3 Tip characterization and MS

Fabricated tips were inspected under optical stereomicroscope equipped with camera EOS 550D (Canon, Tokyo, Japan). SEM (MIRA3, Tescan, Brno, Czech Republic) was used for detailed imaging of the tip surface.

All the MS experiments were conducted on the Velos Pro Dual-Pressure Linear Ion Trap Mass Spectrometer (Thermo Fisher Scientific, Bremen, Germany) in the positive ionization mode. The tip was positioned approximately 2 mm in front of the inlet capillary. For imaging of the ESI plume, the space between the MS inlet and the ESI tip was illuminated by a laser beam (532 nm, 90 mW, ROITHNER LASERTECHNIK, Vienna, Austria) and the diffraction of the laser light on the sprayed droplets was monitored by a CCD camera (G1-0300, Moravian Instruments, Zlín, Czech Republic). The 15 cm long emitter with diameter 25 × 375 μm was attached to a fused silica capillary of 75 × 375 μm and length 50 cm via CapTite™ connector (LabSmith, Livermore, CA, USA) connected to a gas-pressurized electrode chamber to generate the sample flow and provide the high voltage.

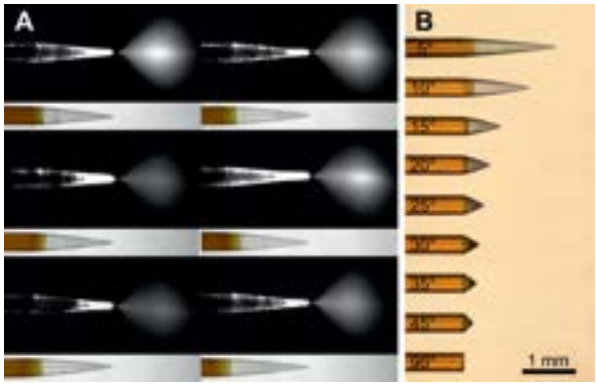

Figure 2. (A) Six nano-ESI tips with ID of 25 μm grinded under 5° with resulting ESI plumes at 5 kV and 150 nL/min; (B) microphotograph of capillary tips grinded at various angles.

2.4 CE-MS

Electrophoretic separation was performed in the sheathless and electrodeless arrangement as described earlier [11]. Briefly, the CE separation in a 60 cm long bare fused silica capillary with the ESI tip was used for a two-step separation. The ID of used capillaries was 25 or 15 μm, respectively. In the first step, high voltage (30 kV) was applied after the pressure sample injection. During this step no flow inside the capillary was generated and the CE separation current was delivered by a Pt electrode placed in the buffer reservoir at the injection side. The ESI tip end of the capillary was placed in front of the grounded MS sampling orifice without any additional electric connection. Under these conditions, all the separation current was conducted by the corona discharge at the capillary tip. In the second step, the voltage was adjusted to nanospray friendly conditions (~5 kV) and the flow inside the separation capillary was initiated by pressurizing the electrode reservoir. Thus, the sample zones, already separated in the first step, were transported to the electrospray tip, electrosprayed, and detected by MS. It is worth noting that the applied high voltage (~5 kV) during the detection step created about 4 kV potential drop along the separation capillary and 1 kV across the electrospray plume.

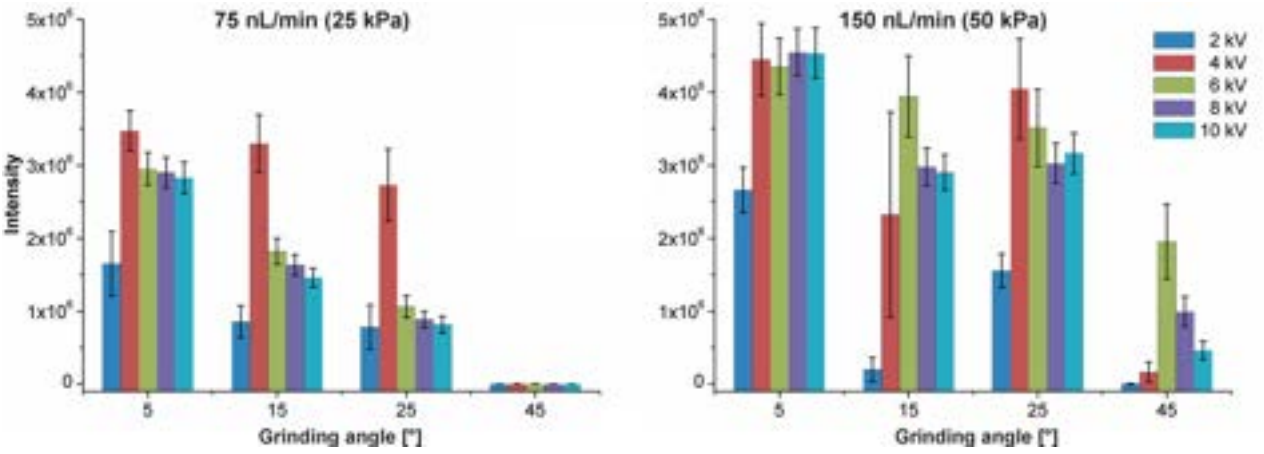

Figure 3. Intensity of reserpine (10^{-6} M) sprayed under different conditions. BGE: 50% methanol, 1% acetic acid v/v. Emitters prepared under four different grinding angles (5°, 15°, 25°, and 45°) were used. Recorded range of *m/z* was 200–1000. The error bars in the graph represent standard deviation for $n = 3$.

2.5 Chemicals

Reserpine, L-histidine, L-alanine, L-methione, and solvents were purchased from Sigma-Aldrich (St. Louis, MO, USA). All solvents were of LC/MS grade. The rabbit plasma sample was deproteinized by mixing with six volumes of acetone. The mixture was centrifuged at 14 000 rpm for 10 min and the supernatant was diluted with two volumes of distilled water prior to injection.

3 Results and discussion

One of the key parameters defining the tip quality is its symmetry. Poor symmetry with off-axis tip opening and/or rough/cracked tip edges results in the spray instability and poor MS signal. In the presented device construction, the symmetricity of the tip was ensured by rotating of both the capillary and the abrasive surface during the grinding process. While higher rotational speed shortens the grinding time, excessive speed may lead to vibrations resulting in an uneven grinding. After thorough optimization, the capillary rotation of 10 000 rpm was chosen as a compromise between these two effects. On the other hand, the rotation of the grinding support minimizes effects of the sandpaper imperfections also assisting to reach symmetrical shape; however, the main benefit is the constant renewal of the grinding surface. Rotational speed of the grinding support (7000 rpm) was chosen according to the optimal linear speed of grinding by the sandpaper recommended by the manufacturer (approximately 10 m/s). Higher speed can cause burning of the sandpaper, lower speed would result in longer grinding times.

To investigate the repeatability of the tip shape prepared with the presented device, six capillaries were sharpened at the grinding angle 5° as shown on the photographs in Fig. 2A together with the corresponding electrospray plumes of 0.15% formic acid solution. All investigated tips provided stable symmetric electrospray plumes. Generally, there are three main causes of cone shape asymmetricity: (i) vibrations of the capillary during the rotational movement, (ii) the asymmetrical removal of the material during the grinding, and (iii) asymmetrical capillary channel from manufacture. Even if the device is constructed to maximally eliminate all these aspects, we estimate that approximately 15% of produced tips are not desirably shaped and are not suitable for sensitive MS analysis.

The adjustable angle arm allows precise change of the grinding angle in steps of 5° up to 90°. The set of the tips prepared with different tip angle is depicted in Fig. 2B. The mass spectrometric response was investigated for four tips prepared at the grinding angles of 5°, 15°, 25°, and 45°. The suitability of the tips for MS analysis was evaluated for the signal of reserpine ($M = 608.68$ g/mol) during an infusion experiment. The experiment was run under two constant flow rates (75 and 150 nL/min) and five different voltages (2, 4, 6, 8, and 10 kV). The signal of reserpine was evaluated in extracted ion mode as an average intensity recorded for 1 min. The results are graphically summarized in Fig. 3.

The electrospray signal is strongly influenced not only by the tip shape, but also by the flow rate and applied voltage. If the voltage is too low at a chosen flow rate, the Taylor cone at the tip is not stable and large droplets are released causing significant instabilities. As the voltage increases, the Taylor cone becomes stable resulting in excellent sensitivity and stability of the MS signal. At higher voltage, the electrospray plume splits into several parts often accompanied by loss of the MS signal.

The experimental data shown in Fig. 3 demonstrate that the biggest robustness toward voltage changes at 75 nL/min flow rate was obtained for the sharpest tip prepared under the 5° grinding angle. The 15° and 25° tips show a rapid signal decrease above 4 kV and the tips ground at 45° did not provide sufficient signal at the 75 nL/min flow rate. At 150 nL/min

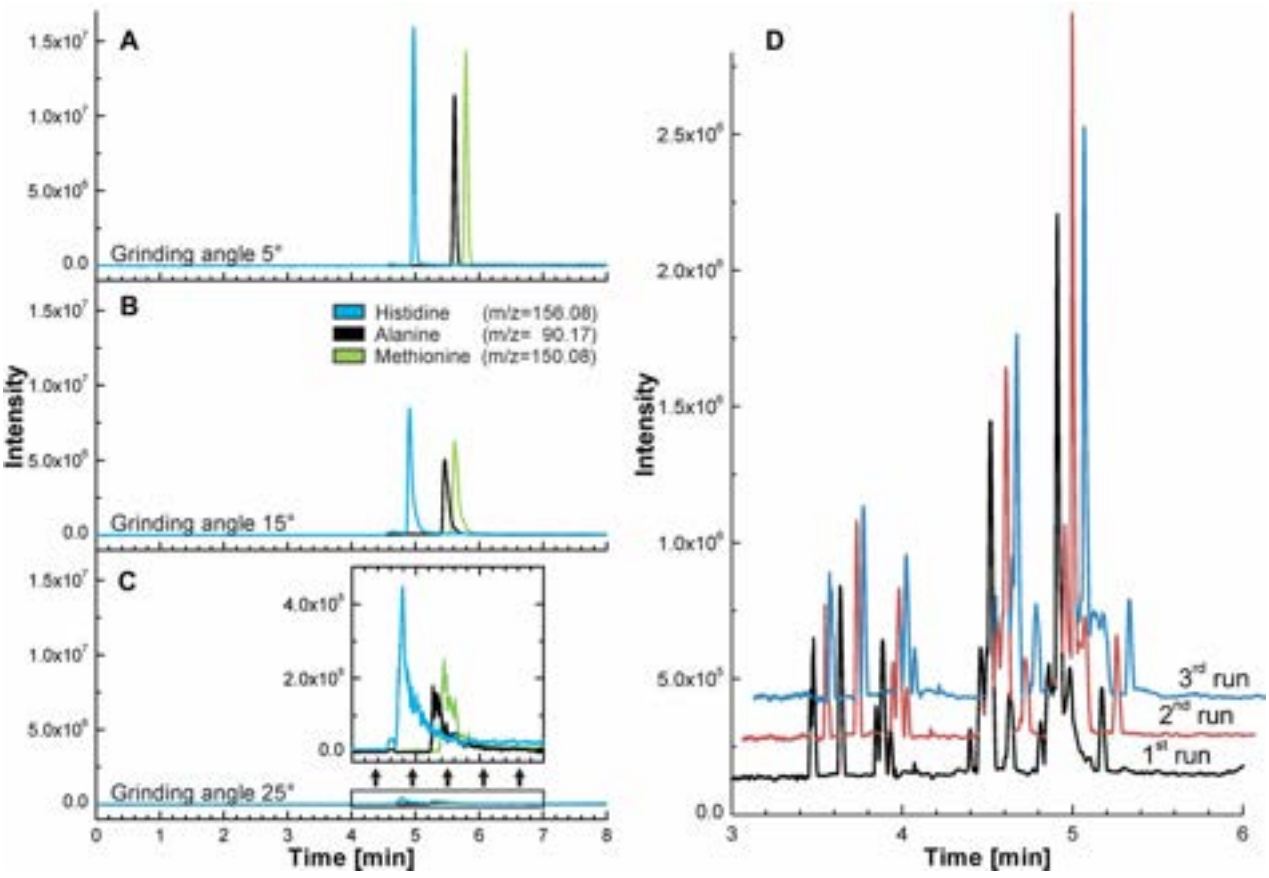

Figure 4. Left, CE-MS analysis of three amino acids of 10 μg/mL concentration. Separations were conducted in capillary ended by tip prepared under grinding angles (A) 5°, (B) 15°, and (C) 25°. The electropherogram is shown in the extracted ion mode; recorded in the *m/z* range of 80–200. BGE: 0.15% HCOOH, 2.5% methanol v/v. Separation capillary: length of 60 cm and dimensions 25 × 375 μm. Separation conditions: 30 kV (0–4 min) at no intended flow rate, 5 kV (4–8 min) at 150 nL/min. Right, (D) base peak CE-MS analysis of rabbit plasma. BGE: 0.15% HCOOH, 2.5% methanol v/v. Separation capillary: length of 60 cm and dimensions 15 × 375 μm. Separation conditions: 30 kV (0–3.5 min) at no flow, 5 kV (3.5–6.0 min) at 20 nL/min. No attempt was made to identify the peaks.

sample flow rate, the analyte signal was more intense for all the tested tips; however, the stability trend was similar to that obtained at the lower flow rate.

The formation of the Taylor cone is given by the equilibrium between the electrostatic force and surface tension of the liquid. Whereas the electrostatic force drags the liquid out of the capillary toward the MS inlet, the surface tension acts in the opposite direction [31]. For tips without sharp ending the liquid does not form a stable plume, since the electric force at a blunt tip is too low. Therefore, the liquid accumulates at the tip surface forming a droplet attracted by the counterelectrode. At the top of this electrically deformed droplet, the electric force is sufficient to surpass surface tension force and form an unstable Taylor cone which is larger than the tip diameter. The size of the Taylor cone affects the diameter of the initial droplets which directly relates to the MS sensitivity [32].

In addition, the larger Taylor cone also leads to higher memory effect resulting in peak broadening. This is demonstrated in Fig. 4 comparing CE-MS traces of the separation of three amino acids in capillaries ended with tips prepared under grinding angles of 5°, 15°, and 25°. While the tip prepared under 5° (Fig. 4A) provided sharp and symmetric peaks, broadening of the zones was significant in capillaries with the tips prepared under 15° (Fig. 4B) or 25° (Fig. 4C) grinding angle. The peak broadening also resulted in a significant loss of the signal intensity. These aspects were taken into account and a tip on a 15 μm ID, 60 cm long capillary was fabricated and tested for the electrodeless CE-MS separation of the deproteinized rabbit plasma (Fig. 4D) further demonstrating the ground tip performance. Three after going separations are shown to present the repeatability of the analysis.

In addition to the tip shape, the ESI stability is also influenced by the surface roughness which affects the wicking of the spray liquid. To support the fine Taylor cone formation only at the tip, its surface should be polished. The sandpaper grains can cause scratches on the fused silica surface with small cracks on the surface leading to higher wettability [33]. The resulting wider base of the Taylor cone leads to an unstable ESI signal. In Fig. 5A, the tip surface was grinded by sandpaper of grain size 2000 and finally polished by fiber-optic lapping film—Fig. 5B. While the surface ground by the

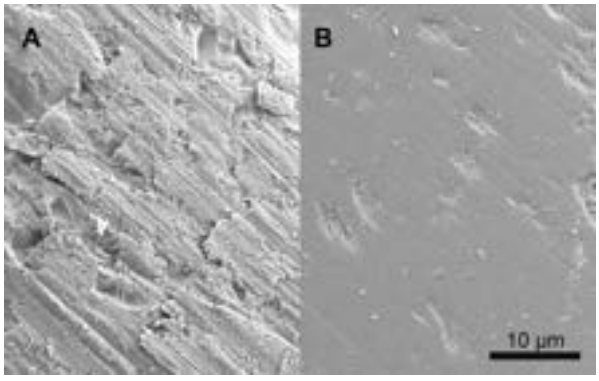

Figure 5. SEM of (A) an emitter surface grinded by sandpaper of 2000 grain size; (B) an emitter surface grinded by fiber-optic lapping film.

sandpaper shows obvious protrusions, the polished surface is much smoother. It should be noted that polishing might be, to some extent, replaced by a hydrophobic coating, e.g. Teflon [34] or acrylic paint [35]. The thickness of the capillary wall at the tip ranging from 5 to 10 μm was routinely achieved, which is comparable to other fabrication procedures [9].

The conducted experiments imply best potential for tips prepared under grinding angle of 5°, with perfectly symmetrical shape and polished by optical paper to eliminate the protrusions and decrease wettability.

4 Concluding remarks

In this work, the low-cost grinding device for sharpening of fused silica capillaries is presented including characterization of the prepared nanospray tips for infusion and CE-MS analysis. 3D printing additive manufacturing was chosen allowing rapid design and construction. Since the sharpen capillaries were aimed to be used as nanospray emitters, the special interest in construction was paid to controllable grinding angle and symmetrical and repeatable shape production. The data observed during MS analysis clearly prove the need for quality sharp emitters for the most robust and sensitive analysis. The CE-MS data showed that the electrospray tip shape can significantly influence the peak shape, sensitivity, and separation resolution.

The adjustable angle arm of the grinding device allows not only sharpening of the capillary tip but also fabrication of the capillary with completely flat end (at the 90° grinding angle), which significantly broadens the potential of applications. While the sharp tips might be also useful for microinjections [13] or micromanipulations [36], the flat ending is a crucial part for capillary connections [37, 38] including the liquid junction CE-MS interfacing [39].

This work was supported by the Czech Science Foundation (P206/12/G014, GA15-15479S) and Institutional support RVO: 68081715. The authors wish to thank Jana Krenkova for the SEM imaging. Part of the work was realized in CEITEC - Central European Institute of Technology with research infrastructure supported by the project CZ.1.05/1.1.00/02.0068 financed from European Regional Development Fund.

The authors have declared no conflict of interest.

5 References

[1] Yamashita, M., Fenn, J. B., *J. Phys. Chem.* 1984, *88*, 4671–4675.

[2] Kebarle, P., Verkerk, U. H., *Mass Spectrom. Rev.* 2009, *28*, 898–917.

[3] Hannis, J. C., Muddiman, D. C., *Rapid Commun. Mass Spectrom.* 1998, *12*, 443–448.

[4] Ek, P., Roeraade, J., *Anal. Chem.* 2011, *83*, 7771–7777.

[5] Valaskovic, G. A., Kelleher, N. L., Little, D. P., Aaserud, D. J., McLafferty, F. W., *Anal. Chem.* 1995, *67*, 3802–3805.

[6] Yuill, E. M., Sa, N. Y., Ray, S. J., Hieftje, G. M., Baker, L. A., *Anal. Chem.* 2013, *85*, 8498–8502.

[7] Lundqvist, A., Pihl, J., Orwar, O., *Anal. Chem.* 2000, *72*, 5740–5743.

[8] Kelly, R. T., Page, J. S., Luo, Q. Z., Moore, R. J., Orton, D. J., Tang, K. Q., Smith, R. D., *Anal. Chem.* 2006, *78*, 7796–7801.

[9] Moini, M., *Anal. Chem.* 2007, *79*, 4241–4246.

[10] Kriger, M. S., Cook, K. D., Ramsey, R. S., *Anal. Chem.* 1995, *67*, 385–389.

[11] Tycova, A., Foret, F., *J. Chromatogr. A* 2015, *1388*, 274–279.

[12] Kusy, P., Kleparnik, K., Aturki, Z., Fanali, S., Foret, F., *Electrophoresis* 2007, *28*, 1964–1969.

[13] Cheng, Y. Q., Su, Y., Fang, X. X., Pan, J. Z., Fang, Q., *Electrophoresis* 2014, *35*, 1484–1488.

[14] Gowers, S. A. N., Curto, V. F., Seneci, C. A., Wang, C., Anastasova, S., Vadgama, P., Yang, G. Z., Boutelle, M. G., *Anal. Chem.* 2015, *87*, 7763–7770.

[15] Prikryl, J., Foret, F., *Anal. Chem.* 2014, *86*, 11951–11956.

[16] Salentijn, G. I. J., Permentier, H. P., Verpoorte, E., *Anal. Chem.* 2014, *86*, 11657–11665.

[17] Anderson, K. B., Lockwood, S. Y., Martin, R. S., Spence, D. M., *Anal. Chem.* 2013, *85*, 5622–5626.

[18] Shallan, A. I., Smejkal, P., Corban, M., Guijt, R. M., Breadmore, M. C., *Anal. Chem.* 2014, *86*, 3124–3130.

[19] Bishop, G. W., Satterwhite, J. E., Bhakta, S., Kadimisetty, K., Gillette, K. M., Chen, E., Rusling, J. F., *Anal. Chem.* 2015, *87*, 5437–5443.

[20] Wei, Q. S., Luo, W., Chiang, S., Kappel, T., Mejia, C., Tseng, D., Chan, R. Y. L., Yan, E., Qi, H. F., Shabbir, F., Ozcan, A., *ACS Nano* 2014, *8*, 12725–12733.

[21] Wei, Q. S., Nagi, R., Sadeghu, K., Feng, S., Yan, E., Ki, S. J., Caire, R., Tseng, D., Ozcan, A., *ACS Nano* 2014, *8*, 1121–1129.

[22] Wei, Q. S., Qi, H. F., Luo, W., Tseng, D., Ki, S. J., Wang, Z., Gorocs, Z., Bentolila, L. A., Wu, T. T., Sun, R., Ozcan, A., *ACS Nano* 2013, *7*, 9147–9155.

[23] Turner, B. N., Strong, R., Gold, S. A., *Rapid Prototyp. J.* 2014, *20*, 192–204.

[24] Turner, B. N., Gold, S. A., *Rapid Prototyp. J.* 2015, *21*, 250–261.

[25] Sidambe, A. T., *Materials* 2014, *7*, 8168–8188.

[26] Deckers, J., Vleugels, J., Kruthl, J. P., *J. Ceram. Sci. Technol.* 2014, *5*, 245–260.

[27] Frazier, W. E., *J. Mater. Eng. Perform.* 2014, *23*, 1917–1928.

[28] Gu, D. D., Meiners, W., Wissenbach, K., Poprawe, R., *Int. Mater. Rev.* 2012, *57*, 133–164.

[29] Murr, L. E., Gaytan, S. M., Ramirez, D. A., Martinez, E., Hernandez, J., Amato, K. N., Shindo, P. W., Medina, F. R., Wicker, R. B., *J. Mater. Sci. Technol.* 2012, *28*, 1–14.

[30] Gross, B. C., Erkal, J. L., Lockwood, S. Y., Chen, C. P., Spence, D. M., *Anal. Chem.* 2014, *86*, 3240–3253.

[31] Wei, J. F., Shui, W. Q., Zhou, F., Lu, Y., Chen, K. K., Xu, G. B., Yang, P. Y., *Mass Spectrom. Rev.* 2002, *21*, 148–162.

[32] Wilm, M. S., Mann, M., *Int. J. Mass Spectrom.* 1994, *136*, 167–180.

[33] Wenzel, R. N., *Ind. Eng. Chem* 1936, *28*, 988–994.

[34] Tomalova, I., Foltynova, P., Kanicky, V., Preisler, J., *Anal. Chem.* 2014, *86*, 647–654.

[35] Bigwarfe, P. M., White, T. P., Wood, T. D., *Rapid Commun. Mass Spectrom.* 2002, *16*, 2266–2272.

[36] Kim, J. Y., Wei, Y. Z., Li, J. H., Kim, S. O., *Biosens. Bioelectron.* 2010, *26*, 555–559.

[37] Shi, L. H., Jin, Y. X., Moon, D. C., Kim, S. K., Park, S. R., *Electrophoresis* 2009, *30*, 1661–1669.

[38] Tong, W., Link, A., Eng, J. K., Yates, J. R., *Anal. Chem.* 1999, *71*, 2270–2278.

[39] Krenkova, J., Kleparnik, K., Grym, J., Luksch, J., Foret, F., *Electrophoresis* 2016, in press, DOI:10.1002/elps.201500357

Journal of Chromatography A, 1466 (2016) 173–179

Contents lists available at ScienceDirect

Journal of Chromatography A

journal homepage: www.elsevier.com/locate/chroma

Interface-free capillary electrophoresis-mass spectrometry system with nanospray ionization—Analysis of dexrazoxane in blood plasma

Anna Tycova[a,b], Marek Vido[b], Petra Kovarikova[c], Frantisek Foret[a,d,*]

[a] Institute of Analytical Chemistry of the CAS, v. v. i., Veveri 97, Brno, 602 00, Czech Republic
[b] Faculty of Science, Masaryk University, Kotlarska 2, Brno, 611 37, Czech Republic
[c] Faculty of Pharmacy in Hradec Kralove, Charles University in Prague, Heyrovskeho 1203, Hradec Kralove, 500 05, Czech Republic
[d] CEITEC – Central European Institute of Technology, Kamenice 753/5, Brno, 625 00, Czech Republic

ARTICLE INFO

Article history:
Received 23 June 2016
Received in revised form 16 August 2016
Accepted 18 August 2016
Available online 23 August 2016

Keywords:
Capillary electrophoresis
Mass spectrometry
Nanospray
Hydrophobic coating
Interface
Dexrazoxane

ABSTRACT

The newly developed interface-free capillary electrophoresis-nanospray/mass spectrometry system (CE-nESI/MS) was applied for rapid analysis of the cardioprotective drug dexrazoxane and its hydrolysed form ADR-925 in deproteinized blood plasma samples. The aim of this study was to test the simplest possible CE-nESI/MS instrumentation for analyses of real samples. This interface-free system, utilizing single piece of a narrow bore capillary as both the electrophoretic separation column and the nanospray emitter, was operated at a flow rate of 30 nL/min. Excellent electrophoretic separation and sensitive nanospray ionization was achieved with the use of only one high voltage power supply. In addition, hydrophobic external coating was developed and tested for additional stability of the nanospray ionization. To our knowledge this is the first study devoted to the analysis of dexrazoxane and ADR-925 by capillary electrophoresis-mass spectrometry.

1. Introduction

Capillary electrophoresis (CE) can provide efficient separation of ionic species according to their electrophoretic mobility. The separation is usually performed in fused silica capillaries with inner diameters of 50–150 μm, where narrower tubes result in lower Joule heating and allow the use of higher electric field strength and/or background electrolyte (BGE) with higher conductivity [1–4]. Another important aspect of separations in narrow bore channels is a substantial decrease of the sample consumption making CE useful especially if limited sample is available, e.g., in single cell lysates [5]. The diameter reduction of the separation capillary results also in the reduction of flow rate necessary for transporting the separated zones into the electrospray. At the very low flow rates (below 100 nL/min) the ionization efficiency increases together with the robustness towards the solvent composition and ion suppression effects decrease [6,7]. This was recently demonstrated by Moini and Rollman running CE-nESI/MS analysis at a flow rate of 10 nL/min, allowing high sensitivity analyses even with nonvolatile chiral selector (sodium salts of cyclodextrin) in the BGE [8]. Similarly, Mayboroda et al. investigated signal of multiply phophorylated peptides within 6.6–100 nL/min during MS infusion. An increase in ionization efficiency of phophorylated peptides was observed at decreased flow rates. Moreover, nanospray operated at ≤20 nL/min provided nearly equimolar response of the tested analytes as a result of significantly reduced ion suppression effect [9].

While it is clear that nanospray brings the best ionization performance, there are different ways of coupling it with the capillary electrophoresis. Two basic groups can be distinguished based on the interface construction with respect to the electric current connection at the electrospray end of the separation capillary. In the first group of the coaxial sheath liquid arrangement [10], an additional conductive liquid (spray liquid) is added for the transport of the separated ions into the nanospray tip. Similar arrangement called a liquid junction [11–13] allows the use of additional liquid with or without any additional flow (pressure or electroosmotic). The electric currents circuits for both the electrophoretic separation and electrospray ionization can be closed via an electrode in contact with the spray liquid. This design has been recently optimized for high sensitivity separations [14–16]. The same principle can be also used in microfabricated devices for mass spectrometry [17,18]. The second group uses a conductive component e.g. attached tip, tip coating or porous glass membrane for electrical connection [19]. Generally, the interfaces implementing a spray liquid provide wider

* Corresponding author at: Institute of Analytical Chemistry of the CAS, v. v. i., Veveri 97, Brno 602 00, Czech Republic.
E-mail address: foret@iach.cz (F. Foret).

http://dx.doi.org/10.1016/j.chroma.2016.08.042
0021-9673/

operation range with respect to the capillary size and buffer composition, whereas sheathless designs may reach better sensitivity [20,21].

Recently, we have proposed a type of interface-free design [22] where the electrophoretic separation is performed in a long narrow bore capillary (ID ≤15 μm) serving also as the nanospray tip. In this design the electrospray current was connected at the injection end of the separation capillary and the resistance of the narrow separation channel created sufficiently high potential drop for the CE separation. Thus only one high voltage power supply was needed with no additional electric connection at the electrospray capillary end making the instrument extremely simple.

It should be mentioned, that the shape of the electrospray tip strongly influences the ionization performance. If the tip is blunt, asymmetric or its surface is rough (cause of higher wettability), the base of the Taylor cone tends to spread resulting in the loss of ionization efficiency, signal stability and resolution of separated zones [23–25]. The volume of Taylor cone can be held at minimum level if the emitter tip is sharp and smooth [26]. Significant improvement can also be achieved with emitters from hydrophobic materials or with hydrophobic surface coating [27,28].

Here we present the interface-free system for CE-nESI/MS with hydrophobically coated nanospray tip for repeatable and sensitive simultaneous analysis of dexrazoxane and its metabolite ADR-925 in blood plasma.

2. Material and methods

2.1. Chemicals

Dexrazoxane, ammonium formate, formic acid and all the solvents were purchased from Sigma Aldrich, (MO, USA). ADR-925 was synthesized by procedure described previously [29].

2.2. Sample preparation

Stock solution of dexrazoxane was dissolved in methanol in 1 mg/mL concentration. ADR-925 was prepared in concentration of 0.1 mg/mL in 50% methanol (v/v).

The rabbit plasma sample was deproteinized by mixing with six volumes of acetone and vortexed approximately for 30 s. The mixture was centrifuged at 14 000 rpm for 10 min. To concentrate the analytes and to avoid the difficulties resulting from high acetone percentage, 100 μL of supernatant was evaporated in the vacuum evaporator (20 min) and dissolved in 10 or 50 μL deionized water.

Samples for in vivo study were obtained from a rabbit treated by 60 mg/kg dose of dexrazoxane. Blood was collected after 10, 20, 60, 120 and 180 min post dose and processed to plasma. The dose, route of administration and experimental setting of the in vivo experiment was used as described previously in the study of dexrazoxane-afforded cardioprotection [30]. Each sample was divided into three aliquots to quantify dexrazoxane by the method of standard addition. Dexrazoxane was added to the sample to reach its final concentrations of 0, 25 and 50 μg/mL. The rest of the sample treatment was the same as described above for the spiked plasma samples. All the plasma samples were kindly provided by Dr. Sterba (Faculty of Medicine in Hradec Kralove, Czech Republic).

2.3. Fabrication of nanospray tip

The nanospray tip was fabricated at the end of a 60 cm long fused silica capillary with 15 μm ID (Polymicro Technologies, AZ, USA) by grinding. The inner capillary diameter remains unchanged during the grinding process. The tip angle was set to 5° using the grinding device assembled from 3D printed components [26]. To support the electrospray Taylor cone stability the tip was treated by a hydrophobic coating prepared from a mixture of the Teflon® AF in the form of 60% water dispersion (DuPont CZ, Prague, Czech Republic) and transparent UV top coat nail polish (Dermacol, Brno, Czech Republic) in volume ratio 3:1. The tip was horizontally dip-coated into the dispersion for 5 s. To prevent tip clogging the capillary was flushed by nitrogen at 4 atm. The coating was dried at laboratory temperature in vertical position for 5 min, treated by heat gun at 370 °C for 3 min and exposed to UV lamp for 30 s to harden the coating.

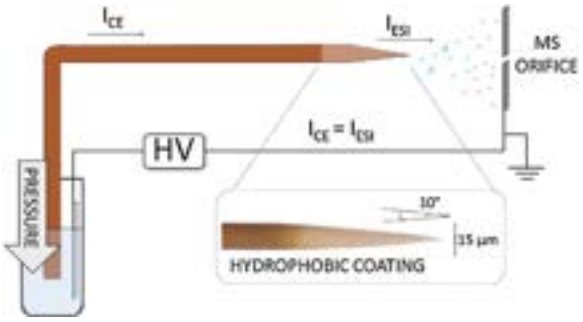

Fig. 1. The scheme of the CE-nESI/MS instrumentation.

2.4. Characterization of tip surface

The surface of fabricated tips was inspected under scanning electron microscopy (MIRA3, Tescan, Brno, Czech Republic). The hydrophobicity of the coating was investigated by contact angle measurement on See System (Department of Physical Electronics, Masaryk University, Brno, Czech Republic).

2.5. CE-nESI/MS

Electrophoretic separations were performed in the sheathless and electrodeless arrangement as described earlier [22]. Briefly, the CE separation was conducted in a bare fused silica capillary (60 cm, 15 μm ID) with the nanospray tip at one end. The tip was positioned in front of the MS sampling orifice without any additional electrical connection. The opposite (injection) capillary end was placed in a polypropylene vial inside a nitrogen pressurized chamber allowing control of the flow rate in the capillary as well as sample injection. Using a 0.5 atm pressure for 10 s, approximately 1 nL of the sample was loaded. The CE separation current was delivered by SL 10 W–300 W power supply (Spellman High Voltage Electronics, United Kingdom) via a Pt electrode inserted into the polypropylene vial. Aqueous solution of 1.5% formic acid (v/v; pH = 1.9) was used as the BGE. The analysis was divided into two steps. In the first step, after the sample injection, high voltage (30 kV) was applied under no flow conditions. During this step, the separation current (3.5 μA) caused fast migration and separation of the sample ions and also resulted in the formation of corona discharge at the capillary tip, unsuitable for mass spectrometry analysis. After 4 min, the voltage was adjusted to the nanospray friendly level of 5 kV (the ESI current was measured in an independent experiment as ~0.1 μA) and the BGE flow of 30 nL/min inside the separation capillary was initiated by pressurizing the electrode reservoir. Thus, the sample zones, already separated in the first step, were transported to the nanospray tip, electrosprayed, and detected by MS under optimum nanospray conditions. The scheme of used CE-nESI/MS instrumentation is in Fig. 1.

All MS experiments were conducted on the Velos Pro Dual-Pressure Linear Ion Trap Mass Spectrometer (Thermo Fisher Scientific, Germany) in the positive ionization mode. The nanospray

tip was positioned axially approximately 2 mm in front of the MS inlet capillary. The precise position of the tip was adjusted with a translation stage and monitored by a CCD camera. For MS/MS experiments CID fragmentation was used with the collision energy of 35 eV for monitoring of specific fragments of dexrazoxane (269.1 → 155.3) and ADR-925 (305.1 → 173.3) [29].

All experiments were conducted in a clean laboratory with air filtration and minimum of dust particles. The potential risk of capillary clogging was therefore limited and no special sample manipulation was necessary. Under these conditions, the lifetime of the capillary/emitter was usually 2–3 weeks.

3. Results and discussion

The cardioprotective drug dexrazoxane is administered during treatment with anthracycline chemotherapeutics to reduce their side effects, including hair loss, indigestion, faintness and, especially, fatal damage of the heart tissue. It has been in use since 1995; however, details on the mechanifsm of its cardioprotective effect are still poorly understood. The traditional theory supposed that the key point is the drug activation based on hydrolysis into a chelating active metabolite – ADR-925. However, the recent investigations suggest that the other mechanisms associated with the parent drug may also be involved [31]. Therefore, and the analysis of dexrazoxane and its putative active metabolite ADR-925 is important to investigate the mechanism of the drug cardioprotection. Simultaneous chromatographic analysis of both agents has been challenging. In past reverse-phase HPLC with ion-pairing agents was successfully used, however, the method was not suitable for online mass spectrometric detection and insensitive UV detection was therefore used instead [32]. Later, HPLC–MS method for determination of both compounds in biological materials was validated within the concentration range of 8–100 μM in cell culture media and 4–80 and 7–70 pmol/10^6cells in cardiac cells, for dexrazoxane and ADR-925 respectively, with relatively long (over 20 min) analysis time [29]. The fact, that both substances of interest are under acidic conditions positively charged and differ in their steric properties, makes CE-MS a promising method for their analysis.

3.1. Nanospray tip treatment

Quality of the nanospray tip is a key for achieving stable and reproducible MS results. With the tip diameter of 15 μm only very low flow rates («100 nL/min) result in a stable electrospray. It is possible to fabricate the tip by three basic procedures – grinding, etching in hydrofluoric acid or capillary pulling. The process of grinding was chosen based on our previous experience, providing the best compromise between the sharpness and robustness. Under ideal conditions, the Taylor cone base is given only by the inner diameter of the electrospray capillary. Unfortunately, the wettability of the tip surface (especially at higher flow rates) often results in the base extending over the tip edges leading to signal instabilities and broadening of the separated zones [23,26]. The tip wettability depends on the material it is made of and its surface morphology. The hydrophilic property of fused silica, used in this work, was further boosted by microscopical scratches originating from tip grinding (Fig. 2A). While the scratches could be further minimized by thorough polishing or different fabrication procedure (e.g. etching in HF), the wetting properties of the surface remained unchanged. To eliminate the tip surface wetting a new durable hydrophobic coating was tested based on a water dispersion of Teflon and UV curable polish. Despite the fact, that Teflon has brilliant hydrophobic properties [33], it suffers from poor mechanical stability especially in the presence of organic solvents. The polish in the coating mixture contributed to better adhesion to the tip surface, mechanical durability and stability towards water and organic solvents, usually used in MS experiments (e.g. methanol). After treating the glass surface the contact angle of water droplet increased from 38 ± 3° to 123 ± 3° (Fig. 2B). Moreover, the coating reduced the need of time consuming tip polishing. The small cavities ranging in size from 20 nm to 1 μm did not influence the hydrophobic properties of the coating. The water droplet exiting through the tip has no tendency to spread past the edge thus stabilizing the Taylor cone during analysis (Fig. 2C). The stability towards solvents was good and the lifetime of the emitter was mostly limited by the tip breakage or clogging, typically once in 2 weeks.

3.2. Analysis of dexrazoxane and ADR-925

In the past both the prodrug dexrazoxane and its hydrolyzed form called ADR-925 were separated by chromatographic techniques [29,32]; however, the presence of secondary amines in dexrazoxane ($pK_a \sim 2.6$) [29] and amidic groups in ADR-925 ($pK_a \sim 2.0$) [29] indicate a good potential for sensitive CE-MS under acidic conditions with positive ESI. Given the pK values of the analytes 1.5% formic acid (v/v) with the pH 1.9 was selected as the background electrolyte.

In this study, we have used the rabbit plasma samples spiked with dexrazoxane and ADR-925 for investigation of dexrazoxane metabolism. The high plasma protein levels typically lead to their strong adsorption on the capillary wall and sample pretreatment is usually required. Although there are many ways of sample deproteinization (e.g. ultrafiltration, size-exclusion chromatography or salt precipitation), organic solvent precipitation was evaluated as the most convenient approach. From the tested solvents, acetone provided the best efficiency of deproteinization. Unfortunately, the low conductivity of supernatant prevented (due to high acetone percentage) from its direct injection for analysis. Moreover, acetone volatility caused gradual changes of the sample concentration during analyses. Therefore, the supernatant was completely evaporated in a vacuum concentrator and re-dissolved in water. In Fig. 3 the separation of deproteinized spiked blood plasma (Fig. 3A) and extracted ion electropherograms of both analytes of interest (Fig. 3B) are shown.

The separation was finished within 7 min being about 3 times faster when compared with the validated HPLC–MS [34]. The repeatability of the measurement was calculated from five replicated analyses. Despite the extreme system simplicity and manual operation of the instrumentation, the migration times of both symmetric peaks were repeatable within 0.28% and 0.21%, with peak heights RSDs of 3.97% for dexrazoxane and 6.76% for ADR-925, respectively. Number of theoretical plates would provide clear information about the separation efficiency; however, here it is not easy to calculate number of theoretical plates directly from the migration times. While the motion of separated zones is driven by electromigration to different velocities in the first step, hydrodynamic flow in the second step is the main transport force moving all zones with a constant velocity. It can be assumed that RSD of the mass spectrometric response can be significantly improved by automation of the sample loading. The lower repeatability of the ADR-925 peak intensity can be attributed to its higher tendency towards sodium and potassium adducts formation. The system provided also very good linearity over four orders of magnitude. Both the linearity and sensitivity was investigated in the MS/MS mode with CID fragmentation and monitoring of the fragments with masses of 155.3 (dexrazoxane) and 173.3 (ADR-925). The sensitivity, linearity and repeatability values are summarized in Table 1.

It should be noted that the LODs obtained for the spiked plasma samples (see Fig. 4B) are more than an order of magnitude worse

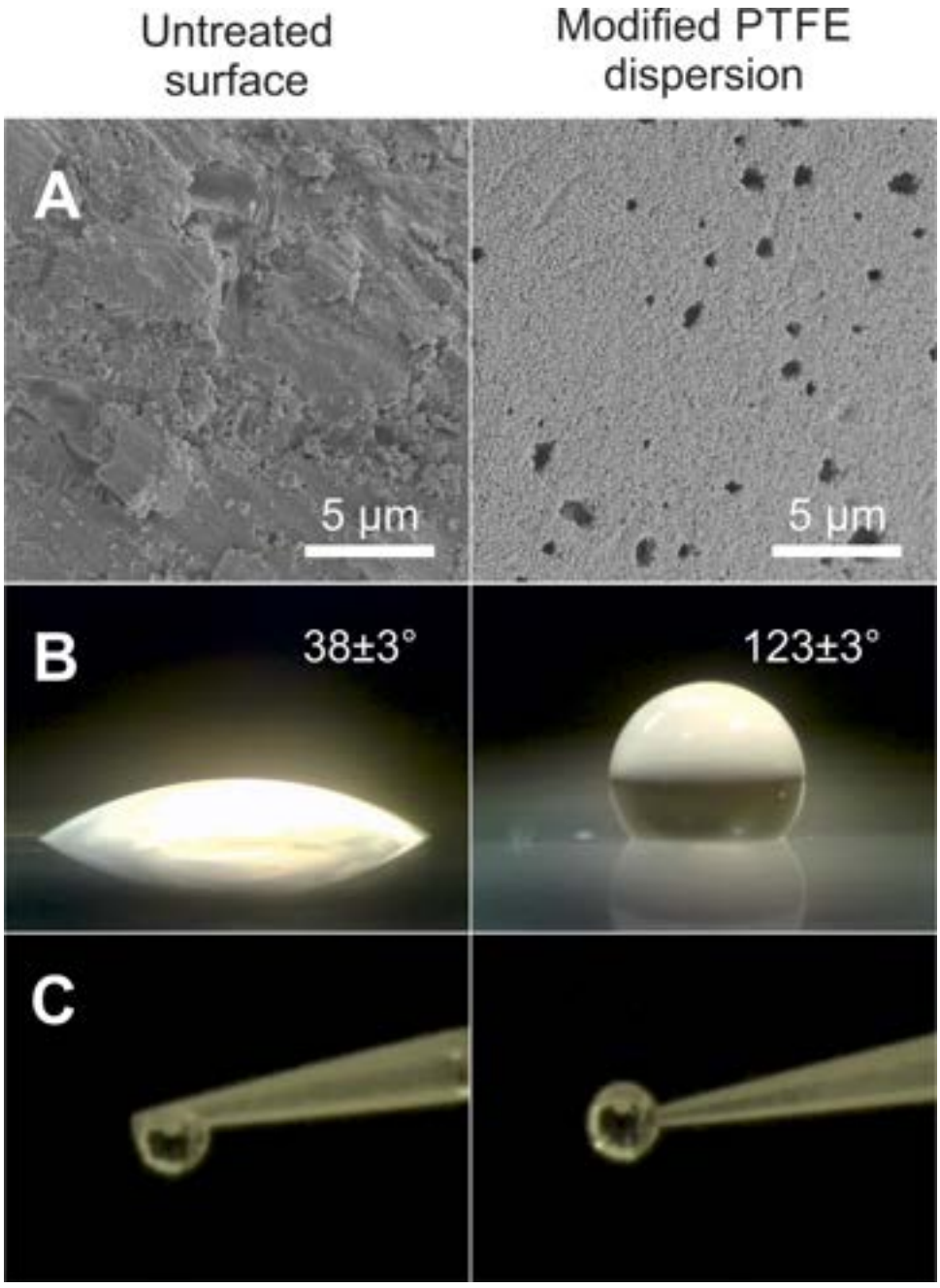

Fig. 2. Characteristics of untreated and hydrophobicaly treated surface: A – SEM image of the tip surface, B – contact angle, C – behavior of water at the tip ending.

Table 1
Repeatability, linearity and sensitivity of dexrazoxane and ADR-925 in the spiked plasma. For measurement of repeatability standard concentration of 1.25 μg/mL was used. The LOD and LOQ was determined as a signal-to-noise ratio of 3:1 or 10:1, respectively.

	Repeatability (n = 5)		Linearity			Sensitivity	
	RSD tr [%]	RSD intensity [%]	Concentration range [μg/mL]	Linear regression equation	Correlation coefficient [R^2]	LOD [ng/mL]	LOQ [ng/mL]
DEX *(m/z 269.1)*	0.28	3.97	50–0.05	y = 15,925x + 5055	0.9977	25	83
ADR-925 *(m/z 305.1)*	0.21	6.76	100–0.1	y = 41,692x – 58,470	0.9926	50	167

y – peak intensity, x – analyte concentration (μg/mL).

than those obtained when separating standards dissolved in the buffer only. The LODs for standard solutions were determined to be 0.9 ng/mL for dexrazoxane and to 0.6 ng/mL for ADR-925, respectively (2 attomoles injected). Clearly, the poor sample recovery during the protein precipitation by acetone together with the matrix effect was responsible for the reduced sensitivity during

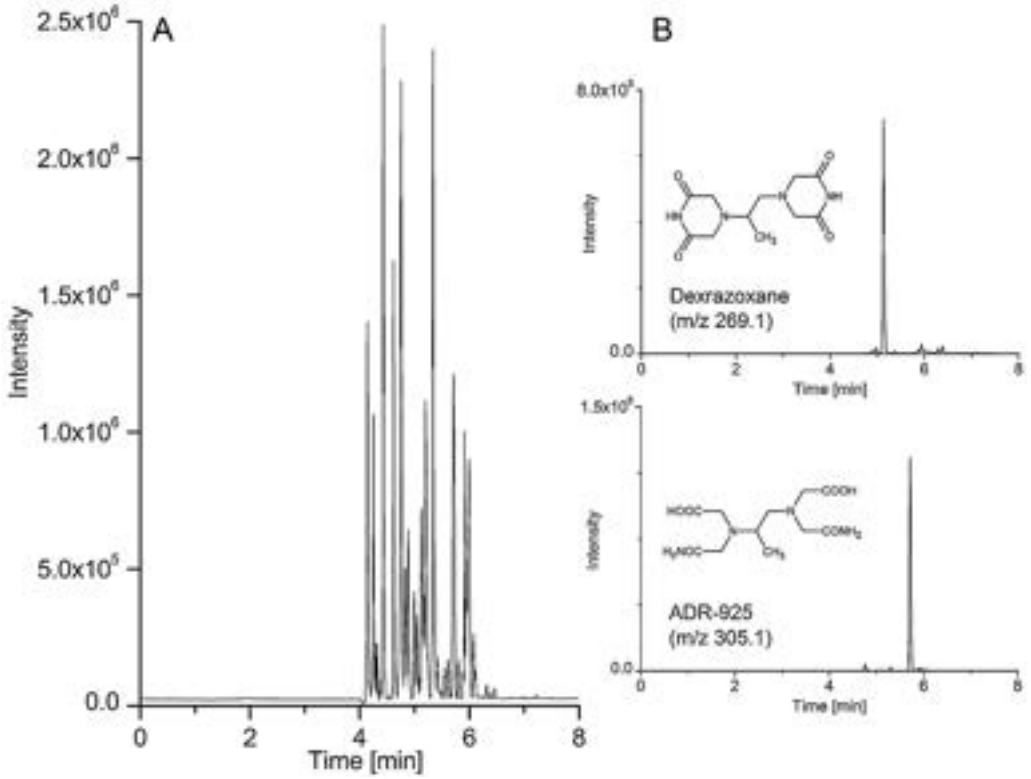

Fig. 3. A – Base peak electropherogram of spiked rabbit blood plasma, B – extracted ion electropherogram of dexrazoxane and ADR-925.

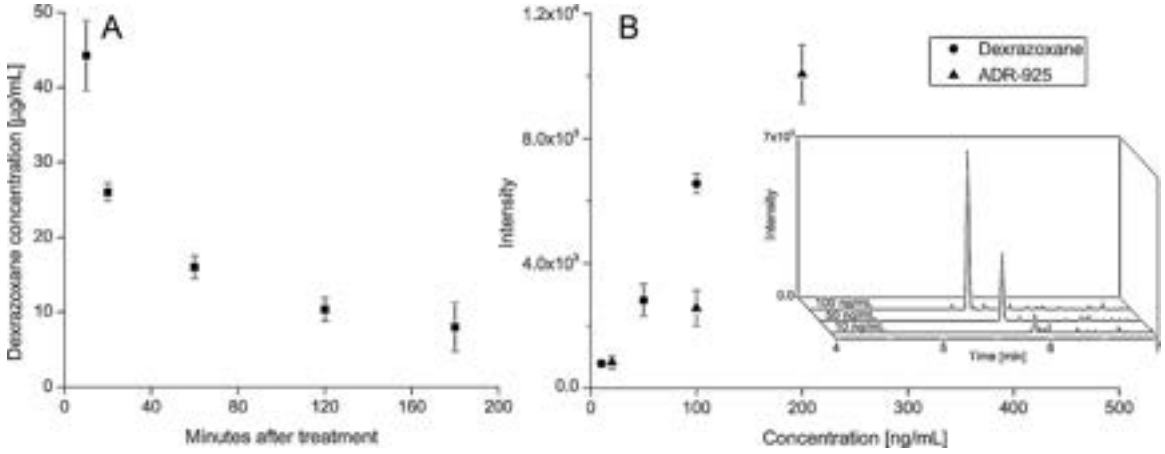

Fig. 4. A – Concentration-time profile of dexrazoxane administered to a rabbit (60 mg/kg, i.p.). B – Intensity of dexrazoxane and ADR-925 in the range of 10–100 ng/mL and 20–200 ng/mL, respectively. Extracted ion electropherograms of dexrazoxane in MS/MS experiment (269.1 → 155.3) is shown in the inserted window. Error bars in the graphs represent standard deviation for n = 3.

the plasma analysis at low analyte concentrations; however, reproducible results could still be obtained.

3.3. Samples from in vivo study

Dexrazoxane was administered intraperitoneally to a rabbit at the dose 60 mg/kg. Its blood plasma was sampled after 10, 20, 60, 120 and 180 min to quantify dexrazoxane by a method of standard addition. The concentration-time profile of dexrazoxane in the rabbit plasma is displayed in Fig. 4. The data clearly show the exponential decrease of its concentration where in the first sample (taken after 10 min) the dexrazoxane amount was 44 μg/mL dropping to 8 μg/mL after 3 h. These analyses proved method applicability for the determination of dexrazoxane in complex biological samples.

3.4. Online transient isotachophoretic concentration

Transient isotachophoresis (tITP) has been shown to provide a substantial sample concentration effect with the common electrophoretic instrumentation using larger bore capillaries [35]. In cationic separations ammonium ions can be used as the transient leading zone since ammonium formate (acetate) does not interfere with the ESI process. Ammonium ions were added to the sample to the final concentration of 400 mM and the sample was loaded into the separation capillary at 0.5 atm for 40 s (approximately 4 nL

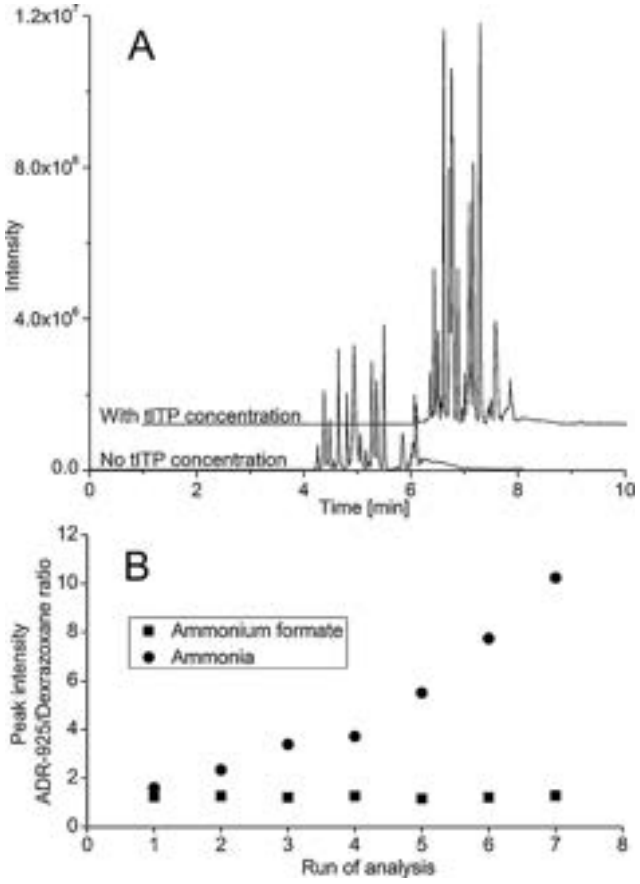

Fig. 5. A – Comparison of base peak electropherograms of spiked plasma without and with concentration of effect, B – change of the ADR-925/Dexrazoxane ratio as a result of hydrolysis in the presence of ammonium cations (400 mM) in the form of ammonium formate (■) and ammonia (●).

loaded and zone length 24 mm). Since the migration time of analytes was slowed down during the concentration process, the 30 kV separation step was extended to 5 min with the remaining conditions identical to those described in Section 2.5 about CE-nESI/MS. As expected, sharper and taller peaks were detected as shown in Fig. 5A, comparing base peak electropherogram of blank plasma without and with concentration effect. The effect of transient isotachophoresis resulted in three times higher sensitivity.

It should be noted that for analysis of dexrazoxane and its metabolite the ammonium cations must be added in the form of a salt to sustain acidic (or neutral) pH of the solution. Addition of ammonia would increase pH resulting in dramatic increase of the dexrazoxane hydrolysis during the sample storage and handling [36]. We have observed that the ADR-925/Dexrazoxane ratio was shifted within 7 analyses (70 min) more than 5 times towards the ADR-925. If ammonium cations were presented in the form of ammonium formate, the ratio remained practically unchanged (Fig. 5B).

4. Conclusions

In this study dexrazoxane and its hydrolyzed form ADR-925 was analyzed by CE-MS for the first time. The separation of analytes from the biological material (rabbit blood plasma) took only 7 min, three times faster than a validated HPLC–MS method. With the injected sample volume of only 1 nL the LODs values were in the low attomole range and the concentration sensitivity could be further improved by the concentrating effect of the transient isotachophoresis. The stability of the ESI was further supported by the newly developed hydrophobic coating of the outer surface of the nanospray tip. The system provided very good linearity over four orders of magnitude and excellent repeatability of migration times. It clearly shows the potential of the CE-nESI/MS system with interface-free design for real complex sample analyses. Although there is still a space for improvement (e.g. automation of the sample loading), the presented design has already proven its potential for analyses with minimal sample consumption while sustaining the sensitivity and analysis repeatability. Further decreasing of the capillary diameter may also result in a single step analysis procedure.

Conflict of interest

The authors have declared no conflict of interest.

Acknowledgements

The authors wish to thank Jana Krenkova (Institute of Analytical Chemistry of the CAS, v. v. i., Brno) for the SEM imaging and Martin Sterba (Faculty of Medicine in Hradec Kralove, Charles University in Prague) for providing us plasma samples from a in vivo experiment. This work was founded by the Ministry of Education, Youth and Sports of the Czech Republic under the project CEITEC 2020 (LQ1601) and by the Czech Science Foundation (P206/12/G014) and Institutional support RVO: 68081715.

References

[1] M. Grundmann, F.M. Matysik, Fast capillary electrophoresis-time-of-flight mass spectrometry using capillaries with inner diameters ranging from 75 to 5 μm, Anal. Bioanal. Chem. 400 (2011) 269–278.
[2] M. Moini, B. Martinez, Ultrafast capillary electrophoresis/mass spectrometry with adjustable porous tip for a rapid analysis of protein digest in about a minute, Rapid Commun. Mass Spectrom. 28 (2014) 305–310.
[3] E.D. Guetschow, S. Kumar, D.B. Lombard, R.T. Kennedy, Identification of sirtuin 5 inhibitors by ultrafast microchip electrophoresis using nanoliter volume samples, Anal. Bioanal. Chem. 408 (2016) 721–731.
[4] M. Moini, C.M. Rollman, Portable, battery operated capillary electrophoresis with optical isomer resolution integrated with ionization source for mass spectrometry, J. Am. Soc. Mass Spectrom. 27 (2016) 388–393.
[5] A.D. Hargis, J.P. Alarie, J.M. Ramsey, Characterization of cell lysis events on a microfluidic device for high-throughput single cell analysis, Electrophoresis 32 (2011) 3172–3179.
[6] R. Juraschek, T. Dulcks, M. Karas, Nanoelectrospray – more than just a minimized-flow electrospray ionization source, J. Am. Soc. Mass Spectrom. 10 (1999) 300–308.
[7] I. Marginean, K.Q. Tang, R.D. Smith, R.T. Kelly, Picoelectrospray ionization mass spectrometry using narrow-bore chemically etched emitters, J. Am. Soc. Mass Spectrom. 25 (2014) 30–36.
[8] M. Moini, C.M. Rollman, Compatibility of highly sulfated cyclodextrin with electrospray ionization at low nanoliter/minute flow rates and its application to capillary electrophoresis/electrospray ionization mass spectrometric analysis of cathinone derivatives and their optical isomers, Rapid Commun. Mass Spectrom. 29 (2015) 304–310.
[9] A.A.M. Heemskerk, J.M. Busnel, B. Schoenmaker, R.J.E. Derks, O. Klychnikov, P.J. Hensbergen, A.M. Deelder, O.A. Mayboroda, Ultra-low flow electrospray ionization-mass spectrometry for improved ionization efficiency in phosphoproteomics, Anal. Chem. 84 (2012) 4552–4559.
[10] R.D. Smith, C.J. Barinaga, H.R. Udseth, Improved electrospray ionization interface for capillary zone electrophoresis – mass-spectrometry, Anal. Chem. 60 (1988) 1948–1952.
[11] E.D. Lee, W. Muck, J.D. Henion, T.R. Covey, Online capillary zone electrophoresis ion spray tandem mass-spectrometry for the determination of dynorphins, J. Chromatogr. 458 (1988) 313–321.
[12] F. Foret, H.H. Zhou, E. Gangl, B.L. Karger, Subatmospheric electrospray interface for coupling of microcolumn separations with mass spectrometry, Electrophoresis 21 (2000) 1363–1371.
[13] V. Hezinova, Z. Aturki, K. Kleparnik, G. D'Orazio, F. Foret, S. Fanali, Simultaneous analysis of cocaine and its metabolites in urine by capillary electrophoresis-electrospray mass spectrometry using a pressurized liquid junction nanoflow interface, Electrophoresis 33 (2012) 653–660.
[14] J. Krenkova, K. Kleparnik, J. Grym, J. Luksch, F. Foret, Self-aligning subatmospheric hybrid liquid junction electrospray interface for capillary electrophoresis, Electrophoresis 37 (2016) 414–417.

[15] X.F. Zhong, E.J. Maxwell, D.D.Y. Chen, Mass transport in a micro flow-through vial of a junction-at-the-tip capillary electrophoresis-mass spectrometry interface, Anal. Chem. 83 (2011) 4916–4923.
[16] L.L. Sun, G.J. Zhu, Z.B. Zhang, S. Mou, N.J. Dovichi, Third-generation electrokinetically pumped sheath-flow nanospray interface with improved stability and sensitivity for automated capillary zone electrophoresis-mass spectrometry analysis of complex proteome digests, J. Proteome Res. 14 (2015) 2312–2321.
[17] E.A. Redman, J.S. Mellors, J.A. Starkey, J.M. Ramsey, Characterization of intact antibody drug conjugate variants using microfluidic capillary electrophoresis-mass spectrometry, Anal. Chem. 88 (2016) 2220–2226.
[18] B.L. Zhang, F. Foret, B.L. Karger, A microdevice with integrated liquid junction for facile peptide and protein analysis by capillary electrophoresis/electrospray mass spectrometry, Anal. Chem. 72 (2000) 1015–1022.
[19] M. Moini, Simplifying CE-MS operation. 2. Interfacing low-flow separation techniques to mass spectrometry using a porous tip, Anal. Chem. 79 (2007) 4241–4246.
[20] K. Kleparnik, Recent advances in combination of capillary electrophoresis with mass spectrometry: methodology and theory, Electrophoresis 36 (2015) 159–178.
[21] R. Ramautar, J.M. Busnel, A.M. Deelder, O.A. Mayboroda, Enhancing the coverage of the urinary metabolome by sheathless capillary electrophoresis-mass spectrometry, Anal. Chem. 84 (2012) 885–892.
[22] A. Tycova, F. Foret, Capillary electrophoresis in an extended nanospray tip-electrospray as an electrophoretic column, J. Chromatogr. A 1388 (2015) 274–279.
[23] V. Gonzalez-Ruiz, S. Codesido, J. Far, S. Rudaz, J. Schappler, Evaluation of a new low sheath-flow interface for CE-MS, Electrophoresis 37 (2016) 936–946.
[24] E.J. Maxwell, X.F. Zhong, D.D.Y. Chen, Asymmetrical emitter geometries for increased range of stable electrospray flow rates, Anal. Chem. 82 (2010) 8377–8381.
[25] H. Tojo, Properties of an electrospray emitter coated with material of low surface energy, J. Chromatogr. A 1056 (2004) 223–228.
[26] A. Tycova, J. Prikryl, F. Foret, Reproducible preparation of nanospray tips for capillary electrophoresis coupled to mass spectrometry using 3D printed grinding device, Electrophoresis 37 (2016) 924–930.
[27] Y.S. Choi, T.D. Wood, Polyaniline-coated nanoelectrospray emitters treated with hydrophobic polymers at the tip, Rapid Commun. Mass Spectrom. 21 (2007) 2101–2108.
[28] T.P. White, T.D. Wood, Reproducibility in fabrication and analytical performance of polyaniline-coated nanoelectrospray emitters, Anal. Chem. 75 (2003) 3660–3665.
[29] P. Kovarikova, J. Stariat, J. Klimes, K. Hruskova, K. Vavrova, Hydrophilic interaction liquid chromatography in the separation of a moderately lipophilic drug from its highly polar metabolites-the cardioprotectant dexrazoxane as a model case, J. Chromatogr. A 1218 (2011) 416–426.
[30] O. Popelova, M. Sterba, P. Haskova, T. Simunek, M. Hroch, I. Guncova, P. Nachtigal, M. Adamcova, V. Gersl, Y. Mazurova, Dexrazoxane-afforded protection against chronic anthracycline cardiotoxicity in vivo: effective rescue of cardiomyocytes from apoptotic cell death, Br. J. Cancer 101 (2009) 792–802.
[31] M. Sterba, O. Popelova, A. Vavrova, E. Jirkovsky, P. Kovarikova, V. Gersl, T. Simunek, Oxidative stress, redox signaling, and metal chelation in anthracycline cardiotoxicity and pharmacological cardioprotection, Antioxid. Redox Signal. 18 (2013) 899–929.
[32] P.E. Schroeder, B.B. Hasinoff, Metabolism of the one-ring open metabolites of the cardioprotective drug dexrazoxane to its active metal-chelating form in the rat, Drug Metab. Dispos. 33 (2005) 1367–1372.
[33] P. Podesva, F. Foret, Metal nano-film resistivity chemical sensor, Electrophoresis 37 (2016) 392–397.
[34] P. Kovarikova, I. Pasakova-Vrbatova, A. Vavrova, J. Stariat, J. Klimes, T. Simunek, Development of LC-MS/MS method for the simultaneous analysis of the cardioprotective drug dexrazoxane and its metabolite ADR-925 in isolated cardiomyocytes and cell culture medium, J. Pharm. Biomed. Anal. 76 (2013) 243–251.
[35] F. Foret, E. Szoko, B.L. Karger, On-column transient and coupled column isotachophoretic preconcentration of protein samples in capillary zone electrophoresis, J. Chromatogr. 608 (1992) 3–12.
[36] B.B. Hasinoff, An HPLC and spectrophotometric study of the hydrolysis of ICRF-187 (dexrazoxane (+)-1,2-bis(3,5-dioxopiperazinyl-1-yl)propane) and its one-ring opened intermediates, Int. J. Pharm. 107 (1994) 67–76.

Anal. Chem. **1997,** *69,* 426−430

Multichannel Microchip Electrospray Mass Spectrometry

Qifeng Xue, Frantisek Foret, Yuriy M. Dunayevskiy, Paul M. Zavracky,[†] Nicol E. McGruer,[†] and Barry L. Karger*

Barnett Institute and Department of Chemistry, Northeastern University, Boston, Massachusetts 02115

Microfabricated multiple-channel glass chips were successfully interfaced to an electrospray ionization mass spectrometer (ESI-MS). The microchip device was fabricated by standard photolithographic, wet chemical etching, and thermal bonding procedures. A high voltage was applied individually from each buffer reservoir for spraying sample sequentially from each channel. With the sampling orifice of the MS grounded, it was found that a liquid flow of 100−200 nL/min was necessary to maintain a stable electrospray. The detection limit of the microchip MS experiment for myoglobin was found to be lower than 6×10^{-8} M. Samples in 75% methanol were successfully analyzed with good sensitivity, as were aqueous samples. The parallel multiple-channel microchip system allowed ESI-MS analysis of different samples of standard peptides and proteins in one chip.

Recently, miniaturized analytical instrumentation has attracted increasing attention as a means of handling small amounts of sample and increasing analysis speeds. Microfabricated chips for both chemical separations, e.g., microchip CE,[1,2] and chemical procedures, e.g., micro-PCR reactions,[3] have been under active development. Technology available from the electronics industry has been directly utilized in the construction of microfabricated analytical devices in order to manipulate nanoliter quantities of sample in a fully integrated design.[4] Large-scale production of such integrated systems can lead to disposable devices using inexpensive materials, eliminating carryover or cross contamination problems of routine analysis. In addition, multiple channels on a chip open up the possibility of high-throughput analysis.[5]

An important aspect of chemical analysis that is not yet a focus with respect to microchip devices is structure elucidation and thus identification of individual sample components. Mass spectrometry (MS) is one of the most powerful tools available for this purpose. Moreover, the specificity of MS often permits analysis with minimal sample preparation. The recent development of electrospray (ESI) MS with low liquid flow rates has allowed the analysis of very small amounts of substances. Microspray ESI-MS, with flow rates in the microliters per minute range, have been successfully utilized in LC/MS.[6,7] More recently, even lower flow rates, nanoliters per minute, have been demonstrated to sustain a stable electrospray for infusing a few microliters of sample in several hours (nanospray).[8,9] During this period, sufficient information can be extracted from the sample, i.e., detection of the molecular ions and their structural characterization in subsequent collision-induced dissociation (CID) experiments. Related to nanospray is the use of gold-coated capillaries for conducting sheathless CE/MS, with flow rates again in the nanoliters per minute range.[10,11] Such approaches not only minimize the amount of sample analyzed, but also more efficiently transfer the ions from the liquid to the gas phase.[7]

In this work, multiple-channel glass microchips have, for the first time, been directly interfaced to ESI-MS to provide the potential for high-throughput analysis at the nanoscale level. A stable electrospray from a flat edge is shown to be feasible by applying the voltage for ESI from the buffer reservoir at the sample side, with the MS orifice grounded. In this first design, consecutive sample injection from the multichannel device into the ESI/MS at a flow rate of 100−200 nL/min has been achieved with a 3D stage and a syringe pump. The characterization of the system is demonstrated using standard proteins and peptides as model samples. The goal in this initial phase of the work has been to design and utilize the simplest and least expensive system possible. Enhanced designs involving sample pretreatment steps and other means of controlling liquid flow will be incorporated later for specific applications. The coupling of the microchip to ESI-MS represents a powerful addition to the integration of a total analysis system (μ-TAS),[12] offering the potential of high-throughput MS analysis.

EXPERIMENTAL SECTION

Microfabrication of Multiple-Channel Microchip. The chip, made of glass, was designed with nine parallel channels. Each channel was connected to two wells, which allowed for fluid

[†] Barnett Institute and Department of Electrical and Computer Engineering, Northeastern University.

(1) Manz, A.; Harrison, D. J.; Verpoorte, E. M. J.; Fettinger, J. C.; Paulus, A.; Ludi, H.; Widmer, H. M. *J. Chromatogr.* **1992**, *593*, 253−258.
(2) Jacobson, S. C.; Hergenröder, R.; Koutny, L. B.; Warmack, R. J.; Ramsey, J. M. *Anal. Chem.* **1994**, *66*, 1107−1113.
(3) Shoffner, M. A.; Cheng, J.; Hvichia, G. E.; Kricka, L. J.; Wilding, P. *Nucleic Acids Res.* **1996**, *24*, 375−379.
(4) Burns, M. A.; Mastrangelo, C. H.; Sammarco, T. S.; Man, F. P.; Webster, J. R.; Johnson, B. N.; Foerster, B.; Jones, D.; Fields, Y.; Kaiser, A. R.; Burke, D. T. *Proc. Natl. Acad. Sci. U.S.A.* **1996**, *93*, 5556−5561.
(5) Woolley, A. T.; Mathies, R. A. *Proc. Natl. Acad. Sci. U.S.A.* **1994**, *91*, 11348−11352.
(6) Emmett, M. R.; Caprioli, R. M. *J. Am. Soc. Mass Spectrom.* **1994**, *5*, 605−613.
(7) Davis, M. T.; Stahl, D. C.; Hefta, S. A.; Lee, T. D. *Anal. Chem.* **1995**, *67*, 4549−4556.
(8) Wilm, M.; Mann, M. *Anal. Chem.* **1996**, *68*, 1−8.
(9) Valascovic, G. A.; Kelleher, N. L.; Little, D. P.; Aaserud, D. J.; McLafferty, F. W. *Anal. Chem.* **1995**, *67*, 3802−3805.
(10) Wahl, J. H.; Gale, D. C.; Smith, R. D. *J. Chromatogr. A* **1994**, *659*, 217−222.
(11) Fang, L.; Zhang, R.; Williams, E. R.; Zare, R. N. *Anal. Chem.* **1994**, *66*, 3696−3701.
(12) van den Berg, A., Bergveld, P., Eds. *Micro Total Analysis System;* Kluwer Academic Publishers: Dordrecht, The Netherlands, 1995.

S0003-2700(96)00711-1 CCC: $14.00

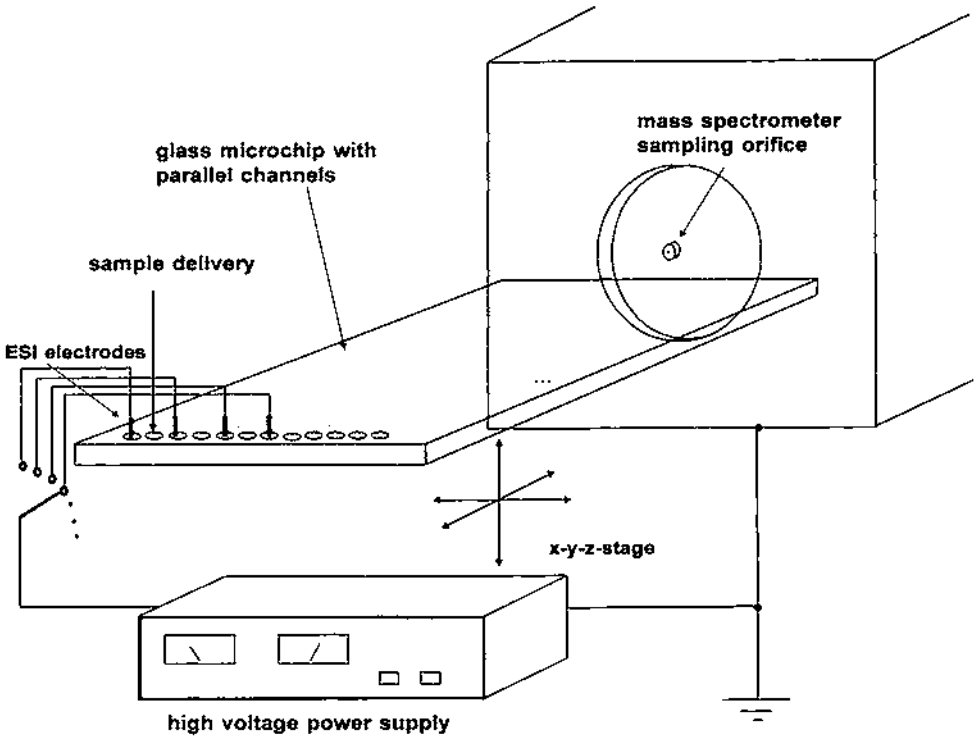

Figure 1. Schematic diagram of the microchip ESI-MS interface. The voltage for ESI was sequentially applied to one well of each channel containing buffer and a platinum electrode. The second well of each channel contained sample and was connected to a syringe pump to provide a flow rate of 100−200 nL/min. The exit ports of the microchip were aligned sequentially with the orifice of the MS using a 3D stage. See Experimental Section for details.

filling and sample injection into the channel (see Figure 1). If separation were required, a third well could be easily implemented for sample injection.[2] To avoid electric field cross talk between channels, in this first design, there was 6 mm spacing between the channels. (Narrower channel spacings have recently been implemented.) The glass disks (Scott D-265) with low sodium content were purchased from S.I. Howard Glass (Worcester, MA).

The multiple-channel microchips were fabricated in class 100 clean rooms, following a procedure similar to that described in ref 13. A laser-machined mask for photolithography was made with all channels of width of 10 μm. The fabrication process included thorough cleaning of the glass, metal deposition (first 300 Å Cr and then 1000 Å Au), photolithography, chemical etching, and thermal bonding. Smooth channels were obtained by isotropic etching with a solution of $HF/HNO_3/H_2O$ (20:14:66 v/v). For a 6 min etching time, the channel width was 60 μm and the depth 25 μm. The channel lengths varied from 3.5 to 5 cm, depending on their location on the glass chip. The microchip device was enclosed by thermal bonding to a flat glass disk containing the wells. The thermal bonding was accomplished over 3 h at 620 °C, after a temperature ramp of 10 °C/min from room temperature. A comparison of scanning electron microscopic photographs before and after bonding showed no noticeable alteration in channel shape.

Interface of Microchip to ESI-MS. A laboratory-constructed three-dimensional stage was used to hold the microchip and to align sequentially each channel outlet with the MS inlet for optimum electrospray performance and sensitivity. The distance from the microchip channel exit to the MS inlet was between 3 and 8 mm. The surface of the outlet edge was coated with a hydrophobic reagent, either Imunopen (Calbiochem, La Jolla, CA) or *n*-octyltriacetoxysilane (Sigma, St. Louis, MO), to prevent the analyzed solution from spreading from one exit port to another. To simplify the experiment, the interface was operated at atmospheric pressure and room temperature. With this configuration, the channel outlet could be visually aligned with the MS inlet.

A 300 μL syringe pump (Model 22, Harvard Apparatus, South Natick, MA) was connected to the appropriate well for delivery of a sample in either 0.1% HAc, 75% MeOH, or 0.1% HAc aqueous solution at a rate of 100−200 nL/min through the channel. All buffer reservoirs were made airtight with plastic stoppers to ensure that the sample solution flowed through only the appropriate channel. The voltage for electrospray was applied from one of the buffer reservoirs with the electrode present. The triple-quadrupole mass spectrometer used in this work was a TSQ-700 (Finnigan Instruments, San Jose, CA).

Infusion from Capillary. To assist in the design of the microchip, an infusion experiment was conducted with a fused silica capillary (50 μm i.d., 360 μm o.d., 30 cm; Polymicro Technologies, Phoenix, AZ) using ESI voltage applied from the sample reservoir and grounding the MS inlet. The basic design was similar to Figure 1, except for substitution of a nonmetalized tipped capillary interface to the MS rather than the microchip interface. An HF-etched capillary tip (~80 μm o.d.) was used for infusion of the sample into the MS, with the reservoir being raised 5 cm higher than the MS orifice level in order to provide the liquid flow for stable ESI.

Chemicals. The sample proteins for the MS experiments were purchased from Sigma, except recombinant human growth

(13) Ko, W. H.; Suminto, J. T. In *Sensors: A Comprehensive Survey*; Granke, T., Ko, W. H., Eds.; VCH Press: Weinhein, Germany, 1989; Vol. 1, pp 107−168.

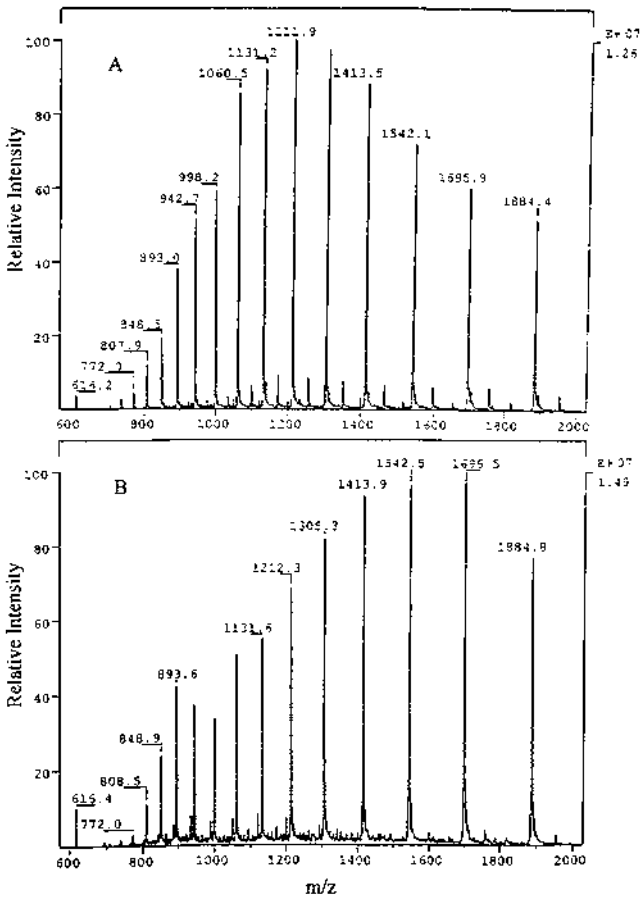

Figure 2. Comparison of ESI-MS spectra of 6 μM myoglobin in 75% MeOH, 0.1% HAc from capillary (A) and microchip (B). (A) HF-etched 50 μm i.d. capillary (80 μm o.d. at tip), 800 nL/min, 2.1 kV. (B) Microchip, 60 μm wide and 25 μm deep, 200 nL/min, 4.3 kV. The edge was covalently coated with *n*-octyltriacetoxysilane.

hormone, which was a kind gift of Genentech, Inc. (South San Francisco, CA). All samples were prepared at a concentration of 1 mg/mL as a stock solution in aqueous buffer (0.1% HAc) and then diluted to the desired concentration with either 0.1% HAc aqueous or 0.1% HAc, 75% MeOH solution.

RESULTS AND DISCUSSION

Off-Line Microchip Electrospray Studies. Initially, experiments were performed to examine infusion of sample from a channel with a nonmetalized exit port. These studies provided the necessary information for design of individual channels for successful electrospray operation. The experimental setup was identical to that shown in Figure 1, but without the MS interface. Instead, a ground electrode was positioned next to the chip at varying distances from a channel outlet, and a microscope was used to follow electrospray behavior from that channel with sample solution exiting at specific flow rates.

It was observed that under a variety of conditions the solution exiting the channel rapidly moistened the edge surface of the glass microchip. This wetting prevented the formation of a well-focused electric field essential for the generation of a stable electrospray. In addition, wetting from one channel to another could potentially lead to cross contamination of samples. To prevent wetting, the edge surface of the microchip was coated with a hydrophobic reagent. This coating prevented the sample solution from spreading over the edge surface of the chip and helped to focus the

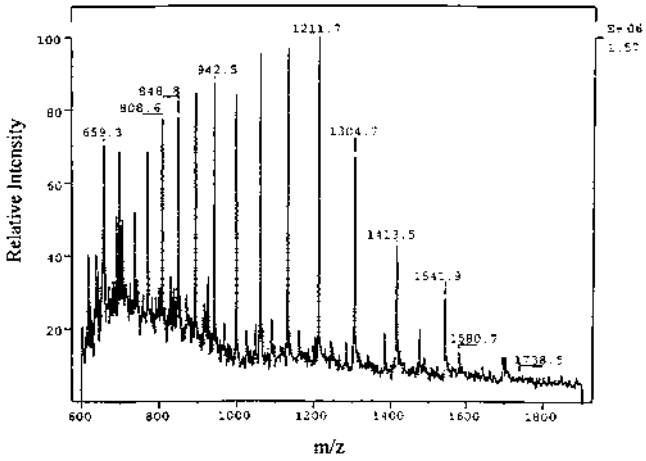

Figure 3. ESI-MS spectrum of infusion of 60 nM myoglobin from a microchip; 200 nL/min, 4.3 kV. The edge of the chip was coated with Imunopen, a silicone grease. All other conditions are as in Figure 2B.

electric field at the surface of the liquid exiting the channel. A microchip made of suitable plastic may have a hydrophobic surface useful for direct electrospray without coating the edge of the chip.

During operation, it was observed that the electrospray plume was stable only when there was sufficient liquid flow at the channel outlet. At the beginning of the run without pressure-assisted flow, a slow increase in the voltage drop across the channel gradually caused a small amount of solution to exit the outlet. When the applied voltage was set at 4.2 kV, the electrospray became observable; however, the plume would gradually diminish, as the electric field was the sole force for delivering the solution. Since the electrospray current was less than 100 nA and the resistance of the buffer solution inside the channel was relatively low, the voltage drop along the channel was very small. This low field strength in combination with the acidic sample solution (pH ~3.6) resulted in a negligible electroosmotic flow. As a consequence, a stable electrospray could not be established. While several approaches could be considered to provide bulk flow within the chip, for simplicity at this stage, we decided to use a syringe pump to deliver the flow necessary for a stable electrospray. A flow of 100−200 nL/min was found sufficient to maintain a stable electrospray with the applied voltage of roughly 4.2 kV. Work is in progress on employing other approaches for sample delivery on the multichannel chip for ESI/MS.

Microchip ESI-MS. Based on the studies of the off-line experiments, the microchip was then interfaced to the triple-quadrupole mass spectrometer. As a measure of performance, we first decided to compare the results obtained by capillary tube infusion with those from a channel on the microfabricated chip. Figure 2 shows the ESI-MS results obtained with infusion of a 6 μM myoglobin solution from a 50 μm i.d. capillary with a nonmetalized tip (A) and from a channel, 60 μm × 25 μm on the microchip (B). While the geometric conditions were different, comparable results for the two cases were obtained in terms of signal intensity, background noise, and charge distribution of the myoglobin ESI-MS spectrum. It should be noted that the spectrum in Figure 2B was acquired from a microchip with a covalently attached hydrophobic (*n*-octyl) coating on the edge surface. The operational lifetime of this monolayer in terms of providing a stable electrospray was 5 min/channel, even with the 75% MeOH solution, a time more than sufficient to acquire the

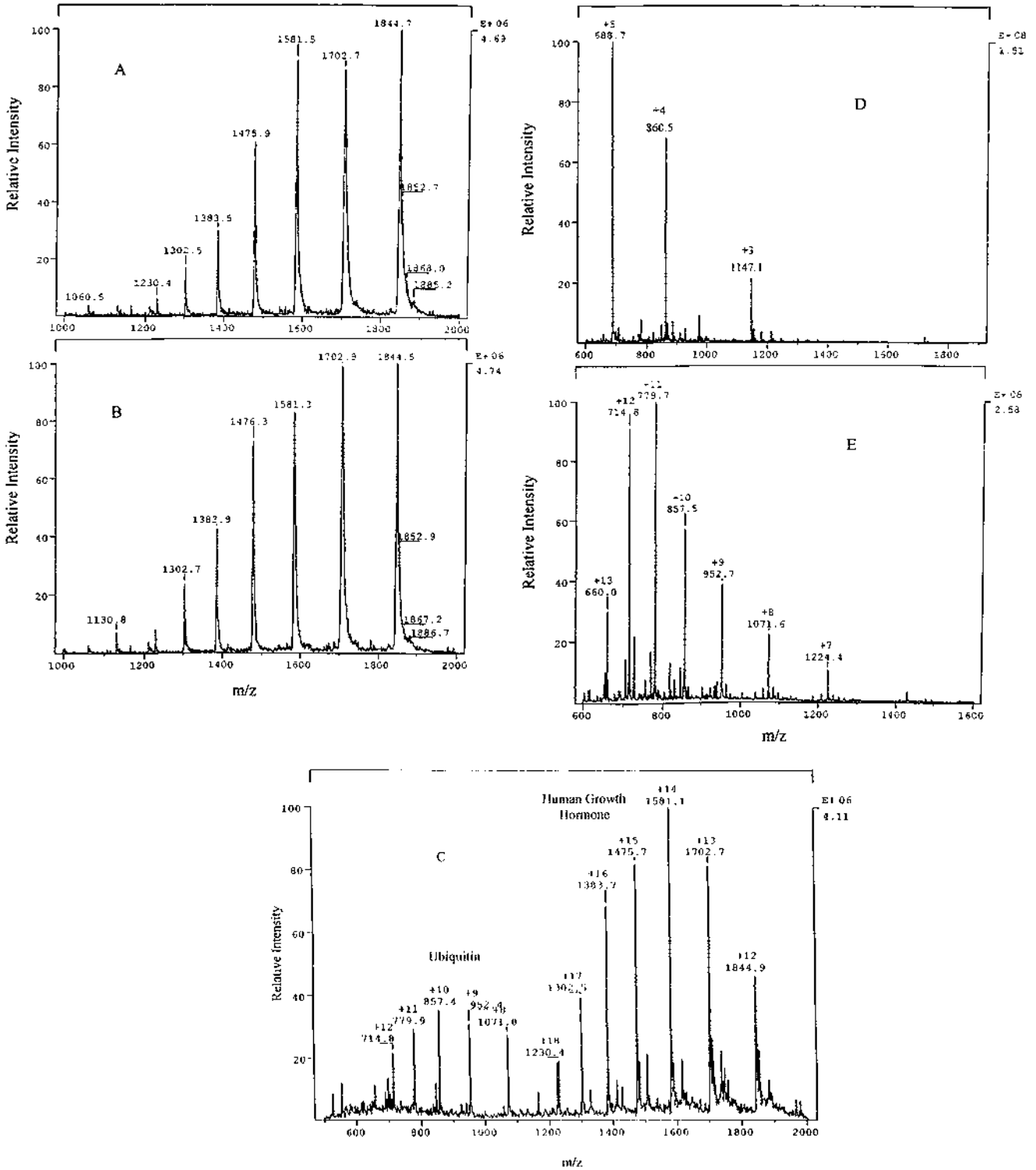

Figure 4. Microchip ESI-MS sequential analysis of different samples in five channels. See Figure 2B for other conditions except those listed below: (A) 2 μM recombinant human growth hormone, aqueous solution; (B) 2 μM recombinant human growth hormone; (C) 2 μM recombinant human growth hormone and 6 μM ubiquitin; (D) 30 μM endorphin; and (E) 10 μM ubiquitin.

MS data. This time is compatible with the requirements for monitoring separation conducted on microchip. The edge could be dried after this period and reused. When the edge surface was noncovalently coated with a silicon grease (Imunopen), a much thicker layer was obtained, which allowed stable electrospray for more than 30 min with the 75% MeOH solution. The results in Figure 2 demonstrate that good ESI spectra can be obtained from individual channels on a microchip interfaced to an MS.

We next explored the reproducibility of ESI-MS spectra from different channels. In this case, a 0.6 μM myoglobin sample in 75% MeOH was infused from five different channels of the same dimension. Similar spectra were acquired from the five channels, illustrating the close agreement in the sensitivity of the spectra between channels. The determined molecular masses were within 0.02% of the known value in all cases, 16 953 Da (16 950 Da known).

The detection limit for myoglobin from the infusion experiments on the microchip was also estimated. Figure 3 shows an ESI-MS spectrum of myoglobin at 60 nM. Again, an accurate molecular mass (16 953 Da) was obtained which agreed with the known molecular mass within 0.02%. Based on the signal intensity in Figure 3, meaningful spectra of myoglobin should be possible lower than 60 nM. It is interesting to note that, as the concentration of the protein was reduced, the charge distribution envelope shifted to lower m/z values. A similar shift was observed for the capillary ESI-MS experiment, possibly a result of an increase in the charging efficiency at low concentration.

Finally, to demonstrate that the microchip ESI-MS can be used to conduct sequential analyses, five different samples yielded the spectra shown in Figure 4, each sample being sprayed from a different channel. Parts A and B of Figure 4 compare the ESI-MS spectra of recombinant human growth hormone obtained from solutions of 100% H_2O and 75% MeOH. As can be seen, similar sensitivities were found for both solutions, and the accuracy in determination of the molecular mass was within 0.02% for both MS spectra [22 120 Da (exptl) and 22 124 Da (known)]. The results indicate that, at the flow rates employed, aqueous solutions can be successfully sprayed into the MS.

A simple mixture was next infused into the MS from a single channel of a microchip. Figure 4C shows the results for ubiquitin and recombinant human growth hormone, in which two distinctive ion envelopes were observed for the mixture. From the mass spectrum, molecular masses for both ubiquitin and recombinant human growth hormone were determined to be 8565 Da (8557 Da known, 0.09% accuracy) and 22 120 Da (0.02% accuracy), respectively. This demonstrates that, as expected, simple mixtures may be characterized directly by microchip MS without the need for separation. More complex samples would undoubtedly require some separation. Figure 4D,E shows ESI spectra for endorphin and ubiquitin, respectively, with comparable molecular masses and accuracies being obtained (endorphin 3438.3 Da [exptl], 3438.0 Da [known], 0.01% accuracy; ubiquitin 8559 [exptl], 0.02% accuracy).

For all the analyses in Figure 4, each determination was performed in less than 2 min with the system operating in the sequential analysis mode. It was not found to be necessary to optimize the ESI conditions when moving from channel to channel. The results suggest that sample preparation (or separation) can be conducted in one channel (or reservoir) while another channel is used to obtain the MS spectrum of a different sample. In this manner, instrumental utilization would be very efficient, since setup and readjustment of the system (required for a single-capillary operation mode) would not be necessary. This would allow many analyses to be performed on a large multichannel microchip with minimum time required for moving from one channel to the next.

CONCLUSIONS

A microfabricated multichannel chip was successfully interfaced to ESI-MS. The microchip ESI-MS showed high sensitivity in analysis of proteins (low nanomolar). Even though organic solvent (75% MeOH) was used in most experiments, aqueous solutions could also be successfully sprayed with a similar ESI-MS sensitivity. A series of sequential experiments were conducted by infusing various samples from different channels, demonstrating that rapid analysis with high throughput can be implemented. The microchip device presented here can be enhanced to include sample pretreatment prior to infusion. For example, on-chip sample desalting can be incorporated for analysis of more complex samples. If a separation is required prior to ESI-MS, a modified microchip can be fabricated in which metal is deposited at the channel outlet, e.g., sheathless CE-MS.[10,11] Such an approach can also be used to infuse electroosmotically the sample for electrospray. By treating the surface of the channel to generate a layer of polymer stationary phase,[14] miniaturized LC/MS would also be possible.

In summary, microchip MS opens up the possibility for microscale sample handling and MS analysis in an integrated system. Importantly, the multichannel approach leads to the possibility of high-throughput MS analysis in screening and diagnostic applications. Further application of the microdevice MS system for on-chip sample treatment followed by MS characterization of the products will be reported separately.

ACKNOWLEDGMENT

The authors thank NIH under GM 15847 for support of this work. The authors further acknowledge Dan Kirby for useful discussions and Keith Warner for help in mask design and chip fabrication. The gift of recombinant human growth hormone from Genentech, Inc. was greatly appreciated. This work is contribution no. 675 from the Barnett Institute.

Received for review July 19, 1996. Accepted October 16, 1996.[⊗]

AC9607119

(14) Jacobson, S. C.; Hergenröder, R.; Koutny, L. B.; Ramsey, J. M. *Anal. Chem.* **1994**, *66*, 2369−2373.

[⊗] Abstract published in *Advance ACS Abstracts*, December 15, 1996.

Integrated Multichannel Microchip Electrospray Ionization Mass Spectrometry: Analysis of Peptides from On-chip Tryptic Digestion of Melittin

Qifeng Xue, Yuriy M. Dunayevskiy, Frantisek Foret and Barry L. Karger*

Barnett Institute and Department of Chemistry, Northeastern University, Boston, MA 02115, USA

SPONSOR REFEREE: Dr. Pierre Thibault, Institute for Marine Biosciences, NRC, Halifax, Nova Scotia, Canada, B3H 3Z1

In continuation of our work to develop an integrated multichannel microchip interfaced to electrospray mass spectrometry (ESI-MS), this paper demonstrates one of several applications of this approach in monitoring tryptic digestion products. The multichannel microchip allowed integration of sample preparation onto the microchip to facilitate the analysis process. Melittin was selected as a model oligopeptide because it possesses a cluster of four adjacent basic residues which enable probing the site specificity of trypsin as a function of digest times. Reactions were performed on-chip in different wells for specific time periods and then analyzed by infusion from the microchip by ESI-MS, using leucine enkephalin as internal standard. The rate of formation and disappearance of the molecular ion and individual fragments was followed for a melittin to trypsin concentration ratio of 300:1. The results indicate the potential of integrating enzymatic reactions with multichannel microchip ESI-MS for automated optimization of reaction conditions while consuming only small amounts of sample. © 1997 by John Wiley & Sons, Ltd.

Received 19 June 1997; Accepted 19 June 1997
Rapid. Commun. Mass Spectrom. **11**, 1253–1256 (1997)
No. of Figures: 4 No. of Tables: 0 No. of Refs: 10

We have recently demonstrated the efficient coupling of a multichannel microfabricated chip to electrospray mass spectrometry (ESI-MS).[1] In this approach the microchip serves as the microfluidic device for rapid and facile delivery of fluid to the electrospray interface with flow rates of 100–200 nL per minute. In the cited work, we showed that electrospray from the flat edge of a microchip is possible with comparable sensitivity to that of capillary ESI-MS for single protein analytes.

Microchip devices are of high interest since they have many potential advantages over traditional instrumental systems.[2] First, such devices can in principle be made inexpensively in that they can be manufactured in large quantities and be disposable. Thus, microchips may be used only once, and the issue of sample carryover from run to run can be eliminated. Secondly, with proper injection procedures, only small amounts of sample and reagents are required.[3] Thirdly, since multiple channels or wells can be placed in small dimensions, high density – high throughout devices for direct infusion[4] or fast separation[5] are possible. Fourthly, a variety of sample steps can be incorporated onto a microfabricated device,[6] and this integration can lead to significant advantage. It is this last aspect of multiple steps on the microfabricated device coupled with ESI-MS on which we wish to focus in this paper.

This paper demonstrates that on-chip tryptic proteolysis can be monitored by direct peptide analysis of the digested products in the mass spectrometer. Furthermore, through the use of an internal standard, the relative amounts of each peptide formed as a function of time can be estimated. Thus, a variety of proteolytic conditions can be studied in order to optimize the tryptic digest in a rapid and automated fashion, using sub-picomol amounts of peptide for each channel monitored. We use melittin as a model oligopeptide, because of the ease with which it can be digested to a few peptide products, and because of multiple adjacent basic amino acids, a variety of peptide products can be formed as a function of time.[7]

MATERIALS AND METHOD

Instrumentation

The instrumental setup was similar to that used in Ref 1. A multichannel microchip was fabricated out of glass following standard photolithographic and wet chemical etching procedures. The microchip contained 9 channels, each 25 μm deep and 60 μm wide with two attached wells, one to be used as a buffer reservoir to apply high voltage for electrospray and the other as a reaction chamber for sample preparation. A 3-dimensional stage was constructed to align each channel outlet of the microchip sequentially with the mass spectrometer inlet for optimum electrospray performance and sensitivity. The edge of the chip containing the exit ports was coated with a hydrophobic layer using Immunopen (Calbiochem. LaJolla, CA, USA) to minimize solution wetting of the edge surface. The liquid sample infusion rate was 200 nL/min, controlled by means of a syringe pump (Harvard Apparatus, South Natick, MA, USA). A TSQ-700 triple quadruple mass spectrometer (Finnigan Instruments, San Jose, CA, USA) was used in this work.

*Correspondence to: B. L. Karger
Contract grant sponsor: NIH; Contract grant number: GM 15847

CCC 0951–4198/97/121253–04 $17.50

Chemicals

All chemicals were purchased from Sigma (St. Louis, MO, USA) and used as received without further purification. A stock solution of melittin (1 mg/mL) was prepared in 20 mM Tris acetate buffer (pH 8.2). Trypsin (1 mg/mL), dissolved in 2% acetic acid solution, was diluted to the desired concentration before using with 20 mM Tris acetate buffer (pH 8.2).

Digest conditions

The tryptic digest protocol was similar to that described previously.[7] Melittin was digested at room temperature in the 20 mM Tris acetate buffer (pH 8.2), with an enzyme to protein ratio of 300:1 (w/w). Identical conditions were used for both on- and off-chip proteolysis; only the volumes of digestion varied, 2 μL for on-chip and 20 μL for off-chip digestion, respectively. The initial concentration of melittin in the digest mixture was 0.01 mg/mL. To stop digestion, 1 μL of 2% acetic acid solution (one-half of the reaction volume) was added. To ensure the final composition of the sample would contain 50% methanol before the ESI-MS analysis, 3 μL methanol, containing 0.01 mg/mL of leucine enkephalin as internal standard, was then added to result in the final volume of 6 μL. For the off-chip experiments, 5 μL of 2% acetic acid was added, followed by 25 μL of methanol.

RESULTS AND DISCUSSION

The microchip consisted of a multichannel network which allowed easy introduction and manipulation of small volumes of sample. Separate reservoirs and channels provided independent mixing of reagents and facilitated on-chip sample preparation prior to ESI-MS analysis. A constant flow syringe pump was used at a flow rate of 200 nL/min to introduce sample to the mass spectrometer. Since the channels on the microchip were of identical dimensions, a stable electrospray could be readily achieved for each channel used in a sequential manner. A 3-dimensional stage was employed for lateral movement of each successive channel to the proper sampling position. Initially, the first channel was manually aligned with the mass spectrometer orifice to achieve maximum signal sensitivity. The alignment of each sequential exit port of a channel with the orifice was rapid, since each port was equally spaced from adjacent outlets. While not used in these studies, a stepper motor-driven operation would allow automated movement of the multichannel chip.

Proteolytic digestion of peptides and proteins is widely used in protein mapping and characterization, with the composition of the digest optimized for a particular goal, e.g. full digestion, partial proteolysis for epitope mapping, etc. This optimization includes the adjustment of the time of the digestion, using different enzymes and protein/enzyme ratios. Other conditions include pH, temperature and extent of denaturation prior to digestion. A multichannel microchip device coupled with a mass spectrometer should facilitate the optimization of all relevant digestion parameters while lending itself to automation.

We chose melittin as a model substance to demonstrate the microchip performance in integrating the proteolytic digestion steps with direct analysis of the resulting sample with ESI-MS. The composition of the tryptic digest of melittin and digestion profiles have been thoroughly investigated.[7] The structure of melittin, the possible peptide fragments and their molecular masses are presented in Fig. 1. When a protein contains repetitive basic residues, as in this case, complete tryptic digestion results in very short peptide fragments and potential loss of structural information. Therefore, to obtain overlapping fragments, it is desirable to employ incomplete digestion to enable formation of overlapping peptide fragments. Thus, control of experimental parameters that influence the degree of proteolysis is important.

The experimental design consisted of melittin and trypsin simultaneously to individual reservoirs, each connected to nine channels for a total sample volume of 2 μL per reservoir. Digestion in each reservoir was allowed to proceed for a specific period of time at room temperature. The reaction was stopped by adding 2% acetic acid and methanol, containing the internal standard, leucine enkephalin, to form a 50% methanol solution. Methanol also aided in achieving stable electrospray conditions. The reaction mixture was delivered to the mass spectrometer inlet using a syringe pump which introduced a buffer of 75% methanol, 0.1% acetic acid through the reservoir at a constant flow rate of 200 nL/min. In separate work, we have also implemented liquid pumping by electro-osmotic flow and gas pressure.[8] Electro-osmotic liquid pumping and off-chip electrospray formation has also been shown by others.[9]

The mass spectral results of the tryptic digest as a function of time with a 300:1 ratio of melittin to trypsin are shown in Fig. 2. It can be seen that the pattern of fragmentation was substantially different for digestion times of 10 min and 40 min. After 10 min, (Fig. 2(a)), the triply protonated molecule of melittin was the most intense ion, and six major product peptide fragment species were identified. On the other hand, after 40 min, the multiply protonated molecules, $[M + 2H]^{2+}$ and $[M + 3H]^{3+}$, were of much lower abundance

fragment no.	1	2	3	4	5	6	7	8	9
residues	T_1T_2	T_1T_2-R	T_1T_2-RK	T_1T_2-RKR	T_2	T_2-R	T_2-RKR	T_2-RKR-T_1	T_1

fragment no.	masses (Da)
1	2150.5
2	2307.1
3	2436.0
4	2590.7
5	1510.9
6	1667.3
7	1951.2
8	2208.1
9	656.6

Figure 1. Primary structure of melittin and possible tryptic peptides and their molecular masses. The fragmentation positions are indicated.

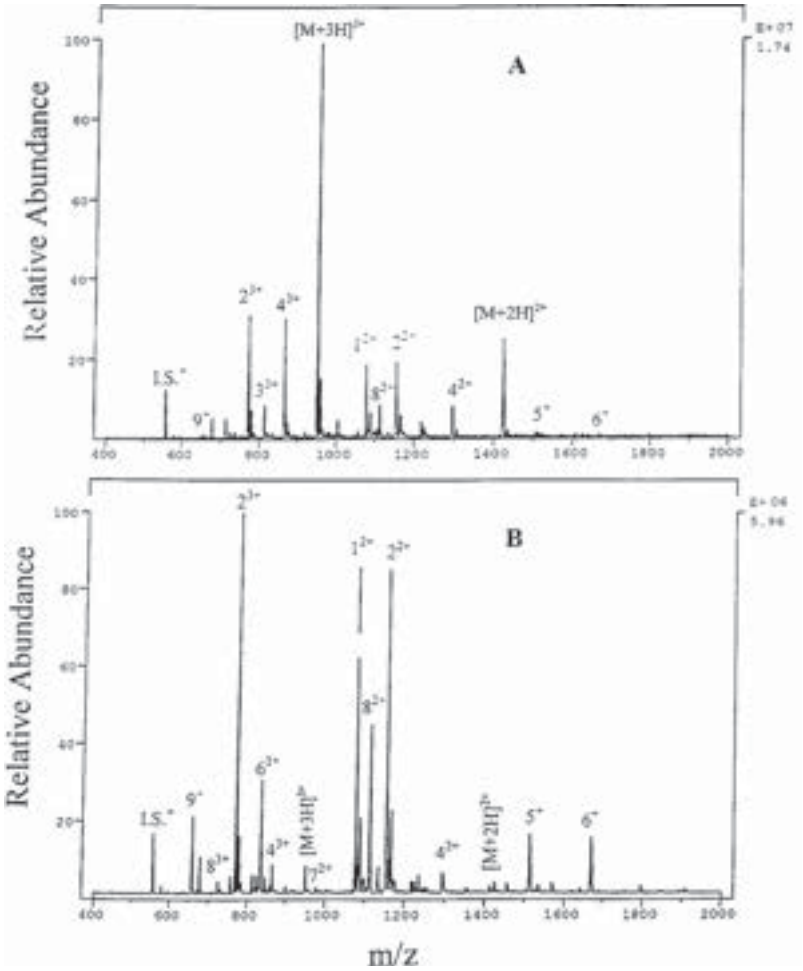

Figure 2. On-chip digestion of melittin at an initial concentration of 0.01 mg/mL (a) for 10 mins and (b) for 40 mins. Note the decrease in the multiple protonated molecule $[M + nH]^{n+}$ for melittin and increase in product ions with digestion time. The concentration of melittin to trypsin was 300:1. The numbers correspond to the peptide digest fragments in Fig. 1, and I.S. represents the internal standard, leucine enkephalin. For a detailed description of the conditions for digestion and electrospray, see the experimental section.

relative to the corresponding fragment ions. Additionally, peptide fragments 5, 6, 8 and 9 increased at the expense of fragments 3 and 4 as the digestion proceeded to completion. Increasing the digestion time resulted in further proteolysis of fragments containing multiple K(lys) and R(arg) residues. It should be noted that while the buffer contained 20 mM Tris, no signal suppression or Tris adduct formation was observed, which removed the need for buffer exchange for compatibility with mass spectrometric analysis.

Next, an off-chip digest was conducted using 20 μL sample volume and the same melittin to trypsin ratio of 300:1. A similar fragmentation pattern to that of the on-chip digestion was observed (results not shown), indicating good correlation between off-chip and on-chip digestion experiments. Clearly, integrating the digestion process and the microfluidics directly on the chip is preferable, to reduce sample consumption. In comparison with classical approaches, describing a similar application,[10] the integrated microchip interface should provide more flexibility in optimizing reaction conditions, with the use of a small volume of the sample.

The peptide fragments are known in this model system, and proper identification is achieved from the mass measurements of individual peaks. However, for unknown peptides, tandem mass spectrometry (MS/MS) experiments can be performed for further characterization. As an example, peptide fragment 9 was subjected to collision-induced dissociation (CID) immediately following full mass spectral acquisition, while the digest sample was still being delivered to the mass spectrometer. The MS/MS spectrum, shown in Fig. 3, contained product ions (a, b and y series) characteristic of the peptide backbone structure. All spectra were acquired within a few seconds, and, given the flow rate of 200 nL/min, the entire digest could be analyzed in the same run, because the initial sample volume was 2 μL.

Using the internal standard, leucine enkephalin, it was possible to follow the changes in relative composition of the peptide fragments as a function of the digestion time. For simplicity, it was assumed that the electrospray ionization of individual fragments was unaffected by other peptides in the digest, as these species were of relatively low concentration (~ 1 μM). It was then possible to plot the logarithmic intensities of individual peptides normalized to the intensity of the internal standard (to account for electrospray ionization variations from run to run) vs. tryptic digest time

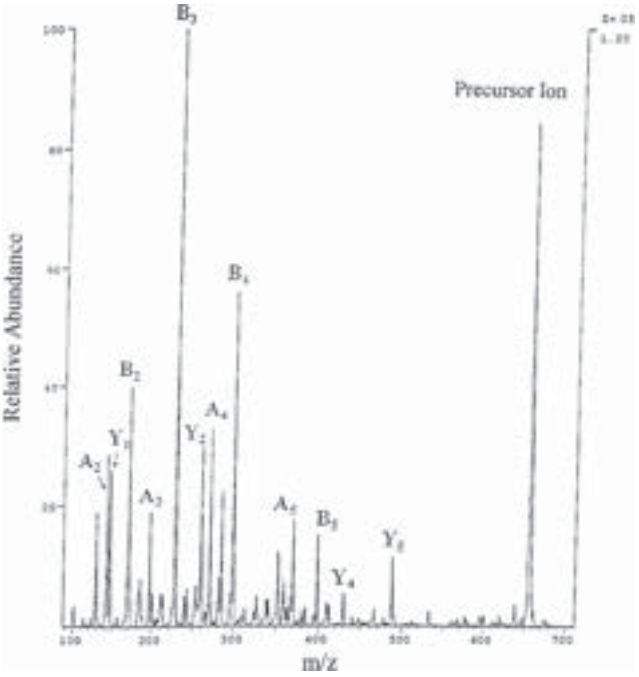

Figure 3. Production spectrum of fragment 9, *m/z* 656.6. The CID conditions were: 1 mTorr argon collision gas and 60 eV collision energy. The sequence of this peptide is GIGAVLK (see Fig. 1).

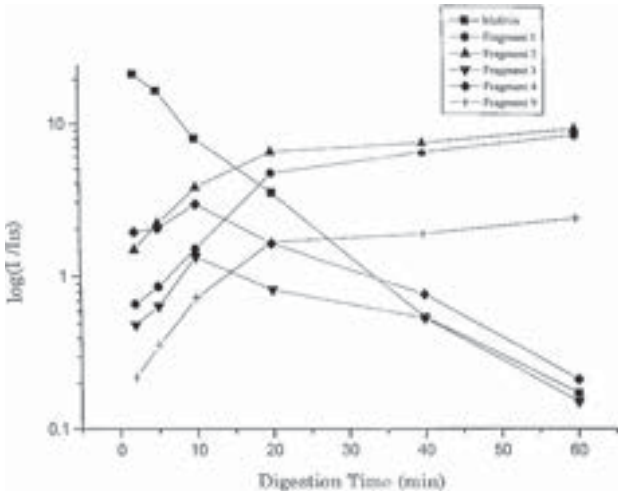

Figure 4. Plot of log relative intensity of individual peptide fragment ions, I, to the internal standard, leucine enkephalin, I_{IS}, vs. on-chip tryptic digestion time. Melittin to trypsin concentration ratio 300:1.

(Fig. 4). The decay of the signal due to multiply protonated molecules associated with mellitin and the increase in product ions with digest time are readily apparent. Moreover, intensity maxima as a function of time are observed for fragments 4 and 3, as expected given their respective positions within the substrate peptide (Fig. 1). Fragments 5–8 are not included in Fig. 4 for purposes of clarity; however, as seen in Fig. 2, their appearance would be observed later in the digestion reaction. From Fig. 4, it is evident that microchip ESI-MS can be used to automate optimization of digest conditions and time, using small amounts of material.

CONCLUSION

This paper demonstrates the integration of tryptic digestion on a microchip with mass spectrometric detection. The integrated microchip has potential in handling small volumes of sample, as sample preparation can in principle be incorporated onto the microchip. In addition, each channel is used only once, thus eliminating the possibility of cross-contamination. Alignment of each channel with the sampling orifice of the mass spectrometer is straightforward and lends itself to automation. For more complex digests, or in cases where the electrospray ionization of individual peptides could be affected by other components present, separation on the chip, e.g. electrophoresis, may be required. This capability is currently under study for on-line coupling to mass spectrometry.

The example presented here is only one of a variety of sample preparation processes that could be performed with the present design. For example, salt exchange and desalting using small packed columns in a multichannel format has been achieved in our laboratory.[8] The integration of these steps in a single chip system confers flexibility to the current approach while simultaneously offering the capability of handling small amounts of material. Furthermore, such chips, in principle, need to be used only once, as costs of production are expected to decrease significantly.

We envision that the multichannel microchip will be a convenient microfluidic device for high-throughput mass spectrometry. The recent introduction to electrospray - time-of-flight mass spectrometry opens up the possibility of conducting analyses on a time scale of only a few seconds per sample. We are continuing work in this area of microchip-mass spectrometry with particular emphasis on the application of online separation on integrated chip systems, and results from these investigations will be reported separately.

Acknowledgements

The authors thank NIH GM15847 for support of this work. The authors further thank Drs. Paul Zavracky and Nicholas McGruer for use of the Northeastern University Microfabrication Center, and Dr. Pierre Thibault for a thorough reading of the manuscript. Contribution No. 694 from the Barnett Institute.

REFERENCES

1. Q. Xue, F. Foret, Y. M. Dunayevskiy, P. M. Zavracky, N. E. McGruer and B. L. Karger, *Anal. Chem.* **69**, 426 (1997).
2. *Micro Total Analysis Systems*, A. van den Berg and P. Bergveld (Eds), Kluwer Academic Publishers (1995).
3. D. J. Harrison, K. Fluri, K. Seiler, Z. Fan, C. S. Effenhauser and A. Manz, *Science* **261**, 895 (1993).
4. A. T. Woolley and R. A. Mathies, *Proc. Natl. Acad. Sci. U.S.A.* **91**, 11348 (1994).
5. S. C. Jacobson, R. Hergenöder, L. B. Koutny, R. J. Warmack and J. M. Ramsey, *Anal. Chem.* **66**, 1107 (1994).
6. M. A. Shoffner, J. Cheng, G. E. Hvichia, L. J. Kricka and P. Wilding, *Nucleic Acids Res.* **24**, 375 (1996).
7. E. P. Morgorodskaya, O. A. Mirgorodskaya, S. V. Dobretsov, A. A. Shevchenko, A. F. Dodonov, V. I. Kozlovskiy and V. V. Raznikov, *Anal. Chem.* **67**, 2864 (1995).
8. Q. Xue, Y. M. Dunayevskiy, F. Foret and B. L. Karger, HPCE'97: Anaheim, CA (1997) poster no. 340.
9. R. S. Ramsey and J. M. Ramsey, *Anal. Chem.* **69**, 1174 (1997).
10. R. M. Caprioli, *Trends in Anal. Chem.* **7**, 328 (1988).

Anal. Chem. **1999,** *71,* 3258−3264

Microfabricated Devices for Capillary Electrophoresis−Electrospray Mass Spectrometry

B. Zhang, H. Liu, B. L. Karger, and F. Foret*

Barnett Institute and Department of Chemistry, Northeastern University, Boston, Massachusetts 02115

Two fundamental approaches for the coupling of microfabricated devices to electrospray mass spectrometry (ESI-MS) have been developed and evaluated. The microdevices, designed for electrophoretic separation, were constructed from glass by standard photolithographic/wet chemical etching techniques. Both approaches integrated sample inlet ports, preconcentration sample loops, the separation channel, and a port for ESI coupling. In one design, a modular, reusable microdevice was coupled to an external subatmospheric electrospray interface using a liquid junction and a fused silica transfer capillary. The transfer capillary allowed the use of an independent electrospray interface as well as fiber optic UV detection. In the second design, a miniaturized pneumatic nebulizer was fabricated as an integral part of the chip, resulting in a very simple device. The on-chip pneumatic nebulizer provided control of the flow of the electrosprayed liquid and minimized the dead volume associated with droplet formation at the electrospray exit port. Thus, the microdevice substituted for a capillary electrophoresis instrument and an electrospray interface—traditionally two independent components. This type of microdevice is simple to fabricate and may thus be developed either as a part of a reusable system or as a disposable cartridge. Both devices were tested on CE separations of angiotensin peptides and a cytochrome *c* tryptic digest. Several electrolyte systems including a transient isotachophoretic preconcentration step were tested for separation and analysis by an ion trap mass spectrometer.

The current advances in the biological sciences have brought increasing demands on the speed and throughput of the analytical systems capable of handling minimum sample amounts. Rapid, high-throughput analysis of subpicomolar quantities of DNA, proteins, and peptides, as well as a variety of small molecules, is today significant not only for genomics and proteomics but also for new drug development, environmental studies, and chemical and biological warfare detection. It is widely expected that a new generation of "lab-on-the chip" microdevices[1] will have a significant impact on all of the above fields. A number of microdevices are being developed for applications ranging from on-chip cell manipulations,[2,3] PCR analysis,[4,5] immunoassays,[6,7] and DNA separations[8−12] to high-throughput DNA hybridization analysis[13,14] and parallel chemical synthesis.[15]

While many of the above applications target a specific sample for analysis on the microdevice, positive identification of the sample components, not often available with on-chip spectroscopic detection, is frequently required. Miniaturized, chip-based, matrix assisted laser desorption ionization/time-of-flight mass spectrometry (MALDI-TOF)[16] has recently been described; however, the approach has focused mainly on miniaturization of the MALDI analysis rather than following the lab-on-a-chip concept. Despite their small size, the microdevices hold great potential for use in biological mass spectrometry. In this combination, (chip-MS), rapid handling (desalting, digestion, separation, etc.) of multiple samples on a small-volume scale could be performed on the microdevice with subsequent fast MS analysis.

Recently, our laboratory, as well as several others, introduced the coupling of microfabricated devices to electrospray ionization mass spectrometry.[17−20] In these initial designs, the focus of the work has mainly been on sample manipulation on the chip

* Corresponding author: (tel.) 617-373-2867; (fax) 617-373-2855; (e-mail) fforet_franta@yahoo.com.

(1) Manz, A., Becker, H., Eds. *Microsystem Technology in Chemistry and Life Science*; Springer-Verlag: Berlin, 1998.
(2) Li, P. C. H.; Harrison, D. J. *Anal. Chem.* **1997**, *69*, 1564−1568.
(3) Wilding, P.; Kricka, L. J.; Cheng, J.; Hvichia, G.; Shoffner, M. A.; Fortina, P. *Anal. Biochem.* **1998**, *257*, 95−100.
(4) Shoffner, M. A.; Cheng, J.; Hvichia, G. E.; Kricka, L. J.; Wilding, P. *Nucleic Acids Res.* **1996**, *24*, 375−379.
(5) Woolley, A. T.; Hadley, D.; Landre, P.; deMello, A. J.; Mathies, R. A.; Northrup, M. A. *Anal. Chem.* **1996**, *68*, 4081−4086.
(6) Koutny, L. B.; Schmalzing, D.; Taylor, T. A.; Fuchs, M. *Anal. Chem.* **1996**, *68*, 18−22.
(7) Chiem, N.; Harrison, D. J. *Anal. Chem.* **1997**, *69*, 373−378.
(8) Woolley, A. T.; Mathies, R. A. *Proc. Natl. Acad. Sci. U.S.A.* **1994**, *91*, 11348−11352.
(9) Effenhauser, C. S.; Paulus, A.; Manz, A.; Widmer, H. M. *Anal. Chem.* **1994**, *66*, 2949−2953.
(10) McCormick, R. M.; Nelson, R. J.; AlonsoAmigo, M. G.; Benvegnu, J.; Hooper, H. H. *Anal. Chem.* **1997**, *69*, 2626−2630.
(11) Schmalzing, D.; Koutny, L.; Adourian, A.; Belgrader, P.; Matsudaira, P.; Ehrlich, D. *Proc. Natl. Acad. Sci. U.S.A.* **1997**, *94*, 10273−10278.
(12) Waters, L. C.; Jacobson, S. C.; Kroutchinina, N.; Khandurina, J.; Foote, R. S.; Ramsey, J. M. *Anal. Chem.* **1998**, *70*, 158−162.
(13) Saizieu, A.; deCerta, U.; Warrington, J.; Gray, C.; Keck, W.; Mous, J. *Nature Biotech.* **1998**, *16*, 45−48.
(14) Zanzucchi, P. J.; Cherukuri, S. C.; McBride, S. E.; US Patent 5 681 484, Oct 28, 1997.
(15) Cheng, J.; Sheldon, E. L.; Wu, L.; Uribe, A.; Gerrue, L. O.; Carrino, J.; Heller, M. J.; O'Connell, J. P. *Nature Biotech.* **1998**, *16*, 541−546.
(16) Little, D. P.; Cornish, T. J.; O'Donnell, M. J.; Braun, A.; Cotter, R. J.; Koster, H. *Anal. Chem.* **1997**, *69*, 4540−4546.
(17) Xue, Q.; Foret, F.; Dunayevskiy, Y. M.; Zavracky, P. M.; McGruer, N. E.; Karger, B. L. *Anal. Chem.* **1997**, *69*, 426−430.
(18) Xue, Q.; Foret, F.; Dunayevskiy, Y. M.; Foret, F.; Karger, B. L. *Rapid Commun. Mass Spectrom.* **1997**, *11*, 1253−1256.
(19) Ramsey, R. S.; Ramsey, J. M. *Anal. Chem.* **1997**, *69*, 1174−1178.
(20) Figeys, D.; Ning, Y.; Aebersold, R. *Anal. Chem.* **1997**, *69*, 3153−3160.

10.1021/ac990090u CCC: $18.00
Published on Web 06/16/1999

followed by off-chip infusion or capillary electrophoresis[20] with electrospray sample ionization. Besides simple sample infusion, either with pressure or electroosmotic sample delivery, other analytical procedures, such as enzymatic digestion performed on the chip, have also been demonstrated.[18]

One of the most important features of these devices is the design of the electrospray exit port on the chip, which should provide stable and efficient ionization of the sample exiting the microdevice. In a typical electrospray ionization interface used in current mass spectrometry practice, the flowing liquid sample is electrosprayed from a sharp pointed tip biased at 1−5 kV with respect to the sampling orifice of the mass spectrometer.[21] Generally, the finer the tip the more efficient and stable the electrospray process. For example, with a widely adopted miniaturized version of electrospray, called nanospray, the sample is sprayed from a tip with an internal diameter of only a few micrometers at a flow rate in the low nL/min range.[22] Obviously, such an arrangement can be accommodated on a microdevice. Unfortunately, the fabrication of chips with integrated electrospray tips is not a simple task. Preliminary reports indicate success in microfabrication of electrospray tips by either casting from plastic materials[23] or by complex microfabrication procedures.[24] Alternatively, the electrospray tips can be fabricated separately and attached to the microfabricated device;[20,25] however, at present, these approaches are not practical for manufacture.

In previous work,[17−19] infusion analysis was performed with electrospray generated from the channel opening at the chip surface. In these cases, an electrospray tip was not necessary since the electric field strength at the exposed liquid surface was sufficiently high to form the electrospray cone. Thus, the analyzed liquid itself served as the ESI tip. Unfortunately, while infusion was readily achievable, the dead volume associated with the droplet formed at the electrospray exit port prevented the use of such a design for performing on-chip capillary electrophoresis/electrospray mass spectrometry (CE/ESI-MS).

In this work, we have developed and evaluated two alternatives for coupling microdevices with electrospray mass spectrometry. In the first design, a short transfer capillary was attached to the microdevice as an extension of the separation channel. The use of the transfer capillary allowed the incorporation of an external electrospray interface as well as on-line UV detection. Since attachment of the transfer capillary may add to the fabrication complexity, this type of device will be most suitable for use in a complex modular system, in which the microdevice would be used for many analyses before replacement. In the second design, a microfabricated pneumatic nebulizer was integrated directly into the microdevice at the electrospray exit port. The nebulizer eliminated the dead volume due to the formation of the droplet at the exit port and improved the stability of the electrospray. This device was fabricated as a one-piece system and could be used as a disposable chip, especially if made out of plastic. Both microdevices were tested for analysis of peptide samples by CE/ESI-MS.

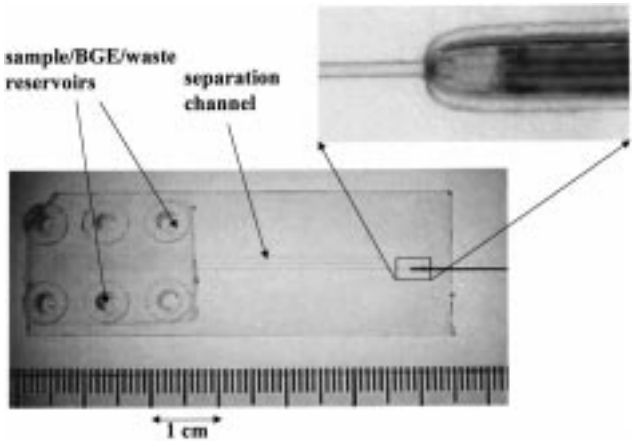

Figure 1. Photograph of the microdevice with attached transfer capillary. The scale is in mm.

EXPERIMENTAL SECTION

A. Microdevice with the Capillary Transfer Line. Fabrication. Standard photolithographic/wet chemical etching techniques were applied for fabrication[26] using Schott 263 glass wafers, (S. I. Howard Glass, Cambridge MA). The microdevice, shown in Figure 1, was fabricated using 1.1-mm-thick glass. First, two glasses with mirror images of identical structures were etched. The diameter of the semicircular separation and sample inlet channels was ∼75 μm. Next, a 6.5-mm-long portion of the separation channel on the exit side was further etched to ∼400 μm, and after drilling the 2-mm access holes and visual alignment, the two glass plates were thermally bonded to form a circular channel. The length of the separation channel was 11 cm. A 4-cm-long piece of a 380-μm od, 75-μm id fused silica transfer capillary (Polymicro Technologies, Phoenix, AZ) was epoxy glued into the 400-μm channel opening with the edge of the capillary being tapered to match the shape of the channel. Finally, a block of sample and buffer reservoirs, cast from a silicone resin (Sylgard 184, Dow Corning, Midland, MI), was attached to the microdevice using a DAP silicone sealant (Dow Corning, Midland, MI).

MS Interfacing. A subatmospheric, liquid-junction-based electrospray interface with an on-line fiber optic detector was used for coupling, as described previously.[27] The device was positioned in front of the mass spectrometer using a laboratory-made plexiglass holder with a removable electrode module on an $x-y-z$ translational stage (Oriel, Stratford, CT).

A modified spectrophotometric detector (Spectra 100, Spectra Physics, San Jose, CA) was used for UV absorbance detection at 214 nm. The modification included an increase in the gain of the input current amplifier by a factor of 15 and attachment of the holder of optical fibers in place of the original flow cell. Two, 1-m-long optical fibers (FVP300330360, Polymicro Technologies) were used for transmission of light between the detector and the on-

(21) Gaskell, S. J. *J. Mass Spectrom.* **1997**, *32*, 677−688.
(22) Wilm, M.; Mann, M. *Anal. Chem.* **1996**, *68*, 1−8.
(23) Foret, F.; Xue, Q.; Dunayevskiy, Y.; Karger, B. L. *Proc. 45th ASMS Conf. Mass Spectrom. Allied Topics*, Palm Springs Convention Center, Palm Springs, CA, 1997; p 377.
(24) Desai. A.; Tai, Y. C.; Davis, M. T.; Lee, T. Transducers '97, Chicago, IL, 1997; pp 927−930.
(25) Liu, H.; Foret, F.; Felten, C.; Zhang, B., Jedrzejewski, P.; Karger, B. L. *Proc. 46th ASMS Conf. Mass Spectrom. Allied Topics*, Orlando, FL, 1998; p 1028.
(26) Madou, M.; *Fundamentals of Microfabrication*; CRC Press: Boca Raton, FL, 1997.
(27) (a) Foret, F.; Kirby, D.; Karger, B. L. *Proc. 44th ASMS Conf. Mass Spectrom. Allied Topics*, Portland, OR, May 12−16, 1996; p 913. (b) Zhou, H.; Foret, F.; Karger, B. L. *Electrophoresis*, submitted.

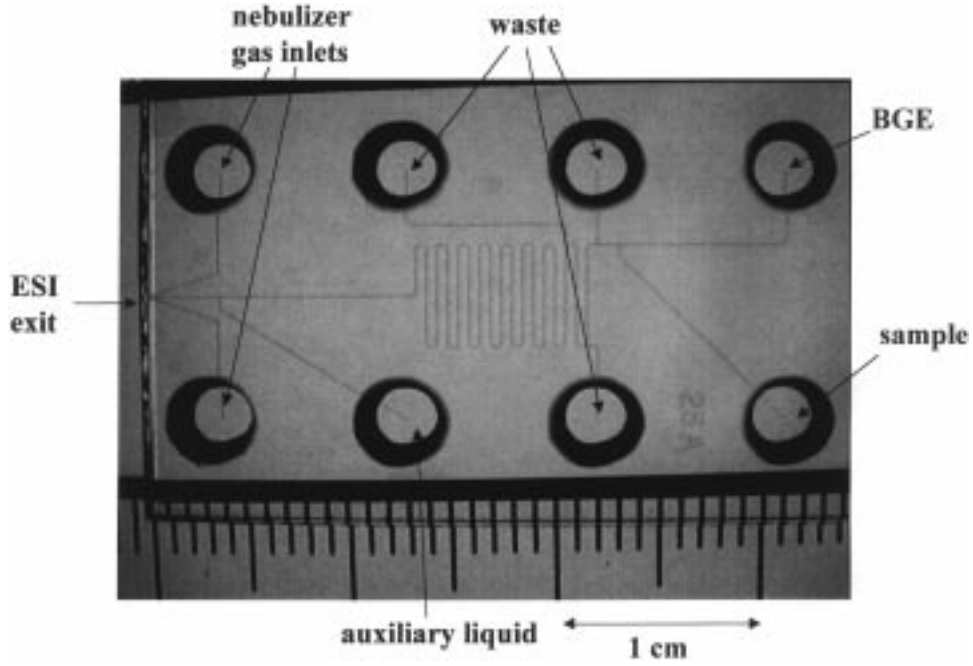

Figure 2. Photograph of the microdevice with the pneumatic nebulizer. The scale is in millimeters.

line capillary detection cell. Two millimeters of the polyimide coating were removed in the middle of the 4-cm transfer capillary, and the optical fibers were positioned at this point. A single high-voltage power supply (CZE 1000R, Spellman, Plainview, NY) was used for both CE separation and electrospray ionization. A high-voltage, high-resistance photoresistor, used to control the potential at the exit port, was constructed with 20 photoresistors (stock no. 699 9514, Allied Electronics, Forth Worth, TX) connected in series. The final resistance could be controlled in the range of ~1 MOhm to several TOhm by illuminating the photoresistors with a 5-V incandescent lamp.

B. Microdevice with the Integrated Nebulizer. Fabrication. For the microdevice with the integrated pneumatic nebulizer (Figure 2), the separation channel and the channels connecting the sample and buffer reservoirs, respectively, were etched on one 500-μm-thick glass plate. The channels with a semicircular cross section were 80 μm wide and 29 μm deep. The size of the auxiliary channel was roughly 35 μm × 160 μm × 10 mm and 29 μm × 80 μm × 0.6 mm at the junction with the separation channel. The size of the gas channels was 35 μm × 160 μm × 10 mm. A 2.25-mm-thick cover plate, with drilled 4-mm diameter holes for the background electrolyte and sample reservoirs, was thermally bonded to the etched glass plate. The electrospray exit port was formed by cutting the chip using a dicing saw.

MS Interfacing. As in the previous design, the microdevice was positioned in the plexiglass holder mounted on the $x-y-z$ stage. The distance between the exit port of the microdevice and the MS sampling orifice was set at 3 mm. The sheath gas was supplied from a nitrogen gas tank, which is a standard accessory of the mass spectrometer. Rubber O-rings were used to seal the gas sheath channel inlet. The electrical connection was the same as in the previous case.

Mass Spectrometry. Mass spectrometry was performed on a Finnigan LCQ ion-trap mass spectrometer (San Jose, CA). The original electrospray interface, supplied with the instrument, was removed and the electrospray high voltage power supply disabled. The heated capillary in the sampling orifice was operated at 200 °C.

Chemicals. All peptides, cytochrome *c*, trypsin, and 6-aminocaproic acid were purchased from Sigma Chemical Co. (St. Louis, MO) and were used without further purification. Ammonium acetate, acetic acid, and formic acid were from J. T. Baker (Phillipsburg, NJ), and methanol was obtained from E. M. Science (Gibbstown, NJ). Deionized water (18.2 MΩ) was prepared using a Milli-Q system from Millipore (Bedford, MA). The tryptic digest was prepared by incubating 1 mg of cytochrome *c* with 20 μg of trypsin at 37 °C in 1 mL of 20 mM ammonium acetate buffer (pH 8.2). After 20 h, the digest was adjusted to pH 4 with acetic acid and was then ready for injection in CE analysis.

RESULTS AND DISCUSSION

In our previous work on the ESI microdevices,[17,18] flow rates in the 100 nL/min range were generated using an external syringe pump. In this work, we have eliminated external pumps to minimize system complexity. We have also excluded simple electroosmotic pumping[19,20] to avoid possible analyte interaction

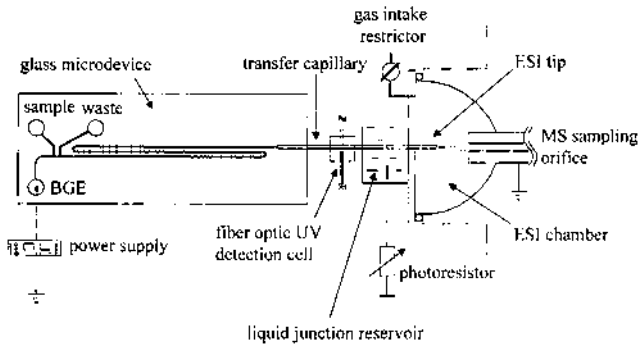

Figure 3. Diagram of the microdevice with the capillary transfer line and the subatmospheric electrospray interface.

with the charged wall of the separation channel. An important design criterion was that the device be universal, allowing all modes of CE separation including where bulk flow inside the chip is negligible, e.g., when the inner surface of the CE separation channel is coated or filled with a sieving matrix. Two different designs were tested: (a) the microdevice coupled to an external (liquid junction based) electrospray interface and (b) the microdevice with an integrated (pneumatic nebulizer based) electrospray interface. Both configurations are instrumentally simple and universally applicable for all modes of CE (as well as LC or CEC) separation performed on the microdevice.

Microdevice with External Transfer Capillary. Our first design consisted of a microfabricated structure that was suitable for sample introduction and CE separation and could be a part of a more complex stationary (nondisposable) system. A short transfer capillary was used to connect the microdevice to a previously developed subatmospheric electrospray interface.[27] This interface allows the use of fine (20 μm or less) electrospray needles which allow for excellent stability and ionization efficiency while not contributing significantly to band broadening.[27] The interface used the pumping action at the mass spectrometer sampling orifice to lower the pressure in the enclosed electrospray region. This created a pressure drop that initiated the flow of the analyzed liquid through the electrospray needle, thus eliminating the need for an external pump.

A diagram of the microfabricated system is shown in Figure 3. The microdevice with a 11-cm-long (~75-μm id) round separation channel was connected to the electrospray interface through a short piece of fused silica capillary (4 cm, 370 × 75 μm id). Since the electrospray current is typically on the order of 100 nA, the CE high-voltage power supply is sufficient to drive both the CE separation and the electrospray ionization. The required potential at the electrospray exit port (in the range of 1−3 kV) was set by the photoresistor, R_{phot}, connected between the liquid junction reservoir and the ground electrode of the high-voltage power supply.[27] Optical control of the R_{phot} protected the operator from contact with high voltage. Alternatively, a high-voltage power supply connected as a current sink can be used in place of the photoresistor R_{phot}.

The pressure in the electrospray chamber was maintained at 70 kPa (~0.7 atm), resulting in a 150 nL/min flow rate through the electrospray needle. The sample was injected into the separation channel as a 0.6-mm-long plug by applying 1 kV between the sample and the waste reservoirs for 10 s. We coated the surface of the separation channel with linear polyacrylamide[28] to eliminate adsorption and band broadening. Although the adsorption could be minimized by using a highly acidic solution as the separation electrolyte (e.g., 0.1 M formic acid solution), the selectivity under acidic conditions was not sufficient for complete resolution of the sample peptides. The transfer capillary (coated with linear polyacrylamide as well), besides transporting the bands to the ESI interface, also served as an inlet port for filling the channels with the reagents.

The CE/MS separation of a mixture of angiotensins, using the microdevice in Figure 3, is shown in Figure 4. The observed separation efficiency of as many as 47 000 plates, (313 000 plates/m) was similar to that which we separately obtained with a fused

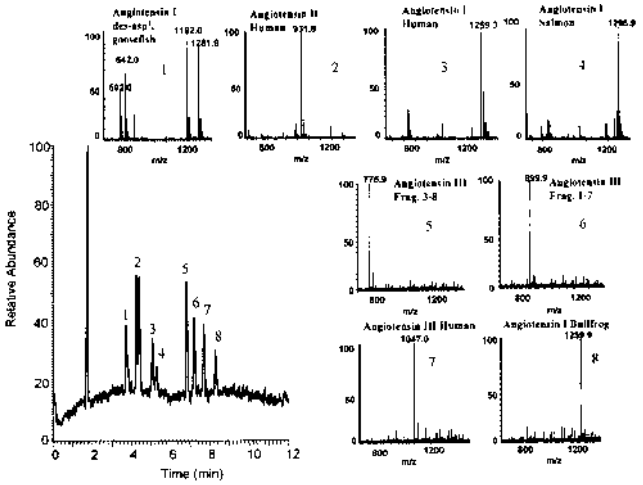

Figure 4. CE separation of a mixture of angiotensin peptides using the system in Figure 3. The sample concentration was 5 μg/mL of each peptide. BGE: 20 mM 6-aminocaproic acid/acetic acid, pH 4.4. Liquid junction solution: 0.8% (v/v) acetic acid in 50% (v/v) methanol/water. Electric field strength: 300 V/cm. ESI voltage: 2 kV. Plate count for peak 5 is 32 000 and 47 000 for peak 8.

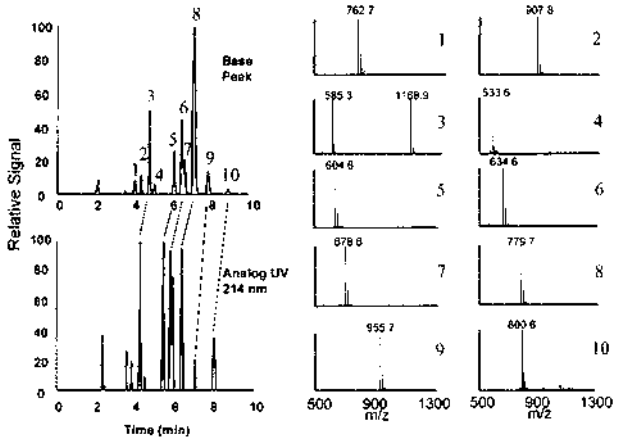

Figure 5. CE separation of cytochrome *c* tryptic digest on a microdevice using the transfer line and subatmospheric ESI interface. Peak identification: 1-KKIFVQKC, 2-KMIFAGIKKK, 3-KTGPNLHGLFGRK, 4-KKTERE, 5-KGITWKE, 6-KIFVQKC, 7-KYIPGTKM, 8-KMIFAGIKK, 9-GITWKEETLMEYLENPKKYIPGTK, 10-RKTGQAPGFTYTDANKN. Plate counts: 26 000 (peak 3), 42 000 (peak 5), 24 000 (peak 9). Other conditions as in Figure 2.

silica capillary column of identical length and diameter attached to the same electrospray interface. Figure 5 shows separation of a cytochrome *c* tryptic digest on the same microdevice with ESI-MS analysis. Also included is the 214-nm trace of the UV absorbance detector placed in the middle of the transfer capillary—see Figure 3. By searching a protein database,[29] all the peaks labeled in Figure 5 could be assigned to the respective tryptic peptides with an accuracy better than 0.3%. The above on-line UV detector in the CE/MS system, useful for quantitative analysis, also served as a valuable diagnostic device. The comparison of the UV and MS signals allowed the clearly distinguishing of CE separation problems (band broadening, adsorption, low sample concentration, etc.) from ESI related problems such as electrospray instability.

(28) Hjerten, S. J. *J. Chromatogr.* **1985**, *347*, 191−194.

(29) EMBL Protein and Peptide Group. http://www.mann.embl-heidelberg.de/Services/PeptideSearch/FR_PeptideSearchForm.html (accessed 6/8/99).

The hybrid microdevice−capillary is useful for testing the features of the microfabricated system such as injection, sample preconcentration, and separation performance. The fused silica transfer capillary allows the use of on-line optical detection (UV absorbance, fluorescence) without the need to fabricate the microdevice from expensive optical quality materials such as quartz or fused silica. Integration of the separation channel with the injector on the microdevice provided the overall system miniaturization.

Assuming that sample losses in the microdevice are minimal, the sensitivity of the mass spectrometric detection will be dependent on the performance of the external electrospray interface. The subatmospheric interface[27] used in this study proved to be well-suited for this application. Depending on the analyte, sensitivity in the submicromolar concentration range (low fmol to high amol amounts injected into the microdevice) should be possible with the present setup.

The hybrid device in Figure 3 is mechanically complex, which could lead to increased production costs when compared with a completely integrated microdevice, i.e., one without the need of a post fabrication attachment of external parts. Thus, the hybrid construction is a preferable means of miniaturization of complex systems in which the microfabricated parts would not be disposable. Such an approach has recently been used for frontal analysis of samples deposited on a microdevice using a C_{18} packed capillary.[30]

Microdevice with an Integrated Nebulizer. As noted, the critical point of an integrated microdevice for mass spectrometric analysis is the electrospray exit port. In earlier work, the opening of the sample delivery channel, created by cutting off the edge of the microfabricated device, was used as the electrospray exit port.[17−19] In this design, the sample exited the channel, forming a small droplet with a volume of 20−200 nL. Depending on the surface tension of the liquid solution and the surface properties of the material of the microdevice, e.g., hydrophobicity, this droplet was either contained in a relatively small area or spread over a larger area around the channel exit. Upon application of the high voltage, the droplet was shaped by the electric field into a cone, and the liquid itself formed the electrospray tip.[17] Obviously, the less wettable the surface of the microdevice, the smaller the droplet and the better the electrospray stability at a given applied voltage. Additionally, the surface around the exit port could be chemically modified to minimize wetting.[17] While successful for infusion analysis, a "flat" electrospray exit port cannot be used in conjunction with on-chip microcolumn separations because of the relatively large extra-column volume of the liquid drop, which destroys any separation in the chip. One possible solution to reduce this extra-column effect would be to use a flowing stream of an auxiliary liquid, which would transport the separated zones toward the electrospray exit port. In analogy to the liquid sheath or liquid junction arrangement of the standard electrospray interface,[31,32] the flow of the auxiliary fluid would also provide an environment for optimum electrospray ionization.

In this work, we have explored the design of a microdevice with an integrated pneumatic nebulizer.[33] The nebulizer removes the droplet formed at the electrospray exit port, minimizing the extra-column volume and the subsequent degradation of separation. Moreover, the nebulizer also serves as a means to control the flow rate of the auxiliary fluid. A photograph of the microdevice is shown in Figure 2. The size of the semicircular separation channel was 29 μm × 80 μm × 100 mm. A serpentine shaped separation channel was used to extend the CE separation path and to increase the sample volume that can be injected, thus aiding MS detection. As in the case of the microdevice with the transfer capillary, the migration time was increased to be compatible with the data acquisition requirements of the mass spectrometer used in this study, i.e., 1 s/scan. Of course, fast mass spectrometers such as time-of-flight instruments may be employed for faster separation with a short, straight separation channel.[34]

The sample, deposited in the sample inlet port, could be injected as a zone of variable length by electromigration. During injection, the electric voltage was applied between the sample inlet port and a selected waste reservoir. CE separation was then conducted with the electric voltage connected between the background electrode reservoir and the reservoir containing the auxiliary fluid. Two gas channels in a V-shape arrangement merged at the electrospray exit port. These channels delivered nitrogen gas (0.3 L/min) to induce suction and dispersion of the auxiliary liquid at the electrospray exit port. At the same time, the gas flow also aided evaporation of the electrosprayed droplets. The flow rate of the auxiliary liquid could be controlled by the nitrogen flow, independent of the electromigration or electroosmotic flow of the liquid in the separation channel. It should be emphasized that, in the design of the microdevice, the distance of the electrospray exit port from the edge of the chip is important. If the gas and separation channels merge more than 500 μm below the edge, gas pressure will cause fluid flow toward the injection port. On the other hand, if the channels do not merge, the gas flow will not disperse the liquid from the exit port. In our experience, stable electrospray signal was achieved when the electrospray exit port with the two merging gas channels formed a single 100−300 μm opening on the surface of the chip. These dimensions could be easily achieved using a precision dicing saw.

During separation, the potential of the electrospray exit port could be set to a desired value (2−5 kV) through a series of photoresistors in the same way as discussed in the previous section with the subatmospheric electrospray interface. The high voltage of the CE was connected to the electrode in the background electrolyte reservoir on the injection side of the separation channel. The scheme of an equivalent electrical circuit is shown in Figure 6. During operation, the high voltage power supply delivered separation current I_{CE} (1−10 μA). This current was divided at the electrospray exit port into one part flowing to the ground through the auxiliary channel and photoresistor, R_{phot}, and the other, I_{ESI} (50−200 nA), transported to the grounded sampling orifice of the mass spectrometer by the plume of the electrosprayed ions.

(30) Figeys, D.; Aebersold, R. *Anal. Chem.* **1998**, *70*, 3721−3727.
(31) Smith, R. D.; Barinaga, C. J.; Udseth, H. R. *Anal. Chem.* **1988**, *60*, 1948−1952.
(32) Lee, E. D.; Muck, W.; Henion, J. D.; Covey, T. R. *Biomed. Environ. Mass Spectrom.* **1989**, *18*, 844−850.
(33) Lazar, I. M.; Xin, B. M.; Lee, M. L.; Lee, E. D.; Rockwood, A. L.; Fabbi, J. C.; Lee, H. G. *Anal. Chem.* **1997**, *69*, 3205−3211.
(34) Zhang, B.; Karger, B. L.; Foret, F. *Proc. 44th ASMS Conf. Mass Spectrom. Allied Topics*, Orlando, FL, May 31−June 4, 1998; p 757.

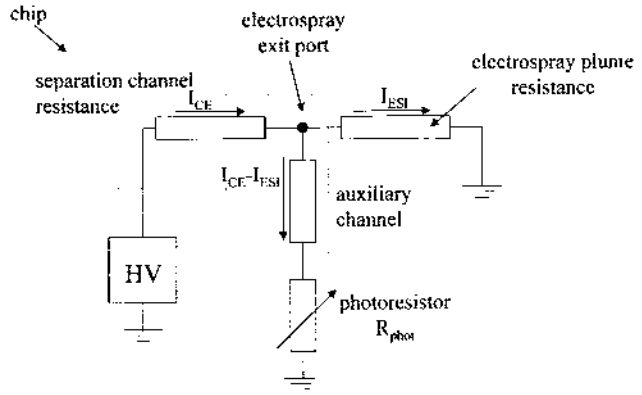

Figure 6. Electrical scheme of the microdevice in operation. The electric current I_{CE}, delivered by the high voltage power supply (HV), transports the ions in the separation channel. The potential of the electrospray exit port can be controlled by an incandescent lamp illuminating the photoresistor, R_{phot}. A small fraction of the electrophoresis current I_{CE} is transported toward ground by the electrosprayed ions while the remaining current returns to ground through the auxiliary channel and the photoresistor, R_{phot}.

To characterize the performance of the electrospray interface with the nebulizer, liquid infusion was first examined. In this experiment, 10 μL of myoglobin solution in 50% methanol/water (v/v) with 0.8% acetic acid was placed in the auxiliary liquid reservoir. The high-voltage power supply was connected through the electrode inserted into the auxiliary liquid reservoir, nitrogen gas was turned on, and the mass spectrum was recorded. Interestingly, the spectrum of myoglobin could be observed even without the application of the electrospray high voltage, similar to that previously reported for a sonic spray.[35] This behavior result is thought to be due to the rapid breaking of larger droplets in the gas stream creating a small charge imbalance in the resulting smaller droplets. The signal intensity, however, was ~100 times weaker compared with the case when 4 kV of electrospray high voltage was applied. Also, the electrospray created ions of higher charge states with a concentration detection limit in the 0.1 μM range.

The sample was electrosprayed at a flow rate of ~200 nL/min, and since the solution evaporates during the analysis, the sample volume of 15 μL (the volume of the auxiliary liquid reservoir) could be electrosprayed for about 20 min. This evaporation is inherent to all chip designs described in the literature. Since the analysis time is typically very short (10 min or less), the control of evaporation is not critical.

To test the nebulized electrospray with on-chip CE separation, we have selected 1% (v/v) formic acid solution (pH ~ 2.3) as the background electrolyte (BGE) for separation of a peptide mixture. At low pH, the electroosmotic flow was negligible, and the only transport phenomena were related to electromigration and suction of the liquid by the nebulizer.

To minimize the contribution of the hydrodynamic flow to zone broadening, the distance between the junction of the CE and auxiliary channels and the electrospray exit port was minimized. Also, the hydrodynamic resistance of the auxiliary fluid channel relative to the separation channel was minimized. In the current design, the auxiliary liquid channel had a cross section more than 2 times larger than the separation channel, but 12 times shorter than the separation channel (i.e., 100 mm long). The measured nebulizer-driven hydrodynamic flow in the separation channel was less than 0.1 mm/s, as determined by observing the mass spectrum with the ESI nebulizer on, but the CE voltage off. No signal was observed after more than 20 min. Since the total time of the CE analysis was less than 5 min, the residual hydrodynamic flow therefore did not significantly contribute to the zone transport, and influence of this flow on the zone broadening is expected to be low.

An important effect, which could potentially result in a decrease or complete loss of the ESI signal, is possible migration of sample zones into the auxiliary electrolyte channel. In practice, the sample ions will not migrate into the auxiliary channel if their electrophoretic velocity is lower than the velocity of the flow of the auxiliary liquid. Thus, the following relation must be fulfilled

$$uE < v \tag{1}$$

Here, u is the effective electrophoretic mobility of the analyte ions, E the electric field strength in the auxiliary channel, and v the velocity of the auxiliary liquid flow. Equation 1 can be rearranged using Ohm's law into the following:

$$uI/\kappa < Q \tag{2}$$

Here, I is the electrophoretic current, κ the conductivity of the auxiliary liquid, and Q the volume flow rate of the auxiliary liquid. For typical experimental conditions ($I \sim 5\ \mu$A, $u \sim 3 \times 10^{-8}$ m^2/Vs, $\kappa \sim 0.2$ S/m), the minimum flow rate was calculated to be 45 nL/min. The flow rate during the present experiments was 4 times higher, and thus, no sample loss due to the sample electromigration into the auxiliary channel would be expected.

An example of the CE/ESI-MS separation of an angiotensin peptide mixture performed with the microdevice is shown in Figure 7. In this experiment we have used transient isotachophoretic (t-ITP) sample preconcentration[36] to increase the analyte concentration. For this purpose, the sample was dissolved in 100 mM ammonium acetate. Ammonium ions served as the leading electrolyte with the H^+ reaction boundary as the terminating zone.[37] The t-ITP preconcentration allowed injection and focusing of a 6.5-mm-long injection plug of the ~10^{-5} M peptide mixture. Both resolution and sensitivity was ~ 10 times less without the t-ITP sample preconcentration (data not shown).

Although in the current design the separation efficiency is lower than that in the microdevice with the transfer line (~ 70 000 vs 300 000 plates/m, respectively), it can be further improved by minimizing the two significant sources of the band broadening. First, the serpentine shape of the separation channel contributes to the band broadening because of the different separation path lengths in the curved channel.[38,39] The required length of the

(35) Hirabayashi, A.; Sakairi, M.; Takada, Y.; Koizumi, H. *Trends Anal. Chem.* **1997**, *16*, 45−52.

(36) Foret, F.; Szökö, E.; Karger, B. L. *Electrophoresis* **1993**, *14*, 417−428.

(37) Bocek, P.; Deml, M.; Gebauer, P.; Dolnik, P. *Analytical Isotachophoresis*; VCH Publishers: Weinheim, Germany, 1988.

(38) Wicar, S.; Vilenchik, M.; Belenkii, A.; Cohen, A. S.; Karger, B. L *J. Microcolumn Sep.* **1992**, *4*, 339−348.

(39) Culbertson, C. T.; Jacobson, S. C.; Ramsey J. M. *Anal. Chem.* **1998**, *70*, 3781−3789

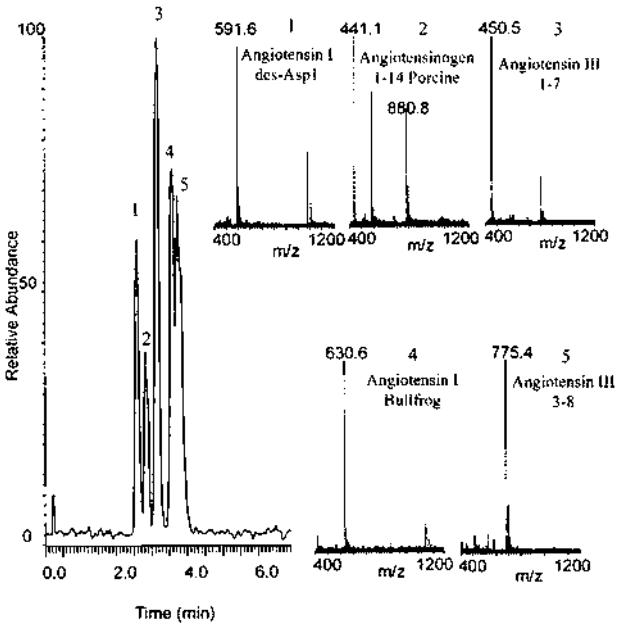

Figure 7. CE/ESI-MS analysis of a peptide mixture in the microdevice with a pneumatic nebulizer using transient isotachophoretic sample preconcentration. Sample concentration: 20 μg/mL of each peptide dissolved in 100 mM ammonium acetate. Injection size: 6-mm plug (~11 nL). BGE: 1% (v/v) formic acid in water. Auxiliary liquid: 1% (v/v) formic acid in 50% (v/v) methanol/water. Electric field strength: 400 V/cm. ESI voltage: 4 kV. Nebulizer gas flow rate: 0.3 L/min, 141 kPa (1.4 atm).

separation channel may be achieved by other geometrical shapes (e.g., as in Figure 1), minimizing the related band dispersion. Second, the hydrodynamic flow in the channel between the junction of the auxiliary liquid channel and the electrospray exit port likely contributed to band broadening. In the current design, this distance was 5 mm, which can be decreased by an order of magnitude in the future design. Finally, the residual flow in the separation channel can be practically eliminated by making the auxiliary liquid channel much wider than the separation channel. These future modifications will significantly enhance the performance of the present microdevice; however, this first-generation design has clearly demonstrated feasibility of a simple, fully integrated microsystem for separation/ESI-MS.

(40) Bing, N. H.; Skinner, C. D.; Wang, C.; Colyer, C. L.; Harrison, D. J.; Li, J.; Thibault, P. *Proc.μTAS'98*, Banaff, Canada, 1998; p 141.

CONCLUSIONS

This paper presents two fundamentally different approaches for coupling of the chip separation with on-line electrospray ionization mass spectrometry. The first design with the transfer capillary and an external subatmospheric electrospray interface represents a universal approach for coupling of external devices to microfabricated systems. The coupling is straightforward and suitable for hybrid systems in which the microfabricated device is not discarded after each analysis. It allows UV absorbance detection regardless of the optical quality of the material used for microdevice fabrication. A related system using a coaxial sheath fluid electrospray interface has recently been described in an independent study.[40]

The second design, with an integrated pneumatic nebulizer, allows use of a flat electrospray exit port without the need to microfabricate or attach an external electrospray tip. The pumping action of the nebulizer provides the control of the flow rate of the electrosprayed liquid regardless of the presence or absence of electroosmosis. The combination of the pneumatic nebulizer with the separation channel represents integration of two commonly independent systems (CE and electrospray interface) on one chip. Since all the separation and gas channels are etched in one step, the microfabrication process is simple and inexpensive. Hence, such a device can be either a part of a more complex hybrid instrument or serve as an inexpensive disposable cartridge. Since neither of the described systems depends on an internal electroosmotic to deliver sample into the electrospray, all modes of separation can be utilized including the CE in a channel with a neutral surface coating or in a polymer-filled separation channel. Further work is in progress on improvements and practical applications of both types of the microdevices.

ACKNOWLEDGMENT

The authors gratefully acknowledge NIH GM 15847 (B.L.K.) for support of this work. The authors further thank Luc Bousse from Caliper Technologies, Inc. for help with fabrication of the microdevices and Dr. Shaorong Liu, Molecular Dynamics, for development of the microdevice−capillary coupling procedure. This paper is contribution no. 755 from the Barnett Institute.

Received for review January 28, 1999. Accepted April 28, 1999.

AC990090U

Anal. Chem. **2000,** *72,* 1015−1022

A Microdevice with Integrated Liquid Junction for Facile Peptide and Protein Analysis by Capillary Electrophoresis/Electrospray Mass Spectrometry

Bailin Zhang, Frantisek Foret,* and Barry L. Karger*

Barnett Institute and Department of Chemistry, Northeastern University, Boston, Massachusetts 02115

A novel microfabricated device was implemented for facile coupling of capillary electrophoresis with mass spectrometry (CE/MS). The device was constructed from glass wafers using standard photolithographic/wet chemical etching methods. The design integrated (a) sample inlet ports, (b) the separation channel, (c) a liquid junction, and (d) a guiding channel for the insertion of the electrospray capillary, which was enclosed in a miniaturized subatmospheric electrospray chamber of an ion trap MS. The replaceable electrospray capillary was precisely aligned with the exit of the separation channel by a microfabricated guiding channel. No glue was necessary to seal the electrospray capillary. This design allowed simple and fast replacement of either the microdevice or the electrospray capillary. The performance of the device was tested for CE/MS of peptides, proteins, and protein tryptic digests. On-line tandem mass spectrometry was used for the structure identification of the protein digest products. High-efficiency/high-resolution separations could be obtained on a longer channel (11 cm on-chip) microdevice, and fast separations (under 50 s) were achieved with a short (4.5 cm on-chip) separation channel. In the experiments, both electrokinetic and pressure injections were used. The separation efficiency was comparable to that obtained from conventional capillary electrophoresis.

Mass spectrometry (MS) is currently one of the most important techniques for analysis of biological samples.[1] Both scanning and time-of-flight MS instruments are employed for analysis of a broad range of samples related to genomics, proteomics, and drug discovery research.[2−4] The need for analysis of a large number of samples (chemical libraries, screening of protein expression, etc.) requires development of high-throughput procedures for sample pretreatment (desalting, separation) and delivery for mass spectrometric analysis. Additionally, increased mass sensitivity is needed as the amount of the analyzed samples rapidly decreases.

Over the past few years, microfabricated devices (microdevices, chips, microchips) have attracted a great deal of attention as a possible means of increasing the throughput and mass sensitivity of analytical procedures via miniaturization. A variety of microdevices for total microanalysis systems (μ-TAS[5]) have been constructed including chemical separation techniques, e.g., capillary electrophosesis (CE), HPLC, CEC,[6−11] and miniaturized systems for PCR or combinatorial library synthesis.[12,13] Compared to standard instrumentation, the microdevices offer the means for handling small liquid volumes without the interferences from excessive dead volumes typical in "tube and ferrule"-based instruments. In addition, short CE or LC columns can be easily created for fast separations. At the same time, the reduced device footprint has potential for lower cost, relative to standard instrumentation.

The coupling of a microfabricated device to ESI-MS initially involved sample infusion from the flat surface[14,15] along with on-chip ion exchange and enzymatic digestion performed on the chip prior to the ESI-MS.[16] In an alternative approach, the glass microdevice, serving as a sample delivery system, was coupled to a standard capillary column using a Teflon connector.[17−19] Although effective for infusion analysis, the above approaches are unsuitable for coupling with on-chip separations due to the large dead volume associated with the droplet formed around the flat electrospray exit port or the Teflon connector. This dead volume problem can be circumvented by using an on-chip integrated pneumatic nebulizer;[20] however, most of the designs are now

(1) Costello, C. E. *Curr. Opin. Biotechnol.* **1999**, *10*, 22−8.
(2) Ross, P.; Hall, L.; Smirnov, I.; Haff, L. *Nature Biotechnol.* **1998**, *16*, 1347−1351.
(3) Yates, J. R. *J. Mass Spectrom.* **1998**, *33*, 1−19.
(4) Siuzdak, O.; Lewis, J. K. *Biotechnol. Bioeng.* **1998**, *61*, 127−134.
(5) Manz, A.; Harrison, D. J.; Verpoorte, E. M. J.; Fettinger, J. C.; Paulus, A.; Ludi, H.; Widmer, H. M. *J. Chromatogr.* **1992**, *593*, 253−258.
(6) Effenhauser, C. S. In *Microsystem Technology in Chemistry and Life Science;* Manz, A., Becker, H., Eds.; Springer-Verlag: Berlin, Germany, 1998; pp 51−82.
(7) Kutter, J. P.; Jacobson, S. C.; Matsubara, N.; Ramsey, J. M. *Anal. Chem.* **1998**, *70*, 3291−3297.
(8) Regnier, F. E.; He, B.; Lin, S.; Busse, J. *Trends Biotechnol.* **1999**, *17*, 101−106.
(9) Rodriguez, I.; Lee, H. K.; Li, S. F. Y. *Electrophoresis* **1999**, *20*, 118−126.
(10) Jacobson, S. C.; Culbertson, C. T.; Daler, J. E.; Ramsey, J. M. *Anal. Chem.* **1998**, *70*, 3476−3480.
(11) Schmalzing, D.; Koutny, L. B.; Taylor, T. A.; Nashabeh, W.; Fuchs, M. *J. Chromatogr., A* **1997**, *697*, 175−180.
(12) Woolley, A. T.; Hadley, D.; Landre, P.; deMello, A. J.; Mathies, R. A.; Northrup, M. A. *Anal. Chem.* **1996**, *68*, 4081−4086.
(13) DeWitt, S. H. *Curr. Opin. Chem. Biol.* **1999**, *3*, 350−356.
(14) Xue, Q.; Foret, F.; Dunayevskiy, Y. M.; Zavracky, P. M.; McGruer, N. E.; Karger, B. L. *Anal. Chem.* **1997**, *69*, 426−430.
(15) Ramsey, R. S.; Ramsey, J. M. *Anal. Chem.* **1997**, *69*, 1174−1178.
(16) Xue, Q.; Foret, F.; Dunayevskiy, Y. M.; Foret, F.; Karger, B. L. *Rapid Commun. Mass Spectrom.* **1997**, *11*, 1253−1256.
(17) Figeys, D.; Ning, Y.; Aebersold, R. *Anal. Chem.* **1997**, *69*, 3153−3160.
(18) Figeys, D.; Aebersold, R. *Anal. Chem.* **1998**, *70*, 3721−3727.
(19) Pinto, D. M.; Ning, Y.; Figeys, D. *Electrophoresis* **2000**, *21*, 181−190.

10.1021/ac991150z CCC: $19.00
Published on Web 01/21/2000

focusing on development of microdevices with fine electrospray tips.[20−26]

Two different approaches have been adopted for construction of the microdevices with electrospray tips. In one, the tip was microfabricated at the outlet of the channel on a silicon device using a back-etching method.[22] In an alternative design, an array of ESI nozzles was made from silicon by dry etching.[23] To date, both approaches have only been used in the infusion mode.

In another approach, the electrospray tip was formed by a piece of fine fused-silica capillary (10−50 μm i.d.) glued to the exit of the separation channel. A microdevice cast from a solvent-resistant polymer with 96 capillary tips was developed for high-throughput infusion analysis.[24] Several groups have reported the use of capillary ESI tips glued to the glass microdevices.[20,21,25−27] The guiding channel for alignment of the ESI tip with the separation channel was fabricated either by a double-etching protocol[20] or by hand drilling.[27]

In the above designs, permanent coupling of the ESI tips to the separation channel has been a problem. Precision drilling followed by gluing the electrospray tips requires skilled operators, and the impurities released from the glued joints may cause sample contamination or clogging of the tip. In this paper, we report a new approach to the liquid junction interfacing method for direct coupling of the microdevice with ESI-MS.[20] The liquid junction reservoir with a guiding channel for the ESI tip was integrated with the separation channel and sample/background electrolyte (BGE) inlets directly on the glass microdevice. Concurrently, the electrospray tip was a part of a miniaturized subatmospheric ESI interface.[28] During operation, the microdevice was inserted onto the free end of the ESI tip. Since the internal diameter of the guiding channel was etched to match closely the outer diameter of the ESI tip, no glue was necessary to secure the tip in place, and the fixed chip structure permitted easy alignment. In practice, either the ESI tip or the microdevice could be readily replaced. The design is inexpensive and suitable for mass production.

EXPERIMENTAL SECTION

Microdevice Fabrication. The microdevice (shown in Figure 1) was fabricated using standard photolithographic/wet chemical etching techniques, as described previously.[20] First, two borofloat glass wafers (S. I. Howard Glass, Cambridge, MA) with mirror images of identical structures were etched. The diameter of the semicircular separation and sample inlet channels was ∼75 μm.

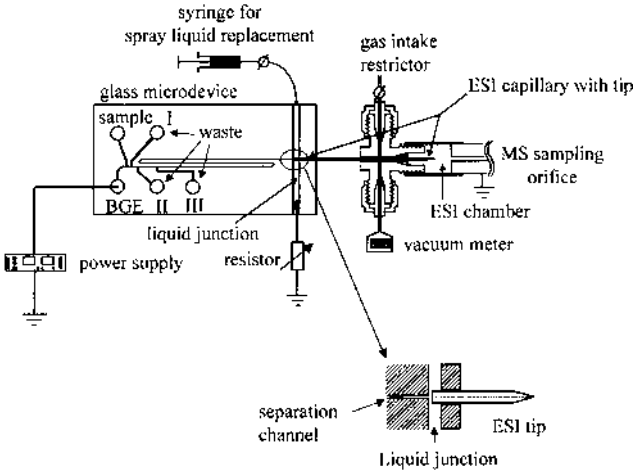

Figure 1. Diagram of the microdevice with a subatmospheric electrospray interface. The expanded view shows the coupling of the ESI tip with the separation channel in the liquid junction. See Experimental Section for details.

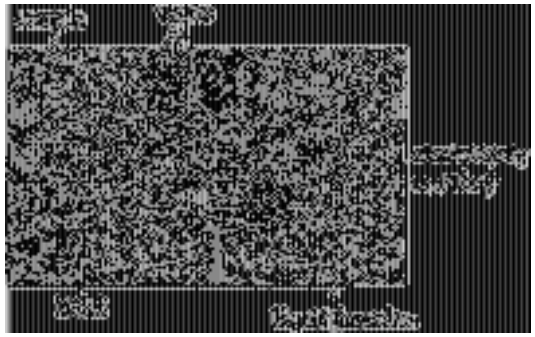

Figure 2. Photograph of the microdevice in Figure 1 with the replaceable electrospray capillary tip. The subatmospheric electrospray chamber and liquid junction connections are not shown for clarity.

Next, an ∼5 mm long portion of the separation channel on the exit side was further etched to ∼400 μm. The liquid junction channel (see Results and Discussion) was created using a dicing saw. After drilling of the 2 mm diameter access holes and visual alignment, the two glass plates were thermally bonded to form circular channels. A block of sample and buffer reservoirs, cast from a silicone resin (Sylgard 184, Dow Corning, Midland, MI), was attached to the microdevice using a DAP silicone sealant (Dow Corning).

A miniaturized subatmospheric ESI interface[28] was constructed using a microcross (P-777, Upchurch Scientific, Oak Harbor, WA). The hole in the microcross was modified to hold a 2.5 cm long fused-silica ESI capillary with a 380 μm o.d. and a 25 μm i.d. (Polymicro Technologies, Phoenix, AZ). The ESI tip was tapered by HF etching to a final outer diameter of ∼30 μm. A silicone rubber septum (∼1 mm diameter) was positioned in the center of the ESI capillary, allowing easy handling. The microcross was then attached to the sampling orifice of the mass spectrometer using 2 cm of silicone tubing. The two remaining outlets of the microcross were coupled to a pressure meter (TIF Instruments, Miami, FL) and to capillary tubing which served as a gas flow restrictor. During the experiments, the vacuum in the chamber was maintained at 78 kPa to produce a stable electrospray.[28] The microdevice was positioned in front of the mass spectrometer

(20) Zhang, B.; Liu, H.; Karger, B. L.; Foret, F. *Anal. Chem.* **1999**, *71*, 3258−3264.
(21) Xiang, F.; Lin, Y. H.; Wen, J.; Matson, D. W.; Smith, R. D. *Anal. Chem.* **1999**, *71*, 1485−1490.
(22) Desai. A.; Tai, Y. C.; Davis, M. T.; Lee, T. *Transducers '97*, Chicago, IL, 1997; pp 927−930.
(23) Schultz, G. A.; Corso, T. N. The *47th ASMS Conf. Mass Spectrom. Allied Topics*, Dallas, TX, 1999; ThOE 3, p 40.
(24) Liu, H.; Foret, F.; Felten, C.; Zhang, B.; Jedrzejewski, P.; Karger, B. L. *Proc. 46th ASMS Conf. Mass Spectrom. Allied Topics*, Orlando, FL, 1998; p 1028.
(25) Bing, N. H.; Wang, C.; Skinner, C. D.; Colyer, C.; Thibault, P.; Harrison, J. D. *Anal. Chem.* **1999**, *71*, 3292−3296.
(26) Lazar, I. M.; Ramsey, R. S.; Sundberg, S.; Ramsey, J. M. *Anal. Chem.* **1999**, *71*, 3627−3631.
(27) Li, J.; Thibault, P.; Bing, N.; Skinner, C. D.; Wang, C.; Colyer, C.; Harrison, J. *Anal. Chem.* **1999**, *71*, 3036−3045.
(28) (a) Foret, F.; Kirby, D.; Karger, B. L. *The 44th ASMS Conf. Mass Spectrom. Allied Topics*, Portland, OR, 1996; WPH 147. (b) Foret, F.; Zhou, H.; Gangl, E.; Karger, B. L. *Electrophoresis*, in press.

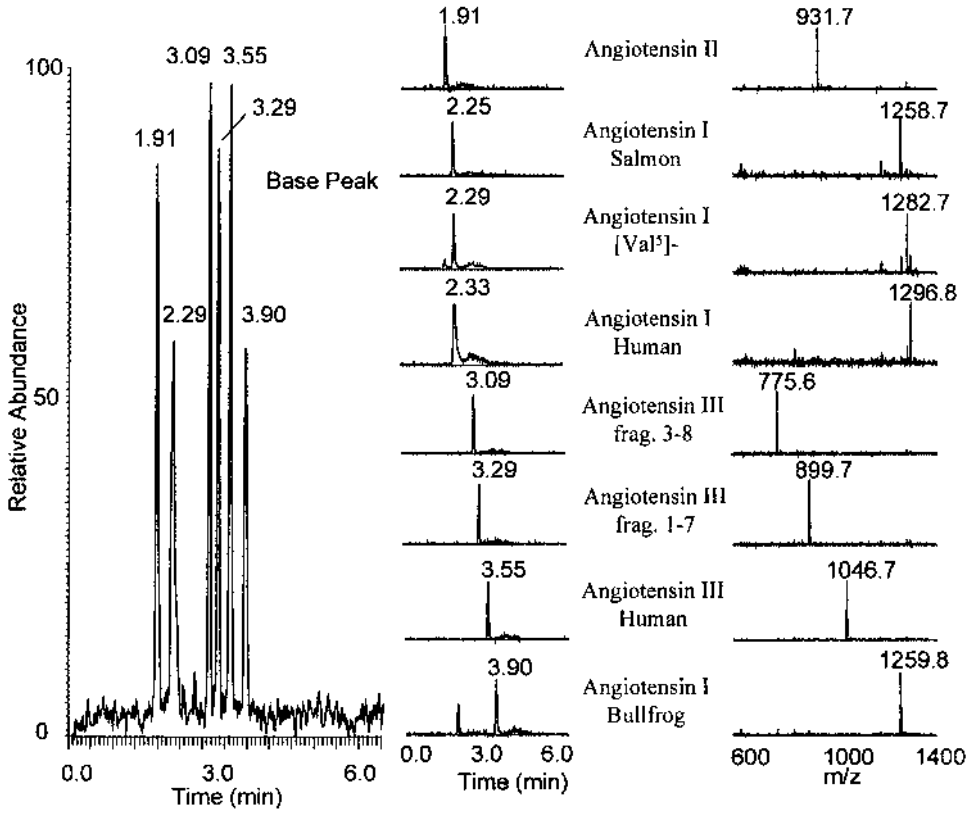

Figure 3. CE/MS analysis of a mixture of angiotensin peptides using the microdevice in Figure 1. The sample concentration was 10 μg/mL of each peptide. BGE, 20 mM 6-aminocaproic acid/acetic acid, pH 4.4. Liquid junction solution, 0.8% (v/v) acetic acid in 50% (v/v) methanol/water. Electric field strength, 500 V/cm. Pressure in the electrospray chamber, 78 kPa. ESI voltage, 2 kV. The signals from base peak monitoring (left), selected ion monitoring (middle), and single-scan mass spectra corresponding to the peak maximums (right) are shown.

using a plexiglass holder with a removable electrode module on an $x-y-z$ translational stage. The distance between the electrospray tip and the MS sampling orifice was ~5 mm.

Electrophoresis. Before each separation, the channel was flushed with the background electrolyte (20 mM ϵ-aminocaproic acid titrated with acetic acid to pH 4.4) using a syringe connected to waste reservoir III (Figure 1). Next the liquid junction was flushed with the spray liquid—1% acetic acid in 50:50 (v/v) methanol/water solution. The sample was injected by electromigration or pressure. In experiments with pressure injection, a laboratory-built pressure controller was used employing a miniature membrane pump (Ohlheiser, Newington, CT) and fast pneumatic switches (SMC, Indianapolis, IN).

Mass Spectrometry. A Finnigan (San Jose, CA) LCQ quadrupole ion trap mass spectrometer was used for all experiments. The heated inlet capillary was maintained at 200 °C. On-line ESI-MS was performed in the positive ion mode with a typical ESI voltage of ~2.2 kV. For CE/MS experiments with the microdevice, the maximum sample injection time was 200 ms, and two microscans were summed for each scan. For the CE/MS/MS experiments, the maximum sample injection time was 300 ms, and two microscans were summed for each scan. The collision energy was set at 25%.

Materials. All peptides and proteins were purchased from Sigma Chemical Co. (St. Louis, MO) and used without further purification. Ammonium acetate, acetic acid, and formic acid were from J. T. Baker (Phillipsburg, NJ), and methanol was obtained from E. M. Science (Gibbstown, NJ). Deionized water (18.2 MΩ) was prepared using a Milli-Q system from Millipore (Bedford, MA), and ϵ-aminocaproic acid was from Fluka (Milwaukee, WI).

The protein digest mixture was prepared as follows: First, the protein (cytochrome *c* or bovine serum albumin (BSA)) was dissolved in 20 mM ammonium bicarbonate to a concentration level of ~1 mg/mL. Trypsin was then added at a substrate-to-enzyme ratio of 50:1, and the whole solution was incubated overnight at 37 °C. Before injection, the sample was adjusted to pH ~4 with acetic acid.

RESULTS AND DISCUSSION

In this work, we have incorporated the external liquid junction interface[20] directly on the microdevice. The ESI tip is not integral to the microdevice structure but forms a removable part of a miniaturized subatmospheric ESI interface. Since a precise guiding channel can easily be microfabricated on the chip, exact positioning of the electrospray capillary tip is assured without the need for gluing it in place. Sample transport into the ESI tip was assured by the pressure difference between the subatmospheric ESI chamber and the liquid junction, the latter being at atmospheric pressure. The positioning of the liquid junction on the microdevice decoupled the separation channel from the ESI capillary. In this way, any band broadening, which could arise due to flow imbalance between the separation channel and the electrospray capillary, was eliminated.[28] Additionally, the spray fluid in the liquid junction could be optimized for electrospray ionization, regardless of the composition of the separation buffer.

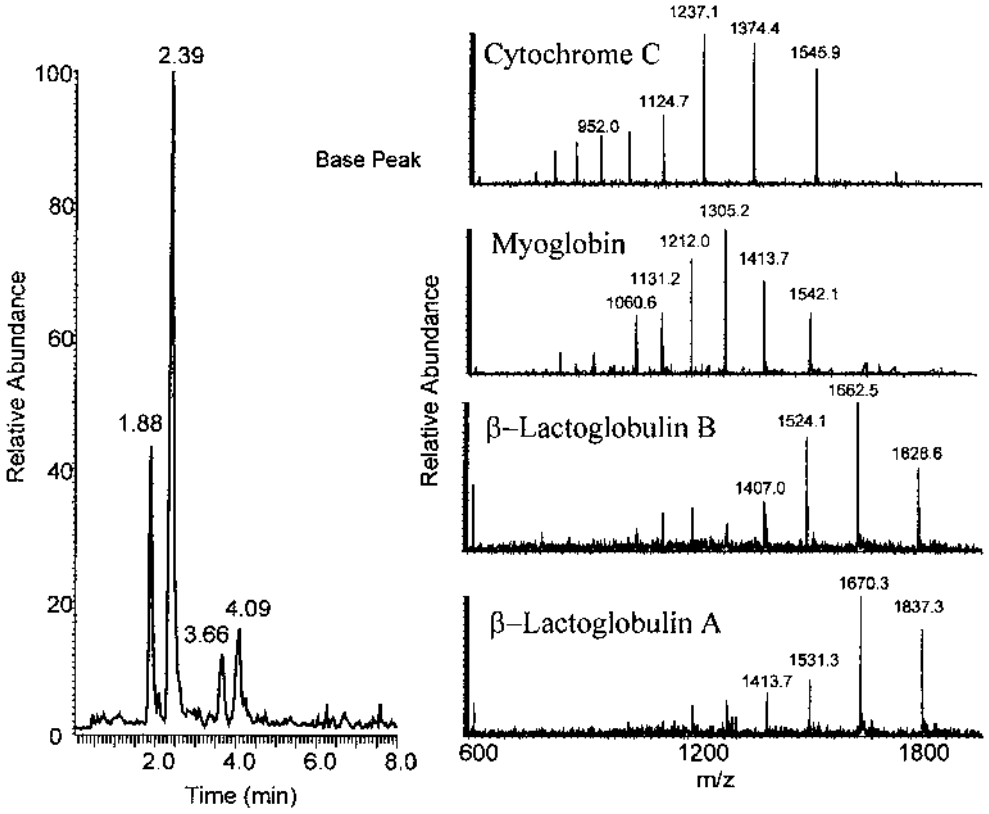

Figure 4. CE/MS analysis of a four-protein mixture using the microdevice in Figure 1. The sample concentration was 2 μM of each protein in 5 mM NH_4Ac/HAc (pH ~4.4). Other experimental conditions as in Figure 3.

Microdevice Design with ESI-MS. Figure 1 presents the design of the system, and Figure 2 shows a photograph of the actual microdevice. A two-step etching procedure was developed in which the separation channel was first etched and protected with a layer of photoresist, followed by microfabrication of a guide channel for the electrospray capillary. The liquid junction (1 mm × 1 mm) was directly cut using a dicing saw. The ends of the junction channel were connected to Teflon tubing, allowing replacement of the BGE or the spray liquid on the microdevice. Since the capillary outer diameter (380 μm) closely matched the size of the guiding channel (400 μm), the tip could be inserted without using any glue to fix its position. The electrospray capillary was inserted into the guiding channel until touching the end of the separation channel. Care was exercised to cleave the end of the electrospray capillary leaving smooth edges without flaking material. No further edge polishing was necessary. The resulting gap between the end of the separation channel and the electrospray capillary was estimated at ~50 μm with a corresponding volume of ~230 pL. It should be noted that since the sample was hydrodynamically focused in the spray fluid, the liquid junction did not significantly contribute to band broadening. A detailed study of the subatmospheric electrospray interface with replaceable ESI tip can be found in ref 28. No liquid leakage around the guide channel was observed during operation. With this design, the electrospray capillary or the microdevice could be easily replaced when broken or blocked. The performance was essentially unchanged upon the change of the electrospray capillary.[28]

It had previously been determined that a flow rate of ~50−200 nL/min provided the most stable electrospray from a 25 μm i.d. capillary.[25,28] To generate the desired flow, we have enclosed the spray end of the electrospray capillary in a chamber maintained at ~78 kPa (~0.77 atm), resulting in a measured flow of 100 nL/min. Dilution of the sample zones was minimized since the spray liquid flow rate was comparable to the volumetric rate of electromigration of the zones (50−150 nL/min).[28]

The channels of the microdevice were coated with either linear polyacrylamide[29] or polyvinyl alcohol (PVA)[30] to minimize adsorption of sample components to the channel wall. Although we used a low-pH BGE, the initial separations obtained in uncoated channels revealed broad tailing peaks for peptides. Moreover, for a variety of protein samples, no peaks could be detected due to significant adsorption on the channel wall. This adsorption is likely related to the fact that the microdevice surface provided a high density of binding sites formed by the release of alkali ions from the glass material. Coating of the electrospray capillary is less important since the sample is transported in the stream of the methanol-containing spray liquid. No surface treatment was used in this study; however, any of the standard capillary coatings could be applied, if necessary.

CE/MS with Electrokinetic Sample Injection. To evaluate the performance of the microdevice in Figure 1, capillary electrophoretic separations of model peptide and protein mixtures were examined. Each sample was injected into the separation channel as a 1 mm long zone (~5 nL) by applying 1 kV for 10 s between the sample well and waste reservoir I in Figure 1. Waste reservoirs II and III, allowing injection of larger sample amounts, were not used in this study. The electropherograms were plotted

(29) Hjerten, S. J. *J. Chromatogr.* **1985**, *347*, 191−195.
(30) Karger, B. L.; Goetzinger, W. U.S. Patent 5,840,388, 1998.

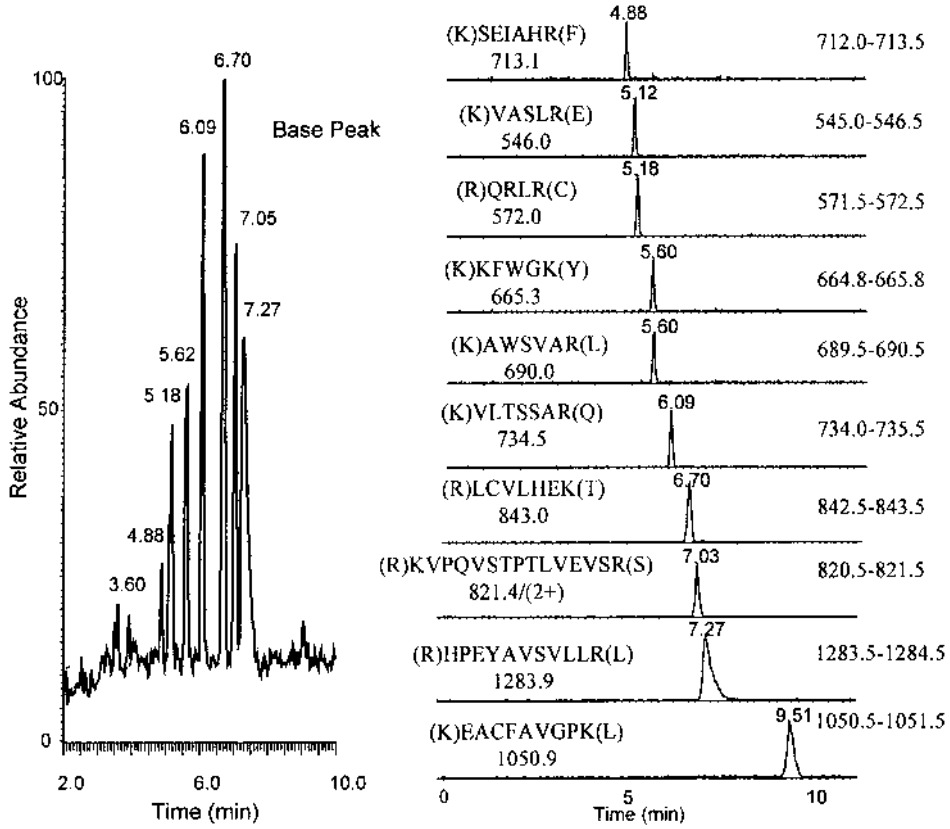

Figure 5. CE/MS analysis of BSA tryptic digest using the microdevice in Figure 1. Electric field strength, 300 V/cm. Other experimental conditions as in Figure 3.

in the base peak mode; i.e., each point in the plot corresponds to the most intense signal in the mass/charge scan. The mass electropherograms and single-scan mass spectra corresponding to the peak maximums of a mixture of angiotensin peptides are presented in Figure 3 and of proteins in Figure 4. Individual components in the mixture could be easily identified according to their corresponding mass-to-charge ratios. The peak widths at half-height in Figure 3 ranged from 3 to 8 s, with separation efficiencies as high as 31 000 total theoretical plates for the 11 cm channel. This efficiency was found to be comparable to that obtained in conventional capillary electrophoresis mass spectrometry under the same conditions, i.e., capillary diameter, length, buffer, and electric field strength. Thus, extracolumn effects in the microstructure design were minimized. The detection limits for the peptides were found to be below 1 μM, corresponding to a mass detection limit in the attomole range for the injection volume of 0.5 nL.

Although the separation channel with two half-turns was used in order to achieve a longer migration distance, no significant band broadening was expected. At the observed separation efficiencies (<100 000), the contribution of the channel curvature to the total band broadening in the CE format is generally assumed to be negligible.[31,32] Hence, the curved channel was not a source of band broadening in this application, as seen in a performance identical to that of a straight capillary in CE/MS.

The mass electropherogram shown in Figure 4 demonstrates the rapid analysis of basic (cytochrome *c*, p*I* 9.3), neutral (myoglobin, p*I* 7.7), and acidic (lactoglobulins, p*I* 5.1) proteins in the glass microdevice with the separation channel coated with linear polyacrylamide. The peak shape clearly shows that the coating effectively screened the surface and minimized the protein adsorption. Both the separation and the quality of the single-scan mass spectra obtained at the peak maximums are comparable to that obtained in standard CE under the same conditions.

Another example, in Figure 5, shows the separation of peptides from a tryptic digest of BSA. Both the base peak and selected ion monitoring of 10 of the tryptic peptide fragments are shown. Database searching[33] allowed easy identification of all of the detected peaks.

Since the separation channel on this microdevice was relatively long (11 cm), good resolution of a number of peaks could be obtained; however, the analysis time was also comparable to that of a standard capillary column of the same length.

One important feature of microfabrication is the ease with which microdevices with a short separation channel can be produced, leading to the potential for fast CE separation. Although the shorter separation distance cannot provide good resolution of sample components with low selectivity, the use of mass spectrometric detection, which in part serves as a second dimension of separation, can compensate for the lower resolution. We have tested a microdevice with the separation channel length of

(31) Wicar, S.; Vilenchik, M.; Belenkii, A.; Cohen, A. S.; Karger, B. L *J. Microcolumn Sep.* **1992**, *4*, 339−348.

(32) Culbertson, C. T.; Jacoson, S. C.; Ramsey J. M. *Anal. Chem.* **1998**, *70*, 3781−3789.

(33) http://www.mann.embl-heidelberg.de/Services/PeptideSearch/FR_peptideSearchForm.htm.

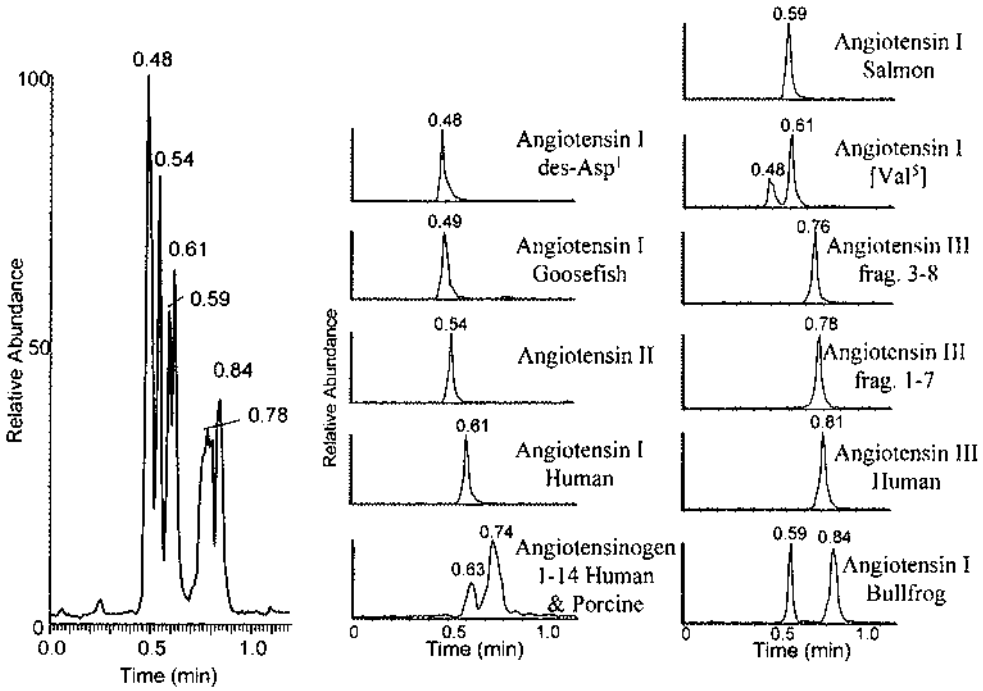

Figure 6. CE/MS separation and identification of a 12-angiotensin peptide mixture on the microdevice with the 4.5 cm separation channel. The sample concentration was 20 μg/mL of each peptide. BGE, 20 mM 6-aminocaproic acid/acetic acid, pH 4.4. Liquid junction solution, 0.8% (v/v) acetic acid in 50% (v/v) methanol/water. Electric field strength, 650 V/cm. Pressure in the electrospray chamber, ~78 kPa. ESI voltage, 2.2 kV. Both the base peak monitoring (left) and selected ion monitoring (right) traces are shown.

4.5 cm for fast CE/ESI-MS separation. Except for the short straight channel, the device was identical to that described in Figure 1. The length of the sample injection plug defined by the double-T injector was 0.6 mm, and an electric field of 650 V/cm was applied.

Figure 6 shows the separation in less than 50 s of a mixture of 12 angiotensin peptides under these conditions. As expected, not all the peaks were baseline resolved; however, all peaks could be readily identified using selected ion monitoring. The observed separation efficiency was in the range of 5000−9000 total theoretical plates for the 4.5 cm column. The contribution of the electrospray capillary transfer time to total analysis time from the microchip to the MS was small (~5 s); if necessary, this time could be further reduced by use of a shorter electrospray capillary. Even higher separation speeds could be attained by increasing the electric field strength. However, the resulting peak width of <1 s would require the use of a mass spectrometer with higher data acquisition rate, such as the time-of-flight instrument.[26]

CE/MS with Pressure Sample Loading and Injection. Most of the CE microdevices currently under development use on-chip electrodes and sample reservoirs. The sample, first loaded on the microdevice at the volume of several microliters, is injected electrokinetically, as above. After analysis, the remaining sample is removed and the reservoir carefully washed before the next analysis. Electrokinetic injection may result in sample bias when the concentrations of the sample matrix ions vary.[34]

In this work, we have tested sample introduction (loading) into a microreservoir inside the microdevice using pressure drop, followed by injection into the separation channel and CE analysis. Instead of the typical electrode reservoirs, short pieces of fused-silica capillary (200 μm i.d., 370 μm o.d. × 15 mm) were fixed to the channels (see Figure 7). After the separation channel was filled with the BGE, the sample (located in an 0.5 mL Eppendorf tube or a microtiter well plate) was siphoned into the reservoir channel, R (5 mm × 200 μm), by applying suction at port 2 for several seconds to a total volume of ~1 μL. In the next step, the sample was injected into the separation channel by suction (or electrokinetically) via ports 3 and 4 (see Figure 7). Three different injected amounts could be selected by filling either section A (4 mm) or B (3 mm) or both (7 mm). After injection, port 1 was inserted into a tube with the BGE, and the sample reservoir channel (R) was washed with the BGE using a short vacuum pulse applied at port 2. The separation voltage was then applied between the liquid junction reservoir and port 1. After each run, the separation buffer was again replaced by pressurizing the liquid junction. The whole cycle of device washing and sample injection could be completed in <1 min. We are currently working on a completely automated system based on the presented design.

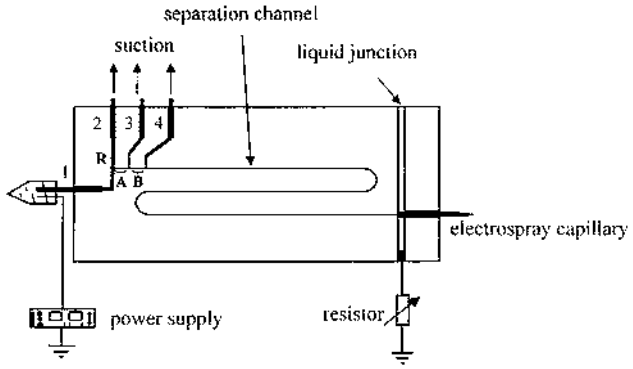

Figure 7. Diagram of the microdevice for pressure sample introduction. See Results and Discussion for details.

(34) Shultz-Lockyear, L. L.; Colyer, C. L.; Fan, Z. H.; Roy, K. I.; Harrison, D. J. *Electrophoresis* **1999**, *20*, 529−538.

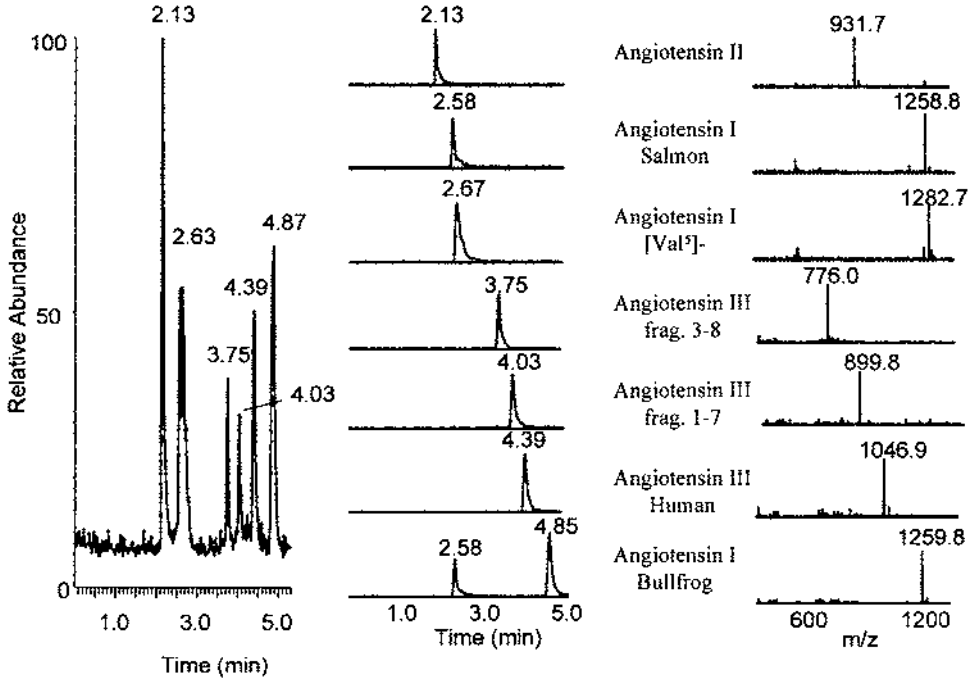

Figure 8. CE separation of a mixture of angiotensin peptides using the system in Figure 7 with pressure sample injection. The sample concentration was 10 μg/mL of each peptide. BGE, 20 mM 6-aminocaproic acid/acetic acid, pH 4.4. Liquid junction solution, 0.8% (v/v) acetic acid in 50% (v/v) methanol/water. Electric field strength, 400 V/cm. ESI voltage, 2 kV. Pressure in the electrospray chamber, ~78 kPa. Base peak monitoring.

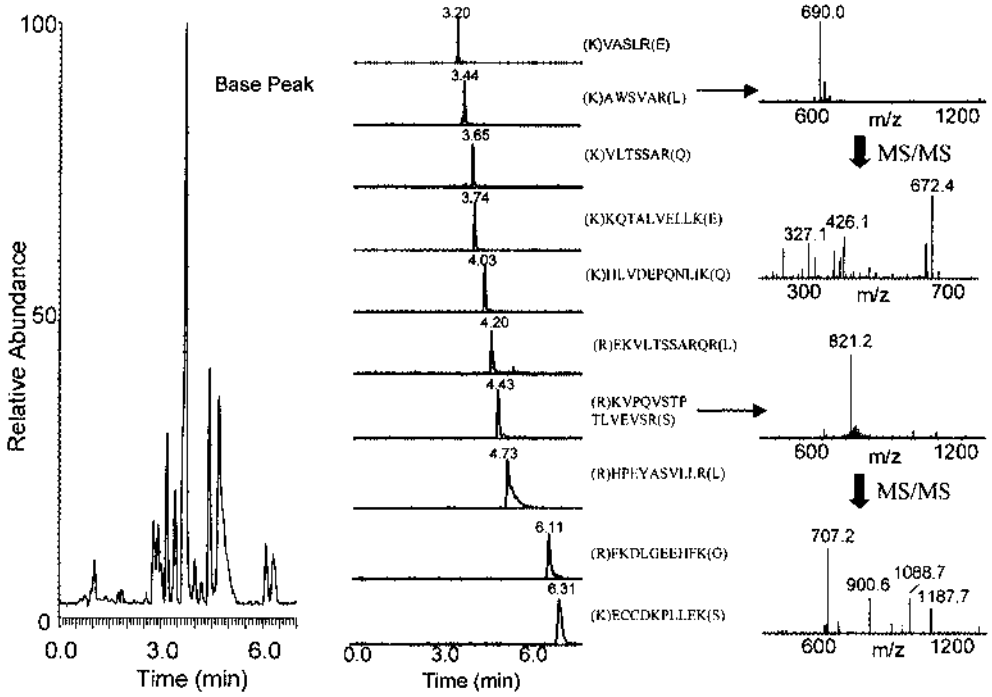

Figure 9. CE separation of BSA tryptic digest on a microdevice with pressure injection. Other conditions as in Figure 8. Base peak monitoring (left), selected ion monitoring (center), and MS/MS spectra of two selected peaks (right) are shown.

The performance of the device was first evaluated again with a mixture of angiotensin peptides. In the experiment, ~14 nL (3 mm sample zone) of sample was pressure injected, resulting in the mass electropherogram shown in Figure 8. As seen in the figure, individual components in the mixture were easily identified according to the corresponding mass-to-charge ratios. A separation efficiency in excess of 20 000 total theoretical plates could be achieved with this design. A similar performance was obtained with electrokinetic injection. Figure 9 presents the separation of the tryptic digest of BSA. In contrast to that shown previously for the microdevice with electrokinetic injection (see Figure 3), the sensitivity in the experiment with pressure injection was 3-fold higher, due to the transient isotachophoretic sample focusing[35] induced by the ammonium ions from the sample buffer. It is also

(35) Foret, F.; Szoko, E.; Karger, B. L. *Electrophoresiss* **1993**, *14*, 417−428.

worth noting that, unlike electrokinetic injection, sample introduction by pressure does not suffer from the bias due to the differences in electrophoretic mobilities of the sample components.[34]

Plate numbers as high as 40 000 were achieved with the limit of detection in the attomole range (concentration of 10^{-7} M). All the peaks were again identified and assigned according to database searching.[33] For selected zones, on-line tandem mass spectrometry (MS/MS) was conducted to facilitate the structure identification of the peptide. Since new sample could be easily loaded onto the microdevice, a miniaturized system for continuous and automatic operation is feasible. Further improvement of the present device, including the full automation of a high-throughput system, is under development.

CONCLUSION

A new generation of microfabricated devices for facile coupling with electrospray mass spectrometry was developed with a miniaturized liquid junction interface. The design integrated the liquid junction into the chip, with the electrospray capillary tip being a part of a miniaturized subatmospheric electrospray interface. The electrospray capillary tip was removable, and no glue was required for coupling it with the microdevice. Importantly, this arrangement is suitable for mass production.

The microdevice was readily implemented for CE/ESI-MS analysis of peptide and protein samples with a limit of detection in the attomole region. High-efficiency and high-resolution separation was achieved on an 11 cm separation channel microdevice. Alternatively, fast separation in less than 50 s was obtained on the microdevice with a short separation channel (4.5 cm). Additionally, pneumatic sample injection modes were developed. Combined with the sensitivity and high efficiency of the microfabricated devices, this design opens up the future potential of fully automated miniaturized high-throughput systems. The microdevice is presently being implemented to process samples automatically from a microtiter well plate.

ACKNOWLEDGMENT

The authors gratefully thank NIH (Grant GM 15847) for support of this research. Contribution No. 775 from the Barnett Institute.

Received for review October 5, 1999. Accepted December 13, 1999.

AC991150Z

Anal. Chem. **2000,** *72,* 3303−3310

Development of Multichannel Devices with an Array of Electrospray Tips for High-Throughput Mass Spectrometry

Hanghui Liu,[†] Chantal Felten, Quifeng Xue,[‡] Bailin Zhang, Paul Jedrzejewski, Barry L. Karger,* and Frantisek Foret*

Barnett Institute and Department of Chemistry, Northeastern University, Boston, Massachusetts 02115

The basic principles of multichannel devices with an array of electrospray tips for high-throughput infusion electrospray ionization mass spectrometry (ESI-MS) have been developed. The prototype plastic devices were fabricated by casting from a solvent-resistant resin. The sample wells on the device were arranged in the format of the standard 96-microtiter well plate, with each sample well connected to an independent electrospray exit port via a microchannel with imbedded electrode. A second plastic plate with distribution microchannels was employed as a cover plate and pressure distributor. Nitrogen gas was used to pressurize individual wells for transport of sample into the electrospray exit port. The design of independent microchannels and electrospray exit ports allowed very high throughput and duty cycle, as well as elimination of any potential sample carryover. The device was placed on a computer-controlled translation stage for precise positioning of the electrospray exit ports in front of the mass spectrometer sampling orifice. High-throughput ESI-MS was demonstrated by analyzing 96 peptide samples in 480 s, corresponding to a potential throughput of 720 samples/h. As a model application, the device was used for the MS determination of inhibition constants of several inhibitors of HIV-1 protease.

The acceleration of drug discovery in recent years has presented significant analytical challenges. The number of compounds to be analyzed has increased dramatically since the introduction of combinatorial chemistry with automated parallel synthesis.[1−4] High-throughput analytical techniques have become critical for determining the identity and purity of synthesized substances,[5] as well as for clinical screening,[6] pharmacokinetics,[7] and proteome-related research.[8]

Most of the current protocols for high-throughput analysis are based on 96 (or larger) microtiter well plate technology where a large number of samples can be processed in parallel. Robotic work stations for such formats are used for sample dispensing and handling. Optical absorbance or fluorescence readers monitor the respective sample/reaction properties directly in the arrays,[9] or flow injection analysis (FIA) systems deliver samples to an external detector for measurement.[10]

Mass spectrometry has become an indispensable tool for pharmaceutical research because of its sensitivity, capability of sample identification, structure elucidation, and quantitation. Electrospray ionization (ESI) and atmospheric pressure chemical ionization (APCI) are the frequently used sample ionization techniques for automated high-throughput MS analysis, often coupled on-line with liquid chromatography (LC) or capillary electrophoresis (CE).[11−14] Nevertheless, a significant portion of ESI-MS applications are also performed in the direct infusion mode.[15] Typically, infusion ESI-MS is carried out with a FIA system equipped with an autosampler. Since every sample flows through the same conduit from the sampling probe through the injection valve to the ESI tip, the sampling probe must be carefully washed and the flow conduit appropriately flushed to minimize sample cross-contamination.[16] Thus, useful mass spectrometric information can be observed only during a fraction of the total analysis time, leading to a low duty cycle.

Recently, microfluidic devices or microchips fabricated on glass, quartz, or plastic substrates have emerged as a means of handling small quantities of samples and achieving high analysis

[†] Present address: Coelacanth Corp., 279 Princeton-Hightstown Rd., East Windsor, NJ 08520.

[‡] Aclara BioSciences, 1288 Pear Ave., Mountain View, CA 94043.

(1) Wilson; S. R.; Czarnik, A. W. *Combinatorial Chemistry: Synthesis and Application*; John Wiley & Sons: New York, 1997.
(2) Gorlach, E.; Richmond, R.; Lewis, I. *Anal. Chem.* **1998**, *70*, 3227−3234.
(3) Czarnik, A. W. *Anal. Chem.* **1998**, *70*, 378A−388A.
(4) Kyranos, J. N.; Hogan, Jr. *J. Chromatogr., A* **1998**, *70*, 388A−395A.
(5) Zeng, L.; Bruton, L.; Yung, K.; Shushan, B.; Kassel, D. B. *J. Chromatogr., A* **1998**, *794*, 3−13.
(6) Van Breemen, R. B.; Huang C. R.; Nikolic D.; Woodbury, C. P.; Zhao, Y. Z.; Venton, D. L. *Anal. Chem.* **1997**, *69*, 2159−2164.
(7) Korfmacher, W. A.; Cox, K. A.; Bryant, M. S.; Veals, J.; Ng, K.; Watkins, R.; Lin, C. C. *DDT* **1997**, *2*, 552−537.
(8) Lottspeich, F. *Angew. Chem., Int. Ed.* **1999**, *38*, 2477−2492.
(9) Ashour, M. B.; Gee, S. J.; Hammock, B. D. *Anal. Biochem* **1987**, *166*, 353−360.
(10) Onnerfjord, P.; Eremin, S. A.; Emneus, J.; Marko-Varga, G. *J Chromatogr., A* **1998**, *800*, 219−230.
(11) Niessen, W. M. A. *J. Chromatogr., A* **1998**, *794*, 407−435.
(12) Dunayevskiy, Y. M.; Vouros, P.; Wintner, E. A.; Shipps, G. W.; Carell, T.; Rebek, J. *Proc. Natl. Acad. Sci. U.S.A.* **1996**, *93*, 6152−6157.
(13) Jiang, L. F.; Moini, M. *Anal. Chem.* **2000**, *72*, 20−24.
(14) Xia, Y. Q.; Whigan, D. B.; Powell, M. L.; Jemal, M. *Rapid Commun. Mass Spectrom.* **2000**, *14*, 105−111.
(15) Chen, S.; Carvey, P. M. *Rapid Commun. Mass Spectrom.* **1999**, *13*, 1980−1984.
(16) Wang, T.; Zeng, L.; Strader, T.; Burton, L.; Kassel, D. B. *Rapid Commun. Mass Spectrom.* **1998**, *12*, 1123−1129.

10.1021/ac000115l CCC: $19.00
Published on Web 05/31/2000

speed.[17,18] In previous work, we,[19] as well as others,[20−22] described the use of such microfluidic devices for generation of electrospray with MS detection. Single- and multiple-channel glass chips were successfully interfaced to ESI-MS for sample infusion,[23] as well as for CE separation.[24−29]

Considering the wide acceptance of the microtiter well plate format in automated analysis and the potentially low cost of plastic devices, a disposable device equipped with an independent electrospray exit port for each sample well represents an attractive alternative to FIA. A device with sample reservoirs positioned in the format of a standard microtiter well plate could be used as the final receiving plate in a parallel sample-processing scheme, such as selective enrichment, affinity capture, and desalting. The advantage of such a device compared to the standard FIA method would be significantly simplified instrumentation, fast switching times for analysis of consecutive samples (high duty cycle), and elimination of sample cross-contamination. Especially, the latter advantage leads to a significantly decreased number of runs required to validate that sample cross-contamination did not occur.

In this work, we have developed a prototype plastic multisprayer device interfaced to ESI-MS. Each of the sample wells was connected by an independent microchannel to a separate sprayer. All samples loaded onto the well plate could be analyzed in rapid sequence without need for injection or washing. When coupled to a quadrupole ion trap mass spectrometer, all 96 sample wells could be scanned in 8 min, corresponding to a throughput as high as 720 samples/h (5 s/sample). Even shorter analysis times could, in principle, be obtained with a fast mass spectrometer, such as time-of-flight instrument. It is important to note that unlike the case of flow injection, a useful signal could be observed practically immediately and as long as needed (e.g., MS/MS) before advancing to the next sample.

EXPERIMENTAL SECTION

Fabrication of the Multisprayer Device. The 96-channel device was fabricated by casting[30,31] from a solvent-resistant polymer resin (EpoFix, EMS, Ft. Washington, PA), as shown in Figure 1. The required patterns of channels and wells (master plates) were first created on rectangular plastic sheets (Lucite S-A-R, Small Parts Inc., Miami Lakes, FL) using a digital drilling machine. Second, the master plates were placed in a plastic box and silicone polymer (Silastic L-RTV silicone rubber kit, Dow Coming Corp., Midland, MI) was cast over the plates. Figure 1A shows the fabrication of the silicone rubber negative with recessed channels of semicircular shape with a diameter of ~300 μm. Figure 1B shows the complete flow diagram of the fabrication of the device (only one of the 96 sample wells is depicted). The silicone negative imprints (c and d in Figure 1B) of the Lucite master plates (a and b) were created, as described above. The master

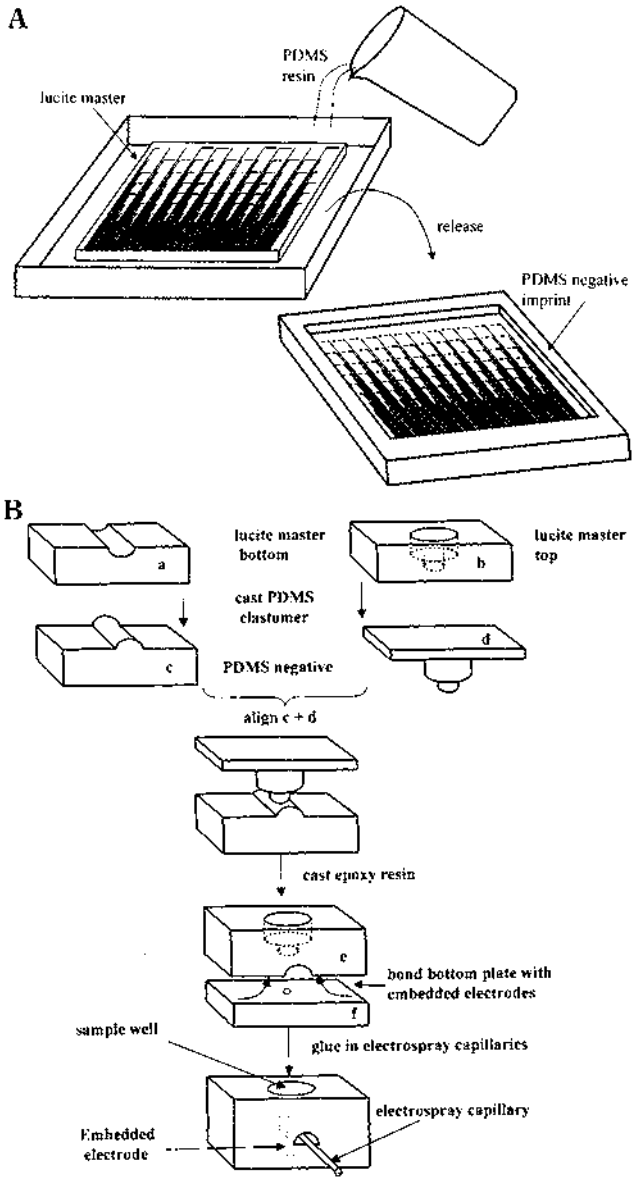

Figure 1. Fabrication of the 96-ESI channel, 96-well device. (A) Preparation of the silicone rubber negative imprint used for epoxy casting. (B) Flowchart of the device fabrication. Lucite master plates (a, b) were used for preparation of the silicone rubber negative imprints (c, d). After alignment, the final well plate (e) and the bottom plate (f) were cast from the epoxy resin (EpoFix). The device was assembled by bonding the bottom plate to the well plate and gluing the electrospray tips. The channels are semicircular with 300 μm diameter and length of 3−10 cm, depending on the location of the respective well on the plate. Not to scale. See Experimental Section for details.

(17) Manz, A.; Harrison, D. J.; Verpoorte, E. M. J.; Fettinger, J. C.; Paulus, A.; Ludi, H.; Widmer, H. M. *J. Chromatogr.* **1992**, *593*, 253−258.
(18) Jacobson, S. C.; Hergenroder, R.; Koutny, L. B.; Warmack, R. J.; Ramsey, J. M. *Anal. Chem.* **1994**, *66*, 1107−1113.
(19) Xue, Q.; Foret, F.; Yuriy, M. D.; Zavracky, P. M.; McGruer, N. E.; Karger, B. L. *Anal. Chem.* **1997**, *69*, 426−430.
(20) Ramsey, J. M.; Ramsey, R. S. *Anal. Chem.* **1997**, *69*, 1174−1178.
(21) Desai, A.; Tai, Y.; Davis, A T.; Lee, T. D. *Transducers'97*, Chicago, IL, 1997; pp 927−930.
(22) Figeys, D.; Ning, Y.; Aebersold, R. *Anal. Chem.* **1997**, *69*, 3153−3160.
(23) Xue, Q. F.; Dunayevskiy, Y. M.; Foret, F.; Karger, B. L. *Rapid Commun. Mass Spectrom.* **1997**, *11*, 1253−1256.
(24) Zhang, B.; Liu, H.; Karger, B. L.; Foret, F. *Anal. Chem.* **1999**, *71*, 3258−3264.
(25) Zhang, B.; Foret, F.; Karger, B. L. *Anal. Chem.* **2000**, *72*, 1015−1022.
(26) Bings, N. H.; Wang, C.; Skinner, C. D.; Colyer, C. L.; Thibault, P.; Harrison, D. J. *Anal. Chem.* **1999**, *71*, 3292−3296.
(27) Li, J. J.; Thibault, P.; Bings, N. H.; Skinner, C. D.; Wang, C.; Colyer, C.; Harrison, J. *Anal. Chem.* **1999**, *71*, 3036−3045.
(28) Wen, J.; Lin, Y.; Xiang, F.; Matson, D. W.; Udseth, H. R.; Smith, R. D. *Electrophoresis* **2000**, *21*, 191−197.
(29) Lazar, I. M.; Ramsey, R. S.; Sundberg, S.; Ramsey, J. M. *Anal. Chem.* **1999**, *71*, 3627−3631.
(30) Verheggen, T. P. E. M.; Everaerts, F. M. *J. Chromatogr.* **1982**, *249*, 221−230.
(31) Foret, F.; Krivankova, L.; Bocek, P. *Capillary Zone Electrophoresis*; VCH: Verlagsgesellschaft, Weinheim, 1993; p 149.

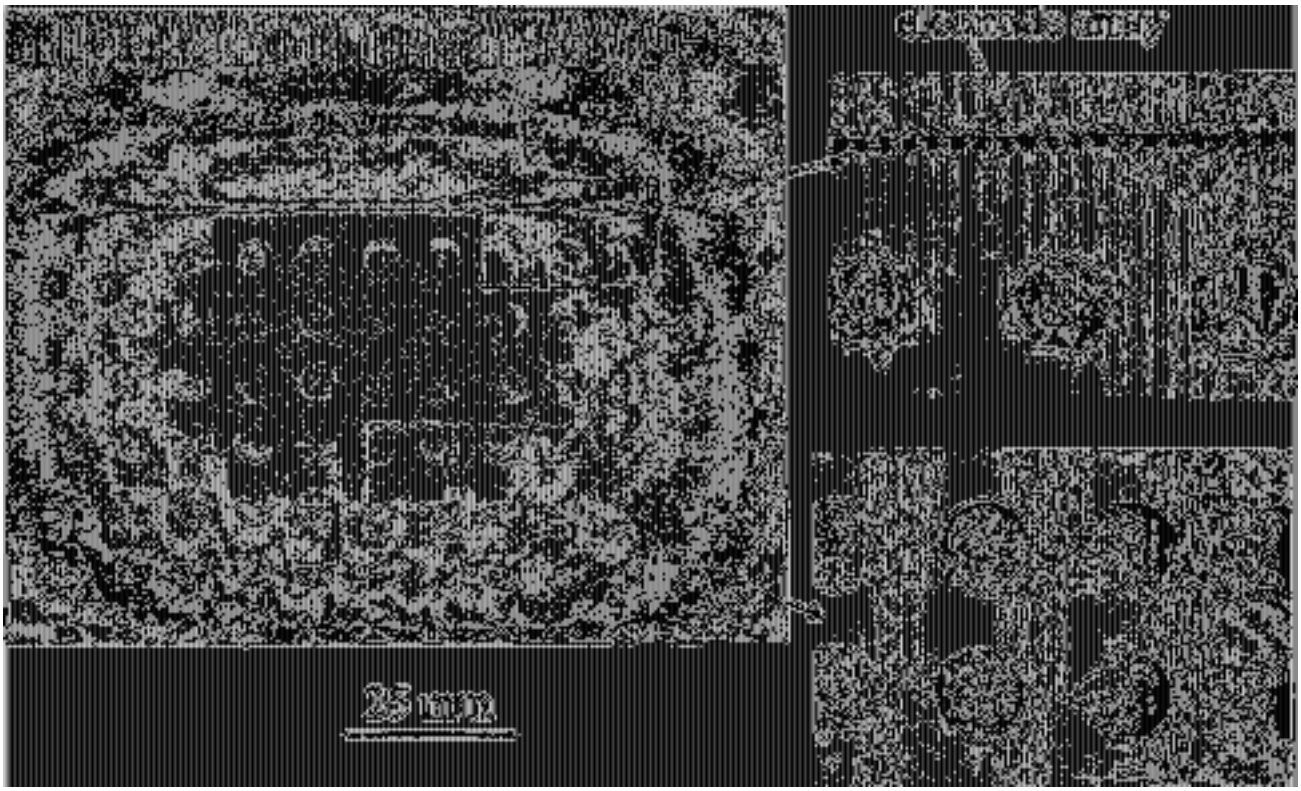

Figure 2. Photograph of the device fabricated from the EpoFix resin with embedded electrodes and attached 96 ESI capillaries (the last row of 12 wells is not visible due to the picture cropping). The expanded sections on the right show the detail of the wells connected to the 300-μm-wide semicircular distribution channels (bottom) and of the array of embedded electrodes for sequential connection of the electrospray high voltage.

plate (a) contained 96 channels with starting points distributed in the standard 96-well plate pattern and ending in an array arrangement at the edge of the plate. The master plate (b) contained 96 wells with 5 mm diameter, 5 mm deep, connected to a 0.5-mm-diameter, 0.5-mm-deep hole in the bottom. In the next step, both rubber imprints (c and d) were aligned to form a cavity, which was then filled with the liquid EpoFix resin. Two other polymeric resins were also tested: Acrylic−polyester-based Casolite AP (AIN Plastics, Mt. Vernon, NY) and epoxy-based Araldite (Fluka, Buchs, Switzerland); however, the EpoFix resin exhibited the best mechanical and chemical resistance properties. After hardening, the EpoFix part (e) was recovered and glued together with a bottom plate (f). The bottom plate, also prepared by casting, had 96 embedded electrodes (0.5 mm in diameter, 1.125 mm center-to-center distance). The electrodes were prepared from electrically conductive epoxy (Epo-Tek 415G, Epoxy Technology, Billerica, MA).

Finally, fused-silica capillaries (2.5 cm in length, 26 μm i.d., 140 μm o.d.) were inserted into the exits of the channels to a depth of 1.5 cm and glued in place. About 1 mm of the polyimide coating at the capillary tips was removed by heat. This procedure produced a 96-well plate with closed channels and embedded electrodes connecting each well with a separate capillary electrospray tip. The dimensions of the final device, shown in Figure 2, were 16 cm $\times$ 10 cm $\times$ 0.9 cm. The details on the left side of this figure show the individual wells with the channels (bottom) and the array of the electrodes embedded into the channels (top) just prior the attachment of the electrospray tips.

Mass Spectrometry. An ion trap mass spectrometer (LCQ, Finnigan MAT, San Jose, CA), operated in the positive ion mode, was used throughout this study. Since the sampling orifice of the instrument was located in a small hemispherical indentation that cannot accommodate the size of the device, an orifice extension was used to overcome the space restriction around the mass spectrometer inlet. The orifice extension was machined from an aluminum rod (2.5 cm long, 8 mm. o.d.) with a 0.35-mm-i.d. channel drilled axially. The extension was connected to the sampling orifice by a 2-cm-long piece of silicone rubber tubing. The signal intensity obtained by electrospraying a standard solution (10^{-6} M myoglobin, 1% (v/v) acetic acid in 50% methanol/water (v/v)) was ~15% lower with the attached sampling orifice extension, and no further improvement was necessary. The MS data were recorded in the mass-to-charge ranges of 800−1400 (protein samples), 400−1200 (peptide samples), and 300−400 (protease inhibitors).

System Design and Operation. The exploded schematic diagram in Figure 3 shows the total system design. During operation, the 96-well/96-ESI tips plate (sample plate) was positioned on a computer-controlled translation stage so that the ESI tips were aligned with the MS sampling orifice extension. The sample plate was then closed by a pressure distribution plate. A thin sheet of silicone rubber with 96 properly positioned holes was placed between the two plates to seal the connection (not shown in Figure 3).

Sequential sample flow through the ESI tips was initiated with the aid of a stationary gas pressure nozzle (200-μm-i.d., 1-mm-

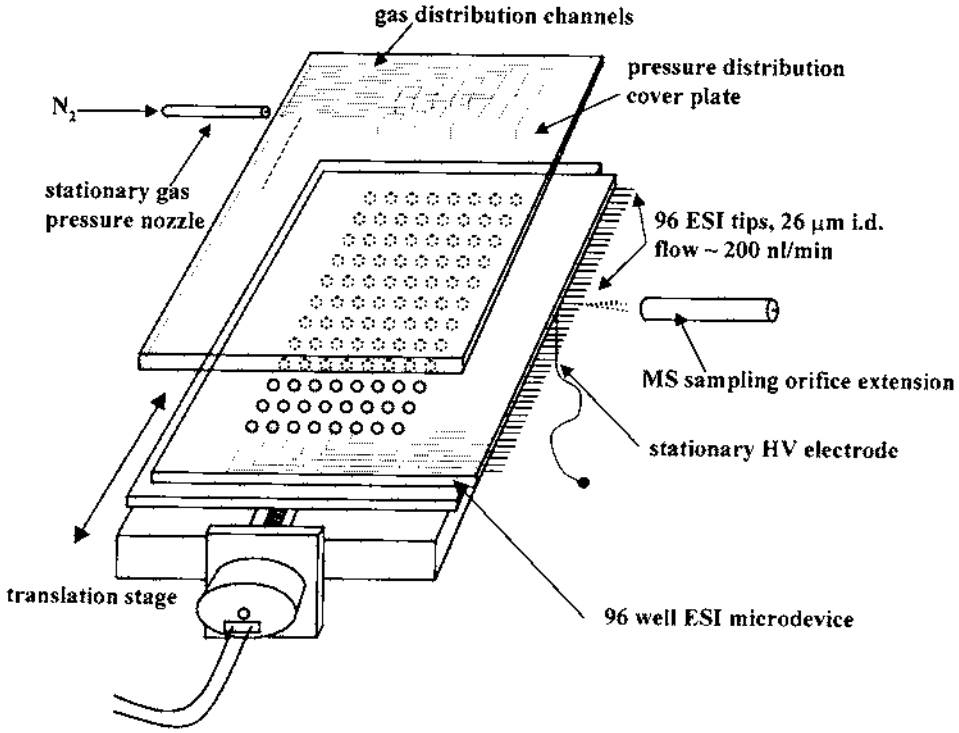

Figure 3. Exploded view of the total system design. The 96-well plate with individual channels and electrospray tips was positioned on a translation stage in front of the extension of the MS sampling orifice. The electrospray analysis of individual samples was activated by sequential pressurization of the sample wells through the pressure distribution cover plate and connection of the ESI high voltage (HV) through the stationary HV electrode positioned under the ESI device. The silicone rubber sealing gasket placed between the ESI device and the pressure distribution cover plate as well as the aluminum clamping plate was omitted for simplicity. See Experimental Section for details.

o.d. Teflon tube) connected to a nitrogen tank. The nozzle contacted the surface of the pressure distribution cover plate so that channels were individually pressurized during the movement of the translation stage. The pressure distribution cover plate, with well and channel patterns as a mirror image of the sample well plate, was made by the same casting procedure as the sample plate. The stationary high-voltage electrode (1-mm-diameter stainless steel wire) was positioned so that the during the movement of the translation stage the high voltage was connected only to the pressurized channel. The high voltage and nitrogen supply were applied during the course of analysis; as the translation stage moved the device to the next position, pressurized gas and high voltage were automatically connected to the respective sample well and channel. An aluminum plate was placed on top of the gas distributor to ensure gastight sealing of all the wells. The linear translation stage (LS3-6-B 10, Del-Tron Precision, Inc., Bethel, CT) was driven by a NEMA 23 step motor controlled by a computer through a motor driver (6006-DB, American Scientific Instrument Corp., Smithtown, NY). A simple computer routine (written in Basic) was used to control the translation stage.

Chemicals. Myoglobin, cytochrome *c*, and angiotensins II and III, purchased from Sigma (St. Louis, MO), were each prepared at a concentration of 1 mg/mL and then diluted to the desired concentration with 0.2% (v/v) acetic acid in 50% (v/v) methanol. Fmoc amino acids and H-val-2-chlorotrityl resin were purchased from Anaspec (San Jose, CA). 1-hydroxybenzotriazol (HOBt), 2-(1*H*-benzotriazole-1,1,3,3-tetramethyluronium) hexafluorophosphate (BBTU), diisopropylethylamine (DIEA), dimethylformamide (DMF), dichloromethane (DCM), potassium cyanide, phenol, ninhydrin, pyridine, and piperidine were obtained from Fluka (Ronkonkoma, NY). HPLC-grade acetonitrile (ACN) and methanol were also from Fluka. HIV-1 protease was obtained from Pharmacia and Upjohn (Kalamazoo, MI), and pepstatin A and *N*-acetyl-Thr-Ile-Nle-ψ-[CH2N]-Nle-Gln-Arg amine (MVT 101) were from Sigma. The organic compounds 158393, 117027, and 32180 were kindly donated by the Drug Synthesis & Chemistry Branch, Development Therapeutics Program, Division of Cancer Treatment, National Cancer Institute (Bethseda, MD). Hack's balanced salt solution (HBSS) was obtained from Parker-Davis. Milli-Q water (Millipore, Medford, MA) was used throughout.

Sample Preparation for HIV-1 Protease Inhibition Assay. An 8-mer peptide substrate (Ser-Gln-Asn-Tyr-Pro-Ile-Val) and a 3-mer peptide internal standard (Glu-Ile-Val) were prepared, following the procedure described in the Anaspec solid-phase synthesis catalog (San Jose, CA). Peptide synthesis was begun from 0.5 mmol of H-val-2-chlorotrityl resin, and coupling was performed by adding 1 mmol of FMOC amino acid in 1 mmol of HBTU/HOBT, 2 mmol of DIEA. The final peptide was then cleaved from the resin with a mixture of acetic acid/trifluoroacetic acid in dichloromethane and precipitated in ice cold ether. HIV-1 protease inhibition was measured by monitoring the concentration of the enzymatic degradation product—Pro-Ile-Val. The total assay volume was 100 μL, containing 50 μg/mL HIV-1 protease, 1 mM substrate, and a defined amount of inhibitor (pepstatin A or MVT 101) in a MES buffer (100 mM MES, 300 mM KCI, 5 mM EDTA, 4.5% (v/v) DMSO, pH 5.5). The solution was incubated at 37 °C for 90 min and then quenched by addition of 10 μL of TFA. Finally, the solution was spiked with 600 μM Glu-Val-Ile, the internal standard.

Aliquots of sample reaction products of 25−50 μL were taken and desalted on a 96-well C_{18} solid-phase extraction (SPE) plate (Varian, Harbor City, CA). The plate was washed with 3 × 200 μL of methanol followed by 3 × 200 μL of water. The sample was introduced on the resin and washed extensively (4 × 300 μL acidified water (10% (v/v) formic acid)). The sample was then eluted from the SPE resin with 3 × 20 μL of 1% (v/v) formic acid in 50% (v/v) ACN/H_2O. The eluate solutions were used for direct infusion or were stored in Eppendorf vials at −15 °C for future analysis.

RESULTS AND DISCUSSION

The aim of this work was to develop a prototype device for high-throughput infusion ESI-MS with the following features: (1) compatibility with the 96 (or higher)-well plate technology; (2) independent electrospray port attached to each of the sample wells to prevent any sample cross-contamination; (3) potential for fully automated operation.

Although current techniques allow microfabrication of very small devices, the compatibility with current technology is an important issue. At present, 96 (384, 1536)-well plates are used for most of the high-throughput sample processing (enrichment, desalting, etc.).[32−34] Thus, we have designed the device as the final receiving plate in the sample-processing scheme to avoid any need for additional pipetting. Hence, the plate can also be used for sample storage and, if produced from an inexpensive plastic material, can be disposable. These requirements led to a design shown in Figures 2 and 3 where all the sample wells were connected by microchannels to an array of independent electrospray tips on the edge of the device. The size of the device was selected to be compatible with the standard microtiter well plates. Since this size is too large for microfabrication using a standard photolithographic technology with wet chemical etching in glass, we have selected construction by casting with polymeric resins for rapid prototyping.[30,31,35,36] The optimum design, suitable for commercial use, could then be produced using injection molding techniques.

In the early stages of this work, we tested several polymeric resins for fabrication of a variety of multichannel devices. Since on-chip fluorescence or absorbance detection was not necessary, the optical properties of the material were not critical; however, the resin could still release impurities (monomers, hardeners, additives, etc.), increasing the MS background and suppressing the analyte signal. During ESI-MS tests with infusion of a myoglobin solution, we found that a device made of Castolite resin generated a strong signal of cluster peaks around m/z 857 that dominated the spectrum and suppressed the protein signal. When the same sample was sprayed from a device made of either Araldite or EpoFix resins, a clean spectrum with strong signal was observed. EpoFix resin was finally selected for fabrication of the 96-well/96-sprayer device due to its superior mechanical properties and ease of use.

Since the diameter of the channels connecting the sample wells with the respective electrospray tips (300 μm) was much larger than the ESI tip inner diameter (26 μm), the channel length (3−10 cm) had an insignificant effect on the sample flow rate. Thus, practically all the flow resistance was due to the capillary tip. After application of gas pressure and high voltage, the electrospray stabilized in 1 s, as observed by monitoring the total ion current. At the start of the run, the first of the 96 tips was aligned with the mass spectrometer sampling orifice, with the remaining tips being sequentially positioned automatically at the orifice by means of the fixed step movement of the stage controlled by the computer.

The device was first tested with an aqueous solution of 10 μg/mL angiotensin II at various pressures (3−40 psi) and voltages (2.5−7 kV), as well as distances between the ESI tip and the MS sampling orifice (1−8 mm). On the basis of signal intensity and stability, 5 psi, 4.5 kV, and 3 mm, respectively, were chosen for all further experiments. Under these conditions, the samples were electrosprayed at a flow rate of ∼200 nL/min, i.e., within the optimum range for the capillary electrospray tip.[37] With the motor and the motor driver used, the minimum time required to move from one channel to the next was 1 s; however, much faster stages would be commercially available, if necessary.

High-Throughput ESI-MS Infusion Analysis. To demonstrate the high-throughput capability of the system, several sample solutions were alternately deposited in the microtiter wells and then analyzed sequentially and automatically. The spectra of cytochrome *c* and myoglobin from EIGHT consecutive channels are shown in Figure 4A. Strong signals with well-defined envelopes of the multiply charged protein ions were obtained every 5 s for each consecutive sample. Since fine electrospray capillary tips were used, the electrospray stabilized practically instantly, and no sample cross-contamination was observed.

In a similar experiment shown in Figure 4B, angiotensins II and III were electrosprayed in 8 min from all 96 wells, with singly charged ions of the two peptides being observed. The data demonstrate the validity of the approach to high-throughput infusion analysis where all the samples loaded on the plate can be analyzed in a rapid sequence. Although several channels were blocked during the manual gluing of the device, it can be expected that this would be completely eliminated with improved protocol. Further simplification may also be expected by using a microfabricated array of sprayers instead of individual capillaries[38,39] or microfabrication of the whole device in one piece. It is also worth noting that even higher throughput could be achieved with the use of a time-of-flight, instead of an ion trap, mass spectrometer. Although, a lower limit of detection test was not included in this study, it is reasonable to expect the sensitivity to be equal to that achieved with a single sprayer under the same conditions (tip dimension, sample flow rate, ESI voltage). At a flow rate of 200 nL/min, the sample consumption will be minimal even after extended data accumulation (minutes or more) and the unused

(32) Berry, C. O.; Kauvar, L. M. *Biotechniques* **1993**, *14*, 340.
(33) Krakowski, K.; Bunville, J.; Seto, J.; Baskin, D.; Seto, D. *Nucleic Acids Res.* **1995**, *23*, 4930−1.
(34) Felleisen, R.; Zimmermann, V.; Gottstein, B.; Muller, N. *Biotechniques* **1996**, *20*, 616−20.
(35) Qin, D.; Xia, Y.; Whitesides, G. M. *Adv. Mater.* **1996**, *8*, 917−919.
(36) McDonald, J. C.; Duffy, D. C.; Anderson, J. R.; Chiu, D. T.; Wu, H.; Schueller, O. J. A.; Whitesides, G. M. *Electrophoresis* **2000**, *21*, 27−40.
(37) Bateman, K. P.; White, R. L.; Thibault, P. *Rapid Commun. Mass Spectrom.* **1997**, 11, 307−315.
(38) Schultz, G. A.; Corso, T. N. *The 47th ASMS Conf. Mass Spectrom. Allied Topics*, Dallas, TX, 1999; ThOE 3:40.
(39) Licklider, L.; Wang, X.; Desai, A.; Tai, Y.; Lee, T. *Anal. Chem.* **2000**, *72*, 367−375.

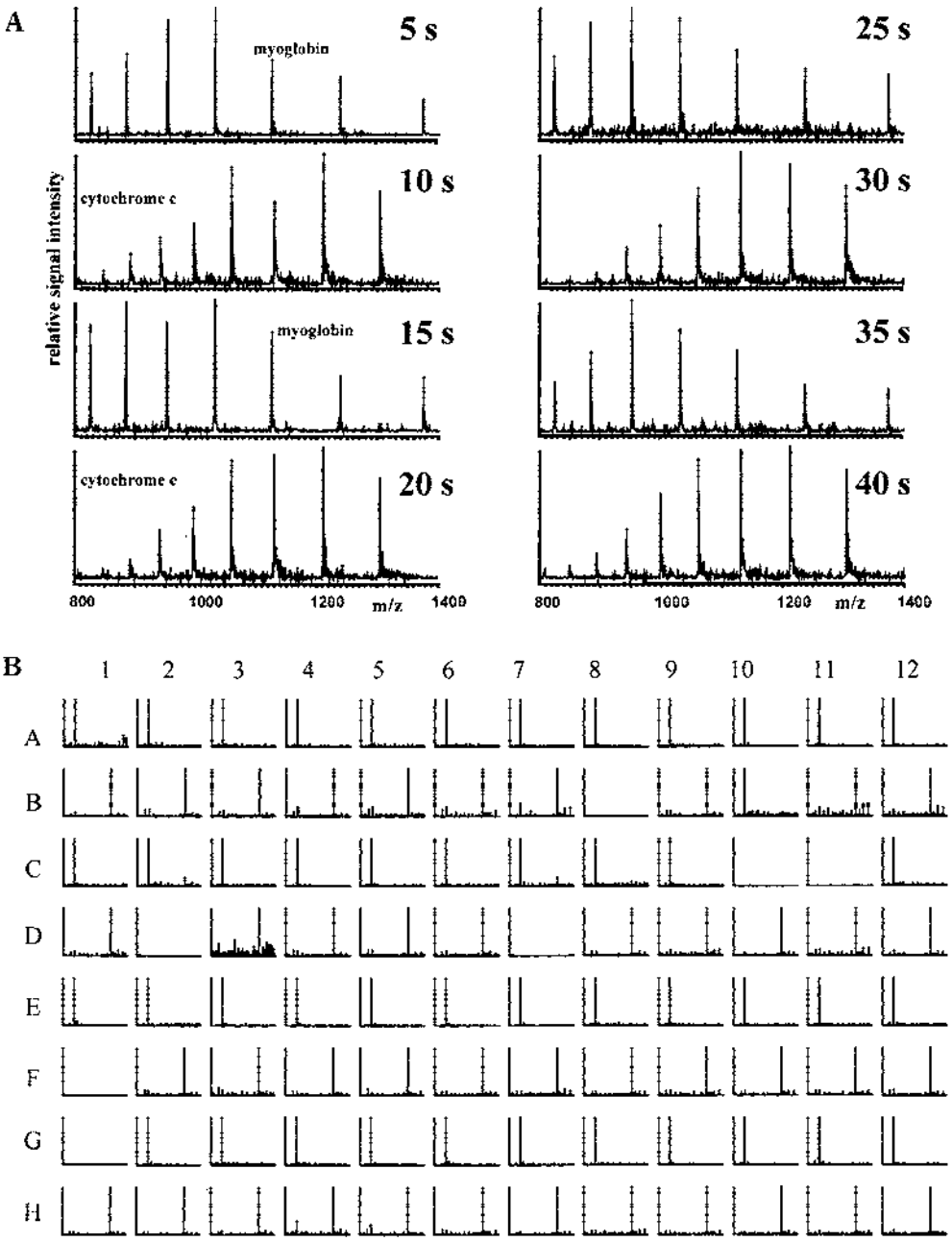

Figure 4. High-throughput ESI-MS analysis using the plastic microwell plate with 96 electrospray tips. (A) cytochrome *c* and myoglobin solutions (5 μL) were alternately loaded into consecutive sample wells, and each well was analyzed every 5 s over a 40-s time period. The concentrations for both proteins were 0.1 mg/mL. (B) angiotensin II and angiotensin III solutions (5 μL) were alternately loaded into the sample wells, and all 96 samples were analyzed as in (A). Concentrations of both peptides were 10 μg/mL.

samples may be used for additional studies, e.g., enzymatic digestion.

Besides higher throughput, the current device design has additional advantages compared to the ESI-MS analysis performed in the FIA mode. In the latter, the MS signal can be observed for only a limited time, as a result of the fixed injected sample volume and flow rate. In the present system, the signal can be observed almost immediately and as long as desired, allowing a short time to acquire strong signals or a longer time to acquire weak signals of lower concentration samples. Of course, the analysis may be programmed in such a way that the next sample would be analyzed only after sufficient information, e.g., MS, MS/MS, is obtained. Switching to the next sample is not accompanied by any delays related to the system washing and sample injection. Furthermore, the sample amount consumed can be maintained small (~15 nL or 150 fmol in examples shown in the Figure 4). Moreover, if necessary, practically all the sample deposited in the sample wells can reach the ESI tip and generate useful signal. This would be important with very low concentrated samples or when MS/MS analysis were necessary. In this respect, the device can be viewed as an array of independent nanoelectrosprays allowing extended MS/MS analyses. Since a separate channel and

ESI capillary is used for each channel, there is no danger of sample cross-contamination or carryover, which is always a concern in serial flow injection systems.

HIV-1 Protease Inhibition Assay and IC_{50} Determination. As an illustration of the use of the infusion device, we selected to examine the in vitro inhibition of HIV-1 protease The IC_{50} values (the concentration of an inhibitor necessary to inhibit the enzyme reaction by 50%) were compared with the published data.[40−42] The preparation of a series of samples with increasing concentration of the HIV-1 inhibitor (pepstatin A) was described in detail in the Experimental Section. Prior to ESI-MS analysis, 25-μL sample aliquots were desalted on a 96-well C_{18} SPE plate. The substrate and standard, with no HIV-1 protease added, were also analyzed by direct infusion ESI-MS. No side product formation was observed, except Ser-Gln-Asn-Tyr(*tert*-butyl)-Pro-Ile-Val (MW 875), which was expected from the substrate synthesis. This side product, however, had no influence in the present study since the m/z value was far removed from the internal standard (MW 359) and the enzymatically formed tripeptide Pro-Ile-Val (MW 327).[43] Figure 5A presents selected ion monitoring (SIM) mass spectra with increasing amounts of inhibitor (pepstatin A), and the corresponding data are plotted in Figure 5B. Inhibition by another peptidomimetic inhibitor *N*-acetyl-Thr-Ile-Nle-ø-[CH_2N]-Nle-Gln-Arg amine, MVT 101) and some other small organic molecules were also studied, and the IC_{50} obtained are listed in Table 1. The experimental IC_{50} value of pepstatin A and the K_i value of MVT 101 were in agreement with those found in the literature[44,45] within the experimental error, typical for this type of analyses (~20%, or more). Since more than 10 MS scans must typically be averaged to obtain a reliable quantitative information, each measurement shown in Figure 5 took ~30 s (10−30 scans averaged). An order of magnitude higher throughput could be obtained with a faster time-of-flight MS instrument. Nevertheless, the model application demonstrates the potential of automated analysis with the present device design.

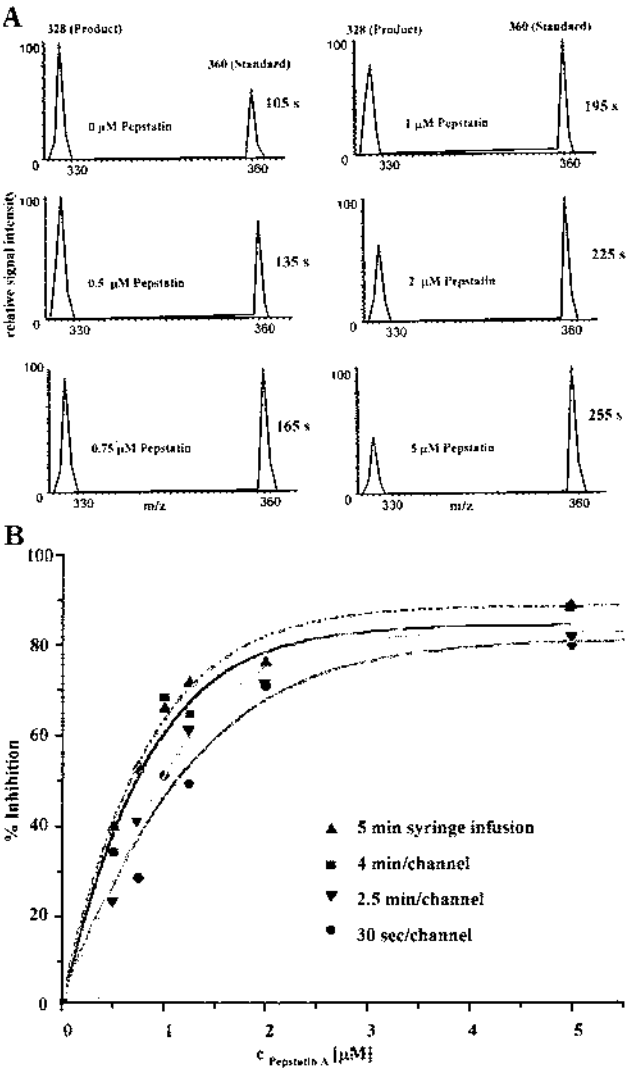

Figure 5. MS determination of HIV-1 protease inhibition using the device. (A) Relative signals of SIM spectra of the product tripeptide (Pro-Ile-Val, $m/z = 328 \pm 4$) and the internal standard (Glu-Ile-Val, $m/z = 360 \pm 4$) after incubation with increasing concentrations of pepstatin A (0−5 μM). (B) Plot of the data extracted from (A); the IC_{50} was determined to be 0.75 μM with an RSD of 13%.

Table 1. IC_{50} Values of Investigated HIV-1 Protease Inhibitors[a]

inhibitor	inhibitor concn range (μM)	IC_{50} (μM) this work	IC_{50} (μM) refs 4 and 45
pepstatin A	0−5	0.75	0.55
MVT 101	0−10	0.65	0.8
compd 117027	0−12.5	9.5	
compd 15839**3**	0−40	6	
compd 32180	0−30	24	

[a] Assay conditions: 5 μL of 1 mg/mL HIV-1 protease in a 100-μL total assay volume, incubation for 90 min at 37 °C.

CONCLUSIONS

This work presents design principles of a disposable device for high-throughput ESI-MS analysis. The dimensions of the described device were selected to be compatible with the current standard sizes of the microtiter well plates; however, devices with much smaller dimensions can easily be microfabricated, if needed. Since each sample is restricted to its independent fluid path, sample cross-contamination and/or carryover is eliminated. This can significantly simplify the validation of new analytical protocols since the tests for carryover are not necessary. The multichannel device can be viewed as a logical extension of the microtiter well plate technology. All 96 (384, 1536, ...) samples deposited in the microtiter well plate could, in principle, be automatically processed (e.g., incubation, desalting, solid-phase extraction, and affinity capture) in parallel and finally deposited into the microfabricated device with electrospray tips for rapid sequential MS analysis. By combining parallel off-line SPE sample preparation with the multichannel device-based ESI-MS, sensitive and high-throughput quantitation could be realized (low ng/μL, sample/5 s, RSD 13%).

(40) Tomasselli, A. G.; Heinrikson, R. L. *Methods Enzymol* **1994**, *241*, 279−301.
(41) Vacca, J. P. *Methods Enzymol* **1994**, *241*, 311−334.
(42) Kempf, D. J. *Methods Enzymol* **1994**, *241*, 334−354.
(43) Wu, J.; Takayama, S.; Wong, C. H.; Siuzdak, G. *Chem. Biol.* **1997**, *4*, 653−657.
(44) Miller, M.; Schneider, J.; Sathyanarayana, B. K.; Toth, M. V.; Marshall, G. R.; Clawson, L.; Selk, L.; Kent, S. B.; Wlodawer, A. *Science* **1989**, *246*, 1149−1152.
(45) Richards, A. D.; Roberts, R.; Dunn, B. M.; Graves, M. C.; Kay, J. *FEBS Lett.* **1989**, *247*, 113−117.

The device was designed as a disposable counterpart of the standard microtiter well plate and should be a good design strategy in situations where throughput is a key factor, such as compound confirmation and purity estimation of combinatorial libraries, pharmacokinetics studies, and substance aging testing. Arranging ESI tips in a two-dimensional array could further increase the channel density without increasing the size of the device.

ACKNOWLEDGMENT

The authors gratefully acknowledge NIH Grant GM 15847 for support of this work. We also thank Dr. Jill I. Johnson from the Drug Synthesis & Chemistry Branch of the National Cancer Institute for the kind donation of the HIV protease inhibitors 158393, 117027, and 32180. Publication 778 from the Barnett Institute.

Received for review February 3, 2000. Accepted April 18, 2000.

AC000115L

Anal. Chem. **2001,** *73,* 2675−2681

High-Throughput Microfabricated CE/ESI-MS: Automated Sampling from a Microwell Plate

Bailin Zhang,† Frantisek Foret,* and Barry L. Karger*

Barnett Institute and Department of Chemistry, Northeastern University, Boston, Massachusetts 02115

A new design for high-throughput microfabricated capillary electrophoresis/electrospray mass spectrometry (CE/ESI-MS) with automated sampling from a microwell plate is presented. The approach combines a sample-loading port, a separation channel, and a liquid junction, the latter for coupling the device to the MS with a miniaturized subatmospheric electrospray interface. The microdevice was attached to a polycarbonate manifold with external electrode reservoirs equipped for electrokinetic and pressure-fluid control. A computer-activated electropneumatic distributor was used for both sample loading from the microwell plate and washing of channels after each run. Removal of the electrodes and sample reservoirs from the microdevice structure significantly simplified the chip design and eliminated the need both for drilling access holes and for sample/buffer reservoirs. The external manifold also allowed the use of relatively large reservoirs that are necessary for extended time operation of the system. Initial results using this microfabricated system for the automated CE/ESI-MS analysis of peptides and protein digests are presented.

The rapid identification and characterization of large numbers of compounds (protein digests, combinatorial libraries, etc.) are major needs in the postgenome era. Mass spectrometry (MS) plays a key role in this area of structure analysis, and critical to the success of this approach is sample handling prior to MS analysis. Microfluidic devices for MS analysis have been of recent interest because they have the potential to meet the increased requirements in handling very small sample volumes without dead volume connections.[1−14] Short separation channels on the microdevices also provide potential for fast separations. Furthermore, the small size of the device significantly reduces the footprint of the instrumentation, which leads to the potential of high-density parallel processing for high-throughput analysis.

The coupling of a microchip to MS using electrospray ionization was initially demonstrated for infusion analysis using a flat-edged surface.[1−3] More recent reports have demonstrated improved performance with electrospray ESI emitter tips, through the attachment of such tips to the device.[4−11] In the latter case, the guiding channel for the capillary ESI tip was created either by a double-etching procedure,[4,5] polymer casting[6] or hand drilling.[7,8] Highly efficient on-chip CE/ESI-MS separations using external capillary ESI tips have been demonstrated.[4,5,7,8] Some attempts have also been made to microfabricate the ESI tips;[12,13] however, these devices were designed only for infusion analysis.

Although current reports have clearly shown high performance CE/ESI-MS analyses, the practical application of the microdevices has been limited. After the analysis, the devices developed to-date have to be either discarded or manually cleaned before the next sample. In addition, many of the current protocols for high-throughput sample processing are based on microwell plate technology, (e.g., digestion, preconcentration, desalting, etc.). Transfer of the individual samples onto the current microdevices generally requires an additional manual pipetting step.

In the present work, an improved microdevice design for high-throughput MS analysis is introduced. The design strategy is based on maximizing the duty cycle of the analysis, while minimizing unnecessary sample transfer steps. In previous work, we demonstrated high-throughput infusion MS analysis using an automated microwell-plate-positioning system close to the mass spectrometer.[15] Both single capillaries and capillary arrays were used for the analysis of samples infused directly from the microwell plate into an ESI-ion trap[15] or a MALDI-TOF mass spectrometer.[16] To minimize the path length for liquid flow, the sample microwell plate was oriented vertically on a motorized

* To whom correspondence should be addressed.
† Present address: ArQule, Inc., Woburn, MA, 01801.

(1) Xue, Q.; Foret, F.; Dunayevskiy, Y. M.; Zavracky, P. M.; McGruer, N. E.; Karger, B. L. *Anal. Chem.* **1997**, *69*, 426−430.
(2) Ramsey, R. S.; Ramsey, J. M. *Anal. Chem.* **1997**, *69*, 1174−1178.
(3) Xue, Q.; Foret, F.; Dunayevskiy, Y. M.; Foret, F.; Karger, B. L. *Rapid Commun. Mass Spectrom.* **1997**, *11*, 1253−1256.
(4) Zhang, B.; Liu, H.; Karger, B. L.; Foret, F. *Anal. Chem.* **1999**, *71*, 3258−3264.
(5) Zhang, B.; Foret, F.; Karger, B. L. *Anal. Chem.* **2000**, *72*, 1015−1022.
(6) Liu, H.; Felten, C.; Xue, Q.; Zhang, B.; Jedrzejewski, P.; Karger, B. L.; Foret, F. *Anal. Chem.* **2000**, *72*, 3303−3310.
(7) Li, J.; Thibault, P.; Bings, N. H.; Skinner, C. D.; Wang, C.; Colyer, C.; Harrison, D. J. *Anal. Chem.* **1999**, *71*, 3036−3045.
(8) Bings, N. H.; Wang, C.; Skinner, C. D.; Colyer, C. L.; Thibault, P.; Harrison, J. D. *Anal. Chem.* **1999**, *71*, 3292−3296.
(9) Lazar, I. M.; Ramsey, R. S.; Sundberg, S.; Ramsey, J. M. *Anal. Chem.* **1999**, *71*, 3627−3631.
(10) Figeys, D.; Van Oostveen, I.; Ducret, A.; Aebersold, R. *Anal. Chem.* **1996**, *68*, 1822−1828.
(11) Figeys, D.; Aebersold, R. *Anal. Chem.* **1998**, *70*, 3721−3727.
(12) Licklider, L.; Wang, X.; Desai, A.; Tai, Y.; Lee, T. *Anal. Chem.* **2000**, *72*, 367−375.
(13) Schultz, A.; Corso, T. N.; Prosser, S. J.; Zhang, S. *Anal. Chem.* **2000**, *72*, 4058−4063.
(14) Wen, J.; Lin, Y.; Xiang, F.; Matson, D. W.; Udseth, H. R.; Smith, R. D. *Electrophoresis* **2000**, *21*, 191−197.
(15) Felten, C.; Foret, F.; Minárik, M.; Karger, B. L. *Anal. Chem.* **2001**, *73*, 1449−1454.
(16) Hu, P.; Rejtar, T.; Preisler, J.; Foret, F.; Karger, B. L. 48th ASMS Conference on Mass Spectrometry and Allied Topics, Long Beach, CA, 2000.

10.1021/ac001432v CCC: $20.00
Published on Web 04/28/2001

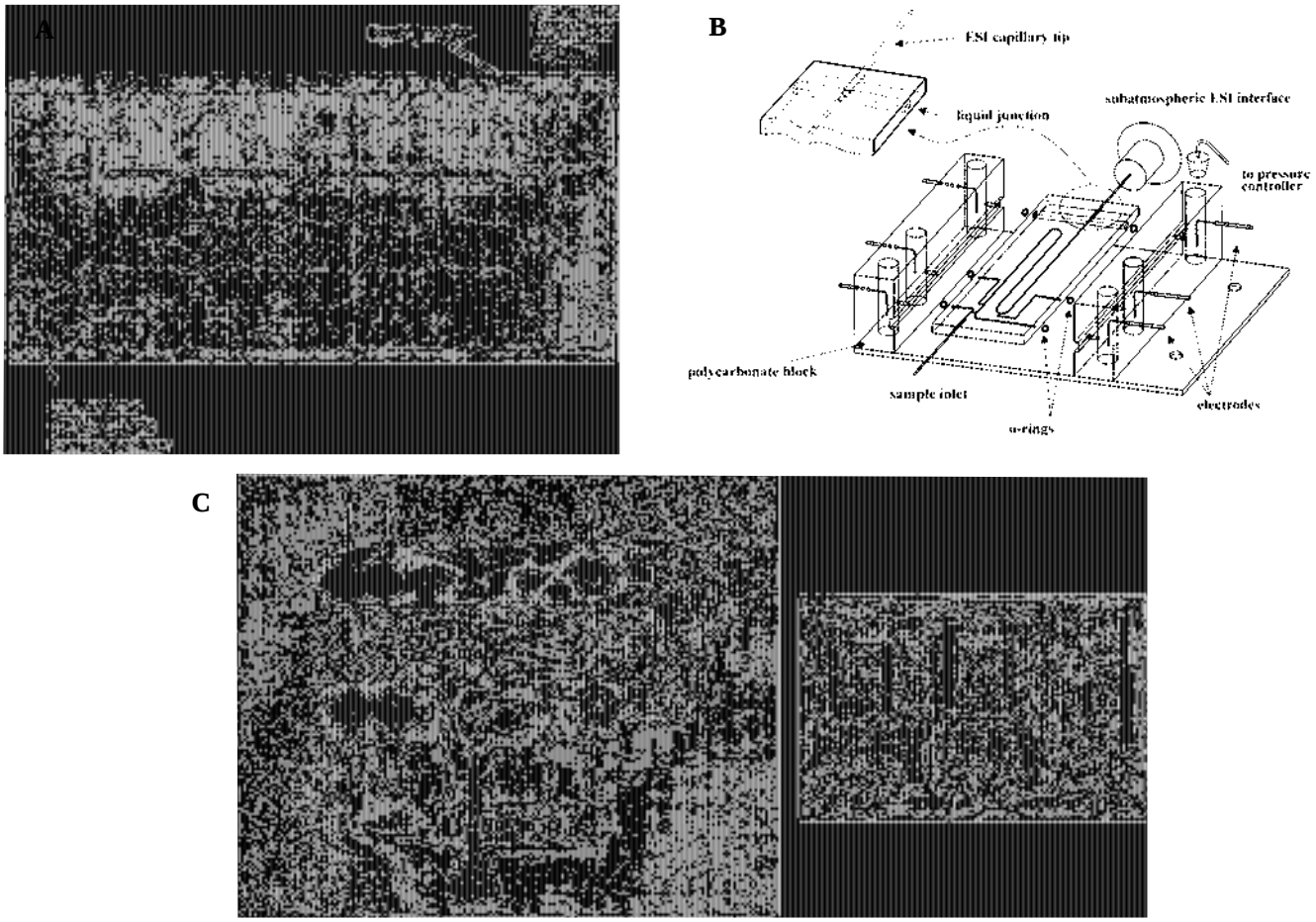

Figure 1. (A) Photograph of the glass chip (5 × 2 cm) used in the system. (B) Diagram of the microdevice design, including the microchip and polycarbonate manifold. (C) Photograph of the microdevice attached to the polycarbonate manifold and subatmospheric ESI chamber. Also shown is a photograph of the pneumatic controller used for sample loading and washing of the microchip.

translation stage. For sample injection, the microwell plate was moved to the stationary sampling capillary or capillary array so that the sample from the desired well was aspirated for analysis.

In this work, we substituted a microdevice with CE separation capability for the above infusion capillary. The microdevice was designed with a polycarbonate device holder that is capable of pneumatic sample manipulation for the automated transfer of samples from the microwell plate onto the microdevice. The holder integrates the microdevice, which contains a sample introduction loop, separation channel, and liquid junction, with an external subatmospheric ESI interface and a manifold of electrode reservoirs. The external pneumatic control system allows direct sample loading from the microwell plate, followed by rapid separation and MS analysis. Both electrokinetic and hydraulic fluid control can be employed, thus allowing use of surface-modified separation channels (to minimize adsorption) without electroosmotic flow and eliminating sample injection bias.[17] In this paper, we present initial results with the system for the CE/ESI-MS analysis of standard peptides as well as protein digests.

EXPERIMENTAL SECTION

Microdevice Fabrication and Instrument Design. The microdevice (Figure 1A) was fabricated using standard photolithographic/wet chemical etching techniques, as described previously.[4,5] The circular separation channel, 75-μm i.d., was 11 cm long, and the loop defining the length of the sample plug was 1.5 mm (sample volume 6.6 nL) long. The liquid junction was cut by a dicing saw as a rectangular channel (1 × 1 mm). The guiding channels for the ESI tip, sample-loading capillary, and outlets on the edge of the microdevice were etched to a circular diameter of 390 μm. The electrospray tip (25-μm i.d., 375-μm o.d., and 3 cm long) was inserted into the guiding hole until it gently touched the end of the separation channel. The tightness of the fit meant that glue did not have to be applied to fix the ESI tip in the hole. Care was exercised to cleave the end of the electrospray capillary to obtain smooth edges without flaking. The gap between the end of the separation channel and the electrospray capillary was measured to be <50 μm. At the sample inlet side, a capillary (200-μm i.d., 375-μm o.d. and 1.5 cm long) was inserted into the guiding channel. In contrast to the ESI tip, which was permanently fixed to the subatmospheric interface, the sample-loading capillary was not attached to any support, and therefore, for robustness, the position of the capillary was made secure by a drop of silicon sealant. The internal volume of the sample-loading capillary (500 nL) represents the sample volume aspirated from the microwell plate for the analysis. The walls of all of the channels inside the microdevice were coated with linear polyacrylamide (LPA)[18] to prevent adsorption and to minimize electroosmotic bulk flow.

(17) Schultz, L. L.; Colyer, C. L.; Fan, Z. H.; Roy, K. I.; Harrison, D. J. *Electrophoresis* **1999**, *20*, 529−538.

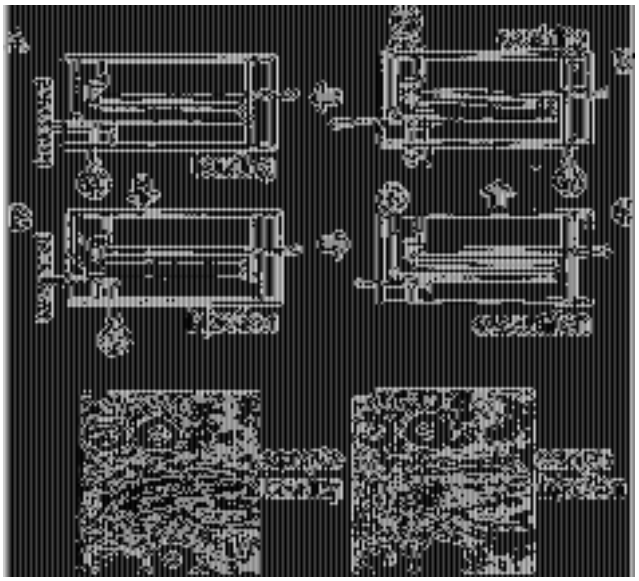

Figure 2. Steps of the operation cycle of the microdevice: A, loading; B, injection; C, separation; D, washing. V, vacuum; P, pressure; +, separation voltage. The colored photographs visualize the sample-loading and injection steps using a solution of methyl green dye.

The glass chip was sandwiched between two electrode reservoir manifolds (12.5 × 23 × 60 mm) machined from polycarbonate (see Figure 1B). A stable, leak-free connection between the chip and the manifold was achieved using miniaturized O-rings (0.38 × 2.36 mm; Apple Rubber Products, Inc.; Lancaster, NY). The O-rings were secured in the chip-positioning groove of the manifold, and the whole chip-manifold assembly was held together by a polyamide screw (see Figure 1C). Each electrode reservoir contained a platinum electrode and a luer connector (Small Parts; Miami Lakes, FL) for connection of the high voltage and gas pressure, respectively. High voltage for electrophoresis was supplied by a CZE 1000 power supply (Spellman; Plain View, NY). A previously described optically controlled resistor 4 connected between ground and the liquid junction reservoir was used to fix the potential of the electrospray capillary at 2 kV. A miniaturized subatmospheric ESI interface 5 was employed to couple the microdevice to the mass spectrometer. The pressure in the ESI chamber was maintained at ~78 kPa, which resulted in a flow of 100 nL/min for efficient ESI.

A laboratory-built pressure control system was utilized for pneumatic sample manipulation (see photograph, Figure 1C). The system incorporated two miniature membrane pumps (Ohlheiser; Newington, CT) and 6 pneumatic switches (SMC; Indianapolis, IN) to control 3 ports for pressure application and 3 ports for vacuum application. The pressure range was ± 13 psi. The system was controlled either manually by switches or by a computer equipped with a digital output port (5V TTL signal) via a program written in LabView (National Instruments; Austin, TX).

A 96-well sample microwell plate with v-shaped bottom was placed vertically in a plastic holder mounted on the *x-y-z* translation stage in front of the microdevice. A laboratory-built computer-operated *x-y-z* translation stage was used to control the movement of the sample microwell plate. The stage was assembled from

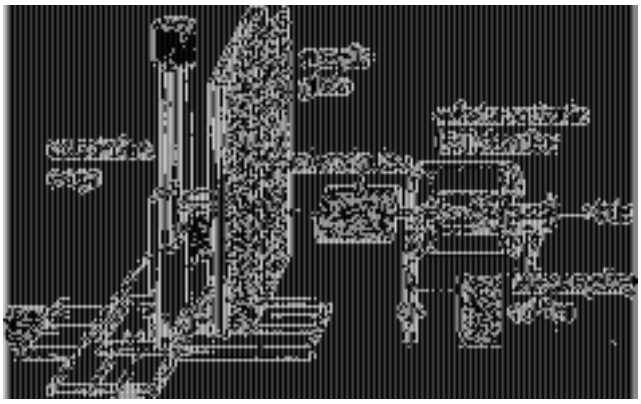

Figure 3. Overall design of the coupling of the microwell plate sample delivery system equipped with a microdevice for high-throughput separation-MS analysis.

three individual Posidrive stages (Deltron; Bethel, CT) connected to NEMA (National Electrical Manufacturers Association) size 23 stepper motors (AMSI Corp.; Smithtown, NY) by high-speed drivers for the stepper motors (AMSI Corp). The stepper motors were controlled by TTL signals from a digital output port (National Instruments) through a software program written in LabView. The stage could directly move to a specific position or perform a sequence of preset movements. The maximum translation speed with the motors was 10 mm/sec (1600 steps/sec).

System Operation. Figure 2 shows the analysis cycle of the microdevice, including sample loading, injection, separation, and washing. The analysis began with loading of the sample from the microwell well plate by applying a vacuum at the sample-loading port (Figure 2A). Next, a short vacuum pulse was applied to the sample injection port to fill the sample loop (Figure 2B). In the following step, the vacuum was turned off, and the voltage was applied for both separation and ESI-MS detection (Figure 2C). After separation, all of the channels were washed by applying positive pressure on the liquid reservoirs and negative pressure on the liquid junction (Figure 2D). Fresh separation buffer and liquid junction solution also filled the respective channels. During the washing step, the *x-y-z* stage moved the microwell plate to the next position so that the next run could begin immediately. Under LabView program control, the times required for sample loading and washing the separation channel were 2 and 3 s, respectively. The separation time varied, depending on the sample mobility and the applied electric field; typically, it was on the order of 30 s to several minutes.

Mass Spectrometry. A ThermoFinnigan (San Jose, CA) LCQ quadrupole ion-trap mass spectrometer was used in all of the experiments. The heated inlet capillary was maintained at 200 °C. On-line ESI-MS was performed in the positive-ion full-scan mode, typically using an ESI voltage of ~2 kV. For CE/MS experiments using the microdevice, the maximum-sample injection time was 200 ms, and two microscans were summed for each scan. For the MS/MS experiments, the maximum sample-injection time was 300 ms, and two microscans were again summed for each scan. The relative collision energy for CID was set at 50%.

Tryptic Protein Digest. The protein digest mixture was prepared as follows: First, the sample was dissolved in 20 mM ammonium bicarbonate to a concentration of ~1 mg/mL. TPCK treated trypsin (Sigma Chemical Co.; St. Louis, MO) was then

(18) Hjertén, S. *J. Chromatogr.* **1985**, *347*, 191−198.

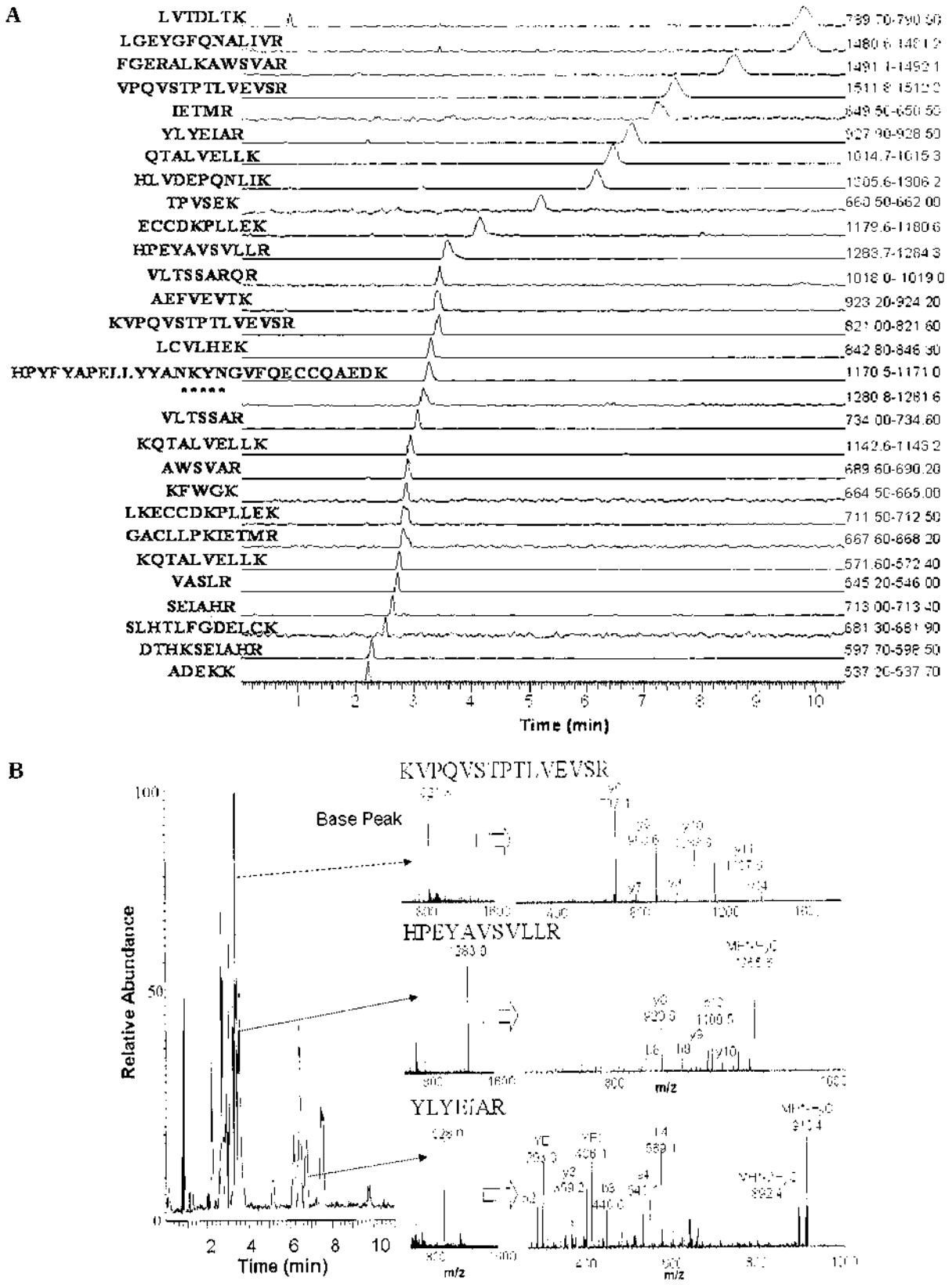

Figure 4. CE/MS analysis of BSA tryptic digest with pressure injection: A, selected ion monitoring; B, MS/MS analysis of selected peaks. Background electrolyte, ϵ-aminocaproic acid/acetic acid, pH 4.4; spray solution, 1% (v/v) acetic acid in 50% (v/v) methanol/water; electric field strength, 600 V/cm.

added at a substrate-to-enzyme ratio of 50:1, and the solution was incubated overnight at 37 °C. The digest was vacuum-dried and reconstituted in water before being loaded onto the microdevice.

Materials. All of the peptides and proteins were purchased from Sigma Chemical Co. and were used without further purification. Ammonium acetate, acetic acid, and formic acid were from

J. T. Baker (Phillipsburg, NJ), and methanol from was from E. M. Science (Gibbstown, NJ). Deionized water (18.2 MΩ) was prepared using a Milli-Q system from Millipore (Bedford, MA), and ϵ-aminocaproic acid was from Fluka (Milwaukee, WI).

RESULTS AND DISCUSSION

Instrument Design. Most microdevice designs to date have integrated sample reservoir(s) directly onto the microchip, thus requiring extensive chip washing or replacement after either each run or a few runs. Automated operation of the system would necessitate robotic replacement of disposable chips with additional sample pipetting. To avoid continual replacement of the single-channel device, we decided on a design in which the microdevice could be easily reused. The system was constructed as a combination of three independent modules, as shown in Figure 3. Each module could be independently optimized for a particular operation, such as CE/ESI-MS described here.

The automated sample-positioning module was designed to minimize the distance between the sample and the microdevice. Thus, we employed vertical orientation of the sample microwell plate so that the length of the sample-loading capillary could be minimized. With the v-shaped microwell plate that was used, sample volumes of 5−300 μL could easily be handled with the plate in the vertical position. Because of the surface tension, the liquid remained in the wells even when the plate was turned upside down. Although not used in this study, the microwell plate can be covered by a protective layer that can be pierced by the sampling capillary prior to each analysis to prevent evaporation.[15]

The samples in the microwell plate were sequentially loaded onto the chip using pneumatic flow control, as described in the Experimental Section. The total sample volume loaded onto the microdevice was ∼500 nL, and a 6.6-nL aliquot was used for the analysis. Unlike in electrokinetic sample injection, the amount of the sample that is injected pneumatically does not depend on the sample composition or the presence of electroosmotic flow. The outside surface of the sample-loading capillary was automatically washed between injections by dipping the capillary into distilled water that was contained in a common well of the microwell plate. No sample carry-over was observed after this simple washing procedure; however, if necessary, a more thorough flow-through washing device could be used.[15]

The subatmospheric electrospray interface was previously described in detail.[19] The lower pressure in the electrospray chamber, relative to the liquid junction, induced constant flow through the ESI capillary. As described in the Experimental Section, the replaceable ESI capillary was not an integral part of the microdevice. The subatmospheric ESI chamber was used to couple the microdevice to an ion-trap MS; however, the same microdevice design can be used to interface to a MALDI/TOFMS instrument.[20]

The requirement for automated operation (continuous use) dictated design changes from the more common approaches.[21,22] Larger reservoir volumes are required to minimize changes in buffer composition due to electrolysis, especially when unbuffered solutions are used.[23] The larger volume reservoirs were also used for pressure washing of the channels after each run. In this initial design, we used an external manifold with electrode reservoir volumes of 250 μL each. By positioning the reservoirs external to the microchip, the need for drilling access holes was eliminated, thus simplifying the microdevice manufacture. The microchip was maintained in the polycarbonate holder by means of a screw, as shown in Figure 1C (also see detail in Figure 1B). After loosening the screw, the microchip could be replaced in the polycarbonate manifold in a matter of seconds. Miniature O-rings, used to seal the chip and the manifold, also helped in the rapid chip replacement. Finally, as shown in Figure 1A, a side channel, connected at the second turn of the separation channel, was added to enhance the washing step. The side channel could also be used for the injection of larger sample volumes (with a preconcentration focusing step). The junction of the side channel and the separation channel was etched to 25 μm (one-ninth of the cross section of the separation channel) to minimize diffusion losses of the sample during separation.

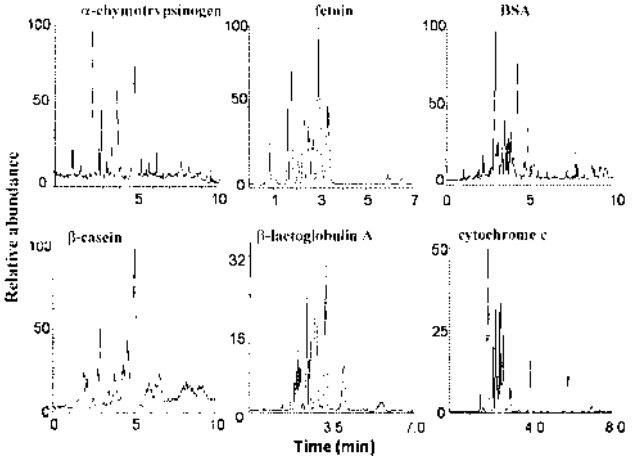

Figure 5. Base-peak electropherograms of sequential CE/ESI-MS analysis of protein tryptic digests. Pressure injection. Each protein digest (1 mg/mL) was diluted 20-fold with water before injection. BGE, formic acid (10 mM, pH 2.9); spray solution, 0.5% (v/v) formic acid in 50% (v/v) methanol/water; electric field strength, 500 V/cm.

CE/MS of Tryptic Peptides. In our initial experiments, conducted to evaluate the overall separation performance of the microdevice for CE/MS analysis, we chose to examine the tryptic digest of BSA. We selected a background electrolyte of pH of 4.4, where the protonation of the N-termini of peptides would be minimized. Because no electroosmotic flow was generated (neutral coating on the walls of the channel), the migrating species would be expected to correspond mainly to basic peptides. Figure 4A shows the selected ion monitoring and partial separation of 29 peaks of tryptic peptides from BSA using the 11-cm channel. The separation was completed in 10 min at an applied electric field of 600 V/cm, with column efficiencies over 10 000 plates (see later), thus demonstrating the resolving performance of the microdevice. A total of 28 of the 29 peaks could be directly identified from the database as digested peptides of BSA. Additional structural information could be obtained by tandem MS/MS analysis of selected peaks performed on the digest peaks, as shown in Figure 4B.

(19) Foret, F.; Zhou, H.; Gangle, E.; Karger, B. L. *Electrophoresis* **2000**, *21*, 1363−1371.
(20) Preisler, J.; Foret, F.; Karger, B. L. *Anal. Chem.* **1998**, *70*, 5278−5287.
(21) Jacobson, S. C.; Hergenröder, R.; Koutny, L. B.; Warmack, R. J.; Ramsey, J. M. *Anal. Chem.* **1994**, *66*, 1107−1113.
(22) Harrison, D. J.; Fluri, K.; Seiler, K.; Fan, Z.; Effenhauser, C. S.; Manz, A. *Science* **1993**, *261*, 895−897.
(23) Macka, M.; Andersson, P.; Haddad, P. R. *Anal. Chem.* **1998**, *70*, 743−749.

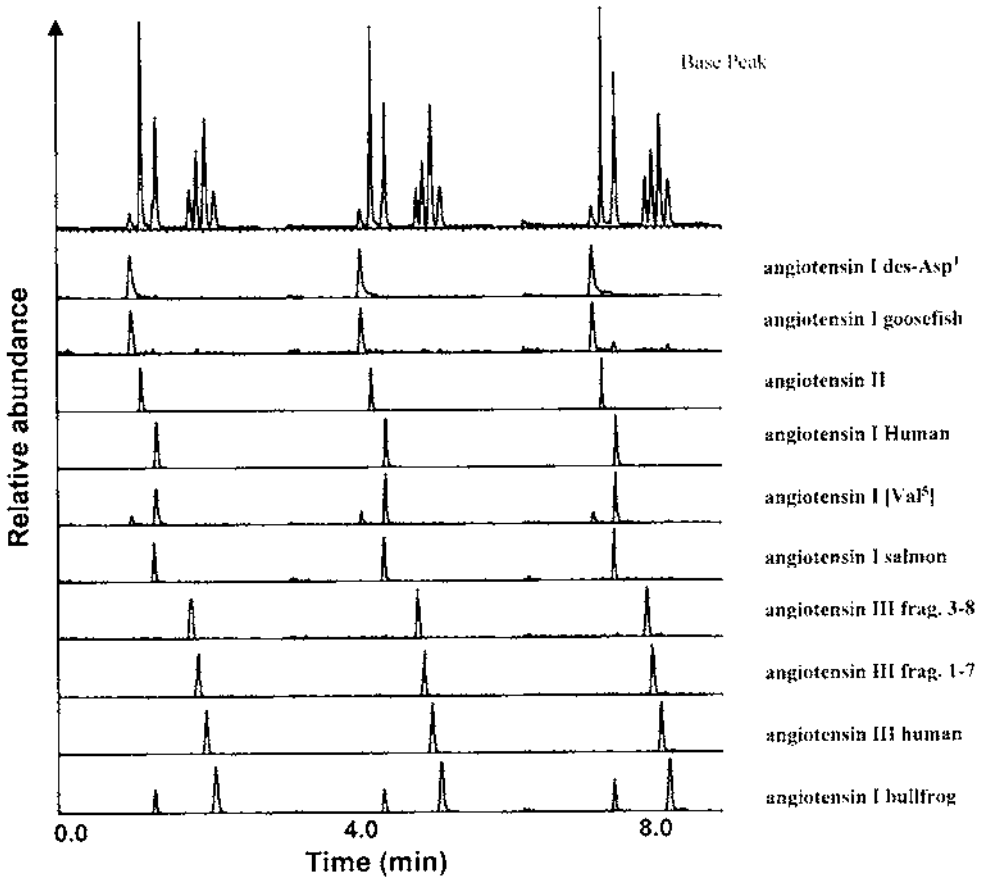

Figure 6. Sequential CE/MS base peak electropherograms of a mixture of angiotensin peptides with pressure injection. Sample, 10 μg/mL of each peptide. Conditions as in Figure 4.

With the above successful initial tests for separation performance, we next examined the automation capabilities of the microdevice system to analyze various protein samples digested in individual microwells of the plate. Figure 5 shows the base peak electropherograms of the sequential analysis of six protein tryptic digests, which were loaded sequentially from the microwell plate, each following a washing step, as described in the Experimental Section. In this example, we selected a background electrolyte at pH 2. 9 to maximize the ionization of the tryptic peptides and speed up the analysis. The measured tryptic peptide masses were used for database search by MS-Fit program (http://prospector.ucsf.edu/). The total sequence coverage of the proteins for this short separation channel was in the range of 69% (BSA) to 97% (cytochrome *c*). Peaks in an individual run were not found to be attributed to peptide digest fragments from a previous run, which suggests that the washing step was sufficient. Even when using pH 4.4 for separation, no sample carryover was observed (data not shown). Thus, individual samples can be sequentially loaded, injected, and analyzed with the microdevice design we describe in this paper.

In the next experiments, we tested the run-to-run reproducibility of the system. A mixture of 10 angiotensin peptides was sequentially injected by the pneumatic injector and separated at pH 4.4. Figure 6 shows an expanded section of a representative base peak electropherogram as well as the list of the peptides. Measured separation efficiencies (10 000−30 000 theoretical plates) were found to be comparable to that obtained using a standard fused-silica capillary of the same length (11 cm), indicating that, in agreement with earlier studies,[5] the microdevice design did not cause additional band-broadening. Although the mixture of peptides was not completely resolved because of the short channel length of 11 cm, individual components could be easily identified by selected ion monitoring, as shown in Figure 6. As an example of reproducibility, the relative standard deviation (RSD) of the migration times and the peak heights for 9 consecutive runs are summarized in Table 1. The reproducibility of the migration times was 2%, and the peak height reproducibility was ∼7%. The lower reproducibility of the peak height was due to the slow scanning rate of the mass spectrometer (∼ 2 scans/sec), which resulted in the peaks' being defined by an insufficient number of data points (peak widths of ∼3 s). Improved reproducibility should be possible with a faster mass spectrometer, for example, ESI/TOFMS.

Table 1. Reproducibility of Migration Times and Peak Heights for 9 Consecutive Injections of a Mixture of Angiotensin Peptides, Each at 10 μg/mL[a]

analyte	RSD of retention time, %	RSD of peak height, %
angiotensin II	1.97	7.1
angiotensin III fragment 3−8	1.10	6.8
angiotensin III human	2.00	7.0

[a] Background electrolyte, ϵ-aminocaproic acid/acetic acid, pH 4.4; liquid junction spray solution, 1% (v/v) acetic acid in 50% (v/v) methanol/water; electric field strength, 600 V/cm.

Figures 4−6 show the performance of the microdevice system with pneumatic fluid control and external reservoirs. At present, the dimensions of the electrolyte reservoirs (5-mm i.d. × 15 mm) allow continuous analysis of up to 46 samples, about one-half of the 96-well microwell plate. Because >1 μL of buffer is flushed through the separation channel, the electrolyte reservoirs have to be replaced after half of the microtiter well plate has been analyzed because of the change in liquid levels in the reservoirs. Because the accumulating liquid rises by ∼1 mm/20 μL, the resulting hydrostatic pressure difference can induce liquid flow in the channels of the microdevice, which in turn can degrade separation efficiency. Fortunately, the volume of the external reservoirs can be easily increased to minimize this difference in liquid height buildup during extended operation. For example, by increasing the diameter of the reservoirs from 5 mm (current system) to 16 mm, the volume would increase 10-fold. This increase would essentially eliminate hydrostatic pressure differences during the analysis of the whole plate. Alternatively, the content of the electrode reservoirs could be designed as a flow-through system[15]. Nevertheless, the results presented in this paper demonstrate that the design strategy of external electrolyte reservoirs as well as sampling directly from the microtiter plate provide good separation performance with the potential for automated high-throughput CE/ESI-MS. Future work will demonstrate the long-term use of this microdevice approach for automated single- and multiple-channel operation with MS detection.

CONCLUSIONS

A new microdevice for automated high-throughput CE/ESI-MS, integrating a separation module equipped with a subatmospheric ESI interface and with injection directly from microwell plates has been introduced. Buffer reservoirs external to the device and an electropneumatic distributor were used for automated device washing and sample loading. The removal of the electrode and sample reservoirs from the microdevice significantly simplified manufacture and operation of the system while the system was tested for CE separation. The system can also be employed for other separation modes, for example, capillary liquid chromatography in a single- or a multiple-channel arrangement. The microdevice provides a possible means for high-throughput peptide identification and analysis, as well as analysis of chemical and combinatorial libraries. High-throughput quantitative analysis for pharmacokinetic studies should also be possible using this approach.

ACKNOWLEDGMENT

The authors gratefully thank NIH (Grant GM 15847) for support of this research and Contribution No. 789 from the Barnett Institute.

Received for review December 5, 2000. Accepted March 20, 2001.

AC001432V

Aerodynamic mass spectrometry interfacing of microdevices without electrospray tips†

Jakub Grym, Marek Otevřel and František Foret*

Received 19th April 2006, Accepted 28th July 2006
First published as an Advance Article on the web 22nd August 2006
DOI: 10.1039/b605599k

A new concept for electrospray coupling of microfluidic devices with mass spectrometry was developed. The sampling orifice of the time-of-flight mass spectrometer was modified with an external adapter assisting in formation and transport of the electrosprayed plume from the multichannel polycarbonate microdevice. The compact disk sized microdevice was designed with radial channels extending to the circumference of the disk. The electrospray exit ports were formed by the channel openings on the surface of the disk rim. No additional tips at the channel exits were used. Electrospray was initiated directly from the channel openings by applying high voltage between sample wells and the entrance of the external adapter. The formation of the spatially unstable droplet at the electrospray openings was eliminated by air suction provided by a pump connected to the external adapter. Compared with the air intake through the original mass spectrometer sampling orifice, more than an order of magnitude higher flow rate was achieved for efficient transport of the electrospray plume into the mass spectrometer. Additional experiments with electric potentials applied between the entrance sections of the external adapter and the mass spectrometer indicated that the air flow was the dominant transport mechanism. Basic properties of the system were tested using mathematical modeling and characterized using ESI/TOF-MS measurements of peptide and protein samples.

Introduction

Miniaturization of analytical instrumentation represents one of the important technology trends. Besides a simple size reduction the microfabrication allows creation of integrated fluidic systems with zero dead volume channel junctions, difficult to achieve by traditional machining. The smaller system dimensions typically also lead to lower reagent and sample consumption and faster analysis times. Additionally, once optimized, the microfabrication provides means for inexpensive, reproducible large scale production of the microdevices. The development of the microfluidic devices, initiated by the pioneering works by Widmer *et al.*,[1–4] is currently rapidly expanding into a number of applications. The interest in microfluidics can be documented not only by the exponentially growing number of scientific reports,[5] and establishment of new specialized periodicals[6,7] including this one, but also by the emergence of the first commercial products.[8–11] An array of applications covering miniaturized chemical sensors,[12,13] DNA arrays[14,15] or microchannel separations[16–18] is more recently being extended by the development of the microdevices for coupling with mass spectrometry.[19–21] It can be anticipated that the importance of the microfluidic systems suitable for direct coupling with mass spectrometry will continue growing in the applications requiring positive sample component identification. Such applications are abundant, *e.g.*, in the omics fields[22] (genomics, proteomics, metabolomics, *etc.*), drug development or diagnostics.[23,24] The first papers on direct coupling of microfluidics with mass spectrometry focused on the electropray ionization (ESI) approach.[25–28]

An important component of electrospray interface is the electrospray emitter, which facilitates stable and efficient sample ionization and transport of the analytes into the mass spectrometer.[29] Typically a fine pointed hollow needle is used as the electrospray emitter creating sufficiently strong electric field and the best results are routinely obtained using the nanospray arrangement.[30] In this case the needles with submicron tip radius can be prepared from glass or fused silica tubing using a pipette puller.[31] Such electrospray tips, allowing very high electrospray ionization efficiency,[32,33] are now commercially available.

While preparation of the electrospray emitters by a pipette puller, etching or by grinding and polishing of the end of the capillary is quite straightforward, the microfabrication of fine electrospray tips seems to be more demanding. This is mainly true for the case where the ESI tip is an integral part of a more complex microfluidic system for sample preparation and/or separation. In some of the first reports the microdevices were coupled to MS using external capillary tips inserted into an opening of the microdevice prepared by etching[34] or drilling[35,36] The preparation of the stand alone ESI tips or arrays of tips for infusion analysis is relatively well developed using batch microfabrication on silicon[37,38] and commercially available systems for automated infusion analysis are

Institute of Analytical Chemistry, Veveri 97, 61142 Brno, Czech Republic. E-mail: foret@iach.cz
† The HTML version of this article has been enhanced with additional colour images.

available.[39] Recently, a simple protocol for preparation of flat pointed ESI microdevices by plasma etching or laser ablation in polyimide has been described[40] and commercialized.[8,41] Additionally a plethora of protocols for microfabrication of suitable emitters in a variety of materials has been described in the past few years[42–47]—for review see ref. 21 and 48.

An attractive alternative to microfabrication of the ESI tips is the use of the opening of the channel on the surface of the microfluidic device. In such a case the fluid opening on the surface of the dielectric material (glass, plastic) can act as the ESI exit port without the need for the tip microfabrication. This arrangement has been tested in the very first works on the coupling of microfluidic devices with electrospray.[25,26] In these studies it has been found that a good quality electrospray can be generated from the semicircular openings with the radius of $\sim$50 μm. Infusion MS analysis of the mixtures of proteins and peptides has been achieved. It has also been found that the hydrophilic surface of the glass microdevice leads to wetting of the surface and droplet formation around the exit port. The size of the droplet generated at the exit port was typically tens to hundreds of nanoliters. While not critical for infusion analysis such a dead volume is not acceptable for coupling with on-chip separations where the zone volumes are typically much less than the dead volume associated with the droplet. The droplet size and surface wetting can be minimized by surface silanization[25] or by the use of a hydrophobic plastic material for microfabrication.[49] Unfortunately, the most frequently electrosprayed liquids often contain over 50% of organic, surface tension lowering, modifiers (*e.g.*, methanol, acetonitrile, isopropanol), which tend to spread even over a hydrophobic surface. Recently, the theoretical and practical aspects of the electrospray emission from non-wetting flat dielectric surfaces have been studied in more detail with emphasis on the potential use as space propulsion thrusters.[50] While these works clearly showed the potential for electrospraying from microchannel openings on flat surfaces, more work will be necessary for routine exploitation of such a simple arrangement.

One possibility for minimizing the dead volume and surface wetting is the use of a flow of a compressed gas for removal of the liquid at the exit port. Such a pneumatic nebulizer has been successfully integrated into the glass microfluidic device designed for capillary electrophoresis[51] where the electrospray exit port has been fabricated in between two converging channels supplied with nitrogen gas. The gas flowing around the ESI exit port continually removed the liquid, effectively preventing the droplet formation. The nebulizing action also induced a liquid flow inside the separation channel of the microdevice. Similar design can also be applied to other operation modes such as atmospheric pressure chemical ionization (APCI).[52] While integration of the pneumatic nebulizer on the microdevice is a feasible way of controlling the spray generation from a single channel microdevice, it also increases the system complexity. In addition, in microdevices designed for multiple sample processing[53,54] the gas connections could increase the size and complexity of the system and preclude its practical use. Recently, alternative designs using porous polymers[55] or integrating piezoelectric element have also been described for a single channel design.[56]

In this work we have decided to minimize the system complexity by moving the nebulizer to the entrance of the mass spectrometer. Additionally the nebulizer included an aerodynamic focusing chamber for directing the electrospray plume into the mass spectrometer sampling orifice. The complete external device comprised a large diameter input nozzle with controlled air intake, aerodynamic focusing chamber attached to the MS sampling orifice and an external pump for creating sufficient air flow for the nebulizing process. During the testing the microdevice was positioned on a rotation stage with the microchannel openings pointing towards the input nozzle.

Experimental

Chemicals

Acetic acid, isopropanol and acetonitrile (both HPLC grade) as well as the bradykinin, neurotensin, angiotensin and myoglobin were obtained from Sigma-Aldrich (Prague, Czech Republic). Distilled water was prepared in house. The conductivity of the sample solutions was measured by a laboratory conductometer CDH-80 (Omega, Stamford, CT, USA).

Microdevice

The microdevice has been modified from the CD format microlaboratory disks (SP1) kindly provided by Gyros, AB, Uppsala, Sweden. These disks, microfabricated from polycarbonate by injection molding, contained 96 microchannel structures originally designed for sample desalting—see www.gyros.com for further details. Disks without the gold coating were used for the experiments in this work. The perimeter rim of the disk was lathed off to expose the exit ports. It was found that machining on a lathe leaves well shaped open channels on the edge of the CD without any need for further processing or cleaning. The photograph in Fig. 1a shows the partial top view of the edge of the CD with two channels merging in the exit ports on the machined edge of the microfluidic disk. The detail in Fig. 1b depicts the structure of the polycarbonate CD disk with the channels closed from the top by the sealing foil. The exit ports with a roughly rectangular cross section (20 × 50 μm) were used for the ESI experiments, Fig. 1b. The larger unlabeled openings correspond to the remnants of the structures, which were removed during the machining (also seen in Fig. 1a). During the experiments the CD microdevice was mounted on a laboratory prepared rotation table driven by a manually controlled stepper motor.

Mass spectrometry

All ESI/MS measurements were performed on the Mariner ESI-TOF mass spectrometer (ABI, Framingham, MA, USA) operated in the positive ESI mode, acquiring 1 spectrum per second in the *m*/*z* range of 100–2000. The high voltage for electrospray was generated by CZE 1000R power supply (Spellman, Hauppauge, NY, USA). In experiments requiring additional high voltage a laboratory constructed power supply adjustable in the range of $\pm$6 kV was used.

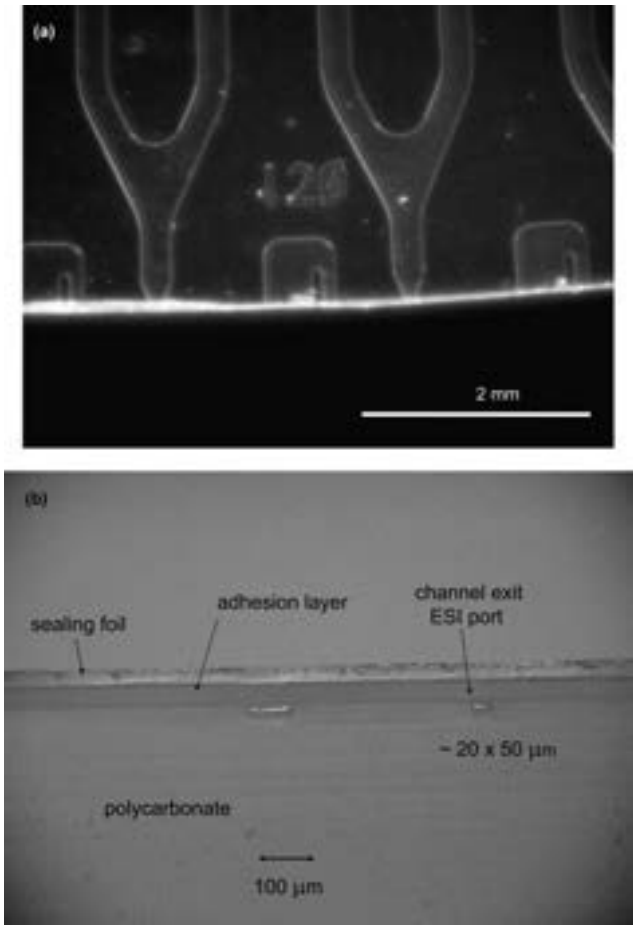

Fig. 1 (a) Top view of the channels on the lathed off edge of the CD microdevice. (b) Side view of the CD perimeter showing the material structure with the exposed exit ports.

Aerodynamic interface

The interface was machined from stainless steel and consisted of three concentric parts. Fig. 2a shows the scheme of the system; the photograph of the attachment of the interface in place of the original sampling orifice of the mass spectrometer is in Fig. 2b. The transfer nozzle was machined as a substitution of the original sampling orifice of the mass spectrometer. Compared to the original sampling orifice with the internal diameter of 0.4 mm the new transfer nozzle was adapted with a 34 mm × 0.6 mm id stainless steel tubing (Small Parts, Miami Lakes, USA). The thread at the end of the transfer nozzle allowed its firm attachment to the focusing chamber with a conical cavity. The opposite side of the focusing chamber was capped by an ESI sampling port with a central opening for collection of the ESI plume with internal diameter of 1.6 mm. The central opening was surrounded by a concentric array of eight 1 mm diameter air inlets. The side opening in the focusing chamber was used for attachment of an external vacuum pump. The dimensions of the 10 mm long focusing chamber were 10 mm diameter at the ESI sampling port and 2 mm at the side of the stainless steel capillary. A rotary pump from the vacuum concentrator (model 5301, Eppendorf, Hamburg, Germany) was attached to the focusing chamber during the operation. The air flow was measured using a mass flowmeter (model 4140 TSI, Shoreview, MN, USA).

Computer simulations

The finite element method was used for flow simulations using routines written in COMSOL 3.2 (COMSOL AB, Stockholm, Sweden), MATLAB 7.1 (The MathWorks, Inc., Natick, USA) and FreePascal (www.freepascal.org/fpc.html).

Results and discussion

Electrospray mass spectrometry is typically performed using a fine pointed electrospray tip. Microfabrication of such electrospray tips can be performed using a variety of the protocols referenced in the Introduction. Generating electrospray directly from the microchannel opening is an attractive alternative, offering a simplification in the microdevice design and fabrication. Additionally, the tipless microdevices could be more rugged in practical use, especially with parallel channels. The size of the channel opening is comparable to a regular microspray needle and sufficient electric field can be achieved by applying a high voltage on the liquid (sample) inside the channel. The main problem related to the wetting of the surrounding surface was previously attacked by selection of the chip material,[43] chemical surface modification,[25,26,57] or by

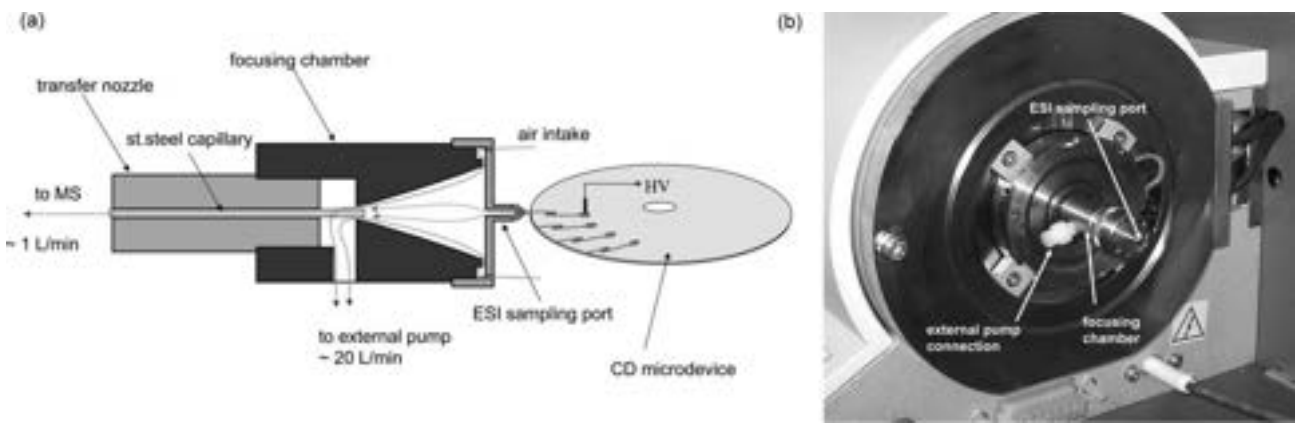

Fig. 2 The scheme (a) (not to scale) and actual view (b) of the interface. For details see Experimental section.

using an integrated pneumatic nebulizer.[51] In this work we have modified the nebulizer concept by moving it from the chip onto the side of the mass spectrometer. This simplifies the chip design and provides the potential for additional functionality of the ESI interface.

During the first experiments we have tried exploiting air intake through the mass spectrometer sampling orifice to assist the nebulization without the use of the external pump. A slot extension made of a fluoropolymer was attached to the sampling orifice of the mass spectrometer and the compact disk microdevice was positioned so that the channel opening was aligned with the mass spectrometer sampling orifice protruding the slot. The vacuum suction through the mass spectrometer sampling orifice assisted the dispersion of the sample stream. Unfortunately, although the ESI mass spectra could be observed, this arrangement proved to be unsuitable for practical use due to the need of very fine position alignment and erratic behavior. The main problem was identified as the low air intake ($\sim$1 L min^{-1}) generated by the mass spectrometer. After these preliminary experiments we have designed an interface with a connection for the external pump as described in the Experimental section. The air intake through the ESI sampling nozzle was increased to 20 L min^{-1} allowing better control of the flow and dispersion of the electrosprayed sample. A piece of fluoropolymer tubing extending 1 mm from the ESI sampling port was used to prevent accidental short circuit and arcing between the ESI exit port and the sampling port. The liquid flow from the microdevice exit port and its nebulization was controlled by the air intake through the sampling nozzle during the operation. This is demonstrated in Fig. 3a where the total ion signal and corresponding spectra were recorded for a solution of 0.2 mg ml^{-1} myoglobin in 50% (v/v) isopropanol/water containing 1% acetic acid electrosprayed at 2.5 kV. Very stable total ion current and good spectra of the myoglobin were observed when the external pump was turned on. After turning the pump off the MS signal decreased rapidly to zero. Note that the signal at the "pump off" state is off set at about 10%. This corresponds to the zero signal level, which was recorded also when no ESI device was connected to the mass spectrometer. Turning the pump on again resulted in restoring the MS signal. This process could be repeated as needed indicating that the air stream generated within the focusing chamber by the external pump was an effective transporter of the electrosprayed ions into the mass spectrometer. It is worth noting that the signal stabilized in only a few seconds after turning the vacuum pump on. The air flow rate generated during the experiments was given by the geometry and physical dimensions of the interface and the capacity of the available pump. From Fig. 3a it is clear that the ion signal is proportional to the pressure and lower ion signals correspond to lower flow rates. Maximum pumping was used during all experiments to maximize the ion signal. The TIC signal plotted in Fig. 3a was acquired in 3 s intervals with typical signal stability on the order of 10% rsd. The typical ESI/MS spectra of the samples containing myoglobin and a peptide mixture are shown in Fig. 3b. In these experiments 10 μL of the samples dissolved in 50% (v/v) isopropanol/water containing 1% of acetic acid were pipetted into the reservoirs on the microdevice and the electrospray voltage (2.5 kV) was connected *via* a platinum wire inserted directly into the sample solutions. Once the signal from one sample was recorded the CD microdevice was rotated and the next sample was analyzed. Since the scope of the study was the design of the interface, no systematic study of the variability in the performance of different CD microdevices was performed. The high device to device reproducibility is inherent to the microfabrication process, which is commonly assumed to be the main advantage of microfluidics. Similarly to the commercial multisprayer device,[39] where each sample is electrosprayed from its own exit port, sample carryover was not observed.

We have also attempted to photograph the Taylor cone at the ESI exit ports; however, without success due to the excessive light scatter at the ESI sampling port. Based on the previous design with the integrated nebulizer[51] we expect similar performance, which could make this arrangement useful also for coupling with separations. Both the stability and signal to noise ratio were similar to those obtained with the standard microspray interface. It is worth mentioning that the electrospray current was conducted by the sample solution in the microchannel connecting the sample reservoir with the electrospray exit port. This current unavoidably generates a potential drop between the sample reservoir and the ESI exit port on the rim of the microdevice. Based on the measured conductivity of the electrosprayed sample (130 μS cm^{-1}), the crossection of the narrowest part of the channel (50 × 20 μm), and the typical ESI current of 100 nA, the maximum electric field strength inside the sample delivery channel, calculated from the modified Ohm's law, was 77 V cm^{-1}. We have also confirmed this value experimentally by measuring the electric current in a fused silica capillary filled with the sample. At 5 kV the elecric current of 900 nA was measured in a 75 μm id × 35 cm long capillary filled with the sample solution. Assuming that the Joule heat effects are negligible at such a low power one can extrapolate that the field strength in the microdevice channel with 4.4 times less cross section area at 100 nA would be about 70 V cm^{-1}. At this field strength the most mobile ions (*e.g.*, potassium with electrophoretic mobility of $\sim$80 $\times 10^{-5}$ cm^2 V^{-1} s^{-1}) electromigrate with the velocity of 0.56 mm s^{-1}. For most analyte ions this velocity will be almost an order of magnitude slower. Given the sample flow rate of 350 nL min^{-1} (see below), the flow velocity at the exit port was almost 6 mm s^{-1}. Thus, with the channel dimensions used in this study, the liquid flow velocity eliminates any effects of electromigration or electroosmosis at any direction. However, it is worth noting that the electromigration effects might become significant in devices with smaller channel sizes.

To estimate the sample flow generated by the vacuum suction during the operation, a series of experiments were performed with larger sample reservoirs attached on top of the microdevice. In this arrangement the sample volume of 30 μL could be continuously sprayed for about 50 min corresponding to the rate of 600 nL min^{-1}. This time includes the effects of air stream nebulization, electrospray action and evaporation. In additional experiments it was found that evaporation of the same sample volume with the ESI voltage and the external vacuum pump off was completed in 120 min (250 nL min^{-1}). Evaporation with the vacuum pump on and ESI voltage off

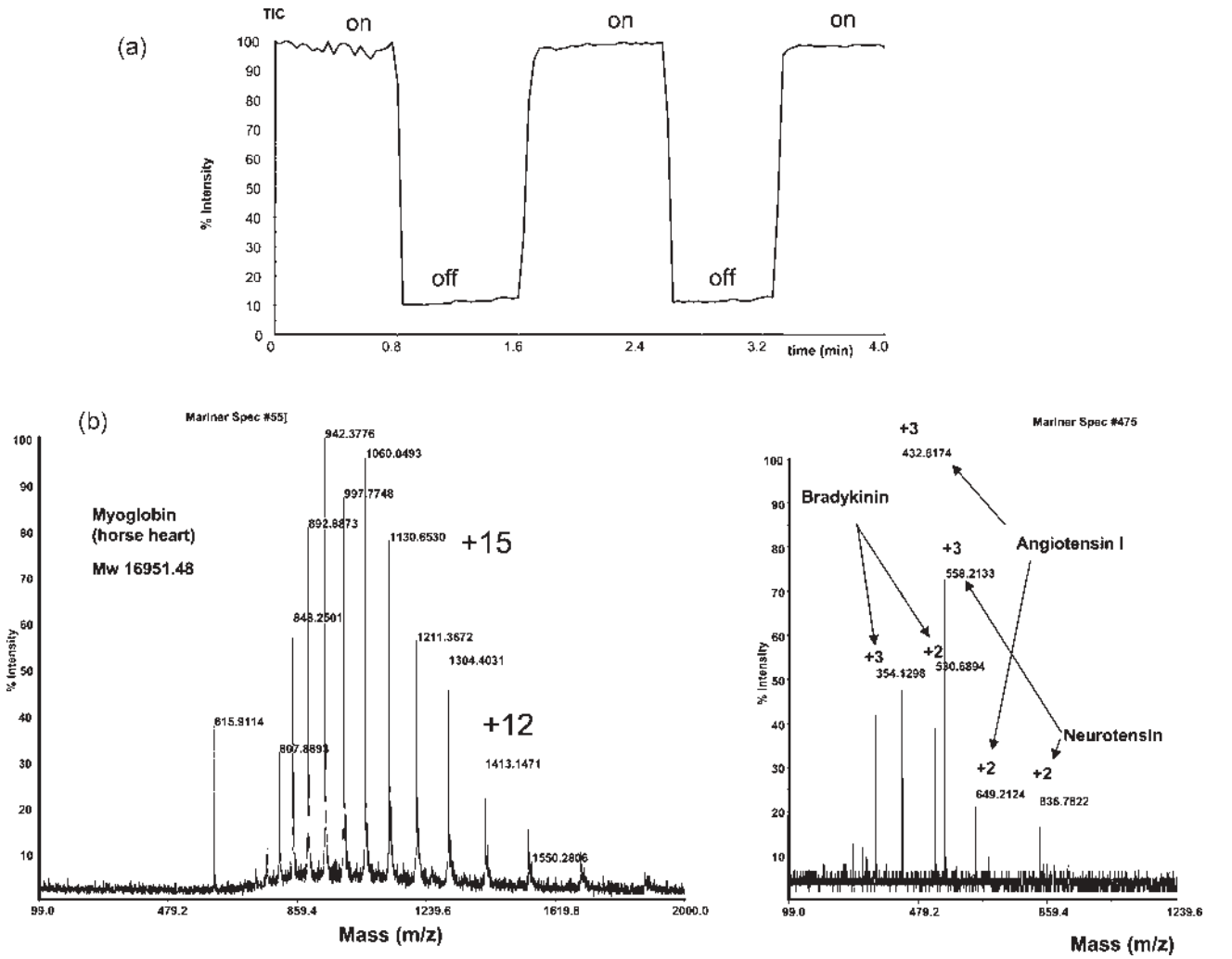

Fig. 3 (a) The effect of the external pumping on the total ion current recorded during the infusion of 20 μM myoglobin at 2.5 kV. The sample was dissolved in 50% (v/v) isopropanol/water containing 1% acetic acid. The labels ''on'' and ''off'' correspond to the periods of the use of the external vacuum pump. (b) The single scan ESI/MS spectra of 1 μM myoglobin (left) and 10 μM each of bradykinin, neurotensin and angiotensin (right). The average molecular masses: bradykinin 1060.23, neurotensin 1672.95, angiotensin I 1296.5. The numbers above the peaks correspond to the charge state of the detected ions. Other conditions as in panel (a).

was completed in about 60 min (500 nL min^{-1}). From these experiments it was concluded that the sample flow rate during the ESI/MS experiments was about 350 nL min^{-1} (600–250). The contribution of the electrospray action to the total flow rate was 100 nL (600–500). Hence the air suction was the main driving force of the flow—250 nL min^{-1}. It is worth noting that the ESI voltage without the vacuum pump on did not increase the rate of evaporation and its contribution was apparent only with the simultaneous action of the vacuum suction. This can be attributed to the fact that the hydrostatic pressure ($\sim$2 mm liquid height) of the sample in the electrode reservoir was not sufficient to create enough flow to sustain the electrospray action. On the other hand the electrospray action is known to contribute to the sample flow.[29] This explains the increased sample flow rate during the ESI ionization compared to the flow generated only by the air suction.

In the second set of experiments we have tested the potential effects of electrostatic field on the transport of the ions inside the focusing chamber. The electrostatic lenses are well established in the vacuum systems and more recently have also been used in the concept of the ion funnel for improvement of the ion transmission in the entrance region of the mass spectrometer.[58] Although the pressure inside the focusing chamber of the presented interface is much higher than inside the mass analyzer (close to the atmospheric pressure), the electrostatic effects might still have a potential effect on the ion transport.[59] A new focusing chamber made of insulator (polyvinylchloride) was prepared for the testing and two high voltage power supplies were connected as shown in Fig. 4. During the experiments the HV1 was adjusted so that potential of the electrospray needle was always at constant 2.7 kV relative to the ESI sampling port. The HV2 power supply was used to adjust the potential between the ESI sampling port and the transfer nozzle (see Fig. 4a). Since these experiments required an extended continuous electrospray action (over 1 h) the microdevice with limited sample capacity was substituted by a standard nanospray needle (ABI, Framingham, MA, USA). The total ion current was continuously monitored and

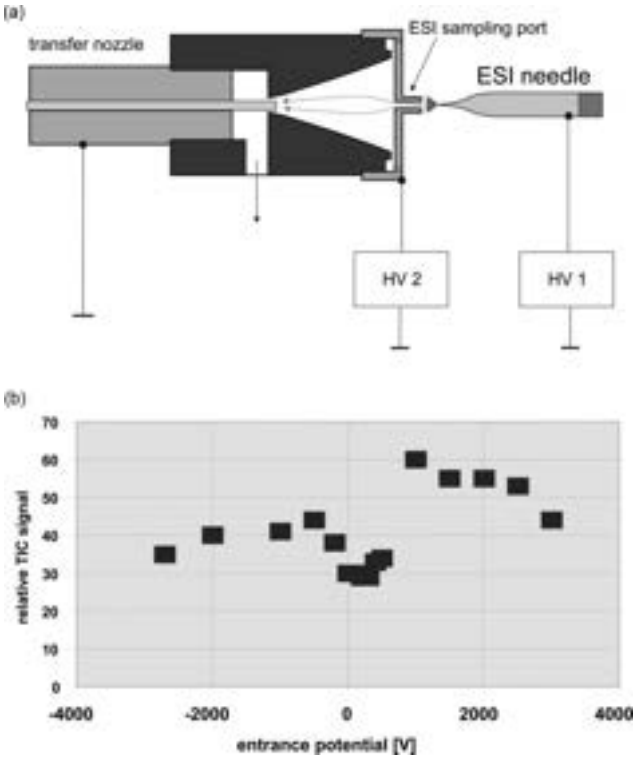

Fig. 4 Effect of the entrance potential on the ion transmission. For details see text.

the average values were recorded for 3 min intervals at any given HV2 value. The transfer nozzle was in direct mechanical and electrical contact with the entrance orifice of the mass spectrometer. According to the manufacturer of the mass spectrometer the potential of the sampling orifice of the MS instrument is kept several volts above the instrument ground. Such a potential is within the measurement error of the typical high voltage power supplies operating at several kV. For simplicity, the transfer nozzle is shown as connected to the instrument ground in Fig. 4a. The MS instrument ground was connected to the zero potential of both the HV1 and HV2. The measurement started with the ESI sampling port at −3 kV with respect to the transfer nozzle and was stepwise increased up to +3 kV. At the same time the voltage at the ESI needle was varied from −0.3 kV to 5.7 kV to keep the ESI potential, and thus the spray action, constant at 2.7 kV relative to the ESI sampling port. Measurements then continued in the reversed order until reaching the −3 kV at the ESI sampling port again. The graph of the average values of the recorded total ion signals *versus* the voltage between the ESI sampling port and the transfer nozzle (entrance potential) is plotted in Fig. 4b. Each data point represents an average of the signal recorded during the two three minute long intervals. The signal variation, including both the noise and drift recorded during this extended measurement period (∼90 min) was about 20%. No apparent differences between the signals recorded at different entrance potentials were observed. Although some signal variations could be detected it has to be concluded that the influence of the voltage is weak at best since the effect was on the same level as the long term signal drift. At this moment it seems that the air flow within the focusing chamber is the dominant, if not the only, transport mechanism of the electrosprayed ions under the experimental conditions.

Computer simulation of the flow

It can be expected that the shape and size of the cavity will play a role in the transmission of the electrosprayed ions into the mass spectrometer. The shape and size of the focusing cavity was designed mainly based on the spatial considerations—the space in front of the mass spectrometer, the sizes of the microdevice and the MS sampling orifice and the pumping capacity of the available external pump. The conical shape was selected on empirical assumption that the beam of the electrosprayed ions entering the sampling nozzle could be focused by the air flow into the center to achieve the best transmission efficiency. Obviously, the optimization of the aerodynamic properties of the focusing cavity is not trivial since aerodynamic flow profile can not be easily estimated. While a separate study will be needed for the rational optimization in this work we have attempted to estimate the mass flow properties using mathematical modeling under simplified conditions. The calculation was performed for the segments of the focusing chamber shown in Fig. 5. First, the air velocity field within the focusing chamber was calculated for a steady-state incompressible Newtonian fluid described by the Navier–Stokes boundary problem:

$$\rho(\boldsymbol{v}\nabla)\boldsymbol{v} = \mu\Delta\boldsymbol{v} - \nabla p \qquad (1)$$

where $\boldsymbol{v}$ is the velocity field, ρ the density, μ dynamic viscosity and p is the pressure field.

Under the experimental conditions the Reynolds number was about 10^5, corresponding to the transition between laminar and turbulent flow. The calculated air velocity profile is in Fig. 6a. The calculations indicate absolute airflow speed exceeding 150 m s^{-1}. It is also clear that, under the experimental conditions the main air transport is axially centered

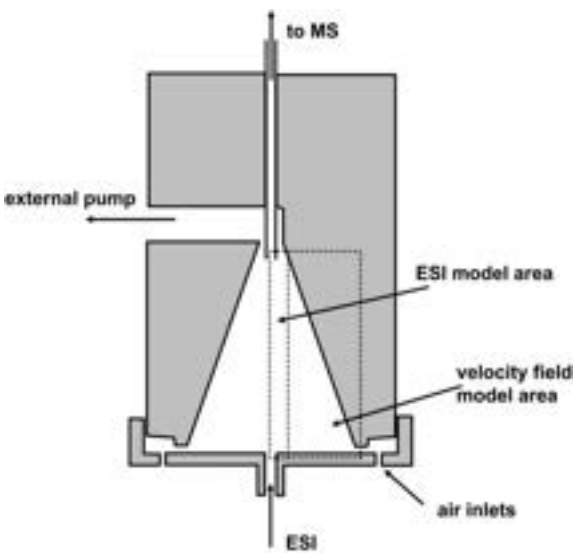

Fig. 5 The geometry and definition of the space included in the simulations.

with little effect of the conical shape of the focusing chamber. In the next step, the behavior of an ion cloud within the focusing chamber was simulated as shown in Fig. 6b. The flow inside this segment was considered to be parallel to the axis (z) and radius (r) dependent. The r-dependence of $\boldsymbol{v}$ shown on the right hand side of Fig. 6b was calculated for a set of identical charged spheres representing the electrosprayed droplets. For simplicity, it was assumed that the forces affecting the spheres

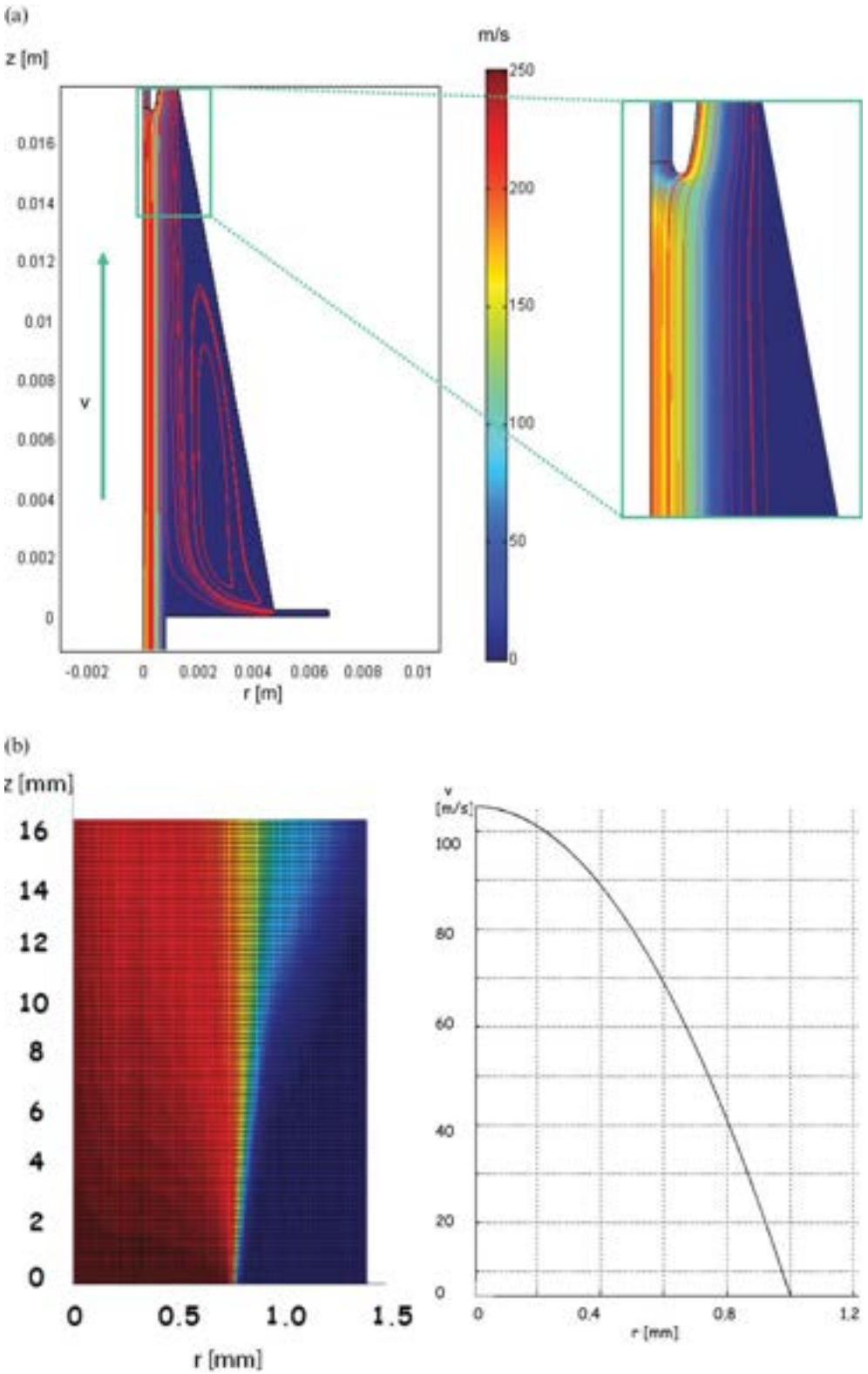

Fig. 6 (a) Computed air velocity field profile within the focusing chamber. (b) Flow profile of the ion cloud within the focusing chamber calculated for a set of 200 nm diameter charged spheres representing the electrosprayed droplets—left.

(electrostatic repulsion and air flow drag) are always in equilibrium. The ESI ion cloud could therefore be described as

$$\nabla(c\,\boldsymbol{u}_{\mathrm{tot}}) = 0$$
$$(\boldsymbol{u}_{tot} - \boldsymbol{V}) = \frac{zq_e\boldsymbol{E}(c)}{6\pi v\rho r} \quad (2)$$

where c is the concentration of the spheres, $\boldsymbol{u}_{tot}$ is the velocity field of the spheres, $\boldsymbol{v}$ is the air velocity field, r and z are the sphere radius and elemental charge count of a sphere, q_e is the element charge, $\boldsymbol{E}(c)$ is the concentration-dependent electrostatic field generated by the ion cloud, v and ρ are the kinematic viscosity and density of the air.

From the known electrospray current, the sample flow-rate and assumption that the spheres are at the Rayleigh limit,[60] the diameters and charges of the spheres were determined, as follows:

$$r = \left(36\varepsilon\gamma\Phi^2/I^2\right)^{\frac{1}{3}}$$
$$z = \frac{8\pi}{q_e}\sqrt{\varepsilon\gamma r^3}$$

Here Φ and I are the ESI flow rate and current, ε and γ are the permittivity and surface tension of the electrosprayed liquid. The following values ware taken for the calculation: I = 100 nA, Φ = 100 nL min^{-1}, the radius r = 186 nm and z = 10140.

From the simulations it follows that the air flow has major influence on the electrosprayed droplets transport. The transit of the droplets in the focusing chamber is very short resulting in a very low electrostatic divergence of the beam of the electrosprayed droplets.

Conclusion

The described concept provides an alternative way for the mass spectrometry coupling of microfluidic devices without the need of electrospray tips microfabrication. Although the aerodynamic properties are not fully optimized in its present form, the external nebulization is an effective way for the control of the elecrospray process at the flat channel opening and transfer of the electrospray plume into the mass spectrometer. The system simplifies the complexity especially of the microdevices designed for multiple sample handling and can be used for rapid switching between the electrospray ports. From both the experiments and computer simulations it follows that the air stream is effective for transporting of the electrospray plume generated outside the region of the mass spectrometry sampling orifice. Potential future enhancements of the ion transmission into the mass spectrometer should be possible by optimization of the flow and aerodynamic shape of the focusing chamber.

Acknowledgements

The authors wish to thank Applied Biosystems (Framingham, MA) for support and donation of the mass spectrometer and Gyros, A.B. (Uppsala, Sweden) for support and donation of the CD microdevices. Additional support was provided by the Grant Agency of the Czech Republic, 203/06/1685, Grant Agency of the Czech Academy of Sciences A400310506 and Ministry of Education, Youth and Sports LC06023. Helpful discussions with Dr Eugene Moskovets and Prof. Barry L. Karger from the Barnett institute in Boston are also appreciated.

References

1 A. Manz, N. Graber and H. M. Widmer, *Sens. Actuators, B*, 1990, 244–248.
2 A. Manz, D. J. Harrison, E. Verpoorte, J. C. Fettinger, A. Paulus, H. Ludi and H. M. Widmer, *J. Chromatogr.*, 1992, **593**, 253–258.
3 D. J. Harrison, A. Manz, Z. Fan, H. Ludi and H. M. Widmer, *Anal. Chem.*, 1992, **64**, 1926–1932.
4 A. Manz, J. C. Fettinger, E. Verpoorte, H. Ludi, H. M. Widmer and D. J. Harrison, *Trends Anal. Chem.*, 1991, **10**, 144–149.
5 C. K. Fredrickson and Z. H. Fan, *Lab Chip*, 2004, **4**, 526–533.
6 μTAS (a virtual journal on micro Total Analysis Systems): http://www.elsevier.com/wps/find/journaldescription.cws_home/672688/description#description.
7 Electrophoresis—Miniaturization Special Issues: www.electrophoresis-journal.com.
8 www.agilent.com.
9 www.caliper.com.
10 www.nanostream.com.
11 www.nanogen.com.
12 M. Ren, E. S. Forzani and N. Tao, *Anal. Chem.*, 2005, **77**, 2700–2707.
13 S. Herber, J. Eijkel, W. Olthuis, P. Bergveld and A. van den Berg, *J. Chem. Phys.*, 2004, **121**, 2746–2751.
14 S. Mocellin, E. Wang, M. Panelli, P. Pilati and F. M. Marincola, *Clin. Cancer Res.*, 2004, **10**, 4597–4606.
15 S. Panda, T. K. Sato, G. M. Hampton and J. B. Hogenesch, *Trends Cell Biol.*, 2003, **13**, 151–156.
16 R. F. Renzi, J. Stamps, B. A. Horn, S. Ferko, V. A. Vandernoot, J. A. West, R. Crocker, B. Wiedenman, D. Yee and J. A. Fruetel, *Anal. Chem.*, 2005, **77**, 435–441.
17 H. Yin, K. Killeen, R. Brennen, D. Sobek, M. Werlich and T. van de Goor, *Anal. Chem.*, 2005, **77**, 527–533.
18 E. Olvecka, D. Kaniansky, B. Pollak and B. Stanislawski, *Electrophoresis*, 2004, **25**, 3865–3874.
19 F. Foret and J. Preisler, *Proteomics*, 2002, **2**, 360–372.
20 W. C. Sung, H. Makamba and S. H. Chen, *Electrophoresis*, 2005, **26**, 1783–1791.
21 I. M. Lazar, J. Grym and F. Foret, *Mass Spectrom. Rev.*, 2006, **25**, 573–594.
22 J. Lederberg and A. T. McCray, *Scientist*, 2001, **15**, 8.
23 J. R. Yates, *Nat. Rev. Mol. Cell. Biol.*, 2005, **6**, 702–714.
24 P. Senk, L. Kozak and F. Foret, *Electrophoresis*, 2004, **25**, 1447–1456.
25 Q. Xue, F. Foret, Y. M. Dunayevskiy, P. M. Zavracky, N. E. McGruer and B. L. Karger, *Anal. Chem.*, 1997, **69**, 426–430.
26 R. S. Ramsey and J. M. Ramsey, *Anal. Chem.*, 1997, **69**, 1174–1178.
27 D. Figeys, C. Lock, L. Taylor and R. Aebersold, *Rapid Commun. Mass Spectrom.*, 1998, **12**, 1435–1444.
28 J. J. Li, P. Thibault, N. H. Bings, C. D. Skinner, C. Wang, C. Colyer and J. Harrison, *Anal. Chem.*, 1999, **71**, 3036–3045.
29 P. Kebarle, *J. Mass Spectrom.*, 2000, **35**, 804–817.
30 M. S. Wilm and M. Mann, *Int. J. Mass Spectrom. Ion Processes*, 1994, **136**, 167–180.
31 G. A. Valaskovic and F. W. McLafferty, *J. Am. Soc. Mass Spectrom.*, 1996, **7**, 1270–1272.
32 M. Karas, U. Bahr and T. Dulcks, *Fresenius' J. Anal. Chem.*, 2000, **366**, 669–676.
33 R. Juraschek, T. Dulcks and M. Karas, *J. Am. Soc. Mass Spectrom.*, 1999, **10**, 300–308.
34 B. L. Zhang, F. Foret and B. L. Karger, *Anal. Chem.*, 2000, **72**, 1015–1022.
35 J. Li, P. Thibault, N. H. Bings, C. D. Skinner, C. Wang, C. Colyer and J. Harrison, *Anal. Chem.*, 1999, **71**, 3036–3045.

36 I. M. Lazar, R. S. Ramsey, S. C. Jacobson, R. S. Foote and J. M. Ramsey, *J. Chromatogr.*, 2000, **892**, 195–201.
37 G. A. Schultz, T. N. Corso, S. J. Prosser and S. Zhang, *Anal. Chem.*, 2000, **72**, 4058–4063.
38 J. Sjödahl, J. Melin, P. Griss, A. Emmer, G. Stemme and J. Roeraade, *Rapid Commun. Mass Spectrom.*, 2003, **17**, 337–341.
39 www.advion.com.
40 T. C. Rohner, J. S. Rossier and H. H. Girault, *Anal. Chem.*, 2001, **73**, 5353–5357.
41 www.diagnoswiss.com.
42 K. Huikko, P. Ostman, K. Grigoras, S. Tuomikoski, V. M. Tiainen, A. Soininen, K. Puolanne, A. Manz, S. Franssila, R. Kostiainen and T. Kotiaho, *Lab Chip*, 2003, **3**, 67–72.
43 M. Svedberg, M. Veszelei, J. Axelsson, M. Vangbo and F. Nikolajeff, *Lab Chip*, 2004, **4**, 322–327.
44 Y. X. Wang, J. W. Cooper, C. S. Lee and D. L. DeVoe, *Lab Chip*, 2004, **4**, 363–367.
45 G. Liljegren, A. Dahlin, C. Zettersten, J. Bergquist and L. Nyholm, *Lab Chip*, 2005, **5**, 1008–1016.
46 Y. Yang, C. Li, J. Kameoka, K. H. Lee and H. G. Craighead, *Lab Chip*, 2005, **5**, 869–876.
47 S. Le Gac, S. Arscott and C. Rolando, *Electrophoresis*, 2003, **24**, 3640–3647.
48 W. C. Sung, H. Makamba and S. H. Chen, *Electrophoresis*, 2005, **26**, 1783–1791.
49 K. Q. Tang, Y. H. Lin, D. W. Matson, T. Kim and R. D. Smith, *Anal. Chem.*, 2001, **73**, 1658–1663.
50 P. Lozano, M. Martínez-Sánchez and J. M. Lopez-Urdiales, *J. Colloid Interface Sci.*, 2004, **276**, 392–399.
51 B. Zhang, H. Liu, B. L. Karger and F. Foret, *Anal. Chem.*, 1999, **71**, 3258–3264.
52 P. Ostman, S. J. Marttila, T. Kotiaho, S. Franssila and R. Kostainen, *Anal. Chem.*, 2004, **76**, 6659–6664.
53 M. Gustafsson, D. Hirschberg, C. Palmberg, H. Jornvall and T. Bergman, *Anal. Chem.*, 2004, **76**, 345–350.
54 M. Inganas, H. Derand, A. Eckersten, G. Ekstrand, A. K. Honerud, G. Jesson, G. Thorsen, T. Soderman and P. Andersson, *Clin. Chem.*, 2005, **51**, 1985–1987.
55 M. F. Bedair and R. D. Oleschuk, *Anal. Chem.*, 2006, **78**, 1130–1138.
56 S. Aderogba, J. M. Meacham, F. L. Degertekin, A. G. Fedorov and F. M. Fernandez, *Appl. Phys. Lett.*, 2005, **86**, 3p.
57 Q. F. Xue, Y. M. Dunayevskiy, F. Foret and B. L. Karger, *Rapid Commun. Mass Spectrom.*, 1997, **11**, 1253–1256.
58 S. A. Shaffer, D. C. Prior, G. A. Anderson, H. R. Udseth and R. D. Smith, *Anal. Chem.*, 1998, **70**, 4111–4119.
59 K. Tang, A. A. Shvartsburg, H. N. Lee, D. C. Prior, M. A. Buschbach, F. M. Li, A. V. Tolmachev, G. A. Anderson and R. D. Smith, *Anal. Chem.*, 2005, **77**, 3330–3339.
60 Lord Rayleigh, *Philos. Mag.*, 1882, **14**, 184–186.

Roman Tomáš
Liushui Yan*
Jana Křenková
František Foret

Institute of Analytical Chemistry, Brno, Czech Republic

Received December 8, 2006
Revised February 23, 2007
Accepted February 26, 2007

Research Article

Autofocusing and ESI-MS analysis of protein digests in a miniaturized multicompartment electrolyzer

Free-solution IEF of protein digests was studied in a newly introduced MicroRotofor multicompartment electrolyzer. The fractionation was performed in a cylindrical separation chamber divided into ten compartments with or without the addition of carrier ampholytes. In the case of autofocusing mode of operation, the tryptic digest itself served as the mixture of ampholytes leading to the separation of the peptides with well-defined p*I*'s. The focusing process was monitored visually using colored p*I* markers. The resulting fractions from both modes of the separation were analyzed by CE and electrospray-TOF mass spectrometer using electrospray tips microfabricated in polyimide. Additional experiments, aiming at visualization of the mass flux within the focusing compartments were performed using isotachophoretic migration of color cationic tracers. The study considered the autofocusing of both the peptides with well-defined narrow p*I*'s as well as those showing negligible net charge in a broader pH range. Although not all peptides in the protein digests have well-defined p*I*'s the autofocusing process can preseparate many of them leading to higher S/N in the ESI-MS signals and improved protein sequence coverage.

Keywords:
Autofocusing / CE / IEF / MS / Peptides DOI 10.1002/elps.200600802

1 Introduction

Protein analysis based on identification of the tryptic peptides belongs to one of the most frequently performed tasks in proteomics. Peptide mixtures typically represent a very complex sample and a separation step is often necessary prior to MS analysis [1]. The most complex samples, generated by global digestion of the whole protein extract, require the highest resolution separations such as those obtained by multidimensional chromatography [2]. The mixtures of less complex samples, *e.g.*, extracted spots from the 2-DE or peptide mixtures prepared by a specific peptide selection/enrichment protocol [3] can often be analyzed directly by an infusion-based ESI or MALDI MS [4]. Unfortunately, the suppression effects during the MS ionization (ESI or MALDI) of peptide mixtures can still result in loss of information [1]. While 2-D chromatography separation is not always necessary, sample preseparation into several fractions may be very helpful in this case. The separation of peptides can be easily performed by column chromatographic or electrophoretic techniques [5, 6].

Correspondence: Dr. František Foret, Institute of Analytical Chemistry, Veveří 97, CZ-602 00 Brno, Czech Republic
E-mail: foret@iach.cz
Fax: +420-541-212-113

Abbreviations: Cas, β-casein; **Cyt,** cytochrome; **Myo,** myoglobin

An alternative option might be the microfractionation of peptides based on IEF. For example, a miniaturized system employing the principle of the multicompartment electrolyzer [7] was constructed for parallel fractionation of 8 samples in 12 compartments separated by gel membranes with defined immobilized pH [8]. Significantly improved protein sequence coverage was obtained by MALDI MS compared to direct analysis of the unfractionated samples. In an alternative approach, the peptides were successfully fractionated in collection reservoirs placed on the surface of the polyacrylamide slab with IPG [9]. This "Off-Gel Electrophoresis" technique has been extensively tested and validated [10] for the shotgun proteomics where it can also form the first separation dimension prior to the nano-LC/MS analysis [11].

In the past, multicompartment electrolyzers have been developed for isoelectric fractionations using either mixtures of carrier ampholytes [12] or membranes with IPGs [7]. Suitable instruments are now commercially available (www.biorad.com, www.amersham.com).

A recently introduced simplified and miniaturized version of a multicompartment electrolyzer (www.biorad.com), was designed for free-solution preparative IEF. The cylindrical separation chamber, divided into ten segments separated

* Permanent address: Nanchang University, Nanchang P. R. China

by permeable polyester screens, allows separation and collection of ten fractions with about 250 μL volumes. The separation chamber slowly rocks during the separation, clamped into the Peltier-driven cooling block, to stabilize the sample against the convective and gravitational disturbances. After focusing, the solution in each compartment can be rapidly collected without mixing using the vacuum-assisted harvesting station that is integrated within the cell. The device was designed primarily for preseparation of protein samples in the pH gradient formed by carrier ampholytes. The separation of peptides is also possible; however, the resulting fractions contain mixtures of both the separated peptides and the carrier ampholytes. This may complicate further analysis, especially with MS, where the ampholytes, with similar molecular masses and high ionization efficiency, can interfere with the separated peptides – see Section 3.

In the pioneering works on the development of IEF [13], before invention of the carrier ampholytes [14], the protein separations based on p*I* differences were performed in the natural pH gradients formed between buffered solutions with selected pH values [13]. During further development peptide solutions prepared by protein fragmentation were utilized as carrier ampholytes for the protein focusing [15]. The introduction of the synthetic mixtures of carrier ampholytes enabled high-performance IEF in smooth and relatively stable pH gradients [16, 17]. These synthetic mixtures containing hundreds or thousands of ampholytes with well-defined p*I*'s and excellent buffering capacity allowed high-resolution IEF and made the original peptide-based gradients obsolete. Today's IEF systems with ampholyte and/or IPGs provide the basis for high-resolution fractionation of proteins.

In this work, we have studied the isoelectric peptide fractionation in free solution with and without the addition of the carrier ampholytes using the miniaturized multicompartment electrolyzer. In the ampholyte-free separation mode the mixture of the tryptic peptides itself formed the pH gradient and autofocused due to the p*I* differences between the individual sample peptides.

2 Materials and methods

2.1 Chemicals and materials

L-1-Tosylamido-2-phenylethyl chloromethyl ketone (TPCK)-treated trypsin (EC 3.4.21.4) from bovine pancreas, myoglobin from horse heart, β-casein from bovine milk, cytochrome *c* from horse heart, dithiothreitol, fuchsin, and ampholyte pH 3–10 electrophoresis reagent for IEF were obtained from Sigma (St. Louis, MO, USA). Ammonium bicarbonate, ammonium acetate and acetic acid were from Lachema (Neratovice, Czech Republic), sodium hydroxide and phosphoric acid from Onex (Rožnov pod Radhoštěm, Czech Republic), iodoacetamide and hydroxyethylmethylcellulose from Fluka (Buchs, Switzerland) and methylgreen-pyronine from Chroma (Stuttgart, Germany). Colored low-molecular weight p*I* markers [18–20] (5-(dimethylamino)-2-(3-pyridylazo)benzoic acid; p*I* 3.9 and 3′,3″-bis(4-morpholinomethyl)-5,5′ dichlorophenolsulfonphthalein; p*I* 5.3) were synthesized and kindly donated by Dr. Karel Šlais from the Institute of Analytical Chemistry.

2.2 Protein digestion

Ammonium bicarbonate (50 mM), pH 8.5, was used for the preparation of both the protein and stock trypsin solutions. The individual protein solutions (7×10^{-5} M) were reduced and acetylated before adding trypsin in the ratio of 1:50 w/w. The digestion proceeded overnight at 37°C and the resulting digests were lyophilized and stored in refrigerator for future use. In the following experiments the peptide aliquots were dissolved in distilled water and combined in the ratio of 1:1:1:1 v/v. The p*I* markers were added as indicated in the respective experiments.

2.3 Micropreparative IEF

The ion-exchange membranes, separating the electrode reservoirs and the focusing chamber, were equilibrated overnight in 0.1 M H_3PO_4 (cation-exchange membrane) and 0.1 M NaOH (anion-exchange membrane), respectively. The sample was injected into the focusing chamber by a 3 mL syringe until all ten compartments were equally loaded. Both the loading and harvesting holes on the opposite sides of the focusing compartments were sealed by an adhesive tape. Focusing assembly was positioned in the cooling block and the oscillating motor gently rocking the focusing assembly was turned on. The separation was conducted using the PowerPac 3000 power supply kindly provided together with the MicroRotofor by Dr. A. Paulus from BioRad (Hercules, CA). Either a constant power of 1 W or a voltage program was applied during the separation as specified in Section 3. The separation was terminated when the current stopped decreasing – typically after 25 min. The pH of the individual fractions was measured with a precision digital pH meter OP-208/1 (Radelkis, Budapest) equipped with a microcombined pH electrode HC 153 (Theta '90). After focusing, the fractions were transferred into polypropylene vials and stored in the freezer at −20°C.

2.4 CE

The laboratory CE setup included SpectraPhysics 100 UV detector for UV detection at 214 nm (Spectra Physics, CA) and high-voltage power supply (CZE 1000, Spellman, NY) operated at constant voltage of 15 kV. The separations, performed in 75 μm id × 55 cm (45 cm to the detector) long bare fused-silica capillary (Polymicro Technologies, AZ) were recorded using a PC-based data acquisition system (Data Apex, Czech Republic). Nonbuffered formic acid solution in water (1% v/v) was used as the BGE. Sample introduction was performed by hydrostatic pressure of 15 cm for 10 s.

2.5 MS

The Mariner electrospray TOF mass spectrometer – ESI/TOF (ABI, Framingham, MA) was used in the positive ion mode in the range of 400–2500 m/z. Each mass spectrum was a sum of ten scans acquired within 2 s. The samples were analyzed using plasma etched polyimide nanospray chips [21] kindly donated by DiagnoSwiss S.A. (Monthey, Switzerland). The samples were diluted ten times in 50% ACN/water v/v with addition of 1% (v) acetic acid. At the applied voltage of 2.2 kV the ESI-induced sample flow rate was about 100 nL/min. The heated entrance capillary of the mass spectrometer was kept at 120°C and no supporting gas was used. The list of detected ions (m/z) was used for protein identification by MS-Fit PMF tool of Protein prospector database (http://prospector.ucsf.edu).

3 Results and discussion

3.1 Peptide autofocusing

The current demand for the peptide separations relates mostly to the proteomics efforts and new separation techniques including IEF for the sample fractionation are in demand [22, 23]. The use of free-solution IEF with the separated peptides serving as the pH gradient medium is an attractive option for crude fractionation since no carrier ampholytes are needed. Additionally, the fractions are free of any interfering compounds, which might be especially useful for consecutive MS analysis. The industrial scale carrier free IEF, termed "autofocusing" [24], was recently adapted for ampholyte-free IEF of peptides in protein hydrolysates in food industry [25]. The applicability of autofocusing for proteomics application was previously demonstrated using either larger scale commercial units for preparative IEF [26] or a capillary format [27]. In cases when a moderate amount of the peptides have to be rapidly prefractionated for further analysis the "mezzo scale" separation of the samples on the mL scale using a miniaturized multicompartment electrolyzer is an attractive option. The instrument used in this study can fractionate the sample in ten ~250 μL compartments. The peptide mixture was prepared from proteins covering wide range of p*I*'s from 5.3 (β-casein), 5.8 (albumin), 7.35 (myoglobin), to 9.6 (cytochrome *c*). It is interesting to note that the tryptic peptides of typically cover a relatively wide range of p*I*'s regardless of the p*I* value of the original protein. This is shown in the plot in Fig. 1 where the molecular masses and p*I*s of the respective tryptic peptides were calculated with the use of the Compute p*I*/Mw tool available at http://us.expasy.org/tools/pi_tool.html. The p*I*'s of the resulting peptides cover the pH range of 3.5–10 and with most masses between 500 and 2000 Da resemble the synthetic ampholyte mixtures.

For comparison of the peptide fractionation the tryptic peptides were separated in two consecutive runs without and with the addition of the carrier ampholytes. Monitoring of the peptide focusing during the focusing was based on the time course of the electric current passing through the electrolyzer. The constant power operation (1 W), used in the first experiments, was soon abandoned due to long separation time and local overheating often leading to the current interruption or leaking of the sample into the electrode assemblies. In all consecutive experiments the voltage program was used with the start at 50 V (30 min) and gradually increasing to 400 V until reaching the power limit of 1 W. The run was terminated after about 2 h, when the current value leveled around 1 mA. The separation progress could be

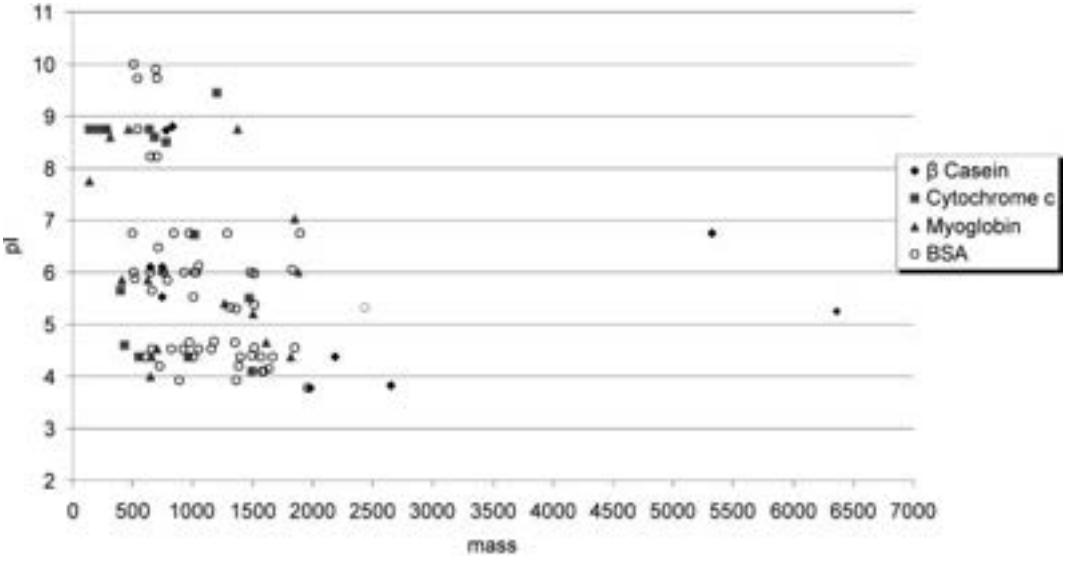

Figure 1. Theoretical molecular masses and p*I*'s of the tryptic peptides used in the experiments.

observed visually with the use of colored isoelectric markers [18] with the p*I*'s of 3.9 and 5.3. The final concentration of the markers added to the focusing cell was 37 μM. The photographs in Fig. 2 show the MicroRotofor electrolysis cell after the separation of the protein digests with the color markers in the absence (bottom left) and in the presence (upper right) of the carrier ampholytes. The photograph on the middle right shows the harvesting tray after the transfer of the focused zones from the electrolysis cell.

In both the autofocusing mode and in the presence of the ampholytes the zones separated according to the corresponding pH in the compartments. It is interesting to note that visually the separation looks better without the use of the ampholytes. This can be attributed to nonlinearity in the pH gradient formed by the autofocusing. We have measured the pH, which, as expected, revealed a smooth pH distribution in the ampholyte containing fractions and wavy distribution in the case of autofocusing. This is shown in Fig. 2b (bottom right). Due to their low concentration the presence of the pH markers did not significantly influence the pH profile in either case. On the other hand, when needed, the focusing pH range can be easily influenced by substituting the catholyte or anolyte (or both) with a solution of a pure ampholyte with the desired p*I*. We have successfully tested this approach by using a 100 mM solution of histidine (p$I \sim 7.6$) to limit the pH range from 2 to 7.6 or from 7.6 to 10 – data not shown. It is also worth noting that the measured pH in the fractions is only an average of the pH distribution inside each compartment. Better pH resolution could, in principle, be achieved for some of the peptides with well-defined p*I*s with the electrolyzer divided into more compartments.

The contents of the ten fractions separated without the pH markers were first analyzed by CE with UV detection at 214 nm – Fig. 3. The fractions were injected without further treatment into the separation capillary by hydrostatic pressure of 15 cm for 10 s. Obviously, the fractions contained different mixtures; however, closer inspection of all the separation records indicated poor focusing of some of the peptides, which were detected in several compartments. This was also confirmed later by the ESI/MS analysis of the frac-

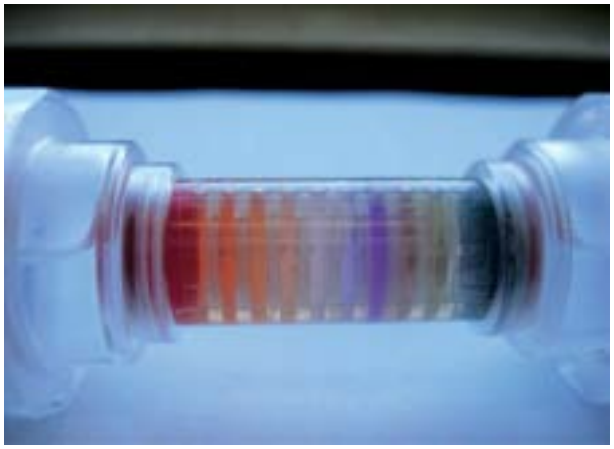

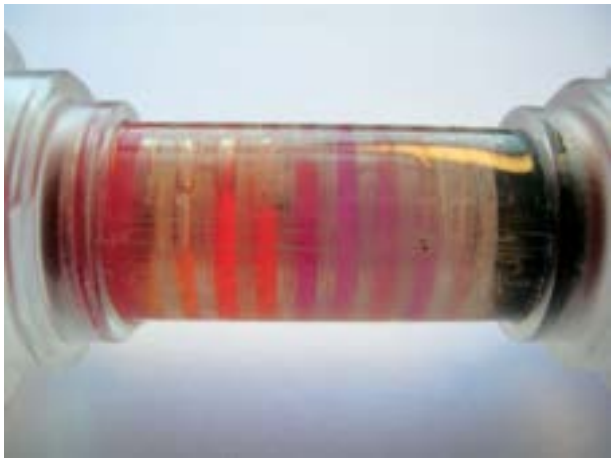

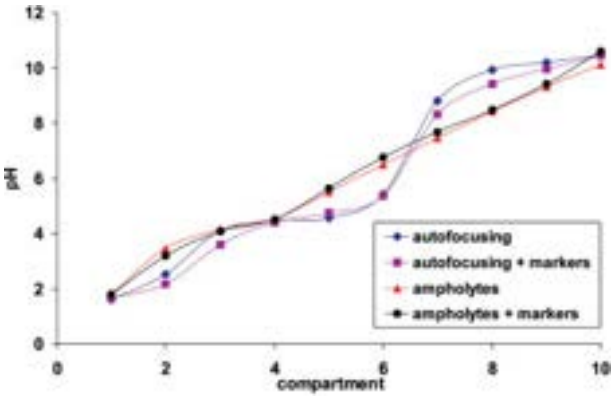

Figure 2. (a) Photograph of the electrolysis cell after the fractionation of the protein digests with the color markers with the p*I* of 3.9 (orange) and 5.3 (purple). (Bottom left) peptide autofocusing; the yellowish color, in the compartment on the left of the purple zone, corresponds to the impurity in the p*I* marker with higher p*I* value. (Upper right) the same sample focused in 2% ampholyte solution. (Middle right) autofocused fractions in the harvesting vessel. The bubbles trapped inside the compartments result from the manual handling of the chamber. No dependence of the amount of air bubbles on the mode of operation was observed. (b) Plot of the pH values measured in the collected fractions.

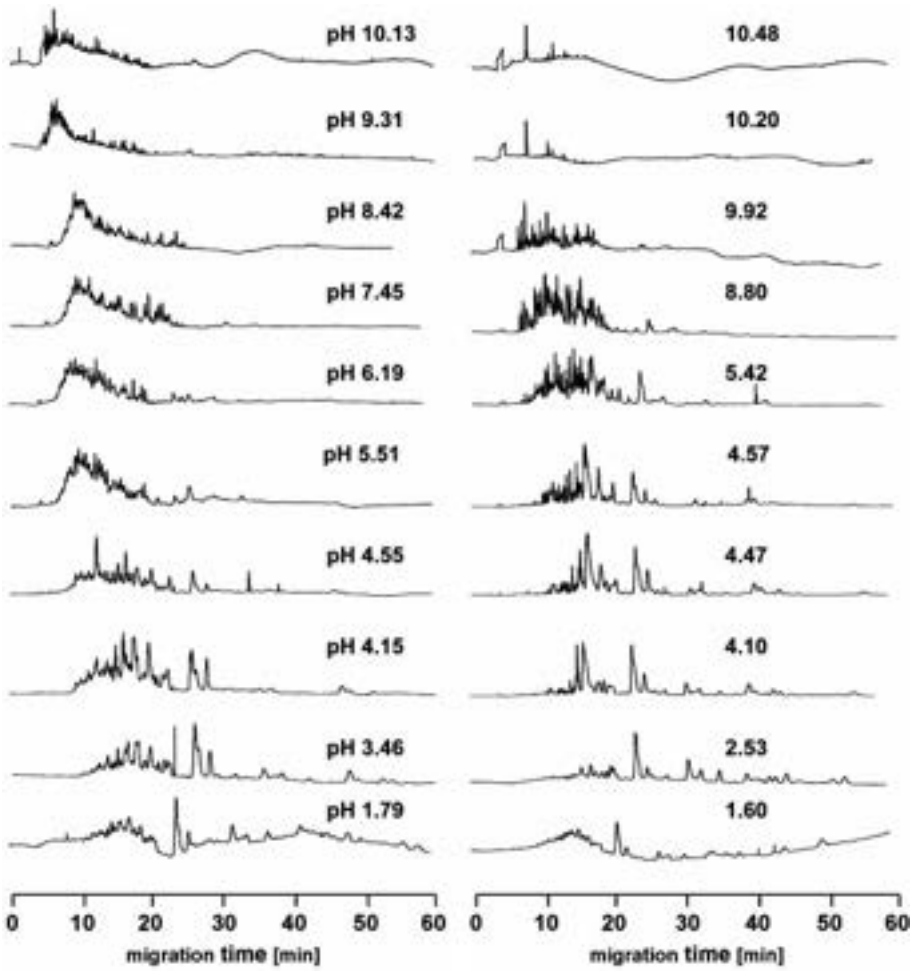

Figure 3. CE separation of peptide fractions separated in 2% ampholytes (left) or by autofocusing (right). Electric field strength 200 V/cm. Acidic fractions start on the top. For details see Section 3.

tions. The spreading of some of the peptides across several separation compartments relates to the fact that these peptides possess very small net charge or are electrically neutral over wide range of p*I*'s.

The colored p*I* marker used in this study to visualize the course of the separation were designed to behave as ideal ampholytes for IEF and their focusing properties are well documented [18, 28]. On the other hand, the focusing properties of protein digests are generally unknown. For good resolution and formation of narrow zones the separated substances must be good ampholytes with the pK_a's of the ionizable groups close to the p*I* value [13]. Thus, for example, most amino acids with pK_a's of the carboxy and amino groups around 2 and 9, respectively, are electrically neutral over a wide pH range and will not focus well in IEF. Similarly, some of the peptides having charge only on the *C*- and *N*-termini may be electrically neutral over a broad pH range. In IEF, the minimum resolvable difference ΔpI can be expressed as [29]

$$\Delta pI = 4\left(\frac{D\mathrm{d(pH)}/\mathrm{d}x}{E\mathrm{d}u/\mathrm{d(pH)}}\right)^{1/2} \quad (1)$$

where D is the diffusion coefficient, E is the applied electric field strength, and u is the electrophoretic mobility. For example, in a linear pH gradient (*e.g.*, using carrier ampholytes or IPG) of 1 pH unit per 10 cm and the diffusion coefficient in the range of 10^{-6} cm^2/s, analytes with well-defined p*I* differing by less than 0.01 p*I* could be resolved. This assumption will not be valid in the case of the peptide autofocusing, where the shape of the pH gradient will differ from sample to sample. Additionally some of the separated (especially smaller) peptides may possess zero net charge over a wide range of pH resulting in focusing regions with peptides spanning several fraction chambers are inevitable.

The speed of the IEF separation depends mainly on the change of the electrophoretic mobility u of the analyte with the change of pH – the term du/d(pH) in Eq. (1). The electrophoretic mobility of chemically similar compounds with molecular mass M and charge z can be expressed as

$$u = za\,M^b + c \quad (2)$$

where *a*, *b*, and *c* are experimentally available constants [30]. For tryptic peptides a modified equation was derived in the form [31]

$$u = \frac{1758 \log(1 + 0.297z)}{M^{0.411}} \quad (3)$$

Since the electrophoretic mobility is only a weak function of the peptide mass and for the MS analysis and database searching the interesting tryptic peptides have masses in a relatively narrow range (*e.g.*, 500–3000 Da) their electrophoretic mobility will be influenced mainly by the net charge of the molecule. Consequently, peptides with a steep change in the net charge with pH will focus well and extending the separation time will provide only marginal improvement. In summary, one can always expect that some tryptic peptides will focus well into a sharp zone and others will stay spread over the portion of the separation compartment. This will be true for all modes of the IEF using carrier ampholytes, IPGs, off-gel electrophoresis or autofocusing. It is also interesting to note that we did not observe any apparent trend in the peptide sequence and its ability to focus into a well-defined zone. Clearly, the final p*I* will depend not only on the content of individual amino acids, but also on their sequence and possible folding of the longer peptides. Additional changes may also result from the presence of additives/denaturants during the focusing. In this respect one should be also careful in accepting the theoretical values of the p*I*'s calculated by the number of available procedures since significant differences may be experimentally observed. Since the autofocusing does not use any additional chemicals its biggest attraction is its simplicity and low cost. While the peptides with well-defined p*I*'s will focus into sharp bands, other species with broad range of electroneutrality will be present in several fractions. This will be also true in other IEF modes employing carrier ampholytes or immobilized gradients. Thus the resolution should, in principle, be similar to other IEF modes.

3.2 MS and sequence coverage

In practice, the limitation of the IEF only to peptides with well-defined p*I*'s may not be critical, since most of the "interesting" peptides (in the mass range suitable for the database searching) will focus. At the same time, the separation modes providing peptide fractions without additional ionic species (autofocusing, off-gel electrophoresis) will be more suitable for direct electrospray–MS analysis. This follows from the fact that the ampholyte mixtures can cause severe ionization suppression as demonstrated in Fig. 4. In this experiment the ESI-MS spectra were obtained from fractions separated with carrier ampholytes and under autofocusing conditions, without the ampholytes. The fractions containing the ampholytes provided strong MS signals; however, none of the peaks corresponded to the separated peptides, which were completely suppressed. On the other hand, the fractions from the autofocusing experiment provided clean ESI-MS spectra allowing identification of the peptides. The ion suppression will be of less of a problem when injecting the fractions into another separation dimension, *e.g.*, HPLC, where most of the ampholytes will be separated from the peptides.

For the ESI-MS analysis each collected fraction was diluted ten times in 1% acetic acid solution in 50% v/v ACN/water. The samples were loaded into the reservoirs of the polyimide nanospray emitters and analyzed by the ESI-TOF mass spectrometer. The peptide fragments were identified using the Protein Prospector (http://prospector.ucsf.edu) database search using MS signals in the range of 400–2000 Da with signal higher than five-fold of the baseline noise. The comparison of the sequence coverage obtained without sample preseparation, with the autofocusing and with IEF separation in the ampholyte pH gradient is summarized in Table 1. Compared to direct infusion the autofocusing in the MicroRotofor provided significantly higher sequence coverage for myoglobin (33% higher sequence coverage) and BSA (24% higher sequence coverage), slight improvement for casein and no improvement for the cytochrome *c* fractions. This finding indicates that the IEF process will leave some of the poorly focusing peptides unfractionated; however, this can be always expected during the separations of very complex samples.

We have also tested the mixing properties inside the multicompartment chamber. The separation compartments of the MicroRotofor were separated by polypropylene screens acting as a flow barrier against the mixing of the separated fractions. During the IEF and especially in the autofocusing mode the differences in conductivity of individual zones lead to the formation of temperature gradients potentially resulting in flow mixing. Additional mixing could be expected during the fraction harvesting when the

Table 1. Comparison of the sequence coverage obtained with autofocusing and with direct infusion

Fractionation mode	Autofocusing				Direct infusion			
Protein	Cyt	Myo	Cas	BSA	Cyt	Myo	Cas	BSA
Sequence coverage	45% (47/104)	67% (103/153)	20% (42/208)	56% (325/582)	52% (54/104)	34% (52/153)	19% (39/208)	32% (189/582)

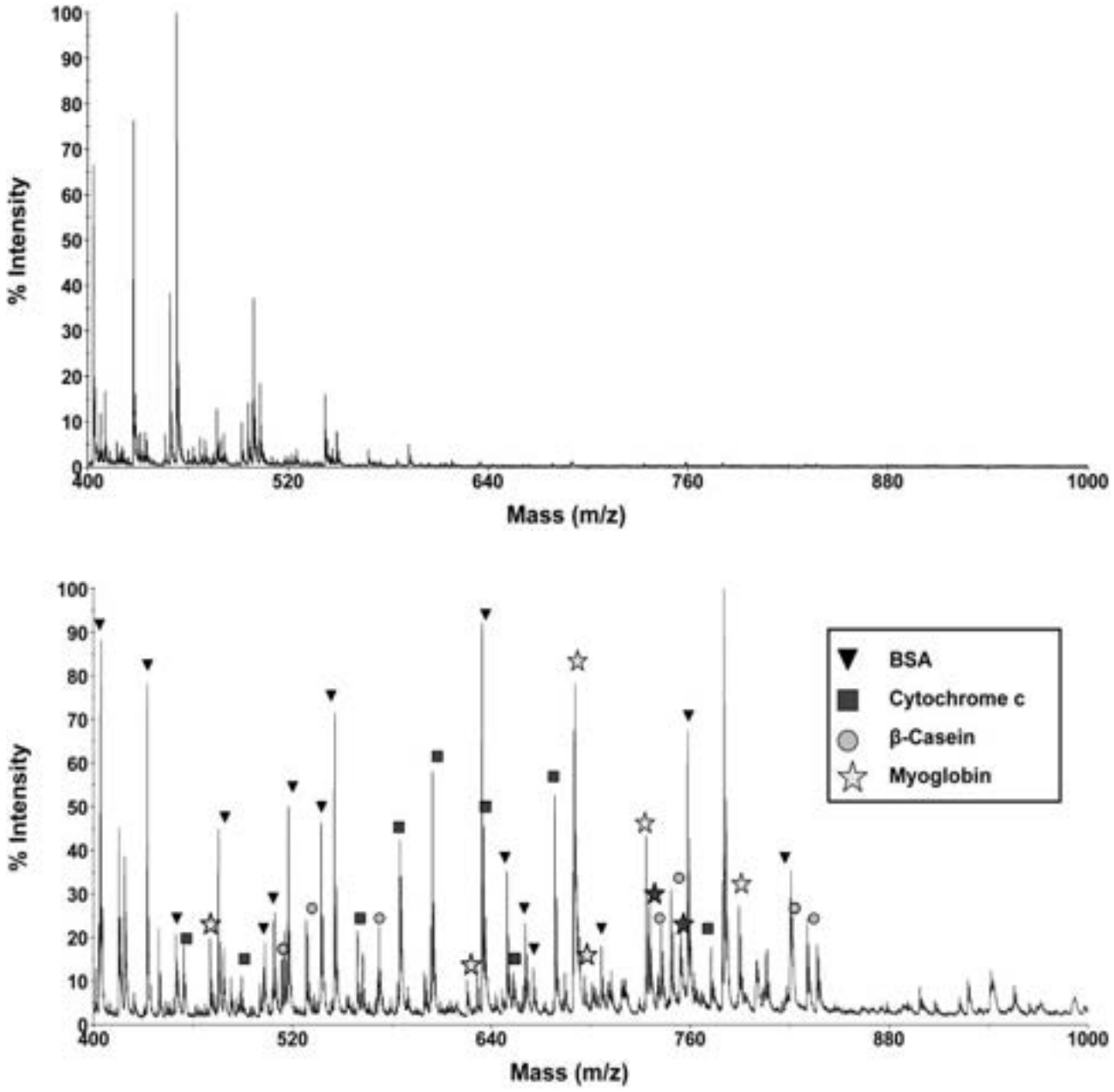

Figure 4. The ESI/MS spectra from the peptide fraction number 8 separated in the presence of the carrier ampholytes (a) and under autofocusing conditions without the ampholytes (b). The identified tryptic peptides corresponded to BSA, cytochrome *c,* β-casein, and myoglobin. No peptides could be identified in the ampholyte containing fraction.

separation voltage is turned off. To test the permeability of the polypropylene screens a colored sample (methylgreen) was isotachophoretically focused into a sharp zone inside one compartment. Nonbuffered ammonium acetate (100 mM solution in water, no additives, pH ~ 7) was used as the leading electrolyte and 1% acetic acid served as a terminating electrolyte. The nonionic detergent Natrosol was added to the solutions in final concentration of 0.25% w/v to minimize sorption and electroosmosis. Once the zone was focused, the separation current was turned off and the color spreading into the neighbouring compartments was observed. It took over 2 h for the focused dye to spread into the adjacent compartments indicating that the polypropylene screens provided excellent barrier virtually eliminating any mixing during the separation and fraction harvesting.

4 Concluding remarks

The tryptic peptides of the selected proteins cover a wide range of p*I*'s and provide a rapid focusing in the Micro-Rotofor device. The use of the color p*I* markers allowed visual monitoring of the separation process and optimization of the separation time. Three milliliters of the protein digests could be fractionated in about 2 h with the voltage programming. The separated fractions were easily harvested from the ten compartments. IEF fractionation was performed either by using the carrier ampholytes or in the autofocusing mode. After harvesting the fractions were analyzed by electrospray MS. While the fractions containing the carrier ampholytes did not provide any useful MS signals, very good spectra were obtained with the autofocused fractions. Total protein sequence coverage was compared using the mass spectra of the autofocused fractions and those obtained from the infusion of the unfractionated sample. As expected, the average value of sequence coverage in the autofocused sample was higher than in the unseparated mixture; however, the ion suppression or surface adsorption could still play a role. From the experiments it can be concluded that the peptide autofocusing leads to improved sequence coverage when analyzing the fractions with ESI-MS, and, in cases of more complex samples, will be useful as the prefractionation tool prior to further separation. The main advantage of the autofocusing is its simplicity without the need of any additional chemicals and the resolution in principle similar to other IEF modes. When needed the focusing pH range can be easily adjusted by substituting the catholyte or anolyte with a solution of a pure ampholyte with the desired pH.

The authors wish to thank Applied Biosystems (Framingham, MA) for support and donation of the mass spectrometer, Dr. Aran Paulus (BioRad) for donation of the MicroRotofor device and Dr. Joël Rossier (Diagnoswiss) for the microfabricated nanospray tips. Additional support was provided by the Grant Agency of the Czech Republic, 203/06/1685, Grant Agency of the Czech Academy of Sciences A400310506, KAN400310651, and Ministry of Education, Youth and Sports LC06023.

5 References

[1] Foret, F., Preisler, J., *Proteomics* 2002, *2*, 360–372.

[2] Wolters, D. A., Washburn, M. P., Yates III, J. R., *Anal. Chem.* 2001, *73*, 5683–5690.

[3] Gygi, S. P., Rist, B., Gerber, S. A., Turecek, F. *et al.*, *Nat. Biotechnol.* 1999, *17*, 994–999.

[4] Strupat, K., *Methods Enzymol.* 2005, *405*, 1–36.

[5] Stroink, T., Ortiz, M. C., Bult, A., Lingeman, H. *et al.*, *J. Chromatogr. B* 2005, *817*, 49–66.

[6] Kašička, V., *Electrophoresis* 2006, *27*, 142–175.

[7] Righetti, P. G., Wenisch, E., Faupel, M., *J. Chromatogr.* 1989, *475*, 293–309.

[8] Tan, A., Pashkova, A., Zang, L., Foret, F. *et al.*, *Electrophoresis* 2002, *23*, 3599–3607.

[9] Ros, A., Faupel, M., Mees, H., van Oostrum, J. *et al.*, *Proteomics* 2002, *2*, 151–156.

[10] Heller, M., Ye, M. L., Michel, P. E., Morier, P. *et al.*, *J. Prot. Res.* 2005, *4*, 2273–2282.

[11] Michel, P. E., Crettaz, D., Morier, P., Heller, M. *et al.*, *Electrophoresis* 2006, *27*, 1169–1181.

[12] Egen, N. B., Bliss, M., Mayersohn, M., Owens, S. M. *et al.*, *Anal. Biochem.* 1988, *172*, 488–494.

[13] Kolin, A., *J. Chem. Phys.* 1954, *22*, 1628–1629.

[14] Vesterberg, O., *Acta Chem. Scand.* 1969, *23*, 2653–2666.

[15] Vesterberg, O., Svensson, H., *Acta Chem. Scand.* 1966, *20*, 820–34.

[16] Stoyanov, A. V., Righetti, P. G., *Electrophoresis* 1998, *19*, 1596–1600.

[17] Mosher, R. A., Saville, D. A., Thormann, *The Dynamics of Electrophoresis*, VCH, Weinheim 1992.

[18] Šlais, K., *J. Chromatogr. A* 1994, *684*, 149–161.

[19] Štastna, M., Travnicek, M., Šlais, K., *Electrophoresis* 2005, *26*, 53–59.

[20] Štastna, M., Šlais, K., *Anal. Bioanal. Chem.* 2005, *382*, 65–72

[21] Rossier, J. S., Vollet, C., Carnal, A., Lagger, G. *et al.*, *Lab Chip* 2002, *2*, 145–150.

[22] Xie, H. W., Bandhakavi, S., Griffin, T. J., *Anal. Chem.* 2005, *77*, 3198–3207.

[23] An, Y. M., Fu, Z. M., Gutierrez, P., Fenselau, C., *J. Prot. Res.* 2005, *4*, 2126–2132.

[24] Sova, O., *J. Chromatogr.* 1985, *320*, 213–218.

[25] Hashimoto, K., Sato, K., Nakamura, Y., Ohtsuki, K., *J. Agric. Food Chem.* 2006, *54*, 650–655.

[26] Xiao, Z., Conrads, T. P., Lucas, D. A., Janini, G. M. *et al.*, *Electrophoresis* 2004, *25*, 128–133.

[27] Storms, H. F., van der Heijden, R., Tjaden, U. R., van der Greef, J., *Electrophoresis* 2004, *25*, 3461–3467.

[28] Šlais, K., Friedl, Z., *J. Chromatogr. A* 1995, *695*, 113–122.

[29] Giddings, J. C., *Sep. Sci. Techol.* 1979, *14*, 869–870.

[30] Foret, F., Křivánková, L., Boček, P., *Capillary Zone Electrophoresis*, VCH, Weinheim 1993.

[31] Simó, C., Cifuentes, A., *Electrophoresis* 2003, *24*, 834–842.

Gabor Jarvas[1,2]
Jakub Grym[3]
Frantisek Foret[1,3]
Andras Guttman[2]

[1]CEITEC – Central European Institute of Technology, Brno, Czech Republic
[2]MTA-PE Translational Glycomics Research Group, MUKKI, University of Pannonia, Veszprem, Hungary
[3]Department of Bioanalytical Instrumentation, Institute of Analytical Chemistry, Czech Academy of Sciences, Brno, Czech Republic

Received August 7, 2014
Revised September 11, 2014
Accepted September 11, 2014

Research Article

Simulation-based design of a microfabricated pneumatic electrospray nebulizer

A microfabricated pneumatic electrospray nebulizer has been developed and evaluated using computer simulations and experimental measurements of the MS signals. The microdevice under development is designed for electrospray MS interfacing without the need to fabricate an electrospray needle and can be used as a disposable or an integral part of a reusable system. The design of the chip layout was supported by computational fluid dynamics simulations. The tested microdevices were fabricated in glass using conventional photolithography, followed by wet chemical etching and thermal bonding. The performance of the microfabricated nebulizer was evaluated by means of TOF-MS with a peptide mixture. It was demonstrated that the nebulizer, operating at supersonic speed of the nebulizing gas, produced very stable nanospray (900 nL/min) as documented by less than 0.1% (SE) fluctuation in total mass spectrometric signal intensity.

Keywords:
CFD / Electrospray / Microfabrication / Modeling / Nebulizer
DOI 10.1002/elps.201400387

1 Introduction

Electrospray ionization interface is the key component for on-line coupling of separations with MS. Since HPLC is the most widely used separation technique most of the interface designs reflect the specifics of the HPLC system, especially with respect to the mobile phase flow rate and connection of the ESI high voltage. The continuous development of microcolumn separations including capillary and chip-based HPLC requires also the development of suitable miniaturized interfaces. In addition due to the continuous development of genomics, proteomics, glycomics, and metabolomics, CE is experiencing a renaissance among separation techniques. Furthermore, regulators requiring orthogonal characterization methods for protein therapeutic candidates and commercially available biopharmaceuticals [1] are also inspiring this emerged status. CE hyphenated with MS is a unique combination of a high performance liquid phase separation technique and a special detection method, providing excellent selectivity and high sensitivity. Albeit, the most widely applied detection modes in CE are UV/VIS absorbance and LIF; MS detection offers extra benefits including sensitivity and ability to identify unknown structures [2]. In bioanalytical applications, where the sample usually contains sensitive molecules with high molecular masses, soft ionization methods (ionization with minimal fragmentation) have particular importance [3]. These methods, namely ESI [4] and MALDI [5], are usually used for a large variety of applications requiring MS analysis. Recently, CE-ESI-MS technique has been used for wide range of proteomics, glycomics, and metabolics applications; see the review of Feng et al. [3] for more details. However, hyphenation of CE with ESI-MS is not straightforward due to their differences in current levels [6] (microampers in CE versus nanoampers in ESI) and flow rates (often no flow in neutrally coated CE capillaries). To this end, numerous interface designs have been developed during the past decade aiming to achieve high selectivity and sensitivity at a simple and low cost way [1, 2, 7].

The coupling tools can be sorted into three main categories: sheathless, sheath liquid, and liquid junction interfaces. Microfabricated devices (microchips) represent an additional specific class, to integrate the separation part with electrospray emitters [8]. Microfabricated interfaces address the issue of handling limited amount of samples, sensitivity, and speed, and avoid cross-contamination. Furthermore, these small footprint devices can have multiple functions (sample extraction, digestion, derivatization, and separation) offering the opportunity of high level automation, which is necessary for fast, low cost—high throughput analyses in the bioanalytical field [9]. Electrospray from microfabricated interfaces has been demonstrated in a wide variety of designs

Correspondence: Dr. Frantisek Foret, Department of Bioanalytical Instrumentation, Institute of Analytical Chemistry, Czech Academy of Sciences, Veveri 97, CZ-611 42 Brno, Czech Republic
E-mail: foret@iach.cz
Fax: +42-0-541-212-113

Abbreviations: CFD, computational fluid dynamics; **PEEK**, polyether-ether-ketone

Colour Online: See the article online to view Figs. 1–3 and 6 in colour.

prepared in glass, plastic, or silicon using single or multiple microtips or fibers of nano/microspray systems [9–20], as well as directly from the chip surface, wherein the emitter is integrated within the body the chip [21–23]. Actually, the channel opening of the dielectric chip material can act as the ESI exit port without the need for the emitter tip. Using such alternative arrangement the hydrophilic surface of the microdevice wets and suffers from droplet formation around the exit port [24]. Using hydrophobic surface coating is one possibility to avoid wetting [9, 25, 26]. Furthermore, the use of compressed gas flow was suggested [9] to continuously remove the spread liquid, effectively preventing droplet formation. As a further benefit, the nebulizing action induced a liquid flow inside the spray channel of the microdevice. The spray liquid was supplied from the spray liquid channel connected at the end of the separation channel. This possible induced flow generated by pressure drop along the separation channel might cause brand broadening. Similar design has been also described for desorption ESI-MS [21]. However, most of the above-discussed systems were developed without deeper theoretical considerations. To speed up the design process, computational fluid dynamic (CFD) modeling techniques could be used to design new microfabricated interfaces. CFD is a simulation tool to help quickly achieve an optimal design at low cost with a minimum number of actual experiments. Albeit, modeling, and simulation are primarily considered as design tools, they can also be used to support experimental data interpretation. They are especially useful to understand the various phenomena occurring in microfluidic environment. For example, the microchannels in the interface systems have very high surface to volume ratio, therefore fluid flow could exhibit unusual behavior that is different than in the macroscopic world. However, in spite of state of the art modeling tools, no computational system is available that would be capable to assist in complete CE-ESI-MS coupling design, both at the molecular and bulk phase levels. Recently, Knapp et al. [10] and also Wu et al. [27] reported a comprehensive study on ESI-MS interface design using CFD, based on Taylor–Melcher leaky-dielectric formulations for solving the electrohydrodynamics and volume-of-fluid method for tracking the formed electrospray cone. In spite of the complexity of their model, the systems could not be applied for tip less interfaces since those were originally developed for the investigation of multi-spray carbon nanofiber emitters and focus more on the repulsion effects of cones on each other's. More recently, Gimelshein et al. [28] published an innovative paper on numerical modeling of ion transition in ESI-MS. Unfortunately, their model only describes the transport of evaporated ions inside the MS under subatmospheric condition.

In this paper, we report on the design, microfabrication, and test of a novel, integrated liquid junction-based pneumatic nebulizer, suitable for the ESI-MS analysis of biological macromolecules. First, numerous alternative chip designs were developed and further selected based on numerical simulations investigating the flow field distribution at the nebulizer gas outlet. Then, the two most promising layouts were microfabricated from glass using standard photolithography followed by wet chemical etching and thermal bonding. Finally, the nebulizers were used to generate electrospray and used to the analysis of a standard peptide mixture of bradykinin, angiotensin, and neurotensin by direct infusion in order to evaluate the performance of the developed devices.

2 Materials and methods

2.1 Numerical simulation-based design

Microfabrication using standard photolithography followed by wet chemical etching and thermal bonding is a time consuming and expensive process, therefore numerical simulation was applied to assist the interface design. Two alternative nebulizer layouts were involved in the simulations and evaluated by numerical methods. In the first design, the outlet ports of the nebulizer gas channels were in a converging arrangement related to the separation channel, while in the second one they run in parallel. Our CFD models for the simulation of the flow field were based on the one phase turbulent form of the Navier–Stokes equation. Figure 1 depicts the schematic representation of the device and its surrounding along with the modeled domain of interest. The nitrogen entered the nebulizer channels at 6 bar and 293 K. Under these conditions of channels the gas exited the chip at a very high velocity, dragging the analyte from the edge of the nearby separation channel. Unfortunately, the commercially available and even the custom-made software packages cannot adequately resolve numerically the droplet formation [29] (by defining the mesh resolution, the minimum droplet diameter is determined), therefore, numerical simulations carried out focusing only on the gas phase. The calculations were done in 2D mirror symmetric mode in order to reduce the computational demand. Based on the theoretical and experimental finding of Grym et al. [24], which refers to a similar interface device, it was assumed that the performance of the electrospray mostly depends on the flow characteristic of the nebulizer, therefore, the effect of electrohydrodynamics due to the applied electric field and the liquid phase (flowing in the separation channel) could be neglected. According to the calculated Reynolds number ($Re \approx 9000$), which indicates the flow characteristic, the fluid dynamics was rather turbulent.

Turbulent fluid flows are chaotic and their trajectory is nearly unpredictable. The flow characteristic was determined by inertial forces [29]. A commonly applied approach, k-ε turbulent model, was used to estimate the kinetic energy dissipation. This model solved for two variables: k; the turbulent kinetic energy, and epsilon; the rate of kinetic energy dissipation [30]. So-called wall functions [31] were used in this model, so the flow in the buffer region was simulated using analytical function. The k-ε model was chosen due to its good convergence rate and reliable performance around sharp geometries.

In our model, the flowing nebulizer nitrogen gas is assumed to be compressible, which means that its density varies

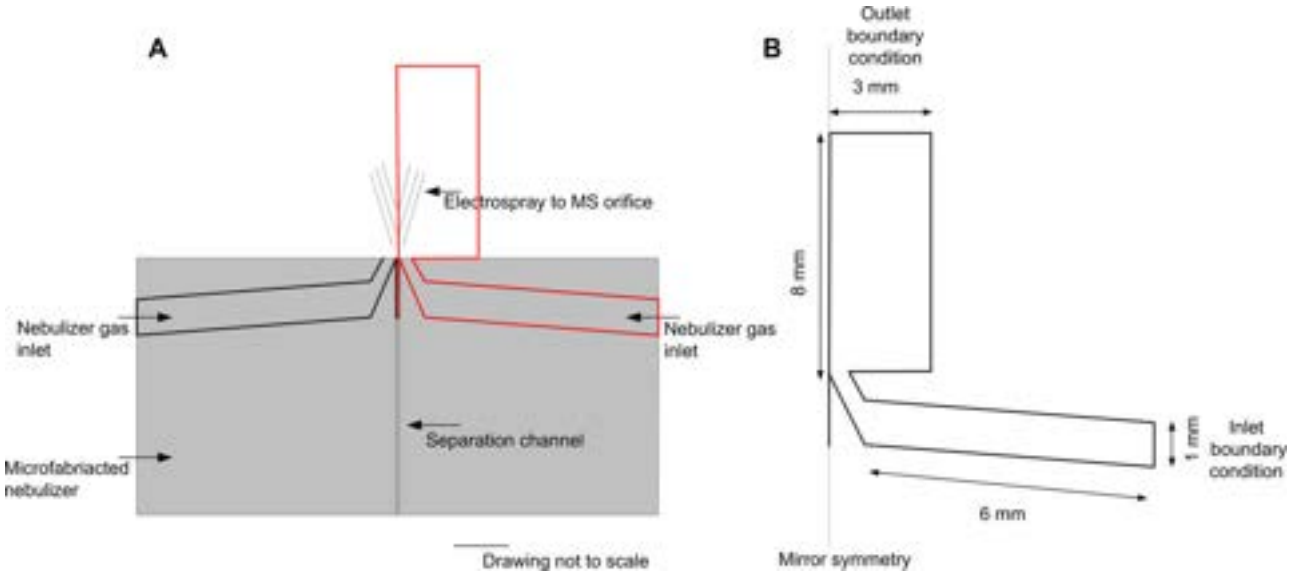

Figure 1. Schematic representation of the device and the modeled domain of interest. (A) The gray part is the body of the micronebulizer (converging design). The red part is the modeled domain covering the chip and the gap between the nebulizer and the MS orifice, this is where the nebulizer gas flows through. (B) The simulated domain (converging design) and its dimensions.

significantly in response to a change in pressure due to the expansion from 6 bar to atmospheric condition. The governing equation, which describes this fluid flow is the compressible vector form of the Navier–Stokes equation:

$$\rho\left(\frac{\partial v}{\partial t}+v\nabla v\right)=-\nabla p+\nabla(\mu(\nabla v+(\nabla v)^T))+\nabla\left(-\frac{2\mu}{3}\nabla v\right)+\rho g. \quad (1)$$

Equation (1) is usually coupled to the continuity equation of compressible flow:

$$\frac{\partial\rho}{\partial t}+\nabla(\rho v)=0, \quad (2)$$

where v is the linear velocity, ρ is the fluid density, μ is the dynamic viscosity of the fluid, t is the time, and p is the pressure. The left hand side of Eq. (1) is the acceleration of the fluid while the first term at the right is the force due to a pressure gradient, the second two terms describe the viscous force, and ρg is the body force.

Initial and boundary conditions are required to solve the governing partial differential equation system. Boundaries are shown in Fig. 1B. Inlet boundary condition is represented as constant pressure of six bar, defined by the nitrogen gas coming from the regulator. Outlet boundary is set to atmospheric pressure using the pressure without stress condition, restricting the numerical solver to keep the pressure at a given level. This is where the flowing fluid exits the computational domain. The boundaries located on the mirror symmetry axis are directly defined as symmetry boundary condition, meaning that no momentum transport occurs across the boundaries. All further boundaries were set as wall boundary condition without slip, meaning that the velocity of the flowing fluid at the wall was zero. Since this problem is highly nonlinear, iterative solving procedure was applied, meaning step-by-step calculation for more and more complex flow/pressure fields. Initial pressure condition for the whole domain was set by using the resulted pressure field of the previous calculation supporting the solver for achieving better convergence (except the first run, where uniform atmospheric pressure distribution was assumed). The meshing (also referred to grid generation or discretization) was done by Delaunay-free triangular method and performed many times with different sizes to obtain grid-independent data [32]. At close to the nebulizer gas outlet point of the chip, the mesh was set denser in order to properly resolve the most intensive change of the flow and pressure fields. Stationer solver of commercially available software COMSOL Multiphysics version 4.3.0.151 was used to obtain time invariant solution including pressure and velocity fields for the whole computational domain.

2.2 Microfabrication

The two numerically simulated microdevices were fabricated for experimental investigations by standard photolithography, chemical etching, and thermal-bonding techniques using borosilicate glass wafers (1.9 mm thickness) precoated with the Cr (2 μm) and photoresist (AZ 1518) layers (Nanofilm, Westlake, CA). Materials and chemicals were purchased form Sigma-Aldrich, Prague, Czech Republic. A μPG 101 laser pattern generator (Heidelberg Ins., Heidelberg, Germany) was used for directly writing the microdevice layouts onto the photoresist. After exposure the etching was carried out in NH_4F buffered hydrofluoric acid at 44°C resulting in 25 μm channel depth. The micromachined

substrate and cover plates were assembled using the standard thermal-bonding process. Finally, the edges of the chip were cut off by a dicing saw using a diamond blade at 3000 rpm exposing the electrospray exit port.

2.3 Instrumentation

The microfluidic devices were designed as part of a stationary manifold eliminating the need of any "glued" connection. To avoid any cross-contamination, polyether-ether-ketone (PEEK), a rather chemically and biologically resistant material was used for all parts of the manifold, which could be in contact with the sample and spray liquid. The PEEK frame was equipped with Luer connections for nebulizer gas and sample inlet/reservoir parts also made from PEEK (25 × 20.8 × 50 mm) were inserted/assembled in a plastic frame (89 × 20.8 × 89 mm). The glass chip was sandwiched between the manifolds as shown in Fig. 2. A stable, leak-free connection between the chip and the manifold was achieved using miniaturized O-rings (0.9 × 2.8 mm; Small Parts; Miami Lakes, FL). The O-rings were secured in the chip-positioning groove of the manifolds, and the chip manifolds in the plastic frame were held by four plastic screws. The PEEK manifolds contained sample reservoirs (Fig. 2A), one for infusion mode and others for further separation purpose. Reservoirs were equipped with platinum electrodes for connection to the high voltage and Luer connectors (Value Plastics; Fort Collins, CO) for gas connections. The high voltage (+3.5 kV) for on-line spray was supplied by the MS instrument. Platinum electrodes, incorporated in the sample reservoirs were connected to the MS ground.

The assembled device (chip, manifolds, and the plastic frame) was positioned in front of an orthogonal TOF mass spectrometer (maXis impact, Burker Daltonics) using an in-house built plexiglass holder and an x-y-z translational stage (Newport, Irvine, CA). Test experiments were performed at atmospheric pressure and room temperature. The nebulizer nitrogen was supplied from a tank and its pressure was regulated by an electro-pneumatic regulator ITV 0050–3N-q (SMC, Tokyo, Japan). ESI-TOF measurements were carried out in positive ion mode with a scan range of 300–1000 m/z. Each mass spectrum was a sum of 2 scans acquired during 1 s. The sample orifice was set to 140°C. The experimental setup was controlled and the data were acquired by Compass Software version 1.5 (Bruker Daltronics).

3 Results and discussion

3.1 Modeling

The 2D meshed geometry consists of 506222 triangular geometry elements together with Cartesian units in the boundary layers. Since the k-ε turbulent model uses the so-called wall function, therefore, wall lift-off in viscous units (a dimensionless number, which indicates the goodness of mesh resolution at the boundary) were calculated in order to test the mesh resolution. Those value matches the 11.06 criteria (determined by the software vendor) meaning that the mesh density is fine enough. Figure 3 shows the calculated velocity fields.

The resulted flow velocity field is not continuous. Free jet with oblique shockwaves are formed due to the applied high input pressure of the nebulizer gas. The presence of expansion–compression fans are not surprising considering the current operation conditions, where the velocity is much above the speed of sound at 293 K. This is further verified by its independence form the applied mesh resolution (maximum discrete element size was varied from 5 to 100 μm).

The right panel in Fig. 3 shows the calculated velocity field in case of nebulizer layout with parallel channels. Comparing left and right plots in Fig. 3, the major difference can be seen around the exit port of the nebulizer gas. In case of parallel

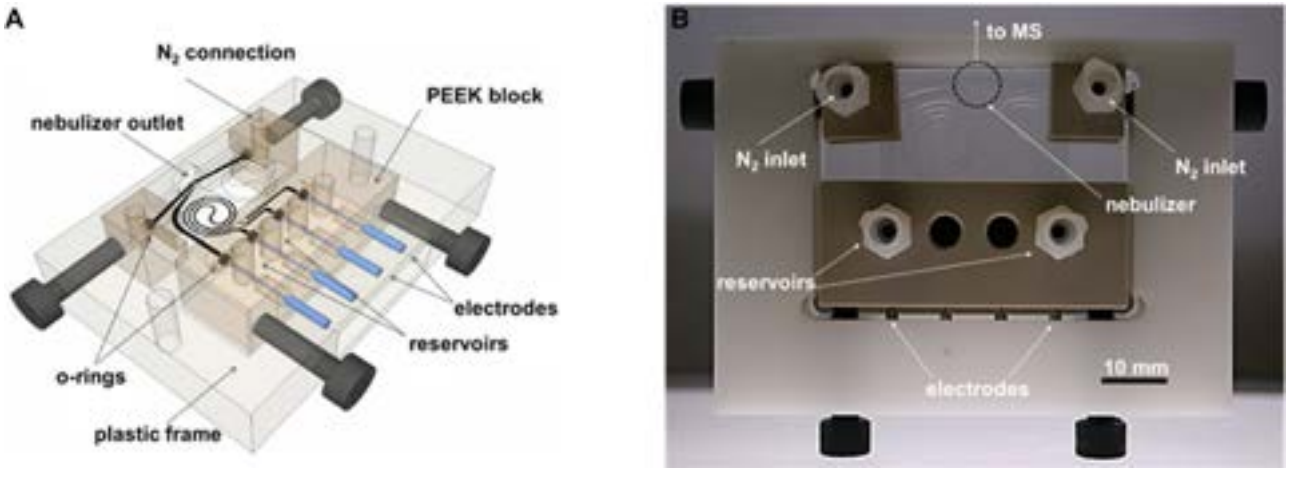

Figure 2. (A) The block scheme of the assembled microfabricated sonic nebulizer setup (the chip, its manifolds and the supporting plastic frame); (B) The experimental setup for test measurments. The chip is fixed by the plastic frame and positioned in front of the MS orifice.

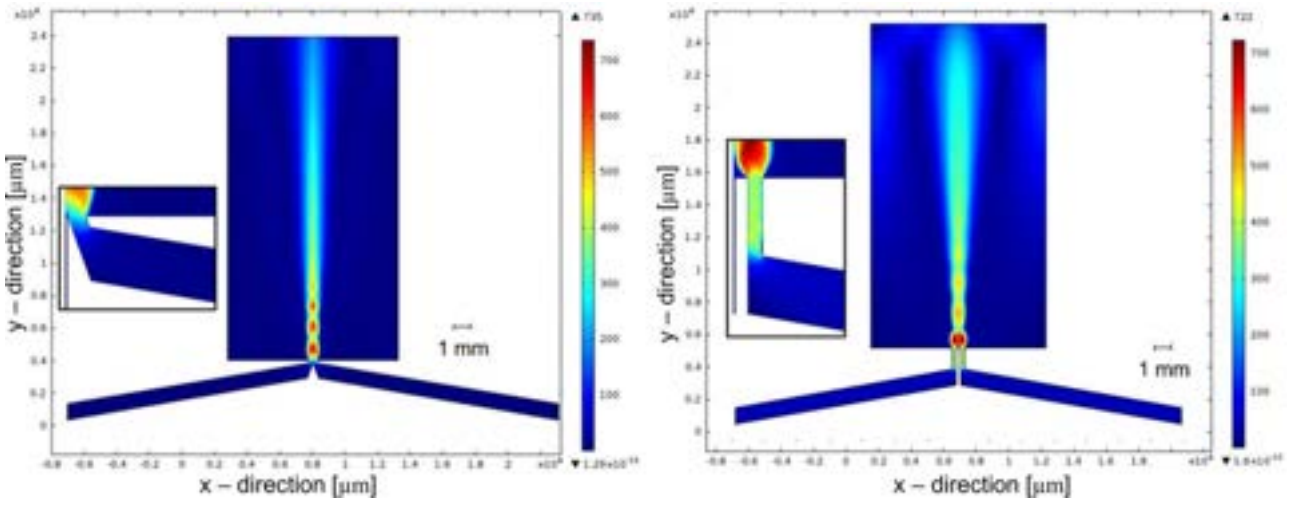

Figure 3. Simulated flow field assuming converging (left) or parallel (right) nebulizer channel layout. For better visualization, the calculated elements are flipped horizontally due to its mirror symmetry. The warmer the color the higher the velocity. Velocity is expressed in m/s.

layout the distance between the outlets of separation and nebulizer channels are 100 μm, while in case of converging one it is practically 0 μm. The outgoing gas accelerates to almost the same velocity in both cases, but on that longer distance the pressure gradient is lower, therefore it produces less effective suction and focusing effects.

3.2 Microfabrication

Based on the simulation results, two different types of chip layouts were fabricated. The nebulizer with converging design was more promising according to the numerical model; however, the parallel setup was also fabricated in order to validate the simulation results. The nebulizer gas channels were 1 mm wide, 25 μm deep and 15 mm long at the wider part and 100 μm × 25 μm × 0.1 mm at the outlet in case of the parallel chip, while the dimension of the converging design was 1 mm × 25 μm × 15 mm and 100 μm × 25 μm × 0.4 mm at the exit port. The separation channel was 50 μm wide and 25 μm deep. In case of the converging layout, the ends of separation and gas channels were merged into a semi-common outlet. The microfabricated nebulizers are shown in Fig. 4.

Positioning of the nebulizer unit was optimized manually by an x, y, z-stage to achieve the strongest ESI signal. Test sample, 1 μg/mL mixture of bradykinin, neurotensine, and angiotensin, was sprayed from the sample reservoir in 1% acetic acid in 50:50 v/v isopropanol/HPLC grade water solution. In case of parallel layout, the MS signal was not observed without applying pressure on the sample reservoir because the nebulizer did not cause sufficient suction and focusing effects. This verified the expectation based on simulation results (considering pressure gradient) that the distance between the exit port of the sample and nebulizer channels is too large in spite of the applied high inlet pressure of nitrogen. Consequently, further investigations were carried out using converging nebulizer design. Using the converging arrangement of nebulizer channels, the MS signal of standard peptides was observed without forcing the sample flow (applying pressure on the sample reservoir). In this situation, the exiting jet of converging pneumatic nebulizer caused sufficient suction and focusing effects. The measured MS spectrum is shown in Fig. 5. The achieved ESI signal intensity was comparable to that of using conventional capillary tips.

While the nebulizer does not create the Taylor cone [33] typical for the electrospray generated from a sharp

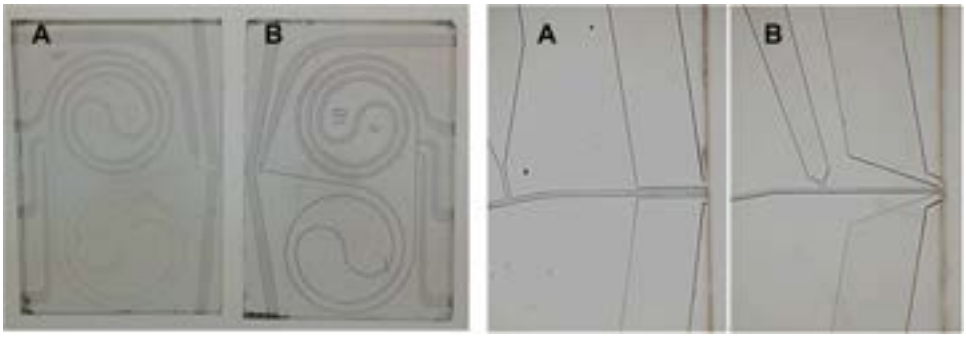

Figure 4. Photograph of the two microdevices tested and details of the nebulizers with parallel (A) or converging (B) pneumatic nebulizer channels.

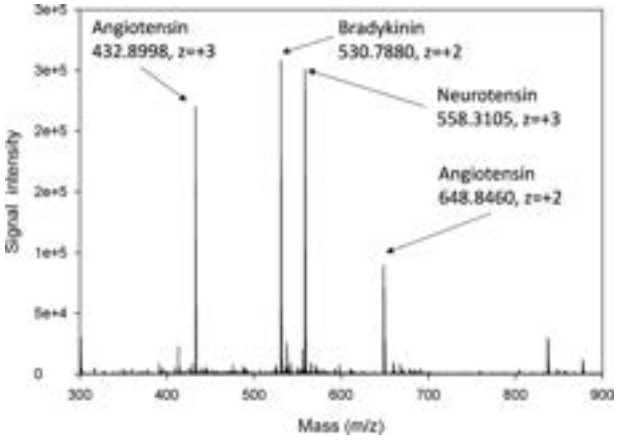

Figure 5. Measured MS spectra using the converging microfluidic nebulizer. Mixture of bradykinin, neurotensin, and angiotensin were sprayed by applying 3.5 kV spray voltage.

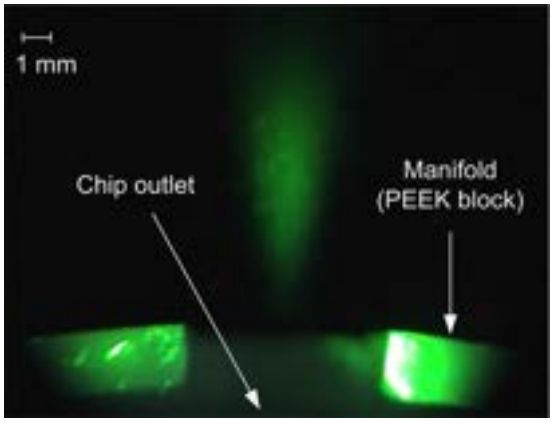

Figure 6. A representative frame of the CCD recorded movie investigating the converging nebulizer layouts. The electrosprayed beam (applying 3.5 kV spray voltage) was illuminated by a 532 nm NdYAG laser.

tip, the electrospray exiting from the edge of the microfluidic device was optically observable upon laser illumination. The spray plume was perpendicularly illuminated by an expanded 532 nm laser beam. The signal was recorded by a CCD camera (Fig. 6). The width of the observed plume agreed well with the simulated one, which was around 1 mm (measured at 3 mm from the exiting hole).

Since the sprayer plume is assisted by the nebulizer gas flow through sucking and focusing effects, it is expected that higher the nebulizer flow rate results in higher MS signal intensity (no signal observed when applying zero flow rate) and there is an optimum, which reflects the current experimental setup and conditions. To find out the optimal flow rate the inlet pressure was varied from zero to eight bars. The measured MS total ion current signal intensity as the function of inlet pressure is shown in Fig. 7A. Under four bars stable MS spectra was not observed. It is figured out that the optimal nebulizer pressure is 6 bar. Below this, the exiting flow is not intensive enough to transmit sufficient amount of ions, while above the optima, trajectories of molecules starting diverge from the main stream due to turbulent eddies. Please note that the MS inlet design also affects the ion transmission efficiency together with the spatial arrangement of the interface, however, further exploration of those was out of the focus of this study.

The long-term electrospray stability, which is one of the most important requirements of ESI-MS interfaces [34], was demonstrated by recording the signal intensity during twenty minutes. The measured total ion current intensity profile is depicted in Fig. 7B. The statistical analysis of the intensity profile—RSD: 71 449 (~1%) and SE: 1888 (~0.03%), based on the overall mean—shows outstanding performance. This stability is comparable or better than the performance (SD: $>$ 1.9%) of a recently published membrane-based emitter [35].

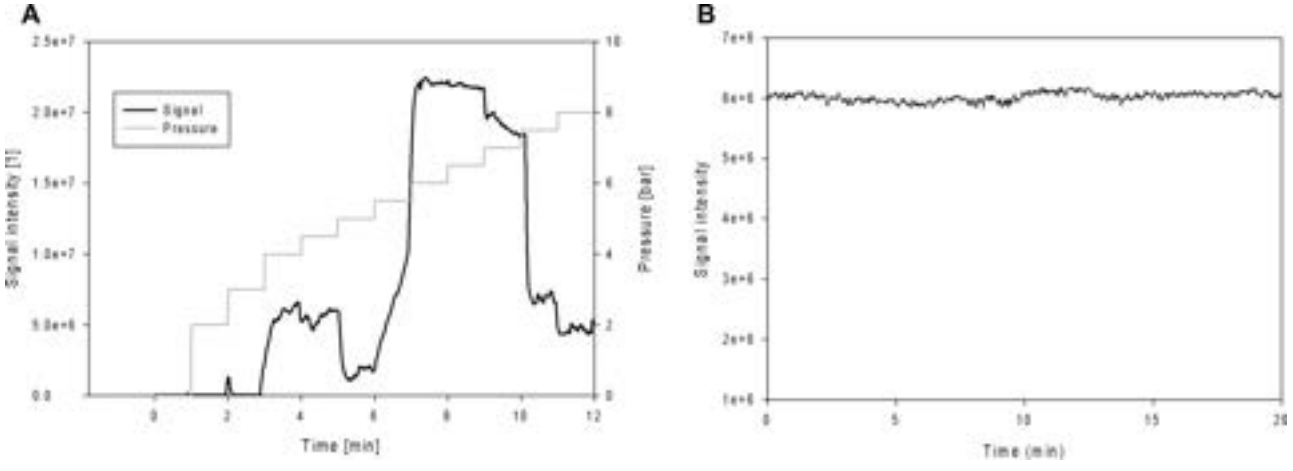

Figure 7. Investigation of the sonic nebulizer performance. Mixture of bradykinin, neurotensin, and angiotensin were sprayed applying 3.5 kV voltage. (A) Measured signal intensity in the function of nebulizer gas pressure. (B) The measured ESI signal stability.

4 Concluding remarks

A novel, tip-less microfabricated ESI-MS interface was developed based on numerical simulation results. The nebulizer gas flow was modeled for various designs, and the two most promising layouts were further investigated experimentally. The experimental findings justified the modeling results, allowing the use of numerical systems to assist in further engagements of the interface for separations-ESI-MS coupling. A converging geometry design showed stable, robust, and high intensity MS signal, furthermore, its optimal nebulizing pressure was determined for the proposed ESI arrangement. Despite of the fact that the microfabricated chip contains separation channels, its CE performance was not tested since it was out of the focus of this study. The described concept, based on the reported results provided an alternative way for MS coupling of microfluidic devices without the need of electrospray tip fabrication. Experimental determination of the gas velocity at the outlet of the semicircular channel opening was rather difficult; however, simulations verified that it was well above one Mach, therefore the term sonic nebulizer ESI would be justified. Further work, including both modeling and microfabrication is in progress for further simplification of sonic nebulizer devices.

This project is cofinanced by the European Social Fund and the state budget of the Czech Republic under project "Employment of Best Young Scientists for International Cooperation Empowerment, reg. number CZ.1.07/2.3.00/30.0037." Part of the work was realised in CEITEC - Central European Institute of Technology with research infrastructure supported by the project CZ.1.05/1.1.00/02.0068 financed from European Regional Development Fund. The support of the Momentum grant #97101 of the Hungarian Academy of Sciences (MTA-PE Translational Glycomics) and P20612G014 of the Grant Agency of the Czech Republic are also gratefully acknowledged.

The authors have declared no conflict of interest.

5 References

[1] Krenkova, J., Foret, F., *Proteomics* 2012, *12*, 2978–2990.

[2] Bonvin, G., Schappler, J., Rudaz, S., *J. Chromatogr. A* 2012, *1267*, 17–31.

[3] Feng, X., Liu, B. F., Li, J., Liu, X., *Mass Spectrom. Rev.* 2014, Doi: 10.1002/mas.21417.

[4] Fenn, J. B., Mann, M., Meng, C. K., Wong, S. F., Whitehouse, C. M., *Science* 1989, *246*, 64–71.

[5] Karas, M., Hillenkamp, F., *Anal. Chem.* 1988, *60*, 2299–2301.

[6] Hau, J., Roberts, M., *Anal. Chem.* 1999, *71*, 3977–3984.

[7] Pantuckova, P., Gebauer, P., Bocek, P., Krivankova, L., *Electrophoresis* 2011, *32*, 43–51.

[8] Lazar, I. M., Grym, J., Foret, F., *Mass Spectrom. Rev.* 2006, *25*, 573–594.

[9] Zhang, B., Liu, H., Karger, B. L., Foret, F., *Anal. Chem.* 1999, *71*, 3258–3264.

[10] Sen, A. K., Darabi, J., Knapp, D. R., Liu, J., *J. Micromech. Microeng.* 2006, *16*, 620.

[11] Sen, A. K., Darabi, J., Knapp, D. R., *Microfluid Nanofluid.* 2007, *3*, 283–298.

[12] Zhang, S., Van Pelt, C., Henion, J. D., *Electrophoresis* 2003, *21*, 3620–3632.

[13] Mao, P., Gomez-Sjoberg, R., Wang, D., *Anal. Chem.* 2013, *85*, 816–819.

[14] Shih, S. C., Yang, H., Jebrail, M. J., Fobel, R., McIntosh, N., Al-Dirbashi, O. Y., Chakraborty, P., Wheeler, A. R., *Anal. Chem.* 2012, *84*, 3731–3738.

[15] Rob, T., Liuni, P., Gill, P. K., Zhu, S., Balachandran, N., Berti, P. J., Wilson, D. J., *Anal. Chem.* 2012, *84*, 3771–3779.

[16] Petersen, N. J., Foss, S. T., Jensen, H., Hansen, S. H., Skonberg, C., Snakenborg, D., Kutter, J. P., Pedersen-Bjergaard, S., *Anal. Chem.* 2011, *83*, 44–51.

[17] Nordman, N., Sikanen, T., Aura, S., Tuomikoski, S., Vuorensola, K., Kotiaho, T., Franssila, S., Kostiainen, R., *Electrophoresis* 2010, *31*, 3745–3753.

[18] Tian, R., Hoa, X. D., Lambert, J. P., Pezacki, J. P., Veres, T., Figeys, D., *Anal. Chem.* 2011, *83*, 4095–4102.

[19] Ohla, S., Belder, D., *Curr. Opin. Chem. Biol.* 2012, *16*, 453–459.

[20] Chambers, A. G., Ramsey, J. M., *Anal. Chem.* 2012, *84*, 1446–1451.

[21] Sen, A. K., Darabi, J., Knapp, D. R., *Sensor. Actuat. B Chem.* 2009, *137*, 789–796.

[22] Schultz, G. A., Corso, T. N., Prosser, S. J., Zhang, S., *Anal. Chem.* 2000, *72*, 4058–4063.

[23] Licklider, L., Wang, X. Q., Desai, A., Tai, Y. C., Lee, T. D., *Anal. Chem.* 2000, *72*, 367–375.

[24] Grym, J., Otevrel, M., Foret, F., *Lab Chip* 2006, *6*, 1306–1314.

[25] Choi, Y. S., Wood, T. D., *Rapid Commun. Mass Spectrom.* 2007, *21*, 2101–2108.

[26] Lord, G. A., *Biomed. Chrom.* 2006, *20*, 1274–1274.

[27] Wu, X., Oleschuk, R. D., Cann, N. M., *Analyst* 2012, *137*, 4150–4161.

[28] Gimelshein, N., Gimelshein, S., Lilly, T., Moskovets, E., *J. Am. Soc. Mass. Spectrom.* 2014, *25*, 820–831.

[29] Jarvas, G., Guttman, A., Foret, F., *Mass Spectrom. Rev.* 2014, Doi: 10.1002/mas.21423.

[30] Rogallo, R. S., Moin, P., *Annu Rev. Fluid Mech.* 1984, *16*, 99–137.

[31] Ojaniemi, U., Riihimäki, M., Manninen, M., Pättikangas, T., *Chem. Eng. Sci.* 2012, *84*, 57–69.

[32] Supeene, G., Koch, C. R., Bhattacharjee, S., *J. Colloid Inter. F Sci.* 2008, *318*, 463–476.

[33] Melcher, J. R., Taylor, G. I., *Annu. Rev. Fluid Mech.* 1969, *1*, 111–146.

[34] Gao, D., Liu, H., Jiang, Y., Lin, J. M., *Lab Chip* 2013, *13*, 3309–3322.

[35] Sun, X., Kelly, R. T., Tang, K., Smith, R. D., *Anal. Chem.* 2011, *83*, 5797–5803.

